Catalytic Conversion of Terpene Feedstocks into value-added Chemicals and Commodity Chemicals

Cunningham, William

Award date:
2018

Awarding institution:
University of Bath

Catalytic Conversion of Terpene Feedstocks into Value-Added Chemicals and Commodity Chemicals

William Cunningham

A thesis submitted for the degree of Doctor of Philosophy

University of Bath

Department of Chemistry

2018

Abstract

There is currently much interest in developing biorenewable alternatives to the multitude of bulk and fine chemicals required by a modern society that are currently sourced from non-renewable petroleum sources. However many of the biomass sources that have been considered as replacement chemical feedstocks for oil such as cellulosic materials or fatty acids are highly oxygenated and are not well suited to constructing the aromatic rings present in many drug molecules. Terpenes, on the other hand, are an abundant class of biomass derived hydrocarbons that are deoxygenated and amenable to aromatisation. Monoterpenes in particular can be easily separated from aqueous environments and can potentially be upgraded into a range of commodity, fine chemicals and drug molecules; complimenting the other biomass chemical sources.

Epoxidation is an especially useful transformation for the formation of important intermediates in the synthesis of fine and bulk chemicals such as pharmaceuticals and polymers. We have optimized a selective, solvent free epoxidation process based upon a tungsten polyoxometalate catalyst that works for a broad range of commonly available terpenes, including crude sulphate turpentine, having expanded its scope and developed an optimal protocol that enables epoxidation in shorter reaction times, with fewer additives, at milder temperatures and without the need for undesirable solvents compared to previous epoxidation protocols. We have also investigated various other catalytic methods to selectively epoxidize the other alkene substitution patterns present in a wide variety of terpene substrates that enables access to a number of key terpene bis-epoxides and this is discussed in chapter 2.

We have also combined the optimal catalytic protocol with flow engineering, to develop a sustainable, catalytic flow epoxidation protocol that is suitable for both laboratory and industrial scale synthesis of biomass derived terpene epoxides. In particular, targeting the replacement of stoichiometric and expensive reagents and environmentally polluting solvents with green H_2O_2 and solvent free conditions and this is discussed in chapter 3.

This catalytic epoxidation protocol was then adapted to enable the sustainable production of terpene and non-terpenoid *anti*-diols without the need for toxic co-solvents, corrosive acid or time consuming neutralisation steps. These *anti*-diol substrates are promising monomers for polymerisation and have other important applications such and this is discussed in chapter 4.

Chapter 5 discusses the development of synthetic routes to sustainable paracetamol *via* the pharmaceutical intermediate 4-hydroxyacetophenone that is economically comparable with current petrochemical routes.

Chapter 6 discusses the development of a number of selective synthetic routes to a number of isomers of the mosquito repellent, *p*-menthane-3,8-diol, with a novel all-*cis* isomer, made with excellent selectivity, that has the potential to have enhanced repellent properties.

Ultimately, this PhD concerns the development of protocols for the conversion of terpene feedstocks into value-added chemicals that will be used as precursors for the synthesis of commodity drug targets such as paracetamol (pain relief); for the synthesis of renewable polymer epoxide and diol monomers and for the synthesis of biologically active molecules such as *p*-menthane-3,8-diol (insect repellent).

Acknowledgements

First and foremost I would like to thank Professor Steven Bull for the opportunity to work in his group and his excellent guidance throughout my PhD. His knowledge of organic chemistry and terpene transformations has been indispensible and I am for always grateful that he has provided me with such useful insights and direction. We have had an excellent few years having been part of the Chemistry football team and having been personally coached by Professor Bull in the ways of football. We have also journeyed together on a number of memorable trips abroad including both Pacifichem and PACCON conferences.

I would also like to thank Dr Pawel Plucinski who has offered advice and use of his equipment throughout my PhD.

I would also like to thank both Dr Marc Hutchby and Dr Robert Chapman for their guidance and help with respect to practical work, report writing and squash whilst they were working as part of the Terpenes consortium and I am very grateful for all the lessons I have learnt from both.

I would like to thank the rest of the Bull, James and Williams groups, both past and present, for their help and support throughout my PhD. I would like to thank in no particular order; Rich, Ruth, Dave, Emma, Adam, Liam, Jordan, Dan and Caroline for making my time in the lab so enjoyable, and would like to thank the more recent members to the groups, Josh, Maria and Maria for making the office and lab such a pleasant environment to work in.

I would also like to thank Steve, again, in particular for taking the time to proof read my thesis and whose advice has been exceptional.

I would like to finally thank my family and friends who have been a constant support to me throughout the PhD process and have offered advice that has helped guide me over the last few years.

Abbreviations

Ac	Acetyl
aq	Aqueous
AIP	Aluminium isopropoxide
Ar	Aryl
Amb-15	Amberlyst 15 solid supported catalyst
A336	Aliquat 336
$Al(O^iPr)_3$	Aluminium isopropoxide
Buli	n-Butyl lithium
Br	Broad
BrAc	Bromo-acetonide intermediate
^{13}C NMR	Carbon 13 Nuclear Magnetic Resonance
J	Coupling constant
^oC	Degrees Celcius
δ	Delta, chemical shift
CST	Crude Sulfate Turpentine
CDC	Centre for Disease Control and Transmission
Cat.	Catalyst
Ca.	Approximately
COSY	Two dimensional homonuclear correlation spectroscopy
$CDCl_3$	Deutetrated Chloroform
DEET	*N*,*N*-diethyl-*m*-toluamide
Dil	Dilute solution
DCM / CH_2Cl_2	Dichloromethane
DMS	Dimethyl sulphide
DMA	Dimethylacetamide
DIBAL	Diisobutylaluminium hydride
DHQD	Dihydroquinidine
DHQ	Hydroquinine
DEAD	Diethyl azodicarboxylate
d	Doublet
DMSO	Dimethyl sulfoxide
DMAP	4-Dimethylaminopyridine
DMDO	Dimethyldioxirane
DMS	Dimethylsulphoxide
DET	diethyl tartrate

DKA	Di-ketone alcohol
DKA-OAc	Di-ketone acetate
Dihydro-PMD	Unsaturated PMD intermediate
eq	Equivalence
ECH	Epichlorohydrin
E.coli	Escherichia coli bacteria
Et	Ethyl
Ent	one enantiomer of a pair
EtOAc	Ethyl acetate
FDA	US Food and Drug Administration federal agency
g	Grams
g/L	Grams per litre
GCMS	Gas chromatography–mass spectrometry
GT	Gum Turpentine
Hz	Hertz
4-HAP	4-hydroxyacetophenone
HexLi	*n*-Hexyl-lithium
h	Hours
HETCOR NMR	Heteronuclear correlation Nuclear Magnetic Resonance
	Nuclear Magnetic Resonance
in vacuo	Under reduced pressure
IR	Infra-red spectroscopy
LTF	Little Things Factory (microreactor manufacturer)
$LiAlH_4$	Lithium aluminium hydride
LimBrOH	Limonene bromo-hydrin
LDA	Lithium diisoprpylamine
L	Litres
m/z	Mass to charge ratio
MHz	Megahertz
Me	Methyl
MTO	Methyltrioxorhenium
MeOH	Methanol
***m*CPBA**	*meta*-Chloroperoxybenzoic acid
min	Minutes
mL	Milliletres

mg	Milligrams
mm	Millimeters
mmol	Millimoles
m	Multiplet
mol%	Mole percent
ml/hr	Millileters per hour
MS	Mass spectroscopy
M	Molar concentration
NBS	N-bromosuccinimide
NMO	*N*-methylmorpholine-*N*-oxide
NEt_3	Triethylamine
nm	Nanometres
Nu	Nucleophile
O	ortho
OPP	Oxygen linked pyrophosphate group
PAAOAc	Pseudo-limonene allylic alcohol acetate
PAA	Pseudo-limonene allylic alcohol
ppm	Parts per million
PL	Pseudo-limonene
Ph	Phenyl
PLimC	Polylimonene carbonate
PTC	Phase transfer agent/catalyst
PTFE	Polytetrafluoroethylene
PTSA	*p*-Toluenesulfonic acid
PNCB	*p*-4-Nitrobenzoic acid
$POCl_3$	phosphorus oxychloride
P	Para-
Py	Pyridine
POM	Polyoxometalates
PPh_3	Triphenyl phosphine
PMD	*p*-menthane-3,8-diol
PMD-Ace	*p*-menthane-3,8-diol acetonide
ppm	Parts per million
^{1}NMR	Proton Nuclear Magnetic Resonance
rt	Room temperature
RT	Residence time

Rpm	Revolutions per minute
R_f	Retention factor
R	Unspecified generic group
rac	Racemic
rt	Room Temperature
s-hydride	Super-hydride (Lithium triethylborohydride)
s	Singlet
S_N2	Binuclear Nucleophilic Substitution
S_N2'	Binuclear Nucleophilic Conjugate Substitution
SARs	Severe acute respiratory syndrome (viral infection)
^{t}	Tertiary
TMP	2,2,6,6-Tetramethylpiperidine
THF	Tetrahydrofuran
tlc	Thin layer chromatography
Tol	Toluene
TBHP	*t*-butyl hydroperoxide
tlc	Thin layer chromatography
t	Triplet
WHO	World Health Organisation

Contents

1 Chapter 1 – Introduction - Overview of Epoxides and their Importance

1.1.1 Sustainability and Green Chemical Technologies

Sustainable development has been defined by the Brundtland report as "… development that meets the needs of the present without compromising the ability of future generations to meet their own needs."[1] As population growth and living standards rise the demand for chemicals will continue to increase, resulting in on-going consumption of natural resources and production of waste. As there are only finite amounts of petrochemical and mineral resources available, they must be used in a responsible, renewable and recyclable manner. The production of waste and toxic reagents must also be minimized and disposed of safely to avoid causing harm.

The chemical industry generates significant revenues worldwide with sales of chemical products reaching ~$3500 bn in 2011[2], with many of these products essential for modern society, including fuels, metals, plastics, pharmaceuticals, agrochemicals and consumer products. However, the chemical industry is also a wasteful and polluting sector of the global economy. Consequently, there is increasing environmental and economic pressures on the chemical industry, including new legislation and rising consumer concern that is compelling industry to think about producing chemical products in a more sustainable manner. Consequently, there are increasing efforts in the chemical and manufacturing sectors to adhere to the principles of "green" chemistry and chemical engineering to make chemical processes more aligned with the concept of sustainability. Paul Anastas defines green chemistry as "utilization of a set of principles that reduces or eliminates the use or generation of hazardous substances in the design and manufacture and application of chemical products".[3] Therefore, the use of catalytic reactions, benign reagents, green solvents and renewable chemical feedstocks are currently key areas of chemical research.

Current bulk and fine chemicals are sourced from unsustainable petrochemical sources, with biomass having been suggested as an alternative source of renewable feedstocks of carbon based chemicals. However, many of these biomass sources (e.g. lignocellulose biomass) are highly oxygenated, difficult to isolate in pure form and are not well suited to the construction of aromatic ring systems that are present in many pharmaceutical molecules.

Terpenes, on the other hand, are a relatively untapped and abundant source of biomass derived hydrocarbons that are generally deoxygenated; contain alkene groups that can be functionalized using existing industrial processes, with catalytic dehydrogenation of the cyclohexenyl rings of monoterpenes potentially affording access to aromatic products. This affords an opportunity to employ terpenes as a source of 'drop-in' biorenewable chemicals that can complement bulk chemical precursors e.g. bioethanol derived from other biomass derived chemical platforms.

Terpene hydrocarbons represent one of the largest and most diverse classes of natural products. They are secondary metabolites,[4] that are produced biosynthetically by plants, insects and microorganisms via incorporation of 5 carbon containing isoprene molecules. They have numerous roles ranging from defence repellents against herbivores or pathogens through animal attractant hormones[5] to agents designed to help disperse seeds and pollen. Terpenes can also function as structural polymers.[4]

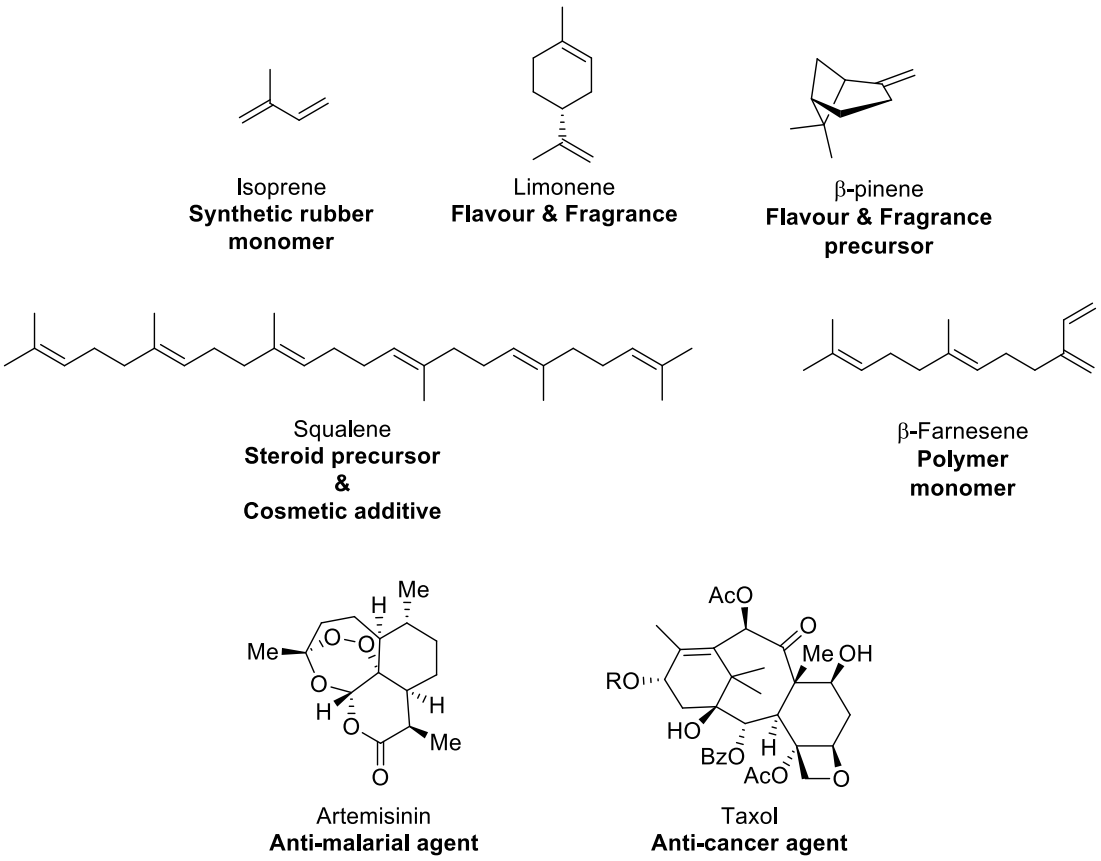

Figure 1. Important terpenes and their applications

Due to the natural abundance of terpenes, they have attracted attention from many industries as a source of chemical products. For example, terpenes are used as solvents (β-pinene) or diluting agents for dyes and varnishes,[6] as cosmetic additives and steroid precursors (Squalene)[7], as polymer monomers (isoprene)[8], as flavours and fragrances (limonene and geraniol (derived from β-pinene))[7] and as medicinally active compounds (artemisinin and taxol)[9]. A number of syntheses of vitamins and insecticides start from terpenes that are employed as synthetic intermediates and chiral building blocks, Figure 1.[10]

Terpenes represent a potentially plentiful biorenewable feedstock for the synthesis of value-added chemical products. Significant volumes of synthetically useful terpenes are commercially available at low cost as by-products of the agricultural and timber industries[11], with an estimated annual volume of around 330,000 tonnes being produced worldwide.[11] The largest source of terpene feedstock is turpentine, with crude sulfated turpentine being produced as a by-product of the Kraft paper pulping process at around $800-1000 per tonne.[12] These volumes and prices suggest that a scalable biorefinery industry based on the use of terpene feedstocks sourced from industrial by-products is potentially feasible.

Industrial biotechnology also provides a potential source of terpene feedstocks. For example the biotechnology company, Amyris, has developed commercial routes to both farnesane and squalene which are used as aviation fuels and cosmetics ingredients respectively.[13] Amyris have genetically modified a synthetic biology platform to convert inexpensive sugars into higher value terpene products. This biotechnology approach not only provides geographic flexibility and a predictable supply of terpene feedstocks, but also allows access to large

volumes of high value monoterpenes, such as perillyl alcohol, that are currently too expensive for widespread use because their natural abundance is too low.

Terpenes have been used since antiquity, typically as flavours and fragrances, but have not been used systematically to produce platform chemicals in a biorefinery context. For these reasons, the development of generic catalytic methods that enable the reliable conversion of terpenes into higher value chemicals are required.

Epoxidation methodologies are used extensively in both academia and industry to upgrade alkene functionality to produce higher value chemical products. Typically, stoichiometric amounts of peracid have been employed to carry out epoxidation reactions on scale, due to low costs and high yields.[14] However, these stoichiometric protocols produce large amounts of waste acid and can be challenging to perform in a safe manner, whilst they often afford lower yields on a large scale.[14]

The development of scalable, safe and catalytic epoxidation methodologies is a difficult undertaking, particularly for the epoxidation of terpene feedstocks. This is because terpenes contain a variety of different types of alkene functionality (e.g. trisubstituted *vs* disubstituted alkenes), that need to be selectively targeted whilst terpene epoxides can undergo competing rearrangement, ring-opening and hydrolysis reactions to afford mixtures of unwanted side products that are difficult to purify. Catalytic epoxidation protocols that employ green oxidants such as hydrogen peroxide typically react in a rapid manner leading to high exotherms that make large batch reactions difficult to control.[14] Nevertheless, epoxidation methodologies involving metal catalysis and green oxidants potentially provide a cheap and waste minimizing route to epoxide products, with the development of solvent free conditions using cheap oxidants (e.g. H_2O_2 / O_2) particularly attractive from a sustainability perspective.

1.1.2 Epoxides

Epoxides (or oxiranes) are strained, 3 membered rings containing one oxygen atom, the general structure of which is shown in Figure 2. Epoxides feature in many industrial processes as key intermediates or products and are also formed as metabolites and biosynthetic intermediates in living organisms.[15]

Figure 2. 3 membered ring structure of epoxides (or oxiranes)

Epoxides are very reactive compared to linear dialkyl ethers because of the strain energy caused by their 3-membered ring structure. This strain makes the carbon-oxygen bonds highly reactive and susceptible to ring opening using a variety of nucleophiles to form a wide range of useful products, as shown in Figure 3.[16]

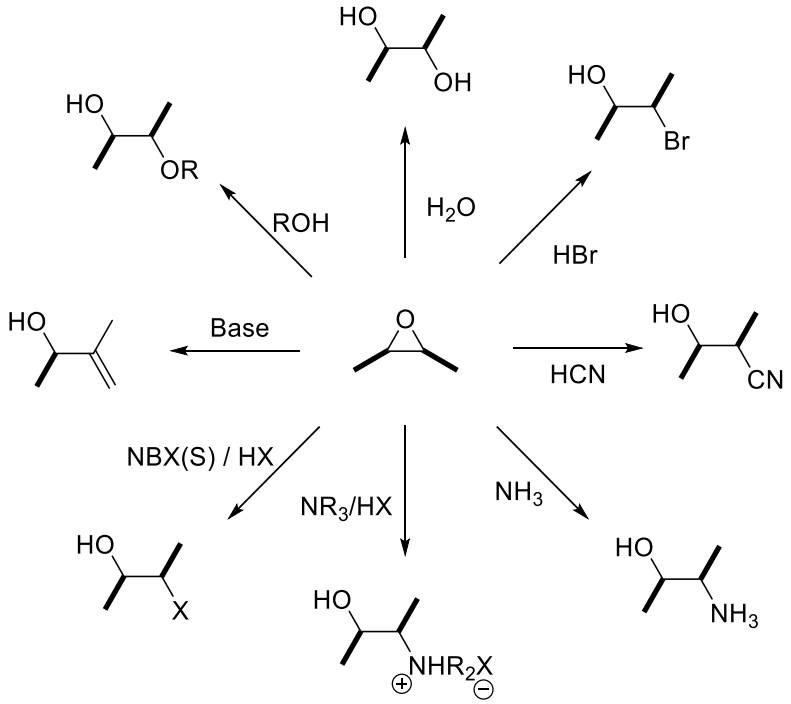

Figure 3. Chemical products obtained from epoxide ring opening

1.1.3 Applications of Epoxides

Epoxides are highly relevant to both the academic and industrial chemical communities. They are important intermediates for the synthesis of polymers such as polyamides, polyglycols and polyurethanes, and are also important in fine chemical manufacture where they are employed to prepare many pharmaceuticals, flavours, fragrances and nutraceuticals.[15]

The largest production of epoxides by volume is in the manufacture of propylene oxide which is used as a monomer for polymer production, with an annual output of 8 million tonnes that is predicted to increase significantly in the future. Ethylene oxide is another major epoxide product that is also used for polymer production, which has been resulted in a large amount of research into the development of epoxidation catalysts.[17]

Other epoxide derived products include glycols, alcohols and polymers such as epoxy resins, polyurethanes and polyesters.[18] Epoxy resins in particular are one of the most versatile types of polymer that are used for many applications such as automotive primers, metal can coatings, printed circuit board materials and semi-conductor encapsulants. For example, the major “epoxy” component, bisphenol A diglycidyl ether, is manufactured from alkylation of bisphenol A with epichlorohydrin, Figure 4.[19]

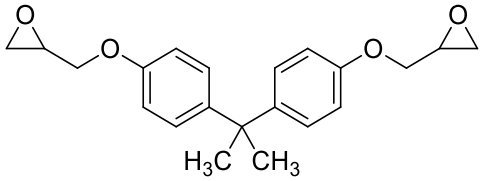

Figure 4 Bisphenol A diglycidyl ether

Currently, large chemical companies such as BASF and Dow use heterogeneous catalysts such as silicate zeolites doped with titania to produce propylene oxide and silver supported on Al_2O_3 supports to produce ethylene oxide. The key reason for using these type of heterogeneous catalysts is their stability, which enables catalyst recycling and the ability to use cheap oxidants such as oxygen and hydrogen peroxide to afford epoxides with high selectivity.[17]

Other potential oxidants such as iodosobenzene, amine/pyridine-*N*-oxides and NaOCl are not widely used by the process industry, because of their safety profile and the fact that they require more complex processing. Other uses of mass produced epoxides are summarised in Table 1 below.[20]

Table 1. Uses of Epoxides

Epoxide	**Application**
Propylene oxide	Polymers
Ethylene oxide	Polymers, Disinfectants, Lubricants, Paints and Cosmetics
Styrene oxide	Epoxy resins
Epichlorohydrin	Epoxy resins
1-octene oxide	Soap
1-decene oxide	Cosmetics

Epoxides exist widely in nature within the structures of biologically active natural products, with Fumagillin[21] and Dynemicin A[22] both exhibiting important medicinal activities as potential antimicrobial and anticancer agents, respectively (Figure 5).

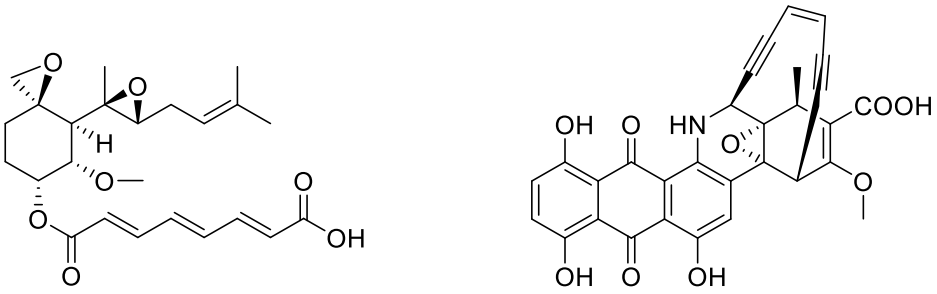

Figure 5. Epoxides in natural products

A His-231 residue in the active site of the methionine aminopeptidase 2 (MetAP2) attacks the epoxide of Fumagillin to trigger its ring opening to form a new covalent nitrogen-carbon bond that results in irreversible inhibition of the enzyme, thus preventing it from hydrolysing the amide bonds of its peptide substrate (Scheme 1).[20,21]

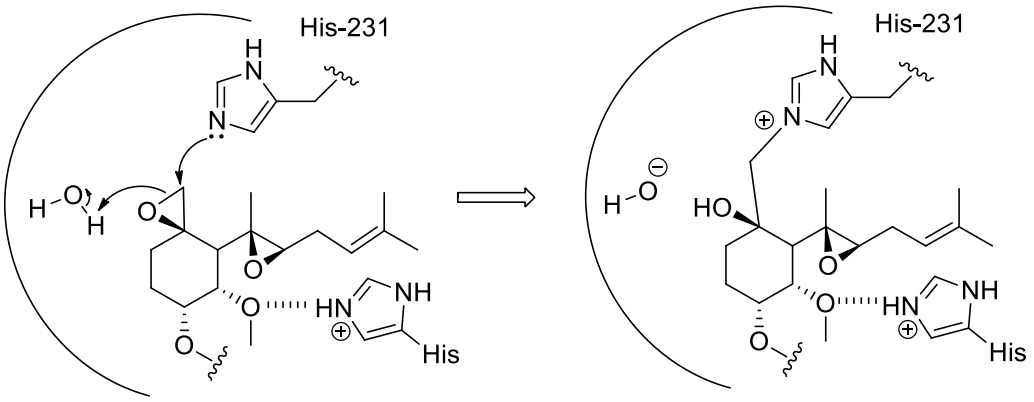

Scheme 1. Proposed mechanism for inhibition of methionine aminopeptidase 2 (MAP2) by Fumagillin

Dynemicin A is an enediyne based anti-cancer drug, whose mechanism of action involves the generation of a diradical species that cleaves specific DNA sequences in the genomes of cancer cells. Cremer *et al*[22] have reported that Dynemicin binds to a double helical DNA strand by intercalation with its base pairs, which causes DNA strand separation to change from 3-4 to 7-8 Angstroms. An enediyne cyclisation reaction is then triggered by NADPH mediated reduction of its quinone fragment and concomitant epoxide ring opening, or *via* direct epoxide ring opening by nucleophiles such as thiols. Bergman cyclisation of the activated ene-diyne fragment then occurs to generate a singlet state didehydrobenzene diradical that can then abstract DNA hydrogen atoms causing both DNA strands to be irreversibly cleaved, leading to cell death (Scheme 2).[22]

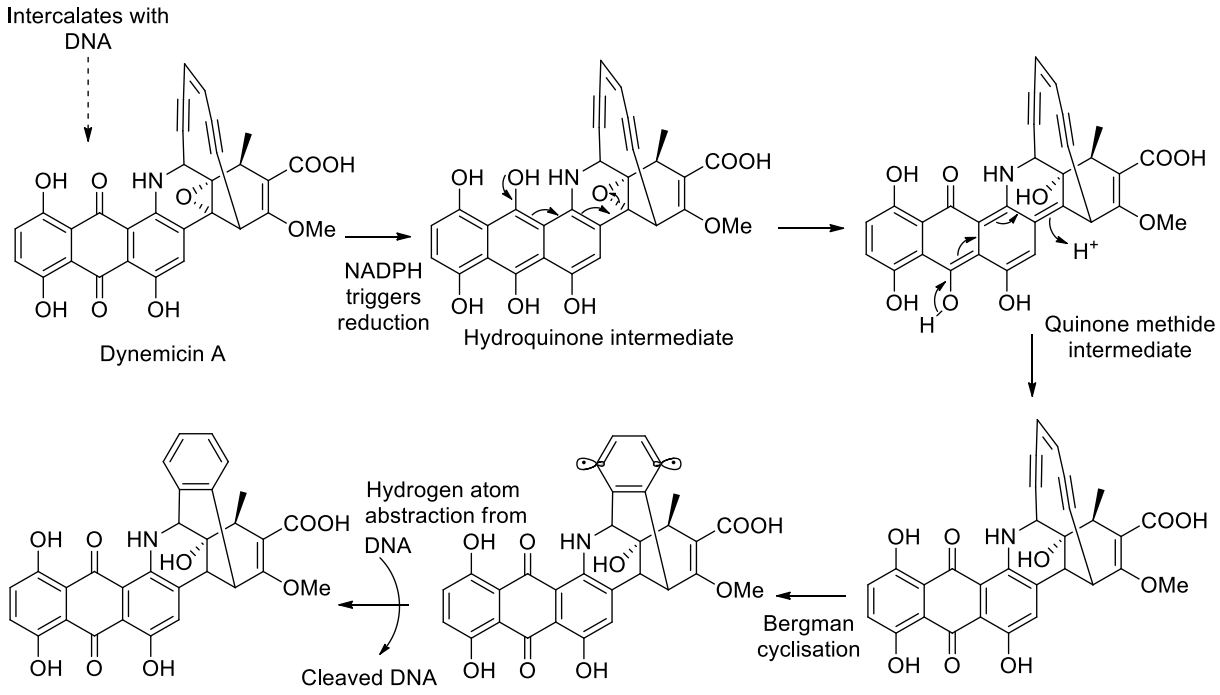

Scheme 2. Mechanism of reductive activation of Dynemicin A

1.1.4 Mechanism of Ring Opening of Epoxides

Epoxides play a major role as organic intermediates for synthesis because their strained cyclic structures readily react with nucleophiles *via* a number of different mechanisms to produce a variety of ring-opened product structures. Epoxides can be opened under either acidic or basic conditions with each pathway potentially affording different products depending on the mechanism of ring opening (Scheme 3).[16]

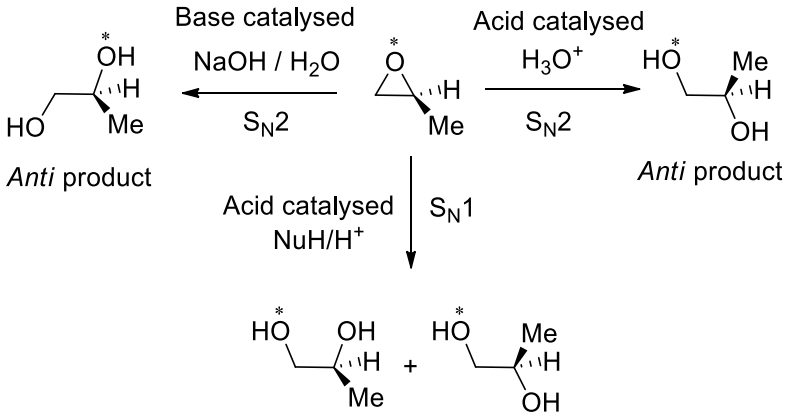

Scheme 3. Different products produced by different epoxide ring opening mechanisms

Acid catalysed epoxide ring opening can occur *via* a S_N2 type fashion with the nucleophile attacking the most substituted carbon with clean inversion of configuration. The use of an acid catalyst can potentially be used to enable weak nucleophiles (e.g. water) to effectively open the epoxide ring (Scheme 4).[16]

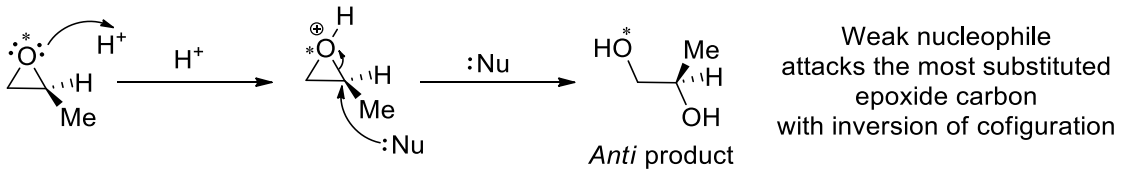

Scheme 4. Acid mediated epoxide ring opening

Alternatively, acid catalysed ring opening reactions can proceed via an S_N1 type ring opening mechanism, which would lead to scrambling of the stereochemistry at the more substituted carbon to give a mixture of *syn*- and *anti*- products (Scheme 5).[16]

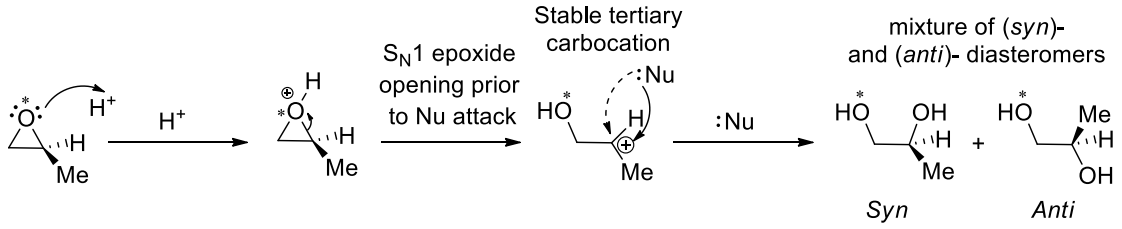

Scheme 5. Acid mediated epoxide ring opening *via* S_N1 mechanism

In comparison, base mediated epoxide opening occurs *via* a S_N2 type fashion with the nucleophile attacking the least substituted carbon to afford a regioisomeric *anti*-product (Scheme 6).[16]

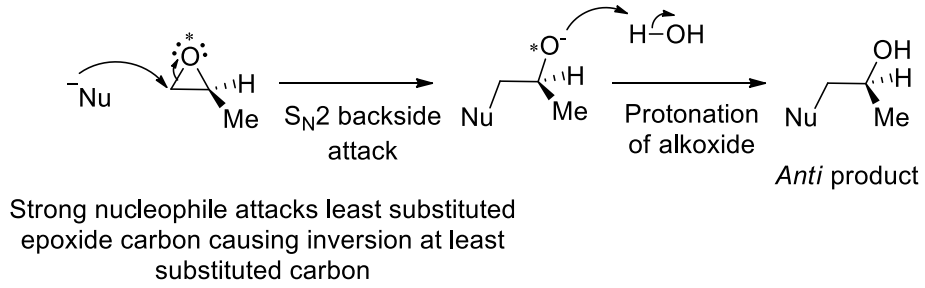

Scheme 6. Base mediated epoxide ring opening

1.1.5 Methodology for the synthesis of epoxides

Epoxides can be synthesised from various different functional groups in numerous ways, with Figure 6 highlighting a range of methodologies that employ stoichiometric and catalytic reagents for the epoxidation of alkenes.

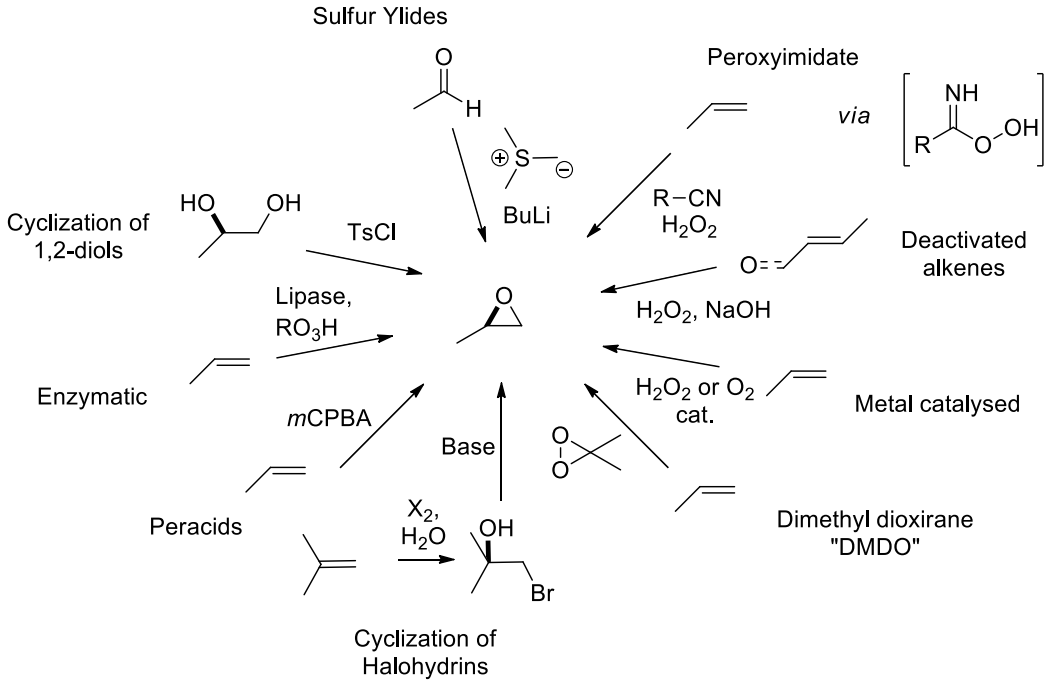

Figure 6. Preparation of epoxides

The following brief discussion describes the most commonly employed strategies that employ non-alkene substrates for epoxide synthesis, followed by a more thorough review of the different approaches that can be used for the direct epoxidation of alkene substrates.

1.1.5.1 Epoxide synthesis from non-alkene starting materials

Diols can be cyclised to prepare epoxides employing strategies involving intramolecular nucleophilic attack of one of the alcohol groups at a vicinal alcohol group that has been converted into an appropriate leaving group. The necessity to convert one of the alcohols into a leaving group, prior to cyclisation, increases the number of steps required for epoxide formation and the amount of waste produced. For example, many epoxide syntheses have been reported involving base mediated cyclisation of secondary hydroxyl group onto a primary *O*-tosylate, which has the benefit of retaining the stereochemistry for the formation of enantiopure epoxides (Scheme 7).

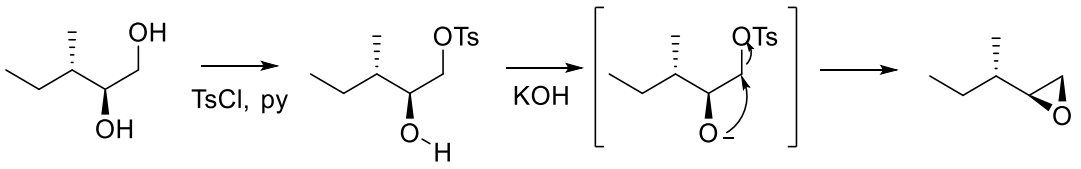

Scheme 7. Epoxide formation *via* cyclisation of α-β-hydroxy-tosylate

For example Kumar *et al*[23] developed a synthesis of the drug (*R*)-clorprenaline hydrochloride which employs this type of strategy for epoxide formation from a styrene (*anti*)-diol followed by ring opening using isopropylamine, as shown in (Scheme 8).

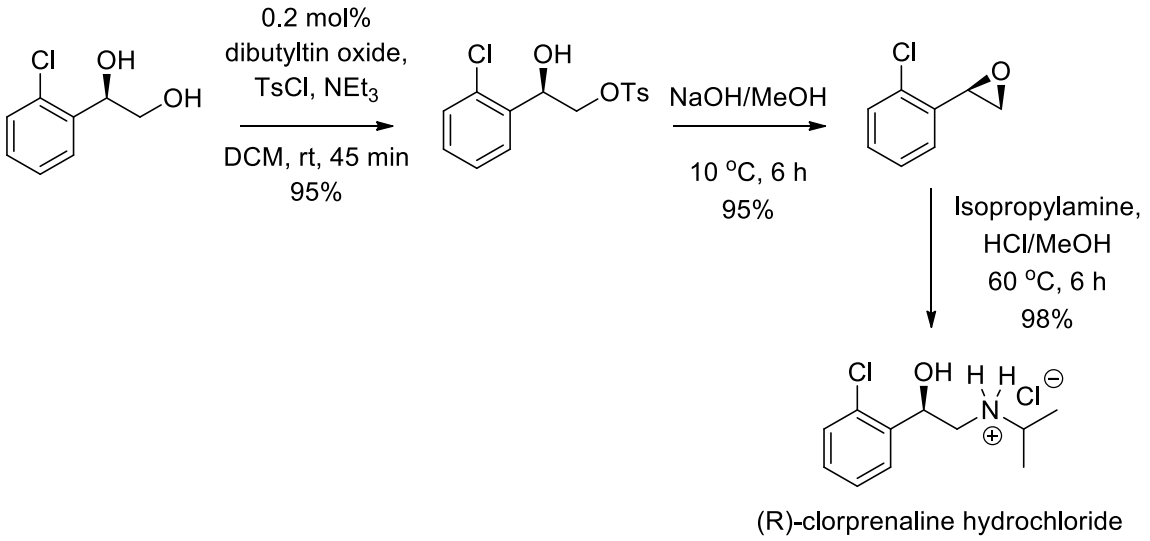

Scheme 8. Epoxide formation from an styrene-diol

Sulfonium ylids can be used to transform aldehydes and ketones into epoxides. The carbanion of a sulfur ylid attacks the carbonyl group of a ketone to form a zwitterionic intermediate that then undergoes intramolecular nucleophilic substitution reaction to form an epoxide and dimethylsulfide. This approach requires the use of a strong base (e.g. butyl lithium) to deprotonate the α proton of a sulfonium halide precursor to form an ylide under strictly anhydrous conditions (Scheme 9).[24]

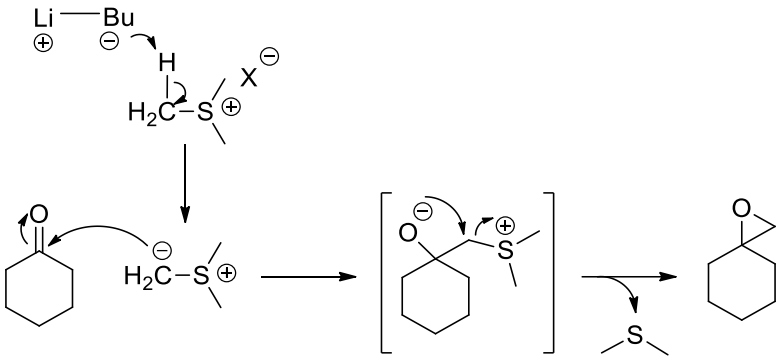

Scheme 9. Epoxide formation using a sulphur ylide

1.1.5.2 Epoxide synthesis from alkene starting materials

1.1.5.2.1 Alkene reactivity towards epoxidation using peracids

The most common way of producing epoxides involves the oxidation of alkenes *via* addition of an oxidant that catalyses the epoxidation of an alkene bond, as shown in Scheme 10.

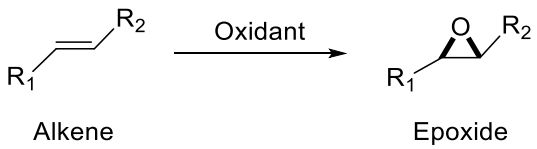

Scheme 10. Alkene epoxidation

The reactivity of alkenes towards oxidants is dependent on the number of alkyl substituents and their substitution pattern, with their general reactivity towards oxidants summarised in Figure . Alkene π-bonds act as electron rich nucleophiles in epoxidation reactions with oxidants such as peracids, with more electron rich alkenes exhibiting greater nucleophilicity. Therefore, increasing the number of alkyl substituents on the alkene bond increases its reactivity, which can be explained by considering inductive and/or hyperconjugation effects. The presence of an adjacent electron donating group such as an alcohol α to the alkene can direct the facial selectivity of an epoxidation reaction, whilst substitution of an alkene with an electron withdrawing group reduces its reactivity towards electrophilic oxidants.[25] Electron donating groups not only stabilises intermediate carbocation character in the transition state of these reactions, but also raise the energy of the alkene π HOMO orbital, thus increasing the alkenes nucleophilicity (Figure 7).[25]

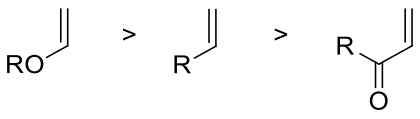

Figure 7. Reactivity of alkenes towards epoxidation

Hyperconjugation is a stabilising effect that occurs from donation of electron density from C-H σ-bonds into adjacent anti-bonding π* orbitals to provide “extended” molecular orbitals that increase the stability of the system.[26] The more adjacent C-H bonds that can donate into the π*-orbitals of the alkene bond, then the more hyperconjugative stabilisation of the alkene bond occurs affording the alkene species (Figure 8).

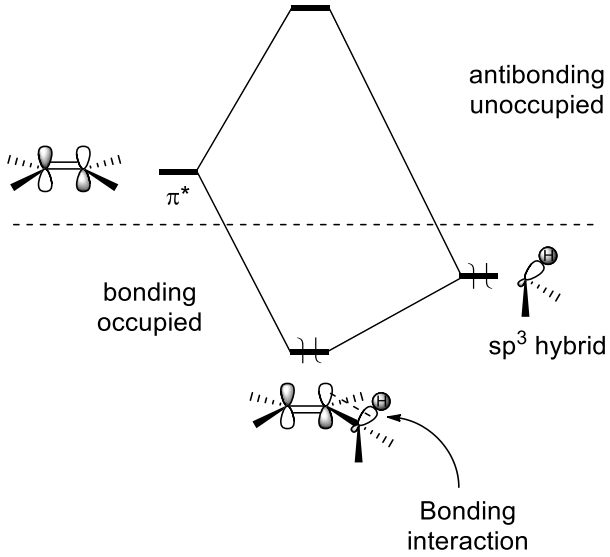

Figure 8. Hyperconjugation stabilisation effect

Peracids are one of the most commonly used types of oxidising reagents used in alkene epoxidation reactions. They react with many different electron rich alkenes with different substitution patterns, but do not generally react with electron poor alkenes such as those adjacent to electron withdrawing ketone groups. For example, the rate of epoxidation of alkenes with meta-chloroperoxybenzoic acid (*m*CPBA) varies significantly, depending on their alkene substitution patterns, as shown in Figure 9.[27]

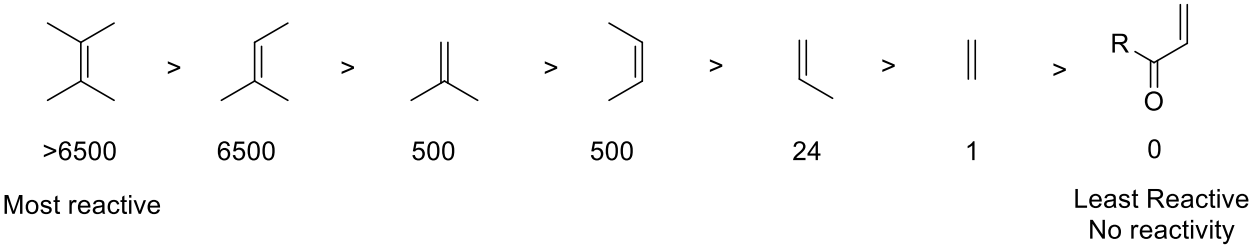

Figure 9. Relative reactivity of different alkenes using *m*CPBA as an epoxidising reagent

Differences in alkene and diene reactivity also exist depending upon their substitution patterns and the electronic and steric properties of their substituents or whether they are conjugated. For example, the tetrasubstituted alkene functionality of diene in Scheme 6 is preferentially epoxidised over its corresponding disubstituted alkene when the amount of *m*CPBA present is limited to 1.0 eq. Alternatively, only one of the alkene bonds of cyclopentadiene is epoxidised when it is treated with 1.0 eq of *m*CPBA key, with 1.0 eq of base being used to buffer the acidic *meta*-chloro benzoic acid produced as a by-product in the reaction to prevent epoxide ring-opening.[28]

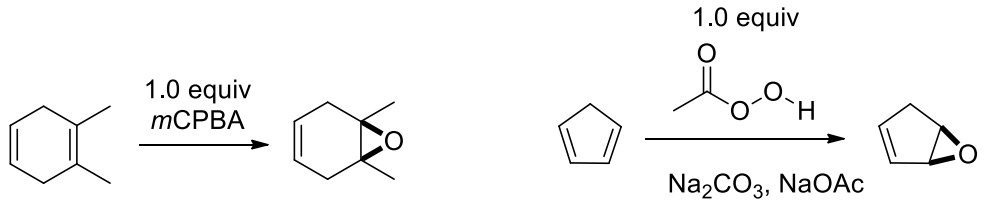

Scheme 6. *m*CPBA mediated monoepoxidation of dienes

Problems that are encountered when peracids are used for epoxidation include their expense, the generation of large amounts of stoichiometric acid waste and handling/safety issues associated with their potentially explosive nature. These issues can be tolerated on a laboratory or kilogram scale, however, it mean that peracids are rarely used on an industrial scale, whilst the high yields observed for *m*CPBA mediated epoxidation reactions on a small scale are often lower on scale-up.[18]

The mechanism of peracid mediated epoxidations is shown in Scheme 7, with this reaction also known historically as the Prilezhaev Reaction.[29] A butterfly transition state involves simultaneous oxygen addition and proton shift, with a concerted mechanism ensuring retention of the alkene stereochemistry in the epoxide product. This means that the relative positions of the R groups in the alkene are maintained after epoxidation ie. a *cis* alkene affords an epoxide whose R groups exhibit a *cis* orientation. This mechanism for the *m*CPBA mediated epoxidation of *cis*-stibene to afford its corresponding *cis*-epoxide is shown in Scheme 8, with *trans*-stilbene affording its corresponding *trans*-epoxide.

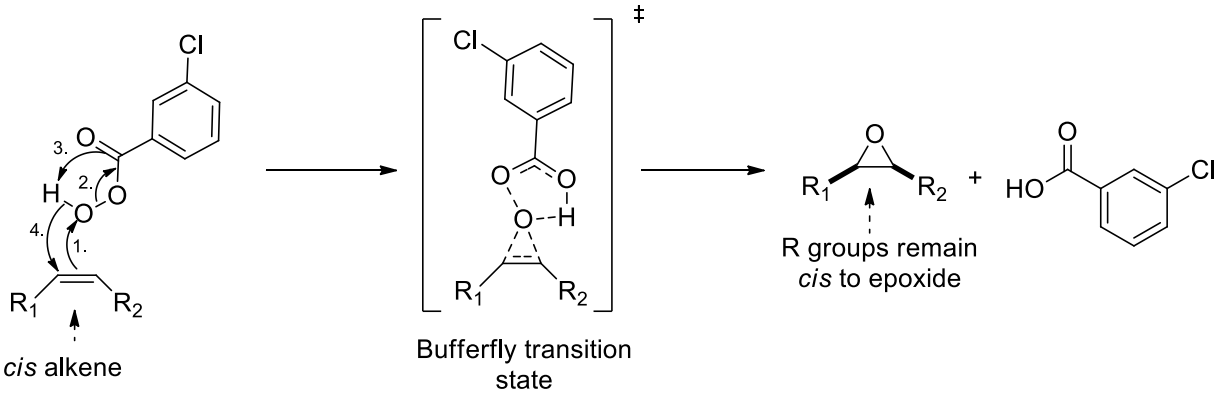

Scheme 7. Butterfly transition state formed when *m*CPBA is used for epoxidation

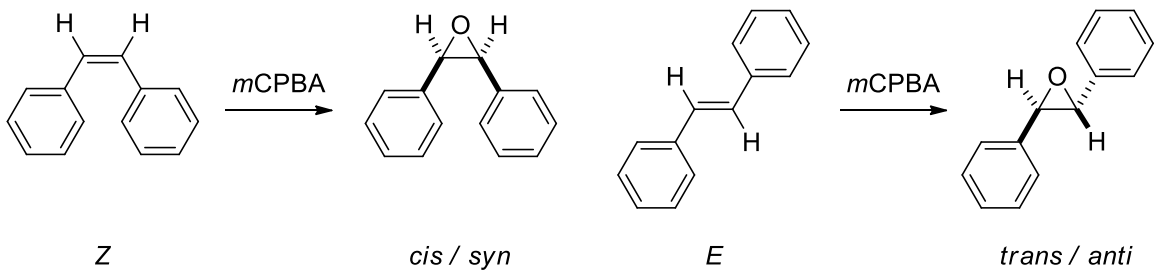

Scheme 8. *m*CPBA mediated epoxidation of *cis*- and *trans*- stilbenes

Another aspect of peracid reactivity concerns their selectivity towards cyclic alkenes, with the peracid normally approaching from the least hindered face to selectively afford *anti*-epoxide

products (see Scheme 8). In this case the electron rich alkene undergoes nucleophilic attack at the electron deficient oxygen atom of the peroxy acid, with the filled HOMO π orbital of the alkene aligning with the empty oxygen-oxygen σ* antibonding LUMO orbital of the peracid, as shown in Scheme 10.[30]

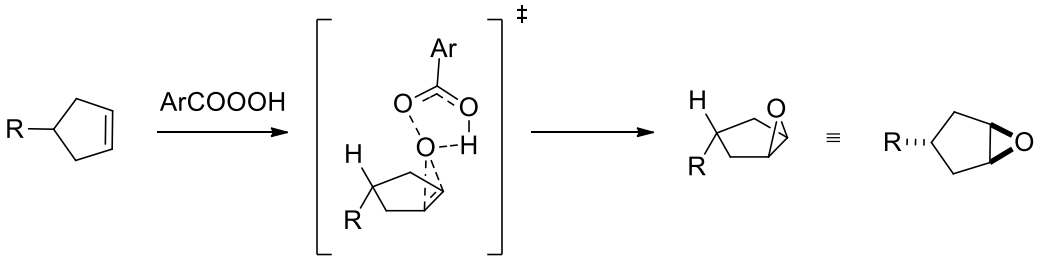

Scheme 9. Selective epoxidation of a cyclic alkene

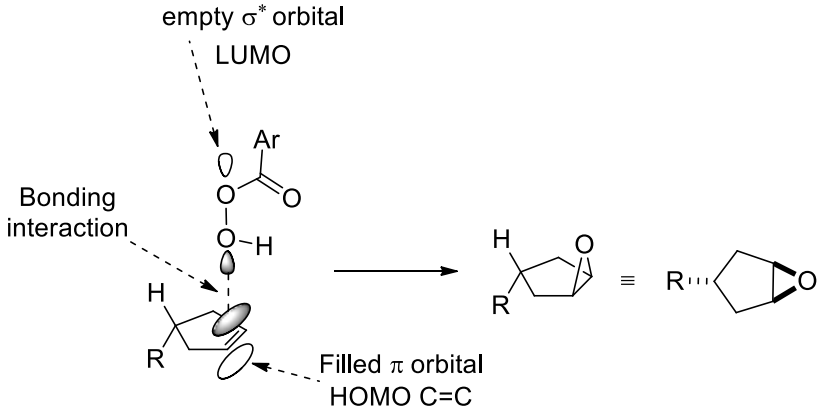

Scheme 10. Molecular orbitals involved in peracid mediated epoxidation

Another feature of peracid mediated epoxidation reactions that needs to be considered is the effect that neighbouring groups present in the alkene may have on directing the trajectory of peracid attack. For example, the OH group of an allylic alcohol can hydrogen bond to the peroxyacid, stabilising the transition state that leads to the *syn*- epoxide (see Scheme 11). If hydrogen bonding of *m*CPBA to the alcohol is prevented by the presence of a alcohol protecting group such as an acetate group, then steric hindrance effects predominate, resulting in preferential formation of the *anti*-epoxide (see Scheme 12).[31]

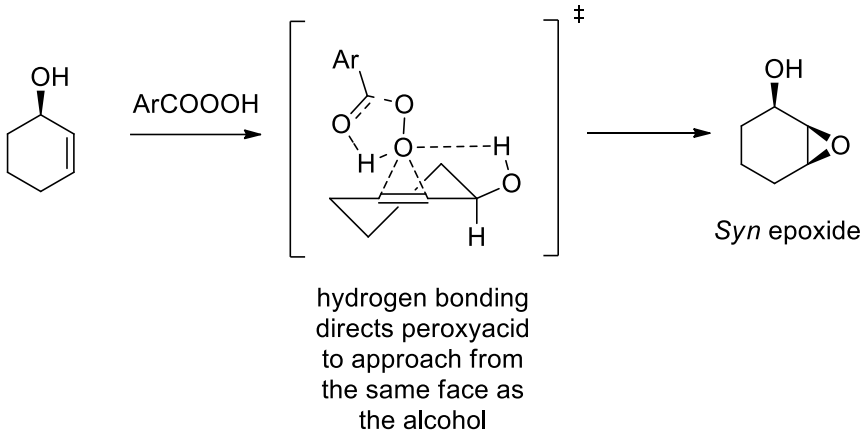

Scheme 11. Hydrogen bonding of *m*CPBA to the hydroxyl group of cyclohexenol results in *syn*-epoxidation

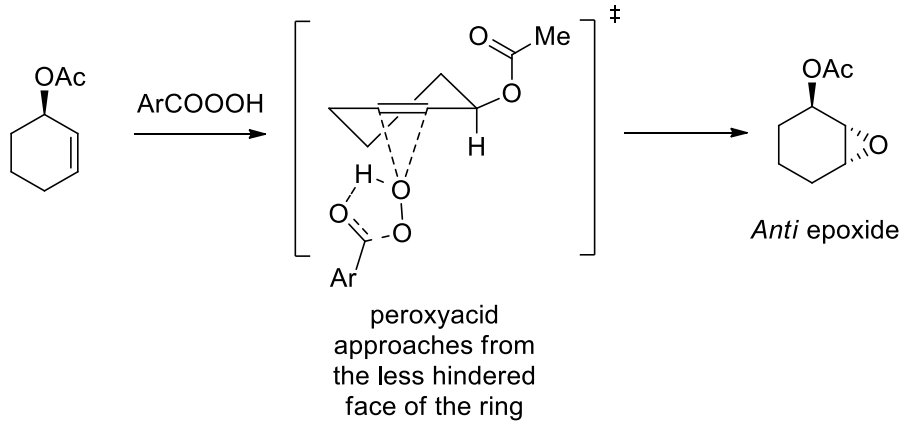

Scheme 12. *m*CPBA mediated epoxidation of cyclohexenyl acetate results in an *anti* epoxide

Peracids are typically prepared by mixing an acid anhydride with high concentrations of hydrogen peroxide (Scheme 13), with the oxidative strength of the resultant peroxide dependent on the leaving group capacity of its carboxylate fragment. A range of typical peracids used in the laboratory are shown below, with *m*CPBA being the most widely used due to its favourable stability profile, and trifluoroperacetic acid being the most reactive (Figure 10).[32]

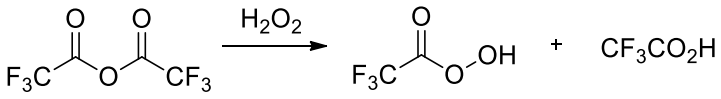

Scheme 13. Peracid formation

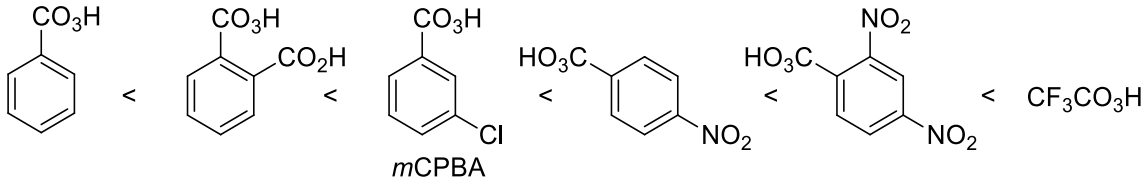

Figure 10. Reactivity profile of a range of commonly used peracids

Peracids are widely used for the epoxidation of alkenes, because their high reactivity enables them to be used under relatively mild reaction conditions with no catalyst being required. However, their use has a number of disadvantages that make them unsuitable for industrial scale epoxidation. Firstly, they all produce 1.0 eq of carboxylic acid by-product (with *m*CPBA being chlorinated), which adds to the cost and environmental impact associated with waste disposal. Peracids are potentially unstable, which means they must be stored under cool conditions, whilst they can potentially undergo explosive decomposition during reaction.[33] They are also corrosive, expensive and have a relatively high oxidative potential that can lead to other functionality present in the alkene substrate undergoing unwanted side reactions. These side reactions[25] include unwanted Baeyer-Villiger reactions of ketones to form esters, oxidation of amines to afford *N*-oxides, and oxidation of thioethers to sulfoxides and sulfones (see Figure 11).[33]

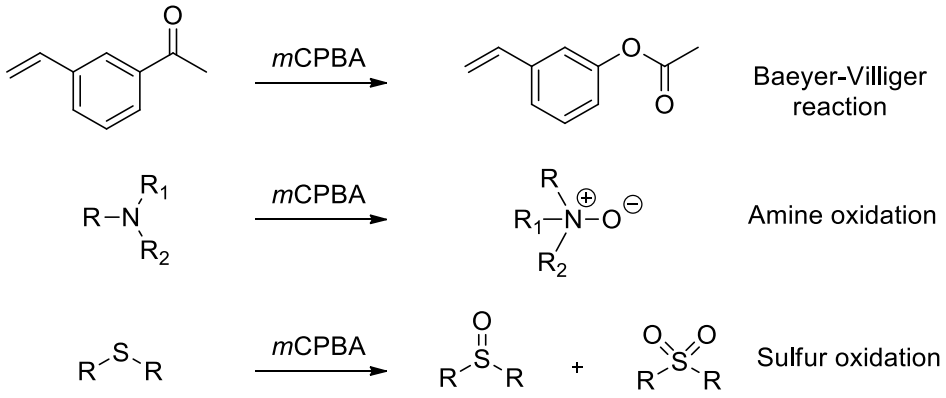

Figure 11. Possible side reactions that can occur when *m*CPBA is used as a peracid in epoxidation reactions

Another drawback of peracid epoxidation concerns their oxidizing strength.[34] Terpene substrates often contain multiple types of alkenes and other acid sensitive functional groups. Therefore, selective epoxidation of terpene substrates is difficult to achieve using peracids with mixtures of mono-, di- and tri- epoxides commonly being formed, alongside unwanted ring opened products such as their corresponding diols (See Scheme 14). These factors can lead to low yields of the desired tri-substituted alkene epoxides, with epoxidation of limonene with *m*CPBA affording a 3:1 mixture of mono-epoxide and bis-epoxide under buffered conditions.[35]

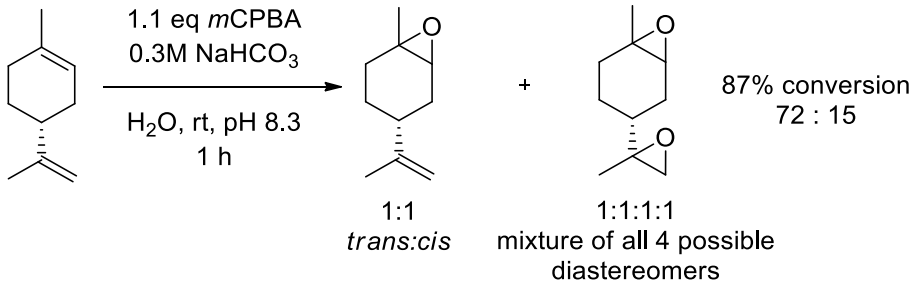

Scheme 14. Epoxidation of (+)-Limonene using *m*CPBA

1.1.5.2.2 Julia-Colonna epoxidation

Peracids cannot epoxidise electron poor alkenes that contain electron withdrawing groups, such as α-β-unsaturated ketones, or α-β-unsaturated esters. The common method for epoxidising electron deficient groups is to use a base such as sodium hydroxide to convert hydrogen peroxide into a nucleophilic, hydroperoxide anion that can then undergo conjugate addition to an α-β unsaturated acceptor (Scheme 15).[36]

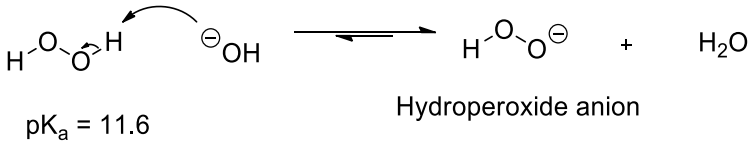

Scheme 15. Hydroperoxide anion formation

The hydroperoxide anion (pK_a = 11.6) is a good nucleophile due to the α-effect, whereby the lone pairs of the vicinal oxygen atom raise the energy of its HOMO, making it a softer nucleophile compared to hydroxide anion.[36] The hydroperoxy anion undergoes conjugate addition to an appropriate α-β-unsaturated acceptor to afford an enolate intermediate, that then undergoes nuclophilic attack at the proximal oxygen of the β-hydroperoxy fragment, with loss of hydroxide, to afford the observed epoxide product (Scheme 16).

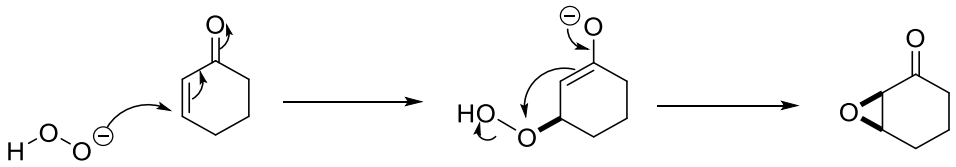

Scheme 16. Hydroperoxide epoxidation mechanism

This epoxidation methodology also uses stoichiometric amounts of reagent; however both the hydrogen peroxide and base are cheap, so this type of methodology is widely used on-scale. Geller at el[37] have developed a modified Julia-Colonna epoxidation methodology that employs a chiral poly-L-Leucine polymer as a catalyst in the presence of TBAB to perform the rapid stereoselective epoxidation of *trans*-chalcone, Scheme 22.

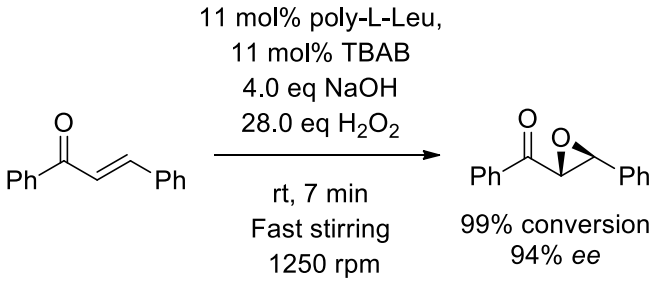

Scheme 22. A catalytic enantioselective Julia-Colonna epoxidation reaction

There are differences between the stereochemical outcomes of reactions carried out using electrophilic peracids when compared to nucleophilic hydroperoxide. Peracid epoxidations are stereospecific because they proceed *via* a concerted transition state, whilst hydroperoxide anion reaction occurs *via* a two-step process. This means that the α-β C-C bond of the enolate intermediate can potentially undergo bond rotation to favour its more stable *trans*-epoxide, regardless of the geometry of the original alkene starting material (see Scheme 17).

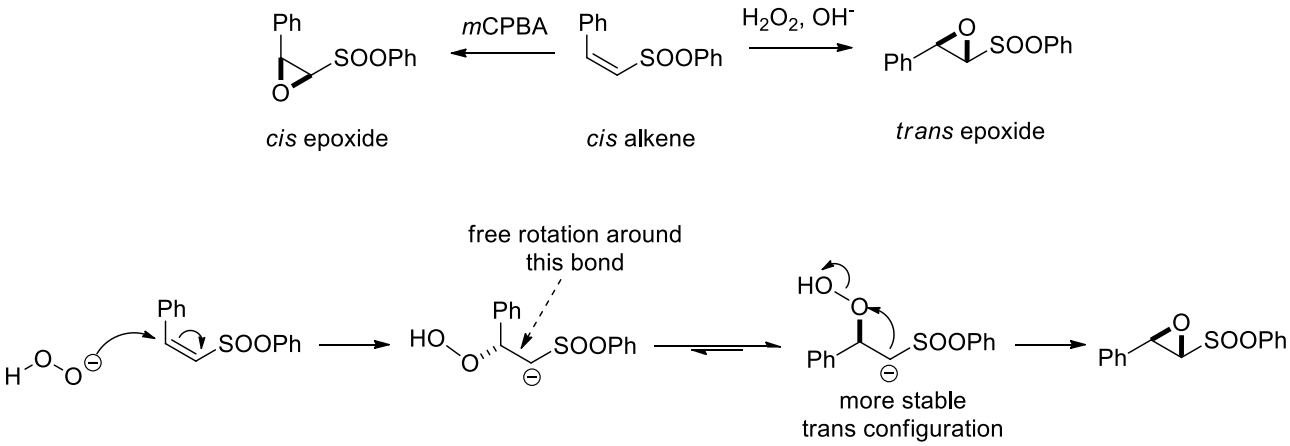

Scheme 17. Peracid and hydroperoxide anion mediated epoxidation reactions of a (*Z*)-α-β-unsaturated sulfone

1.1.5.2.3 Epoxidation using dimethyldioxirane species

Dimethyldioxirane, DMDO, also known as Murray's reagent is a very reactive and selective epoxidising agent for alkenes. Due to its high reactivity, DMDO is only stable as a dilute solution (typically in acetone) and is formed *in situ* from the reaction of acetone with oxone (potassium peroxymonosulfate) (Scheme 18). However, it is particularly challenging to use on scale because of its highly explosive nature.[38] The mechanism of this reaction is shown in Scheme 24, with the only by-product of this epoxidation procedure being acetone, which means that DMDO is often used for the epoxidation of acid sensitive substrates.

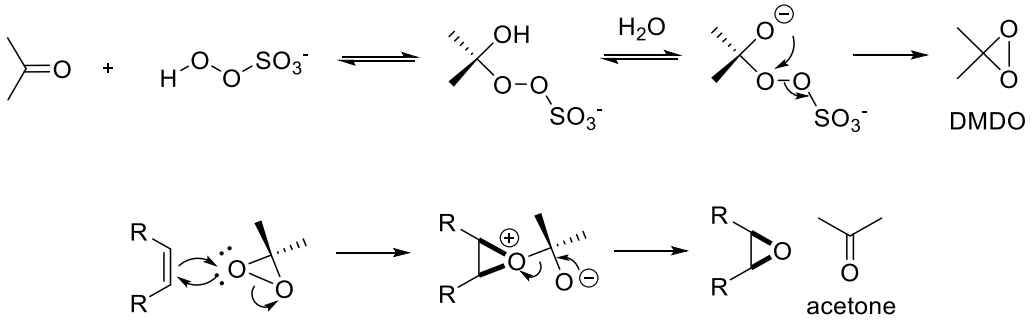

Scheme 18. Synthesis of DMDO and its use for alkene epoxidation

The Shi epoxidation protocol is an asymmetric version of the DMDO epoxidation, which employs an enantiopure fructose based organo-catalyst for the enantioselective epoxidation of alkenes. Since alkene substrates are only soluble in organic solvents, and the oxidant is present in the aqueous layer, then a phase transfer catalyst (e.g. tetrabutylammonium sulphate) is used as a phase transfer catalyst, with a D-fructose derived catalyst affording the (*R*,*R*)-epoxide of β-methyl-styrene in 82% *ee* (Scheme 19).[39]

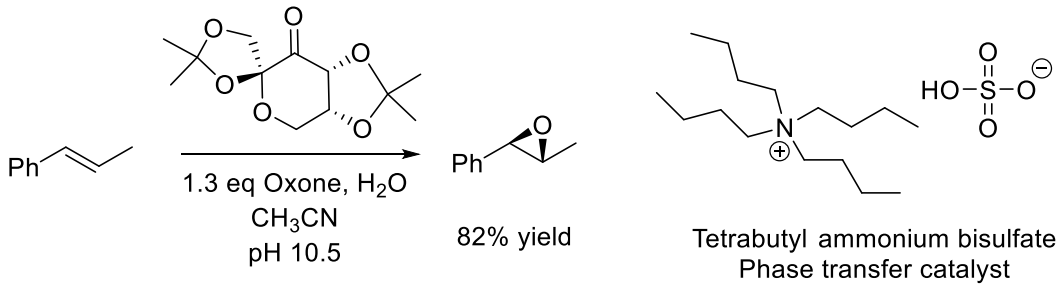

Scheme 19. Shi epoxidation conditions

The DMDO epoxidation reaction is proposed to proceed *via* a concerted mechanism, however oxy-anion intermediates have been observed (see above), suggesting that these reactions may also proceed *via* an S_N2 type mechanism (Scheme 20).[39]

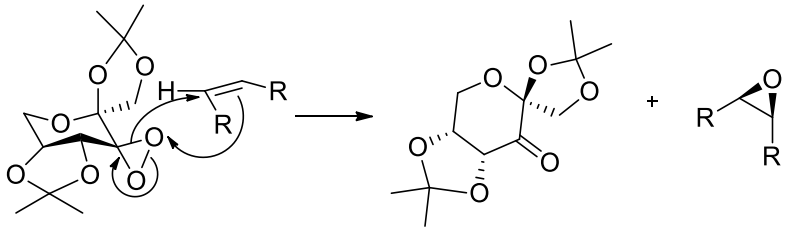

Scheme 20. Concerted mechanism for DMDO epoxidation of alkenes

1.1.5.2.4 Epoxide preparation *via* cyclisation of halohydrins

Alkenes can be reacted with electrophilic halide sources in water to form *anti*-halohydrins that can then be cyclised using base to form an epoxide. This process involves two steps and requires stoichiometric amounts of a brominating agent; however this approach affords the possibility of producing epoxides with opposite facial selectivity to epoxides produced by direct action of a peracid (See Scheme 21).[40]

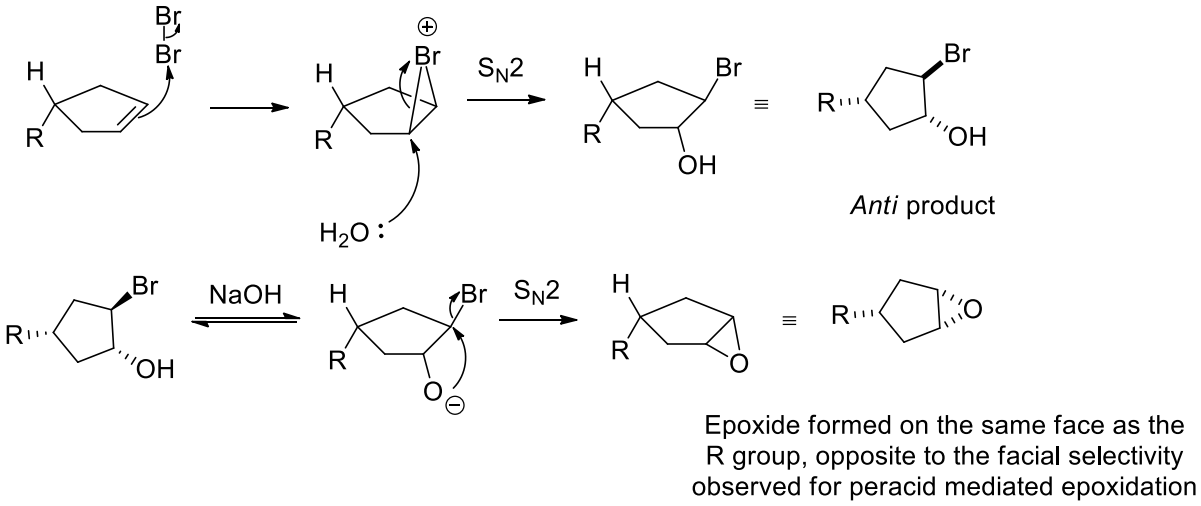

Scheme 21. Epoxide formation *via* halohydrin formation

1.1.5.2.5 Epoxide synthesis using metal catalysts and H_2O_2/O_2 as oxidants

Metal catalysts are often used to activate H_2O_2 for epoxidation reactions of alkenes. These catalytic systems can achieve high selectivity and yields but increase the complexity of the system which can result in increased costs depending upon which type of metal and ligand are used.[41]

A catalytic system based on the use of $VO(acac)_2$ and ^tBuOOH has been used for the epoxidation of allylic alcohols, with the vanadium centre serving to bind the peroxide and allylic alcohol so that they are in close proximity to each other (Figure 12). This binding event resuts in the alkene and peroxy bonds being activated, resulting in transfer of oxygen from a cyclic peroxy species to the alkene to afford an epoxide (See Scheme 22).[41]

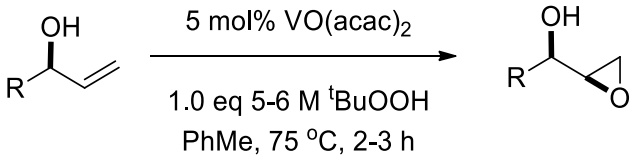

Scheme 22. Vanadium catalysed epoxidation reaction of allylic alcohols

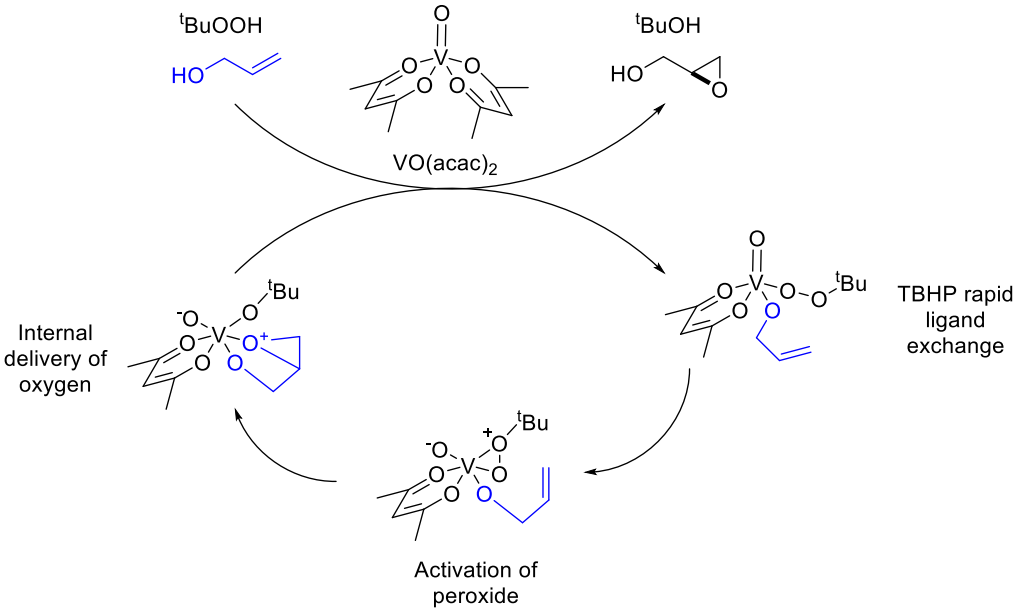

Figure 12. Mechanism of $VO(acac)_2$ mediated epoxidation

Enantioselective variants of this type of transition metal catalysed epoxidation reaction have also been developed, with the well-known Sharpless asymmetric epoxidation employing a titanium isopropoxide catalyst, *t*-butyl hydroperoxide (TBHP) as oxidant, and diethyl tartrate (DET) as a chiral ligand.[42] These conditions can catalyse the enantioselective epoxidation of a wide range of allylic alcohols, with the alcohol group of the allylic alcohol coordinating to the chiral metal catalyst and helping direct epoxidation of its adjacent alkene group. The chiral ligand DET is responsible for establishing a chiral environment within the catalytic complex responsible for epoxidation, as shown in Figure 13. The catalytic cycle begins with the stepwise displacement of isopropoxide ligands of the titanium complex by DET, TBHP, and the allylic alcohol reagent. The resultant chiral complex is thought to exist as a titanium dimer, with TBHP binding to the titanium metal and being activated to afford a cyclic peroxy intermediate that results in epoxidation of the alkene bond of the bound allylic alcohol, with the chiral DET ligand serving to direct enantiofacial selectivity (Scheme 23).[42]

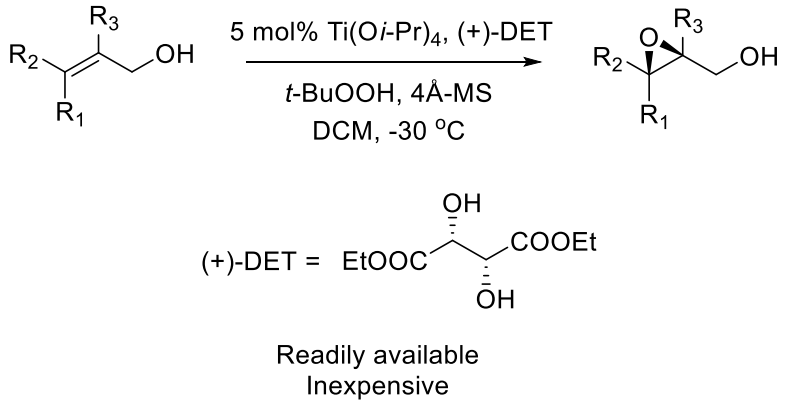

Scheme 23. Sharpless asymmetric epoxidation

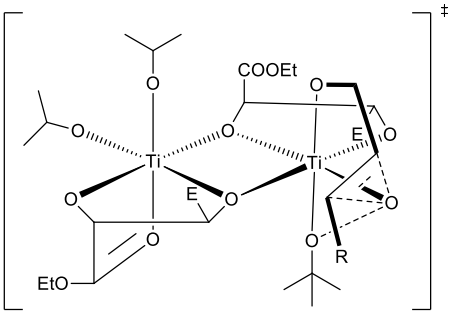

Figure 13. Proposed transition state for the Sharpless epoxidation of allylic alcohols

Another major class of metal catalysed epoxidations is the Jacobsen asymmetric epoxidation reaction[43] that unlike the Sharpless system reacts with most unfunctionalized alkenes, not just those adjacent to alcohol groups. This catalytic system employs a manganese based system with a chiral salen ligand and cheap NaOCl (bleach) as a stoichiometric oxidant for epoxidation. Excellent *ee* values were achieved on a small scale, with some controversy over the mechanism of the epoxidation reaction still existing, with the most commonly accepted 'Katsuki' transition state model shown in Figure 13.[44] Whilst this Jacobsen epoxidation methodology has been widely used for the preparation of a wide range of chiral epoxides,[45] it has proven to be difficult to perform on a large scale, with high catalyst loadings typically required and lower *ee*'s and yields often being obtained (Scheme 24).[44]

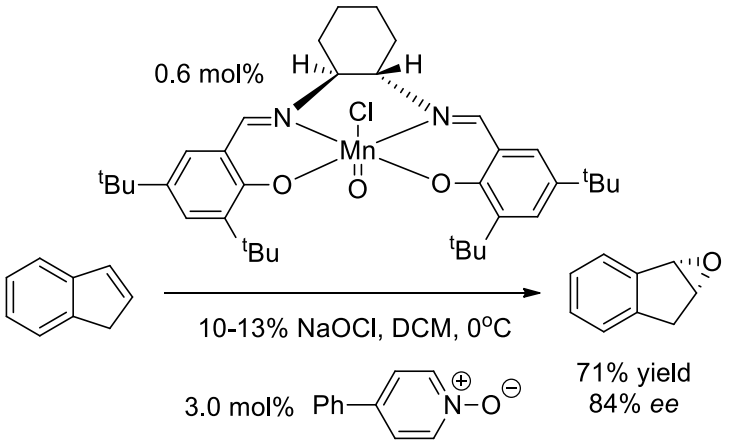

Scheme 24. Jacobsen epoxidation conditions

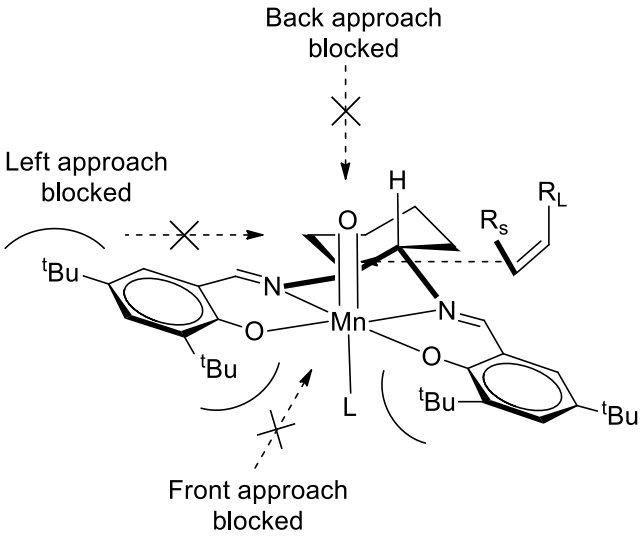

Scheme 25. Katsuki transition state model

In the Katsuki transition state model the substituents on the diamine backbone adopt equatorial positions causing the salen moiety to "lean", which means that all the approach vectors other than from the right-hand side are blocked. The alkene substituents are directed upwards, away from the salen ligands, with the smaller alkene substituent (R_s) positioned in close vicinity to the ^{t}Bu group of the salen ligand (Scheme 25).[46]

1.1.5.2.6 Alkene epoxidations using Lipases

An alternative approach to epoxide formation involves the use of lipases as catalysts that convert an oxygen source into a peracid which then epoxidises an alkene substrate. For example, Li *et al*[47] have applied a lipase catalysed H_2O_2 mediated process for the stereoselective epoxidation of a number of alkene substrates, including α-pinene, as shown in Scheme 26.[47]

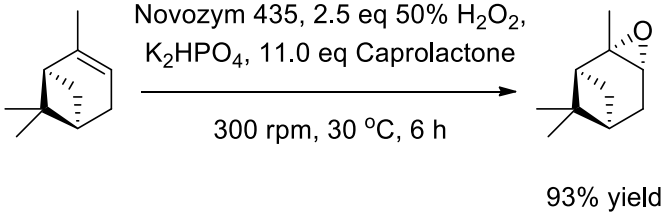

Scheme 26. Lipase mediated α-pinene epoxidation

This method uses hydrogen peroxide and caprolactone as additives with an epoxidation mechanism being proposed that involves lipase mediated H_2O_2 oxidation of the acid functionality of the ring opened form of caprolactone to afford a peracid that epoxidises the alkene (See Scheme 27).[47] However, these type of enzymatic processes can be expensive, with biocatalysts needing to be recycled effectively if an epoxidation process is to be commercialised. Immobilisation of the lipase on a solid support is one way of reducing the cost

and increasing the turnover number of this type of epoxidation reaction, since immobilisation protects the enzyme from degradation and facilitates its recovery and reuse.

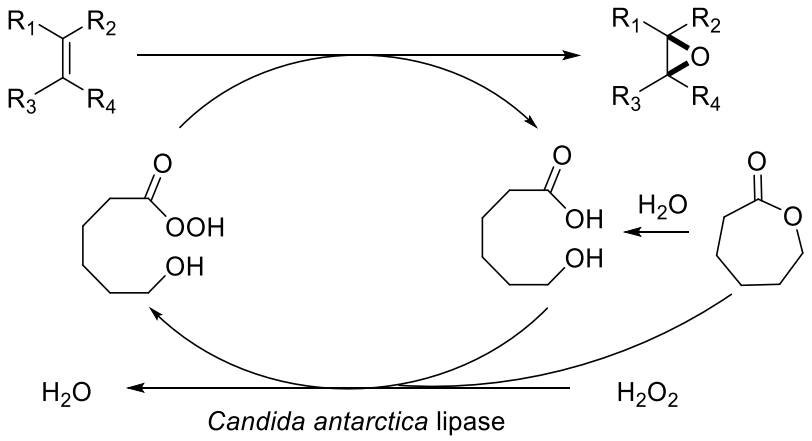

Scheme 27.Proposed mechanism for lipase mediated epoxidation

1.1.5.2.7 Conclusions

Whilst many methodologies have been developed for the epoxidation of alkene substrates, many of these processes are not amenable to scale-up. We wished to develop a solvent-free catalytic route for the epoxidation of common biorenewable terpene substrates using a cheap oxidant such as O_2 or H_2O_2. Therefore the next chapter describes my investigations into the use of the Ishii-Venturello tungsten catalyst for the selective epoxidation and dihydroxylation of terpene substrates in batch and flow under organic solvent free conditions (Scheme 28).

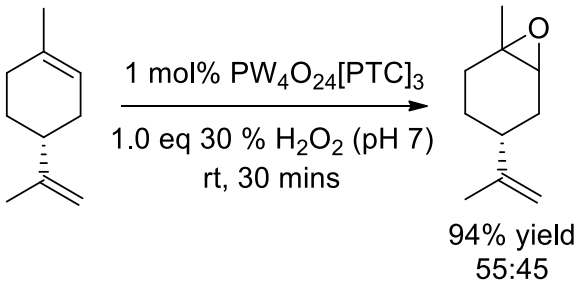

Scheme 28. Ishii-Venturello epoxidation protocol applied to (+)-limonene

2 Chapter 2 - Solvent-free batch epoxidations of terpenes

The research contained within this chapter focuses on the development of catalytic methodology for the synthesis of epoxide compounds using green principles, low impact oxidants and efficient catalysts. The aim of this research was to develop a broadly applicable method for green epoxidation that was compatible with terpene substrates that could be tuned to selectively epoxidise the different types of alkene substitution patterns present in terpene substrates.

2.1 "Green" Alkene Epoxidation methods

Various alternative catalytic systems for the epoxidation of alkenes on scale have been developed, with molecular oxygen and hydrogen peroxide the most widely used stoichiometric oxidants in these reactions. Numerous metal complexes have been investigated to activate these oxidants for epoxidation, with the most successful catalytic systems based on the use of titanium, iron, manganese, vanadium, chromium, molybdenum, tungsten or rhenium complexes.[48]

2.1.1 "Green" Oxidants - O_2 versus H_2O_2

Various organic hydroperoxides have beed used as oxidants, including cumene hydroperoxide, *tert*-butyl hydroperoxide, ethylbenzene hydroperoxides and hydrogen peroxide. These oxidising agents possess a number of advantages such as high reactivity and ease of used, having a better safety profile than peracids and DMDO.[18] However, they are generally much more expensive than H_2O_2 and so are not generally used for catalytic epoxidations on an industrial scale.

Hydrogen peroxide is a relatively stable, clean, and cheap oxidising reagent, whose only by-product is water.[49] However, its use as an effective oxidant requires activation with a suitable catalyst to increase its electrophilicity.[50] A potential problem with using hydrogen peroxide is its hydrophilic nature, which can make it difficult to achieve effective mixing with more hydrophobic organic substrates. The addition of co-solvents such as tert-butanol, methanol and acetonitrile can solve this problem, as can the use of phase transfer catalysts.[51]

Oxygen is another possible green oxidant that is attractive because of its abundancy, low cost and lack of harmful by products. However, pressurised oxygen can spontaneously ignite or explode on a large scale, whilst its potential to make explosive hydroperoxides can result in uncontrolled radical chain reactions, which means that hydrogen peroxide is often the most desirable green oxidant for reactions on-scale.[48]

2.1.2 Selected state-of-the-art catalytic epoxidation methods

Catalytic epoxidation processes have been extensively explored over the past decades due to their importance for producing various important epoxide intermediates for the generation of valuable chemical products. This section highlights a number of recent catalytic epoxidation systems that have been reported in the literature, concentrating on peroxide based oxidants that could potentially be used on a large scale.

Kamata *et al*[52] have developed a selenium peroxytungstate catalyst system that was used for epoxidation of homoallylic alcohols using hydrogen peroxide on a multigram scale. This catalytic epoxidation system required minimal equivalents of oxidant, was high yielding for a range of alkenes and could be performed under mild conditions. The use of selenium and tungsten metal catalysts was beneficial when compared to other metal based systems because it enabled the use of hydrogen peroxide, instead of tert-butyl hydroperoxide, which is both cheaper and more sustainable (Scheme 29).[52]

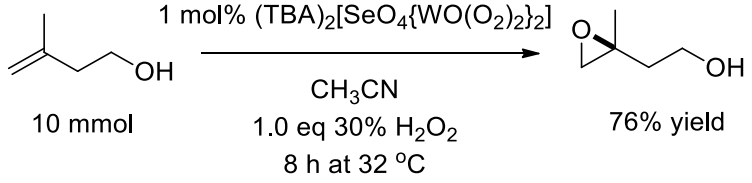

Scheme 29. Selenium-peroxytungstate catalyst for the epoxidation of homoallylic alkenes

In 2014 Kokotos *et al*[53] reported an effective, catalytic epoxidation methodology using polyfluoroalkyl ketones as organocatalysts alongside hydrogen peroxide as an oxidant for a range of alkene substrates. These epoxidation reactions were efficient, occured with short reaction times, employed cheap reagents and were high yielding as the reaction conditions shown for cyclohexene in Scheme 30.

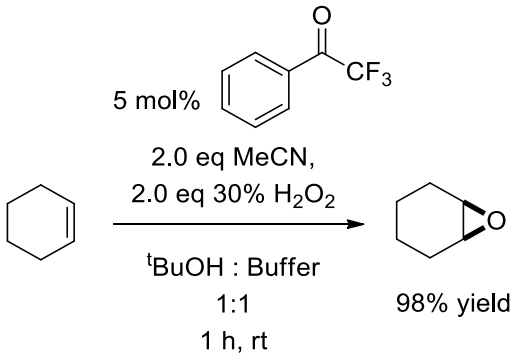

Scheme 30. Organocatalytic epoxidation methodology

Iron tetracarbene systems are highly active homogenous catalysts that have a number of benefits, with Kuhn *et al*[54] developing an iron(III) based catalytic epoxidation system that employs hydrogen peroxide as an oxidant in 2015. Compared to conventional iron(II) systems, use of this catalytic system led to significantly less oxidant decomposition and increased reactivity, relative to established, more expensive metal systems based on Mo and Re (Scheme 31).

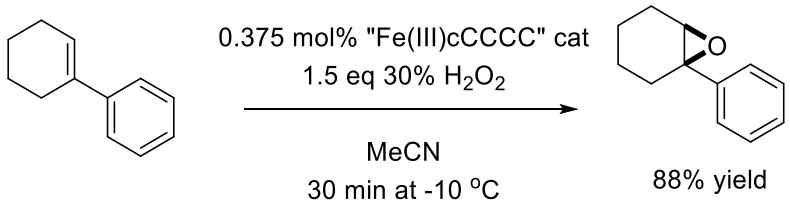

Scheme 31. Novel Iron(III) catalysed epoxidation system

In 2016 Stack *et al*[55] developed a novel manganese based catalytic system for the epoxidation of alkenes using 1.1 eq of peracetic acid as oxidant, with this system exhibiting a wide substrate scope and epoxidation reactions that were completed within minutes. Other key advantages to this manganese based system include its broad selectivity and the use of a cheap picolinic ligand system that self assembles *in situ*, which enabled this system to be scaled up to produce gram quantities of epoxides without loss of activity (Scheme 32).

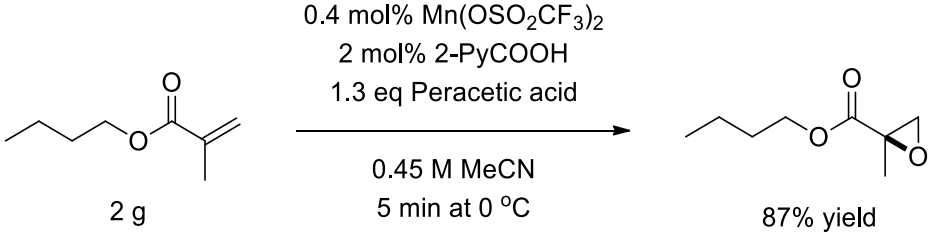

Scheme 32. Gram scale epoxidation using a simple *in situ* generated Mn catalyst

2.1.3 Selected state-of-the-art process scale catalytic epoxidation methods

In 2001 Burgess *et al*[56] developed a manganese catalysed epoxidation methodology using 10.0 eq of hydrogen peroxide in DMF as an oxidant that was scalable to 100 g. This methodology worked on a broad range of alkyl and aryl substrates with good functional group tolerance, however, terminal mono substituted alkyl alkenes were unreactive using this methdology (Scheme 33).

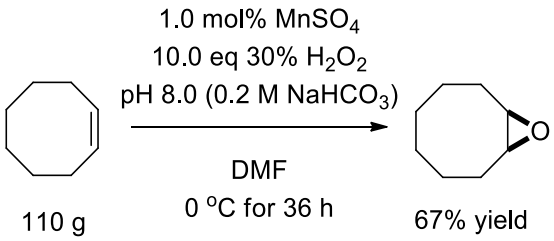

Scheme 33. Large scale mangenese catalysed epoxidation

Effler *et al*[57] have developed vanadium catalysed epoxidation methodology for a large scale synthesis of vitamin E from geranyl geranyl, with one of the key steps in their synthetic route involving epoxidation of the alkene bond of allylic alcohol functionality of phytol on a 100 gram scale (Scheme 34).

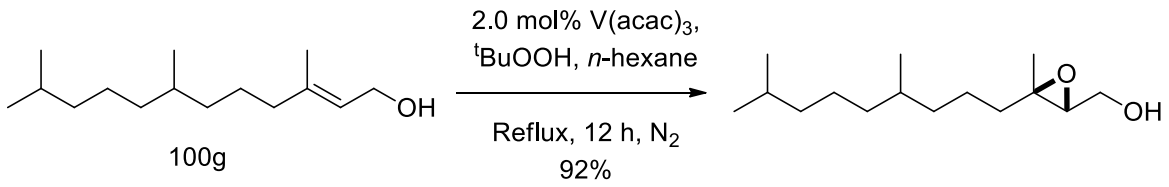

Scheme 34. Large scale catalytic epoxidation using a vanadium catalyst

In 2004 Geller *et al*[58] successfully scaled up a catalytic asymmetric Julia-Colonna epoxidation protocol that enabled epoxidation of a chalcone derivative on a 100 g scale with an excellent 97% *ee* and a high yield of 78%. Poly-*L*-leucine was used as a catalyst with sodium hydroxide and hydrogen peroxide at room temperature for 20 h (see Scheme 35).

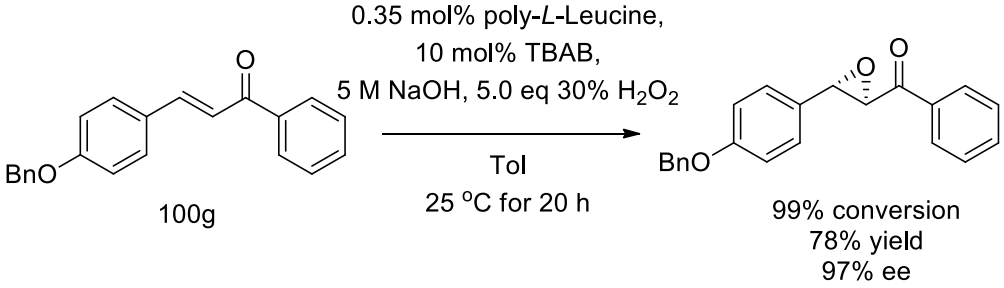

Scheme 35. Large scale Julia-Colonna epoxidation conditions

In 2012 Fuchs *et al*[59] scaled up a Jacobsen asymmetric epoxidation protocol for the epoxidation of cyclic dienyl sulfones. Jacobsen epoxidations are typically much less effective when performed on scale, with large scale reactions normally requiring 5-15 mol% catalyst loadings, 10-40 mol% of co-catalyst and the use of buffered bleach as an oxidant in chlorinated solvent. Fuch's optimised conditions enabled epoxidation to be performed on 350 g scale with much lower catalyst loadings of 0.6 mol%, affording the corresponding epoxide in high yield and *ee* using hydrogen peroxide as an oxidant in methanol. A number of additives were screened to allow for effective pH control that led to higher reaction rates, higher catalyst turnover and improved reliability (Scheme 36).

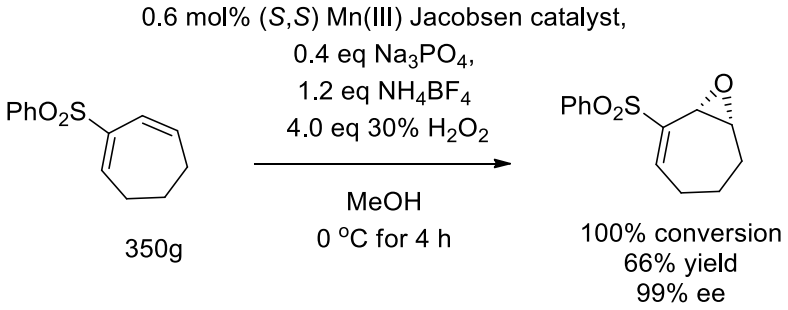

Scheme 36. Large scale Jacobsen epoxidation reaction

Research published in 2017 by Pati *et al*[60] highlights the use of the Sharpless asymmetric epoxidation reaction on an industrial scale. Pati *et al* scaled up the synthesis of "DNDI-VL-2098", a promising drug candidate for the treatment of visceral leishmaniasis, enabling it to be produced on kilogram quantities. The first step in their synthetic route involved a Sharpless asymmetric epoxidation of methyl-2-propen-1-ol on a 2 kg scale as shown in Scheme 37.[60]

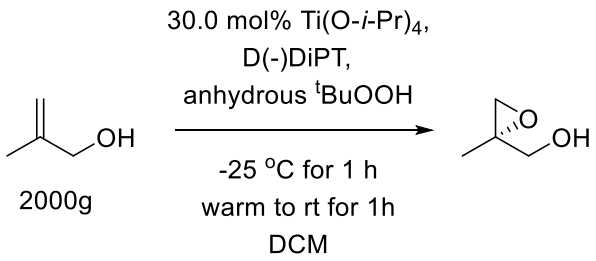

Scheme 37. Large scale asymmetric Sharpless epoxidation reaction

2.2 Catalytic epoxidation of terpene substrates

2.2.1 Previous reports of using polyoxometalate catalysts for epoxidation of the tri-substituted alkenes of terpene substrates

The development of the Ishii-Venturello catalyst system for the epoxidation of terpene substrates can be applied for the epoxidation of alkene substrates in a variety of ways with a number of different additives enabling modification of product yields and selectivities, with previous literature on its use described below.

Many biorenewable terpene substrates contain tri-substituted alkene functional group, which means it would be highly desirable to develop catalytic methodology that would enable their selective epoxidation in the presence of other disubstituted alkene functionality. An ideal catalytic system would afford good yields of terpene epoxides, using a recoverable catalyst and H_2O_2 as an oxidant under solvent free condition, which would produce water as the only byproduct. Many metal based catalysts, such as rhenium, manganese, iron, vanadium, titanium, molybdenum and tungsten have been used as epoxidation catalysts using hydrogen peroxide as oxidants for the selective epoxidation of terpene substrates.[61]

A review of the literature revealed that polyoxometalates (POMs) catalysts have been used for epoxidation of alkenes using H_2O_2, with their rate of epoxidation often dependent on the substitution pattern of the alkene. POMs are anionic metal-oxygen clusters made up of three or more transition metal oxyanions joined together by a network of bridging oxygen atoms that form a 3D framework (Figure 14).[19,62] POMs have received significant attention as both homogeneous and heterogeneous catalysts for a number of oxidative processes, including alkene epoxidation reactions.[49] POMs can be formed with a wide variety of structures and this provides excellent opportunities for tuning their reactivity by altering their atomic structure.[50] Typically, POMs are used as homogenous catalysts that are known to perform well in biphasic systems.[48] POMs that catalyse oxidation reactions are attractive to industry because they are robust and stable at elevated temperatures under oxidative conditions.[61] POMs are resistant to oxidative decomposition and are thermally stable, however, they are known to be decomposed by electricity and light.[49]

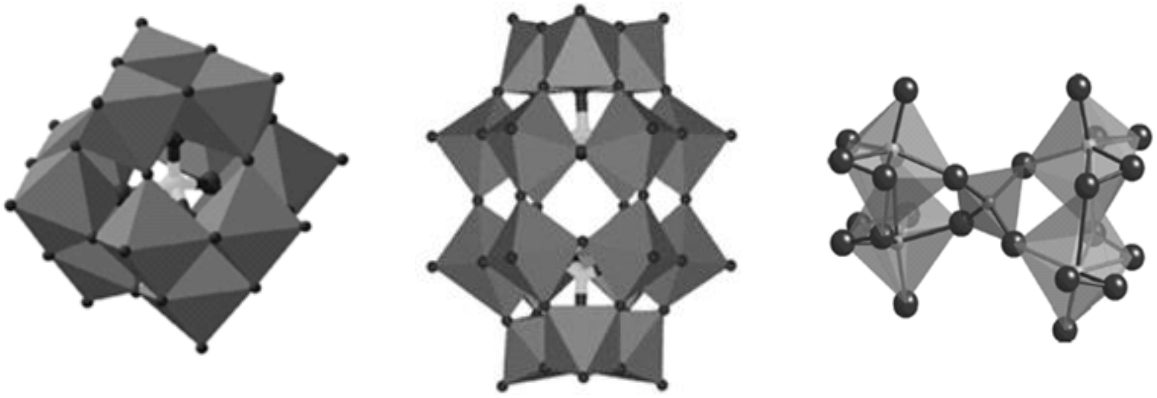

Keggin structure
$PMo_{12}O_{40}^{3-}$

Dawson structure
$P_2W_{18}O_{62}^{6-}$

Venturello structure
$PW_4O_{24}^{3-}$

Figure 14. Classical POM structures

Peroxotungstate derived POMs are efficient epoxidation catalysts because they minimizes peroxide disproportionation and maximize oxygen transfer, reducing the amount of hydrogen peroxide required in the reaction.[48] Their synthesis is straightforward, does not require the use of air sensitive techniques, with POMs able to coordinate to organic ligands that provide an opportunity to immobilize/couple them with phase transfer catalysts that enable their recycling.

The Venturello catalyst is a tungsten oxide based polyoxometalate system, whose tungsten metal centre reacts with H_2O_2 to afford a cyclic peroxy species that delivers an oxygen atom to an alkene to form an epoxide, according to the catalytic cycle shown in Figure 15.[49] The lipophilic nature of its long-alkyl chain quaternary ammonium cation results in the peroxycomplex migrating to the organic phase where epoxidation of the alkene then takes place.[63] Epoxidation of alkenes occurs with similar selectivity profiles to peracids, with epoxidation of more substituted alkene bonds generally occurring from their least hindered face.

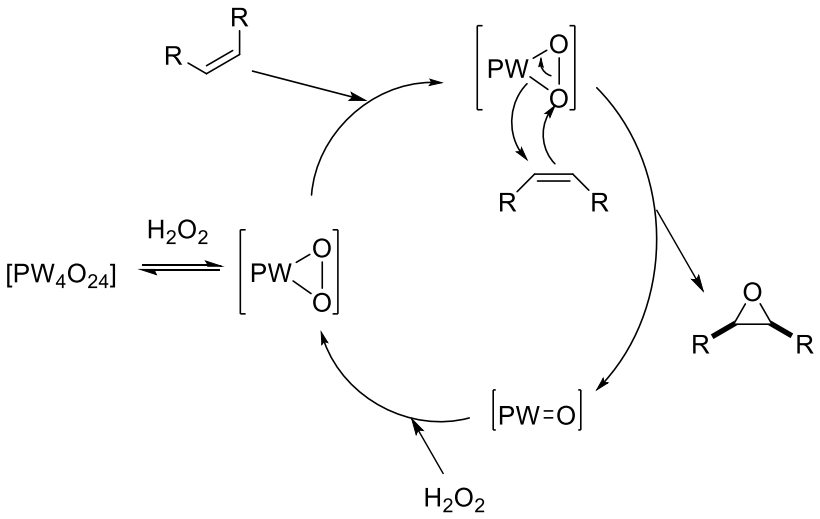

Figure 15. Proposed mechanism for the Venturello catalytic epoxidation reaction

In 1985 Venturello and Aloisio[64] reported the X-ray structure of an isolated POM anion, $[PW_4O_{24}]^{-3}$ (Figure 16),[51,65] and identified that it was an efficient epoxidation catalyst when

combined with a phase transfer catalyst (PTC) under biphasic conditions. This peroxotungsten heteropoly anion $[PW_4O_{24}]^{-3}$ exhibited C_2 symmetry being comprised of four distorted $W(O_2)_2O_3$ pentagonal bipyramids joined centrally by a tetrahedral phosphate group.

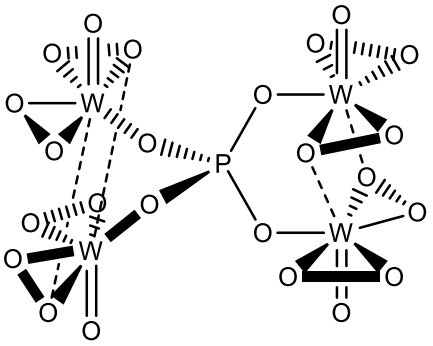

Figure 16. Venturello $[PW_4O_{24}]^{-3}$ anion POM

Venturello *et al*[66] expanded the epoxidation capacity of $[PW_4O_{24}]^{-3}$ catalysts in 1988.[66] They used two different approaches to improve epoxidation of a range of non-terpene alkene substrates containing mono-, di- and tri substituted alkenes. 10 of the 15 substrates were epoxidised with a POM-PTC complex in its preformed state at pH 2.3, because the epoxide products were stable under the acidic conditions employed. A second method was developed to epoxidise more acid sensitive substrates, using different aprotic solvents (DCE, DCM and benzene) and aqueous NaOH to buffer the reaction mixture. Two different PTCs were employed to prepare the $[PTC^+]_3[PW_4O_{24}]^{-3}$ tungsten peroxo complex, PTC-A $[(C_8H_{17})_3NCH_3]^+$ and PTC-B $[(C_{18}H_{37}(76\%)+C_{16}H_{33}(24\%)]_2N(CH_3)_2]^+$ catalysts in a one pot manner, which were obtained as a syrup, and white powder respectively (Scheme 44).[66]

$$4\ H_2WO_4 + H_3PO_4 + 8\ H_2O_2 + 3\ PTC^+Cl^- \xrightarrow[\text{DCM or } C_6H_6,\ 60\ ^oC,\ 1\text{-}3\ h]{H_2O} [PTC]_3[PW_4O_{24}] + 3\ HCl + 12\ H_2O$$

Scheme 38. Synthesis of preformed Venturello-PTC catalyst complex

For example, 1-octene was epoxidised using a preformed catalyst complex under acidic conditions in 89% yield, whilst cyclohexene was epoxidised under buffered conditions in 88% yield (Scheme 45). The epoxidation procedure performed at pH 4.0 led to significantly lower catalytic activity, so extra catalyst was used to counter this loss in activity.

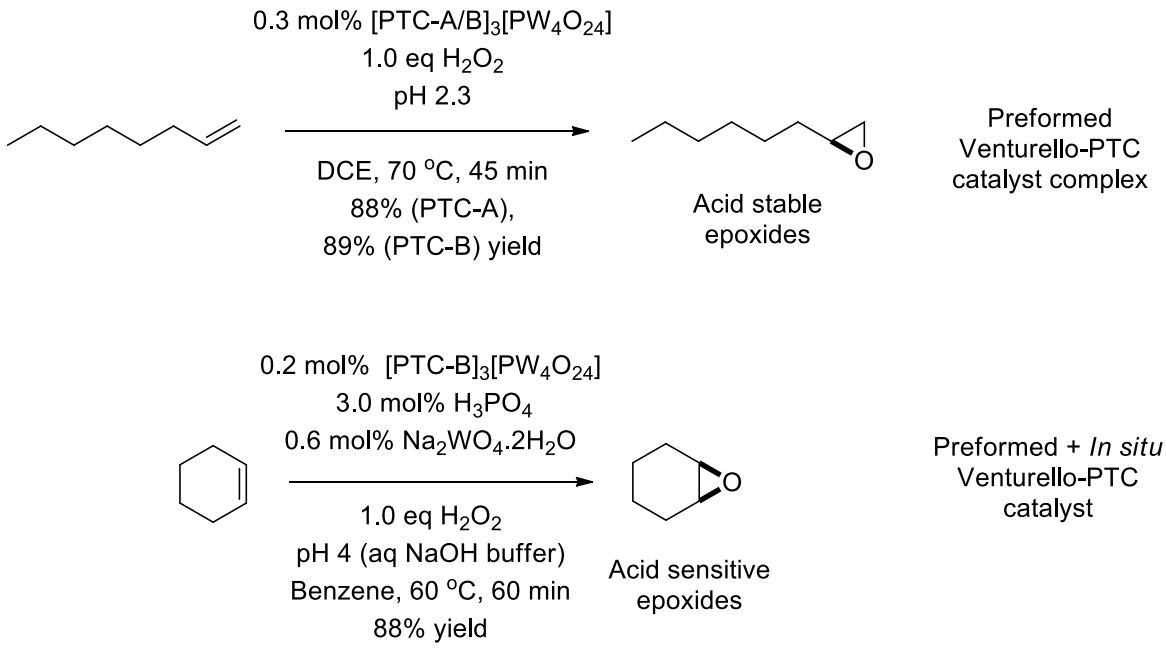

Scheme 45. Epoxidation using a preformed Venturello catalyst under acidic and buffered conditions

In 1996 Noyori and Sato el al[67] reported the use of catalytic Na_2WO_4 as a precursor to generate the catalytic system, $[PTC^+]_3[PW_4O_{24}]^{-3}$ in situ, that was used for epoxidation of three terminal alkene substrates using H_2O_2. A key modification to their procedure was the replacement of chlorine based PTC salts with trialkylmethyl ammonium hydrogensulfates, which resulted in improved catalytic activity. They also employed an α-amino phosphonic acid additive to speed up the epoxidation reaction, although the exact role of this additive was not discussed, whilst its inclusion of is not ideal from an economic perspective due to of its high cost (ca. £100 per 250 mg Sigma-Aldrich). Only three different types of alkyl alkene substrate were screened, with no epoxidation of terpene substrates being reported, with styrene only being epoxidised in a low yield of 23% yield (Scheme 46).[34]

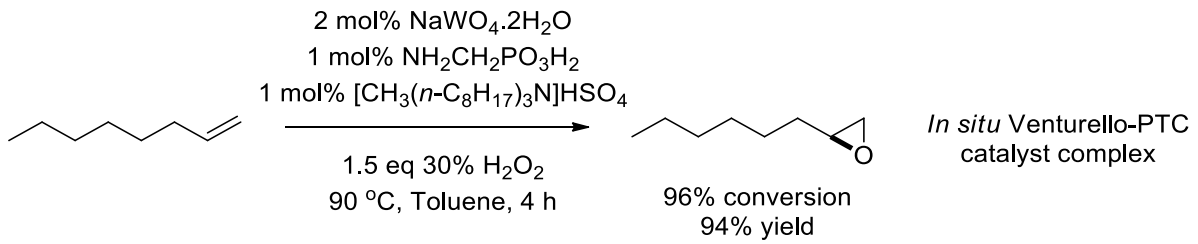

Scheme 46. Noyori and Sato *et al* epoxidation conditions using an *in situ* generated tungsten catalyst

Ishii *et al*[34] reported the use of a preformed Venturello-PTC catalyst complex. ($[C_5H_5N^+(CH_2)_{15}CH_3]_3[PW_4O_{24}]$) to epoxidise a range of monoterpene substrates in chloroform in 1996 using hydrogen peroxide as an oxidant. Nine monoterpene substrates (2 cyclic and 7 acyclic) were screened with high selectivity for epoxidation of the tri-substituted alkene and >80% yields reported. Importantly limonene was epoxidised to afford a 1:1 mixture of α-/β-

epoxides in a high 91% yield with a short reaction time of 1.5 h at room temperature (Scheme 47).[34]

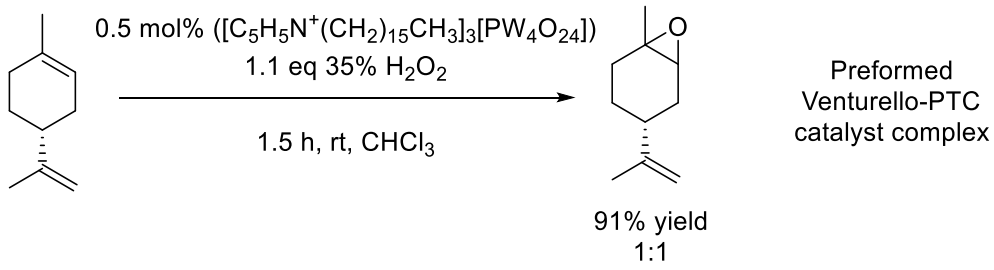

Scheme 47. Ishii-Venturello epoxidation of limonene in chloroform

In 1999 Jacobs *et al*[68] used a preformed heterogeneous macroreticular $PW_4O_{24}[(C_4H_9)_4N]_3$-Amberlite Venturello type catalyst and H_2O_2 for the biphasic epoxidation of a number of terpenes in acetonitrile or toluene, (Scheme 48)[68] with $H_2NCH_2PO_3H$ incorporated as an additive to improve the yields of the acid sensitive epoxide products. 8 (2 cyclic and 6 linear) monoterpene substrates were screened with moderate to high 50-95% yields being achieved. However, this methodology was less efficient at epoxidising the key monoterpenes limonene and 3-carene with only moderate yields of 68% and 53% achieved respectively after long reaction times for 24 h at 35°C.

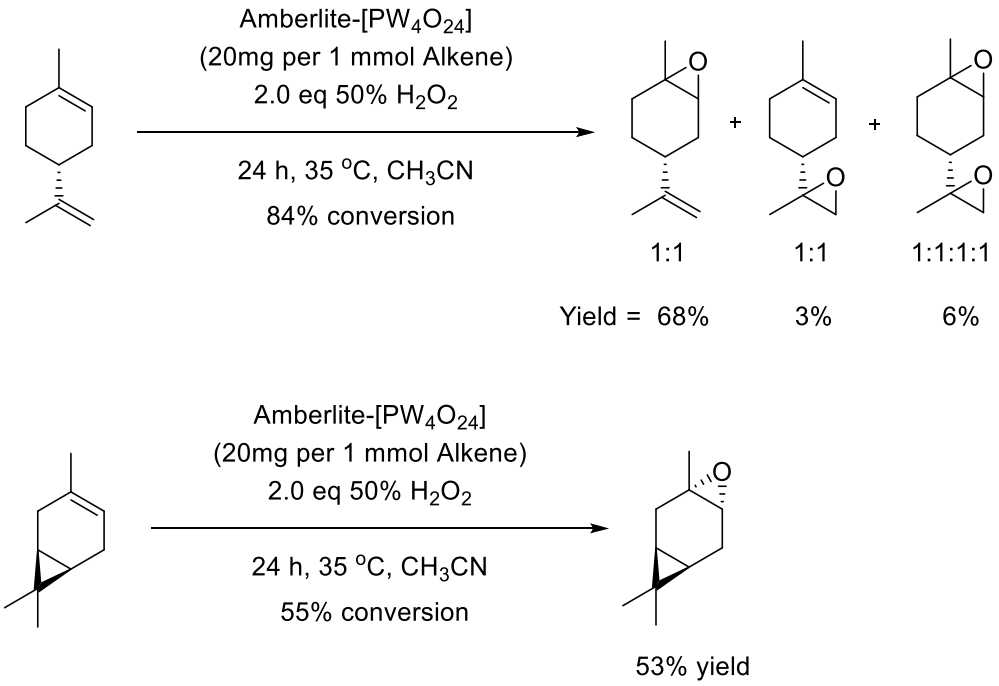

Scheme 48. Epoxidation of limonene and 3-carene using preformed, solid supported Venturello catalyst

They also demonstrated the ability to epoxidise acid sensitive terpenes such as α-pinene and 3-carene using a h***omogeneous*** preformed Venturello-PTC catalyst complex achieving 76% and 94% yields respectively. The use of the additive (aminomethyl)phosphonic acid helped increase the rate of epoxidation, however use of this additive raised the cost of this process, whilst carcinogenic benzene was used as a solvent (Scheme 49).[14, 68]

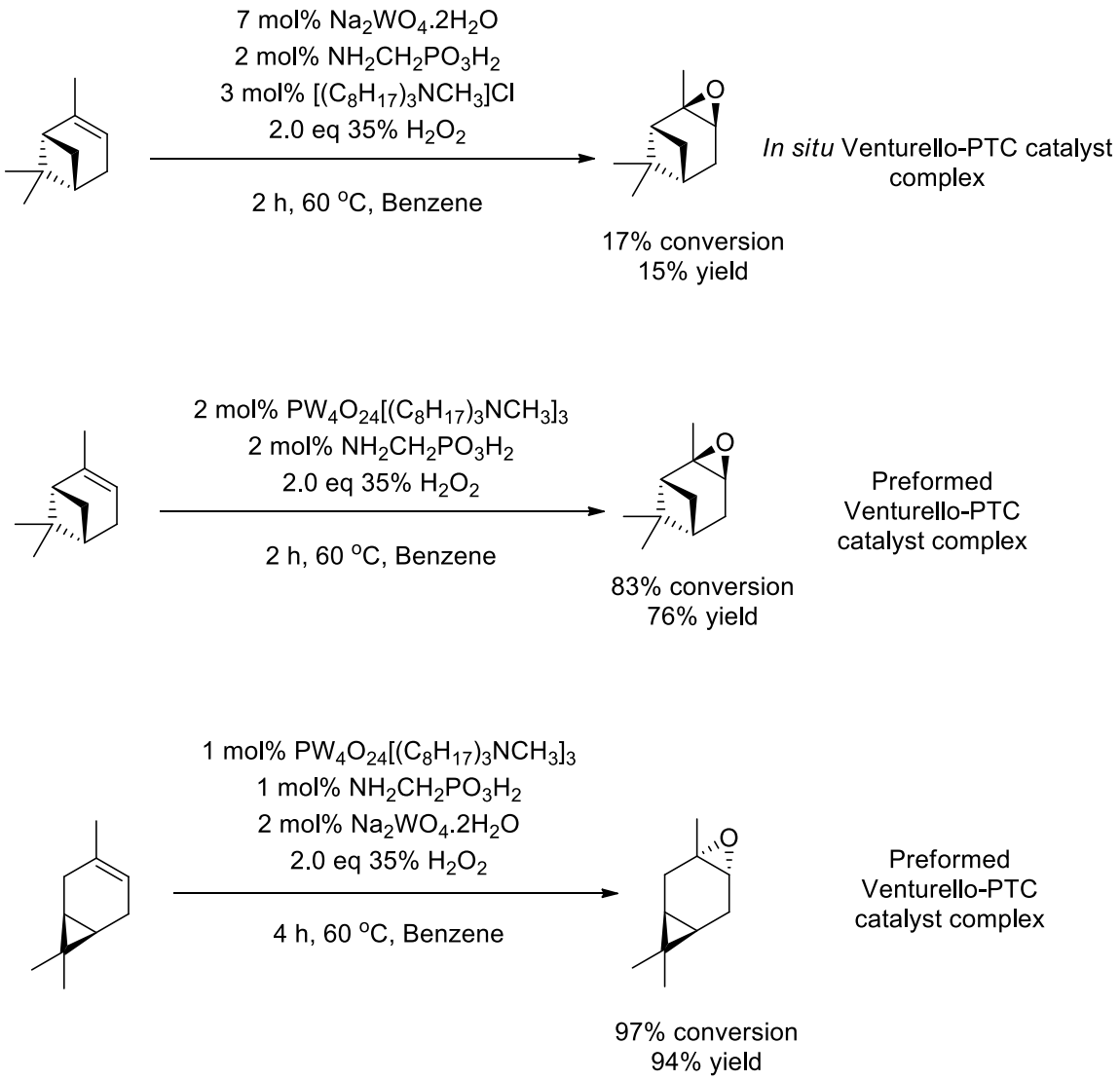

Scheme 49. Epoxidation of acid sensitive monoterpenes α-pinene and 3-carene using *in situ* and preformed homogeneous Venturello-PTC catalysts

In 2006 Clark *et al*[14] reported the first use of a Na_2SO_4 additive in tungsten POM mediated epoxidation reactions employing a phosphate buffer to reduce the rate of competing epoxide hydrolysis, which enabled the pH of the epoxidation reaction to be controlled without the need for expensive phosphonic acid additives. They used an *in situ* generated Venturello catalyst under halide free conditions; however, toluene was still required as a reaction solvent. Seven monoterpene substrates (2 cyclic and 5 acyclic) were epoxidised in 47-95% yields, with this protocol affording high yields of limonene and 3-carene in 76% and 88% yields, respectively. However, this protocol required pre-preparation of a multi-component buffered peroxide solutions, elevated temperatures and large volumes of solvent (Scheme 50).

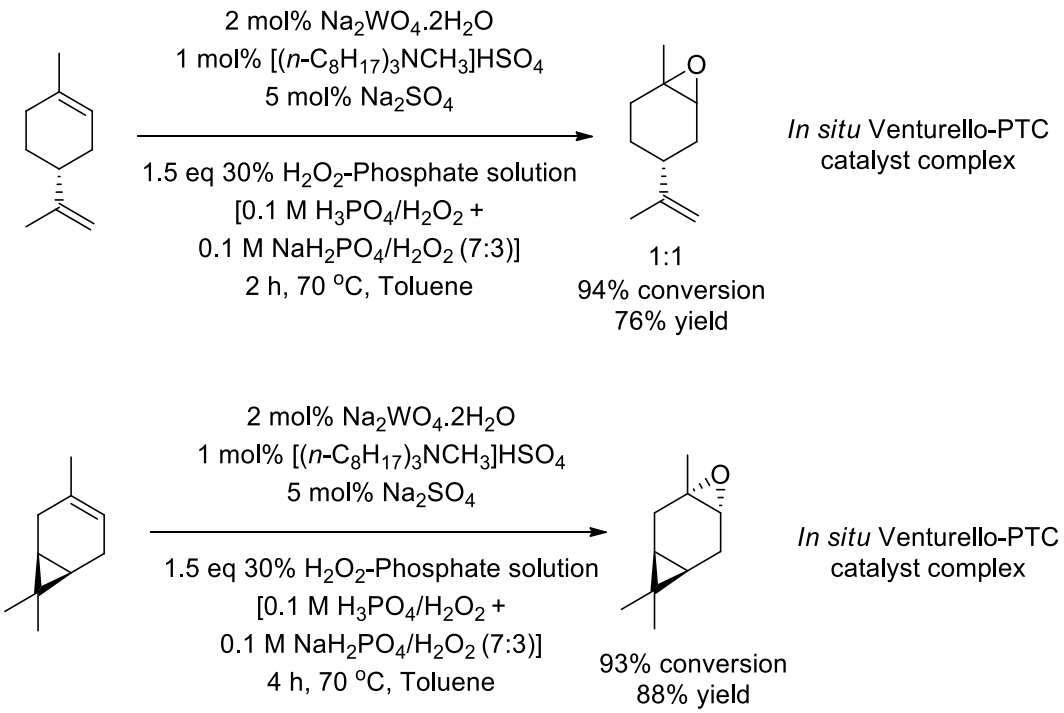

Scheme 50. Clark *et al in situ* generated Venturello catalysed epoxidation of monoterpenes

Further development work by Sato *et al*[69] in 2011 showed that epoxidation using an *in situ* generated Venturello catalyst could be performed under solvent-free conditions in the presence of a phase transfer catalyst [Me(*n*C_8H_{17})$_3$N]HSO_4 and the additive $PhP(O)(OH)_2$ at neutral pH. A range of terpenes (6 cyclic and 1 acyclic substrates) and aromatic alkenes (9 substrates) were epoxidised with moderate to good 55-98% yields. The two improvements for this system were the ability to perform epoxidation under solvent free conditions in high yields and good selectivity observed for trisubstituted alkenes. However, this protocol had a number of disadvantages, including long reaction times (12 h) to reach high conversions, high catalyst loadings of 8 mol%, and the use of phenylphosphonic acid (£0.20 per 1 g Sigma-Aldrich) as an additive.

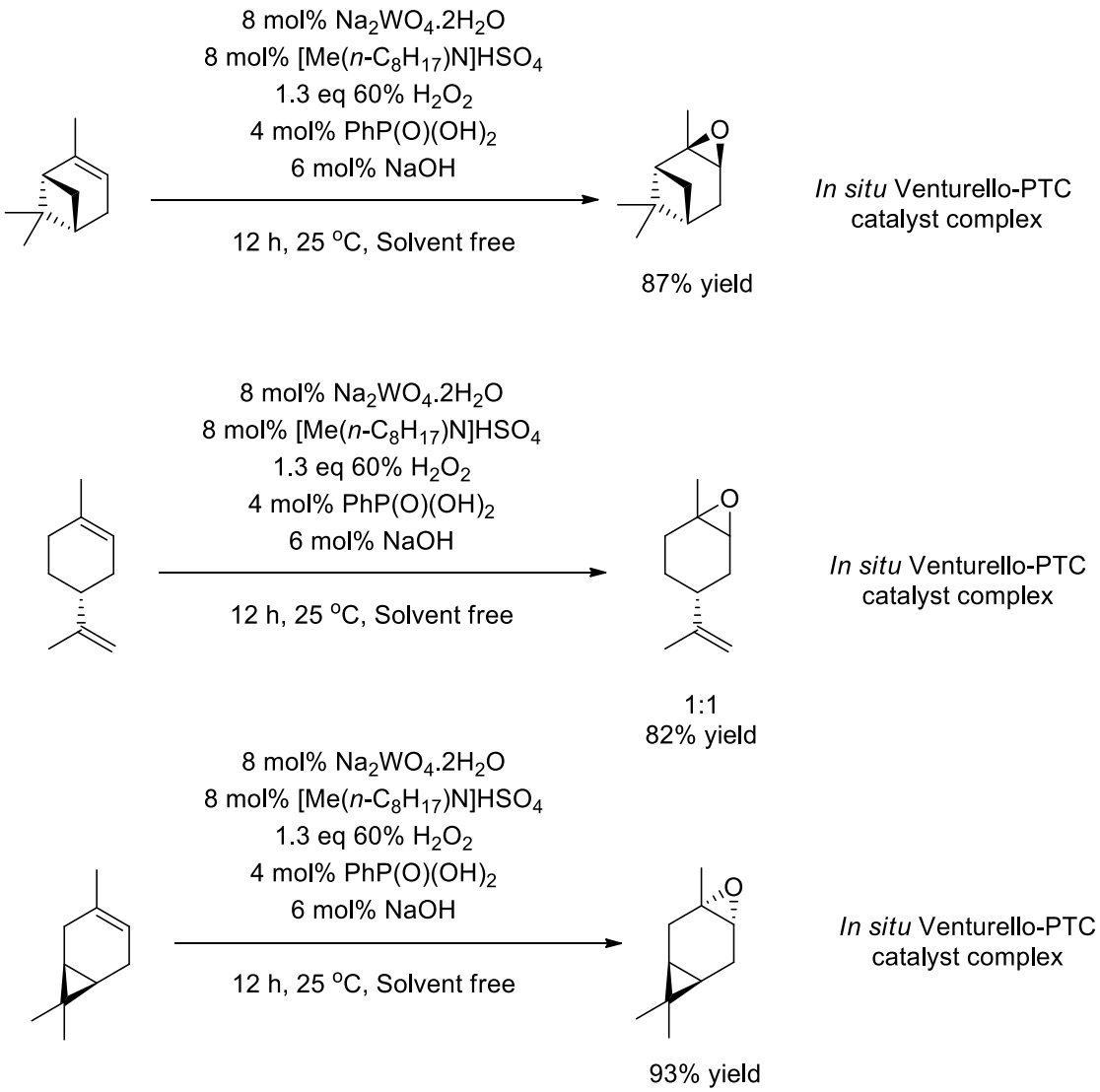

Scheme 51. Solvent free epoxidation of alkenes using *in situ* generated Venturello-PTC catalyst in the presence of a phenylphosphonic acid additive under neutral conditions

Sato *et al*[70] reported a modification to these conditions in 2012 employing high catalyst loadings (8 mol%) and the use of concentrated H_2O_2 (60%). They screened a variety of salts as a replacement for aqueous NaOH to prevent epoxide hydrolysis, without lowering the activity of the catalytic system. Similar to Clark *et al*[14], they found that Na_2SO_4 was the most effective additive for reducing epoxide hydrolysis which enabled high yields of terpene epoxides to be obtained. They found that α-pinene could be epoxidised under acidic conditions, without the need for NaOH buffer, with addition of Na_2SO_4 enabling a 4 fold reduction in the loading of catalyst, and the use of commercially available 30% H_2O_2. Both these changes had no impact on the high yields and selectivities of the epoxidation reactions, however long reaction times (16 h *vs* 12 h) were still needed to achieve high conversions in the presence of the phenylphosphonic acid additive (Scheme 51).

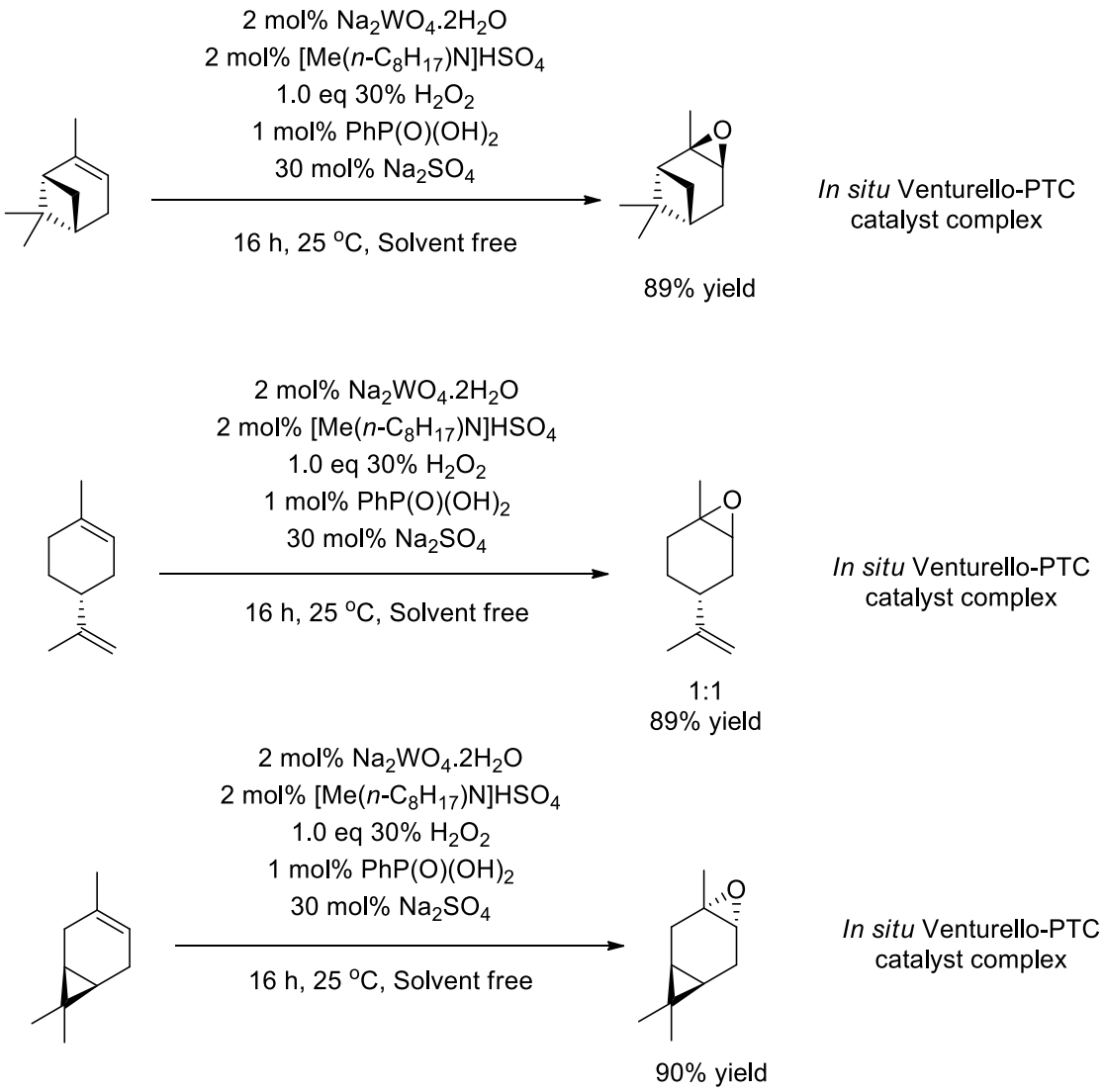

Scheme 52. Organic-solvent free epoxidation of alkenes using lower loadings of *in situ* generated Venturello-PTC catalyst and phenylphosphonic acid additive under acidic conditions

In 2014, Mizuno *et al*[19] reported the use of a Venturello-PTC, $[PW_4O_{24}][(n\text{-}C_6H_{13})_4N]_3$, based system using imidazole as an additive for the epoxidation of 3-carene and a range of cyclic alkenes/dienes (9 substrates with yields of 75-94%). The types of alkene substrate employed were typically difficult to epoxidise in good yield, due to their susceptibility to undergo competing allylic epoxidation reactions, and the instability of the resultant epoxides towards ring opening reactions. However, this protocol required an inert atmosphere, high catalyst loadings, used acetonitrile as a reaction solvent and required lengthy reaction times of 24 h to reach high conversions (Scheme 52).

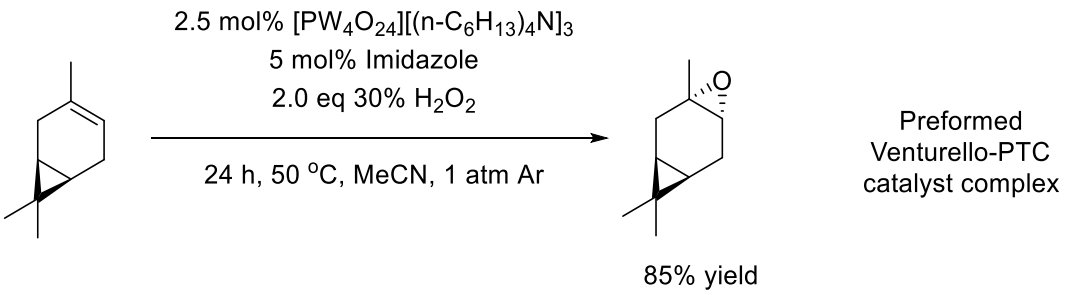

Scheme 53. Mizuno *et al* epoxidation conditions using imidazole additive

Given the promising results obtained for the epoxidation of terpenes using the Ishii-Venturello catalytic system, we wished to investigate its use in flow epoxidation protocols. Prior to carrying out these flow epoxidation studies, it was decided to optimise the Ishii-Venturello catalytic system under conventional batch reaction conditions for the synthesis of terpene epoxides. Once optimal conditions had been established for the batch epoxidation of terpene feedstocks we then envisaged that these conditions would be used as the basis for developing the flow epoxidation protocol (Scheme 53).

It was decided to develop a flow protocol that used a preformed homogeneous catalyst in the absence of any additives, since this would simplify experimental design and facilitate rapid optimisation of the flow protocol for each terpene substrate. A preformed catalyst was desirable, because Sato and Clark had shown that *in situ* formed catalytic systems required longer reaction times to reach full conversion.[71] Whilst, use of an immobilised Venturello catalyst system could potentially allow for more efficient recovery of the catalyst, the selectivities/yields obtained using Jacob's heterogeneous system had been shown to be inferior to those obtained using homogenous catalysts and required significantly longer reaction times.[68]

Therefore, it was decided to develop a preformed Venturello-A336 catalyst to develop an optimal solvent free and additive free protocol for the sustainable epoxidation of terpenes in batch, and then use these conditions as a starting point to optimise conditions that would enable their epoxidations to be carried out in flow.

2.3 Optimisation of the Ishii-Venturello catalyst and H_2O_2 for the solvent free epoxidation of terpene substrates under batch conditions

Limonene (1) was initially chosen as a substrate to optimise our catalytic epoxidation protocol to ensure selectivity for the epoxidation of trisubstituted alkenes over disubstituted alkenes, whilst limonene epoxides have been used widely for numerous applications. For example, 1,2-limonene epoxide (2) has been employed for the synthesis of a range of fine chemicals such as perillyl alcohol,[72] numerous natural products[73-74] and biopolymers,[75-76] (see Scheme 54).

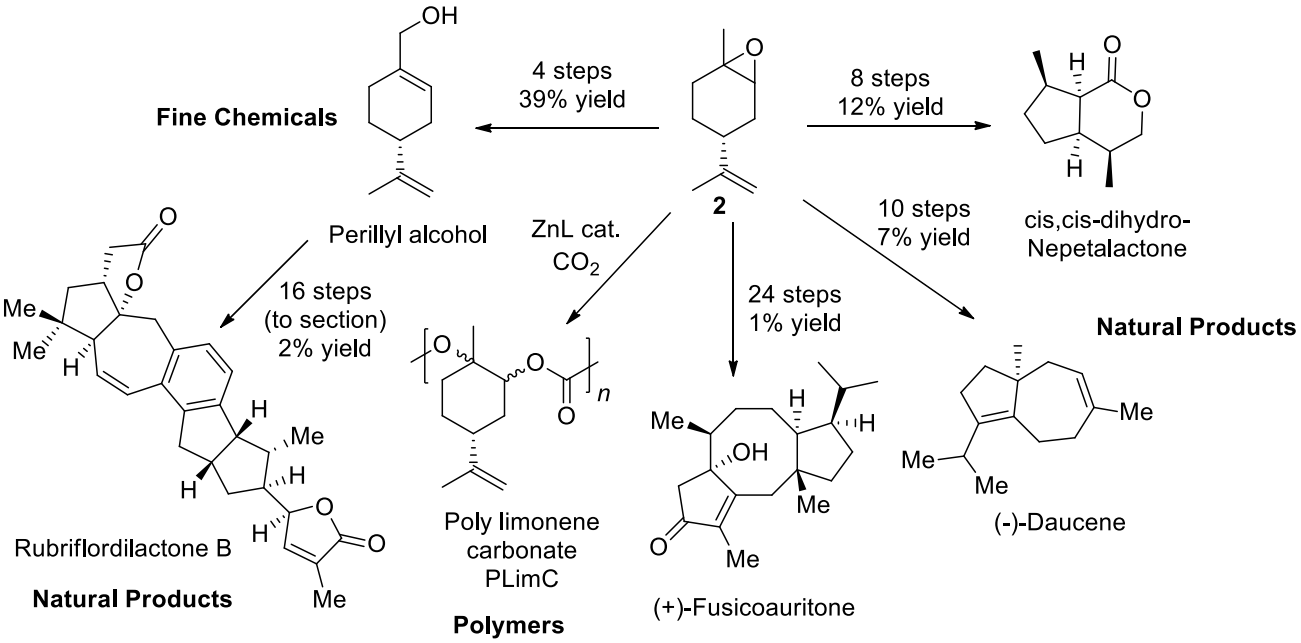

Scheme 54. Range of products derived from 1,2-limonene epoxide

Consequently, our first goal was to develop a versatile protocol for the synthesis of a pre-formed tungsten based Ishii-Venturello type catalyst that could be used under solvent free conditions for the epoxidation of trisubstituted alkene functionality of limonene in terpene substrates. An Ishii-Venturello catalyst containing an Aliquat 336® counterion (PTC) was prepared according to literature precedent.[77,66]

Therefore, Venturello-A336 catalyst complex was prepared by stirring a solution of tungstic acid (H_2WO_4, £2.50 for 10 g) in 30 wt% aqueous H_2O_2 at 60 ^oC for 4 h, before the solution was cooled and an aqueous solution of 85% orthophosphoric acid then added at room temperature. After stirring for 30 min at room temperature, a solution of Aliquat 336 (£0.80 per 10 mL) in CH_2Cl_2 was added slowly with stirring over a period of 15 min. The resulting mixture was stirred vigorously for 1 h at room temperature after which time the organic phase was concentrated under vacuum to give the Venturello-A336 catalyst complex as a viscous, transparent yellow syrup in 70% yield.

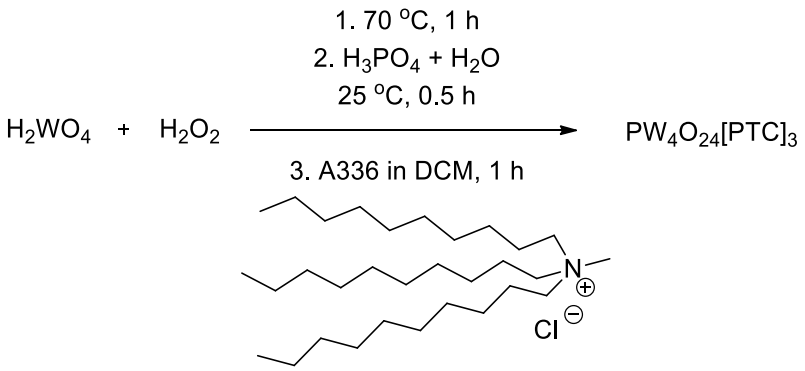

Scheme 55. One-pot synthesis of the Venturello catalyst

The preformed Ishii-Venturello catalyst-PTC was initially screened as a catalyst (1 mol%) for the biphasic epoxidation of limonene, using 1.0 eq of 30% H_2O_2 as an oxidant in CH_2Cl_2 (Scheme 55). Reaction monitoring using gas chromatographic analysis, revealed complete consumption of starting material after 4 h at room temperature, enabling 1,2-limonene epoxide (55:45 mixture of α- and β-epoxides) to be obtained in an excellent 96% isolated yield (Table 2, Entry 1). As reported previously, complete selectivity for monoepoxidation of the more electron rich trisubstituted 1,2 alkene bond of limonene over its disubstituted 8,9 alkene bond was achieved affording 1,2- limonene epoxide with <5% of the corresponding *bis*-epoxide being present.

The catalyst was highly soluble in the neat limonene organic layer and so it was next decided to carry out the epoxidation reaction under solvent free conditions, with 1 mol% of catalyst **1** being dissolved in limonene, followed by addition of 1.0 eq of 30% aqueous H_2O_2 (pH 4.0) and vigorous stirring of the resultant biphasic reaction mixture. This resulted in all of the limonene being consumed after only 1 h, to give 1,2-limonene epoxides in 71% yield, along with 25% of its corresponding diol (3) (mixture of diastereomers), and a small amount (<5%) of limonene bis-epoxide (4) (mixture of four diastereomers).

It was proposed that the diol by-product produced in this epoxidation reaction had been caused by competing hydrolysis of the epoxide ring by water catalysed by the acidic stabilizer (0.5 ppm stannate-containing compounds and 1 ppm phosphorus-containing compounds) that results in the pH of commercial $H_2O_{2(aq)}$ solutions being between 3.0-4.0. Consequently, the pH of the hydrogen peroxide solution was adjusted to pH 7.0 using 0.5M NaOH solution, prior to repeating the epoxidation reaction of limonene. This modification proved effective, resulting in the formation of the desired 1,2-limonene epoxides in an excellent 94% yield, with <5% of any diol by-product being formed.

Changing the phase transfer counterion (PTC) from C8/C10 Aliquat 336 to trioctylmethyl-ammonium showed little change in the performance of the resultant epoxidation catalyst (Table 2, entry 4), whilst using a catalyst containing tetrabutylammonium group counterion, containing shorter alkyl side chains, resulted in no reaction due to rapid precipitation of the catalyst when the hydrogen peroxide was added to the reaction (Table 2, entry 5). The final optimised system for epoxidation of limonene epoxidation, (Scheme 56), with A336 being used as a PTC because of its low cost of £1.50 per 10 g, when compared to pure trioctylmethylammonium counterion of £38.40 per 10 g.

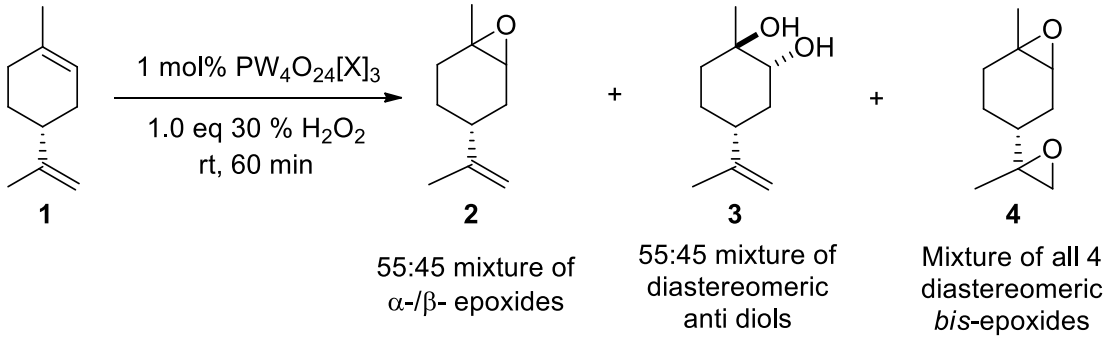

Table 2. Optimisation of Venturello system

Entry	**Solvent**	**pH H_2O_2**	**Counterion X (PTC)**	**1,2 Limonene epoxide Yield**	**1,2 Limonene Diol Yield**	**1,2-8,9 Limonene Bisepoxide Yield**
1	DCM	4	Aliquat 336®	96	4	-
2	Neat	4	Aliquat 336®	71	25	<5
3	Neat	7	Aliquat 336®	94	-	<5
4	Neat	7	Trioctylmethyl ammmonium	93	7	-
5	Neat	7	Tetrabutyl ammonium	-	-	-

[a]Aliquat 336® is a mixture of trioctylmethylammonium and tridecylmethyl-ammonium counterions, which contains excess C_8 cation.

A representative solvent free protocol for the epoxidation of limonene involved dropwise addition (30 seconds) of 30% aqueous hydrogen peroxide (pH 7.0) to a rapidly stirred solution of preformed catalyst-PTC $PW_4O_{24}[PTC]_3$ (1 mol%) dissolved in limonene (10 mmol). This epoxidation reaction was then stirred at room temperature for 0.5 h before the solution was allowed to settle to afford a biphasic system containing two layers (Figure 17). The top organic layer was then decanted and purified *via* column chromatography (or fractional distillation under reduced pressure) to produce the desired 1,2-limonene epoxide as a clear oil in 90-95% isolated yield.

Figure 17. Bi-phasic reactor used for the solvent free epoxidation of limonene

This optimal system had multiple benefits (Scheme 56); no solvent was required, water is the only by-product produced, high yields were achieved at ambient conditions and product separation involved a simple phase separation. In comparison, Sato *et al*[78] reported similar results using a related Ishii-Venturello catalyst that was generated in situ,[79] whilst Sakaguchi *et al*[34] achieved similar at room temperature, however their system required the use of chloroform solvent.

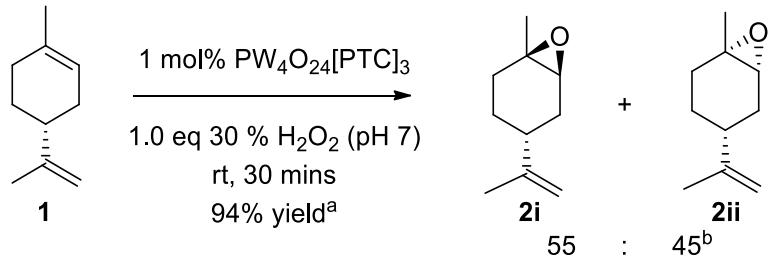

Scheme 56. Optimised Ishii-Venturello system for the epoxidation of limonene

[a]Isolated yields after specified times that were determined by monitoring substrate consumption by tlc. [b]Diastereomeric ratio determined by GCMS and ^{1}H NMR epoxy proton peak integration.

Having established effective catalytic solvent free and additive free conditions for the epoxidation of limonene it was decided to explore the scope and limitation of these conditions for selective epoxidation of the trisubstituted alkene functionalities of a wide range of commercially available terpene substrates shown in Figure 18.

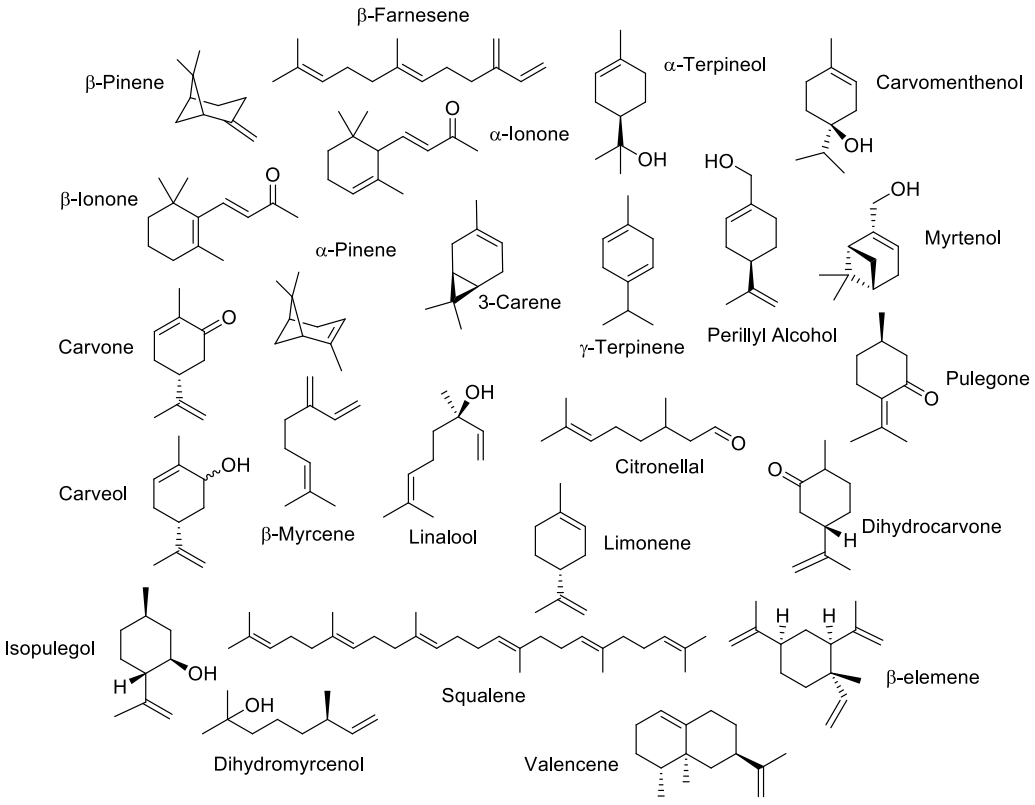

Figure 18. Range of commercially available terpene substrates that were screened for epoxidation using the Ishii-Venturello catalyst/H_2O_2 under solvent free conditions.

2.3.1 Epoxidation of a range of non-oxygenated cyclic terpenes

A range of non-oxygenated cyclic terpenes were epoxidised using our optimised Venturello-A336 epoxidation protocol, with good to excellent yields being achieved with high selectivity for the desired epoxide products being obtained after different periods of time. In some cases, Sato's strategy of using Na_2SO_4 as a salt additive was necessary to facilitate epoxide formation and prevent unwanted diol formation. In those cases where the terpene substrate contained more than one trisubstituted alkene functionality, then greater numbers of equivalents of hydrogen peroxide were employed to ensure that all of the trisubstituted alkenes bonds present were epoxidised. All epoxidation reactions were monitored by tlc and reactions worked up as soon as each terpene substrate had been consumed.

α-Pinene is one of the cheapest and most abundant biorenewable terpenes available in bulk quantities from turpentine sources and this makes it an important test substrate for any sustainable epoxidation methodology. However, epoxidation of α-pinene is often problematic, due to the occurrence of competing acid catalysed rearrangement, fragmentation and hydrolysis reactions that can combine to afford low yields of α-pinene epoxide.[79] When α-pinene was subjected to the standard Ishii-Venturello epoxidation conditions, developed for limonene, no epoxide product was obtained with only starting material or diol-like by-products observed in the crude ^{1}H NMR spectra. However, Clark *et al*[14] had previously reported that good yields of terpene epoxide could be obtained using an *in-situ* formed Ishii-Venturello catalyst in the presence of Na_2SO_4 as a salt additive. Sato *et al*[79] had subsequently applied these salt additive conditions for the epoxidation of α-pinene affording excellent yields of the corresponding epoxide as a single diasteroisomer. They proposed that addition of Na_2SO_4 to these epoxidation reactions slows down competing water mediated epoxide ring opening reactions, by decreasing the availability of water in the organic phase[14].

Incorporation of this salt additive into our preformed Venturello catalyst protocol was achieved by dissolving 0.3 eq of Na_2SO_4 in the buffered hydrogen peroxide solution prior to its addition to the organic phase. This resulted in clean epoxidation of α-pinene to afford a single epoxide diastereomer in 85% yield, with epoxidation of the alkene bond having occurred on its least-hindered face, opposite to the gem-dimethyl group. A similarly high yield of epoxide was reported by Sato after 16 h, however our solvent free system was complete after 4 h.[78] Jacobs *et al*[68] have also used a Venturello catalyst immobilised on Amberlite IRA-900 to perform the epoxidation of α-pinene, achieving a yield of 76% after only 2 h, however, their protocol employed benzene as a reaction solvent, with elevated temperatures of 60 ^{o}C required for complete conversion (Scheme 57)

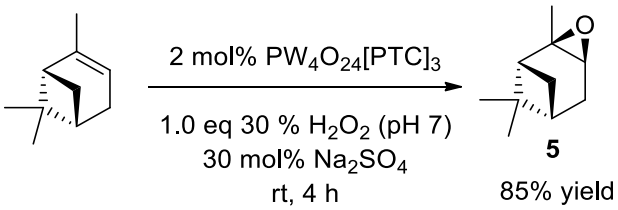

Scheme 57. Epoxidation of α-pinene

α-pinene epoxide (5) is an important target that has been used previously to synthesise a number of high value compounds such as the mucolytic pharmaceutical Sobrerol[80] and natural

products such as Aritasone[81]. A major derivative of α-pinene epoxide is campholenic aldehdyde[82] which is a starting material for the synthesis of a number of natural products such as Necrodol[83] and Triquinanes[84] and synthetic sandalwood-like aroma compounds such as Sandalore[85,86] (Scheme 58).

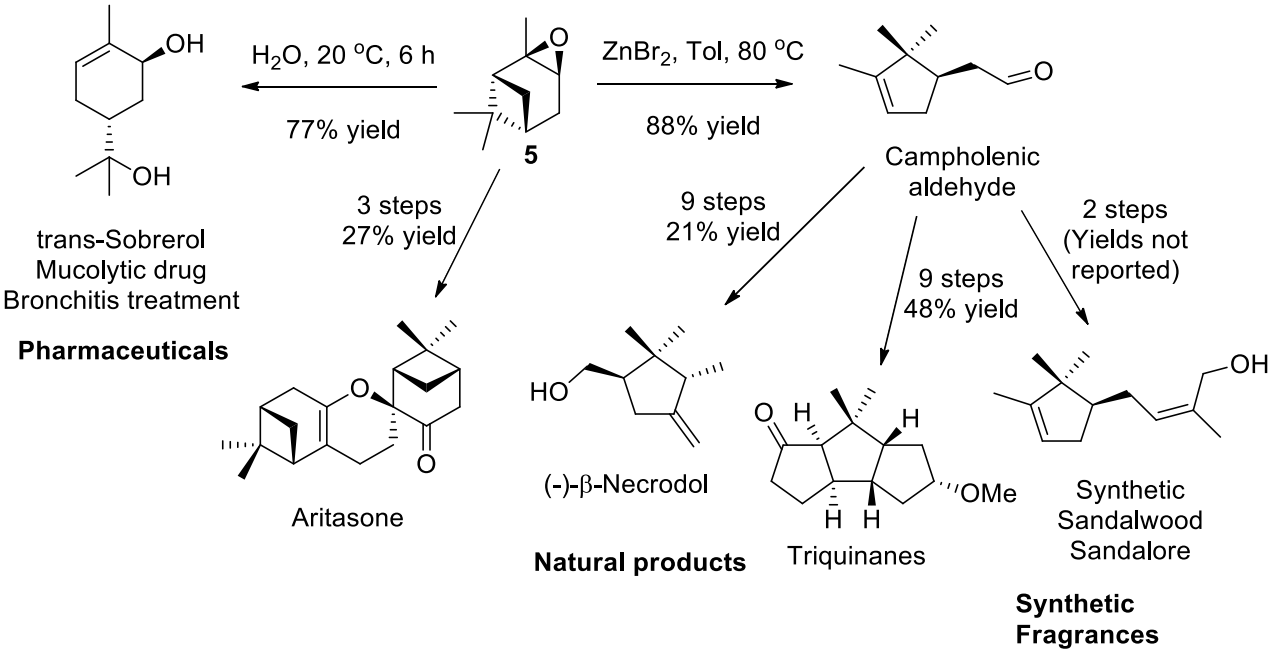

Scheme 58. Key pharmaceuticals, natural products and fragrances derived from α-pinene epoxide

3-Carene is a major biorenewable terpene present in turpentine that is available cheaply in bulk quantities, which was chosen as the next terpene substrate to be epoxidised. 3-carene epoxide was produced as a single diastereomer in a good 92% isolated yield after 4 h. Kamata *et al*[19] have previously used a peroxytungstate catalyst with a tetra-*n*-hexylammonium counterion and hydrogen peroxide as oxidant in acetonitrile at 50 °C to prepare 3-carene epoxide, however their system required the use of imidazole as an additive. Clark *et al*[14] also reported the epoxidation of 3-carene using an *in situ* formed tungstate catalyst in toluene, which required a reaction time of 2 h at 70 °C to proceed to completion (Scheme 59).

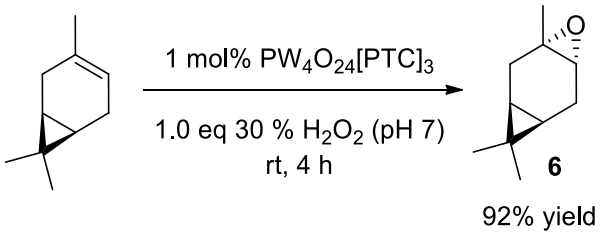

Scheme 59. Epoxidation of 3-carene

3-Carene epoxide (6) is another widely used starting material for synthesis, with this versatile epoxide having been used to prepare Spirochroman[81], the β-lactam side chain in Taxol[87], agrochemicals such as the pyrethroid precursors[88] (+)-butyl chrysanthemate and (-)-caronaldehyde acid hemiacetal and carvone[89], respectively (Scheme 60).

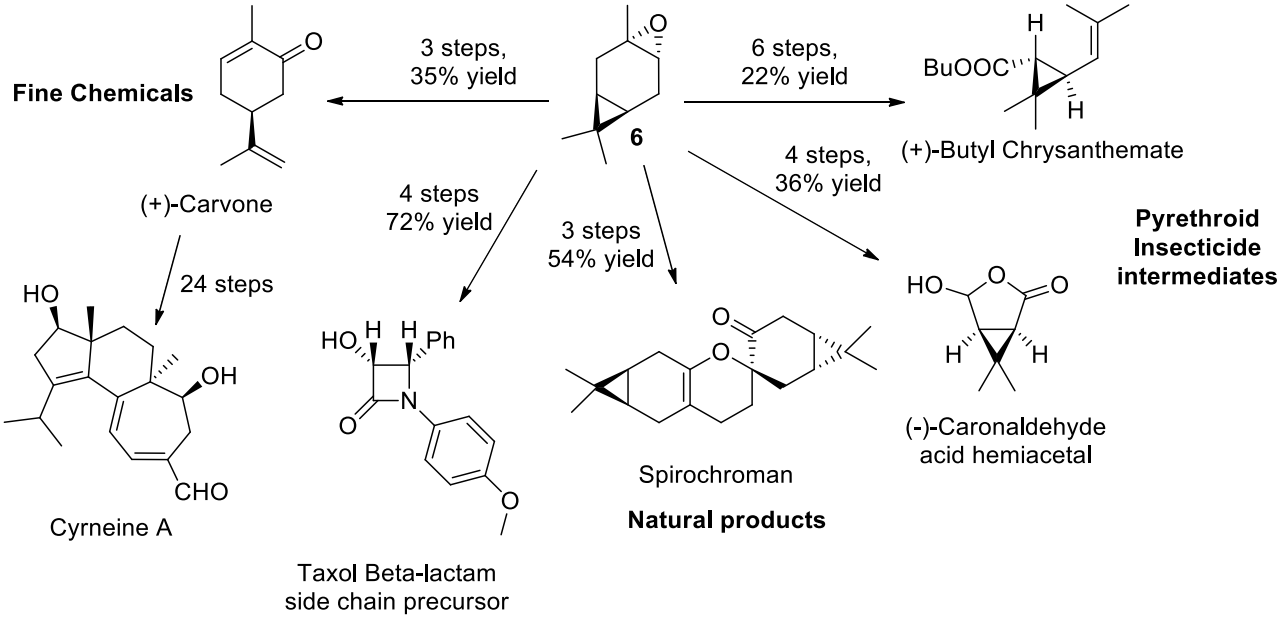

Scheme 60. Key products derived from 3-carene epoxide

γ-terpinene contains two trisubstituted alkene bonds so 2.0 eq of H_2O_2 were used for its catalytic epoxidation using our Ishii-Venturello catalytic system which selectively gave the *cis*-bis-epoxide diastereomer in >90% *de* (as determined by ^{1}H NMR, ^{13}C NMR and GC analysis) in 86% yield (Scheme 61).

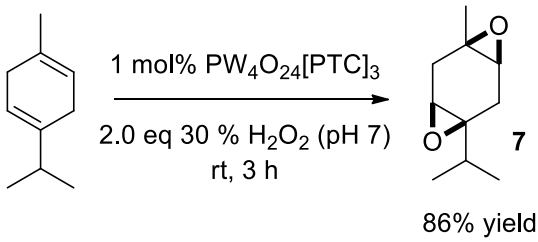

Scheme 61. Epoxidation of γ-terpinene epoxidation

A similar unexpected product selectivity for diepoxide formation was also reported by Ishii *et al* who proposed that monoepoxidation of one of the trisubstituted alkenes of γ-terpinene affords a mono-epoxide that then directs epoxidation of the second trisubstituted alkene on the same face (See Figure 19).

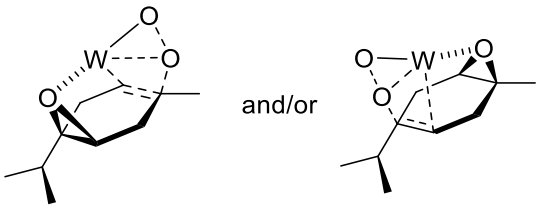

Figure 19. Directing effect model used to rationalise *cis*-bis-epoxide formation[34]

Ishii *et al*[34] have previously employed a tungsten catalytic system to epoxidise both alkene bonds of γ-terpinene, however their protocol required the use of chloroform as solvent. A 2008 patent by Klemarkzyk *et al* describes a process for co-polymerising γ-terpinene bis-epoxide (7) (prepared using stoichiometric amounts of *m*CPBA) with bisphenol F diglycidyl ether for

the manufacture of an epoxy resin that TGA analysis showed had a high melting point of 200 ^{o}C. We repeated the synthesis of this bis-epoxide on a 20 g scale to produce bis-epoxide that other members of the terpene consortium are exploring for the synthesis of biorenewable polymers using the range of polymerisation strategies (Scheme 62).

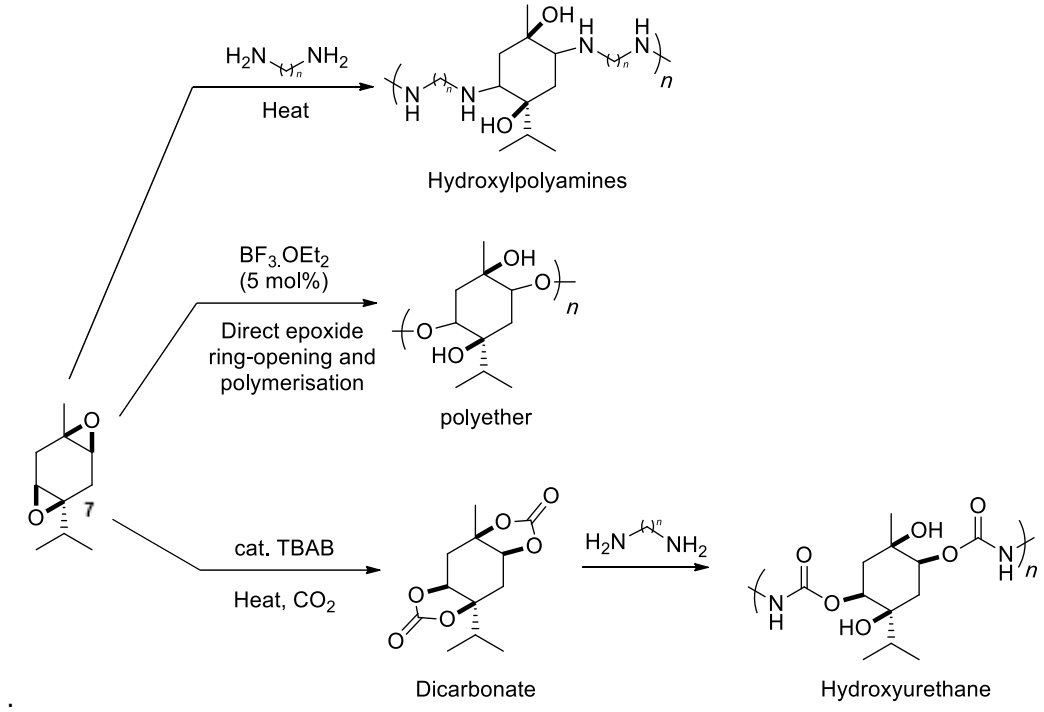

Scheme 62. Possible biorenewable polymers derived from γ-terpinene bis-epoxide

The bicyclic sesquiterpene valencene contains a tri-substituted alkene functionality and an exocyclic di-substituted alkene functionality which is produced by the biotech company Isobionics who have developed a fermentation process that enables it to be produced in multigram quantities. Epoxidation of valencene at 20 ^{o}C using our epoxidation conditions for 24 h resulted in monoepoxidation of its trisubstituted double bond to give a 7:3 mixture of exocyclic and endocyclic epoxides respectively with no epoxidation of the isopropenyl group having occurred (determined by epoxy peak ^{1}H NMR analysis that matched previously reported NMR data reported by Shaffer et al[90]). This is the first time that this sesquiterpene substrate has been selectively epoxidised using a catalytic tungsten system. Shaffer *et al*[90] previously reported the epoxidation of valencene using stoichiometric peracetic acid in benzene produced a mixture of diastereomers (71:29 ratio) in 63% yield. However, Shaffer *et al* reported that the exocyclic epoxide was the major diastereomer formed when using peracetic acid (Scheme 63).

Only two other reports of valencene monoepoxides (8) appear in the literature, the first of which was prepared using cytochrome P450 enzymes to oxidise valencene into a mixture of oxygenated products[91] and the second report by Fdil *et al*[92], who epoxidised valencene using two ruthenium-1,2,4-triazepine catalysts with molecular oxygen in DCM to afford a mixture of valencene monoepoxides in 94% and 65% yields, respectively, in a similar (62:38) *endo : exo* ratio to that obtained using our protocol. They achieved yields of with the oxygen based 1,2,4-triazepine and sulphur 1,2,4-triazepine ligands respectively.

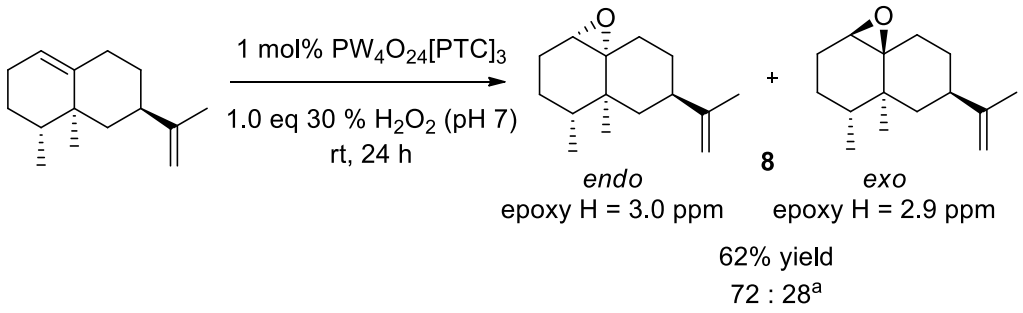

Scheme 63. Epoxidation of valencene

[a]Diastereomeric ratio of 76 : 24 determined by integration of the ^{1}H NMR epoxide C-H protons of the *endo : exo* epoxides at δ 3.0 and δ 2.9 ppm[90], respectively.

β-elemene is a sesquiterpene that is a major constituent of *Rhizoma zedoariae* and *Pterodon emarginatus* that are Chinese and Brazilian medicinal herbs respectively and have been shown to possess anti-tumour/anti-inflammatory properties.[93] It contains two disubstituted alkene groups and one monosubstituted alkene group, making it an ideal substrate to test the selectivity of our epoxidation protocol for trisubstituted alkenes. Catalytic epoxidation of β-elemene with 2.0 eq of H_2O_2 at 50 °C using our standard Ishii-Venturello protocol resulted in bis-epoxidation to afford a 40:40:10:10 mixture of bis-epoxide diastereomers (determined *via* GC and ^{1}H/^{13}C NMR analysis), with the monosubstituted alkene remaining unfunctionalized, even at epoxidation temperatures of 80 °C. This mixture of epoxide diastereomers could not be separated by chromatography and the relative configuration of the major diastereomers produced could not be assigned from examination of the ^{1}H NMR spectra of the crude reaction product (Scheme 64).

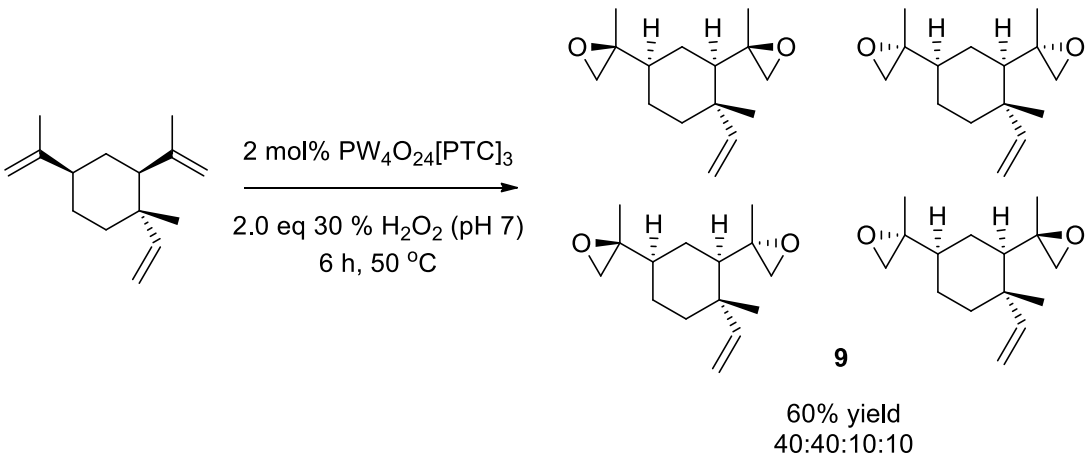

Scheme 64. Epoxidation of β-elemene

These type of β-elemene bis-epoxides (9) are potentially good sources of biorenewable monomers for the production of advanced biopolymers, since they contain two reactive epoxide groups that can potentially be cross-linked, with the additional benefit that they contains an unreactive monosubstituted alkene that can potentially be used for polymer functionalization (e.g. *via* cross methathesis). A range of potential polymerisation approaches that are currently under investigation by other members of the Bath terpene consortium are shown in Scheme 65.

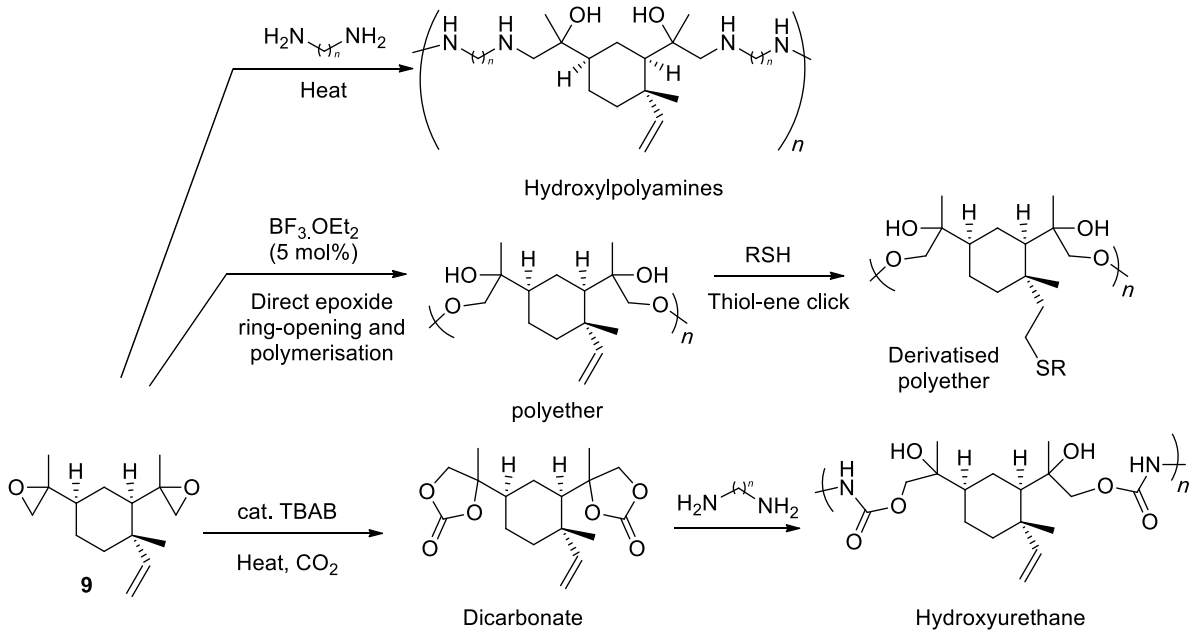

Scheme 65. Potential polymers that could be produced from β-elemene bis-epoxide

2.3.2 Epoxidation of cyclic terpenes containing alcohol functionality

Lett *et al*[94] have proposed a number of different mechanisms to explain the mechanism and stereochemistry of tungsten catalysed epoxidation reactions of allylic alcohols. They suggest that epoxidation occurs *via* coordination of the hydroxyl group of the allylic alcohol to afford an allylic pertungstate ester that then facilitates an intramolecular epoxidation reaction (Figure 20, (1)). Alternatively, hydrogen bonding from the hydroxyl group of the allylic alcohol to a tungsten coordinated hydrogen peroxide species may result in epoxidation (Figure 20, (2)). A third model involves coordination of the hydroxyl group of the allylic alcohol to afford a dimeric tungsten species with a pentagonal bipyrimidal structure, with internal delivery of a tungsten peroxy species affording the epoxide (Figure 20, (3)).[94]

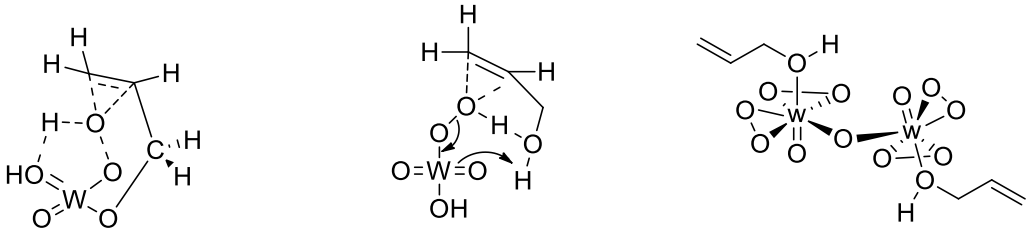

Figure 20. Potential models for tungsten catalysed epoxidation of allylic alcohols

A range of cyclic terpene alcohols were epoxidised using our Ishii-Venturello catalytic system at room temperature to afford a series of monoepoxides in 55-77% yield, with the time taken for epoxidation to occur determined by the relative steric hindrance of their alkene functionalities (Scheme 66). Perillyl alcohol was epoxidised to give clean samples of their α-

β- epoxides (10) in a 58:42 ratio in 2 h in 71% yield, whilst carveol gave their corresponding α-β- epoxides (11) in a 55:45 ratio in 4 h in 55% yield (Scheme 66).

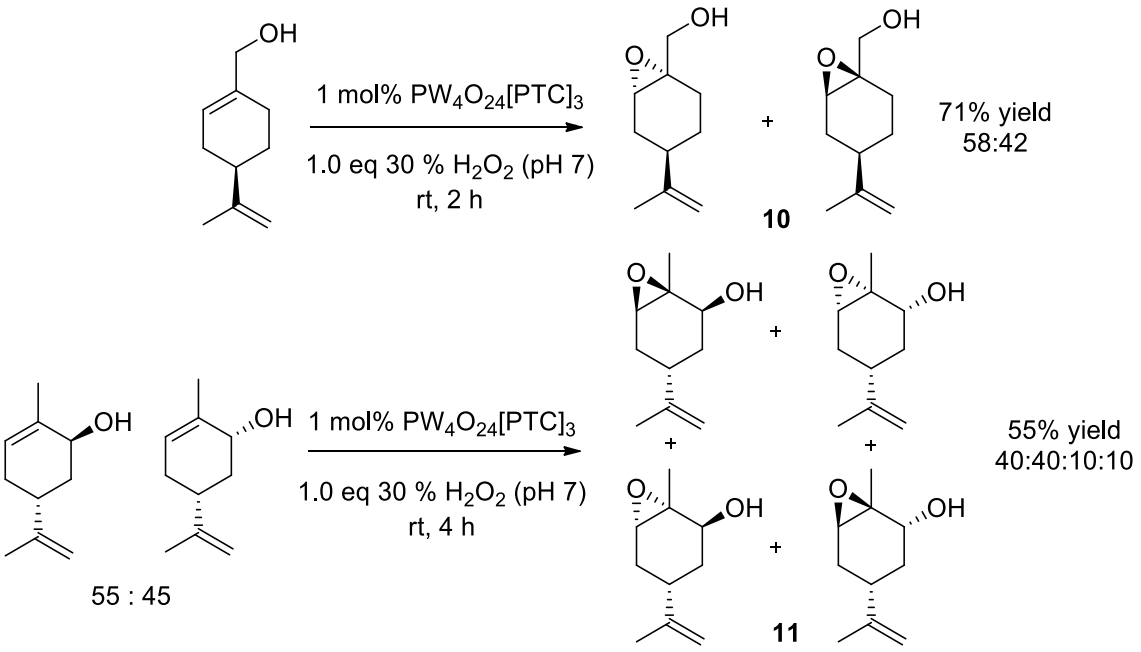

Scheme 66. Optimised perillyl alcohol and carveol epoxidation conditions

Perillyl alcohol epoxide has been used extensively to produce a number of important natural products such as Rubifolide[95], Kallolide B[96], Zoanthamine alkaloid building blocks[97], vigulariol[98], insect pheromone and the fine chemical cryptone (Scheme 67).[99]

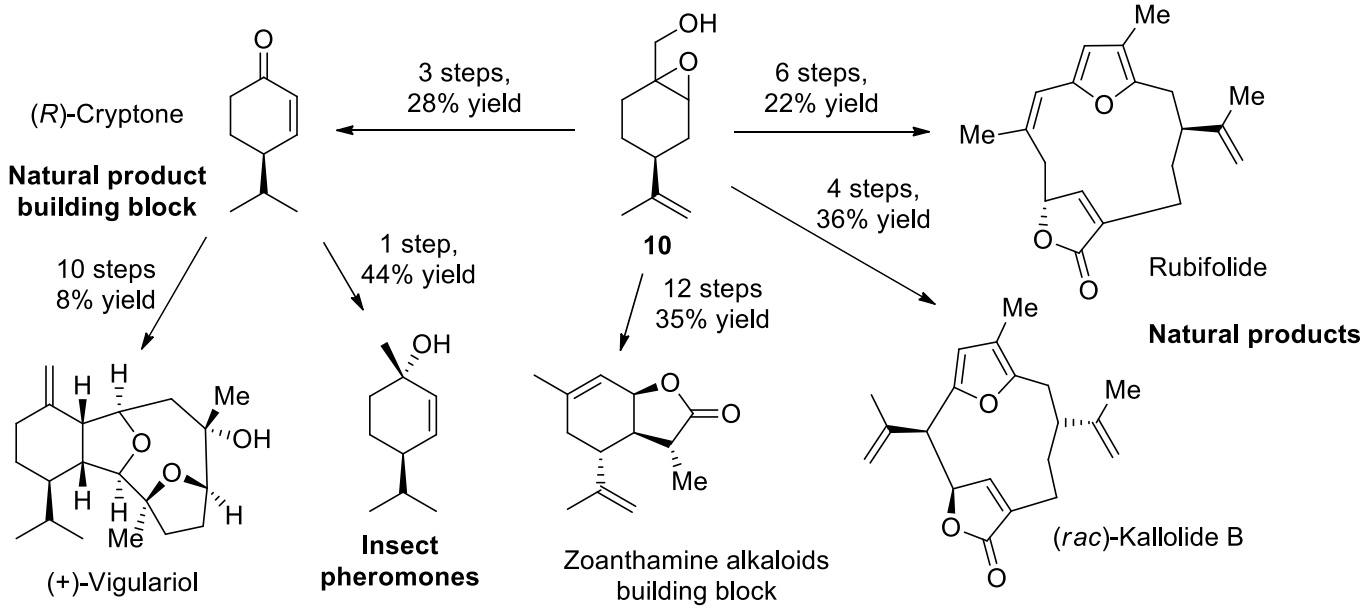

Scheme 67. Key products derived from perillyl alcohol epoxide

Carveol epoxide has also been used as a building block compound for the synthesise of a number of natural products, such as Machaeriol D,[100] Eucannabinolide[101] and Dihydroxyvitamin D3 (Scheme 68).[102]

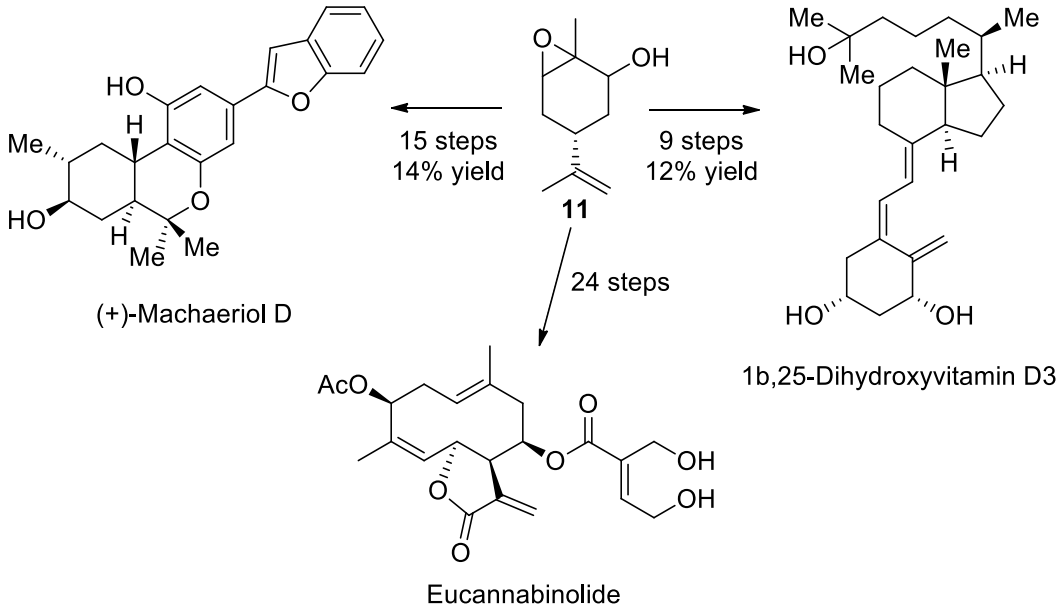

Scheme 68. Natural products derived from carveol epoxide

Myrtenol was epoxidised using an Ishii-Venturello epoxidation catalyst using 30 mol% sodium sulfate as an additive, to give a single diastereomeric epoxide after 2 h in 70% yield, with epoxidation occurring exclusively from the face opposite to the 1,1-dimethyl substituent (Scheme 69). The stereochemistry of this epoxide (12) was confirmed by comparison to literature data reported by Il'ina *et al*,[103] who prepared this epoxide using peracetic acid as a stoichiometric oxidant in 32% yield.

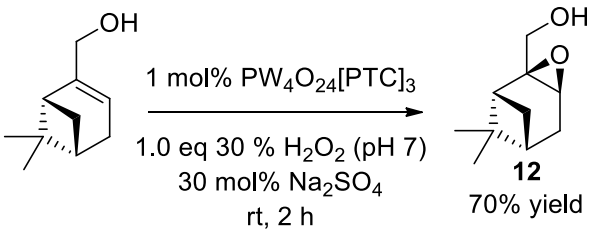

Scheme 69. Epoxidation of myrtenol

Applications of myrtenol epoxide have not been widely explored, however Il'ina *et al*[103] have shown that myrtenol epoxide can be converted *via* an acid catalysed rearrangement reaction to afford campholenic aldehyde in 27% yield (Figure 21).

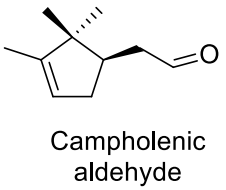

Figure 21. Campholenic aldehyde

The homoallylic alkene bond of carvomenthenol was successfully epoxidised to give a mixture of its epoxide diastereomers (13) in 77% yield with 90:10 selectivity favouring the *cis* isomer, which is formed preferentially due to the directing effect of the cyclic tertiary alcohol group.

This yield is comparable to that reported previously by Sato *et al*,[78] however our preformed catalyst system reached completion in a much shorter reaction time (3 h *vs* 12 h) (Scheme 70).

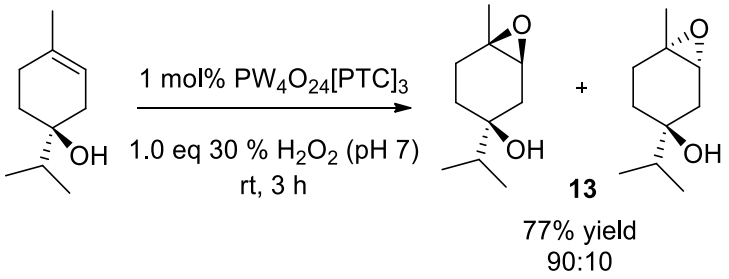

Scheme 70. Epoxidation of carvomenthenol

Carvomenthenol epoxide has been used to synthesise natural products such as dihydropinol (Figure 22),[104] which is an analog of the mucolytic drug, Sobrerol. Carvomenthenol is also a key active ingredient in Tea Tree oil that is responsible for its cytotoxic effect against demodex mites that are a common ectoparasite found on the human skin that is thought to be a major cause of acne.[105]

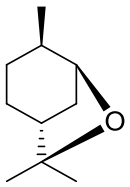

Figure 22. (*1R,4R,5S*)-Dihydropinol

Finally, α-terpineol was epoxidised in 66% yield in 1 h, to give a 56:44 mixture of α-/β- epoxides (14), with no 2-hydroxy cineole products formed from competing intramolecular cyclisation of its tertiary alcohol onto the epoxide ring. Once again, this reaction time was much faster than previously reported by Sato using their protocol that employed an *in situ* catalyst formation step (1 h vs 16 h) (Scheme 71).[79]

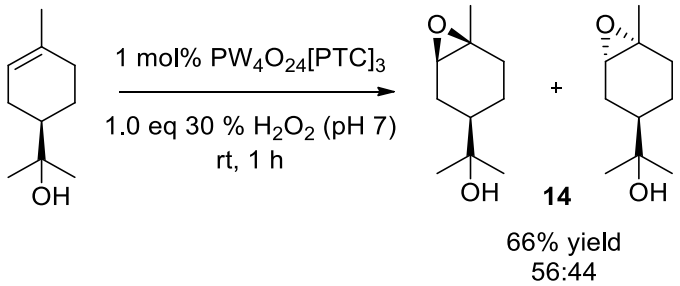

Scheme 71. Epoxidation of α-terpineol

α-terpineol epoxide has previously been used to synthesise 2-*exo*/*endo*-hydroxy-cineoles (Figure 23) that are produced by microorganisms in the digestive systems of marsupials that can hydroxylate cineole, that is the major eucalyptus essential oil found in the Australian bush.[106] Hydroxy-cineoles have also been used as cosmetic ingredients, due to their balsamic,

piney aroma, or as starting materials for the synthesis of other cosmetic compounds containing scented esters.[107]

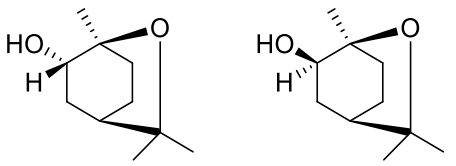

(+)-(1S,4R,6S) (-)-*(1S,4R,6R)*

Figure 23. 2-*exo*/*endo*-cineoles derived from α-terpineol epoxides

2.3.3 Epoxidation of terpenes containing α, β-unsaturated functionality

We then explored the potential of using our preformed Ishii-Venturello catalytic protocol for the epoxidation of trisubstituted alkene functionalities of cyclic terpenes containing α-β-unsaturated ketone functionalities. The more reactive non-conjugated trisubstituted alkene functionalities of (*rac*)-α-ionone were readily epoxidised at room temperature to afford a mixture of its α-/β- mono-epoxides in 79% yield after 4 h (Scheme 72). In comparison Sato's previous epoxidation protocol for (*rac*)-ionone required elevated temperatures of 90 ^{o}C, whilst a methyltrioxyrhenium (MTO) catalytic system used by Sfrazzetto *et al*[108] required DCM as a solvent, pyridine as an additive and 20 h to afford a 5:1 mixture of epoxides (15).

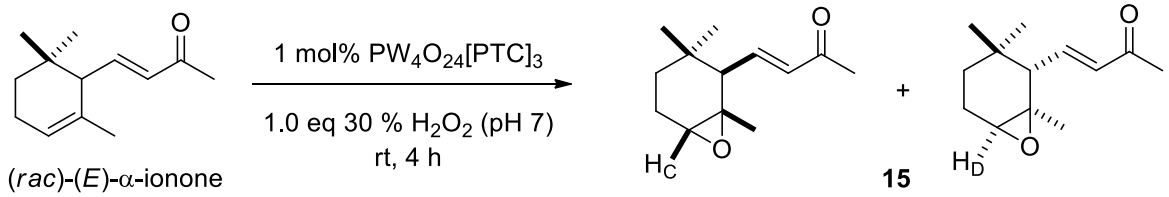

(*rac*)-(*E*)-α-ionone **15**

79% yield
cis:trans
80:20

Scheme 72. Optimised epoxidation of α-ionone using the Ishii-Venturello protocol

This favoured diastereofacial selectivity for formation of the *cis* epoxide was rationalised by Sfrazzetto *et al*, who proposed that formation of the transition state leading to the trans epoxide was disfavoured due to repulsive 1,3-diaxial interactions between its methyl groups as part of a late transition state (Scheme 73).[108]

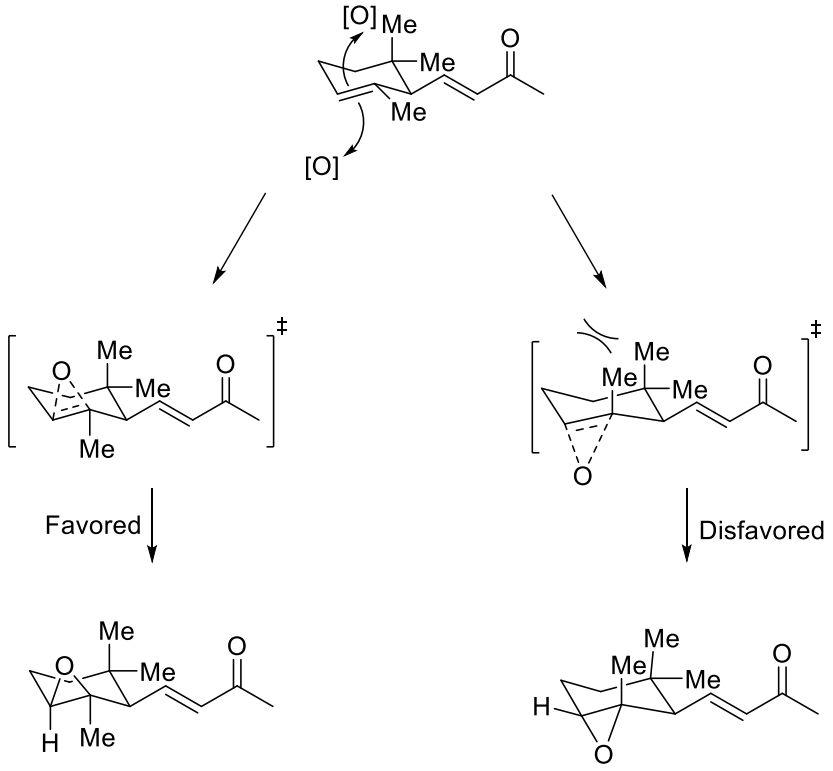

Scheme 73. Model proposed by Sfrazzetto *et al* for *cis* facial selectivity preference

α-ionone epoxide has been used for a number of applications, including the synthesis of (*S*)-(+)-4-hydroxy-β-ionone that is used as a precursor for the synthesis of carotenoid vitamins and the fragrance damascene.[109] The natural products Forskolin[110], *epi*-Ambliol-A[111] and Trisporin A[112] have also been synthesised from α-ionone epoxide (Scheme 74).

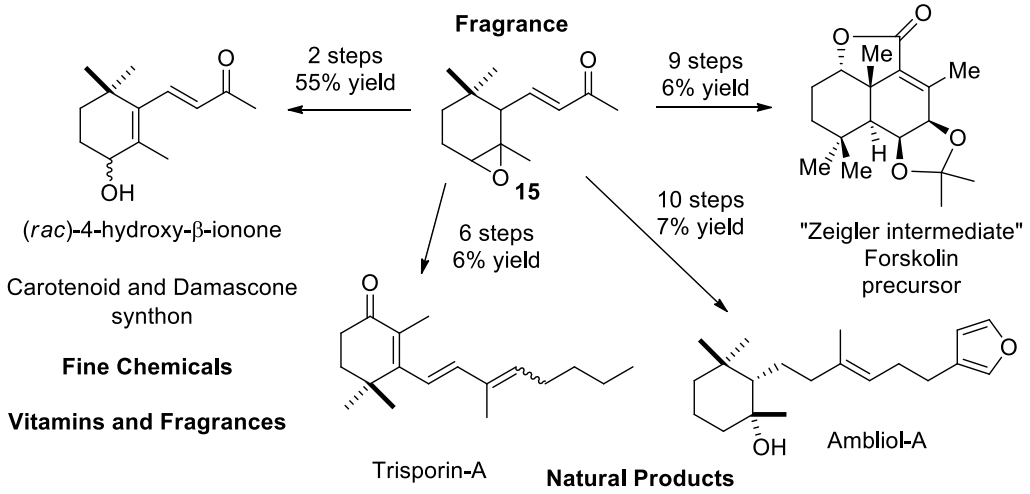

Scheme 74. Products derived from α-ionone epoxide

We then epoxidised the sterically hindered ***tetra***-substituted α-β-alkene functionality of β-ionone using our preformed the Ishii-Venturello/H_2O_2 catalytic protocol at 50°C for the first time, affording a 75:25 mixture of diastereomeric epoxides (16) in 84% yield (Scheme 75).[113] Other catalytic systems using catalytic MTO[108] and selenium[113] species have also been used

for the synthesis of these epoxides, however these protocols require expensive and toxic metal catalysts.

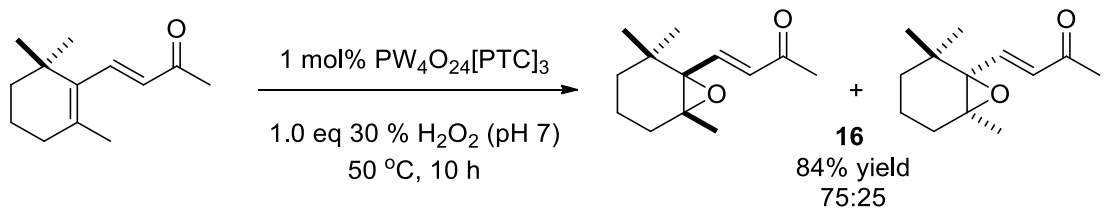

Scheme 75. Epoxidation of β-ionone using the Ishii-Venturello protocol

Importantly, β-ionone epoxide is an important fragrance molecule that is frequently used in perfumery due to its long lasting aroma,[114] and for the synthesis of higher value fragrances and pheromones such as Dihydroactinidiolide.[115] It has also been used to prepare the natural products uparene[116] and secocuparena,l[117] whilst β-ionone epoxide itself has been shown to be a potent inhibitor of cancer cells (Scheme 76).[118]

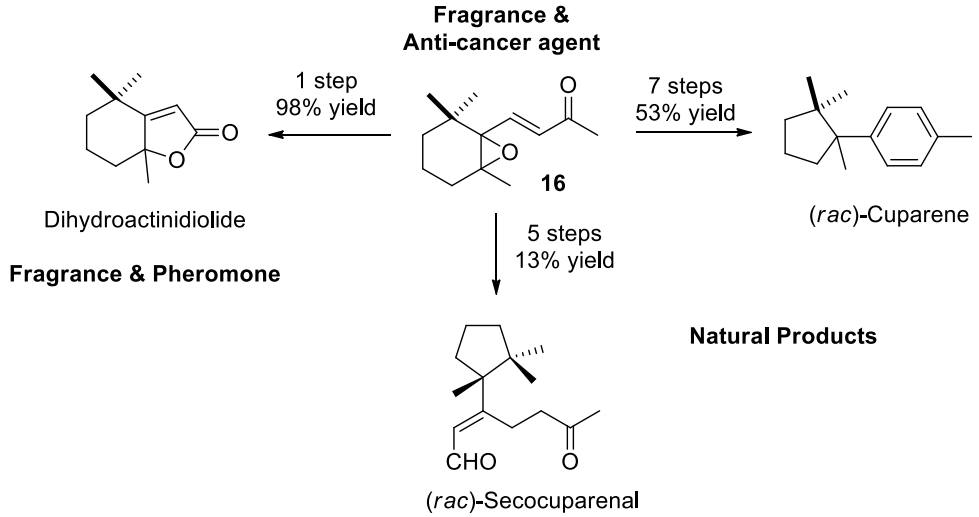

Scheme 76. Products derived from β-ionone epoxide

The tetrasubstituted α-β-unsaturated alkene functionality of pulegone also reacted rapidly using our catalytic epoxidation protocol at 50 °C to give a 55:45 mixture of epoxides, albeit in a relatively low 40% isolated yield. This is the first time that pulegone has been epoxidised using a tungsten based catalyst, with Kaneda *et al*[119] having previously reported that an aluminium-magnesium based catalyst system using benzonitrile and H_2O_2 in methanol *via* potentially explosive peroxyimidic acid oxidant that gave a high yield, 93%, of pulegone epoxide (17) after 48 h (Scheme 77).

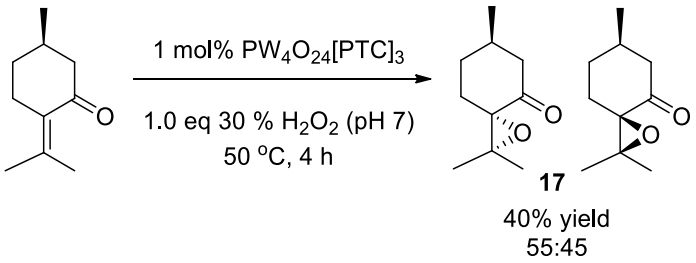

Scheme 77. Epoxidation of pulegone

Pulegone epoxide has been widely used for synthesis, including protocols for the preparation of seven membered trimethylcycloheptane-1,3-dione,[120] fragrances such as α-corocalene[121] and for the synthesis of (-)-lycoposerramine-R[122] and bisabolangelones and liginvolones sesquiterpenes (Scheme 78).[123]

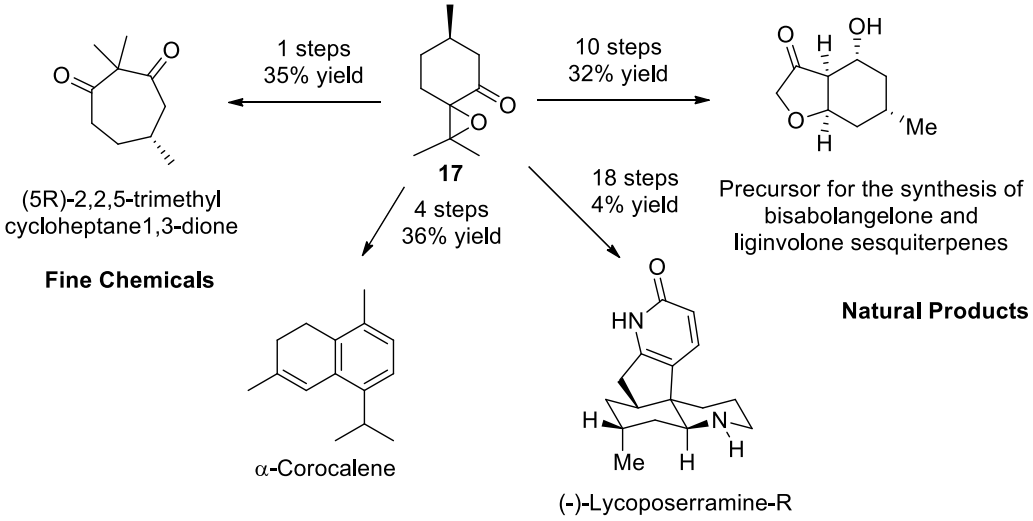

Scheme 78. Products derived from pulegone epoxide

2.3.4 Epoxidation of acyclic terpenes

Our attention then turned to using our preformed Ishii-Venturello catalyst for the epoxidation of a range of acyclic terpenes. The isolated trisubstituted alkene bond of myrcene was epoxidised to give its mono-epoxide as a 50:50 mixture of diastereomers in 82% yield after 3 h, leaving its synthetically useful diene fragment (e.g. for Diels-Alder reactions) unreacted. Sato *et al*[79] also epoxidised myrcene effectively using their *in situ* epoxidation protocol in a slightly lower 75% yield (18) after 12 h (Scheme 79).

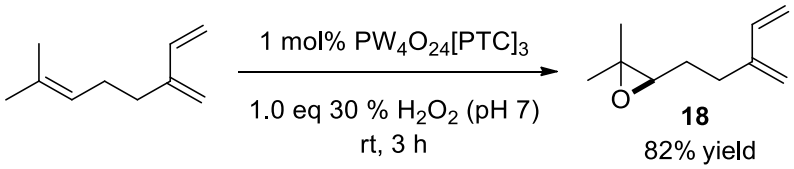

Scheme 79. Epoxidation of myrcene

Unfortunately, use of our preformed Ishii-Venturello protocol for the epoxidation of citronellal consistently produced a low yield of citronellal epoxide (19) (5 h, 40% yield), at 70% conversion along with 30% yield of the corresponding diols (20) formed from epoxide ring opening by water. Increasing the catalyst loading to 3 mol% and lowering the temperature to 15 ^{o}C led to 100% consumption of starting material over 24 h, however a 74% yield of citronellal diol (from hydrolysis of intermediate epoxide) was obtained, even when the solution was buffered at pH 7 (Scheme 80).

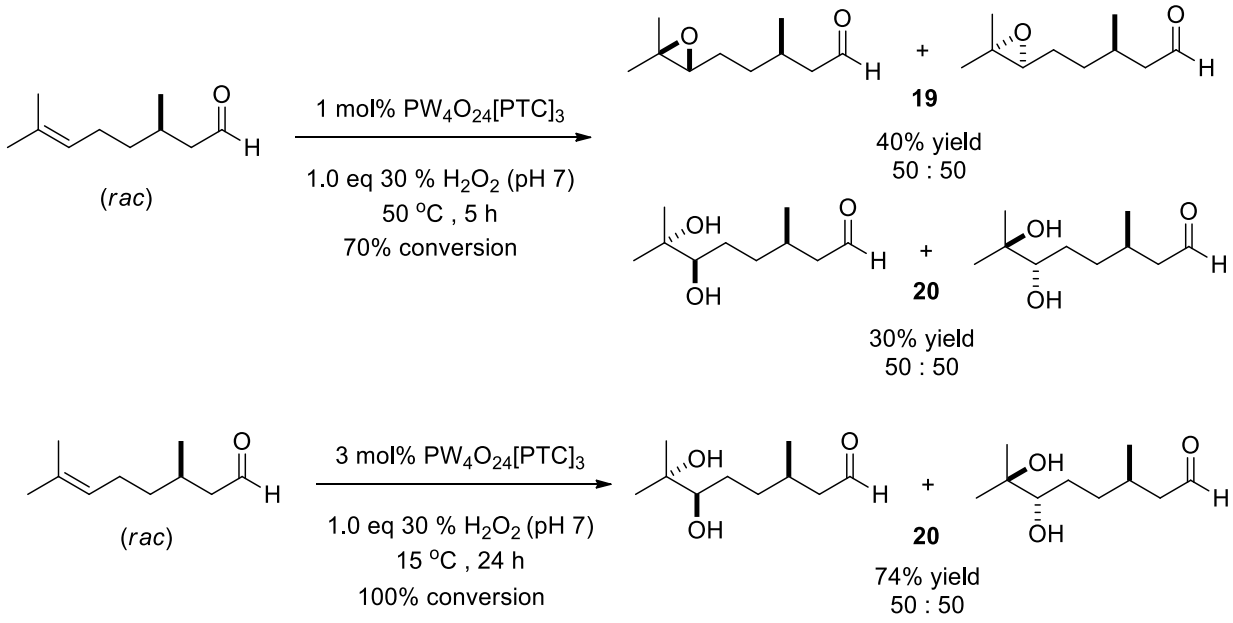

Scheme 80. Unsuccessful epoxidation of citronellal

Both of the trisubstituted alkene bonds of farnesene were epoxidised using our preformed Ishii-Venturello catalyst, using 2.0 eq of H_2O_2, affording its corresponding bis-epoxide (21) as a 50:50 mixture of diastereomers in 86% yield after 18 h, with the less reactive diene not being epoxidised. This selectivity profile is particularly powerful because epoxidation of farnesene using stoichiometric peracids such as mCPBA generally results in competing epoxidation of its diene motif. The only other previous method to produce farnesene bis-epoxide is described in a patent by Woolard *et al*,[124] who employed Novozym-435 as a biocatalyst and a urea-peroxide complex as oxidant in ethyl acetate over a 40 h reaction time. In comparison, our protocol requires no solvent, uses a cheaper oxidant and catalyst and is complete within 5 h (Scheme 81).

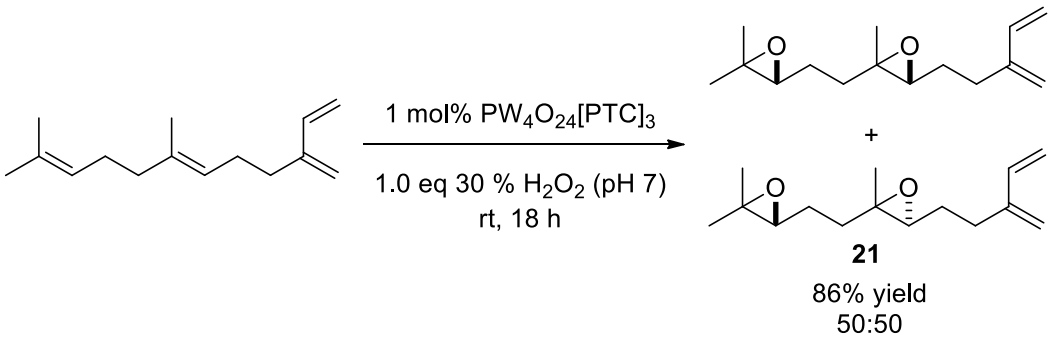

Scheme 81. Epoxidation of farnesene

The Diels-Alder functionality of myrcene epoxide makes it an ideal monomer for the synthesis of thermoset polymers that are produced by irreversible curing (heat or UV irradiation) of biphasic liquid solutions Thermosetting polymers are generally prepared from monomers that contain three or more groups which can polymerise to form multidimensional highly cross-linked structures, which once set cannot be reshaped. Epoxy thermosetting polymers make up 70% of the thermoset market with global volumes of 2 million tonnes in 2014 worth approximately $18 billion dollars.[125] A representative range of transformations that could

potentially be carried out using farnesene bis-epoxide as a monomer for the synthesis of different types of biorenewable polymer are shown in Scheme 82.

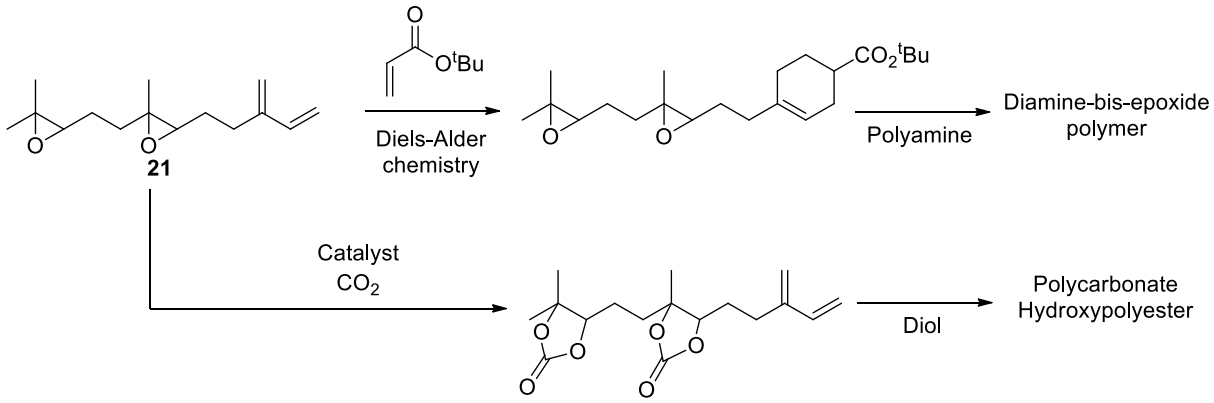

Scheme 82. Potential applications of farnesene bis-epoxide

We next set ourselves the challenging goal of developing an effective protocol for the epoxidation of all six trisubstituted alkene bonds of squalene, which is now widely available as a fermentation product produced through industrial biotechnology. Therefore, squalene was treated with 1 mol% of our Ishii-Venturello catalyst and 6.0 eq of H_2O_2 under solvent free conditions to give a mixture of diastereomeric hexa-epoxides in 89% yield after 12 h (Scheme 83). The impressive formation of the hexa-epoxide (22) was confirmed by MS analysis of the purified reaction product which showed the presence of a broad peak (multiple epoxide diastereomers) that gave a correct molecular ion of 507.3696 m/z.

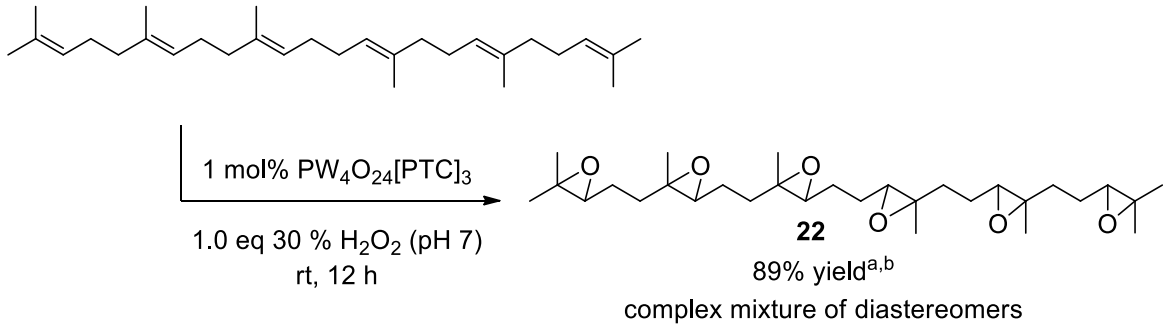

Scheme 83. Optimised epoxidation of squalene using the Ishii-Venturello protocol

[a]Diastereomeric ratio not determinable by NMR or GCMS analysis. [b]Product identity confirmed by GCMS analysis.

2.3.5 Epoxidation of acyclic terpenes containing alcohol groups

We next attempted to employ our Ishii-Venturello protocol for the epoxidation of acyclic terpenes containing alcohol groups. Attempts to epoxidise linalool and β-citronellol were only partially successful, affording their corresponding monoepoxides (50:50 mixture of diastereomers) in only (23) 24% and (25) 35% isolated yields respectively (Scheme 84).

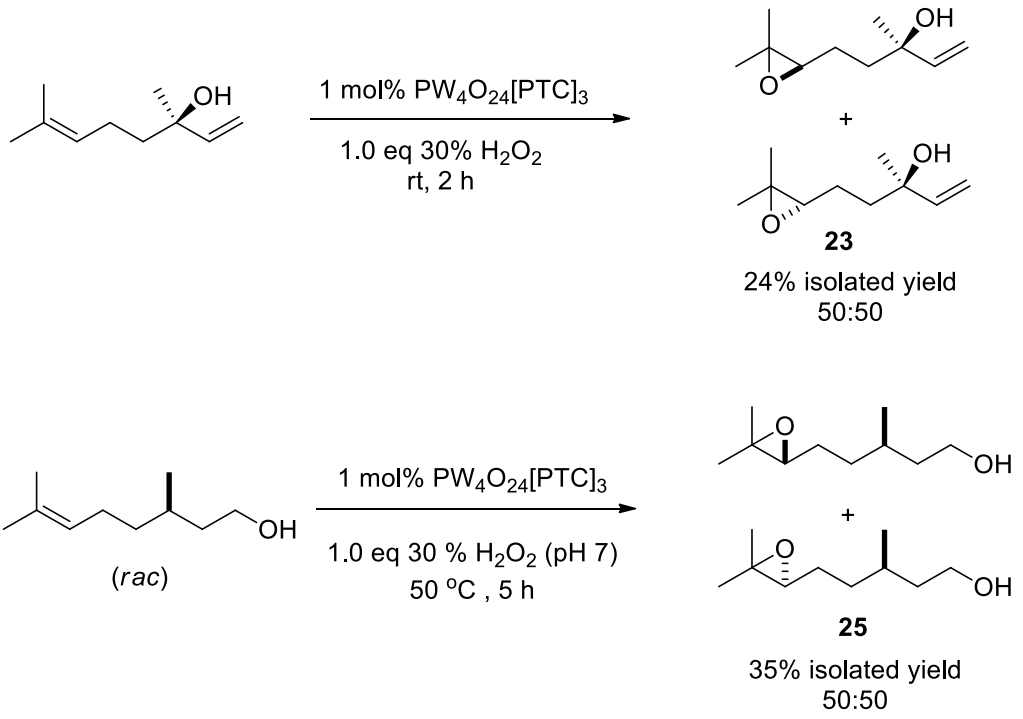

Scheme 84. Low yielding epoxidation of linalool and β-citronellol

Clark *et al*[14] have previously reported poor yields for the synthesis of β-citronellol epoxides, which they proposed was due to its unhindered primary alcohol group competing with H_2O_2 for coordination to the tungsten metal centre of the catalyst, thus inhibiting its catalytic activity. Further investigation into the epoxidation reaction of linalool revealed that the poor yield of epoxide was due to competing formation of the tetrahydrofuran alcohol linalool oxide, which was formed *via* intramolecular 5-*exo*-tet attack of its alcohol group to ring-open the trisubstituted epoxide at its secondary centre (Scheme 85) (24).

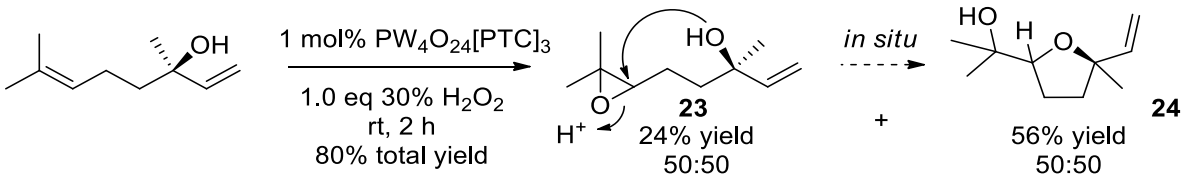

Scheme 85. Epoxide ring opening mechanism for the competing formation of linalool oxide. Product ratios determined by ^1H NMR analysis of crude reaction product.

Therefore, it was decided to investigate epoxidation of analogues of citronellol whose alcohol groups were protected with three common protecting groups that could potentially be removed under mild conditions that were compatible with the presence of an epoxide group. Therefore, the alcohol group of citronellol was *O*-protected with an acetyl group using standard literature protocols in 95% yield (26). The *O*-protected citronellol substrate was then epoxidised using our preformed Ishii-Venturello catalyst to form a 50:50 mixture of *O*-acetyl- β-citronellol (27) in a 55% yields. The *O*-acetyl protecting group was then easily removed *via* hydrogenolysis with K_2CO_3 in MeOH to give β-citronellol epoxide in 80% yield (Scheme 86).

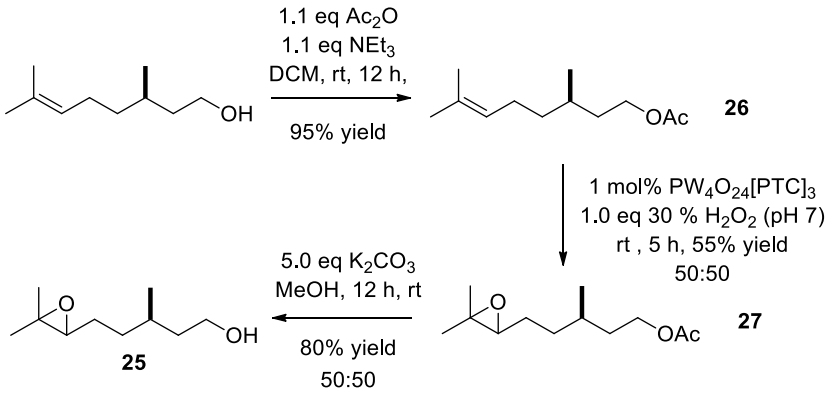

Scheme 86. Epoxidation of *O*-acetyl-β-citronellol derivative

β-citronellol epoxide (25) and *O*-acetyl-β-citronellol epoxide (27) both have a number of useful synthetic applications, with the acetate readily converted into its carbonate monomer for polymerisation,[126] whilst the unprotected epoxide is a precursor for the synthesis of natural products and fragrances (e.g. cytochalasin B[127] and rose oxide[128]). Alternatively, functionalising the primary alcohol of citronellol epoxide with epichlorohydrin can provide a bis-epoxide species that is a versatile monomer for polymerisation (Scheme 87).[129]

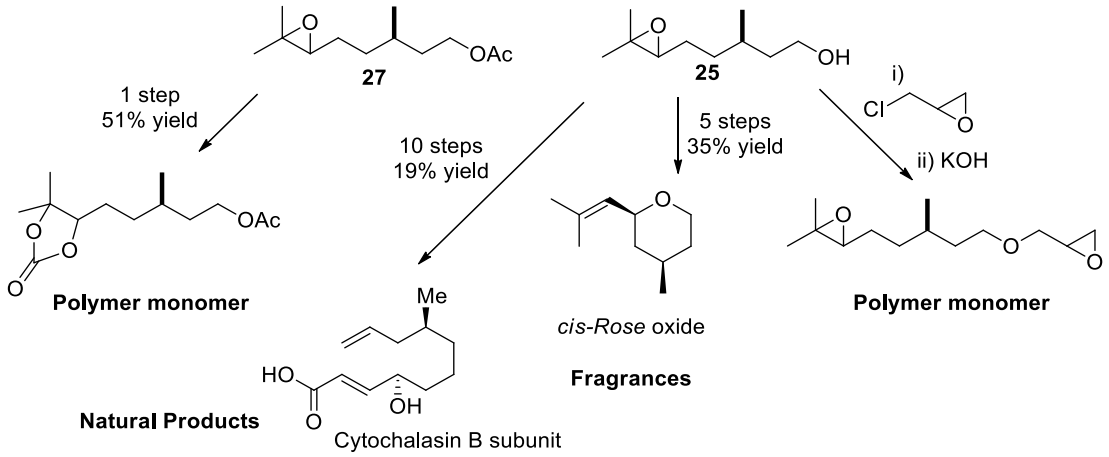

Scheme 87. Products derived from β-citronellol epoxide derivatives

2.3.6 Epoxidation of terpenes containing disubstituted alkenes

Having demonstrated that our a preformed Ishii-Venturello catalyst could be used for the H_2O_2 mediated epoxidation of the trisubstituted alkenes of terpene substrates, we next turned our attention to determining whether it could be used for the epoxidation of terpenes containing less reactive disubstituted alkenes. Epoxidation studies on β-ionone and pulegone had shown that the preformed Ishii-Venturello catalytic system could be used at 50 °C under more forcing conditions for the epoxidation of less reactive alkenes. Therefore, we investigated whether these conditions could be used for the epoxidation of terpene substrates containing disubstituted alkenes. Initial epoxidation of dihydrocarvone (4:1 mixture of *trans:cis* isomers) using 1 mol% preformed Ishii-Venturello catalyst and 1.0 eq of H_2O_2 at room temperature for 12 h gave no epoxide products, however repeating the reaction at 50 °C for 2 h resulted in

formation of a 10:10:1:1 mixture of diastereomeric epoxides (28) in 71% isolated yield. This is the first time that the disubstituted alkene bond of dihydrocarvone had been epoxidised using a tungsten based catalyst, with the only other catalytic method for its synthesis being reported by Stack *et al*[130] who developed a manganese based system using peracetic acid as an oxygen donor (Scheme 88).

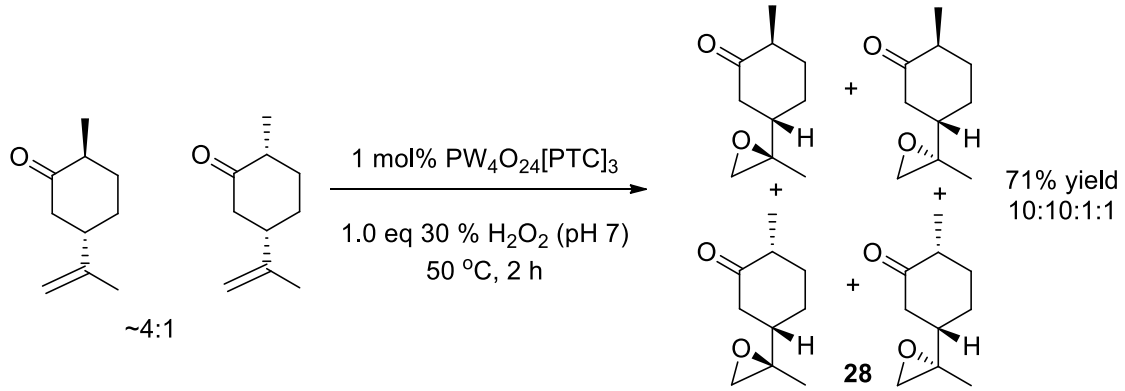

Scheme 88. Epoxidation of the disubstituted alkene functionality of dihydrocarvone

Dihydrocarvone epoxide has a number of useful applications as a monomer precursor for the synthesis of polymers, with Hillmyer *et al* having shown that an epoxylactone derived from dihydrocarvone can be co-polymerised with caprolactone to form a crosslinked polymer with good physical characteristics as polymers for shape memory applications (Scheme 89).[131]

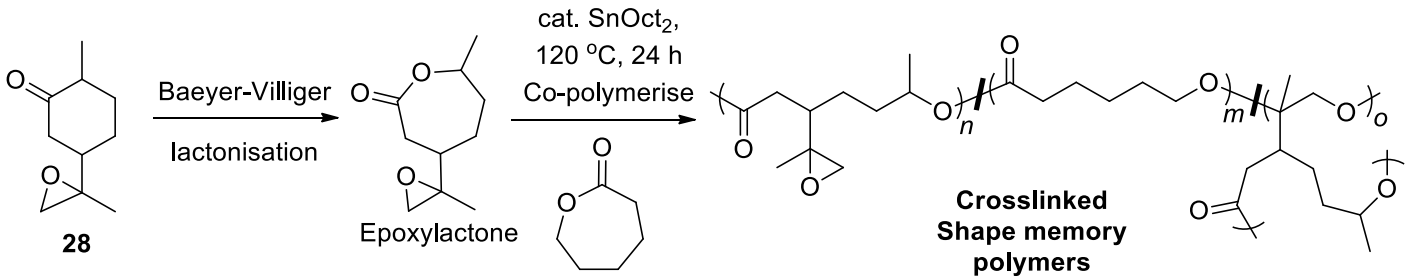

Scheme 89. Polymers that can be produced from dihydrocarvone epoxide

The disubstituted alkene bond of isopulegol could also be epoxidised at 50 °C to give a 60:40 mixture of diastereomeric epoxides (29) in 63% yield after 1 h, which was significantly faster than the rate of epoxidation previously reported using the Sato system which required a reaction time of 16 h (Scheme 90).[79]

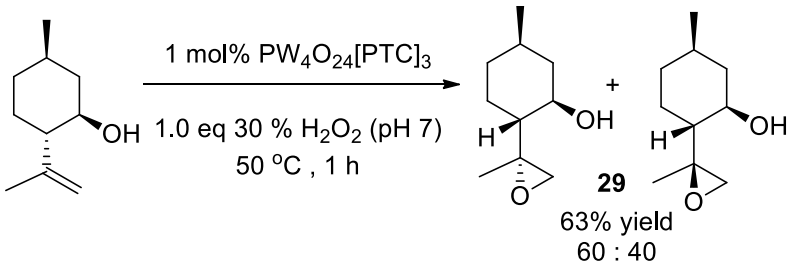

Scheme 90. Epoxidation of isopulegol

Isopulegol epoxide is used as a versatile starting material for the synthesis of fragrances such as menthofuran[132] and hydroxycitronellol,[133] and natural products such as hernandulcin[134] and the pseudopterosins[135] (Scheme 91).

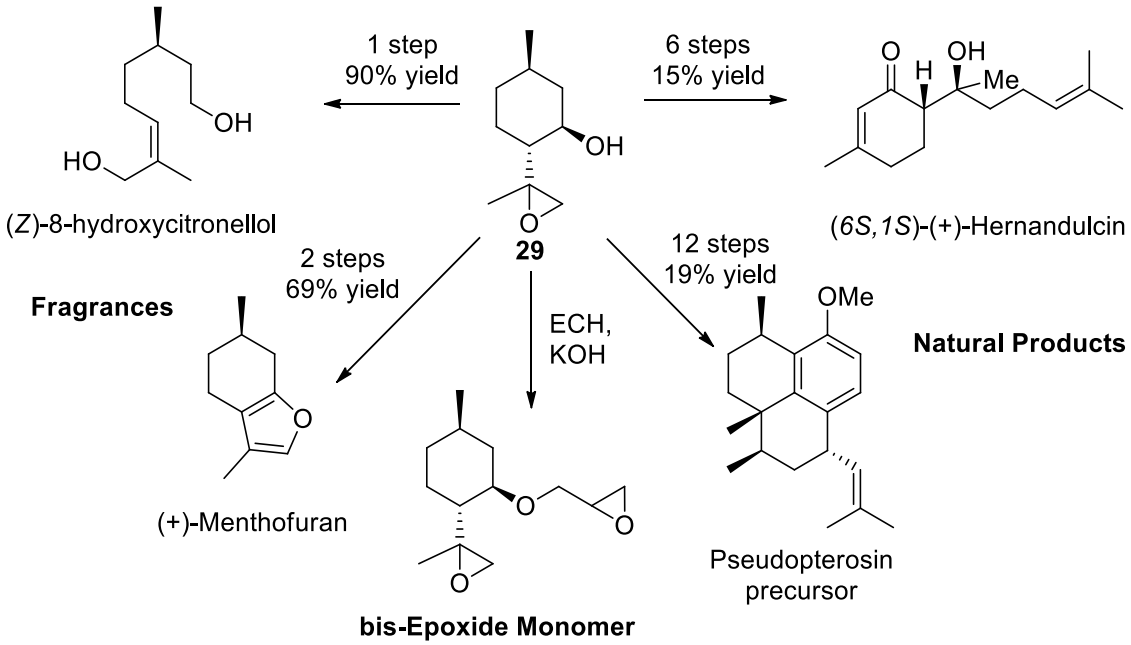

Scheme 91. Products derived from isopulegol epoxide and potential synthesis of bis-epoxide monomer

Acyclic dihydromyrcenol could also be epoxidised at 50 °C to afford their corresponding diastereomeric epoxides in a 50:50 ratio in a yield of 75% after 5 h, which is the first time that this substrate has been successfully epoxidised (30) using a tungsten based catalyst (Scheme 92).

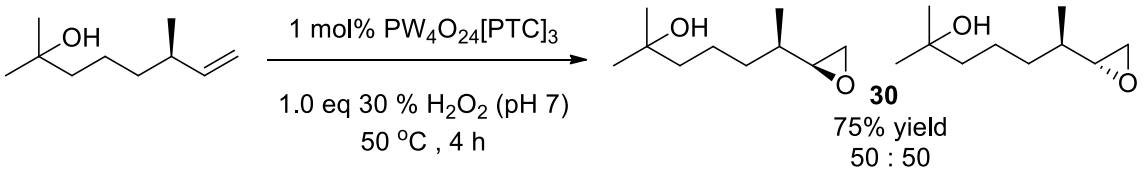

Scheme 92. Epoxidation of dihydromyrcenol

Dihydromyrcenol represents a promising source of monomers for polymerisation, since protection of the tertiary alcohol as an ester, followed by ring-opening carbonylation would give a cyclic carbonate[126] that could be ring opened to form polyester materials. Alternatively, the tertiary alcohol group could be protected with epichlorohydrin to afford a bis-epoxide species that could be ring-opened using diamine co-monomers to form polyhydroxylamines (Scheme 93).[129]

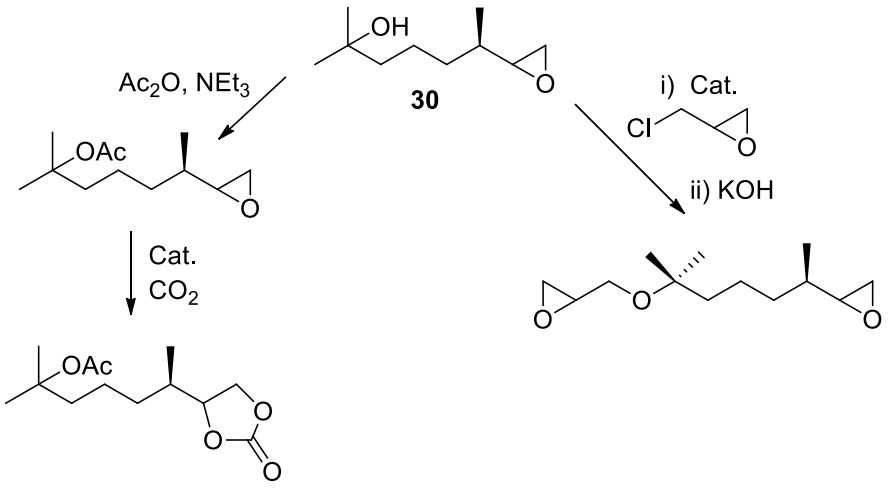

Scheme 93. Prospective monomers derived from dihydromyrcenol epoxide for polymer synthesis

2.3.7 2-step, catalytic synthesis of limonene bis-epoxide

Limonene bis-epoxide is an important chemical intermediate that has applications as a lubricating oil and as a fragrance in cosmetics, whilst it has also been used as a monomer for the production of thermosetting resins and composites, and polyesters. For example, Kleij *et al*[136] have reported the use of an iron based catalyst for the ring-opening copolymerization of limonene bis-epoxide (31) for the synthesis of bio-based semi-aromatic polyesters (Scheme 94).

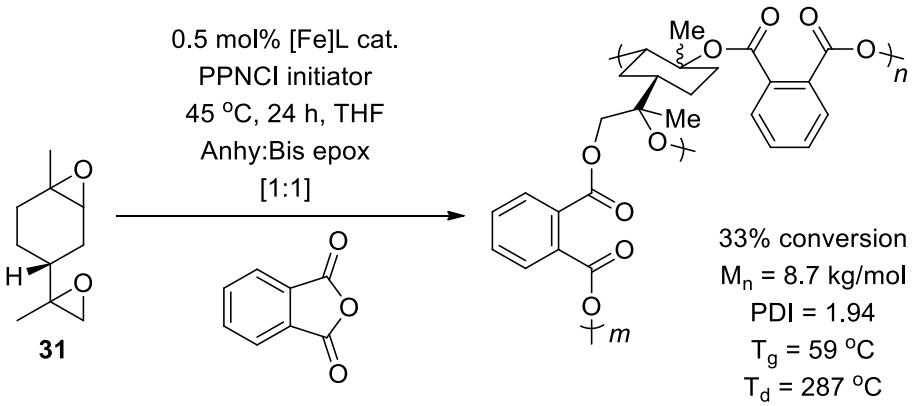

Scheme 94. Ring-opening copolymerization of limonene bis-epoxide with phthalic anhydride

Alternatively, limonene bis-epoxide has been used to prepare limonene bis-carbonate that contains a terminal cyclic carbonate that is highly reactive for the production of bio-based polyurethanes that have many applications ranging from foams, coatings, textile fibres, adhesives and sealants[137] The linear limonene epoxide derived thermoplastic synthesised by Mülhaupt *et al*[137] is 100% bio-based exhibits a high molecular weight (22.8 kg/mol), good tensile strength and stiffness properties with minimal coloration, but unfortunately has a lower PDI/T_g than desired (Scheme 95).

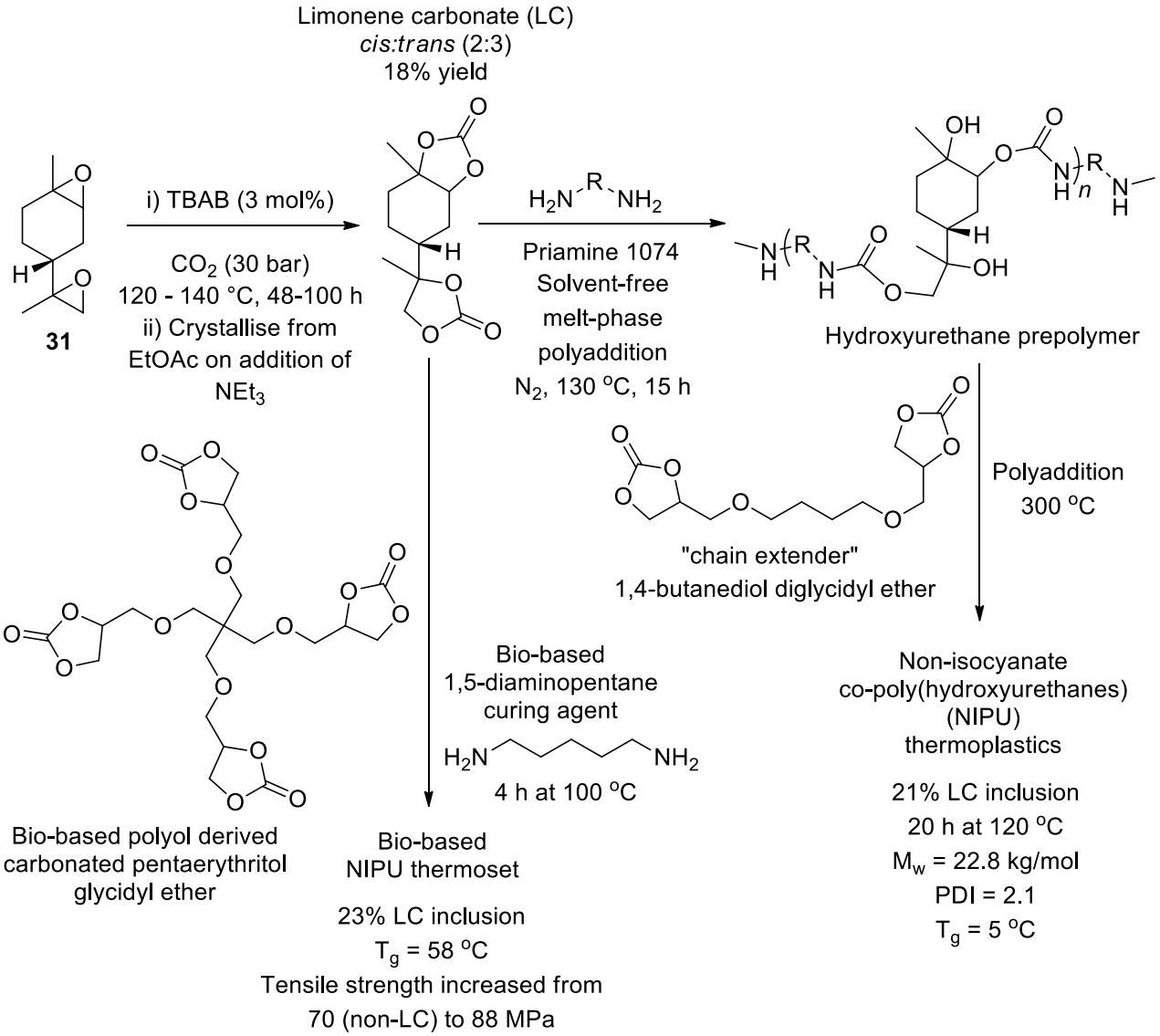

Scheme 95. Application of limonene bis-carbonate for the synthesis thermoplastics and thermosetting materials[137]

The increasing demand for limonene bis-carbonate as a monomer as a monomer for polymer synthesis means that there an increasing demand for the development of efficient catalytic methods for the sustainable production of multigram quantities of limonene bis-epoxide. However, only a handful of catalytic routes currently exist for the synthesis of limonene bis-epoxide, with each of these methods having disadvantages that make them unsuitable for use on a large scale.

In 1998 Jacobs *et al*[138] developed an epoxidation method to synthesise limonene bis-epoxide using MTO, hydrogen peroxide in DCM and using 40mol% pyridine as an additive. This methodology gave an excellent yield of limonene bis-epoxide, however, MTO is costly (£160 per 1 g, Sigma Aldrich), pyridine is toxic and chlorinated solvents and low temperatures were required for extended periods of time (Scheme 96).

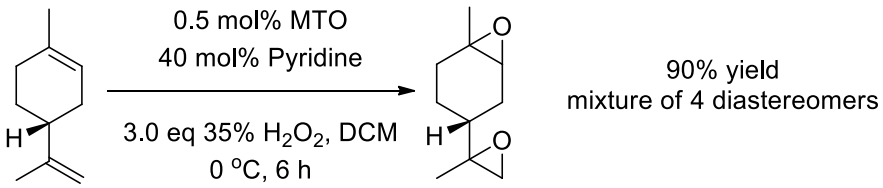

Scheme 96. MTO catalysed route to limonene bis-epoxide

In 2012 Bermejo *et al*[139] reported an iron based catalytic method to synthesise limonene bis-epoxide using hydrogen peroxide, in acetonitrile and AcOH. They achieved a high yield of 90% (a mixture of diastereomers) using 3.0 eq of H_2O_2 as oxidant and 15 mol% catalyst at room temperature for 10 minutes. However, this methodology requires a high loading of a homogeneous iron catalyst that requires a lengthy ligand synthesis and expensive iron(II) triflate (£65 per 1 g) for its synthesis, whilst the epoxidation reaction requires an argon atmosphere and acetonitrile as solvent (Scheme 97).

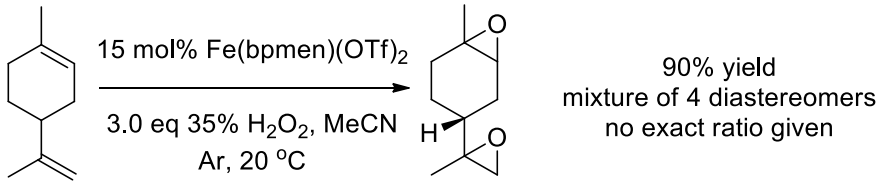

Scheme 97. $Fe(bpmen)(OTf)_2$ catalysed route to limonene bis-epoxide

In 2017 Fomenko *et al*[140] developed a catalytic synthesis of limonene bis-epoxide using hydrogen peroxide and catalytic $MnSO_4$ using salicyclic acid as an additive. The hydrogen peroxide was added gradually over 3.5 h with the reaction mixture cooled to maintain its temperature below 25°C. This reaction requires 10.0 eq of hydrogen peroxide whilst $MnSO_4$ is costly (£273 per 1 g Sigma-Aldrich) (Scheme 98).

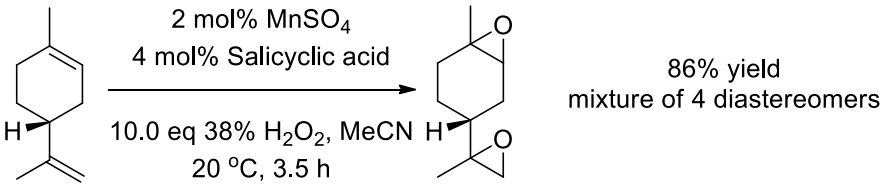

Scheme 98. $MnSO_4/H_2O_2$ catalyst mediated route to limonene bis-epoxide

Given these limitations, it was decided to try and optimise the bis-epoxidation of limonene using our preformed Ishii-Venturello catalytic protocol. Initial optimization studies were carried out, using a variant of the standard conditions used previously for epoxidation of limonene (e.g. solvent-free, 1.0 eq H_2O_2 and 1 mol% catalyst) at both 35 °C and 50 °C. Unfortunately, these conditions gave relatively low yields of the bis-epoxide, with significant amounts of ring opened *anti*-diol also being observed, even when buffered H_2O_2 (pH 7.0) and 30 mol% Na_2SO_4 was employed as an additive (Scheme 99).

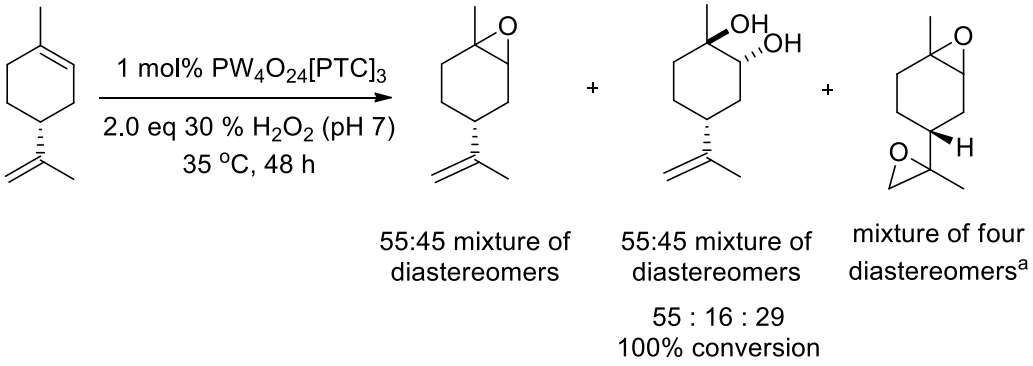

Scheme 99. Limonene bis-epoxide formation using the Venturello catalyst. . [a]Peaks in GCMS and ^{1}H NMR spectrum of 4 epoxide diastereomers were overlapped preventing estimation of their diastereomeric ratio.

We next carried out the bis-epoxidation reaction at a higher temperature of 50 °C, without salt to see whether these conditions would epoxidise both alkene bonds faster, however, even short reaction times of 30 minutes only led to very small amount of the desired diepoxide (6%), with significant amounts of limonene diol (60%) and limonene tetrol (19%) being formed. Attempts to incorporate Na_2SO_4 as a 30% salt additive into the epoxidation protocol at room temperature and 50 °C had no success in suppressing competing diol formation (Scheme 100).

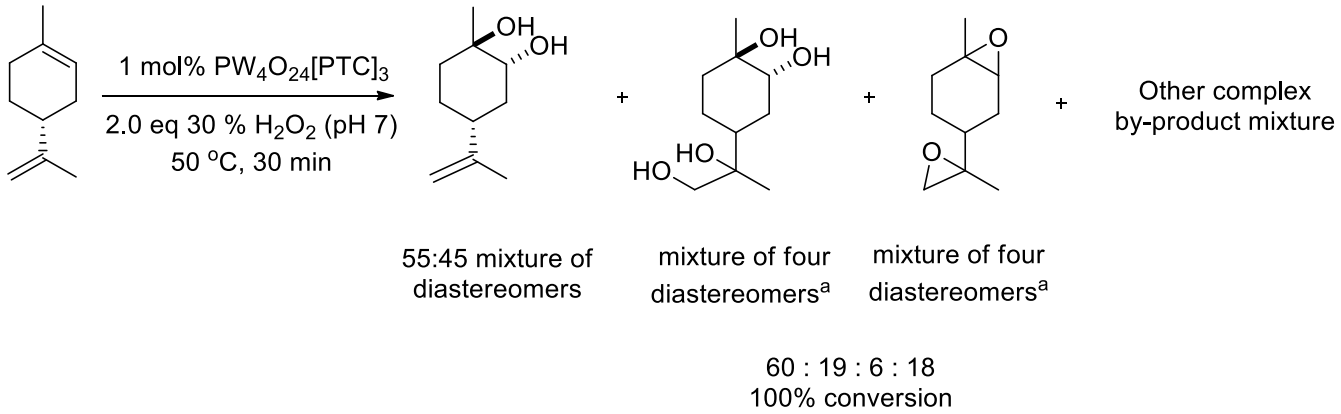

Scheme 100. Limonene bis-epoxide formation using the Venturello catalyst. [a]Peaks in GCMS and ^{1}H NMR spectrum of 4 epoxide diastereomers were overlapped preventing estimation of their diastereomeric ratio.

These epoxidation experiments had shown that the 1,2 epoxide functionality of limonene underwent competing ring-opening to its *anti*-diol at the elevated temperatures (50 °C) required for epoxidation of the disubstituted alkene at its 8,9 position. Consequently, it was decided to employ an alternative epoxidation catalyst to selectively epoxidise the 8,9 position of limonene and then use the Ishii-Venturello conditions at ambient temperatures to catalyse epoxidation of the more substituted 1,2 alkene position of this monoepoxide.

Mizuno *et al*.[141] have developed a selective polyoxometalate catalyst based upon a tungsten and vanadium core that specifically epoxidises di-substituted alkenes over trisubstituted alkenes. These Mizuno catalysts use H_2O_2 as a stoichiometric oxidant at its divanadium oxide centre that has a relatively small binding pocket that only allows binding of less hindered disubstituted alkenes substrate for epoxidation (Figure 24).[141] The mechanism of epoxidation

for the Mizuno catalyst is shown in Figure 25, which reveals that the vanadium catalyst centre initially forms a vanadium-peroxide species that converted into a highly reactive triple bonded oxygen species that then acts as the catalytic epoxidation species.

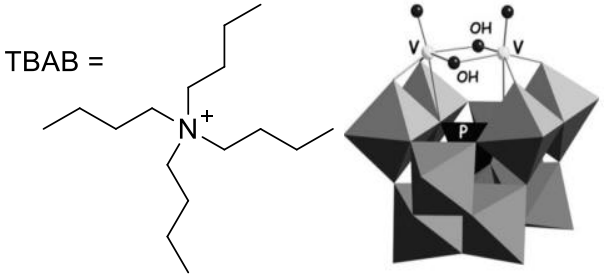

Figure 24.Structure of Mizuno catalyst and ligand

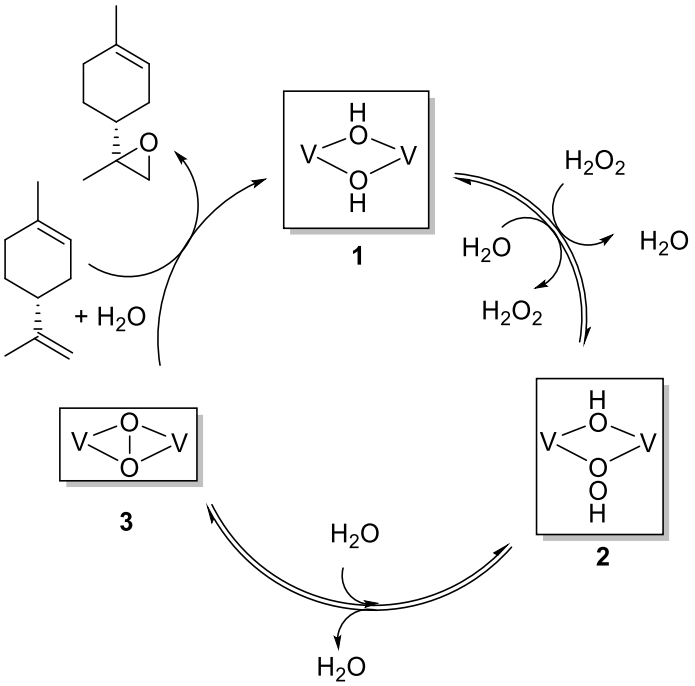

Figure 25.Proposed Mizuno epoxidation mechanism

In 2005, Mizuno *et al*[142] reported the use of a silicon containing polyoxovanadometalate catalyst $HSiV_2W_{10}O_{40}[TBAB]_4$ for the selective epoxidation of the 8,9 position on limonene, with no epoxidation observed at the 1,2 position (Scheme 101). In 2011, they subsequently[141] reported a more active modified polyoxovanadometalate catalyst, γ-$HPV_2W_{10}O_{40}[TBA]_4$ which shortened epoxidation times from 24 h to 1.5 h, which was used to produce multigram quantities of 8,9 limonene epoxide (32) in 73% yield (Scheme 102).

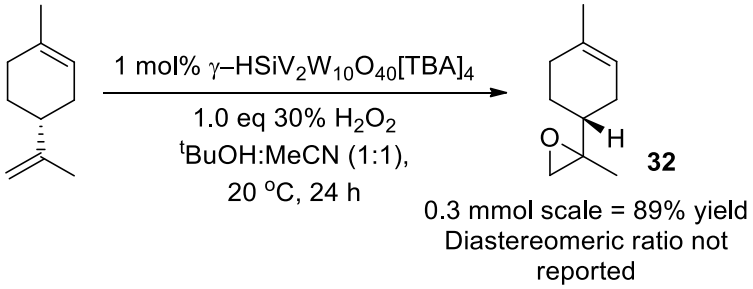

Scheme 101. Silicon containing Mizuno catalytic system

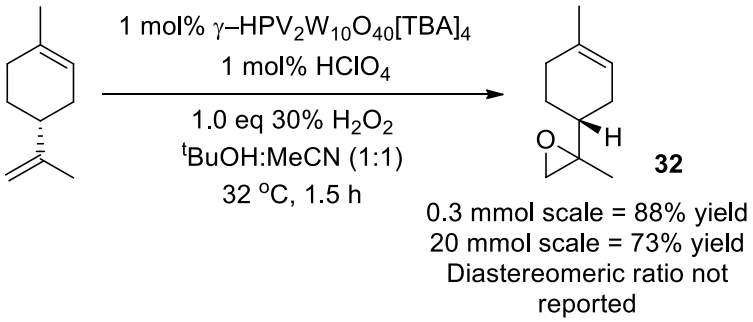

Scheme 102. Phosphorus containing Mizuno catalytic system

Consequently, we were interested to see if we could combine Mizuno's catalytic protocol with the Venturello-Ishii protocol to synthesise limonene bis-epoxide using green methodologies in a two-step high yielding manner. The 2nd generation Mizuno catalyst was prepared by reaction of tungstic acid (H_2WO_4), CsOH and phosphoric acid affording $Cs_7[PW_{10}O_{36}].xH_2O$ that was then treated sequentially with $NaVO_3$, HCl and tetrabutyl-ammonium bromide (TBA-Br) according to the extended protocol described in Scheme 103.

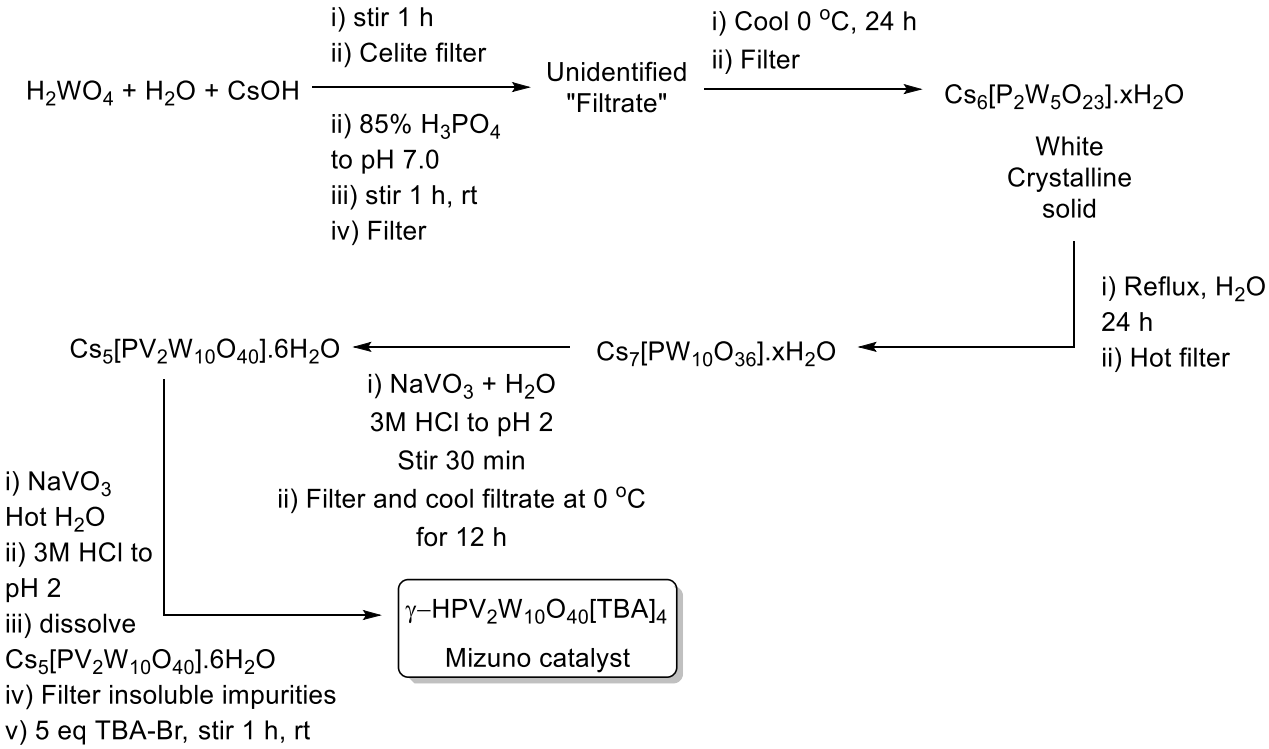

Scheme 103. Preparation of the Mizuno catalyst

Treatment of limonene with 1 mol% of Mizuno catalyst, 1.0 eq of H_2O_2 in CH_3CN at 32 °C for 1.5 h afforded a 60:40 mixture of limonene 8,9-epoxide diastereomers as the sole product. This mixture of 8,9 epoxides was then treated with our preformed Ishii-Venturello catalytic protocol using 1.0 eq of H_2O_2 to give a good yield of limonene bis-epoxide as a mixture of four diastereoisomers in an excellent 70% isolated yield (see Scheme 104).

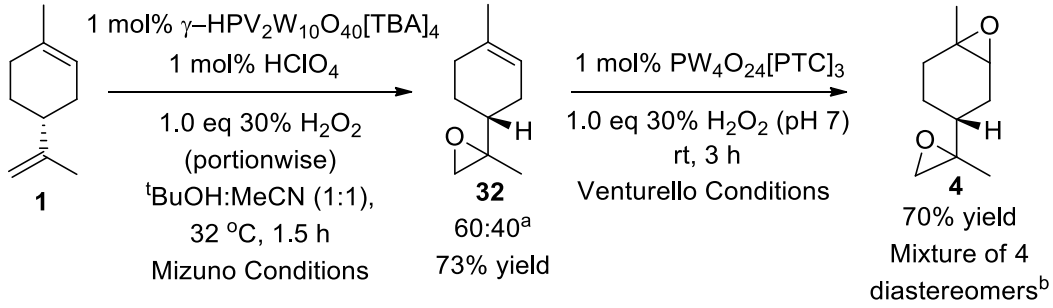

Scheme 104.Two-step catalytic epoxidation of limonene to form limonene bis-epoxide

[a]Assignment of configuration of 8,9-limonene epoxide diastereomers not possible as they were inseparable by chromatography. [b]Peaks in GCMS and ^{1}H NMR spectrum of 4 epoxide diastereomers were overlapped preventing estimation of their diastereomeric ratio.

Given its success in selectively epoxidising the 8,9 alkene bond of limonene, the Mizuno catalyst was then applied for the epoxidation of the isopropylidene bond of carveol which successfully afforded its corresponding carveol 8,9-epoxides (32) as a 60:40 mixture of diastereomers in 60% isolated yield (Scheme 105). The only other route currently available for the synthesis of carveol 8,9-epoxide involves stoichiometric epoxidation of carvone using *m*CPBA followed by reduction of the ketone using $NaBH_4$. Carveol 8,9 epoxide is a key intermediate in the synthesis of the prenylbisabolane diterpene insecticide that can be prepared *via* a 5 step route in 49% overall yield (Figure 26).[143]

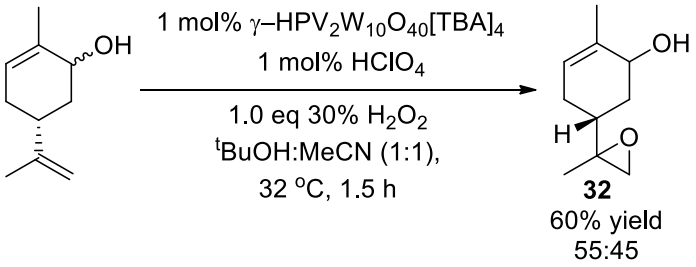

Scheme 105. Epoxidation of the disubstituted alkene functionality of carveol using the Mizuno catalyst

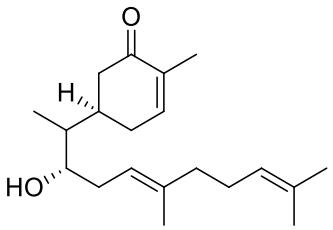

Figure 26. Prenylbisabolane diterpene insecticide

Unfortunately, attempts to use the Mizuno catalyst to epoxidise the di-substituted alkene functionality of perillyl alcohol, farnesene and β-pinene proved unsuccessful, returning starting material in each case. It is possible that competing coordination of the primary hydroxyl group of the perillyl alcohol to the tungsten centre of the Mizuno catalyst prevents the H_2O_2 oxidant from coordinating and carrying out an epoxidation reaction. Alternatively, the Mizuno catalyst is known to be less reactive and more sensitive to the steric demand of

the alkene substrate, thus explaining why the more stable diene functionality of farnesene and the hindered alkene of β-pinene (33) were not epoxidised (Figure 27).

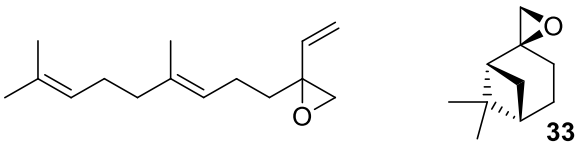

Figure 27. Failed attempts to epoxidise farnesene and β-pinene using the Mizuno catalyst system

2.3.8 2-step synthesis of carvone bis-epoxide

We then decided to try and develop a two-step method to epoxidise both alkene bonds of carvone, to give its corresponding bis-epoxide (34). This bis-epoxide is potentially a useful monomer for polymer synthesis as it contains two orthogonal epoxide bonds with different reactivity profiles, thus providing sites for cross-linking with bifunctional nucleophiles, and functionalisation of the resultant polymers (see Scheme 106).

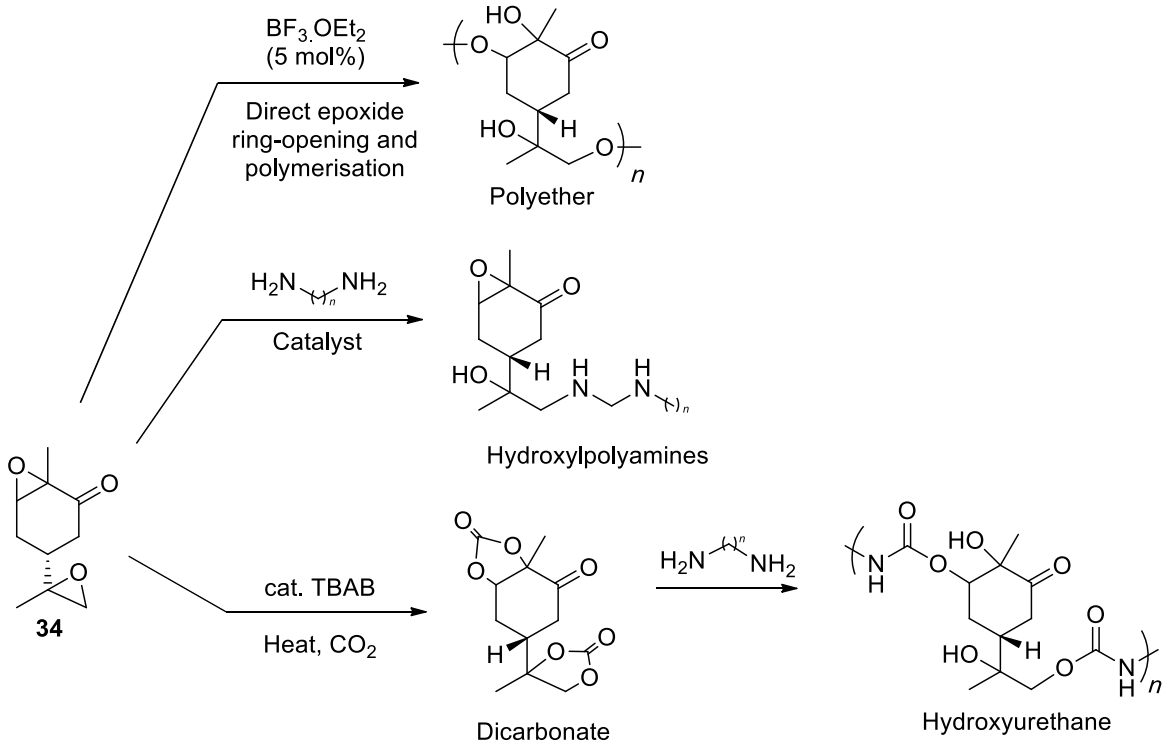

Scheme 106. Potential monomers and polymers obtained from carvone bis-epoxide

A number of catalytic methods exist for the synthesis of carvone bis-epoxide, however they all suffer from some disadvantages. In 2003 Stack *et al*[144] developed a manganese based catalytic system for the synthesis of carvone bis-epoxide in 88% yield in a short reaction time of 5 minutes, however this system requires synthesis of a complex ligand, uses a peracid oxidant and required acetonitrile as solvent (Scheme 107). In 2012 Bermejo *et al*[139] reported an iron based catalytic method to synthesise carvone bis-epoxide in 70% yield using hydrogen

peroxide as an H_2O_2 in acetonitrile, however this methodology requires 3.0 eq of oxidant and 15 mol% of a homogeneous catalyst at room temperature under an argon atmosphere (Scheme 108).

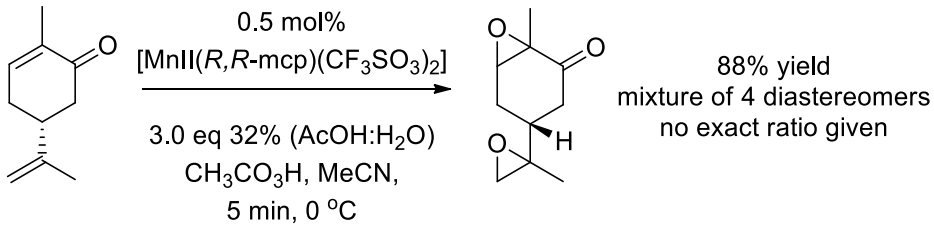

Scheme 107. Catalytic route to carvone bis-epoxide using a Mn catalyst and peracetic acid as oxidant

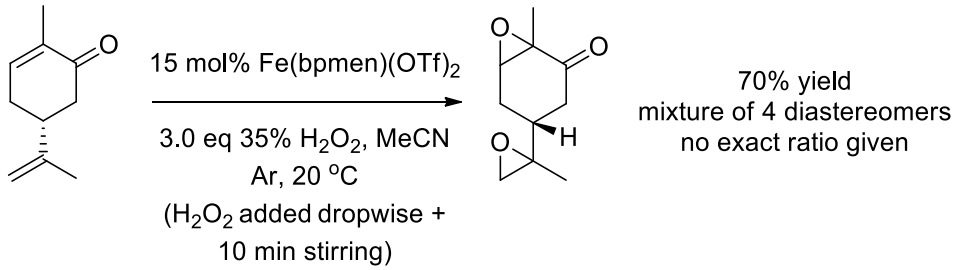

Scheme 108. $Fe(bpmen)(OTf)_2$ catalysed route to carvone bis-epoxide

Epoxidation of carvone using our preformed Ishii-Venturello protocol (2 mol% catalyst, 2.0 eq H_2O_2 (pH 7.0), 50°C (5.5 h) resulted in a mixture of unreacted carvone, mono-epoxide (50:50) mixture of diastereomers) and bis-epoxide (mixture of four diastereoisomers) in a ratio of 17:55:28, respectively (Scheme 109).

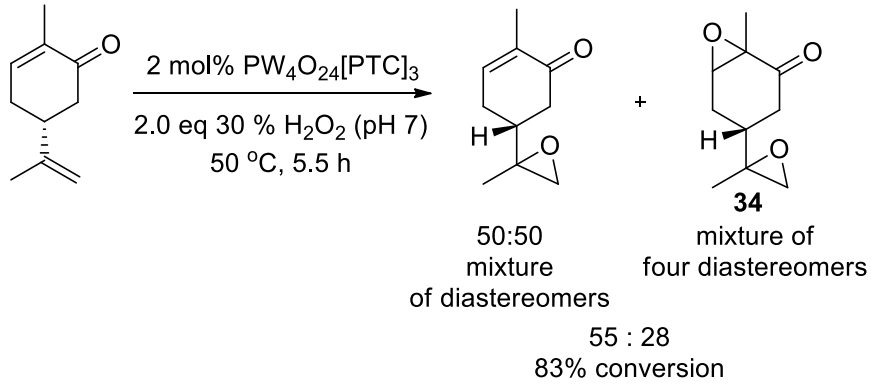

Scheme 109. Epoxidation of carvone using a preformed Ishii-Venturello catalyst

The use of higher temperatures (70 °C) using 2.0 eq of H_2O_2 resulted in complete consumption of carvone, affording a 3:2 mixture of mono-epoxide and bis-epoxide after 2 h, alongside a significant amount of unidentifiable diol mixtures. Unfortunately attempts to run the reaction for longer periods of time resulting in decreased yields of epoxide, due to competing diol formation (Scheme 110).

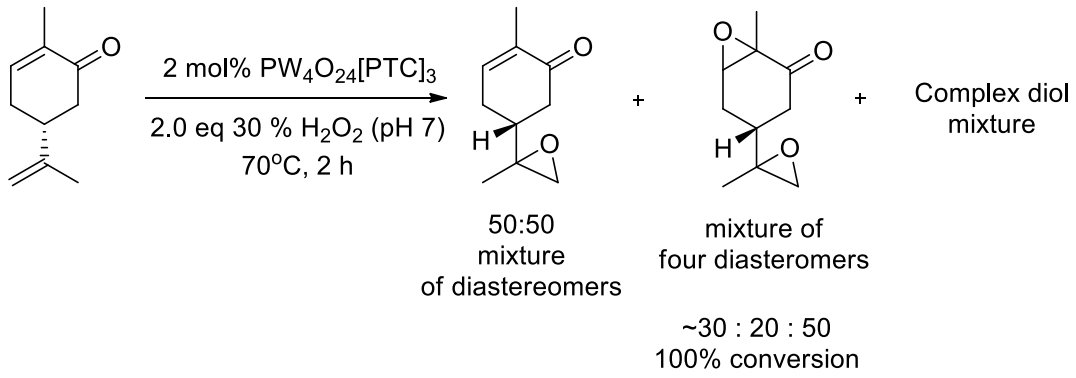

Scheme 110.Higher temperature epoxidation of carvone

These results showed that epoxidation of the α-β-unsaturated alkene functionality of carvone was slow under these reaction conditions, leading to extended reaction times and competing formation of diol side products. Consequently, it was decided to adopt an alternative two-step strategy, involving nucleophilic peroxide mediated epoxidation of the α,β-unsaturated functionality of carvone to afford a 2,3-monoepoxide (35). The isopropylidene group of this mono-epoxide would then be epoxidised using the Ishii-Venturello catalyst (or the Mizuno catalyst) at elevated temperatures. Therefore, treatment of carvone with H_2O_2/OH^- in MeOH at 0 °C for 6 h gave carvone-2,3-monoepoxide in 60% yield, which was then epoxidised using our standard catalytic Ishii-Venturello protocol at 50°C to afford the desired carvone bis-epoxide as a mixture of diastereomers in 60% yield (see Scheme 111).

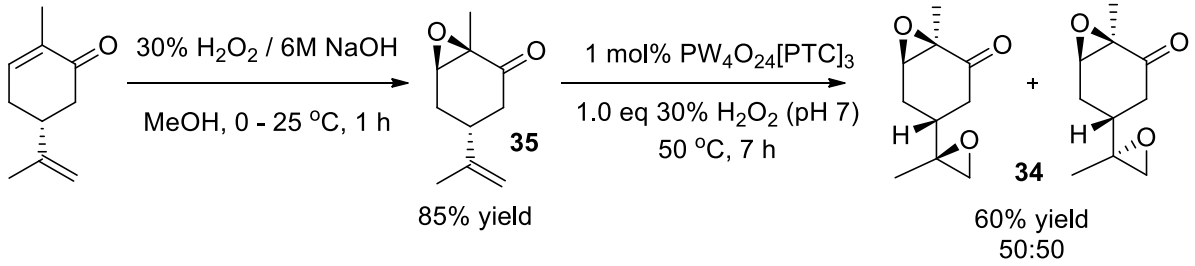

Scheme 111. Synthesis of carvone bis-epoxide

2.3.9 Scale-up of solvent free Venturello catalysed epoxidation reactions

Having established the scope of the preformed Venturello catalyst for epoxidation of a wide range of alkene substrates, it was decided to scale-up this methodology to assess its potential for industrial scale applications. One of the criteria when assessing processes for scale-up is safety, with the heat generated in large scale epoxidation reactions needing to be controlled. For the case of the Venturello/H_2O_2 epoxidation system, temperature control was likely to be necessary to prevent thermal runaway causing accelerated H_2O_2 decomposition that could potentially lead to explosions and diminished yields. In addition to thermal management, effective mixing was required because the reaction was biphasic and run under solvent free conditions. Therefore, it was essential to ensure that proper mass transfer across the aqueous-organic phase boundary would occur during scale-up to ensure high conversions and prevent hot spot formation.

The first attempted epoxidation of limonene using the preformed Ishii-Venturello catalyst was linearly scaled up to 5 g under our standard conditions using standard laboratory equipment. The hydrogen peroxide oxidant was added in one portion at room temperature and vigorous stirring initiated. However, after 5 minutes this experimental setup led to vigorous thermal runaway generating high temperatures that resulted in uncontrolled discharge of water vapour (steam!) and violent expulsion of the reaction contents from the flask! This 5 g reaction was repeated in an 'open' 100 mL beaker that prevented spillage of the reaction solution, enabling us to collect a sample of the reaction product that was present a minute after the thermal runaway reaction had commenced. ^{1}H NMR spectroscopic analysis revealed formation of significant amounts of limonene epoxide, and so it was decided to continue with optimising this epoxidation reaction on-scale.

The 5 g scale epoxidation reaction of limonene with H_2O_2 was repeated using the experimental setup shown in Figure 28. An un-stoppered 250 mL reaction vessel was used to give a large headspace to prevent pressure build-up, the reaction vessel was cooled using a room temperature water bath, with the temperature of the reaction mixture being closely monitored using an internal thermometer. The H_2O_2 solution was added dropwise using a dropping funnel over a 2 h period, with dropwise addition of H_2O_2 halted whenever the temperature of the reaction mixture reached ≥35 °C, which allowed it to cool back to <30 °C. This experimental setup enabled us to perform large scale epoxidation reactions in batch without any thermal runaway occurring, which enabled significant quantities and good yields of 1,2-limonene epoxide to be obtained.

Figure 28. Large scale for the catalytic epoxidation of limonene.

After successfully establishing conditions that enabled limonene to be epoxidised on a 5 g scale, we then scaled these conditions to carry out successive epoxidation reactions of limonene on a 15 g, 50 g and 100 g scale, affording limonene epoxide in 88%, 86% and 85% yields respectively. These scale-up conditions were then applied to the solvent free epoxidation (in the presence of Na_2SO_4) of 15 g of 3-carene and 15 g of α-pinene to afford their corresponding epoxides in 76% and 85% isolated yields respectively (Figure 29). These

results were important, as 3-carene and β-pinene are two of the three major components of crude sulphated turpentine which represents the cheapest source of biorenewable monoterpene feedstock currently available.

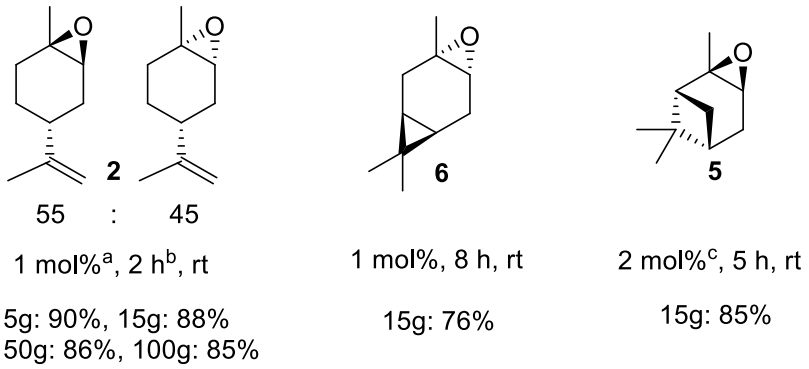

Figure 29. Scale up of epoxidation reactions of limonene, 3-carene and β-pinene.

[a]Isolated yields. [b]Times of reactions were determined by monitoring substrate consumption by tlc. [c]Bicyclic structures required the presence of 30 mol% Na_2SO_4 salt to prevent hydrolysis of their epoxides to their corresponding diols.

2.3.10 Use of the Ishii-Venturello catalyst for epoxidation of β-pinene

Bicyclic β-pinene is an important monoterpene species that is a major component of crude sulphated turpentine which can contain between 10-50% β-pinene, depending on its geographical origin. β-pinene is a particularly challenging substrate to epoxidise, because its terminal disubstituted alkene bond is sterically hindered due to the presence of its cyclobutane ring system. Furthermore, β-pinene epoxide can readily undergo ring-opening reactions with a wide range of nucleophiles (e.g. water) to give unwanted mixtures of products (e.g. diols).

β-pinene epoxide is a valuable synthetic intermediate, with various literature procedures available for its conversion into the commercially valuable monoterpene, perillyl alcohol (ca £240 per 100 g) (e.g., see Scheme 112). Perillyl alcohol itself is a potent anti-cancer agent[145] that has also been used as a precursor to prepare drugs such as Tacrine[146] and Rolipram-POA[147]and bioactive natural products such as Mesembrine[148] and Rubiflordlactone.[73] β-pinene epoxide can also be easily ring-opened using water to form perillyl alcohol hydrate[149] that has insecticidal activity, as well as being oxidised to produce oleuropeic acid[150] that has been used as a synthon for natural product synthesis (Scheme 113).[151]

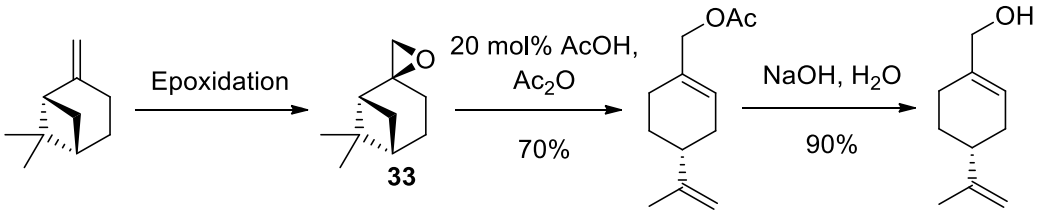

Scheme 112. Literature procedure to convert β-pinene epoxide into perillyl alcohol

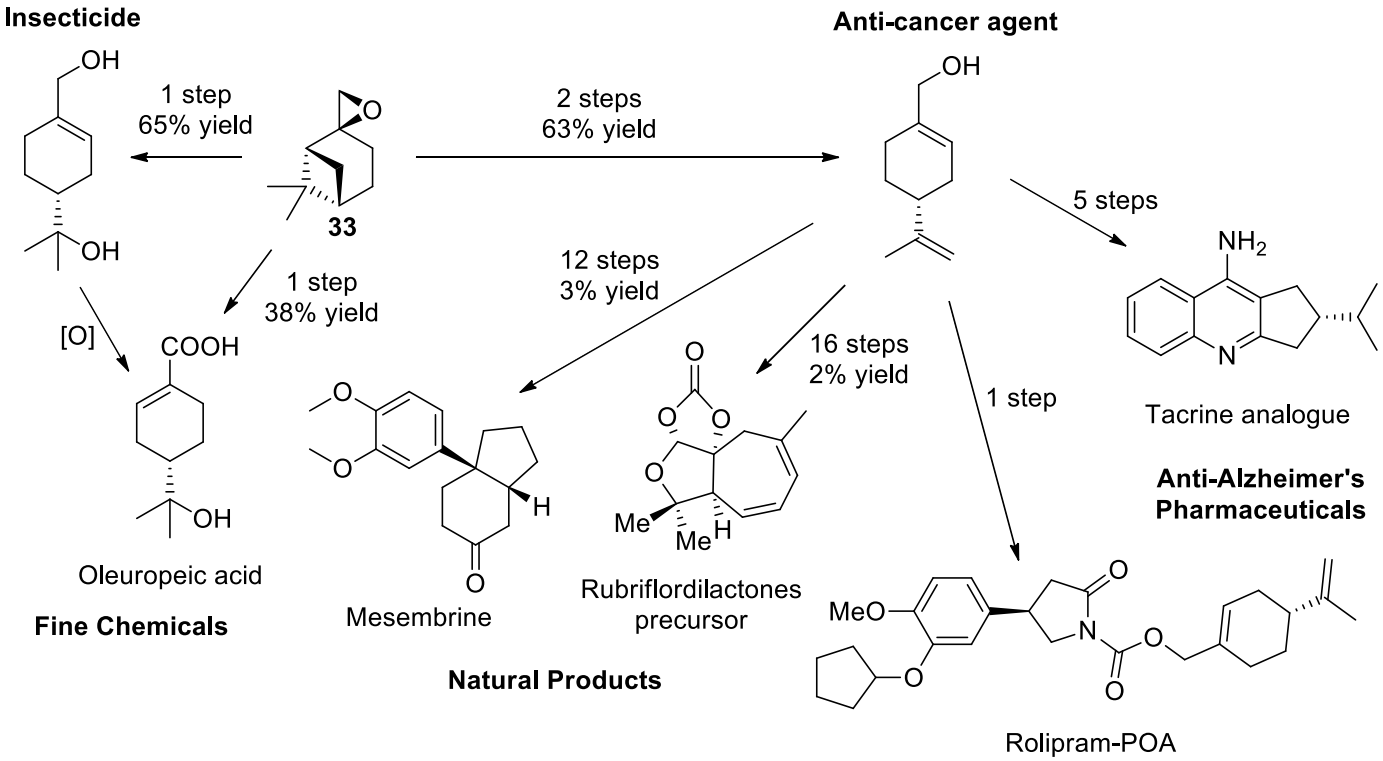

Scheme 113. Products derived from β-pinene epoxide/perillyl alcohol

A review of the literature, revealed that one of the most effective methods for the epoxidation of β-pinene[152] involves the use of peroxyimidic acid that is formed *in situ* by reacting potassium hydrogen carbonate with benzonitrile and hydrogen peroxide. We repeated this method and found it to be highly selective and high yielding for formation of β-pinene epoxide in 90% yield after 2 h on a 5 g scale (Scheme 114). Unfortunately, this method requires the use of stoichiometric amounts of peroxy reagent and the final reaction work-up to quench excess peroxy acid is time-consuming and potentially dangerous to perform on a large scale.

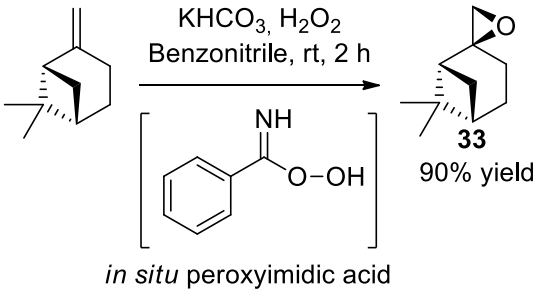

Scheme 114. Stoichiometric peroxyimidic acid conditions for the epoxidation of β-pinene.

Given these limitations, it was decided to try and optimise the epoxidation of β-pinene using our preformed Ishii-Venturello catalytic protocol, with initial optimization studies (Scheme 115) carried out using the standard conditions developed previously for epoxidation of α-pinene (e.g. solvent free, 1.0 eq H_2O_2, 1 mol% catalyst and 30 mol% of Na_2SO_4). As expected the epoxidation reaction product was slow, affording 11% conversion to β-pinene epoxide after 1 h even at an elevated temperature of 35°C (Table 3, Entry 1) and 29% conversion after 7 h (Table 3, Entry 2), with the remaining mass balance being comprised of unreacted starting material. To counter this lack of reactivity the epoxidation reaction was repeated at 50 °C, using higher catalyst and H_2O_2 loadings, which resulted in faster consumption of β-pinene, but which led to lower isolated yields of β-pinene epoxide (<10%), due to ring opening of the epoxide product under these conditions (Table 3, Entries 3-4). Consequently, it was decided to increase the amount of catalyst used in the epoxidation reaction of β-pinene at room temperature to 3 mol% which gave 47% isolated yield of β-pinene epoxide after 7 h on a 5 g scale (Table 3, Entry 6), with < 5% β-pinene remaining (Scheme 116). The remaining mass balance from this optimal epoxidation reaction corresponded to a complex mixture of by-products formed by ring opening of the bicyclic ring, that has been reported to lead up to 9 possible by-products.[153]

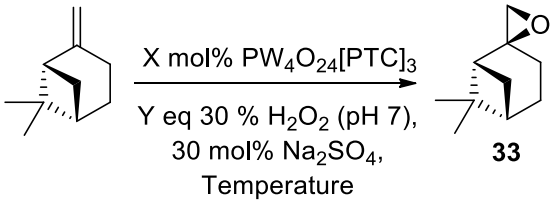

Scheme 115. Conditions screened for the catalytic epoxidation of β-pinene

Table 3. Conditions screened for batch epoxidation of β-pinene

Entry	Venturello Cat Loading (mol%) X	H_2O_2 eq (30%) Y	Time (h)	Temp (°C) Z	Yield of β-Pinene Epoxide/ %[a]
1	1	1	1	35	11 [b]
2	1	1	7	35	29 [c]
3	1	1	1	50	<5[d]
4	1	3	4	35	<5[d]
5	3	1	1	20	14 [e]
6	3	1	7	20	47 [e]

[a]Isolated yields after specified times. [b]Remaining mass balance comprised of starting material. [c] ca. 10% complex by-product formation. [d]No starting material with <5% β-pinene epoxide formed. [e]<5% β-pinene, remaining 40% mass balance comprised of complex mixture of unidentifiable by-products.

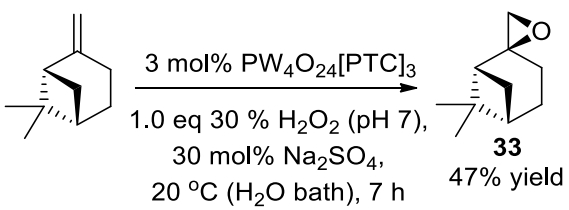

Scheme 116. Optimal protocol for the epoxidation of β-pinene

2.3.11 Batch solvent free Venturello epoxidation of Crude Sulphate Turpentine (CST)

Turpentine represents a cheap mixture of terpenes obtained from extraction of pine trees which is comprised primarily of a mixture of α-pinene, β-pinene and 3-carene, respectively (Figure 30).[154] Three different types of turpentine are available commercially, the composition of which is dependent on their method of extraction; known as gum turpentine (GT), wood turpentine and crude sulfated turpentine (CST). The composition of the terpenes present in the turpentine "blends" are dependent upon their geographical origin; for example pine trees from the western US and India produce turpentine containing around 15% 3-carene, whilst turpentine from pine trees from Western Europe contain around 40% 3-carene.[155]

Turpentine contains many different terpene components that can be separated using fractional distillation under reduced pressure, with α-pinene distilling before β-pinene. Four turpentine fractions are normally obtained; comprising of 3% light extracts, 50-60% α-pinene, 20-25% β-pinene and a final fraction containing phenolic terpineols. Annual worldwide turpentine production ranges between 300,000-330,000 tonnes, with the USA alone producing 100,000 tonnes of CST, so there is potentially a large amount of cheap terpene feedstock available for the synthesis of value-added chemical products.

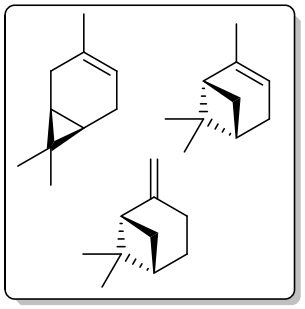

CST

Figure 30. Major terpene components of CST

Although turpentine sources can be fractionally distilled to afford their individual components, this thermal process adds cost to the terpene supply chain, with crude sulphated turpentine from the paper processing industry by far the cheapest source of terpene feedstock available. Crude sulphated turpentine is produced as a by-product of the Kraft paper making process that is used to produce pulp for downstream processing into paper. This process involves heating and stirring wood chips with sulfurous, alkaline liquor to breakdown the hemicellulosic structure of the wood fibres, which produce a volatile oleoresin by-product that is released from the wood chips and collected to give crude sulfate turpentine. The Kraft pulping process generates approximately 200 kg of CST for every 10 tonnes of wood chips that are processed. Typically, CST is then either de-sulfurised and used as a cleaning fluid, or is burnt on site at paper mills as a source of energy, with CST currently costing around $1 per kg on the open market.[12]

We wished to determine whether our preformed Ishii-Venturello catalytic protocol could be used for direct epoxidation of the major terpene components of CST. Consequently, industrial grade CST (that had not been de-sulfurised) was obtained from the Sodra Forestry Cooperative based in Southern Sweden. Its composition was analysed by ^{1}H NMR spectroscopy and GCMS and found to be comprised of 48% α-Pinene, 40% 3-carene and 12% β-pinene, typical of a Northern European source of CST containing a high 3-carene content (Figure 31).

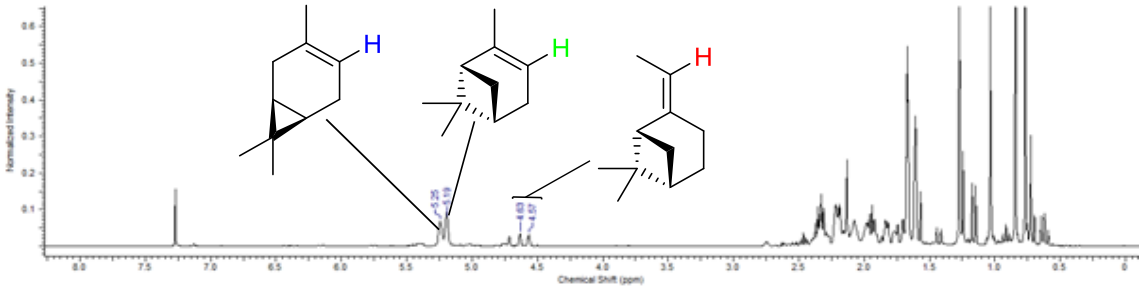

Figure 316. ^{1}H NMR spectrum of CST

Treatment of a sample of industrial CST with 2 mol% of the Ishii-Venturello system (to ensure a high conversion of α-pinene and β-pinene) and 2.0 eq of buffered H_2O_2 (pH 7.0) under solvent free conditions at room temperature resulted in 90% consumption of the 3 major terpene components of CST after 2.5 h, with 3-carene being converted its corresponding epoxide and α-pinene and β-pinene being converted into their corresponding diols (and other ring-opened products) (Scheme 117). No α-pinene epoxide or β-pinene epoxide were present in the crude reaction product as these epoxides were rapidly hydrolysed into their diol derivatives. The 3-carene epoxide product could then be separated from the other oxidised terpene components by chromatography or fractional distillation under reduced pressure. The sulphurous smell associated with the dimethyl sulfide present in the industrial CST disappeared, which we hypothesise is caused by catalytic oxidation of DMS into DMSO. Therefore, this version of our catalytic protocol enables selective conversion of the 3-carene component of CST into its corresponding epoxide.

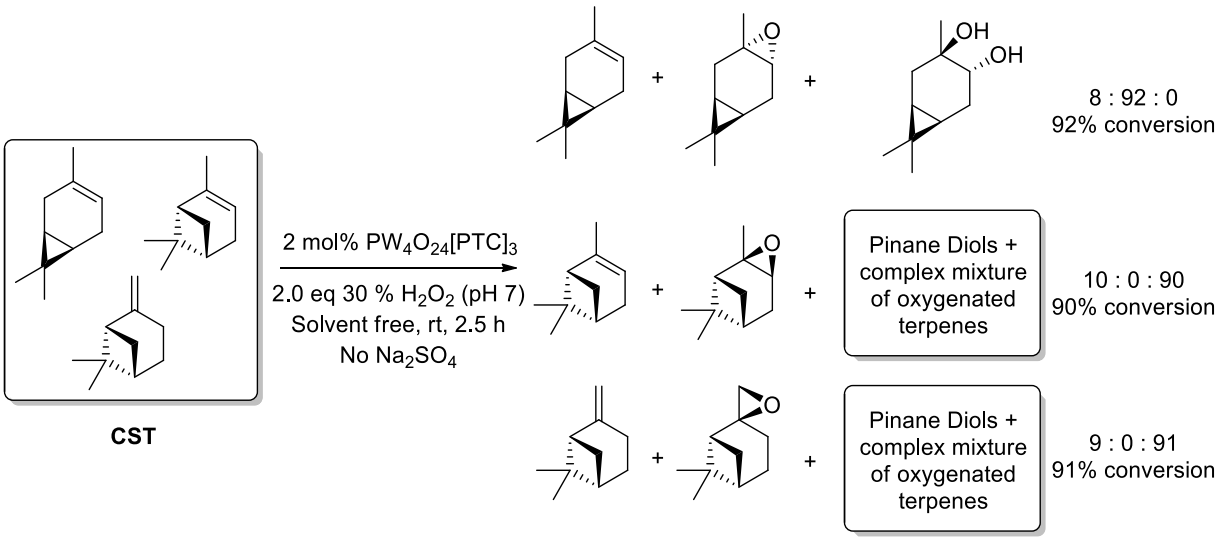

Scheme 117. Epoxidation of CST in the in the absence of 0.3 eq of Na_2SO_4

We then explored using the preformed Ishii-Venturello epoxidation reaction of CST in the presence of 0.3 eq of Na_2SO_4, which had previously been shown to enable epoxidation of α-pinene to its epoxide in good yield. These conditions gave 3-carene epoxide in 94% (Scheme 118), however, once again, no α-pinene epoxide or β-pinene epoxides, with only starting material and their diol derivatives being present. This was unexpected, as using 2 mol% catalyst with 0.3 eq of salt had previously given a good yield of α-pinene epoxide when pure α-pinene starting material was used under these conditions. This lack of epoxide stability was proposed to have been caused by the extra equivalence of hydrogen peroxide, or the presence of dimethylsulfide in the CST.

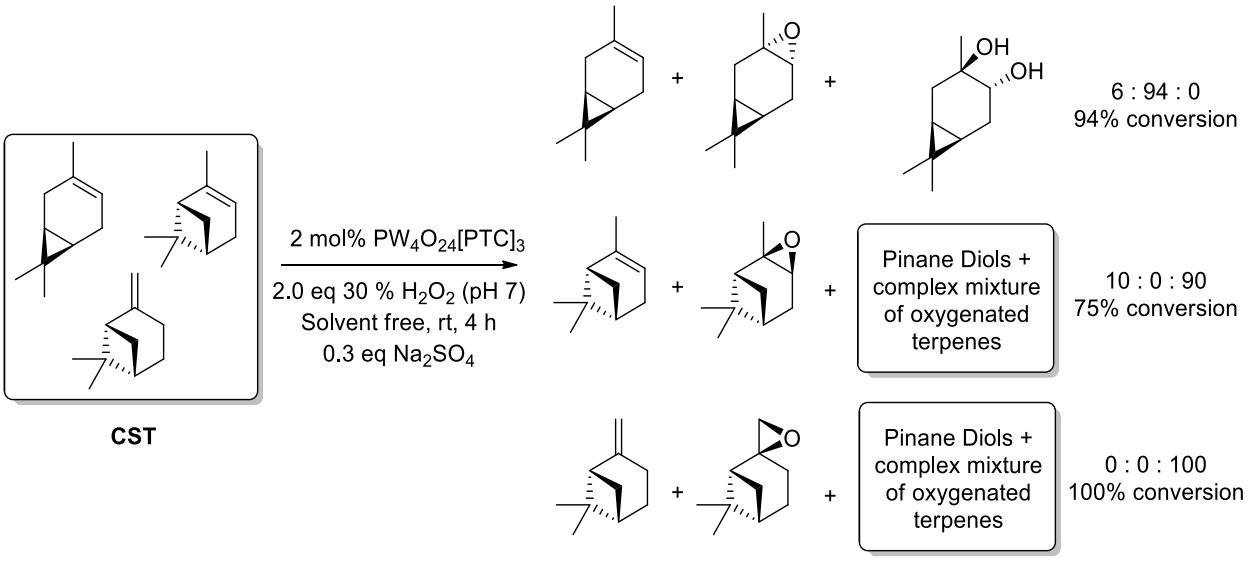

Scheme 118. Epoxidation of CST in the presence of 0.3 eq of Na_2SO_4

We then used 1mol% of catalyst with 1.0 eq of H_2O_2 oxidant to epoxidise CST, which after 6 h gave good yields of 3-carene epoxide and α-pinene epoxide in 91% and 68% yields, respectively. However, small amounts of 3-carene and significant amounts of α-pinene remained, with all the β-pinene epoxide having been converted into its corresponding diol (and other oxygenated terpenes) (Scheme 119).

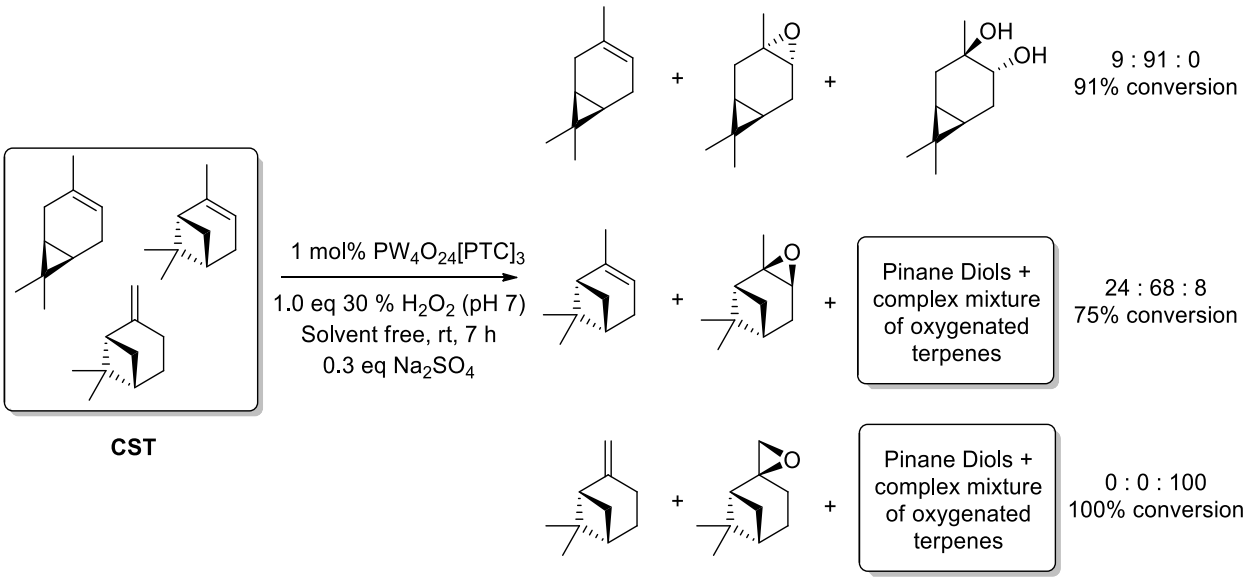

Scheme 119. Epoxidation of CST in the presence of 0.3 eq of Na_2SO_4

Therefore, promising conditions (2 mol% catalyst, rt, 2.0 eq H_2O_2) have been established that enable the selective epoxidation of the 3-carene component of CST, with less forcing conditions (1 mol% catalyst, rt, 1.0 eq H_2O_2, 0.3 eq Na_2SO_4) being partially successful for epoxidation of both the 3-carene and α-pinene components of CST.

2.4 Conclusions

An optimal protocol for the solvent free epoxidation of the alkene bonds of terpene substrates has been developed that employs low loadings of an easily prepared preformed Ishii-Venturello catalyst, using H_2O_2 as a stoichiometric oxidant. This catalytic protocol has been used to selectively epoxidise the trisubstituted and tetrasubstituted alkene bonds of a range of biorenewable terpene substrates in good to excellent yields. Some of these epoxidation reactions (e.g. α-pinene) required the presence of 0.3 mol% of Na_2SO_4 as an additive to minimise competing ring-opening of their epoxides to give their corresponding diols. The scope of this operationally simple solvent free protocol has been extended to the epoxidation of a wide range of new terpene substrates (e.g. β-elemene, farnesene, valencene, dihydromyrcenol, dihydrocarvone, pulegone, β-ionone, perillyl alcohol and myrtenol) in shorter reaction times, with fewer additives, at milder temperatures without the need for undesirable solvents (e.g. benzene, $CHCl_3$ or CH_2Cl_2) that were required in previous protocols (Scheme 56).

Increasing the number of equivalents of H_2O_2 used in this catalytic system enabled epoxidation of terpene substrates containing more than one trisubstituted alkene groups (e.g. formation of γ-terpinene bis-epoxide), with the potential power of this catalytic protocol demonstrated for global epoxidation of the six double bonds of squalene using 6.0 eq of H_2O_2.

Our Ishii-Venturello protocol was modified to enable the less reactive conjugated and disubstituted alkene bonds of terpene substrates such as pulegole and dihydrocarvone, respectively, to be epoxidized at higher temperatures (50 ^{o}C) for the first time. Attempts to use this catalytic system for the selective epoxidation of the exocyclic alkene of β-pinene were only partially successful due to competing ring opening of its epoxide to afford its corresponding diol. Stepwise protocols that combine Mizuno and Ishii-Venturello catalysts for the synthesis of the bis-epoxide of limonene, and nucleophilic peroxide and the Ishii-Venturello catalytic system for the synthesis of carvone bis-epoxide, have also been developed.

Application of our optimised epoxidation conditions to crude sulphated turpentine using 2 mol% catalyst loading and 2.0 eq of H_2O_2 at room temperature in the presence of Na_2SO_4 for 4 h gave a desulfurized mixture of 3-carene epoxide, α-pinene-*anti*-diol and β-pinane-diol. Alternatively, repeating this epoxidation with 1 mol% catalyst loading and 1.0 eq of H_2O_2 at room temperature in the presence of Na_2SO_4 for 7 h gave a mixture of 3-carene epoxide, α-pinane-epoxide and β-pinane-diol.

The potential of this epoxidation process for scale-up has also been demonstrated for the solvent free epoxidation of the major biorenewable feedstocks limonene, α-pinene and 3-carene on 15-100 g scales. These scale-up reactions required modification of the original conditions, involving dropwise addition of the H_2O_2 oxidant into a rapidly stirred mixture of the terpene and catalyst, with efficient cooling required to control the large exotherm that occurred when these reactions are carried out on-scale.

The yields of the 25 terpene epoxides prepared in this study illustrate the scope and limitation of our modified Ishii-Venturello catalytic protocols for the epoxidation of terpene substrates and are summarised in Figure 32.

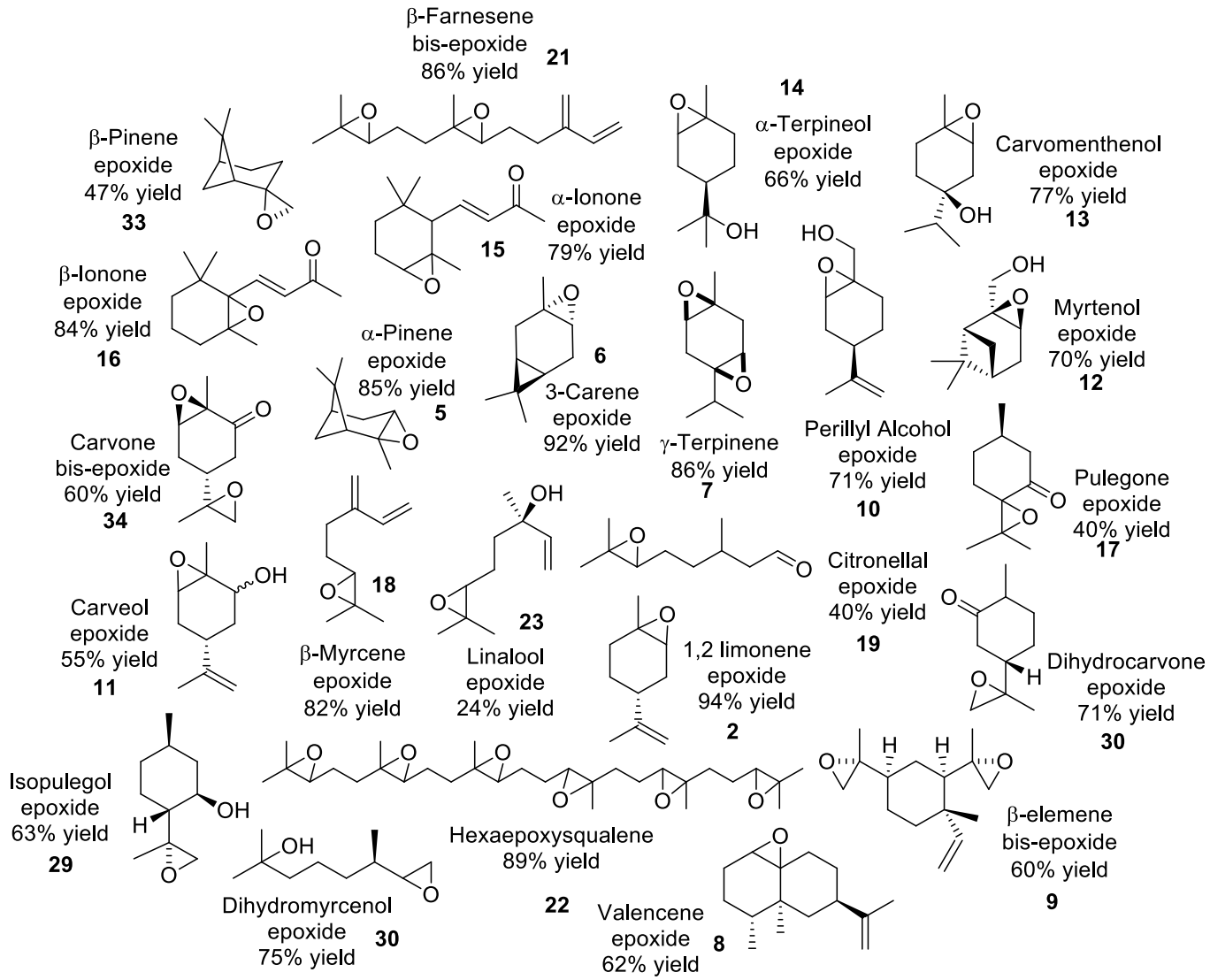

Figure 32. Range of commercially available terpene epoxides prepared via epoxidation using the Ishii-Venturello catalyst/H_2O_2 under solvent free conditions.

3 Chapter 3 – Solvent-free flow epoxidation of terpenes

Having developed an efficient and procedurally simple protocol using a preformed Venturello-A336 catalyst system for solvent-free epoxidation of terpene alkenes in batch, we turned our attention towards developing a viable flow epoxidation protocol using this methodology. It was hoped that the practical benefits of using flow chemistry (e.g. rapid mixing, efficient temperature control, etc.) might enable this epoxidation protocol to be applied to problematic terpene substrates that were difficult to epoxidise in batch. In this respect, we were particularly interested in trying to see whether we could improve the overall efficiency of epoxidation of β-pinene, because it is one of the major components of CST.

3.1 Benefits and Limitations of Batch Synthesis

Batch processes involve stirring all reagents together under controlled conditions until the reaction is complete, with additional steps then required to workup and purify products. Batch processes are typically used in fine chemical and pharmaceutical manufacturing because the technology and processes involved are well understood, with expensive chemical plant infrastructure readily available. However, there are major disadvantages in carrying out batch operations for certain classes of reaction, which can make scale up of these processes difficult, unsafe and low yielding.

The first issue that can occur when using batch conditions on a large scale concerns fast reactions where reactive intermediates and products can potentially degrade under batch process conditions. Poor mixing can lead to the concentration of reactive intermediates building-up to dangerous levels, leading to the formation of unwanted by-products that are difficult to separate or uncontrolled reactions that can lead to explosions or fires.

A good way to appreciate the limitations of batch processing is to consider the physical limitations of carrying out chemical reactions in small and large flasks as shown in Table 4.[156] Mixing of reagents in a small flask results in rapid 'bottom to top' mixing that is not possible in larger reactors, which can result in losses in selectivity in larger batch systems.[156] Smaller flasks also have a higher surface area to volume ratio that allows rapid heat transfer *via* external cooling, which is not possible in larger vessels where poor heat control can lead to localized hot spots that can cause serious safety issues. These scale-up issues can lead to by-product formation, thermal runaway, the need for expensive cooling of exothermic reactions and extended reaction times.[157] Whilst, smaller reactions can be run in parallel using a series of smaller batch reactors to produce large amounts of material, this approach is generally more labour intensive, with associated economic and logistical implications.

Table 4. Physical characteristics of reactions in small and large glass vessels

	25 mL round bottom flask	2 L round bottom flask
Height (sphere, cm)	3.6	34.8
Speed of top to bottom mixing	Rapid mixing possible	Mixing not always rapid
Surface area/volume (cm^2/mL)	1.66	0.17
Heat generated/surface area (cal/g)[a]	36.2	347.1

[a]For a full reactor with a reaction mass generating 60 cal/g of heat.

A key aim of green chemistry and process engineering is to ensure that chemical processes are as efficient as possible, whilst ensuring that they are safe, efficient and generate waste as little as possible. Flow chemistry can achieve this goal by allowing continuous chemical processes to be developed at an early stage of a project that may then be used to produce large quantities of product in an industrially relevant manner.[158]

3.2 Benefits of Flow synthesis

Continuous processing and flow chemistry offer alternative ways to carry out chemical synthesis in a more sustainable and green manner, enabling small scale synthesis and industrial manufacturing to be linked together to provide a more reproducible, scalable, efficient and safe synthetic process.[158] In flow chemistry, chemical reactions are carried out in a network of interconnecting tubes and reactors, where a continuously flowing stream of chemicals are mixed and reacted.[159] There are a number of advantages to flow chemistry and continuous processes, many of which are related to reagent mixing. This is because dosing times are essentially eliminated, resulting in highly efficient mixing of reaction streams that produce more uniform reaction compositions that avoid the build-up of large concentrations of unreacted reagents. These process streams result in efficient mixing of reagents, enabling reaction temperatures to be effectively controlled, thus reducing side product formation caused by inefficient mixing and the presence of temperature hot spots.[160] For example, static mixers can be used to create turbulent micro-mixing that ensure more uniform heat distribution through the generation of vortexed flow streams. Efficient mixing also allows reactions to be run at a higher concentration, thus reducing the amount of solvent used in flow chemical processes.

The high surface area to volume ratio's in small reactors also allow efficient application and removal of heat, which enables closer control of reaction temperatures that can be used to increase reaction rates in a controllable manner, thus leading to shorter reaction times. This means that the energy employed for temperature control and mixing can also be applied more efficiently, enabling smaller flow-reactor tubes that are cheaper to run and more environmentally benign.

An excellent example of the benefits of employing flow chemistry for synthesis was reported by DSM, who reported the use of metal microreactors to manufacture an acrylamide monomer using a highly exothermic Ritter reaction.[160] Key benefits of this protocol included decreased exposure of the operator to acrylonitrile, lower levels of product decomposition, a decrease in overall waste of 15% and an increase in yield of 15%, with this flow protocol producing of 40 tons of acrylamide product per day (Scheme 120).

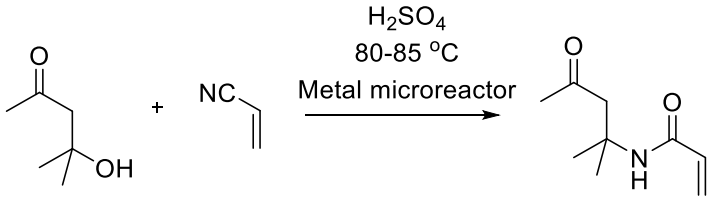

Scheme 120. Use of microreactors for the continuous production of an acrylamide monomer

Continuous processes have also been used for the optimisation of high temperature and cryogenic reactions. Batch reactions often require cooling to proceed safely and achieve selectivity, which is often costly and difficult to achieve in large reaction vessels. However, cooling in flow reactors can be performed much more efficiently, with shorter contact times between the reaction and cooling systems being possible at higher temperatures. This potentially eliminates the need to construct expensive cryogenic batch reactors that consume a lot of energy in maintaining low temperatures on-scale. From a safety perspective, using small reaction streams at high temperatures for short periods of time can minimise the potential damage caused by thermal runaway reactions, because only low volumes of reactants are present at any one time.[160]

Flow chemistry also affords the possibility of re-circulating reaction streams past ultraviolet lamps or other light sources to effectively initiate photochemical reactions, or to use sonication to produce cavitation events that can increase the overall rate of reactions. Its use also affords the opportunity to pass reaction flows through solid-supported reagents, such as immobilized catalysts and polymer supported scavenging reagents, to facilitate reaction purification.

Another advantage of continuous processes is the ability to use dangerous or toxic reagents in a safe manner. For example, highly energetic reagents or toxic compounds such as phosgene, HCN and diazomethane can be continuously generated and consumed, preventing them from accumulating to dangerous levels. It is also possible to use heat exchangers to rapidly cool a reaction stream directly after a heating zone, which means that only small volumes of a potentially dangerous reagent or intermediate are present at high temperatures.[160] Broek *et al*[161] have developed scalable continuous flow methods in glass microreactors to minimize reaction exotherms that cause degradation of reactive chloroiminium intermediates generated in Vilsmaier-Hack formylation reactions, thus making these reactions suitable for industrial application (Scheme 121).

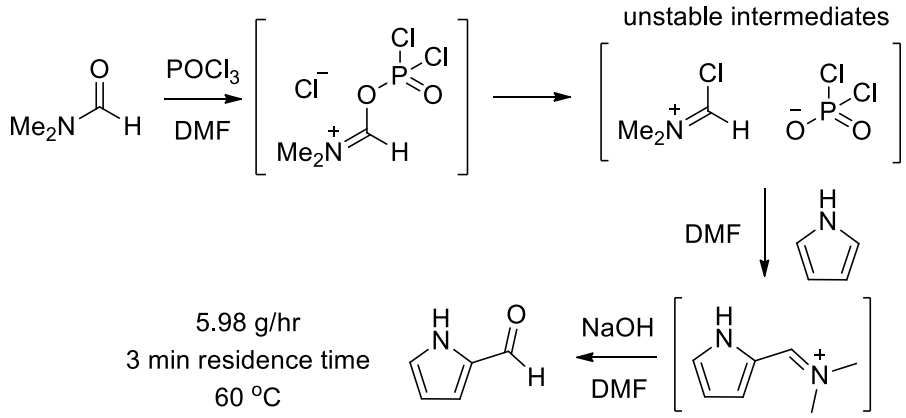

Scheme 121. Vilsmeier-Haack formylation of pyrrole using a glass microreactor

A less obvious advantage of using continuous processes for synthesis concerns intellectual property. Developing a chemical process in flow can sometimes deliver new opportunities to patent a process, with real time process analytical technology (PAT) capable of ensuring high quality chemical products for regulatory purposes and provide in-depth data for mechanistic analysis.

Another benefit of flow chemistry is the ability to make large quantities of product with minimal process re-development. The easiest strategy involves carrying out a continuous flow reactor

for a longer period of time, in a process that is known as “scaling out”. An alternative approach is to run reactions in multiple reactors in parallel, using a “numbering up” process, although this approach can be expensive as it requires access to multiple reactors. The last approach is to construct larger continuous flow reactors, which may need more process development, but have the capacity to deliver large volumes of product. For example, the microreactor technology team at Lonza led by Roberge *et al*[162] developed flow ozonolysis methodology that enabled 500 kg of a cyclopropyl substrate to be produced daily using a 450 litre loop reactor (Scheme 122).

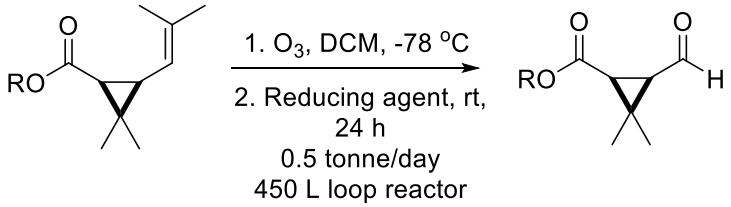

Scheme 122. Large scale flow ozonolysis

Flow chemistry and continuous processing techniques offer many advantages that can be enhanced by using miniaturized micro or millireactors for chemical synthesis. This reactor technology is particularly useful for kilogram scale syntheses using hazardous reactions that cannot be scaled up using conventional reactors.[163] Typically, micro-reactors have volume capacities within the nano-litre to milli-litre range, with applications of continuous micro-reactors for industrial applications well established.[163]

It is estimated that a traditional batch synthesis produces 25 to 100 kg of waste for every 1 kg of product synthesized, which causes a significant environmental impact.[164] The use of micro-reactors can lead to reduction of waste and exceptional reaction control,[164] because their thin channel dimensions and static mixers enable exceptionally efficient mixing within the millisecond range.[164] Their small size also prevents hot spot formation, often leading to better yields and selectivity, whilst fast mixing and efficient heat transfer allows the use of concentrated or solvent-free conditions that reduce the amount of waste generated.

A final consideration on the decision on whether to use flow chemistry for a reaction relates to cost. Continuous operations typically require more specialised equipment, when compared to batch operations. For example, pumps, multiple reactors, product collection vessels, secure fittings, valves, pressure gauges, static mixers, in-line probes and separators are typically required. However, the investment in time and money in developing a flow route to a specific chemical product at an early stage can often be offset by the overall savings that can be produced in a scaled-up industrial process.

A range of recently reported chemical reactions that have been carried out in flow are shown in Scheme 123, which demonstrate the benefits and potential of using flow technology to carry out reactions that would be problematic in batch reactors on a large scale.[158]

The small size of microreactors reduces the volumes of materials used and enables more hazardous transformations to be performed with lower chances of reaction failure.[158] Diazomethane is a useful reagent for performing methylation reactions but is highly toxic and explosive making it dangerous to use in batch. Stark *et al*[165] have shown that microreactor technology can be used to rapidly generate diazomethane *in situ* from Diazald, to avoid the

need to transport and stockpile large quantities, which can be used to methylate benzoic acid in a high yield of 75%.

Other hazardous reagents such as fluorine gas can be generated for direct fluorination of substrates in flow which can reduce the number of steps required to perform highly reactive fluorination reactions. For example in 2017 Sandford *et al*[166] used a 1 step fluorination reaction using 10% fluorine gas to synthesise the antifungal agent, Flucytosine, achieving a high yield of 83%. This process replaced a 4 step procedure performed industrially and significantly reduced the cost of this pharmaceutical which is critical as its primary markets are in low income African nations.

Another major advantage of flow chemistry is its ability to perform scalable photochemical transformations by making use of the high surface area to volume characteristics of flow reactors which allow for more efficient light penetration and higher transfer of photons to reaction mixtures resulting in higher yields. In 2010 Stephenson *et al*[158] demonstrated a catalytic photochemical alkylation cyclisation reaction performed using a ruthenium catalyst, that had previously required the use of toxic tin reagents in batch, that could be scaled to produce grams over 24 h affording a 91% yield whereas the same photochemical reaction in batch resulted in minimal conversion.

The use of ammonia gas in condensation reactions often requires heating for high conversions to be achieved, which can result in the need to use large amounts of ammonia due to its inherent volatility. This difficulty can be minimised under flow conditions, with Ley *et al* having carried out Paal-Knorr reactions of ammonia and 1,4-diketones in flow to afford pyrroles in >90% yields with short 2 h reaction times.[167]

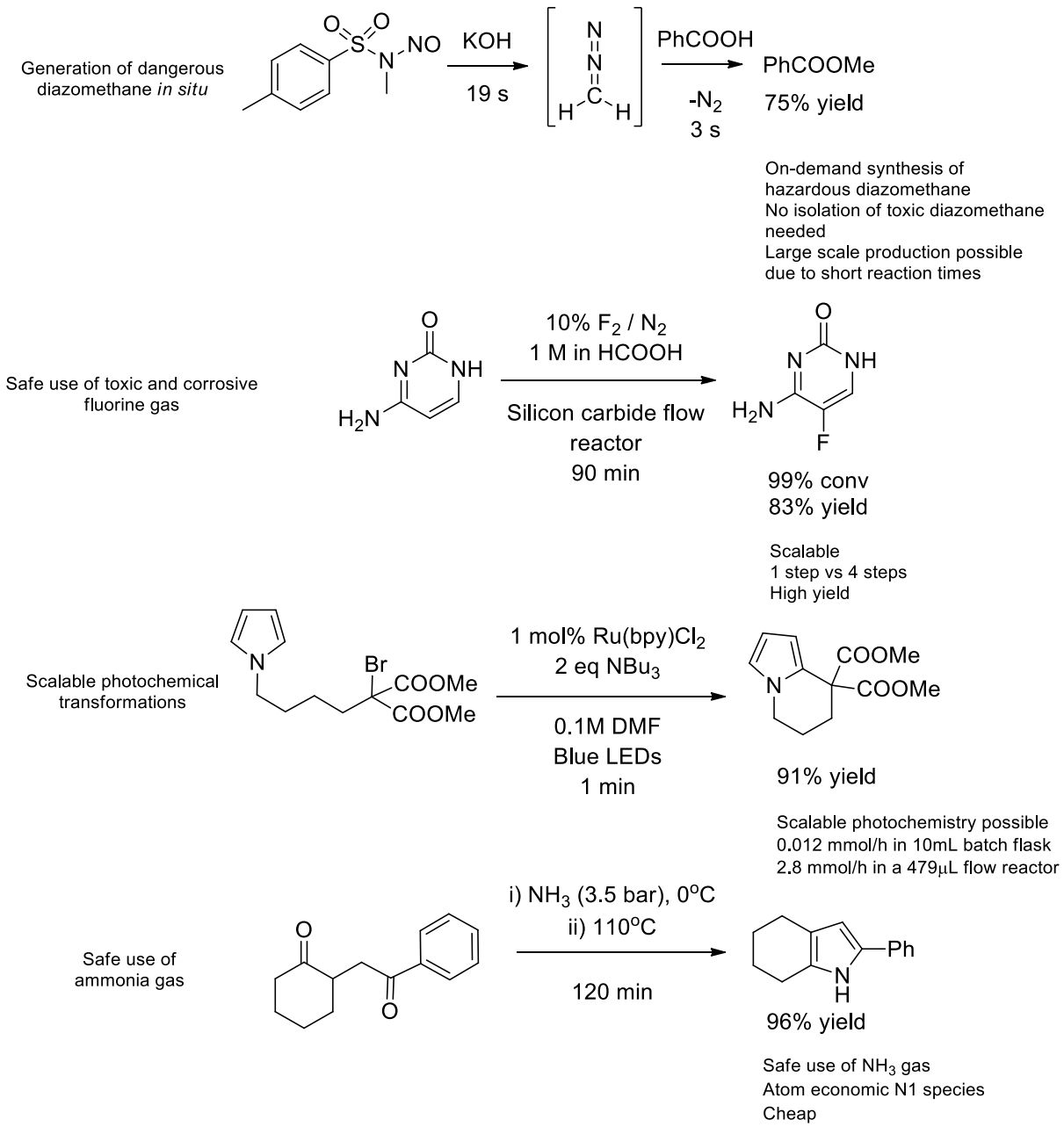

Scheme 123. Scale-up of four difficult transformations that were made possible using flow chemistry

3.3 Flow Epoxidation Reactions

Epoxidation reactions of alkene substrates using stoichiometric amounts of peracids have been developed in flow to mitigate the safety risks and costs associated with carrying out large scale reactions in batch due to the explosive nature of peracids. In 2012 Rutjes *et al*[168] optimised the use of peracetic acid for the synthesis of trans cyclohexane diol in flow. Initially they optimised the flow epoxidation reaction of cyclohexene, before performing a second ring opening step to afford diols using water as a nucleophile. The conditions to achieve the flow epoxidation of cyclohexene involved reaction with 32% aqueous peracetic acid using a 5 minute residency time at 60 °C, which gave the desired cyclohexene epoxide in 67% yield. The reaction time of 5 minutes for the epoxidation reaction to proceed to completion in flow is much faster than the 4 h required for this epoxidation reaction under typical batch conditions (Scheme 124).

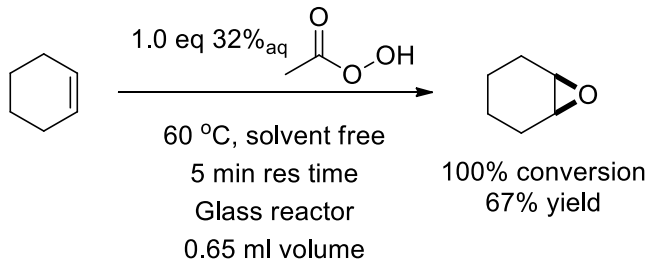

Scheme 124. Peroxyacetic acid mediated flow epoxidation of cyclohexene

In 2016 Guo *et al*[169] developed a flow protocol for the epoxidation of cyclohexene using *in situ* generated *m*CPBA. The high costs associated with using *m*CPBA are in part due to the need to purify it as well as the costs associated with safe transport of this highly reactive reagent, which is highly unstable in its pure form. Flow reaction of *m*-chlorobenzoic acid with 5.0 eq of alkaline H_2O_2 in H_2O/dioxane for 30 seconds afforded *m*CPBA in 85% yield, which was then reacted immediately with a stream of cyclohexene in EtOAc using a capillary microreactor system to afford cyclohexene epoxide in 100% conversion and 95% isolated yield (Scheme 125).

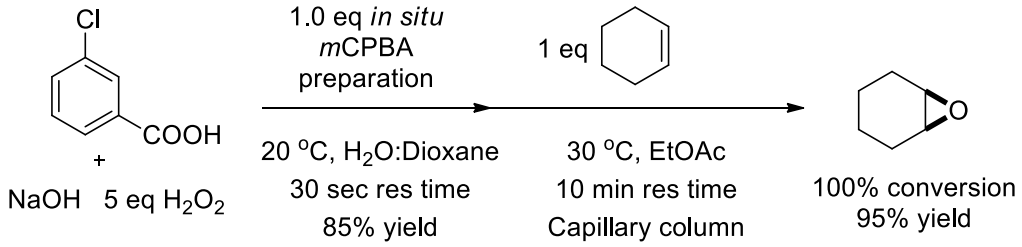

Scheme 125. *In situ* generated mCPBA for the continuous epoxidation of cyclohexene

3.3.1.1 Continuous catalytic epoxidation

A number of catalytic flow epoxidation protocols that employ hydrogen peroxide as a stoichiometric oxidant for the continuous epoxidation of alkenes have also been developed. Gavriilidis *et al*[170] carried out flow enantioselective organocatalytic epoxidation reactions of chalcones. An immobilised polyethylene glycol-poly-L-leucine catalyst was employed in the presence of DBU as a base to generate nucleophilic hydroperoxide anion *in situ*, that reacted

with chalcone to give the desired chiral epoxide in high yield and 88% *ee*, using a short residence time of 16 minutes at 25 °C (Scheme 126).

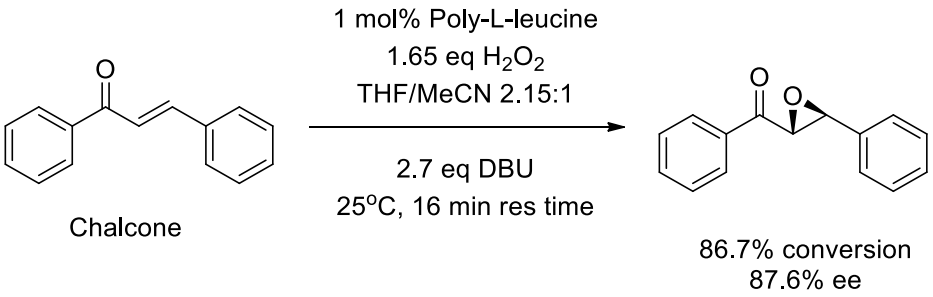

Scheme 126. Enantioselective flow epoxidation of chalcones using hydrogen peroxide as oxidant

In 2017 Schenkel *et al*[171] developed an organocatalytic epoxidation flow protocol that proceeds *via* formation of an imidoyl hydroperoxide species (known as Payne's reagent) to afford a 100% yield of epoxide after a short residence time of 5 minutes, which was much faster than batch conditions that took 1 h to reach complete full conversion (Scheme 127).

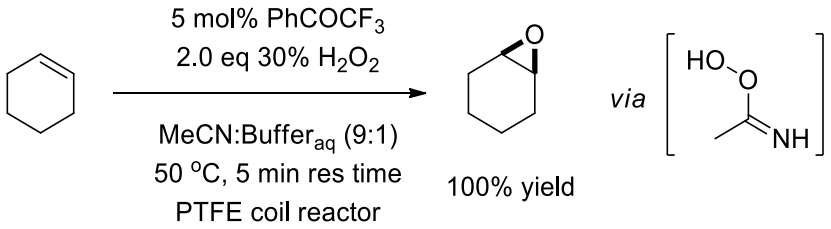

Scheme 127. Continuous organocatalytic epoxidation of cyclohexene

In 2017 Lapkin *et al*[172] reported the continuous epoxidation of waste cocoa butter using an *in situ* generated Ishii-Venturello catalyst and hydrogen peroxide as the oxidant. The long chain alkene sidechains of these fatty ester substrates are highly viscous and prevent efficient mixing in batch epoxidations; therefore the use of a continuous reactor for enhanced thermal transfer and efficient mixing was required. Epoxidation was performed using a Vapourtec flow reactor, which gave good conversion and good selectivities for epoxidation using short reaction times, with toluene and a surfactant required in this process due to the high viscosity of this biorenewable alkene feedstock (Scheme 128).

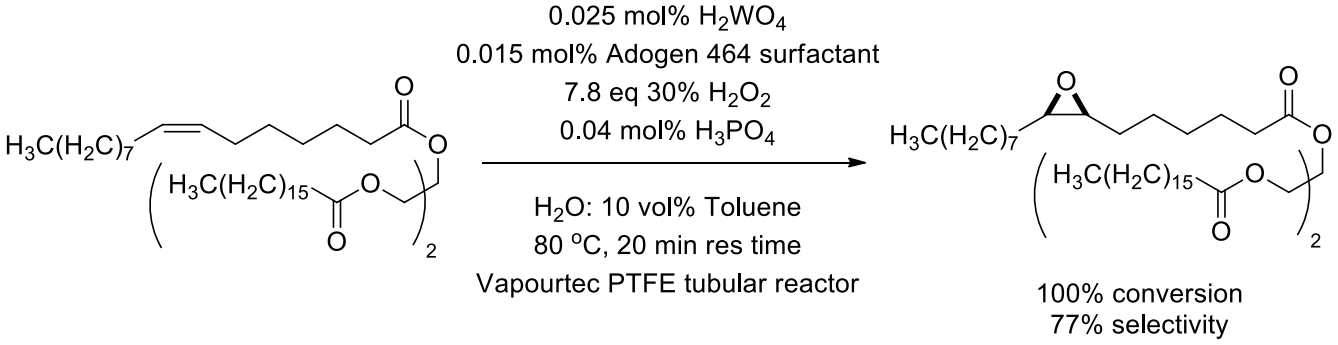

Scheme 128. *In situ* generated Ishii-Venturello catalyst for the continuous epoxidation of waste cocoa butter

3.4 Catalytic Solvent-free Flow Epoxidation Reactions of Terpene Substrates

As the short review above reveals there are currently no previous reports of solvent free flow protocols for the continuous epoxidation of alkenes (including terpene species) using flow protocols. Therefore, it was decided to attempt to explore whether our optimised preformed Ishii-Venturello-A336 epoxidation protocol could be adapted to carry out flow epoxidation of the alkene functionalities of terpene substrates under solvent free conditions.

A factor that needed to be addressed was the known propensity of hydrogen peroxide to decompose to oxygen and water at surfaces, especially at elevated temperatures.[171] Hydrogen peroxide degradation was minimised by employing a number of precautionary measures such as preventing the peroxide solution from being exposed to direct sunlight and only using fresh peroxide reagent that had been stored at low temperatures. Flow reactions that were performed using long residence times (5 minutes or longer) were heated to a maximum temperature of 60 ^{o}C, with only minimal peroxide degradation being observed at this temperature. When "flash" flow epoxidation reactions were carried out at higher temperatures at lower residency times, then some peroxide degradation was observed, so an excess of hydrogen peroxide was used to ensure high conversions. A maximum of 0.3 eq of Na_2SO_4 was used as an additive in the flow epoxidation experiments, with attempts to employ higher amounts of salt failing due to unwanted salt precipitation causing blockages of reactor channels and inlet/outlet tubes.

Three initial flow epoxidation experiments were performed using limonene as a model terpene substrate to compare different flow reactor setups. The first setup involved using PTFE coil tubing (1/16" tube) and a Y-junction submerged in a heated water bath similar to the system used by Lapkin *et al*[172] for the flow epoxidation of cocoa butter. The second setup involved a LTF glass millireactor with smooth channels, whilst the third setup used a LTF glass millireactor containing static mixer channels. A preformed catalyst loading of 2 mol% and a temperature of 50 ^{o}C was used in all reactor setups trialled. The first and second reactor designs gave 30% conversion to limonene epoxide after 5 minutes, however, the static mixer glass LTF millireactor gave significantly higher 65% conversion under these conditions, and so this reactor design was chosen for further flow epoxidation optimisation experiments.

Next, 1 mol% of preformed Ishii-Venturello catalyst was tested at a range of longer residence times in a static mixer glass LTF millireactor, using 1.6 eq of H_2O_2 at a constant temperature of 50 ^{o}C. Two glass milli-reactors fitted with static mixers with a volume of 9 mL were linked together to provide a combined reactor with a total reaction volume of 18 mL that enabled lower flow rates and longer residence times to be screened. The Venturello catalyst (1.36 g, 1 mol%) was then dissolved in the limonene substrate (20 mL, 126 mmol) and the resultant solution loaded into a glass syringe. 30% hydrogen peroxide (11.7 mL, 202) (buffered to pH 7.0 using 0.5 M $NaOH_{(aq)}$) was then loaded into the second glass syringe. These syringes were then loaded onto their respective syringe pumps that could be programmed to pump solutions at different flow rates to achieve the desired reactor residence time and stoichiometries. After flow reaction was commenced, the flow system was allowed to stabilise (for one complete residence time run), before the composition of the organic component of the flow solution was

sampled at the outlet ports using GCMS and NMR analysis. The flow reactor setup that was employed in all the flow reactions carried out in this study is shown below in Figure 33.

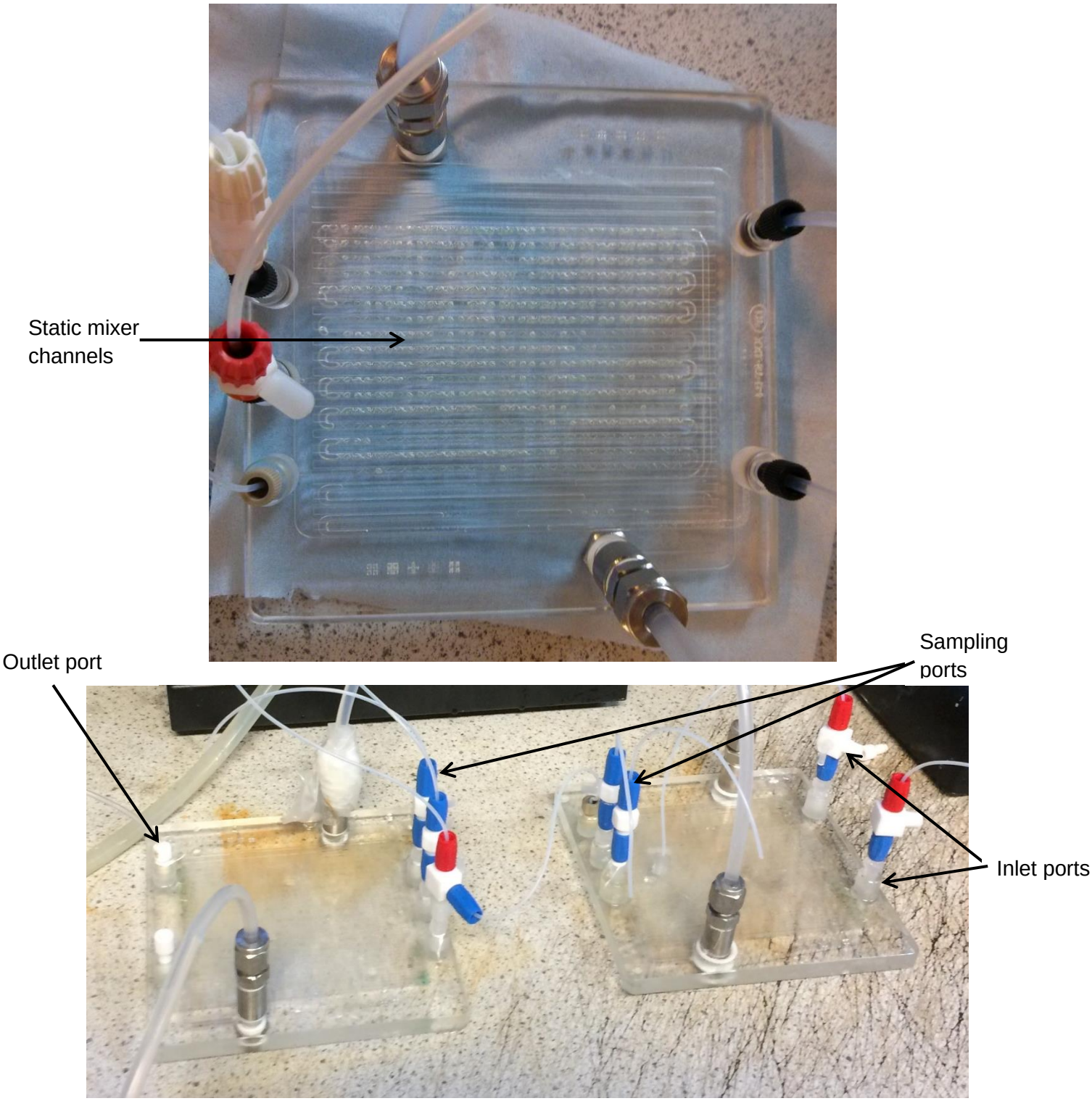

Figure 33. Photographs of flow reactor and LTF static mixer setup used for terpene epoxidation reactions

This simple two-feed flow set-up enabled flow rates and residency times to be adjusted to maximise conversion of limonene into its corresponding mixture of epoxides. The reaction product effluent was collected into a glass beaker, with its biphasic nature resulting in two

layers - with the limonene epoxide product present in the top organic layer. This enabled the limonene epoxide to be easily separated from the aqueous layer, without any solvent extraction procedures being required, with direct distillation *in vacuo* allowing for recovery of 'catalyst free' limonene epoxide in 71% isolated yield (Scheme 129).

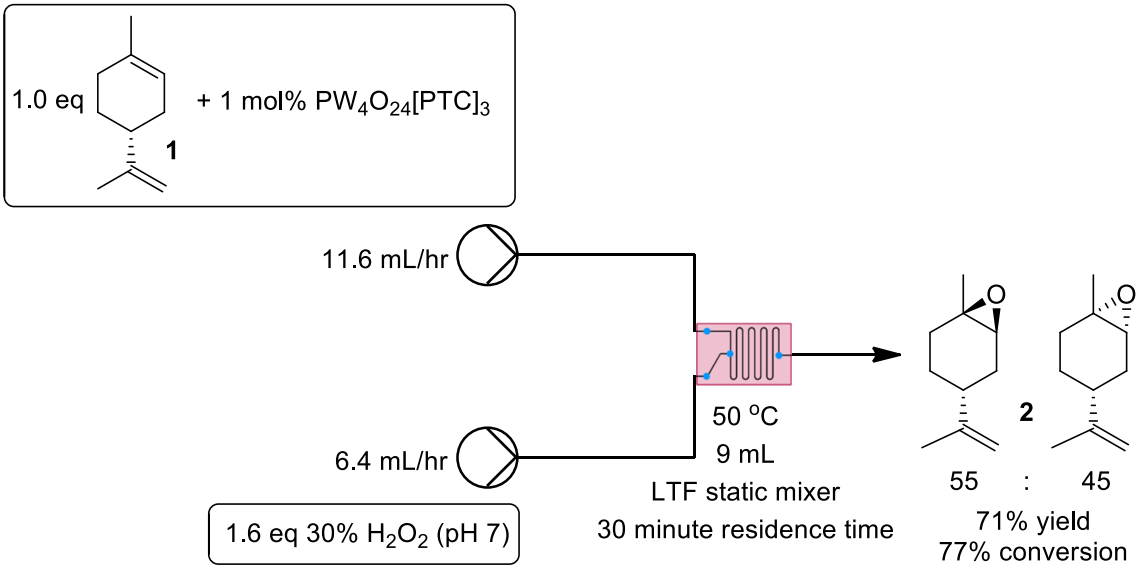

Scheme 129. Conditions used for flow epoxidation of limonene

Figure 34 shows the effect of residence time on the H_2O_2 mediated epoxidation of limonene over time. As expected, higher yields of epoxides were obtained for longer residency times (Figure 34), with a residence time of 20 minutes affording a substrate conversion of 65%, and a residence time of 30 minutes affording 77% conversion and a 71% isolated yield of 1,2-limonene epoxide.

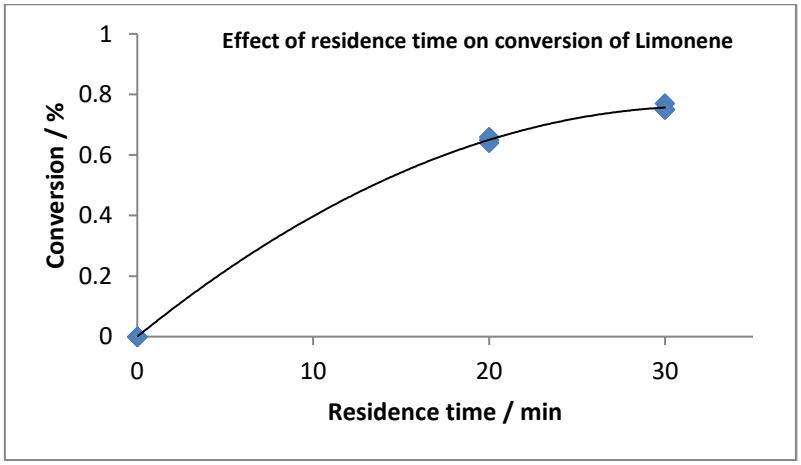

Figure 34. Effect of residence time on flow epoxidation of limonene using 1 mol% catalyst

The flow epoxidation reaction of limonene was then repeated using the same reactor setup employing a higher 3% loading of Ishii-Venturello catalyst to try and achieve total consumption of starting material. This resulted in the limonene substrate reacting at a much faster rate, reaching 95% conversion after 15 minutes residence time, which afforded an 85% isolated yield of 1,2-limonene epoxides (Scheme 130). Unfortunately, ^{1}H NMR spectroscopic analysis of the crude reaction product, revealed that these conditions also resulted in formation of small amounts of limonene 1,2-diol and limonene bis-epoxide in a combined yield of around 10%.

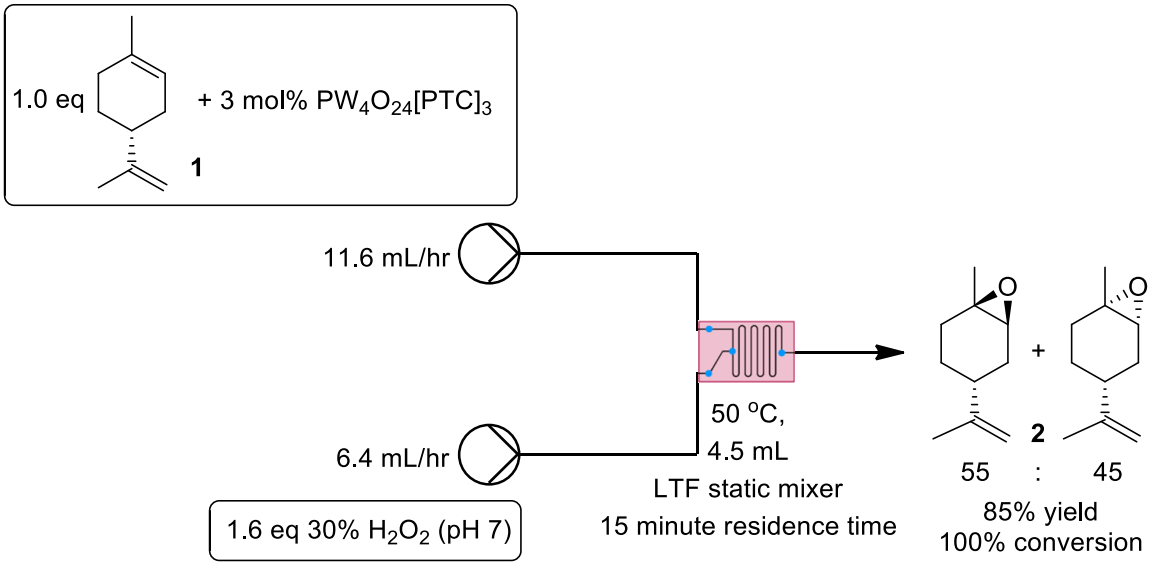

Scheme 130. 3 mol% catalyst loading for the flow epoxidation of limonene

With conditions having been successfully established for the flow epoxidation of limonene, we next explored the flow epoxidation of 3-carene using a catalyst loading of 1 mol%. Three different residence times of 15, 20 and 30 minutes were screened (Figure 35), with increasing residence time resulting in increased amounts of epoxide being formed. Similar to limonene, the flow epoxidation reaction was very clean with only epoxide product and alkene starting material being observed in the product stream, with a 30 minute residence time affording 75% conversion and a 73% yield of 3-carene epoxide (Scheme 131).

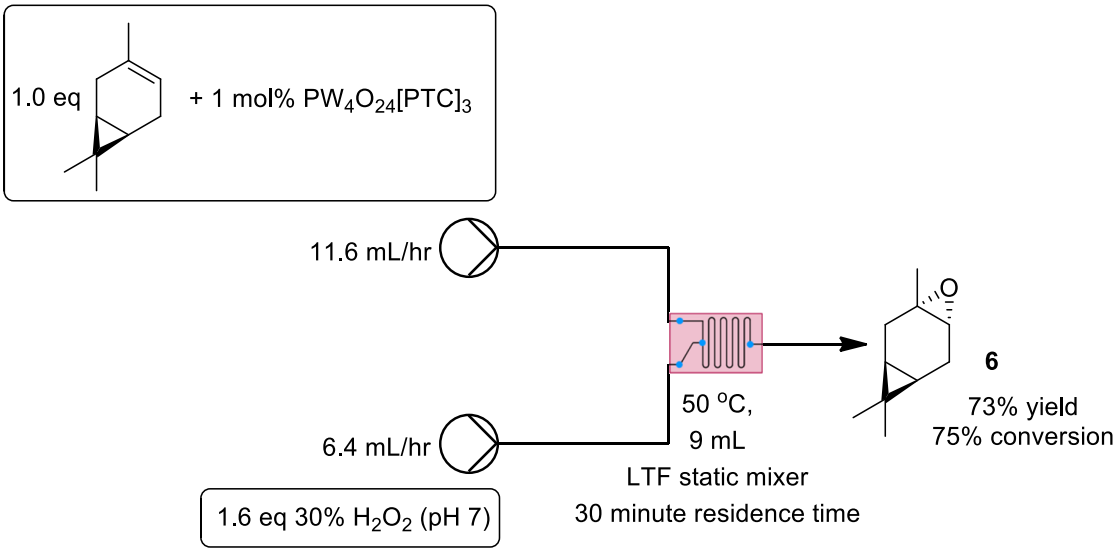

Scheme 131. Epoxidation of 3-carene under flow conditions

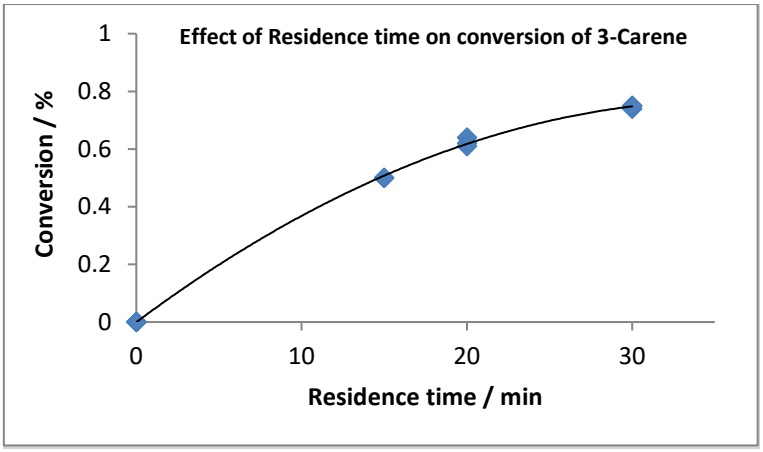

Figure 35. Effect of residence time on flow-epoxidation of 3-carene

The catalyst loading was then increased to 3 mol%, which resulted in complete consumption of 3-carene to afford 3-carene epoxide in 97% yield after a 30 minutes residence time (Scheme 132).

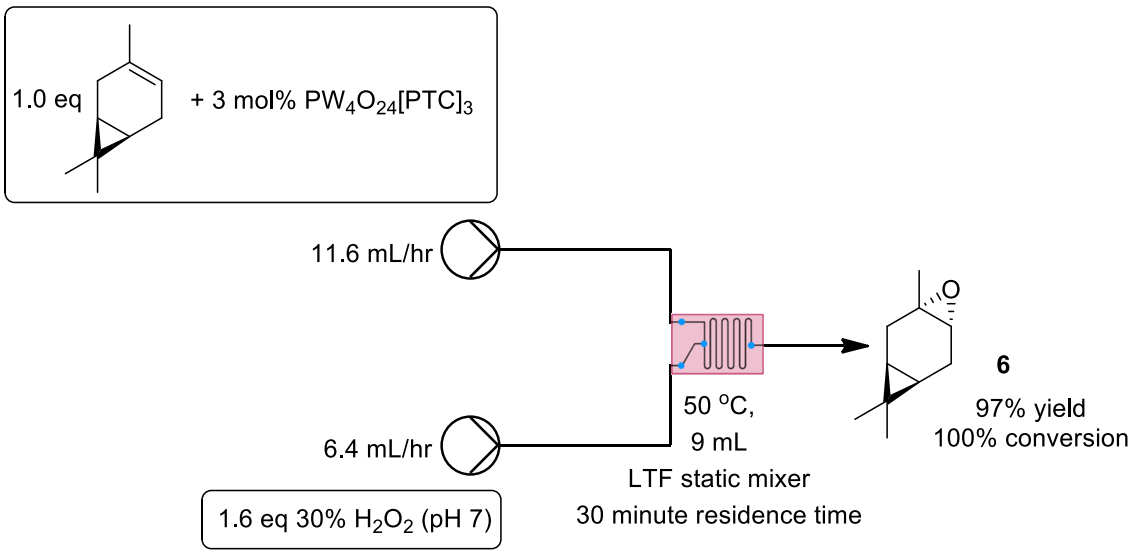

Scheme 132. Flow epoxidation of 3-carene using 3 mol% catalyst

α-pinene was then epoxidised in flow using 1 mol% catalyst, with 30 mol% Na_2SO_4 salt being incorporated into the flow protocol to maximise the yield of cyclic epoxide formation, by minimising competing diol formation. The rate of epoxidation of α-pinene in flow was much slower compared to limonene and 3-carene, with 12% conversion after 20 minutes residency time and 36% conversion after 40 minutes respectively (Scheme 133).

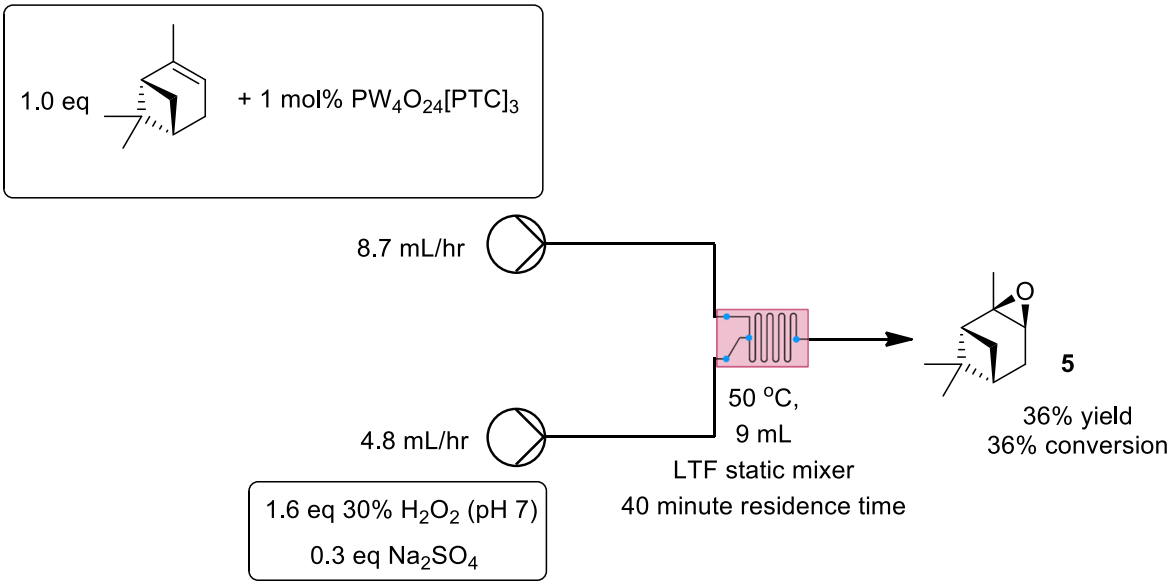

Scheme 133. Flow epoxidation of α-pinene using 1 mol% catalyst.

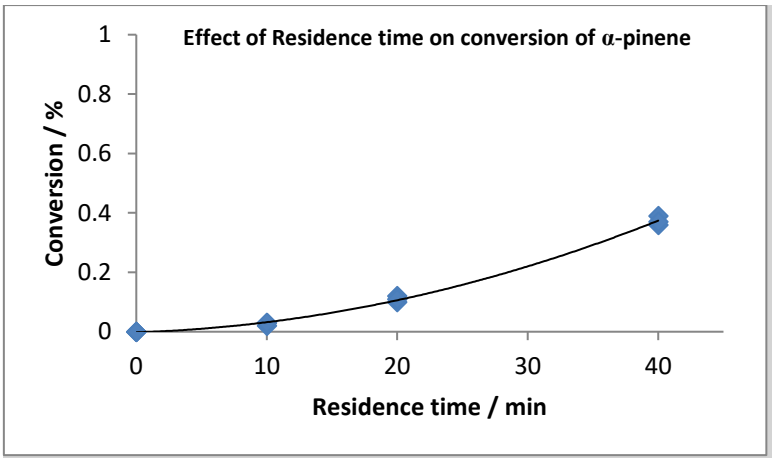

Figure 36.Effect of residence time on flow epoxidation of α-pinene

We next tried to increase the rate of the epoxidation reaction in flow, by increasing the temperature of the reactor to 60 °C and increasing the catalyst loading from 1 mol% to 3 mol% (Figure 36). This led to a significant increase in the rate of epoxidation of α-pinene resulting in 70% conversion with 100% selectivity for the epoxide product to afford α-pinene epoxide after 30 minutes (Scheme 134). No diol by-products were observed with only 30% starting material remaining, which could be easily separated *via* fractional distillation due to the significant difference in boiling point between α-pinene (155 °C) and its epoxide (185 °C) respectively).

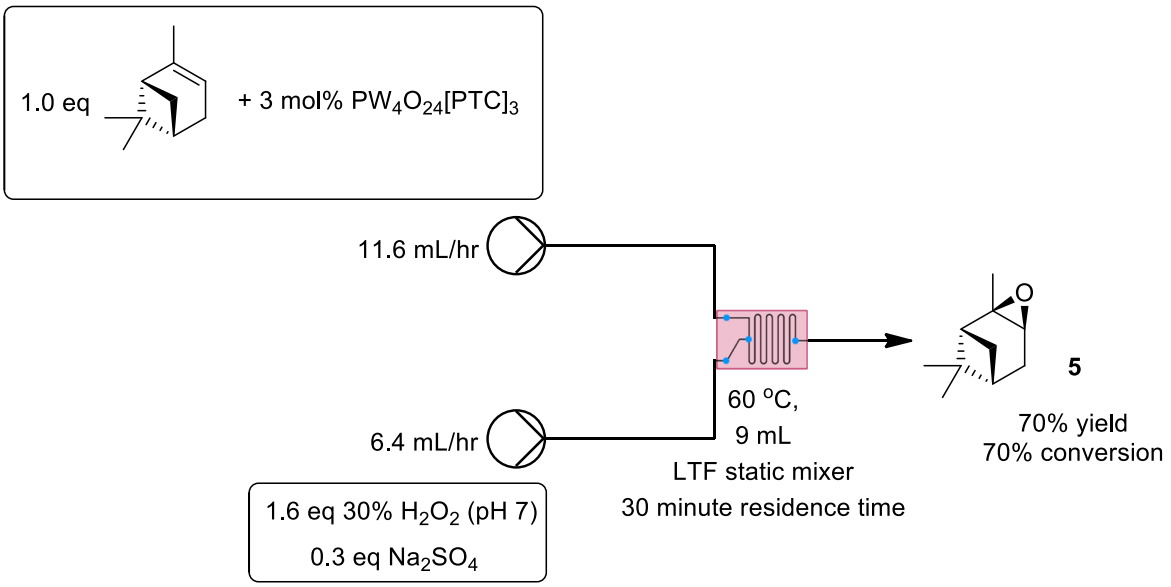

Scheme 134. Flow epoxidation of α-pinene using 3 mol% catalyst

Increasing the catalyst loading further to 6 mol% increased the yield to 78% after a residence time of 15 minutes (and a reactor volume of 4.5 mL). A slightly longer residence time of 20 minutes achieved a conversion of 88% (Scheme 135), but selectivity was lowered with some diol product being formed, with an epoxide yield of 81%. The 6 mol% amount of catalyst used in this epoxidation was near its saturation limit in α-pinene, with a small residue (ca. 100 mg) of catalyst remaining un-dissolved in the beaker.

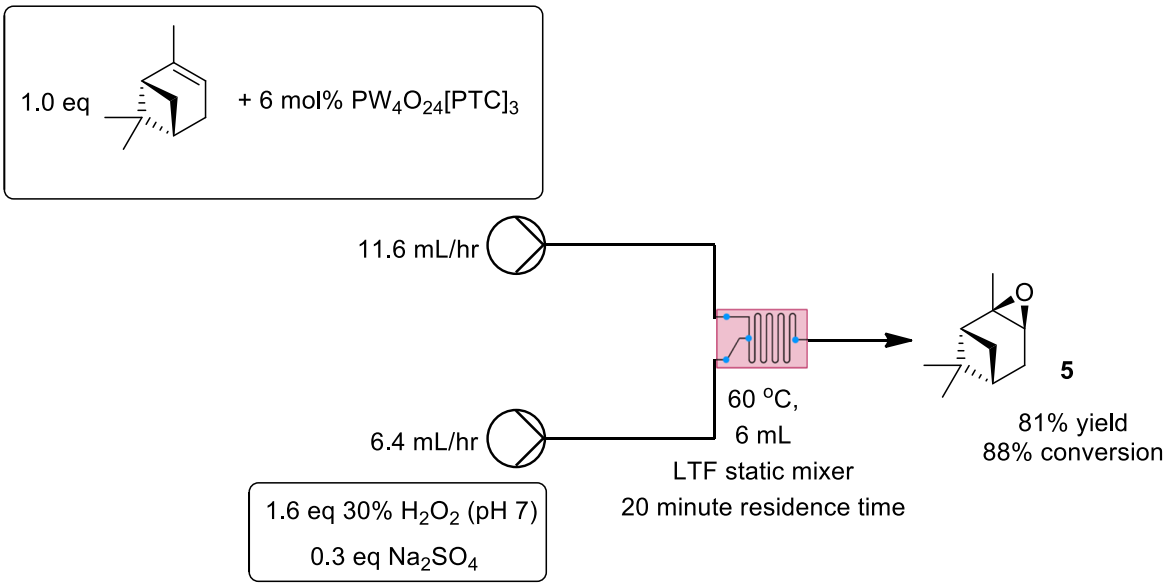

Scheme 135. Flow epoxidation of α-pinene using 6 mol% catalyst

3.4.1 Optimisation of the flow epoxidation reaction of β-pinene

As described previously, Ishii-Venturello epoxidation of β-pinene proved problematic because of the relatively low reactivity if its disubstituted alkene bond and the ease with which its epoxide is hydrolysed to diol by-products. It was hypothesised that the use of flow conditions might result in better results for the epoxidation of β-pinene because more efficient mixing would result in a faster reaction and more precise control of reaction temperature. This might allow for shorter exposure of the epoxide product to water at elevated temperatures, which we hoped would minimize hydrolysis to its ring opened diol.

The optimal flow regime developed previously for the epoxidation of α-pinene (using Na_2SO_4 additive) was screened for the flow epoxidation of β-pinene, however these conditions resulted in formation of a complex mixture of diols after 40 minutes, with < 5% of epoxide and mostly (90%) β-pinene starting material being present. Consequently, an alternative set of more forcing conditions were screened, involving the use of a fast flow rate to minimise reactor residency time, with the increased flow rate achieving greater mixing of the two phases in the static mixer. Higher equivalences of hydrogen peroxide (2.6 eq) were used in this flow epoxidation to compensate for its increased rate of thermal degradation at higher temperatures (Scheme 136).

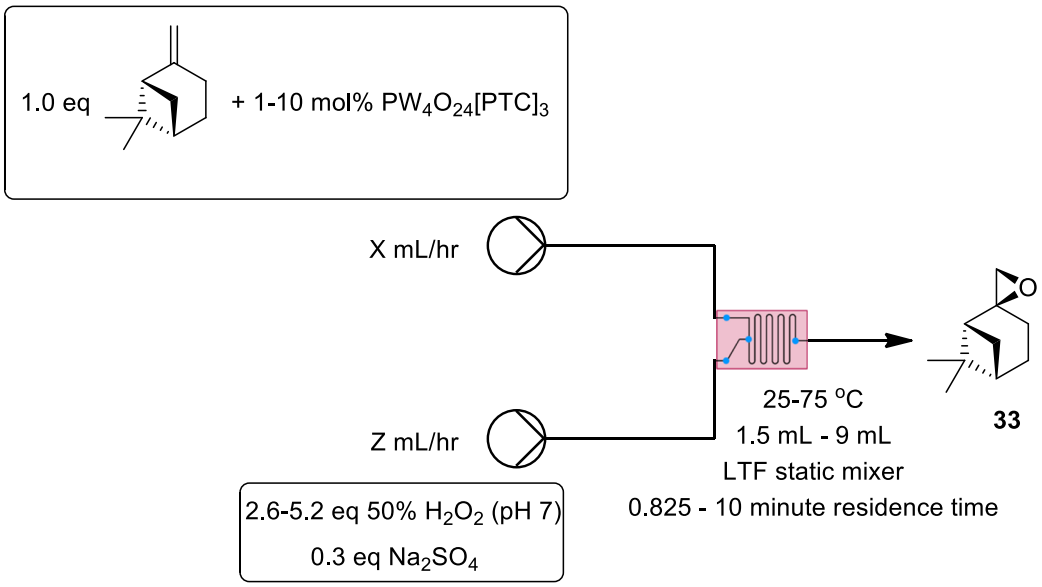

Scheme 136. Range of parameters screened for the flow epoxidation of β-pinene

Initially, epoxidation of β-pinene using a 5 minute residency time was employed at a series of reaction temperatures, with the amount of β-pinene epoxide produced found to increase with increasing temperature (Figure 37). The best conversion rates were obtained at 75 °C which gave a 22% yield of the desired β-pinene. Attempts to carry out the epoxidation reaction at temperatures of >75 °C did not result in any improvement in epoxide yield, because of rapid hydrogen peroxide degradation occurring.

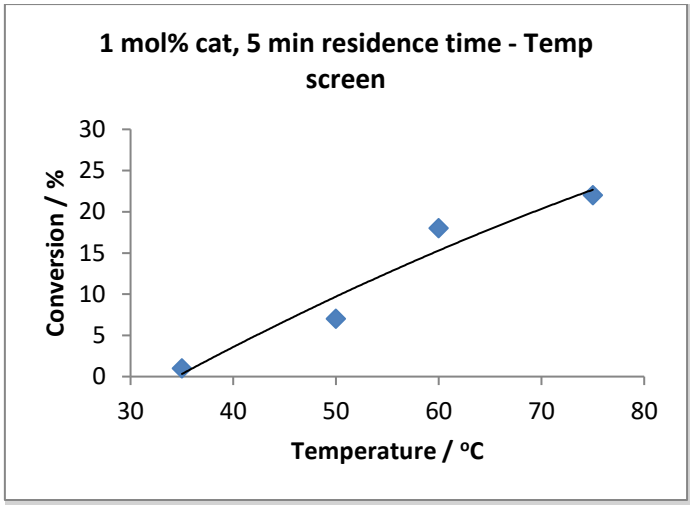

Figure 37.Effect of temperature on yield of β-pinene epoxide

The effect of residence time on epoxide yield was than investigated at a constant temperature of 75 °C, Figure 38. As expected, the yield of β-pinene epoxide increased with increasing residence time until it reached a maximum of around 25% yield at around 6 minutes, after which time it decreased, due to competing hydrolysis of the epoxide to afford its corresponding diol.

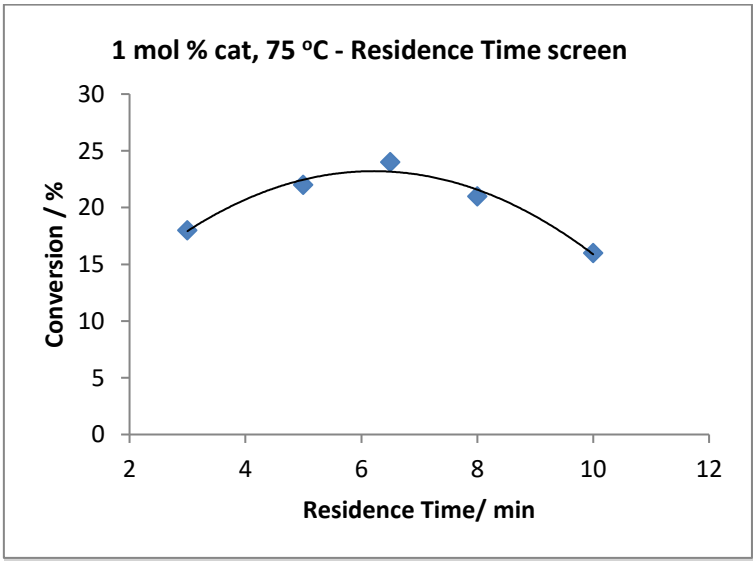

Figure 38.Effect of residence time on β-pinene flow epoxidation conversion

The effect of catalyst loading was then investigated, with 2 mol% catalyst leading to an increase in conversion from 22% to 32% (Figure 39), and an increase in catalyst loading to 5 mol% leading to 38% conversion. However, increasing catalyst loadings, to 5 mol%, led to no increase in β-pinene epoxide yield, primarily due to the catalyst beginning to precipitate out of solution at these higher concentrations.

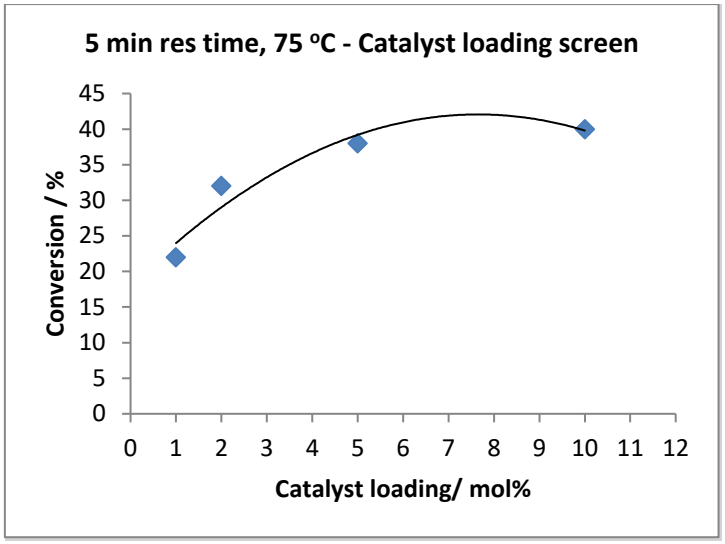

Figure 39. Effect of catalyst loading on β-pinene flow epoxidation conversion

Finally, the shortest possible reactor volume was investigated using 5 mol% catalyst. A reactor volume of 1.5 mL with a residence time of 1.67 minutes was used to give a 55% yield of β-pinene epoxide (Scheme 137), with no diol by-product mixture present. When the reactor volume was increased to 3 mL, significant levels of diol by-product were formed, with no improvement in the yield of β-pinene epoxide.

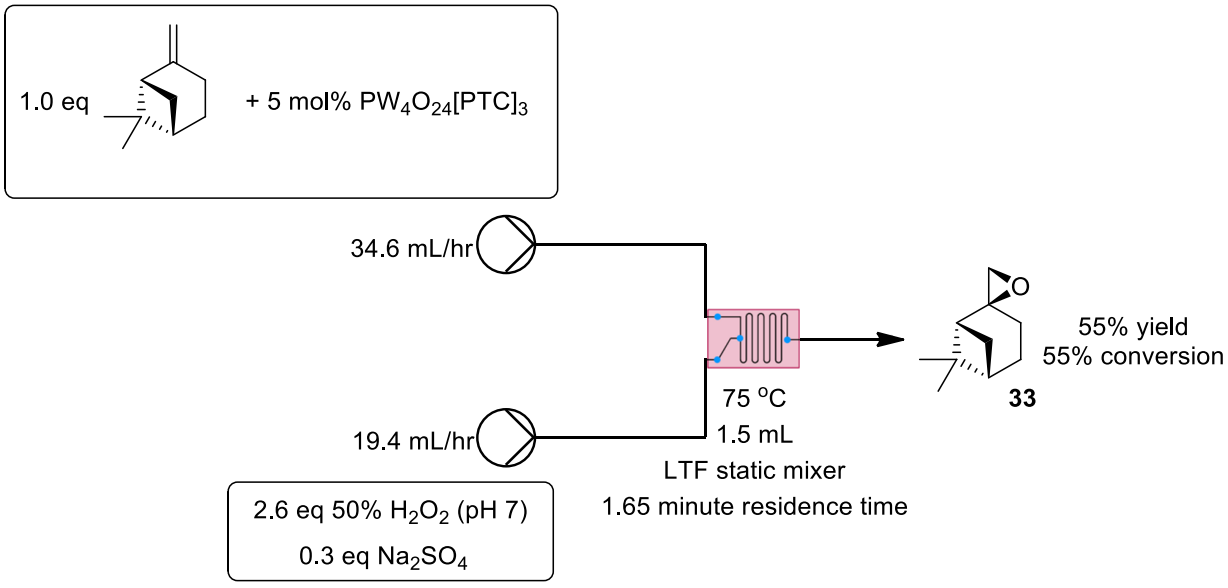

Scheme 137. Optimal β-pinene flow epoxidation conditions

A final experiment was performed to see if a faster flow rate over a short reactor volume might give improved conversion to the β-pinene epoxide product (0.83 min residency time), however these conditions resulted in a reduced 41% yield of epoxide being observed. When the epoxidation reaction was left for longer (1.65 minute residence time with 2 x flow rate), then nearly all the β-pinene epoxide was degraded to a complex diol mixture leaving only 5% epoxide remaining (Scheme 138).

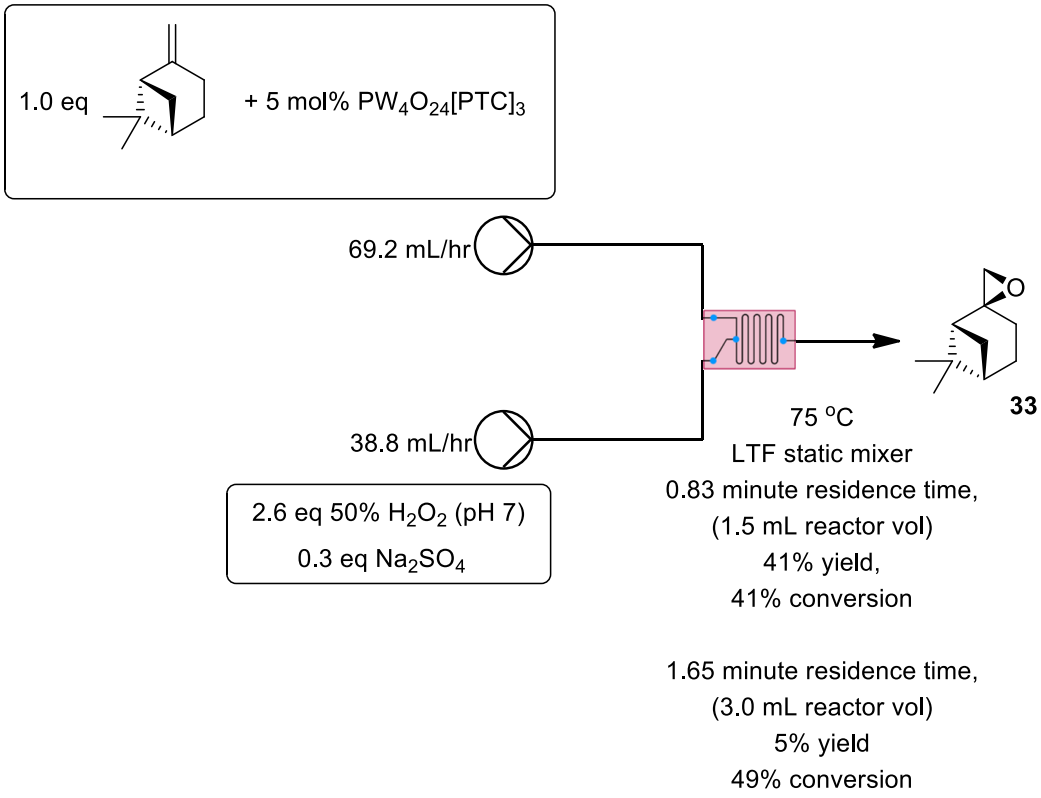

Scheme 138. Fast mixing β-pinene flow epoxidation conditions

3.4.2 CST flow Venturello epoxidation

Given the success of developing a flow protocol for epoxidation of limonene, 3-carene, α-pinene and β-pinene, it was next decided to attempt to epoxidise CST in flow, using a variety of conditions to analyse their effect on product selectivity (Scheme 139).

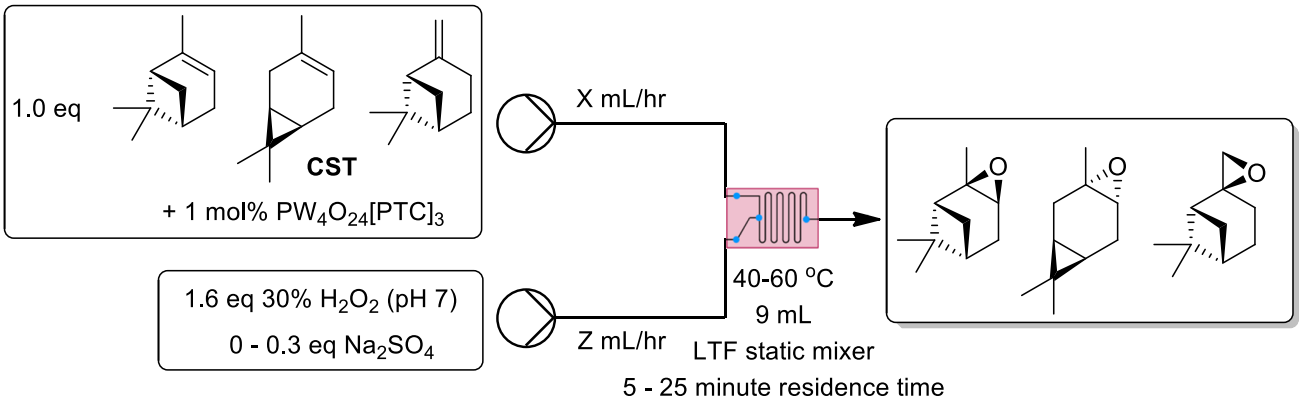

Scheme 139. CST flow epoxidation conditions

Initial flow experiments were performed using 1 mol% catalyst, no Na_2SO_4 salt and a temperature of 40 °C with a 20 minute residence time which led to formation of 47% 3-carene epoxide, 14% α-pinene epoxide and 18% β-pinene epoxide, after 20 minutes.

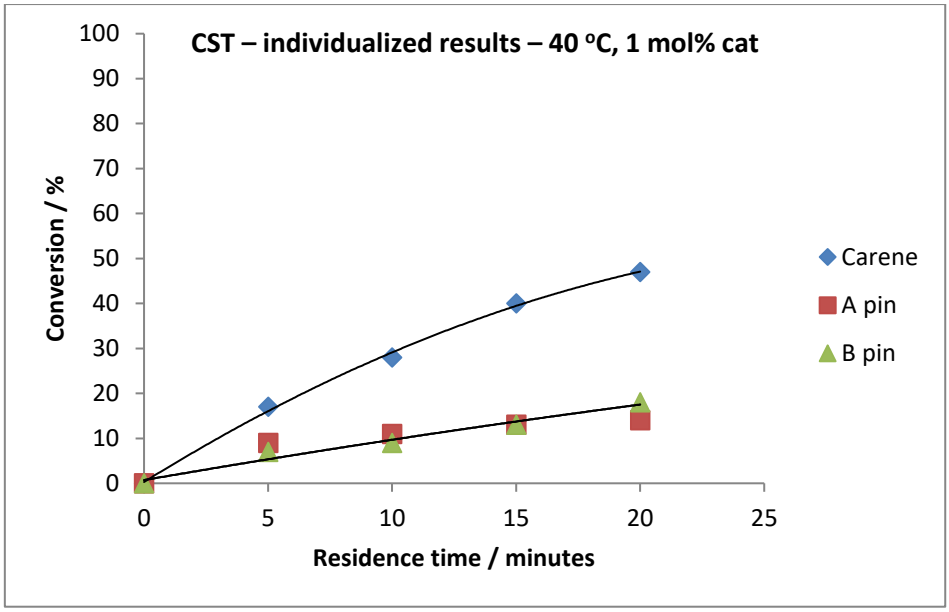

Figure 40. Flow epoxidation of CST at 40 °C

The temperature of the flow epoxidation reaction using 1 mol% catalyst was then increased to 60 °C to increase the rate of epoxidation of the bicyclic α-pinene and β-pinene components of CST. Both did not achieve 100% conversion of the CST starting materials with significant amounts of the pinene components still remaining whilst 40% of the 3-carene component was converted into its corresponding epoxide (Figure 40), however < 20% of the α-pinene and β-pinene components were consumed.

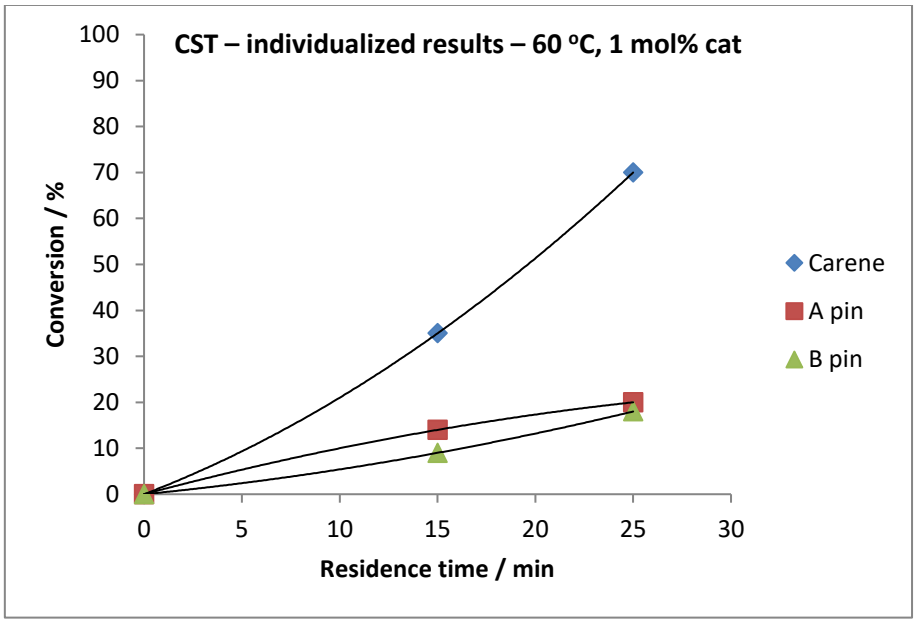

Figure 41. Flow epoxidation of CST at 60 °C

A final experiment was then performed using 5 mol% Venturello catalyst, (1.6 eq 30% H_2O_2, 0.3 eq Na_2SO_4) in an attempt to reach full conversion of each CST component within a shorter residence time, with the aim of minimising epoxide degradation (Figure 41).

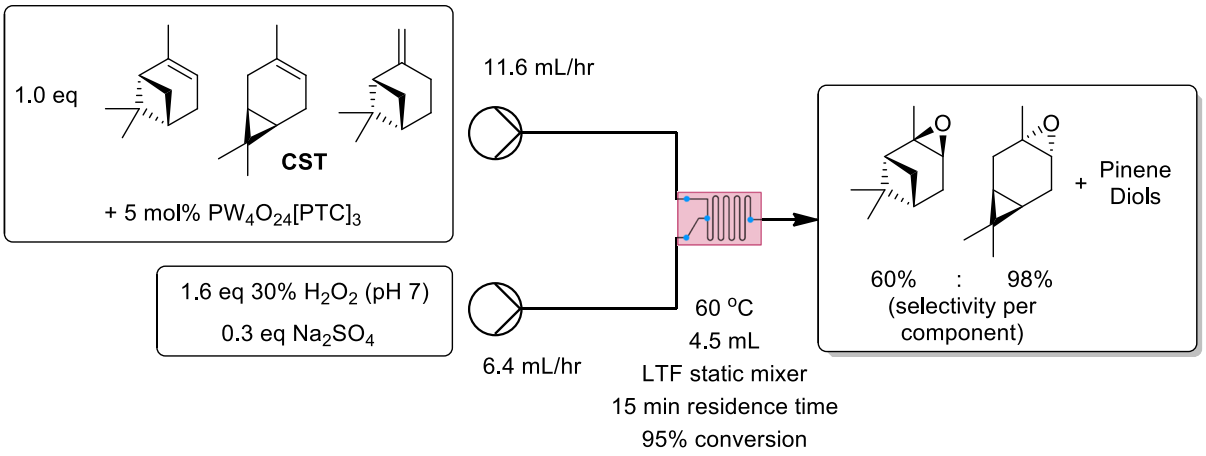

Scheme 140. Flow epoxidation of CST using high catalyst loadings

To our delight, this flow reaction resulted in 98% conversion to 3-carene epoxide and 60% conversion to α-pinene epoxide, however, the β-pinene epoxide proved too unstable under these conditions being converted to its corresponding diol (Scheme 140).

Alternatively, if only 3-carene epoxide is desired, without any α-pinene epoxide being present, the flow reaction can be left longer (25 minutes) which results in full degradation of α-pinene epoxide to its corresponding diol mixture leaving, allowing 3-carene epoxide to be isolated in a 90% yield (Scheme 141).

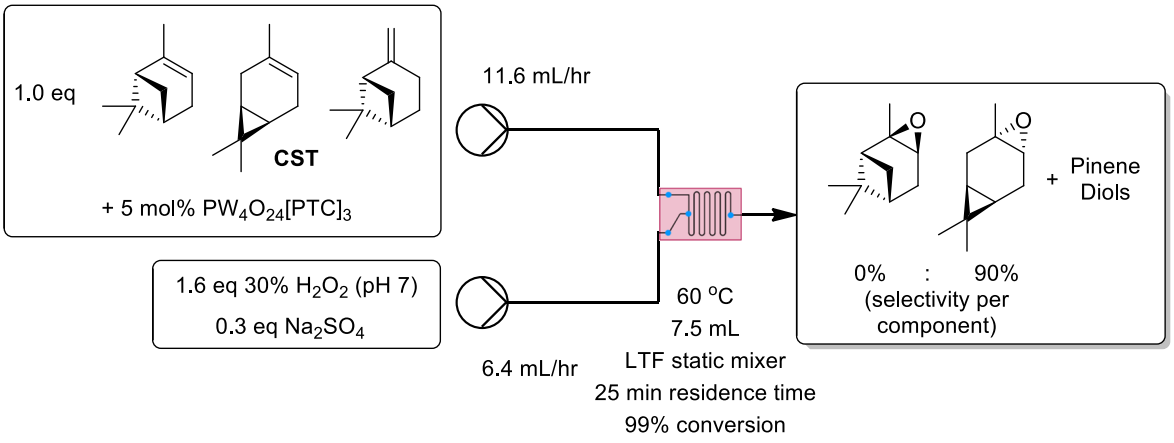

Scheme 141. Flow epoxidation of CST using high catalyst loadings to afford good yields of 3-carene epoxide

3.5 Conclusions

A preformed Ishii-Venturello-A336 catalyst has been used for flow epoxidations of a range of monoterpene substrates using LTF static mixer glass reactors in short reaction times, in an operationally simple two-feed flow set-up and can be used to prepare large volumes of epoxides in a safe and efficient manner.

This flow epoxidation protocol was applied for the epoxidation of bulk terpenes limonene, 3-carene with complete conversion being achieved using 3 mol% Ishii-Venturello catalyst and 1.6 eq H_2O_2 after 15 minute and 30 minute residence times respectively (Figure 42).

A novel “flash” epoxidation protocol for the epoxidation of β-pinene gave a 55% yield of β-pinene epoxide that occurred in a short reaction time (1.65 minutes in flow *vs* 7 h in batch). CST has also been epoxidised in flow for the first time with simultaneous epoxidation/de-sulfurization occurring to afford either 3-carene epoxide, or a mixture of 3-carene and α-pinene epoxides respectively.

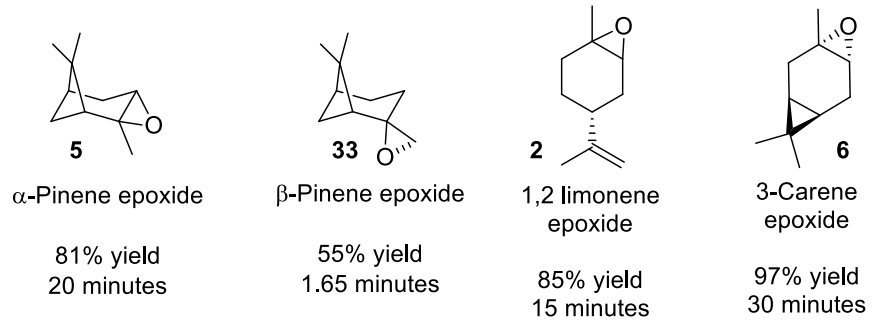

Figure 42. Range of commercially available terpene epoxides prepared *via* epoxidation using the Flow Venturello-A336 catalyst/H_2O_2 protocol under solvent free conditions.

4 Chapter 4 - Catalytic *anti*-diol synthesis from renewable terpenes and non-renewable organic substrates using Venturello-A336 protocol

We next turned our attention to developing 'one-pot' methodology (Scheme 142) that would enable the Venturello/H_2O_2 catalyst to be used for the direct catalytic dihydroxylation of the alkene bonds present in terpene substrates. This would involve optimisation of the minor reaction pathway that that was first observed during epoxidation of limonene (buffer free), that led to the unwanted formation of *anti*-diols in 25% yield.

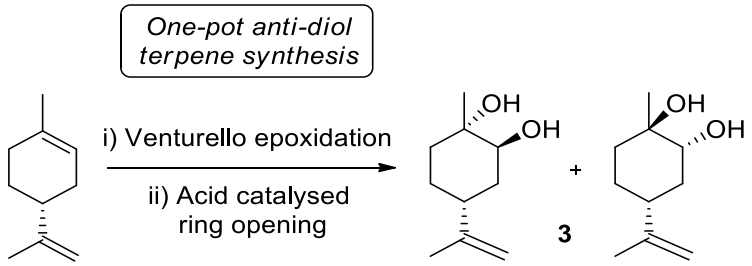

Scheme 142. Envisioned one-pot epoxidation-hydrolysis protocol for terpene substrates

4.1 Importance and uses of vicinal 1,2-Diols

1,2 diols, also known as vicinal diols, are important chemical products, for example, ethylene glycol and propylene glycol (Figure 43) are prepared on a multi-million tonne scales per year for use as anti-freeze agents, or as monomers for polymer manufacture. 1,2 Diols can potentially occur in either their *syn* or *anti* forms (Figure 44).

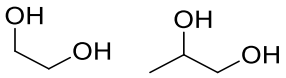

Figure 43. Structure of industrially important vicinal diols

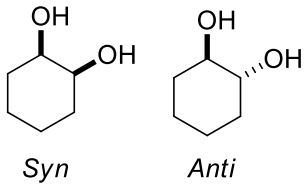

Figure 44. Diastereomeric *syn* and *anti* vicinal diols

1,2-diols are common structural motifs found in pharmaceuticals and natural products as shown in Figure 45. For example, the non-steroidal anti-inflammatory drug Flocafenine and the expectorant Guaifenisin drug contain terminal 1,2 diol motifs (Figure 45).[173] The pharmaceutical Remikiren contains a 1,2-*anti*-diols which is a potent active renin inhibitor that is used to treat hypertension.[174] The natural products Deoxyaltronojirimycin[175] and Hedycoropyran[176] are glycosidase inhibitors that contain both *syn*- and *anti*-diol fragments, (Figure 45).

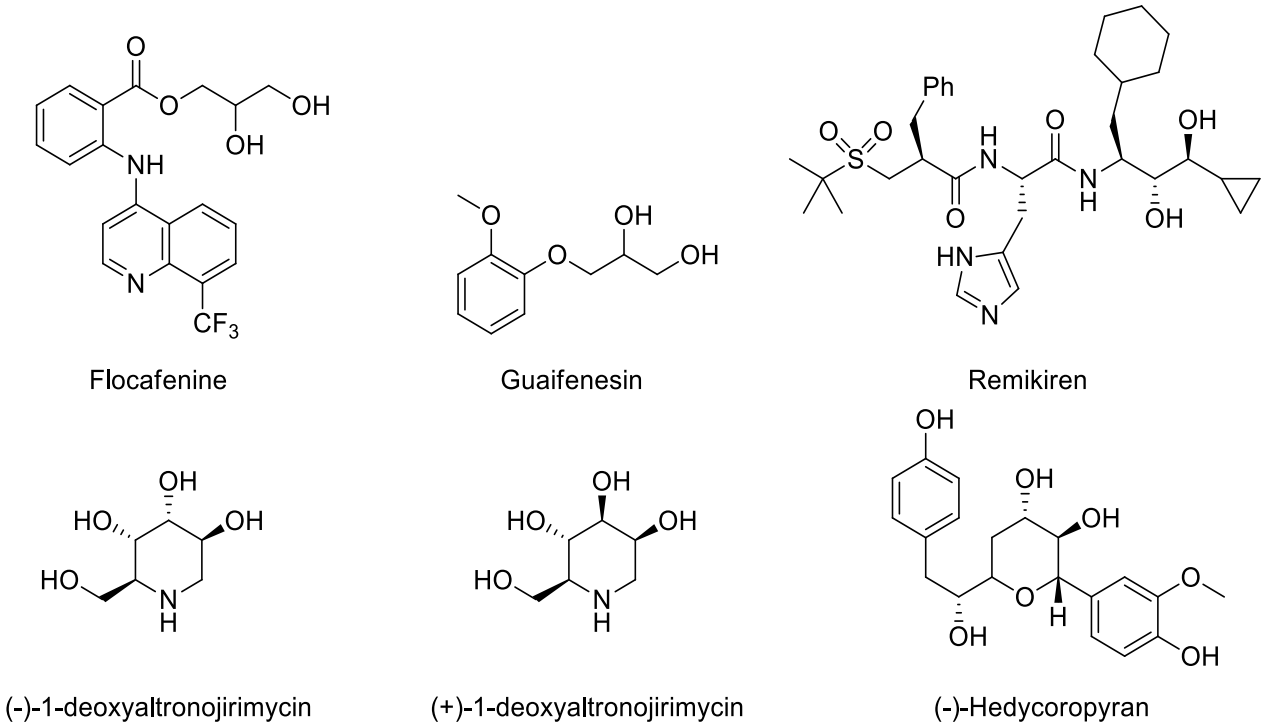

Figure 45. *Syn* and *anti* vicinal diols present in a range of natural products and pharmaceuticals

4.1.1 Methodologies for the synthesis of *syn*- and *anti*-diols

A number of highly effective stoichiometric and catalytic methods have been developed for the direct dihydroxylation of alkenes to afford *syn*-diols in good to excellent yields. Historically, stoichiometric metal based reagents were used for the dihydroxylation of alkenes, with potassium permanganate and osmium tetroxide traditionally employed as stoichiometric oxidants, under relatively dilute conditions (See Scheme 143).[25]

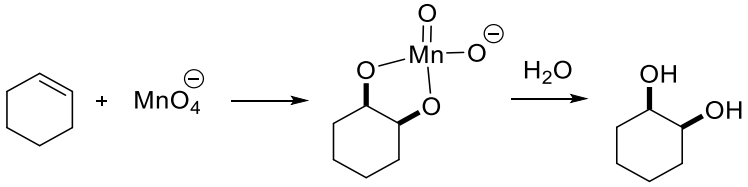

Scheme 143. Permanganate mediated dihydroxylation

These stoichiometric oxidants were superseded by the development of the Upjohn dihydroxylation process which involves the use of catalytic osmium tetroxide in the presence of a stoichiometric amount of *N*-methylmorpholine-*N*-oxide (NMO) or (Fe^{3+}) as a sacrificial re-oxidant. The concerted cycloaddition dihydroxylation mechanism results in both oxygen atoms simultaneously attacking the electrophile to afford an osmate ester of OsO_4 that is then hydrolysed by water to produce a *syn* diol. The role of stoichiometric NMO or Fe^{3+} is to re-oxidize the Os(VI) into the active Os(VIII) form, which enables it to be used in catalytic amounts, which is beneficial from economic green and toxicity perspectives (Scheme 144).[177]

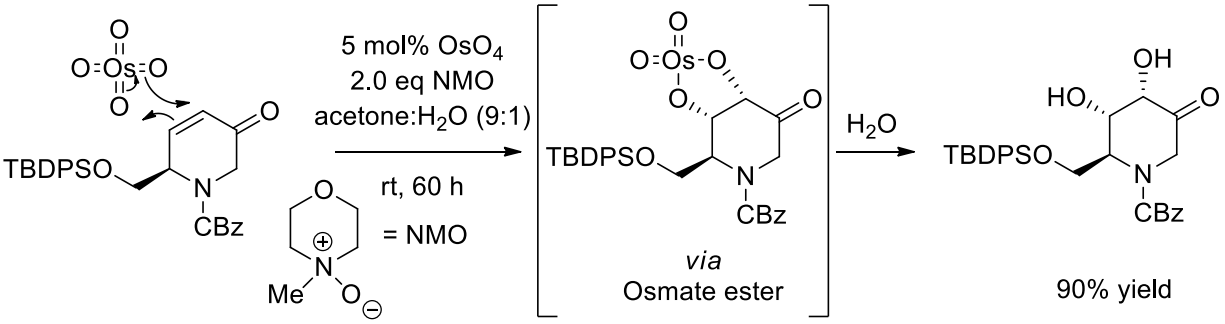

Scheme 144. OsO_4 catalysed Upjohn dihydroxylation reaction

The stereochemistry of the diol produced from acyclic alkenes depends upon the geometry of the alkene, with *syn* dihydroxylation of an (*E*)-alkene affording a *cis*-diol, whilst *syn*-dihydroxylation of a (*Z*)-alkene results in a *trans*-diol (Scheme 145).

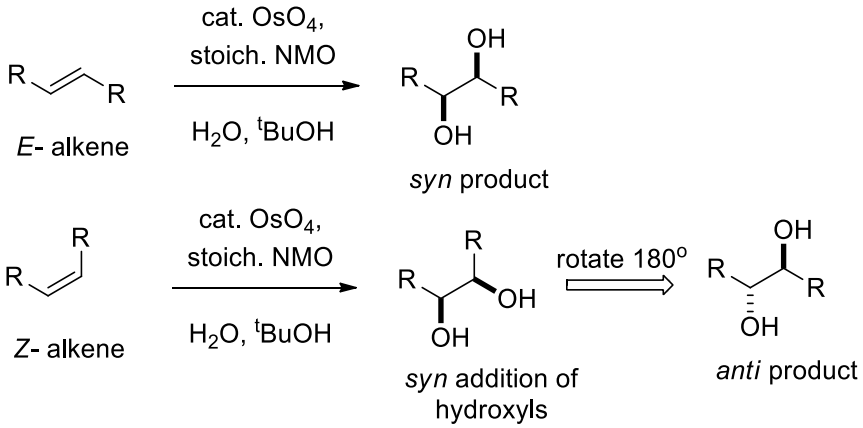

Scheme 145. Diol stereochemistry dependent on the geometry of the alkene starting material

Representative examples developed by Shing *et al*[178] of a related ruthenium catalysed *syn* dihydroxylation reaction demonstrate how *E*- and *Z*- alkenes can be used to prepare *syn*- and *anti*- diols respectively (Scheme 146).

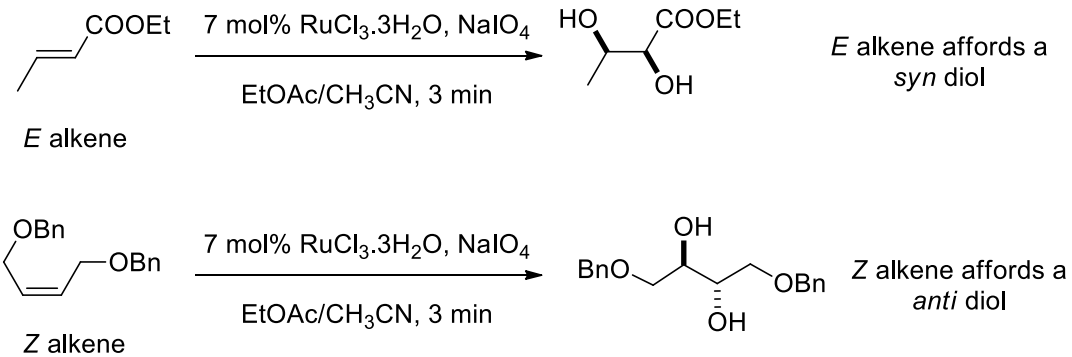

Scheme 146. *Syn*-dihydroxylation strategy for the synthesis of *syn*- and *anti*- diols.

Asymmetric dihydroxylation reactions can be performed using catalytic osmium tetroxide when combined with chiral ligands such as DHQ or DHQD, with these tertiary amine ligands that not only providing a chiral environment, but also accelerating the rate of the

dihydroxylation reaction. Dihydroxylation reagent kits are available commercially as AD-mixes with the AD-mix-α containing DHQPHAL and AD-mix-β containing $DHQD_2PHAL$ (both structures shown in Figure 46).[179] The use of these chiral reagents for the enantioselective dihydroxylation of trans-stilbene highlights why this methodology is one of the most widely used enantioselective catalytic transformations (Scheme 147).[179]

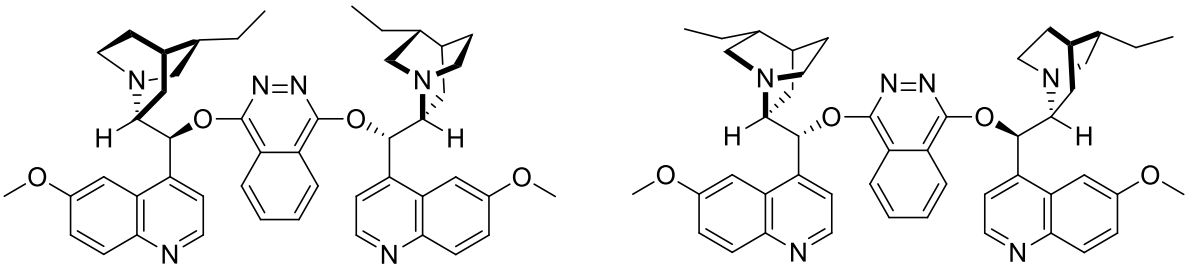

$(DHQD)_2PHAL$
dihydroquinine / phthalazine
based ligand

$(DHQ)_2PHAL$
dihydroquinine / phthalazine
based ligand

Figure 46. $(DHQD)_2PHAL$ and $(DHQ)_2PHAL$ ligand contained in AD-mix-β

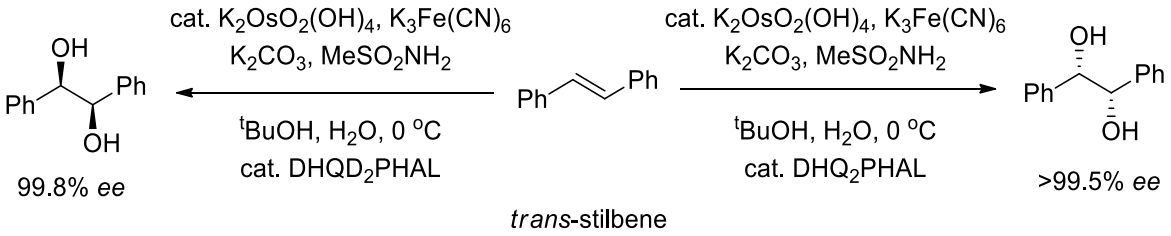

Scheme 147. Asymmetric dihydroxylation of *trans*-stilbene

Niggemann *et al*[180] have developed cheap low loading ruthenium catalysed *syn* dihydroxylation methodology that is considered to produce a cleaner, less toxic waste stream, when compared to osmium catalysed methods. However, it should be noted that this catalyst needs to be activated using 20 mol% H_2SO_4, which makes the workup of the reaction more process intensive (Scheme 148).[180]

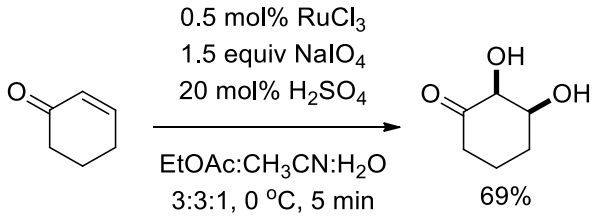

Scheme 148. Ruthenium catalysed *syn*- selective dihydroxylation

Routes for the direct *anti* dihydroxylation of alkenes are less well developed however, with only a handful of catalytic approaches currently available, based on the use of tandem metal/acid catalysed epoxidation-hydrolysis, or biocatalytic protocols (Scheme 149). The

Prevost reaction is a traditional stoichiometric method for producing *anti*-diols, involving treatment of an alkene with iodine and silver benzoate.[25] However, this method requires the use of expensive stoichiometric silver reagents and halides, which generate large amounts of waste (Scheme 150).[25, 181]

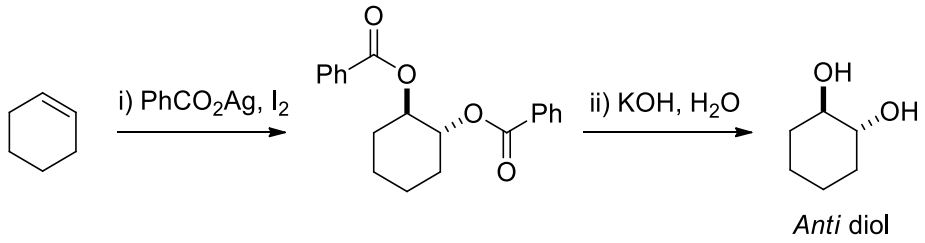

Scheme 149. Prevost conditions for the synthesis of *anti*-diols

.

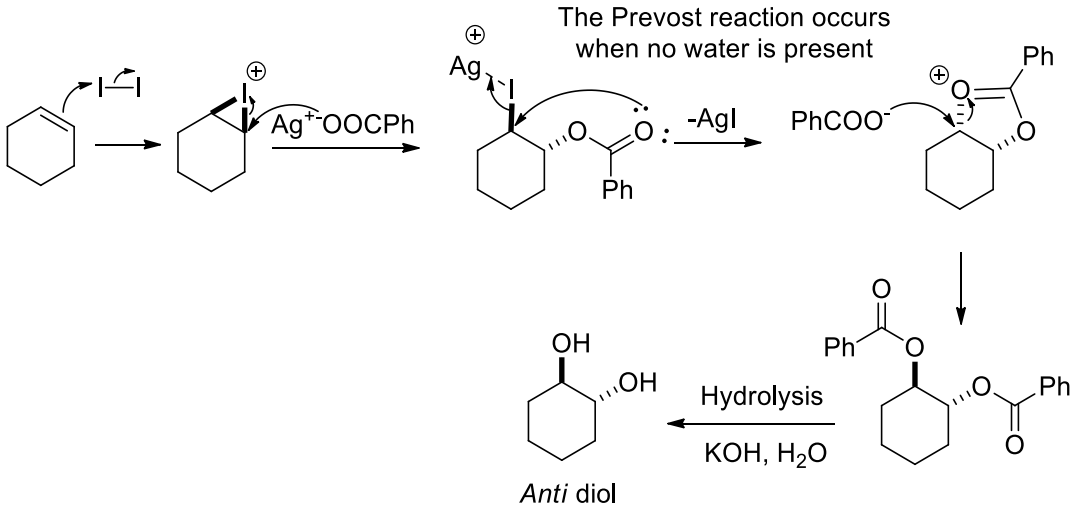

Scheme 150. Mechanism of the Prevost reaction

The Woodward modification of this silver based methodology (Scheme 151)[181], involves addition of water to the reaction mixture which intercepts the benzoxonium intermediate to produce a mono-ester that is then hydrolysed to afford the alternative *syn*-diol product.

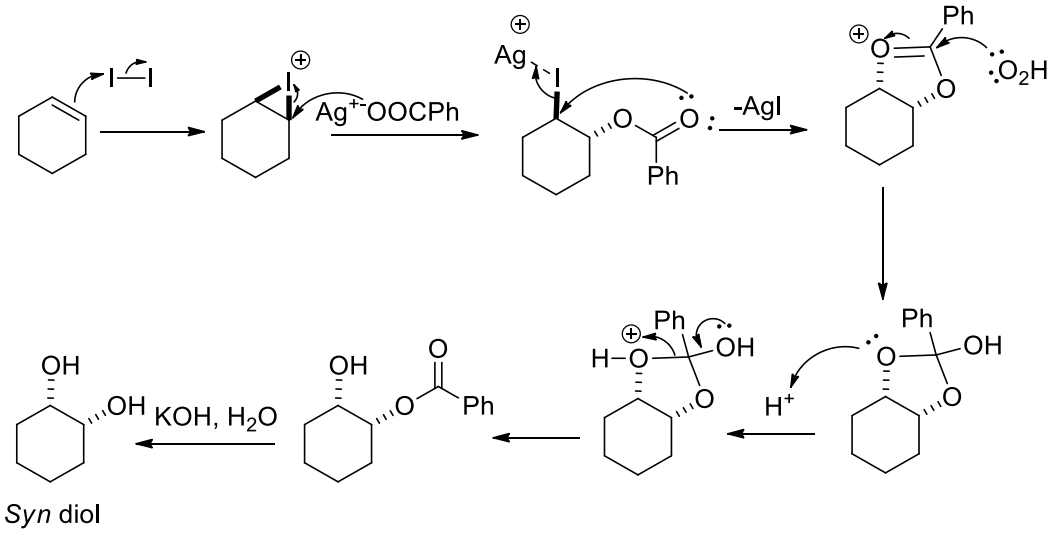

Scheme 151. Mechanism of Woodward modification of the Prevost reaction

Sudalai *et al*[181] have developed a catalytic version of the Prevost-Woodward process using catalytic LiBr alongside a stoichiometric oxidant at elevated temperatures in acetic acid. They found that changing the type of oxidant used in these dihydroxylation reactions enabled either *syn* diols ($NaIO_4$) or *anti* diols ($PhI(OAc)_2$) to be obtained. Excellent selectivity for each class of diol was achieved, however, high temperatures and long reaction times were needed to form the reactive intermediates required for dihydroxylation to occur (Scheme 152).[181]

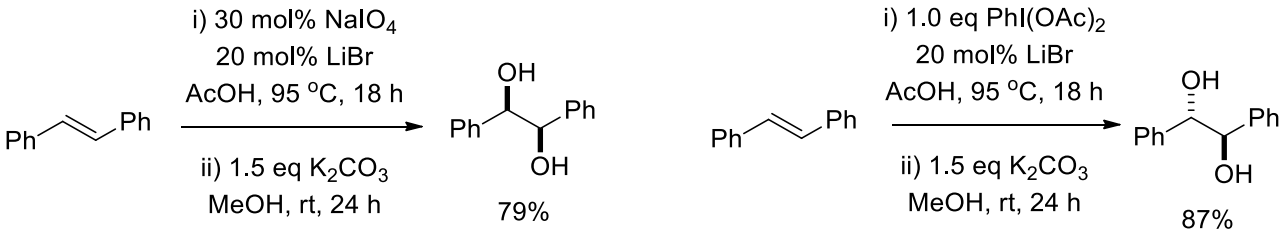

Scheme 152. Catalytic Prevost-Woodward reaction

A recent modification to the Prevost dihydroxylation method has been developed by Tomkinson *et al*[182] involving the use of cyclopropyl malonyl peroxide as a dihydroxylating agent. As shown in Scheme XX, this method is selective and high yielding for the formation of *anti*-diols from a range of alkenes, but requires elevated temperatures, lengthy reaction times and use of stoichiometric amounts of malonyl peroxide and acid (Scheme 153).[182]

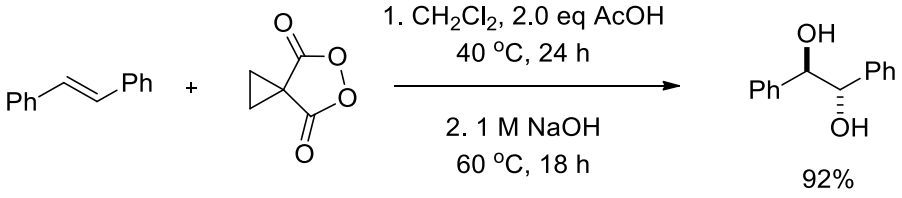

Scheme 153. Tomkinson's *anti*-dihydroxylation method using malonyl peroxides

Tomkinson suggested the following mechanism for the malonyl peroxide mediated *anti*-dihydroxylation reaction. The electron rich alkene reacts with the malonyl peroxide to break the weak oxygen-oxygen bond with its carboyl group then forming a bond to the unstable

secondary carbocation to form a cyclic dioxonium species. Acetic acid then attacks the dioxonium intermediate to afford a non-symmetric bis-ester that then undergoes hydrolysis to give the *anti* diol product (Scheme 154).[182]

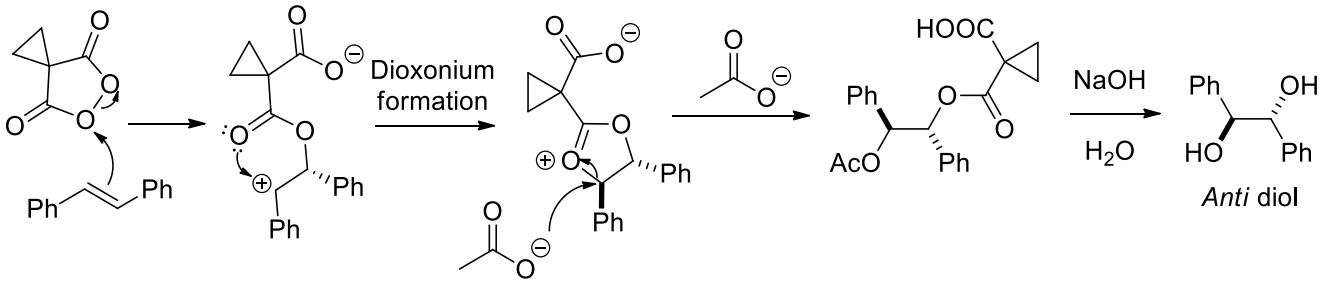

Scheme 154. Mechanism of Tomkinson's *anti* dihydroxylation protocol

4.1.1.1 Synthesis of anti-diol from alkenes via hydrolysis of epoxide intermediates

A common two step method of preparing *anti*-diols involves, treatment of an alkene with a suitable oxidant to afford an epoxide that is then ring opened with water under either acid or base catalysed conditions. This approach often combines a stereoselective epoxidation reaction with a regioselective epoxide ring opening reaction to afford an *anti*-diol as a single diastereoisomer, as shown for synthesis of the piperidine diol shown in Scheme 155.

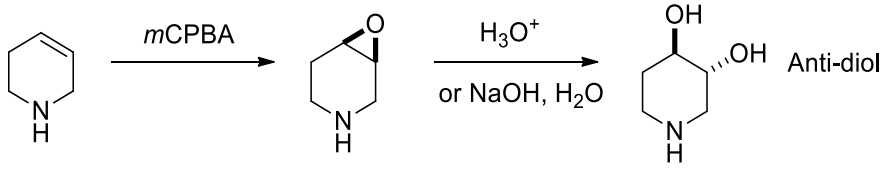

Scheme 155. Epoxide ring opening to *anti*-diols

Selective epoxidation of 1-vinyl-3-cyclohexene has been performed using a combination of phthalic anhydride and 50% hydrogen epoxide.[183,184] with the epoxide product then treated with acid to form the cyclic *anti* diol product which was used for the synthesis of an anti-cancer agent (Scheme 156).

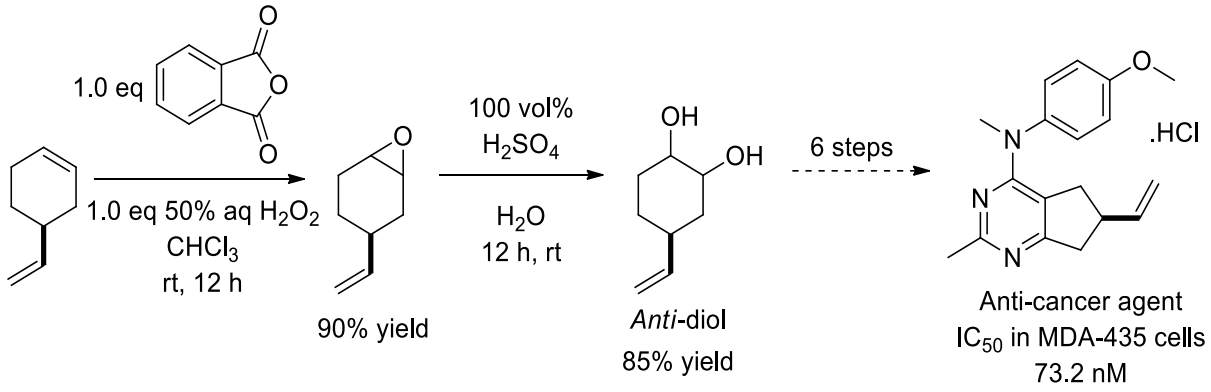

Scheme 156. Acid catalysed epoxide ring opening to *anti*-diolsStoichiometric methods for the synthesis of *anti*-diols

Savelli *et al*[185] published a one-pot two-step method for *anti*-diol formation in 1989, involving the use of stoichiometric *m*CPBA to epoxidise alkenes in water, followed by the addition of 10% aqueous sulphuric acid to afford an *anti*-diol (Scheme 157). This procedure was procedurally simple, fast and proceeded at room temperature, however a stoichiometric amount of *m*-chlorobenzoic acid is generated in the reaction, with lengthy neutralisation of the acid solution required during workup.

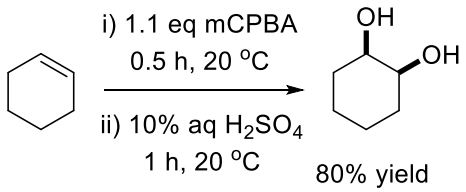

Scheme 157. Savelli's one-pot stoichiometric *anti*-diol synthesis procedure

In 1991 Zhu *et al*[186] reported the use of oxone in water as a method for *anti*-dihydroxylation of alkenes in an organic solvent free manner (Scheme 158). However, whilst this oxidant is commercially available, it is expensive and generates considerable amounts of waste, with high temperatures required to achieve high conversions, with DMDO unsuitable for scale up due to its unstable nature.

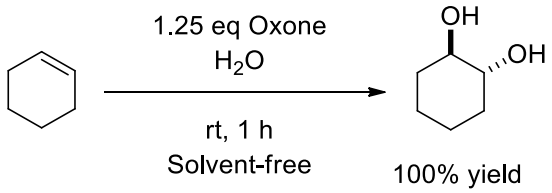

Scheme 158. Stoichiometric oxone mediated *anti*-dihydroxylation method

4.2 Catalytic methods for the synthesis of *anti*-diols

Konwar *et al*[187] developed a methodology for the synthesis of *anti*-diols from alkenes using catalytic selenium dioxide with hydrogen peroxide in 1,4-dioxane. They proposed that this combination of reagents generate perseleninic acid *in situ* which acts as the epoxidising reagent, followed by hydrolysis by water (Scheme 159). This methodology operates at mild temperatures, and tolerates a number of functional groups; however, only moderate yields of diols were achieved, with high loadings of the expensive and toxic catalyst required.

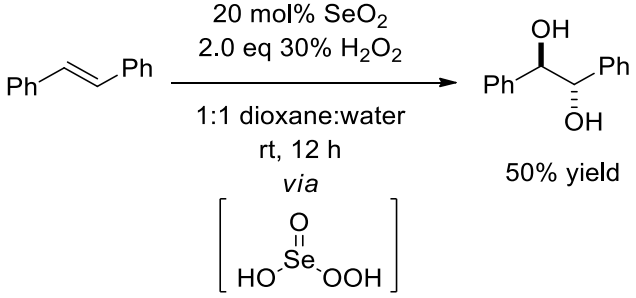

Scheme 159. Selenium catalysed *anti*-dihydroxylation reaction

Li *et al*[188] developed biocatalytic protocol to produce chiral *anti*-diols using an epoxide hydrolase from *Springomonas sp.* H*XN-200* that was expressed in *E.coli*. Excellent enantioselectivities were achieved using this methodology with the epoxides of 14 types of cyclic alkenes being ring-opened with good levels of stereocontrol (Scheme 160).

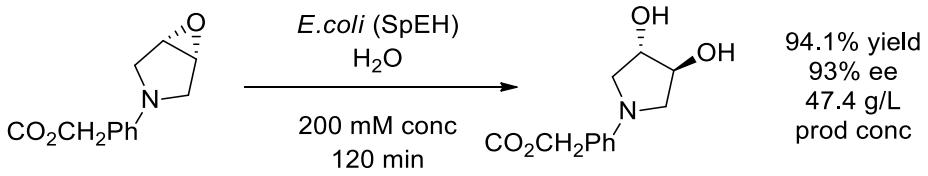

Scheme 160. Enantioselective hydrolysis of epoxides to *anti* diols using resting cells of *E. Coli (SpE*H*)*

Zhou *et al*[189] reported the use of MoO_3 for the synthesis of *anti*-diols from alkenes using *t*-butyl hydrogen peroxide as the oxidant, reporting a moderate aryl/alkyl alkene substrate scope, however this methodology was not suitable for the dihydroxylation of mono-substituted alkenes such as 1-hexene. However, they did report one example where this methodology was used to prepare the *anti* 1,2-diols of limonene in an acceptable 66% yield. This methodology required elevated temperatures over a 10 h period, using toluene as a solvent and a relatively large amount of MoO_3 catalyst (Scheme 161).

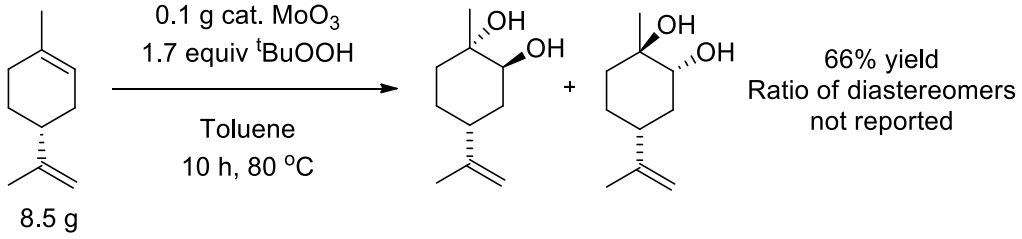

Scheme 161. MoO_3 catalysed *anti*-dihydroxylation of limonene

Sato *et al*[190] developed a one-pot *anti*-diol procedure in 2003 using Nafion NR50 to an acidic ion exchange catalyst in the presence of hydrogen peroxide at 70 °C for 20 h affording 1-hexene *anti*-diol in a relatively low 40% yield. Moderate yields were achieved with acyclic alkenes and higher yields obtained with more substituted alkenes such as cyclohexene. They proposed that the sulfonic acid reacted with hydrogen peroxide to form a sulphurous peracid *in situ* which epoxidises the alkene, with the sulfonic acid then catalysing ring opening of the epoxide by water to form the *anti*-diol (Scheme 162). This procedure is metal free and uses a solid supported acid catalyst that is easily recovered, however, elevated temperatures and extended periods of time were required with only moderate yields were acheived.[177] The use of Nafion NR50 is not ideal from an economic perspective; due to the high cost of Nafion NR50 (£10.00 per 1 g) compared to Amberlyst-15 (£0.05 per 1 g).

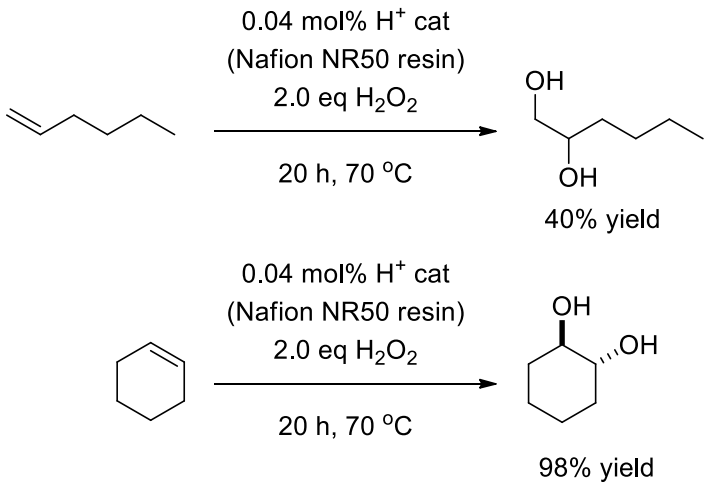

Scheme 162. Sato's one-pot protocol for the synthesis of non-terpene *anti*-diols

Afonso *et al*[177] have employed 20 mol% PTSA as a homogenous acid catalyst in the presence of hydrogen peroxide for the *anti*-dihydroxylation of alkenes under solvent free conditions. This method required elevated temperatures of 50 °C for long periods of time, but achieved excellent yields of *anti*-diols for a range of alkyl and aryl alkene substrates. They also developed a method for recycling the acid catalyst by reusing the aqueous layer for epoxidation of an alkene using a fresh amount of hydrogen peroxide, with seven rounds of catalyst recycling performed without any significant loss in activity (Scheme 163).

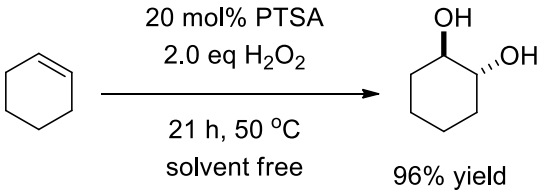

Scheme 163. Solvent free acid catalysed *anti*-dihydroxylation using PTSA catalysis

Kokotos *et al*[191] reported an organo-catalytic method for *anti*-dihydroxylation of homoallylic and aryl alkenes using hydrogen peroxide as oxidant in the presence of 2,2,2-trifluoroacetophenone in acetonitrile at mild temperatures. Large equivalents of hydrogen peroxide were required for all substrates, with two equivalents of camphor sulphuric acid required to ring open the epoxide intermediate species. Only one terpene, limonene, was dihydroxylated with no selectivity for its alkene bonds, resulting in a mixture of its corresponding tetrol product as a mixture of diastereomers in 61% yield (Scheme 164).

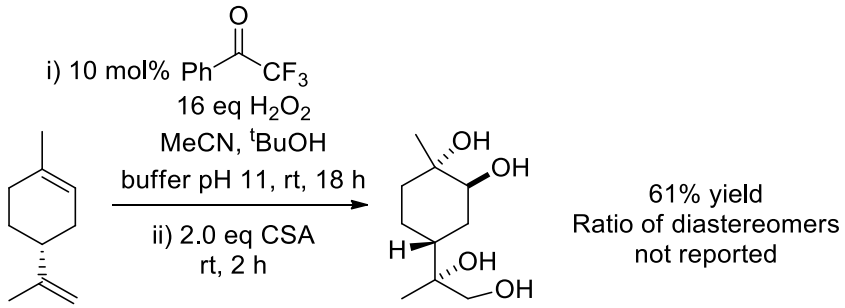

Scheme 164. Organocatalytic *anti*-dihydroxylation reaction of limonene

Saladino *et al*[192] inadvertently developed an *anti*-dihydroxylation protocol using catalytic microencapsulated MTO with hydrogen peroxide whilst attempting to develop an effective epoxidation methodology. The MTO catalyst was highly active with its Lewis acidic properties leading to competing ring-opening of the epoxide intermediates with water to afford *anti*-diol products. Three terpene substrates were dihydroxylated using this methodology with 3,4-carene *anti*-diol, 1,2-limonene *anti*-diols and α-pinane *anti*-diol being produced in 78%, 63% and 75% yields respectively (Scheme 165).

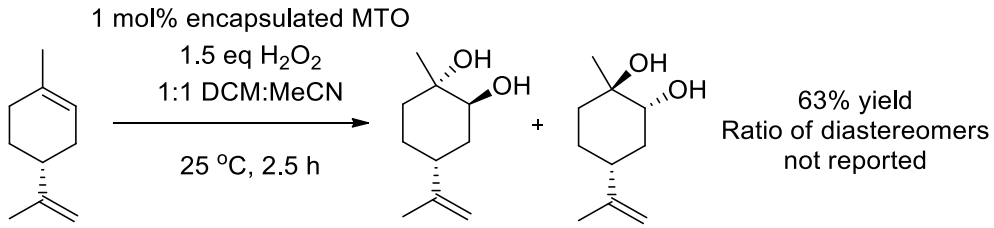

Scheme 165. MTO catalysed *anti*-dihydroxylation of limonene

4.2.1.1.1 Tungsten catalysed synthesis of *anti*-diols

The first reported example of using tungsten catalysts for the dihydroxylation of alkenes was reported by Singh *et al*[193] in 1989, who used high loadings of tungstic acid with hydrogen peroxide in *tert* butyl alcohol to *anti*-dihydroxylate cyclooctadiene in 65% yield (Scheme 166).

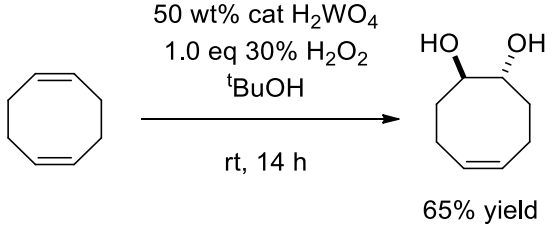

Scheme 166. Dihydroxylation using tungstic acid and hydrogen peroxide

Venturello *et al*[194] then published that low loadings of a preformed Venturello-PTC catalyst could be used for tungsten catalysed *anti*- dihydroxylation reactions under acidic conditions using benzene as a solvent for 6 out of the 10 substrates that were dihydroxylated. A limited

range of alkyl- and aryl alkenes were screened (Scheme 167), however no examples of using this protocol for the dihydroxylation of any terpene substrates was reported.

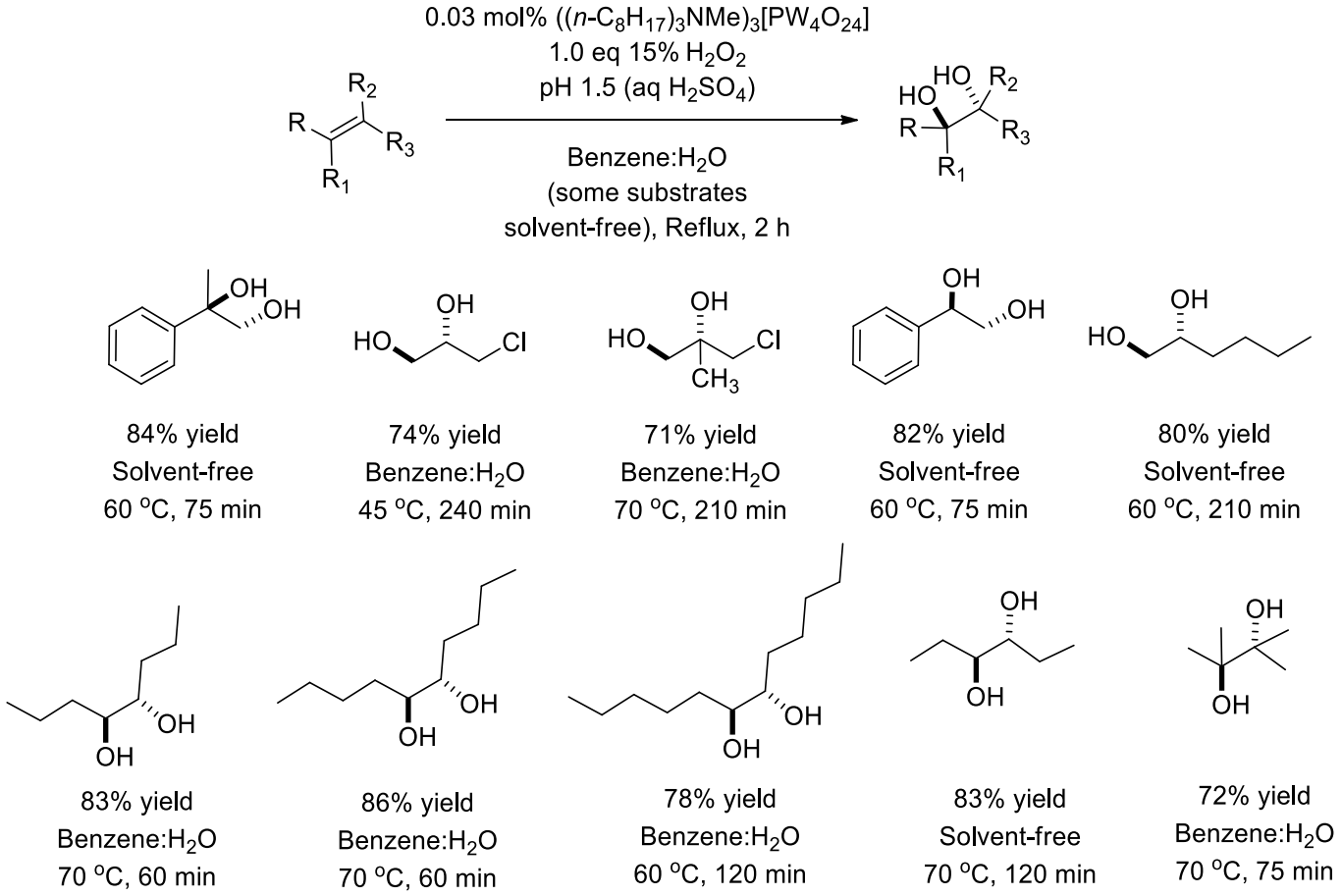

Scheme 167. First use of the Venturello catalyst in a one-pot *trans* dihydroxylation protocol

Given the promising results we had observed with the use of our preformed Ishii-Venturello catalyst for epoxidation reactions that afforded *anti*-diols as by-products under more forcing conditions, it was therefore decided to see whether we could optimise a one-pot epoxidation-hydrolysis reaction, to enable terpene *anti*-diols to be produced as major products.

4.3 A one-pot Ishii-Venturello/H_2O_2 protocol for catalytic *anti*-dihydroxylation of the alkene bonds of terpene feedstocks.

During our optimisation studies into the Ishii-Venturello catalysed epoxidation reaction of limonene, it was found that the use of unbuffered hydrogen peroxide led to formation of large amounts of diols (3) (ca. 25%) that were produced as by-products from hydrolysis of their parent epoxides (2). It was hypothesised that the presence of the acidic stabiliser (0.5 ppm stannate-containing compounds and 1 ppm phosphorus-containing compounds used to stabilize the solution [pH of 3-4]) in commercial hydrogen peroxide was causing acid catalysed ring opening of the epoxide by water present in the aqueous peroxide solution. Significant diol formation was also observed during optimisation of the batch scale-up reaction of the epoxidation of limonene, with the first uncontrolled 5 g scale reaction (non-dropwise addition

of hydrogen peroxide) leading to a thermal runaway that led to large amounts of limonene diol formation (Scheme 168).

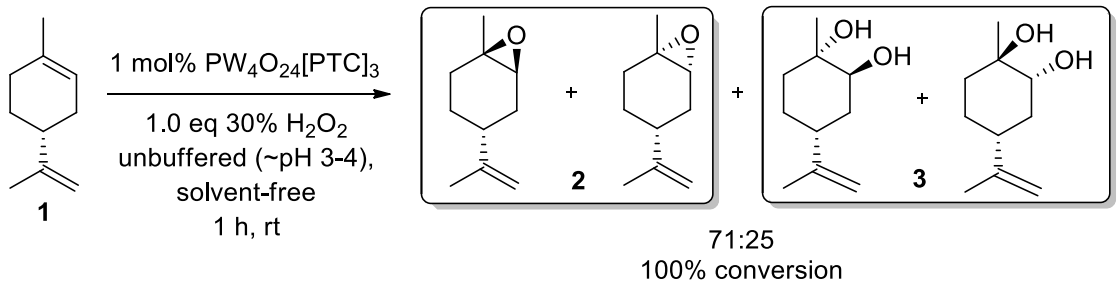

Scheme 168. Venturello epoxidation of limonene using unbuffered H_2O_2.

Both these experiments demonstrated that limonene epoxides were susceptible to ring-opening under acid catalysis, and so it was decided to optimise this 'side-reaction' to develop a one-pot method for the synthesis of terpene *anti*-diols. Catalytic two-step epoxidation-hydration reaction would exclusively afford *anti*-1,2-diols in a one-pot manner, using hydrogen peroxide as a green oxidant, would be extremely attractive. Since, our initial unbuffered epoxidation reactions had resulted in 25% of the limonene epoxide being hydrolysed, it was envisaged that using unbuffered hydrogen peroxide in the presence of an acid catalyst and/or elevated temperatures would result better yields of diol products.

As we wanted our methodology to be as operationally simple as possible we wanted to minimize liquid acid handling and any extra neutralisation steps required before workup of the dihydroxylation. Consequently, it was decided to use Amberlyst-15 (£0.05 per 1 g) as a cheap solid supported acid catalyst to catalyse ring-opening of the epoxide *in situ*.

Amberlyst-15 is a sulfonated styrene polymer (Figure 47) with a macromolecular structure containing pores that allow easy access of gases and liquid reactants to their strongly acidic sulfonic groups. This resin was developed as a heterogeneous catalyst for a variety of acid catalysed reactions (e.g. alkylations, etherifications and esterifications) as an environmentally benign, commercially available heterogeneous acid that is easy to handle and recycle multiple times.

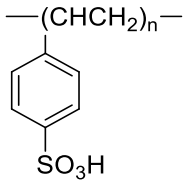

Figure 47. Molecular structure of Amberlyst-15 resin

Our first dihydroxylation optimisation experiment using Amberlyst-15 as an acid catalyst was performed under solvent-free conditions, with limonene first being reacted with 1 mol% of the Ishii-Venturello catalyst in the presence of 1.0 eq of H_2O_2 which resulted in complete consumption of the limonene starting material. 0.13 mol% (140 mg on 5 mmol scale) of Amberlyst-15 (4.6 mmol/g)[195] was then added to the reaction mixture (5 mmol of limonene) and the reaction mixture stirred vigorously, which resulted in hydrolysis of the limonene epoxides to afford its corresponding diols. However, it was found that as the amount of diol present in the reaction increased to beyond 25%, then the viscosity of the reaction increased

to the extent where stirring of the reaction became impossible, with the amount of epoxide hydrolysis then stalling at around 50% conversion (Scheme 169).

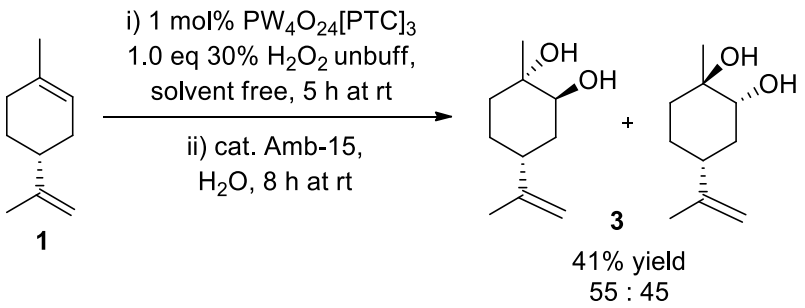

Scheme 169. One-pot solvent free epoxidation-hydrolysis reaction of limonene

Consequently, the epoxidation reaction was repeated on a 5 mmol scale, in the presence of 1.0 mL (10 mmol, 2.0 eq) of ethyl acetate as a co-solvent, which allowed for efficient stirring in the second hydrolysis step, of the reaction after the Amberlyst-15 had been added. The use of Amberlyst-15 also made the workup of this reaction simple, which required no need for neutralisation with base, with filtration of the reaction allowing for the Amberlyst-15 resin to be recovered. Addition of ethyl acetate (10 mL) followed by drying of the organic layer with $MgSO_4$ and removal of solvent *in vacuo*, afforded 1,2-limonene diol in an isolated 76% yield, with <5% of limonene, limonene epoxide or limonene tetrol being present (Scheme 170).

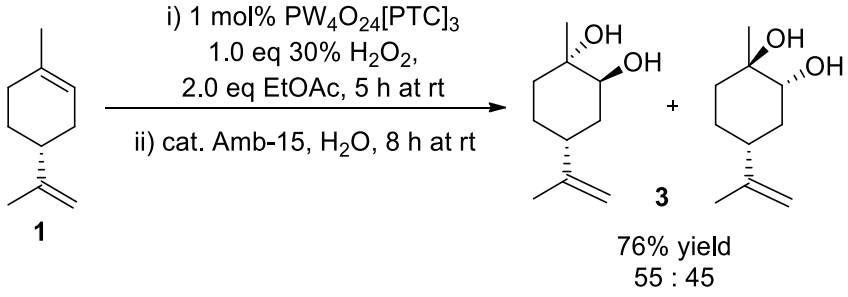

Scheme 170. One-pot catalytic methodology for the synthesis of 1,2-limonene diol

Scheme 171 shows the proposed mechanism for the acid catalysed ring opening of 1,2-limonene epoxide to the corresponding *anti*-diol product, with protonation of the lone pair of the epoxide oxygen resulting in ring-opening due to nucleophilic attack of water at the tertiary carbon occurring with inversion of configuration.

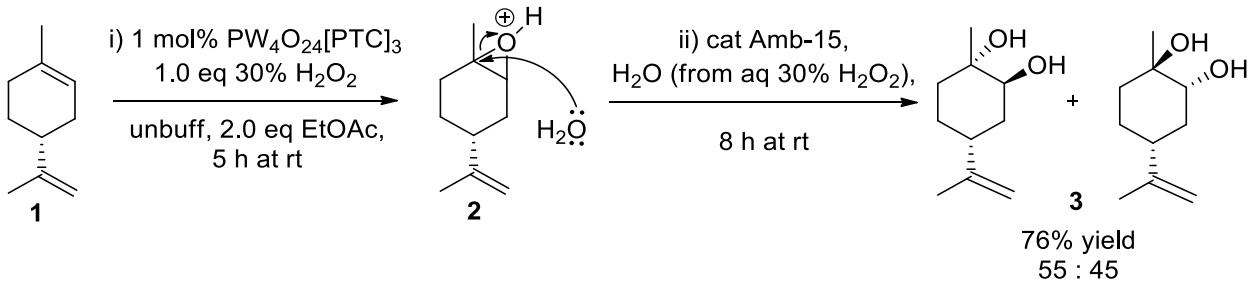

Scheme 171. One-pot solvent free epoxidation-hydrolysis protocol for the synthesis of 1,2-limonene *anti*-diol

Other catalytic methods have been used to synthesise *anti* 1,2- limonene diol, however, they all have various weaknesses. Liu *et al*[196] developed a polymer supported rhenium catalysed protocol using a similar biphasic system to afford *anti* 1,2- limonene diol in a lower 62% yield in 48 h using a more expensive catalyst. This method used an expensive rhenium based catalyst and $KHSO_5$ as an expensive and corrosive oxidant that generated stoichiometric amounts of acidic waste.[196] Balula *et al*[197] reported the synthesis of 1,2-limonene *anti*-diol in 48% yield using a silica supported phosphotungstate catalyst and 4.5 eq of oxidant hydrogen peroxide in acetonitrile for 24 h. Hugel *et al*[198] have developed a two-step stoichiometric route to *anti* 1,2-limonene diol in a 47% yield over two steps using stoichiometric *m*CPBA in DCM followed by treatment with AcOH/NaOAc. In comparison, our new one-pot Ishii-Venturello/H_2O_2 protocol is more convenient, with both epoxidation and ring opening steps occurring in a one pot manner, using a dihydroxylation process that employs a cheap catalyst and oxidant. It creates no waste, requires no neutralisation step or halogenated solvent, employs only 2.0 eq of a low environmentally impacting co-solvent and the water nucleophile coming from aqueous 30% H_2O_2.

1,2-limonene-*anti*-diol has a number of important applications for the synthesis of monomers for polymer synthesis, with limonene carbonate[126] having been used as a monomer for bio-based polycarbonate synthesis.[76] Alternatively, the epichlorohydrin strategy developed by Jaffe *et al*[199] could be applied to limonene diol to attach two epoxy moieties that could then be reacted with polyamines to form bio-based thermoset polymers. Natural products such as vinyldecalin[200] and bio-based insect repellents[201] have also been prepared using limonene diol (Scheme 172).

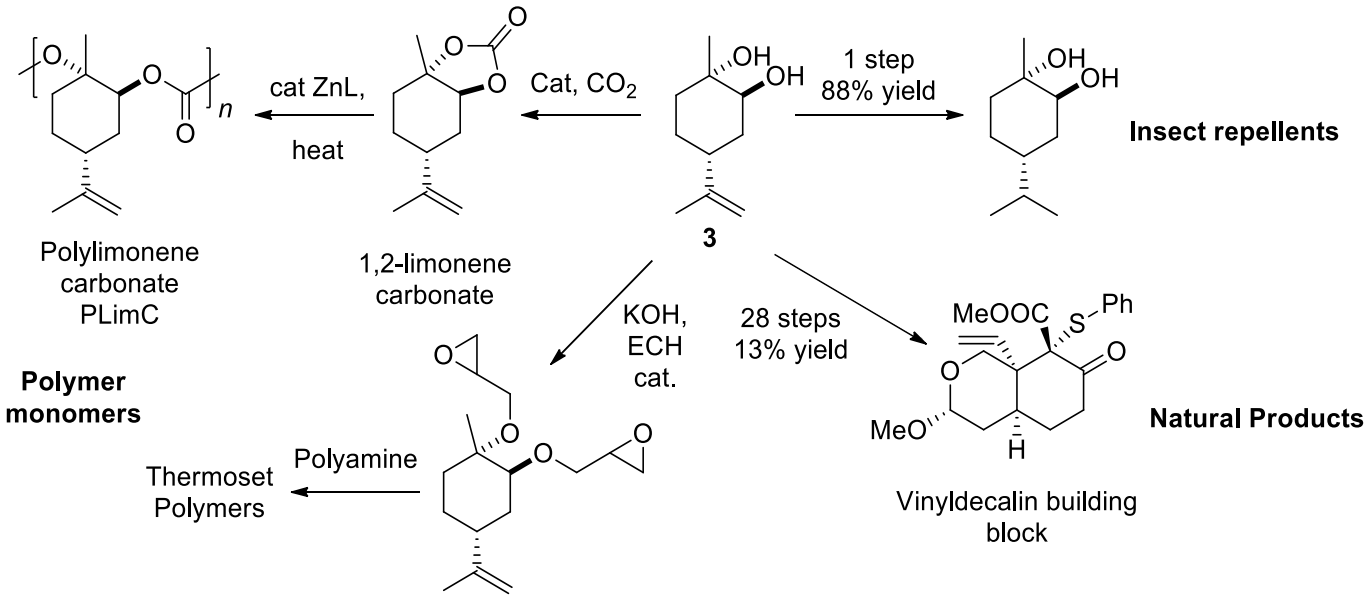

Scheme 172. Value added products from 1,2-limonene diol

Having developed an effective *anti*-dihydroxylation protocol for limonene it was decided to apply this methodology for the dihydroxylation of a range of cyclic and acyclic terpene substrates (Figure 48) to prepare their respective *anti*-diol derivatives.

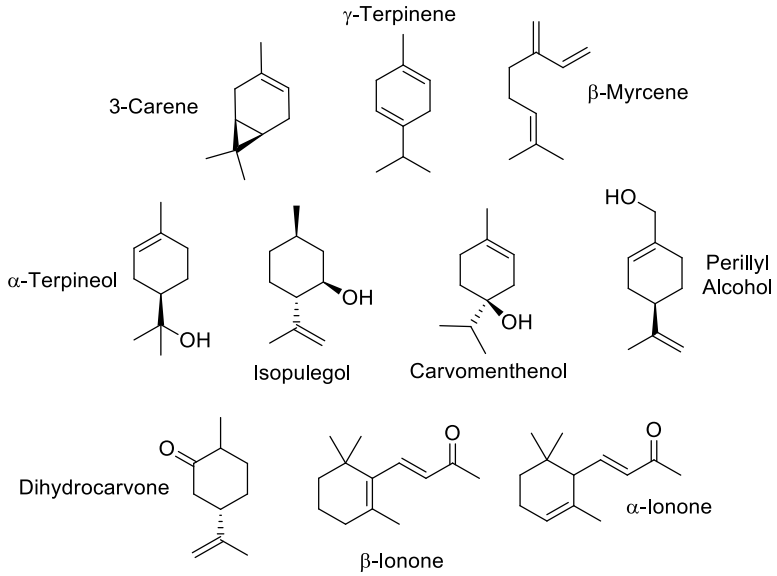

Figure 48. Range of commercially available terpene substrates that were screened using our dihydroxylation protocol using the Ishii-Venturello/Amb-15 conditions.

4.3.1 *Anti*-dihydroxylation of terpene substrates

Our one-pot, catalytic protocol was first applied for the *anti*-dihydroxylation of 3-carene which gave *anti* 3,4-carene diol (37) as a single diastereoisomer in 73% isolated yield, with <5% of 3-carene or its corresponding epoxides being present at the end of the reaction. The dihydroxylation reaction of 3-carene (Scheme 173) and γ-terpinene (Scheme 175) were scaled up successfully enabling their corresponding diols and tetrols on a 10 g scale in 62% and 55% isolated yields respectively.

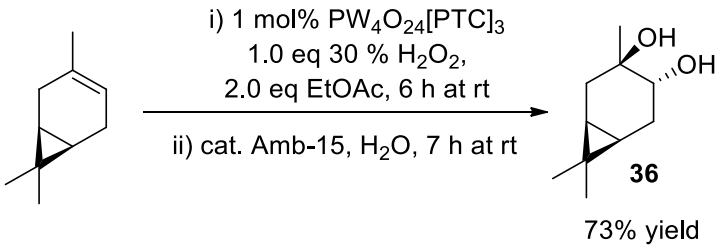

Scheme 173. One-pot two step epoxidation-hydrolysis for the synthesis of *anti* 3,4-carene diol

In comparison, Rocha *et al*[202] have previously used a zirconium phosphate based catalyst/H_2O_2 system in a 1:1 acetic acid:CH_2Cl_2 solvent system at 50 ^oC for 6 h that gave a low 29% yield of *anti* 3,4-carene diol. Saladino *et al*[192] employed microencapsulated MTO and hydrogen peroxide in chlorinated solvent to produce a 78% yield of *anti* 3,4-carene diol using mild temperatures with a relatively short reaction time of 2.5 h. Yoshio *et al*[203] reported a two-step stoichiometric route to *anti* 3,4-carene diol in 79% yield using *m*CPBA and $Ca(OH)_2$.

anti 3,4-carene diol is a potent insect repellent[201], cosmetic moisturiser additive[204] and has been used as a chiral building block for the synthesis of topical anaesthetics[205], polymer monomers[199,126], fragrance precursors[206] and agrochemical building blocks (Scheme 174).[207]

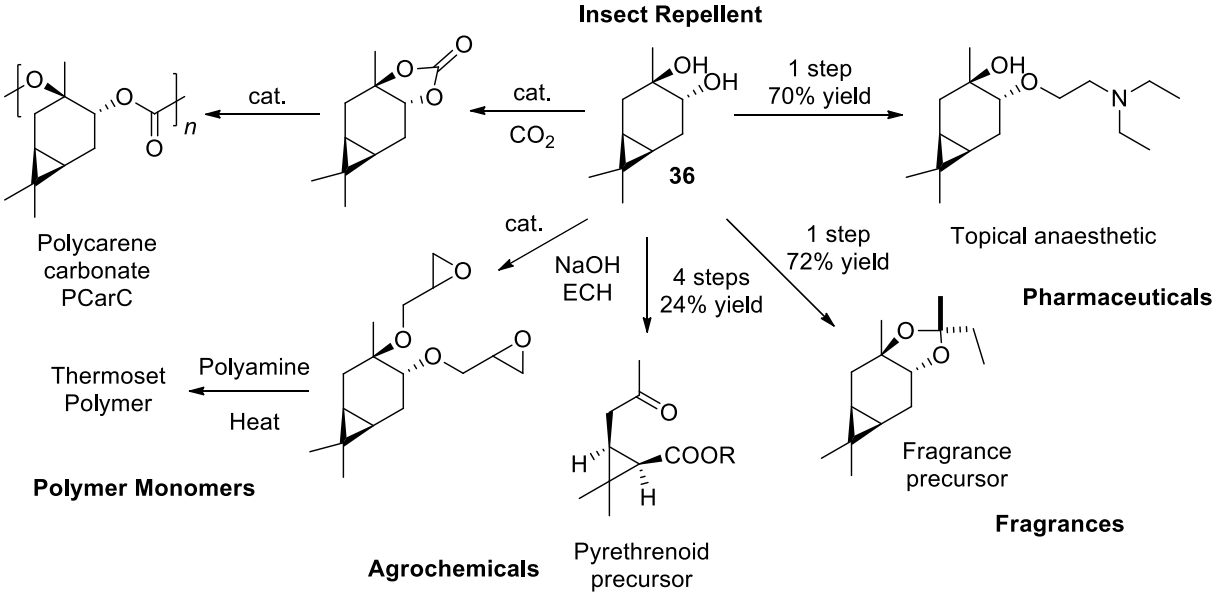

Scheme 174. Current and potential applications of *anti* 3,4-carene diol

γ-terpinene was dihydroxylated using 2.0 eq of hydrogen peroxide in ethyl acetate to form its bis-epoxide and was subsequently opened to give its tetrol form (37) after stirring for 8 h at room temperature using 0.13 mol% (140 mg per 5 mmol) Amberlyst-15 and water. Reaction progress was judged to be complete by tlc and a small amount of saturated brine solution was added to the crude reaction mixture to minimise tetrol dissolution in the aqueous layer. The crude reaction mixture was extracted three times with ethyl acetate (ca. 50 mL total) and the combined organic layer was dried and filtered. The tetrol product was purified by column chromatography using a 9:1 ethyl acetate:petroleum ether solvent system to give a pure white crystalline product. Alternatively, the crude product could be washed with DCM to remove organic soluble impurities leaving the tetrol product in its pure form due to its high insolubility in DCM.

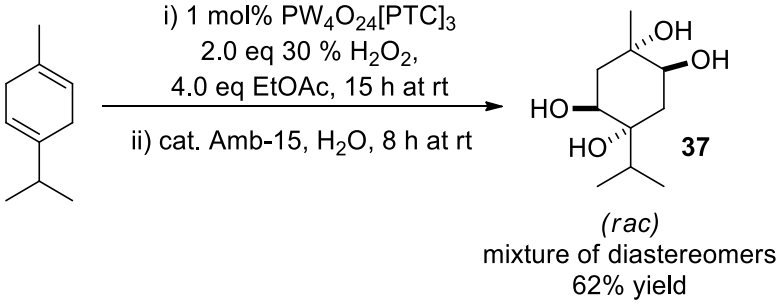

Scheme 175. One-pot two step epoxidation-hydrolysis for γ-terpinene *anti*-tetrol synthesis

γ-terpinene tetrol has been prepared previously as a minor by-product (1.3 g obtained from a 25 g reaction) from the peracetic acid oxidation of sabinene.[208] The only other references to this tetrol relates to small amounts isolated from various plant essential oils, therefore this is the first synthetic route to γ-terpinene tetrol which may have use as a monomer for

biorenewable polymer synthesis. A variety of potential applications employing γ-terpinene tetrol as a monomer for the synthesis of different types of polymer are shown below in Scheme 176[199,209]. Given its potential as a monomer for polymer synthesis, it was decided to scale-up the *anti*-dihydroxylation reaction of γ-terpinene *anti*-tetrol to a 10 g scale to provide sufficient material for polymer synthesis studies by other members of the terpene consortium. This scale-up reaction preceded uneventfully affording multi-gram quantities of a crystalline tetrol product in a 55% yield that could be easily purified by recrystallization of the crude reaction product.

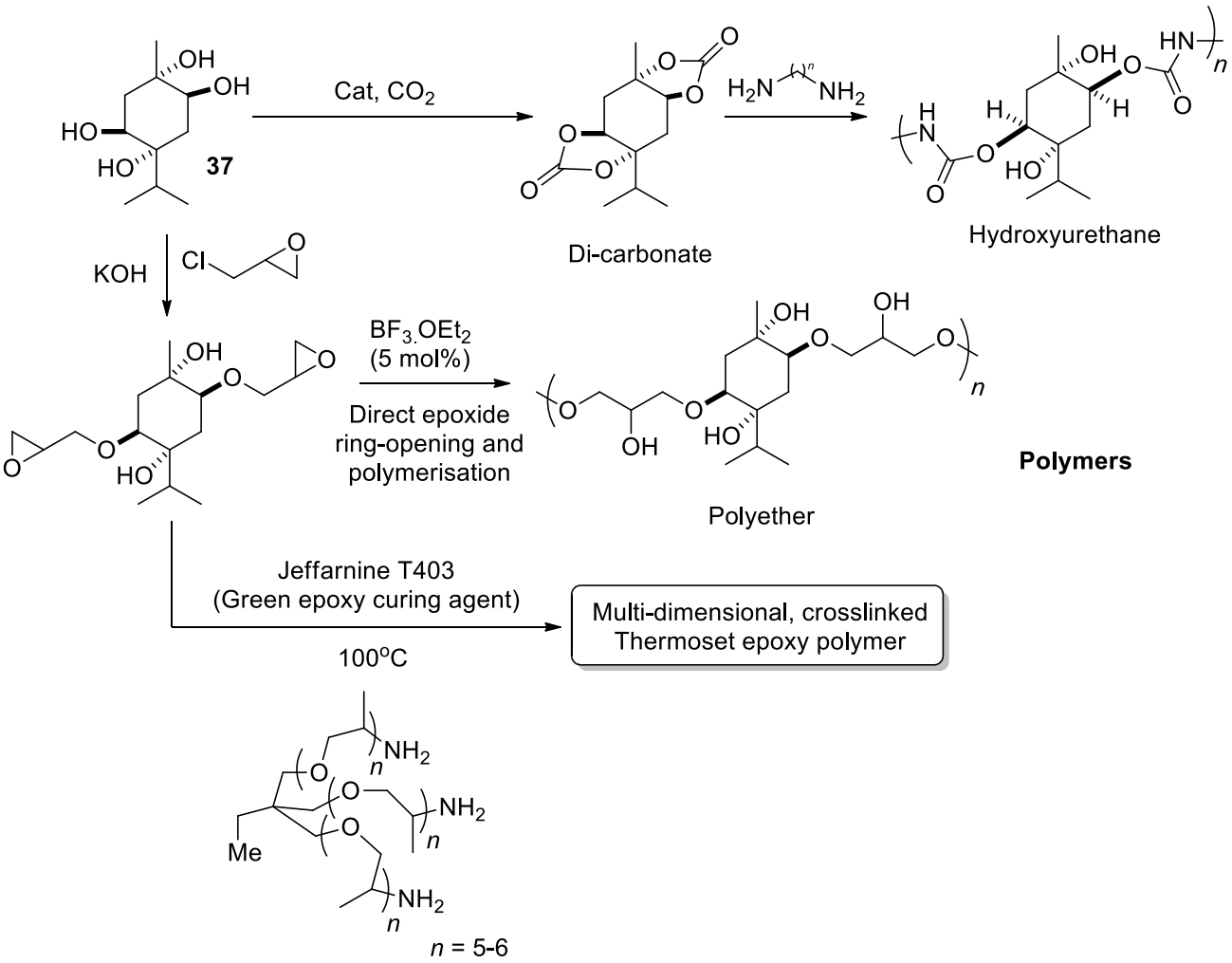

Scheme 176. Possible polymer monomer applications of γ-terpinene tetrol

Perillyl 1,2 *anti*-diol was then synthesised as a 58:42 mixture of diastereomers using our one-pot two-step *anti*-dihydroxylation protocol in 56% isolated yield (38) (Scheme 177). This *anti*-diol species has been reported previously by Kiran *et al*[210], who employed the microbe *Fusarium* h*eterosporium* to dihydroxylate perillyl alcohol in 13% yield. This biocatalytic method required large amounts of substrates, reagents and solvent (20 g glucose, 500 mg perillyl alcohol, 1 L water) to produce only 70 mg of perillyl 1,2 *anti*-diol during their investigations into using various monoterpineols as anti-cancer agents.[210]

α-terpineol 1,2 *anti*-diol (39) was prepared as a 56:44 mixture of diastereomers using our one-pot two-step *anti*-dihydroxylation protocol in 41% yield. Ishikawa *et al* have reported the isolation of α-terpineol 1,2-*anti* diol from water soluble extracts of the herb Dill,[211] with Carman

et al having synthesised various *anti* and *syn* α-terpineol 1,2 diols using stoichiometric amounts of hydrogen peroxide and formic acid. [212] The only other reported route to this *anti*-diol (29 mg) involved use of *Gibberella cyanea* to dihydroxylate α-terpineol (800 mg).[213] α-terpineol 1,2 *anti*-diol has also been isolated from the roots of *Decalepis* h*amiltonii* used in herbal medicine preparations that have been shown to have potent anti-oxidant activity[214].

Carvomenthenol 1,2 *anti*-diol (40) was synthesised as a 90:10 mixture of diastereomers using our one-pot two-step *anti*-dihydroxylation protocol in 77% yield. Most literature references mentioning carvomenthenol diol concerns its isolation from natural resources, whilst it has been reported to exhibit potent anti-algal and anti-bacterial activity against strains such as C*hlorella fusca*, *Esc*he*ric*h*ia coli* and *Bacillus megaterium*.

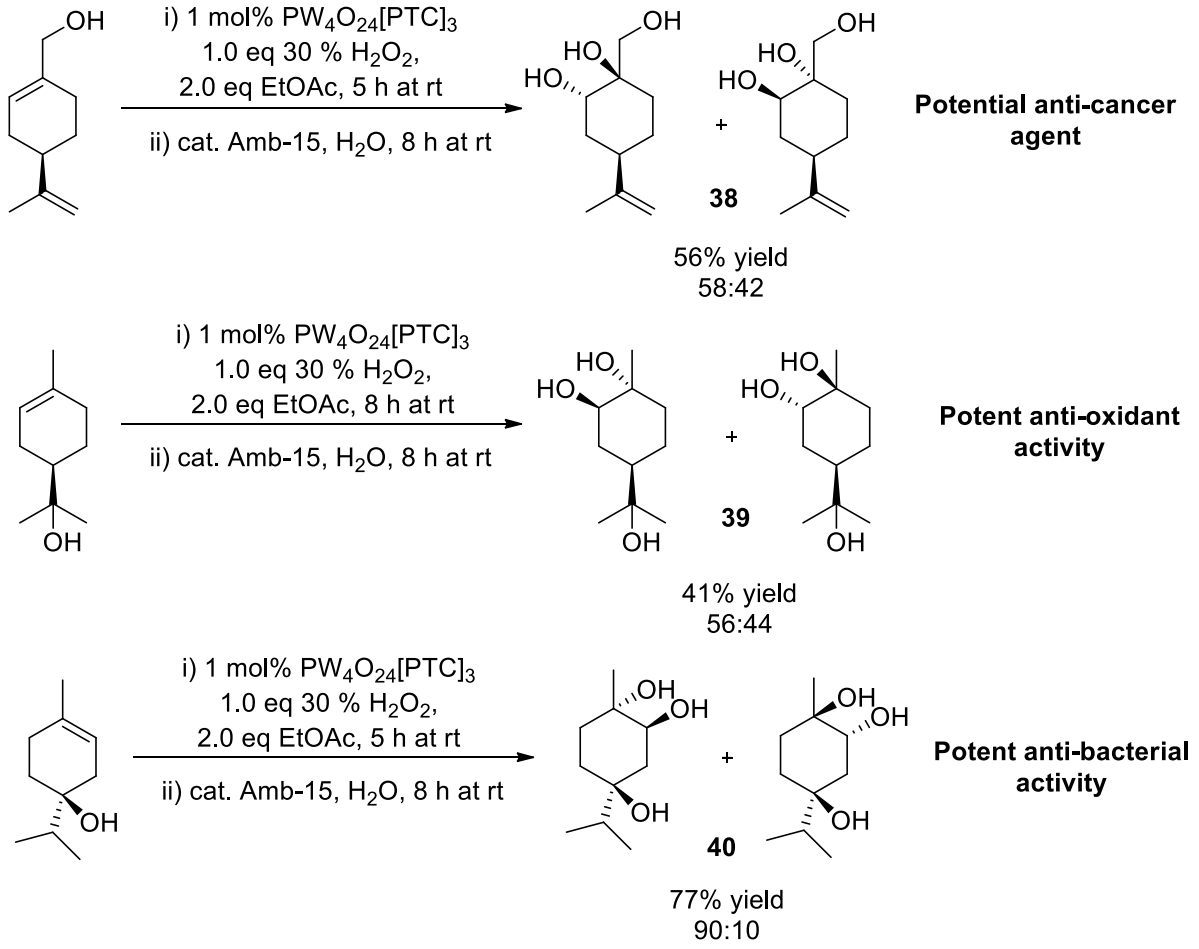

Scheme 177. Cyclic terpenes *anti*-diols derived from monoterpineols

Our Ishii-Venturello *anti*-dihydroxylation protocol was then used to transform the non-conjugated alkene bond of (*rac*)- α-ionone to afford its corresponding α-ionone diols (41) as an 80:20 mixture of *cis-/trans*- diastereomers in 70% yield. Similarly this catalytic one-pot epoxidation/hydrolysis protocol could be used to selectively *anti*-dihydroxylate the trisubstituted α, β-alkene bond of β-ionone to afford its corresponding diols (42) as a 75:25 mixture of *cis-/trans*- diastereomers in 55% yield (Scheme 178).

Bermejo *et al*[215] have previously employed 15 mol% of an iron catalyst and 3.6 eq of hydrogen peroxide as oxidant to *anti*-dihydroxylate α-ionone, achieving a 28% yield of diol after 10

minutes at room temperature. All other reported syntheses involve the use of stoichiometric amounts of peracid to carry out epoxidation of the trisubstituted alkene followed by acid catalysed ring opening of the epoxide to afford the desired diols.[216] The uses of α/β-ionone diols have not been widely investigated, with most references concerning their isolation from natural plant sources,[217] therefore, there is scope to investigate their applications more fully.

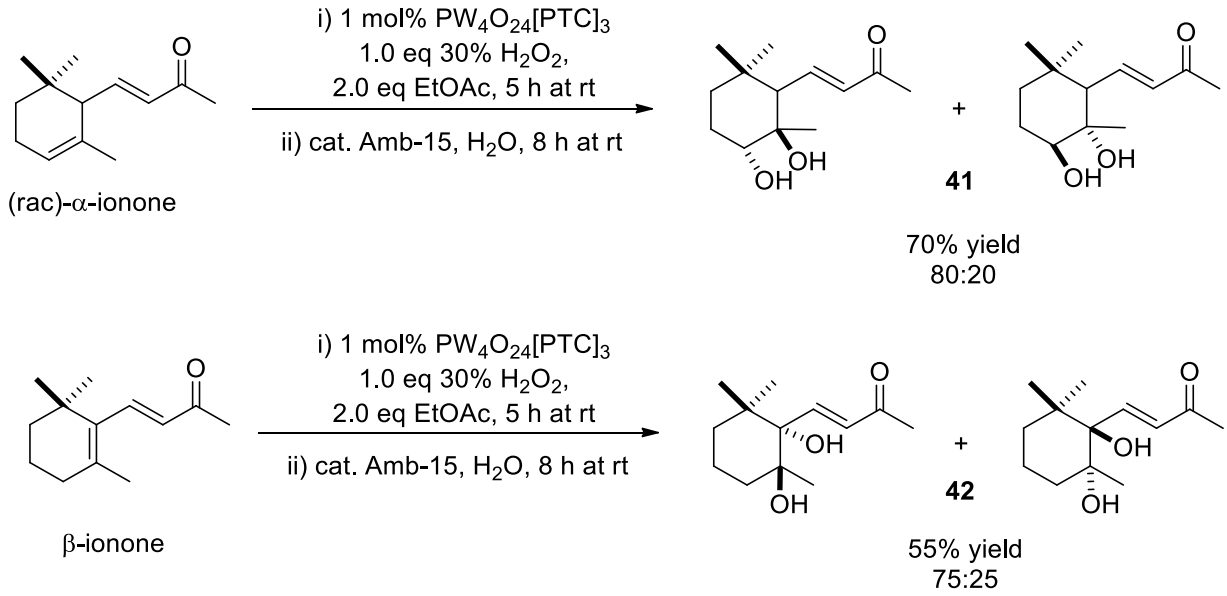

Scheme 178. Cyclic *anti*-diols obtained from α- and β- ionones

Our one-pot two-step *anti*-dihydroxylation-hydrolysis protocol was then used to dihydroxylate the exocyclic disubstituted isopropylidene bond of isopulegol to afford its corresponding 1,2-diol (43) as a 60:40 mixture of diastereomers in 60% yield (Scheme 179). This dihydroxylation reaction was carried out at 50 °C to ensure that the less reactive disubstituted alkene was epoxidised *in situ* within 2 h. This is the first catalytic method for the synthesis of isopulegol diol, with the only previous method of its preparation involving treatment with stoichiometric amounts of formic acid, hydrogen peroxide and aqueous sodium hydroxide.[218] Potential applications of isopulegol diol that are currently under investigation involve its use as an insect repellent[201] (due to its structural similarity to the known mosquito repellent PMD) and as a biorenewable monomer for the preparation of thermoset polymers (Scheme 180).

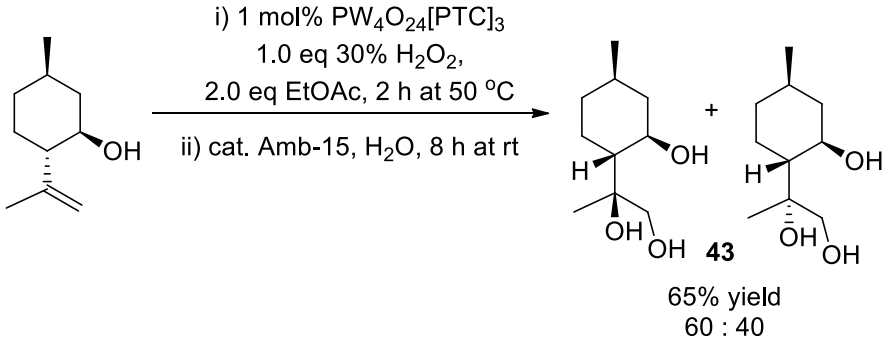

Scheme 179. Catalytic synthesis of cyclic triols derived from isopulegol

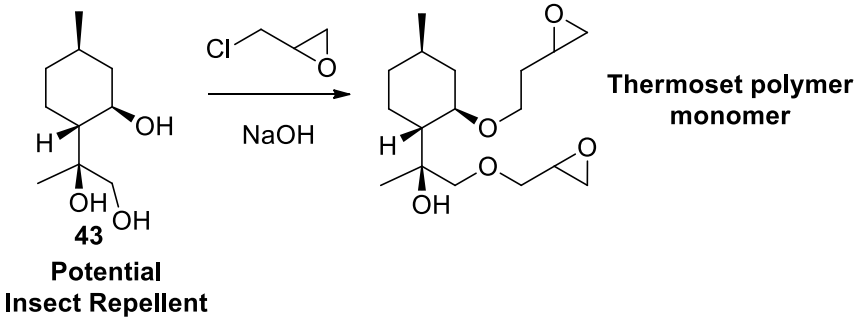

Scheme 180. Possible applications of isopulegol diol

We also used our protocol to dihydroxylate dihydrocarvone (4:1 mixture of isomers) to afford a mixture of 4 diastereomeric diols (44) in 62% yield (Scheme 190), which had previously been isolated from dill extracts by Kitajima *et al*[211]. Applications of dihydrocarvone diol itself have not been investigated, however reduction of its ketone functionality would afford its corresponding *p*-menthane triol derivative, that have applications as food and cosmetic additives[219] and as a fungal growth modifier (Scheme 191).[220]

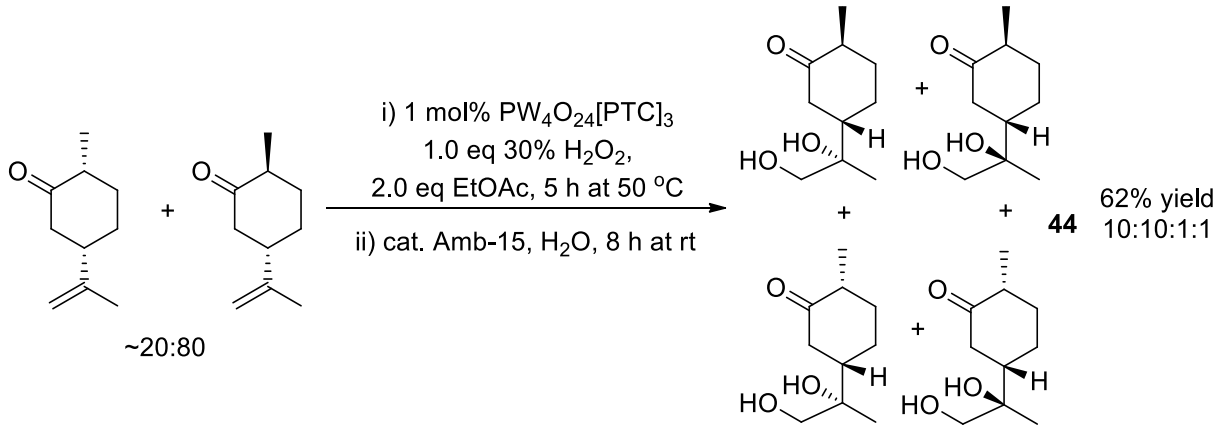

Scheme 190. One-pot synthesis of dihydrocarvone diol

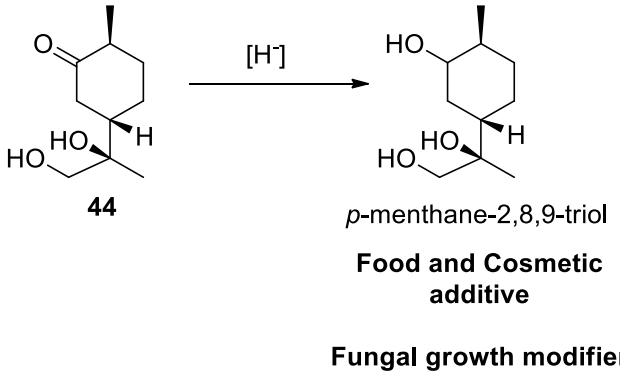

Scheme 191. Potential applications of dihydrocarvone triol

The trisubstituted alkene bond of acyclic myrcene was selectively dihydroxylated using our epoxidation-hydrolysis protocol at room temperature to afford (*rac*)-myrcene diol (45) in 61% yield (Scheme 193). This is the first catalytic synthesis of myrcene diol which has previously been prepared in 82% yield, using a two-step approach using stoichiometric *m*CPBA to form the epoxide, followed by ring opening with 70% aqueous $HClO_4$.[221] Myrcene diol has a number

of applications including as a building block for the synthesis of fragrances[222] and natural products such as halomon[223] and hippospongic acid analogues (Scheme 194).[221]

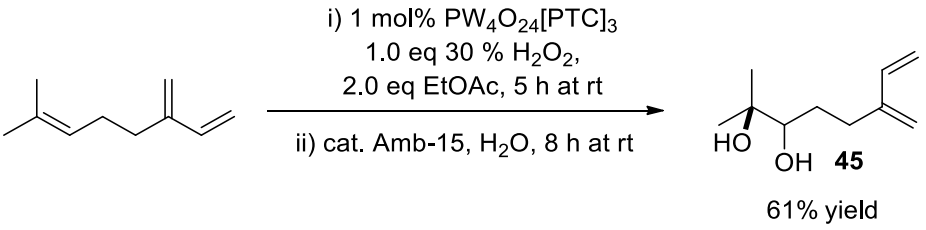

Scheme 193. Acyclic *anti*-diol terpenes

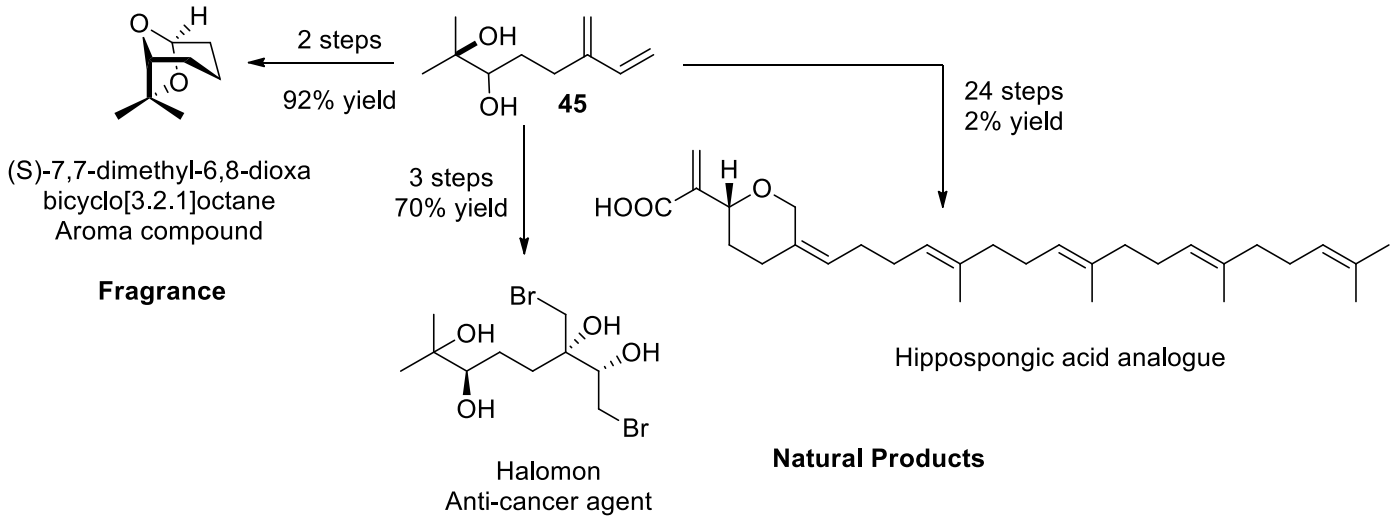

Scheme 194. Applications of myrcene diol

4.3.2 *Anti*-diol synthesis from non-renewable alkenes with Venturello

Having developed a practical catalytic one-pot two step protocol for the dihydroxylation of a range of terpene substrates, we decided to briefly explore the scope and limitation of this methodology for hydroxylation of a range of non-terpene alkenes. Styrene (46) and α-methylstyrene (47) were dihydroxylated using 1 mol% of Ishii-Venturello catalyst and unbuffered H_2O_2 for 2 h at 50 ^oC whose epoxides were unstable under these condition, readily undergoing ring-opening to afford their corresponding diols (without Amberlyst-15) in 82% and 84% yields, respectively. Similarly, the disubstituted alkene bonds of cyclohexene (48) and 4-methyl-cyclohex-1-ene (49) were dihydroxylated at 50 ^oC to afford their corresponding *anti*-diols in 72% and 75% yields, respectively. Dihydroxylation of the trisubstituted bond of 1-methyl-cyclohexene (50) proved to be particularly facile, resulting in formation of its corresponding diol in 73% yield after 1 h at room temperature (Figure 49).

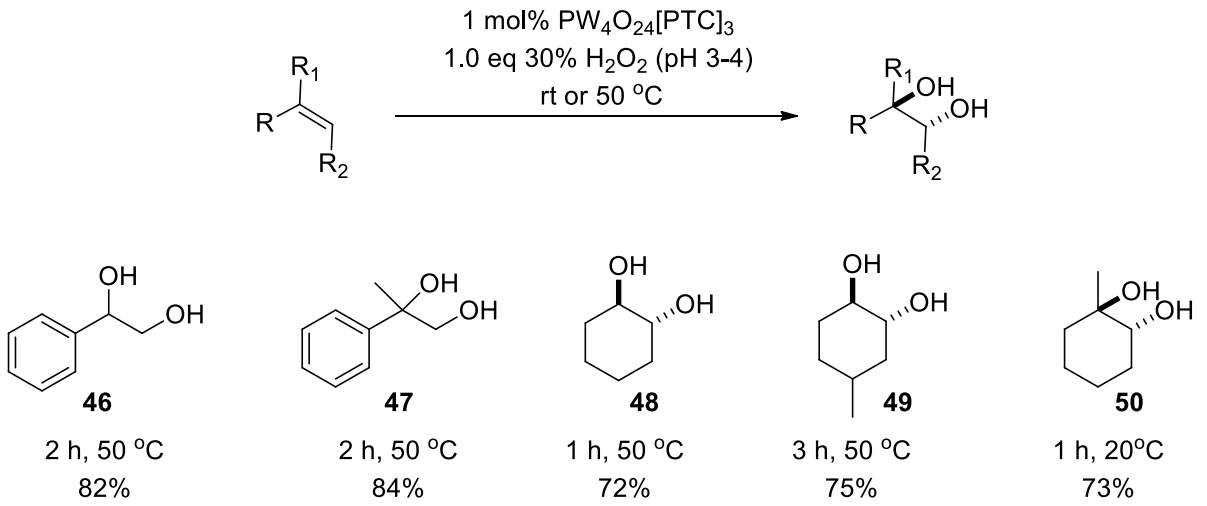

Figure 49. Dihydroxylation of aromatic and cyclohexyl alkenes

Epoxidation of the monosubstituted alkenes of acyclic substrates using our Ishii-Venturello catalytic system required more forcing conditions, with epoxidation occurring at 80 °C under solvent free conditions to form stable epoxides after 1 h. Clean conversion into their corresponding diols (51), (52) required the addition of 0.13 mol% Amberlyst-15 which resulted in clean epoxide hydrolysis at room temperature after 6 h to afford their corresponding diols in 75% yields. Both alkene bonds of cyclohexadiene (53) were *anti*-dihydroxylated *via* treatment with 2.0 eq of hydrogen peroxide, using 2.0 eq of EtOAc (per alkene bond) as a cosolvent to prevent the reaction mixture in the second epoxide hydrolysis step becoming too viscous to stir, which gave its corresponding crystalline tetrol (mixture of 2 diastereomers) in 70% yield (Figure 50).

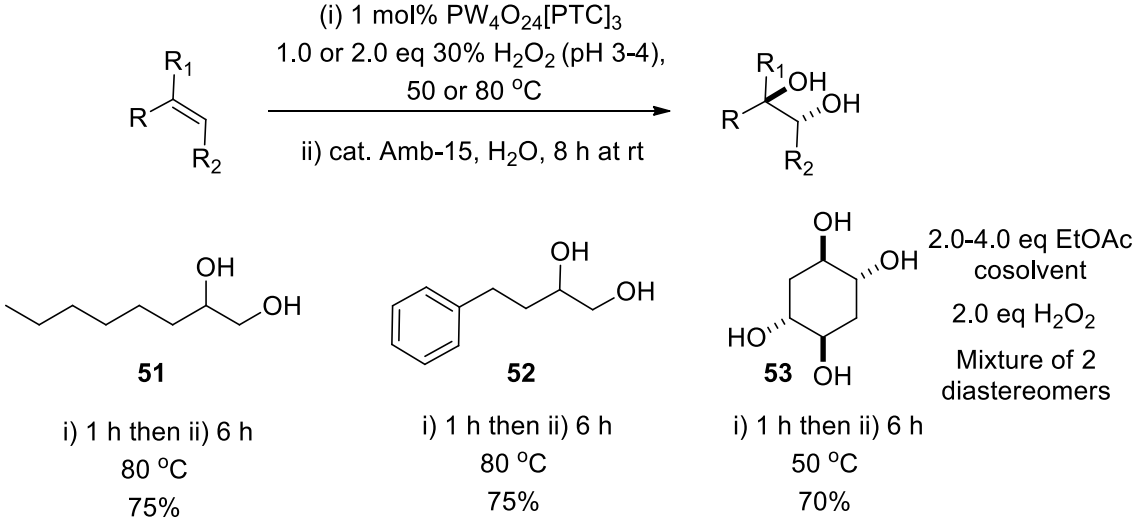

Figure 50. Dihydroxylation of cyclohexyl and acyclic alkenes

4.4 Conclusion

Figure 51 below summarises the terpene *anti*-diols synthesised using our Venturello-A336 catalysed protocol.

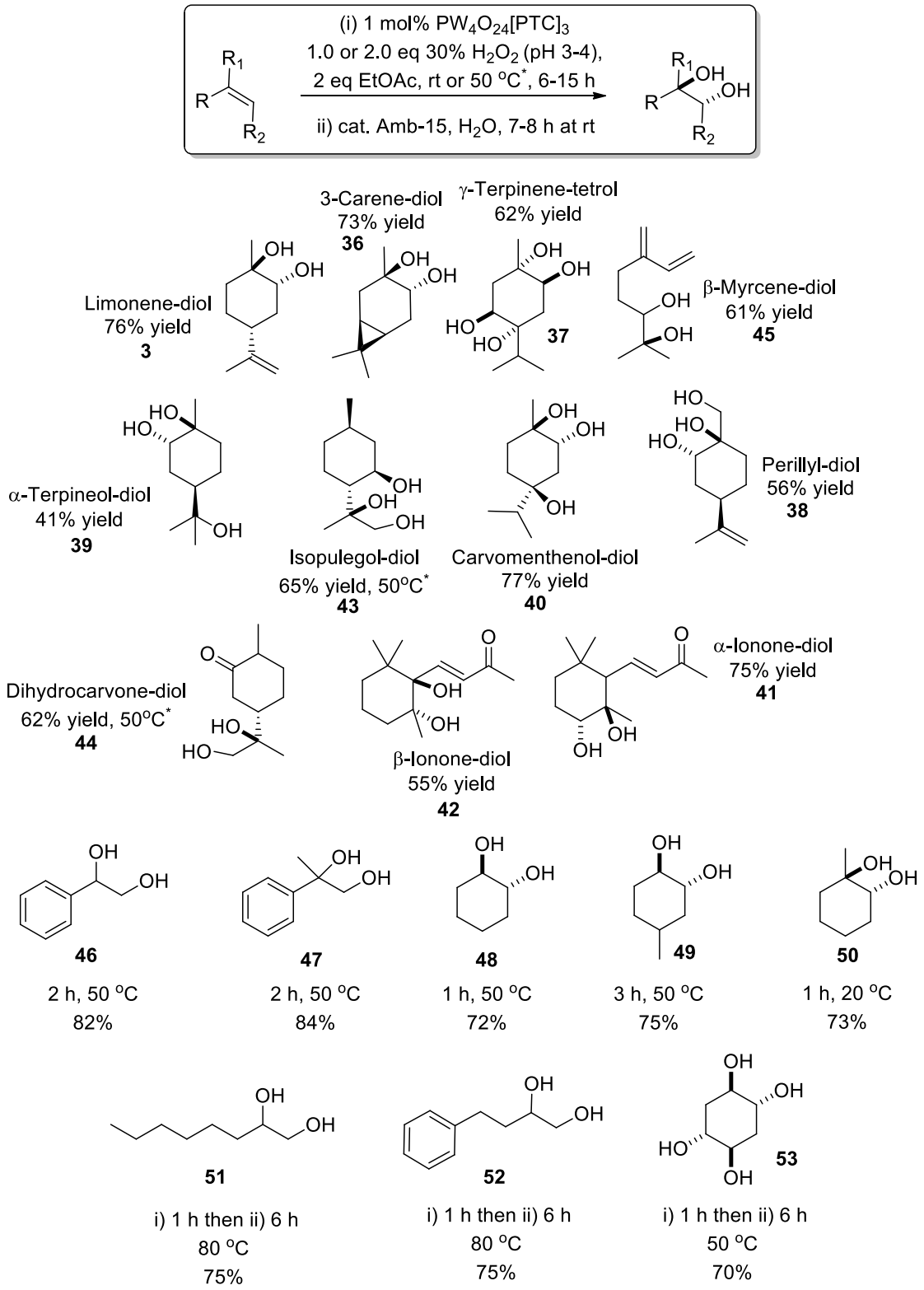

Figure 51. Range of commercially available terpene substrates that were dihydroxylated using the Ishii-Venturello catalyst/H_2O_2/Amb-15 conditions.

A novel one-pot protocol for the catalytic epoxidation-hydrolysis of the alkene bonds of terpenes has been developed giving access to a wide range of useful terpene 1,2 *anti*-diols in good to excellent yields. This methodology combines use of the readily prepared Ishii-Venturello catalyst and cheap H_2O_2 to prepare epoxides that are then treated *in situ* with the cheap heterogeneous acid catalyst (Amberlyst-15) to afford the desired 1,2 *anti*-diols. This protocol employs 2.0 eq of EtOAc as a benign cosolvent (rather than benzene) with the heterogeneous acid catalyst being easily recovered by filtration, which removes the need for carrying out a neutralisation step. Ambient temperatures were used for the most part, with higher temperatures required with less reactive substrates (rt-50 ^{o}C), in the dihydroxylation protocols used to prepare the terpene *anti*-diols, with use of 2.0 eq of H_2O_2 resulting in both alkene bonds of γ-terpinene being dihydroxylated to afford its corresponding tetrol (37). This *anti*-dihydroxylation protocol could also be applied for the *anti*-dihydroxylation the alkene bonds of a range of cyclic and acyclic non-terpene substrates to give their corresponding diols in good yields, with some of their more reactive epoxide intermediates being ring-opened in the absence of Amberlyst-15. The scope and limitation of this one-pot epoxidation-hydrolysis methodology for the *anti*-dihydroxylation of the alkene bonds of 19 terpene and non-terpene substrates are summarized in Figure 51.

5 Chapter 5: Syntheses of Valuable Compounds from Terpene Feedstocks

5.1 Use of terpene derived natural products as pharmaceuticals

Terpenes and terpenoids are used extensively in the flavours and fragrances industry, but also have a broad range of biological activities that have been exploited by the pharmaceutical industry.[224] Terpenes have been used as scaffolds for therapeutic agents such as antimalarials and anticancer drugs,[225] with worldwide sales of terpene-based pharmaceuticals valued at $12 billion in 2002, including sales from Taxol and Artimesinin.[224] Not only does the pharmaceutical industry use significant quantities of terpenes for the synthesis of current drugs, it also needs supplies of terpenes for the production of new drugs using novel synthetic protocols. However, the lack of significant quantities and a reliable supply chains for specific terpene substrates is a major obstacle[224] to the production of terpenoid-based clinical drugs.

Many terpene compounds only occur naturally in very low quantities and it would be un-economical and environmentally harmful to harvest them from nature. Chemical syntheses of these complex compounds are possible, even on an industrial scale; however their structural complexity means that they must be produced using complex, multi-step routes. These routes often involve the use of expensive and/or toxic reagents, environmentally unfriendly temperatures, cryogenic temperatures and the generation of large amounts of waste, which means that they are often economically unfeasible for scale-up.

This demand has helped drive interest into developing metabolically engineered cell cultures, microorganisms and plants for the production of reliable supplies of valuable terpenes.[224] Engineering plant and microbial systems requires an interdisciplinary approach and significant investment involving modification/introduction of isoprene biosynthetic pathways into these systems. Currently the complex pharmaceuticals Taxol and Artemisinin (Figure 52), are manufactured industrially using genetically modified organisms. There are many other complex terpenoids that have excellent bioactivity; however the lack of viable scale up routes to these products prevents their use as medicinal compounds, with advances in biotechnology and genetic engineering potentially providing potential solutions to this supply problem. The use of microorganisms enables the efficient production of complex terpenes using a series of enzyme intracellular systems, which can potentially be used for the production of structural analogues for screening purposes.[9]

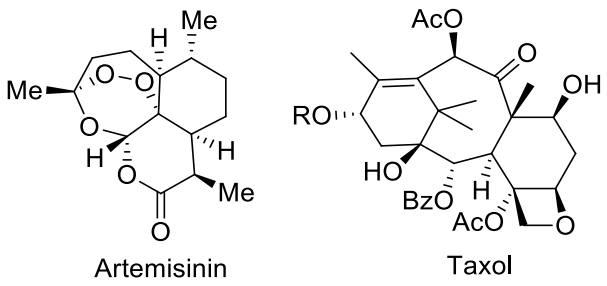

Figure 52. Terpene derived pharmaceuticals currently manufactured using GM microorganisms

Taxol is the trademark name for Paclitaxel which is a potent diterpenoid anti-cancer drug[226] that is worth over one billion dollars per year.[227] Taxol was originally isolated from the bark of the Pacific Yew tree that is particularly slow growing and low yielding (approximately 3000 trees or 10,000 kg of bark to produce 1 kg of drug[227]), with each patient requiring 2.5-3 kg of Pacitaxel,[227] so the supply was insufficient to meet the growing clinical demand for the drug.[226] The method for extracting and purifying Taxol from its natural source is very complex and costly, further increasing the need for an alternative source.

After 15 years of research the biosynthetic pathway leading to Taxol was determined and used to develop alternative biological and semi-synthetic production methods using readily available starting materials (Scheme 195). However, all these approaches are low-yielding and require access to large numbers of slow-growing Yew trees that must be farmed in a biorenewable manner.

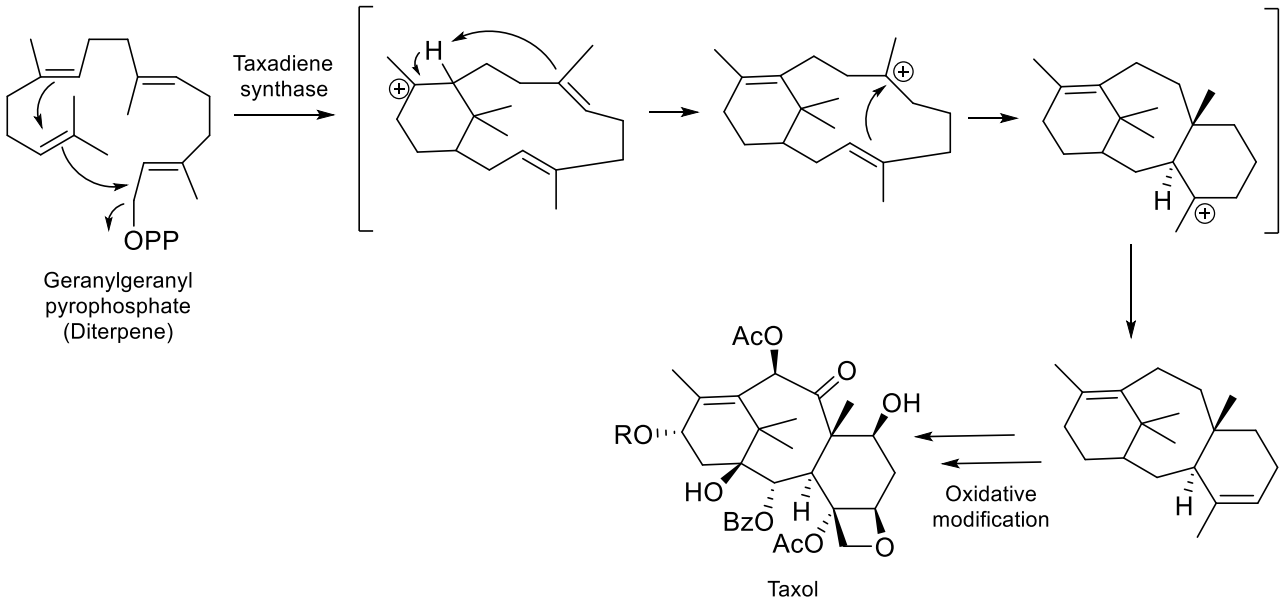

Scheme 195**.** Simplified biosynthesis of Taxol from the geranylgeranyl pyrophosphate

An alternative and sustainable route to Taxol and its analogues is to use genetically engineered plant cell cultures that express genes for its biosynthetic pathway for its production.[227] These cultures can be grown in fermenters using cheap raw materials, with the Taxol products being excreted into the extracellular medium and harvested for use. There are various advantages to this biotechnological approach, with Taxol production not being constrained by seasonal variations in yields, that enable Taxol to be produced at the correct location under the correct environmental conditions.[227]

The yield of Taxol from the cultures has been increased by optimising conditions, selection of higher producing strains, the addition of mediators and precursors, and the use of metabolic engineering techniques to overexpress genes controlling the rate limiting steps controlling its production.[227] Python biotech currently produces the large volumes of Taxol using this method, utilizing a fermenter with a 75,000 L capacity.[227]

Another important terpenoid related drug is Artemisinin which is a potent antimalarial agent isolated from Sweet Wormwood that is used for the treatment of malaria (Scheme 196). It is

especially useful for the treatment of resistant Plasmodium strains that are unaffected by existing antimalarials such as quinine and sulfadoxine-pyrimethamine combination therapy.[225]

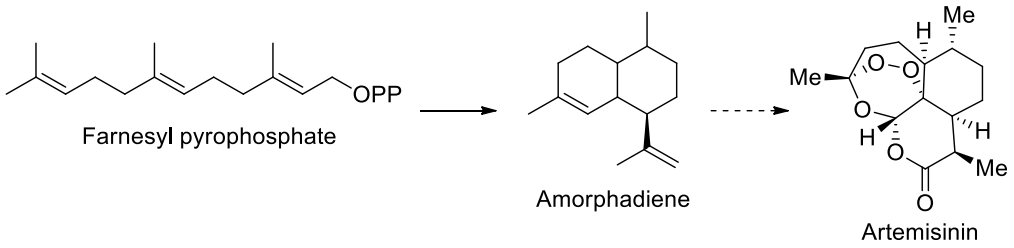

Scheme 196. Simplified biosynthetic route from the sesquiterpene farnesyl pyrophosphate to artemisinin.

Current production of artemisinin relies upon extraction and purification from plant sources, with this process suffering from low yields that result in a costly anti-malarial drug that prevents its widespread use in the 3rd World. Microbial hosts have been investigated as a means to produce artemisinin in higher yield, which was achieved by altering the mevalonate-dependent pathway to introduce a high flux heterologous isoprenoid pathway into *E. coli.*[225] Genes for the production of amorphadiene were overexpressed in *E.coli*, leading to the production of high levels of amorphadiene (27 g/L),[10] that can be isolated and used as a substrate for the semi-synthetic conversion into artemisinin.[228] Alternatively, some researchers have tried to overexpress the genes involved in artemisinin biosynthesis to produce transgenic plants for its production.[225] Since nature produces all terpenoids using the same biosynthetic precursors, it is feasible that these pathways of host microbes can be altered to produce large amounts of other types of commercially valuable terpenes, and a large amount of costly research is currently underway worldwide to achieve this aim.

5.1.1 Terpenes as synthons for natural product synthesis

Both enantiomers of a number of cheap monoterpenes (e.g. carvone (industrial derivative of limonene)) are available as chiral building blocks for the stereoselective synthesis of fine chemicals, perfumes, drugs, insecticides, and natural products. For example, Ghosh et al[229] employed (*S*)-carvone for the synthesis of the potent antibacterial (-)-Platensimycin that has activity against vancomycin-resistant gram-positive strains, whilst Brimble et al[230] used it to synthesise the anti-cancer agent Phorbin A. Alternatively, Gademann et al[231] used (*R*)-carvone for the synthesis of the anti-degenerative agent, Cyrneine A, whilst Mehta et al[232] used it to prepare the anti-cancer agent (-)-Isocelorbical (Scheme 197).

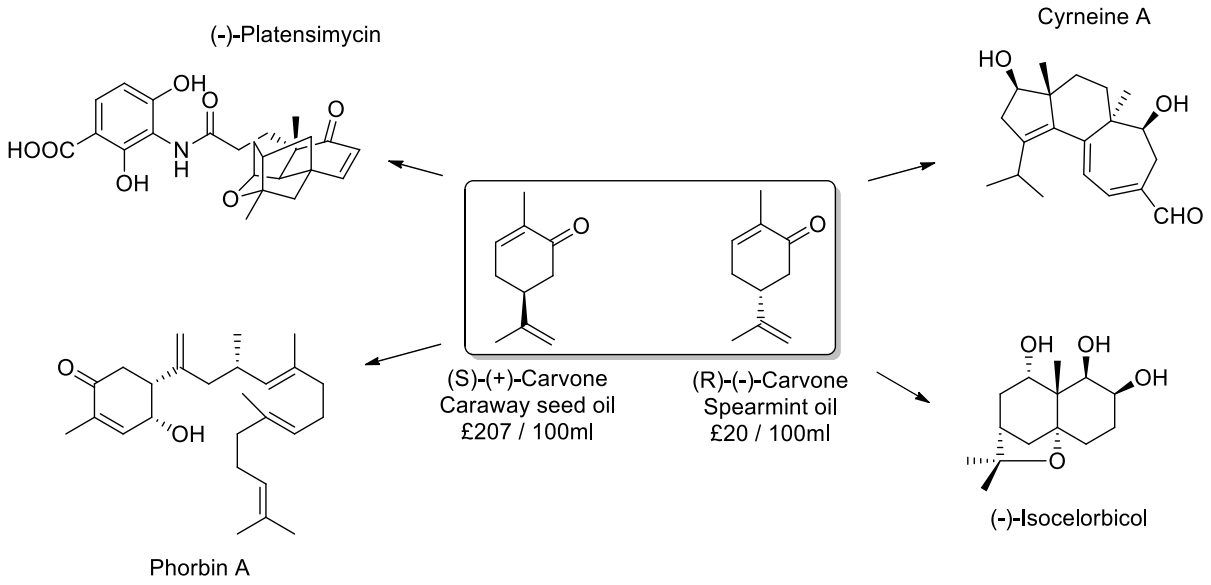

Scheme 197. Natural products synthesised using enantiopure carvone

5.1.2 Terpenes as feedstocks for the synthesis of pharmaceuticals *via* 4-Hydroxyacetophenone

Traditional drug molecules typically contain aromatic and heteroaromatic fragments with various substituents attached to their core ring systems. For example, a number of well-known traditional aromatic containing pharmaceuticals are shown below, including Albendazole which is an antiparasitic agent; Ibuprofen which is an analgesic and anti-inflammatory; and the statin Lipitor which has anti-cholesterol activity (Figure 53).[233,234]

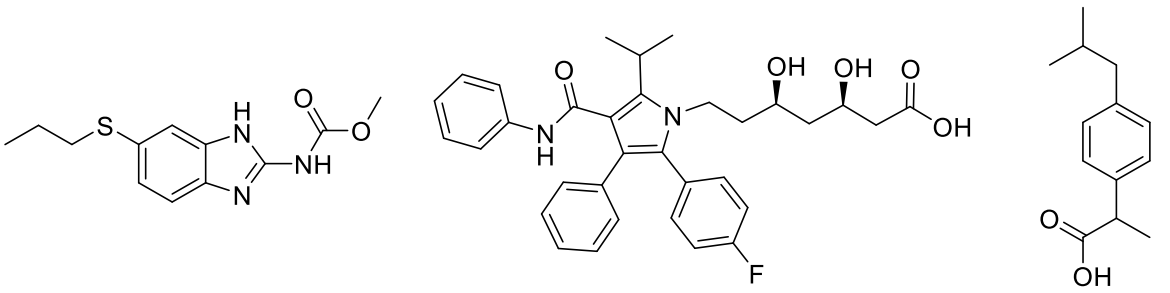

Figure 53. Drugs containing aromatic and heteroaromatic fragments

All of these pharmaceuticals are derived from oil derived aromatic building blocks and hence are synthesised from non-renewable sources. In comparison, monoterpenes such as limonene, 3-carene, α-pinene and β-pinene are renewable C10 compounds (Figure 54) containing 6 membered rings that could potentially be converted into aromatic rings, either directly (for limonene), or using ring opening procedures to afford monocyclic 6 membered ring systems.[11]

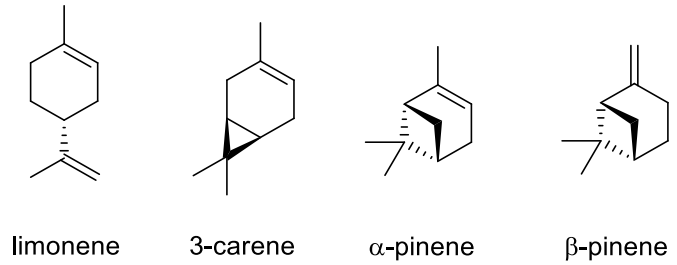

Figure 54. 6 membered rings contained in monoterpenes

Nature uses a similar aromatisation approach to prepare biologically important metabolites containing aromatic fragments, such as the biosynthetic pathway leading from androstenedione to the female sex hormone estrone.[235] In this pathway, the α-keto-ring of the steroid skeleton is oxidatively metabolised by an aromatase enzyme, with cleavage of its angular methyl group, to afford the phenolic ring of estrone.

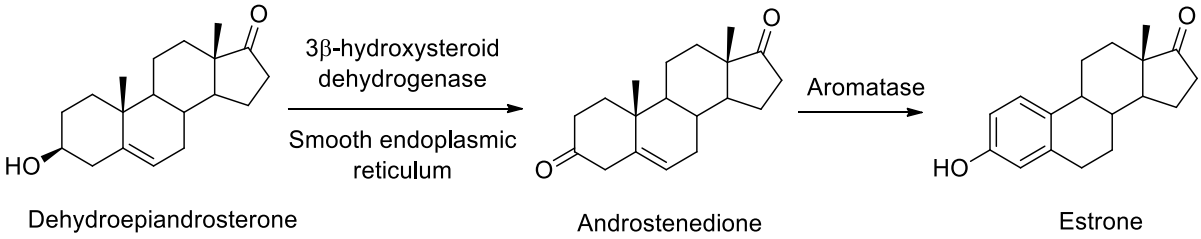

Scheme 198. Biosynthetic aromatisation of 6 membered ring of androstenedione

The biosynthetic pathway leading to estrone employs a catabolic strategy that converts the chiral cyclohexyl ring (one stereogenic centre) in androstenedione into the aromatic phenolic ring of estrone (Scheme 198). We envisaged employing a similar strategy to convert the sp^3 centres of 6 membered rings of monoterpenes into the sp^2 centres of aromatic rings for the synthesis of drug molecule. This approach would inevitably involve destruction of stereogenic centres and the removal of redundant carbon fragments. The biosynthetic pathways used by

Nature produce a wide range of chiral molecules, with many mono terpenes (e.g. the pinenes) being produced in vast amounts from plant sources. Therefore, the use of these type of cheap chiral biorenewable carbon sources for the synthesis of economically valuable achiral aromatic products that results in the destruction of multiple chiral centres is perfectly feasible. In comparison, this approach of transforming chiral biological molecules into useful products *via* destruction of their stereogenic centres is at the heart of the lignocellulose fermentation process that results in transformation of the 5 stereocentres of glucose into bioethanol.[236]

Large volumes of useful terpenes are commercially available at low cost as by-products of the agricultural and timber industries with an estimated 330,000 tonnes produced worldwide.[237] The largest source of terpene feedstocks is turpentine, with crude sulfate turpentine (CST) being produced as a by-product of the Kraft pulping paper available at around $1000 per tonne.[12] Gum turpentine, also obtained from tapping the sap of trees, is available at around $1000-1500 per tonne.[12] Turpentine is comprised primarily of α- and β-pinene, with some sources also containing significant amounts of 3-carene. Limonene ($3000 per tonne)[10] is also available as a by-product of the citrus juice industry from extraction of waste fruit peel, with global production estimated to be approximately 30,000 tonnes/year.[11] These volumes and prices suggest that a scalable biorefinery industry based on the use of terpene feedstocks sourced from industrial by-products is potentially feasible for the production of pharmaceuticals from renewable feedstocks in an economic manner.[10] Furthermore, it is predicted that the rapid development of genetically modified biological organisms[238] will result in an increasing number of monoterpenes becoming available as cheap feedstocks for synthesis on an industrial scale.[239]

A wide range of traditional pharmaceuticals are currently synthesised from the common aromatic intermediate 4-hydroxyacetophenone (4-HAP) (54), including a significant number of drugs that are prescribed annually to millions of patients worldwide (Figure 55). For example, isoprenaline[234] is a non-selective β adrenoreceptor agonist that is available from multiple generic sources (>25 brands) which is widely used as a highly potent treatment for bradycardia (slow heart rate). Metoprolol is a selective β1 receptor blocker that is used to treat high blood pressure and abnormally fast heartbeat,[240] which is a WHO essential medicine. It is currently sold as a generic drug, being the 19th most prescribed drug in the USA in 2013, with annual worldwide sales in 2011 of $1.53 billion.[241] Salbutamol[234] causes dilation of small airways in the lungs which is used as medication to treat asthma attacks and chronic obstructive pulmonary disease.[242] Asthma is estimated to affect 30 million people worldwide and its incidence is expected to rise significantly in the future. Salbutamol is administered through an inhaler, by injection, or in pill form, which acts within 15 minutes of being administered and lasts up to 6 hours.[241] It is also on the WHO list of essential medications because of its high effectiveness and lack of severe side effects. Currently, Salbutamol is sold as a generic drug with a 200 dose inhaler costing £1.50 in the UK in 2015, with worldwide sales in 2011 of $1.57 billion.[241] It should be noted that isoprenaline, metoprolol and salbutamol are all sold as racemates, so routes for their stereoselective synthesis in enantiopure form are not required.[234]

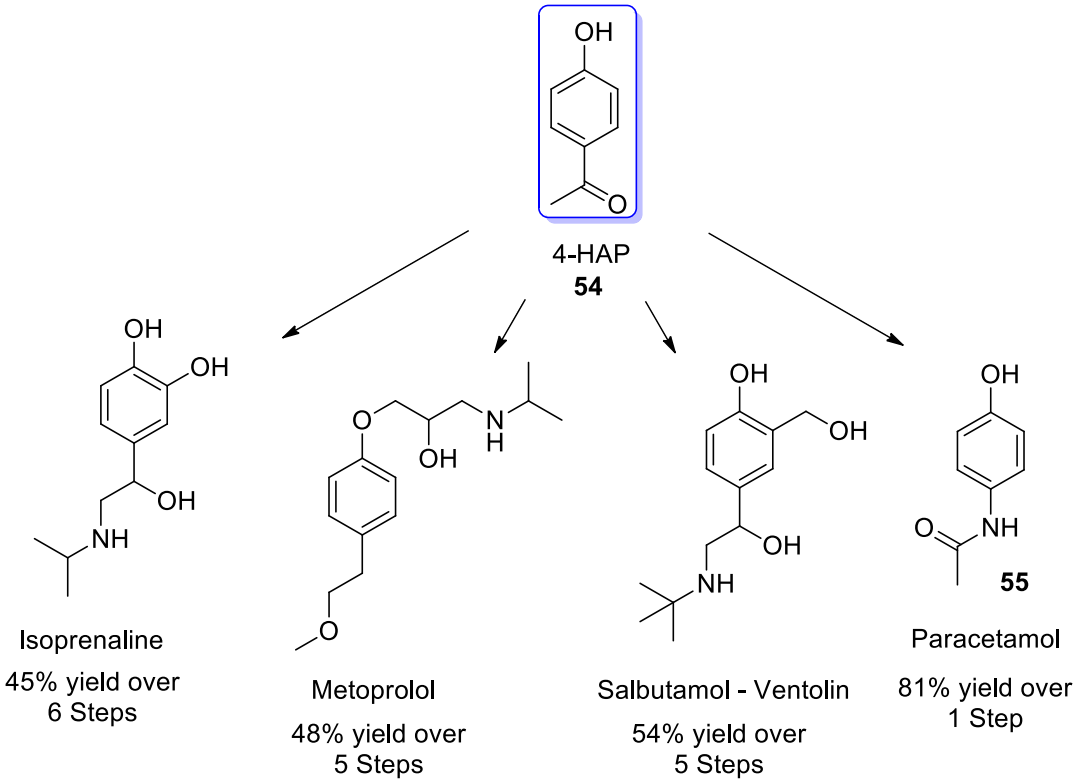

Figure 55. Pharmaceuticals derived from 4-HAP using known chemical transformations

Paracetamol (55) was first synthesised in 1878 by Morse [243]. It is one of the most popular and widely used drugs for the treatment of pain and fever [244] and is on the WHO essential medications list. Global demand in 2004 was estimated at 100,000 tonnes per annum.[245] 20 million packets of paracetamol are sold in the UK annually, corresponding to one packet for every 4 people, which represents around two-thirds of the over-the-counter analgesics purchased in the UK. [246] Global paracetamol sales were $6.12 billion in 2011[241] and are expected to grow in the future, due to a rising need for pain medication associated with disorders such as flu, fever and arthritis that require quick pain relief. Demand for Paracetamol is highest in the USA, followed by Europe and then the Asia-Pacific region.

Paracetamol is also used as a starting material for the synthesis of higher value pharmaceuticals (Figure 56) such as Ambroxol which is a mucolytic agent and potential treatment for Parkinson's disease[247], and the anti-malarial, Amodiaquine.[248] Amodiaquine is on the WHO list of essential medications and is widely used on the African continent for the treatment of malaria, which still causes millions of deaths worldwide.[248]

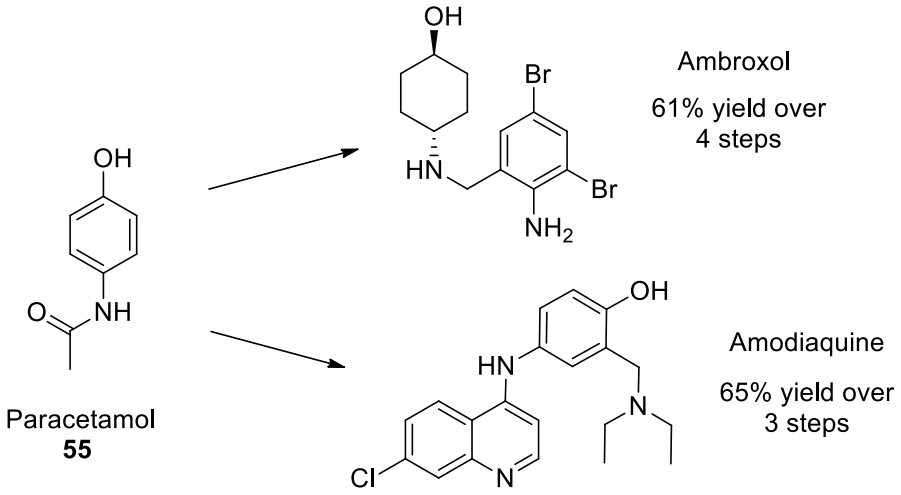

Figure 56. High value pharmaceuticals derived from Paracetamol

All of these generic medicines are prepared using 4-HAP as a substrate and sold in large volumes worldwide. Therefore, the development of a commercially viable route to 4-HAP from a cheap biorenewable terpene feedstock would represent a significant demonstration of the strategy of using a biorenewable feedstock to target ‘drop-in’ intermediates for the synthesis of green pharmaceuticals.

5.1.3 Petrochemical routes to 4-hydroxyacetophenone and paracetamol

At present, there are four major industrial routes to afford paracetamol: these are the phenol route; the p-nitro-chloro benzene (PNCB) route; the Hoeschst-Celenese route; and the nitrobenzene route – all of which are shown in Scheme 199.[249] Industrially these four routes make use of petrochemical feedstocks to produce an estimated 180,000 tonnes of Paracetamol annually.[245,250,34, 36]

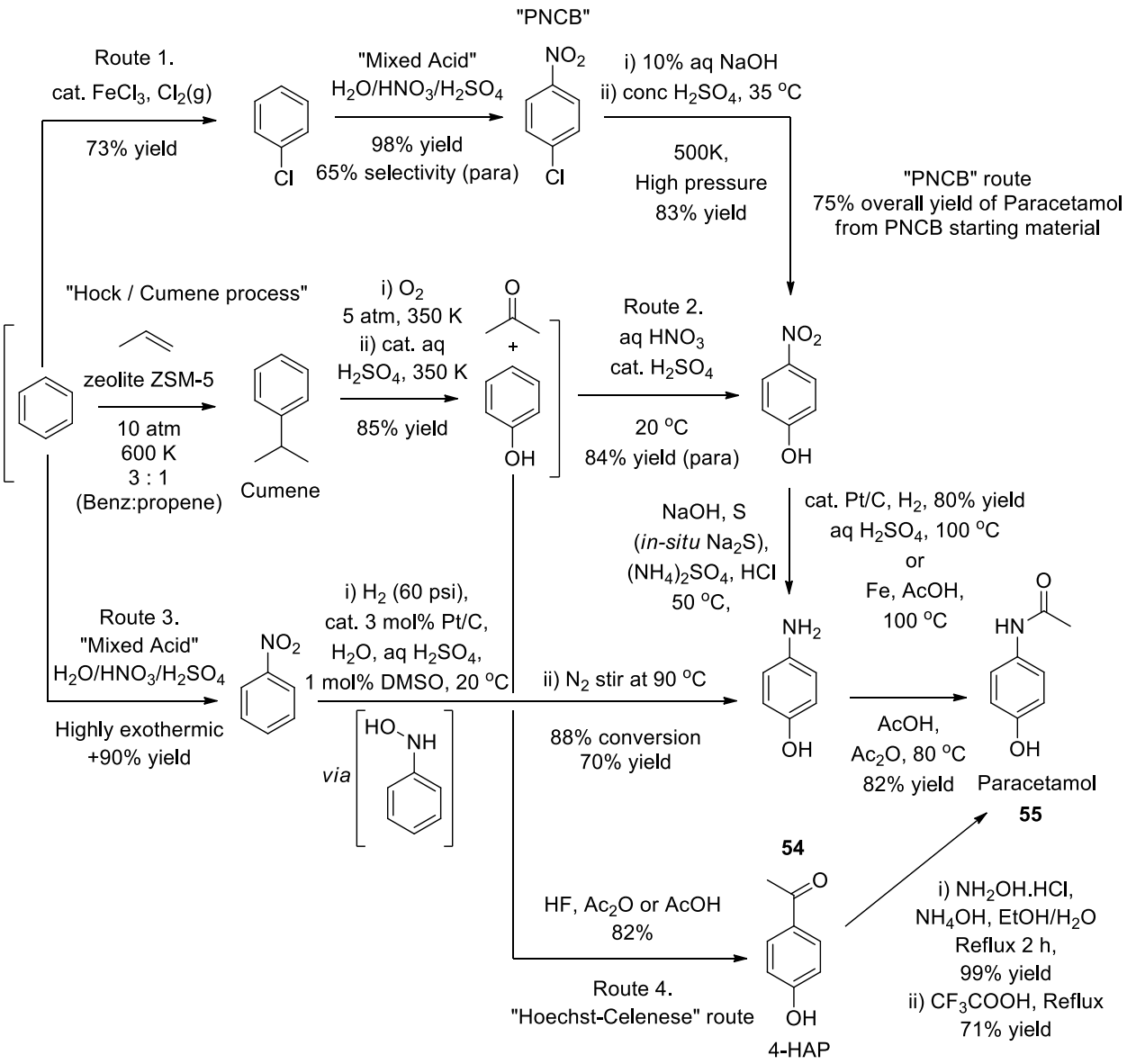

Scheme 199. Commercial routes to paracetamol from petrochemical feedstocks

The yield and atom economy of each of these industrial routes to Paracetamol is summarised in the Table 5 below, which demonstrates how inefficient and wasteful some of these processes are. A large number of manufacturers of paracetamol exist worldwide including: Angene International Limited, BOC Sciences, Granules India, Haihang Industry Co., Ltd., Rhone Poulenc, Jinan Haohua Industry Co., Ltd., Kemcolour International, Mallinckrodt Inc, McNeil, ORGANICA Feinchemie GmbH Wolfen, Parchem Fine & Specialty Chemicals, Hoechst Celanese, Sterling Organics, Wuxi Feipeng Imp. & Exp. (Group) Co., Limited and

Zhejiang Hisun Chemical Co., Limited. Mallinckrodt Inc (USA) and Hoechst Celanese are currently the largest producers of paracetamol.[254]

Table 5. Metrics for the industrial manufacture of paracetamol.[245,250,34, 36]

Route	Major Manufacturer[245]	Volume[245] (2004)	Approximate Industrial Yield[a]	Atom Economy[b]	Liquid effluent waste per tonne of Paracetamol[245]
1. PNCB route	Mallinckrodt Inc, USA / Sterling Organics, UK	12000, 3000	35% (75% from PNCB)	38%	35,000 litres
2. Phenol route	Rhone Poulene, USA and France	7000	47% (52% from phenol)	54%	40,000 litres
3. Nitrobenzene route	McNeil, USA	(Not reported)	52%	52%	(Not reported)
4. Hoeschst-Celenese route *via* 4-HAP (newest route 1990's)	Hoeschst-Celenese, USA	9000	46%	49%	(Not reported)

[a] Yields calculated using data reported in the literature relating to industrial processes, with yields dependent on the efficiencies of individual plant design and conditions used. Yields calculated by Eynde 2016[255] using data gathered from laboratory scale processes. [b]Atom economies calculated for routes using Ac_2O as a reagent for the final *N*-acetylation step to paracetamol.[249]

The first industrial route to paracetamol requires 5 steps from benzene ((i) aromatic chlorination; (ii) aromatic nitration; (iii) S_NAr; (iv) nitro reduction, (v) *N*-acetylation), with a lot of acidic waste and numerous salts being generated as by-products using this route. This leads to a low atom economy for this process of 38%.[249] The Lewis acid catalysed chlorination step from benzene requires purification to remove dichlorinated aryl products; whilst the second nitration step requires purification to remove *ortho* substituted nitroaryl regioisomers. Approximately 35,000 tonnes of liquid waste is generated for every tonne of paracetamol produced using this route,[245] with this route having a relatively low yield of 35%.[249]

The second industrial route to paracetamol requires 5 steps from benzene which employs the Hock process ((i) Friedel-Crafts alkylation; (ii) cumene oxidation) to convert benzene into phenol (via cymene) which is then nitrated to afford p-nitro-phenol, which are then reduced to afford 4-HAP that can then be *N*-acetylated Nitration of phenol produces the undesired *ortho* nitro phenol that must be removed, which contributes to an atom economy of 54% and a moderate yield for paracetamol of 47%.[249]

The third industrial route to paracetamol involves a highly exothermic mononitration reaction of benzene that poses a significant safety hazard. Hydrogenation of nitrobenzene then occurs through a phenylhydroxylamine intermediate that undergoes a Bamberger rearrangement to afford *para*-aminophenol that is then *N*-acetylated. The difficulty with this process is the need

to minimise competing formation of aniline as a by-product in the hydrogenation step, whilst the generation of large amounts of sulphate salts lower the atom economy of this route.[249]

The fourth industrial route involves a 4-step process which was developed by the American company Hoechst-Celenese that afford paracetamol in 49% overall yield. This process employs the two-step Hock process to convert benzene into phenol that then undergoes Friedel-Crafts acetylation to afford 4-hydroxyacetophenone.[255] Stoichiometric amounts of acidic HF are required in the acetylation step which represents a significant toxicity and corrosion risk. The final step involves an acid mediated Beckmann rearrangement of 4-HAP which is a highly atom economic step that affords paracetamol in good yield.[249]

BASF also produce 4-HAP using a different industrial process which employs aluminium chloride as a Lewis acid to mediate the Fries rearrangement of phenyl acetate of to give 4-HAP (54) (and 2-hydroxyacetophenone (2-HAP)) (Scheme 200). The BASF route suffers from low selectivity for formation of the desired *para* product however its isolation is facilitated by direct crystallisation of 4-HAP from the crude reaction mixture, with the major 2-HAP isomer remaining in solution.[256]

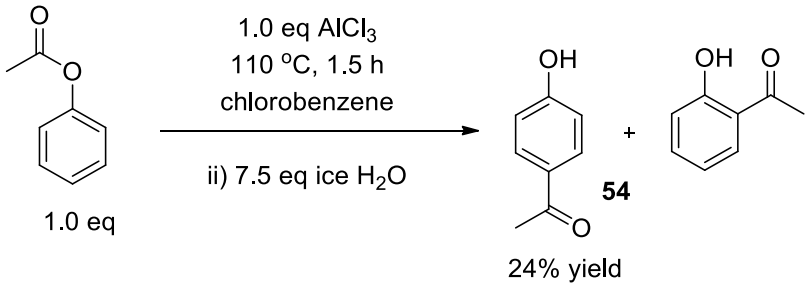

Scheme 200. BASF Fries reaction for the industrial synthesis of 4-HAP

As discussed above, there are many disadvantages associated with each of the current commercial routes to paracetamol that affords an opportunity to demonstrate that terpenes could be used as renewable feedstocks for the scalable and green synthesis of a common pharmaceutical. Therefore, 'green' paracetamol was chosen to demonstrate the potential of using a monoterpene such as limonene or β-pinene as a biorenewable feedstock for the sustainable production of a bulk commodity pharmaceutical. It was decided to target a sustainable route to paracetamol using catalytic protocols that would afford 4-HAP as an intermediate, since this would allow direct access to paracetamol in one step using an industrially validated Beckmann rearrangement reaction. Furthermore, an efficient catalytic synthesis of 4-HAP would represent a route to a 'drop-in' intermediate that could be used as a green aromatic building block for the synthesis of more expensive drugs, such as isoprenaline, propranolol and salbutamol.

5.2 1st Generation route to paracetamol

A first generation sustainable route to transform biorenewable limonene into paracetamol was devised according to the 6 step synthetic route shown in Scheme 201, with the first step of the synthesis employing the catalytic Ishii-Venturello epoxidation reaction of limonene developed previously. The overall strategy employed would incorporate eight of the carbon atoms of limonene into the core structure of 4-HAP and paracetamol, with no new C-C bond forming reactions being required. Specific challenges highlighted at the start of this synthesis, included the ability to selectively ring open the epoxide in step 2 to afford an exocyclic disubstituted alkene and the ability to catalytically aromatise the keto-enone intermediate in step 5.

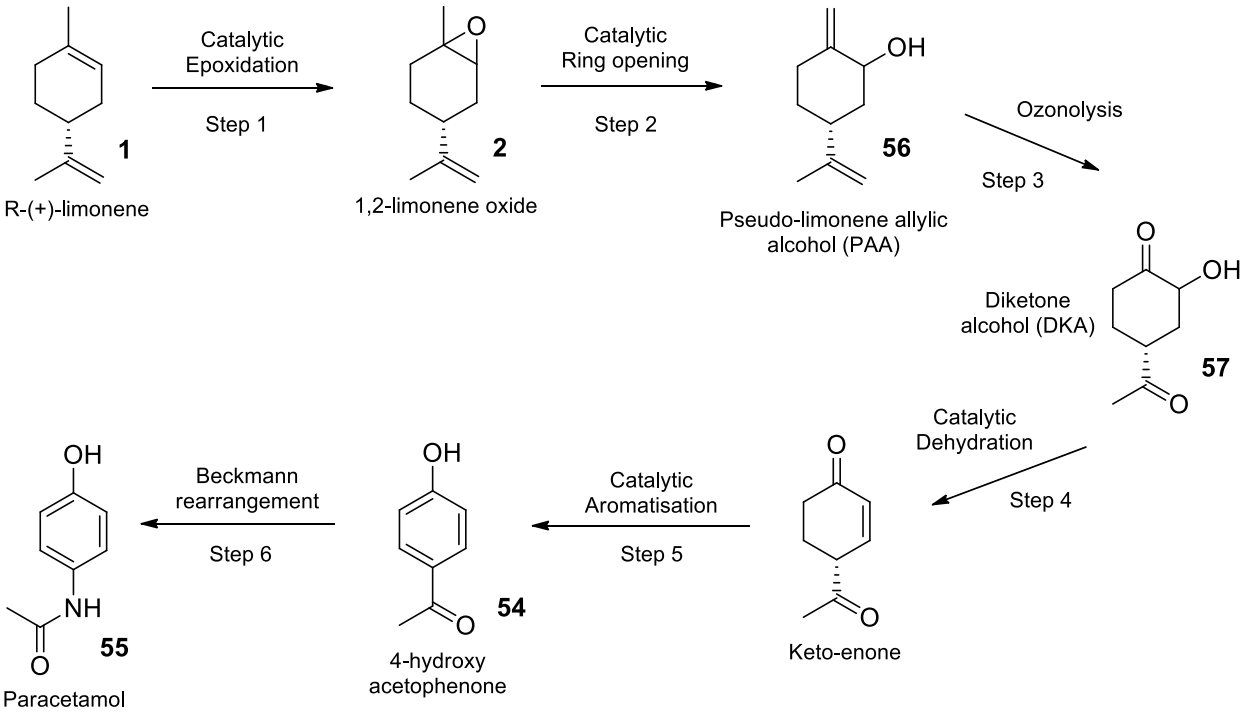

Scheme 201. 1st generation six step route from limonene to paracetamol

5.2.1 Steps 1 and 2. Epoxidation of limonene and ring-opening of limonene epoxide to afford pseudo-limonene allylic alcohol

The initial selective 1,2-epoxidation step of limonene (1) had been optimised using the catalytic Ishii-Venturello/H_2O_2 system described in the previous chapter, so this reaction was repeated to provide 10 g batches of limonene epoxide as 55:45 mixture of α-/β- diastereomers in 94% yield (Scheme 202).

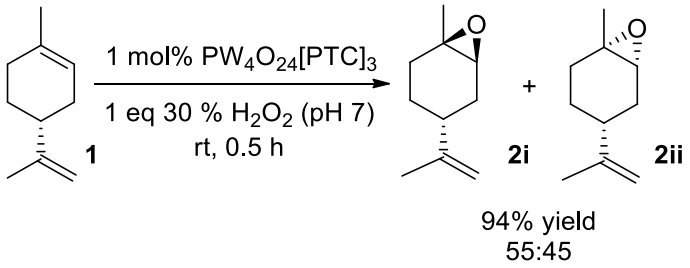

Scheme 202. Solvent free epoxidation of limonene

With 1,2-limonene epoxide in hand, a review of the literature revealed that Uroos et al[257] had employed a stoichiometric amount of Yamamoto's aluminium amide[258] to ring open (*R*)-(+)-limonene epoxide (2i/ii) to afford the desired pseudo-limonene allylic alcohols (PAA) (56) in 96% yield, which was used for the total synthesis of (+)-cymbodiacetal (Scheme 203).[257]

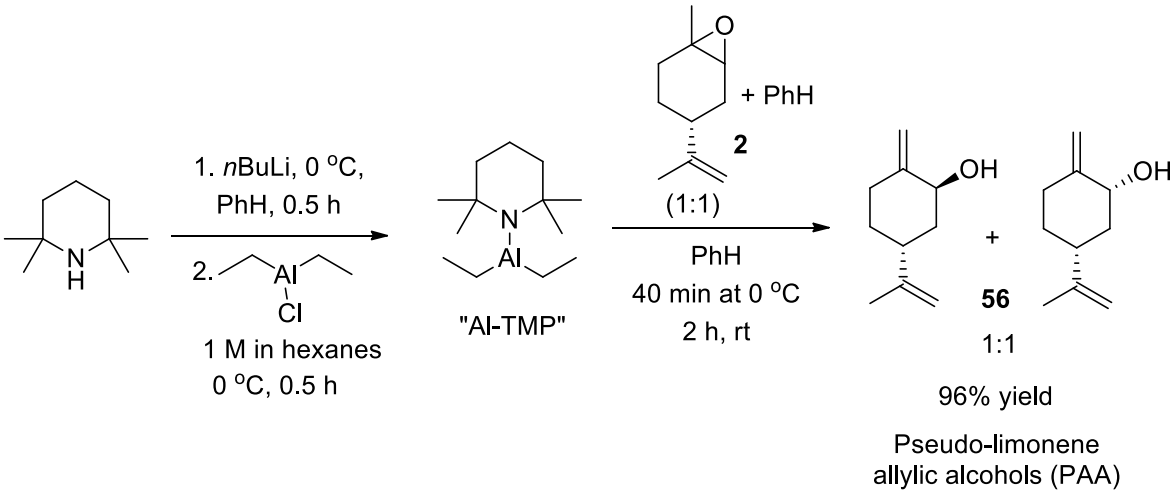

Scheme 203. Ring opening of 1,2-limonene epoxide using Al-TMP

This protocol was repeated, with similar results being achieved to afford the desired allylic alcohol in 83% isolated yield, however the use of benzene as a solvent was far from ideal from a green perspective. Consequently, a solvent screen (Table 6) was performed to find a more environmentally benign alternative, with excellent 77-86% yields for the allylic alcohols being produced using toluene, hexane and THF (Scheme 204).

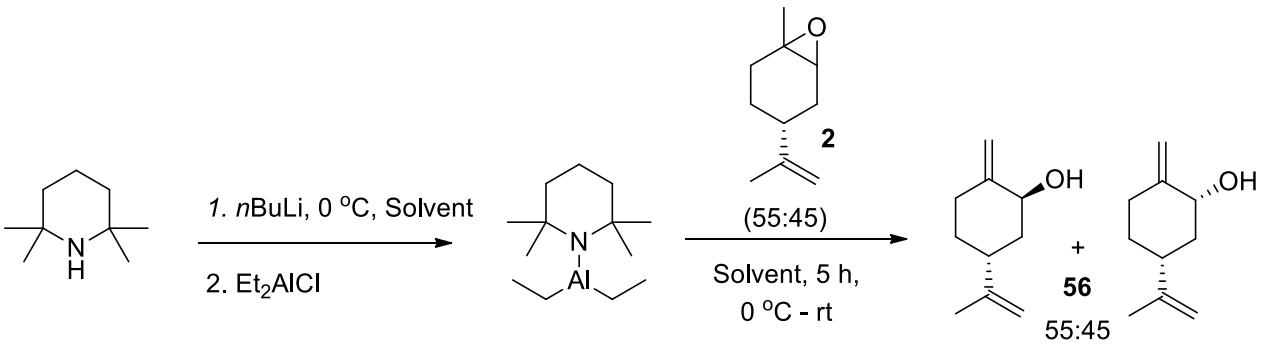

Scheme 204. 1,2-limonene epoxide ring opening using Al-TMP

Table 6. Solvent screen of Aluminium-TMP for the ring opening of 1,2-limonene epoxide

Solvent	**Yield % of PAA[a]**
Benzene	83
Toluene	86
Hexane	77
THF	83

[a] Reactions carried out on 750 mg 1,2-limonene epoxide using 1.7 mL 2,2,6,6-tetramethylpiperidine, 4.3 mL of 2.3 M *n*BuLi in hexanes, 11.3 mL diethyl aluminium chloride solution (1.0 M in hexanes) in 15 mL of solvent, 0 °C to rt, 5 h.

It is proposed that this regioselective epoxide ring-opening reaction proceeds *via* a mechanism whereby its aluminium counterion coordinates to a lone-pair of the epoxide oxygen atom resulting in the nitrogen fragment being positioned in the correct orientation to act as a base to selectively deprotonate the exocyclic methyl proton, to trigger epoxide ring-opening (Scheme 205).

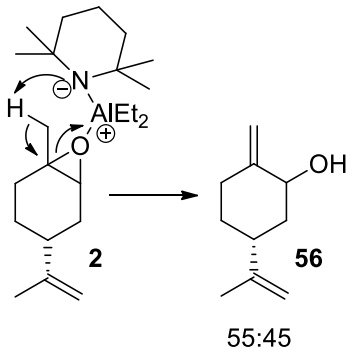

Scheme 205. Proposed mechanism of base-mediated ring opening of limonene epoxide (2)

Attempts to employ sterically hindered lithium amides (e.g. LDA) as a replacement for the aluminium amide of TMP in this epoxide ring-opening reaction using Et_2O as a solvent at 35 °C were successful, resulting in selectivity for the desired allylic alcohol (56) over its carveol isomer dependent on the steric bulk of the lithium amide used for deprotonation. Therefore,

lithium TMP gave a 94:6 ratio, LDA gave a 90:10 ratio and lithium diethylamide gave a 80:20 ratio of pseudo-limonene allylic alcohol (56) over carveol (58), respectively (Scheme 206).

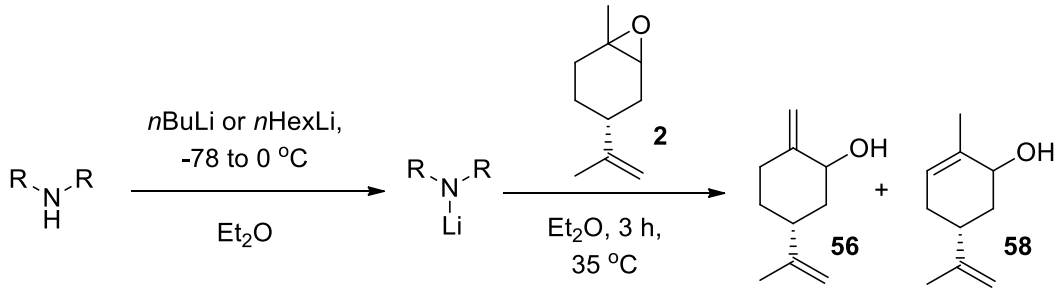

Scheme 206. Lithium amide mediated ring opening reactions of 1,2-limonene epoxide

Table 7. Screen of lithium amides used as bases for ring opening of 1,2-limonene epoxide

Amine	**% Yield**	**% Selectivity for PAA**	**% Selectivity for Carveol**
TMP	95	94	6
*i*Pr	90	90	10
Et	91	80	20

[a]Isolated yields; reactions carried out using 750 mg 1,2-limonene epoxide in 15 mL Et_2O

Although these metal amide protocols gave excellent selectivity (Table 7) for the desired regioisomeric pseudo-limonene allylic alcohol, they unfortunately required the use of stoichiometric reagents, dry solvents and inert atmospheric conditions, so an alternative ring opening procedure was required from a process scale-up perspective.

A literature search revealed that aluminium based reagents had previously been used to perform Lewis acid mediated epoxide ring opening reactions to afford allylic alcohols with exocyclic methylene bonds. For example, Basabe *et al.*[259] had shown that that aluminium isopropoxide (AIP) had been used to ring open a cyclohexyl epoxide to afford an allylic alcohol containing an exo-methylene group for the synthesis of a Spongolactam C analogue (Scheme 207).[259]

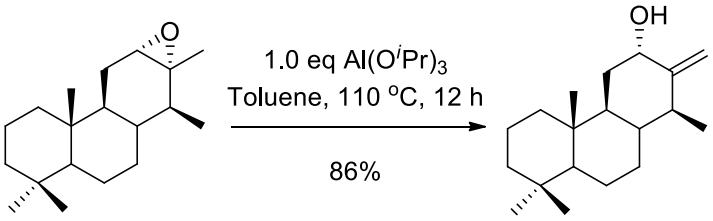

Scheme 207. AIP used to ring open the cyclohexene epoxide of a Spongolactam C analogue

We found that refluxing limonene oxide with 0.1 or 1.0 equivalent of AIP or 1.0 equivalent of aluminium *tert*-butoxide in toluene resulted in ring-opening to form a 2:1 mixture of pseudo-limonene allylic alcohol and carveol in a combined yield of 83-94% yield. These conditions were then modified to allow for ring-opening under solvent-free conditions at 140 °C using 0.1mol% of AIP (homogeneous solution at 110 °C) to give a 3:2 mixture of pseudo-limonene allylic alcohol (56) (kinetic product) and carveol (58) (thermodynamic product) in 86% yield

(Scheme 208). Examination of the ^{1}H NMR spectrum of the crude reaction mixture also revealed the presence of 14% of 1,2-limonene-diol (3), that had been formed from competing hydrolytic ring opening of 1,2-limonene epoxide (2).

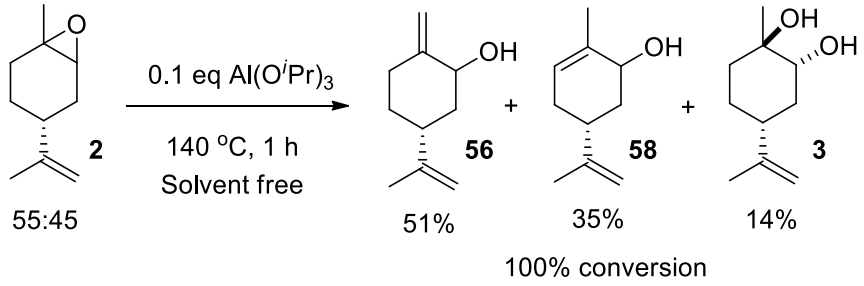

Scheme 208. Lewis acid catalysed ring opening of 1,2-limonene epoxide

The mechanism of epoxide ring-opening is thought to proceed through an acid catalysed ring opening mechanism *via* an E_2-like mechanism that must proceed under kinetic control, since it affords the thermodynamically less stable exocyclic methylene group of PAA. Therefore, ring opening *via* pathway (a) results in formation of the exocyclic methylene group of pseudo-limonene allylic alcohol, whilst elimination *via* pathway (b) leads to formation of the trisubstituted alkene bond of carveol (Scheme 209).

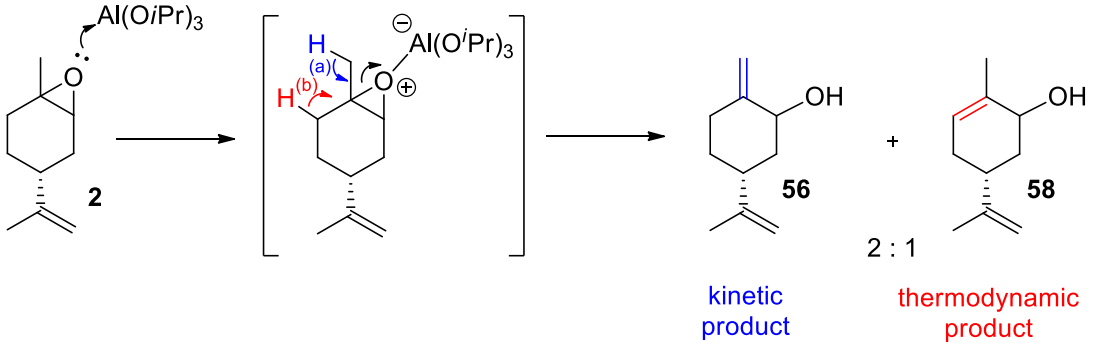

Scheme 209. Proposed acid catalysed mechanism for epoxide ring opening

It was then decided to determine whether ring opening the diastereomers of limonene epoxide with AIP would give different ratios of PAA and carveol. Single diastereomers of 1,2-limonene epoxide were prepared using a reactive separation protocol developed by Steiner et al,[260] based on separate reaction of the mixture of epoxides with pyrrolidine or pyrazole, respectively. Therefore, reaction of the mixture of limonene epoxides (2) with pyrrolidine resulted in fast ring open of the *trans*-epoxide (2ii) diastereomer at its 2-position, which enabled the less reactive *cis*-epoxide (2i) to be recovered. Alternatively, reaction of the mixture of limonene diastereomers with pyrazole and water resulted in selective hydrolysis of the *cis*-epoxide (2i) at its 1-position, allowing for the *trans*-epoxide (2ii) to be recovered (Scheme 210).[260]

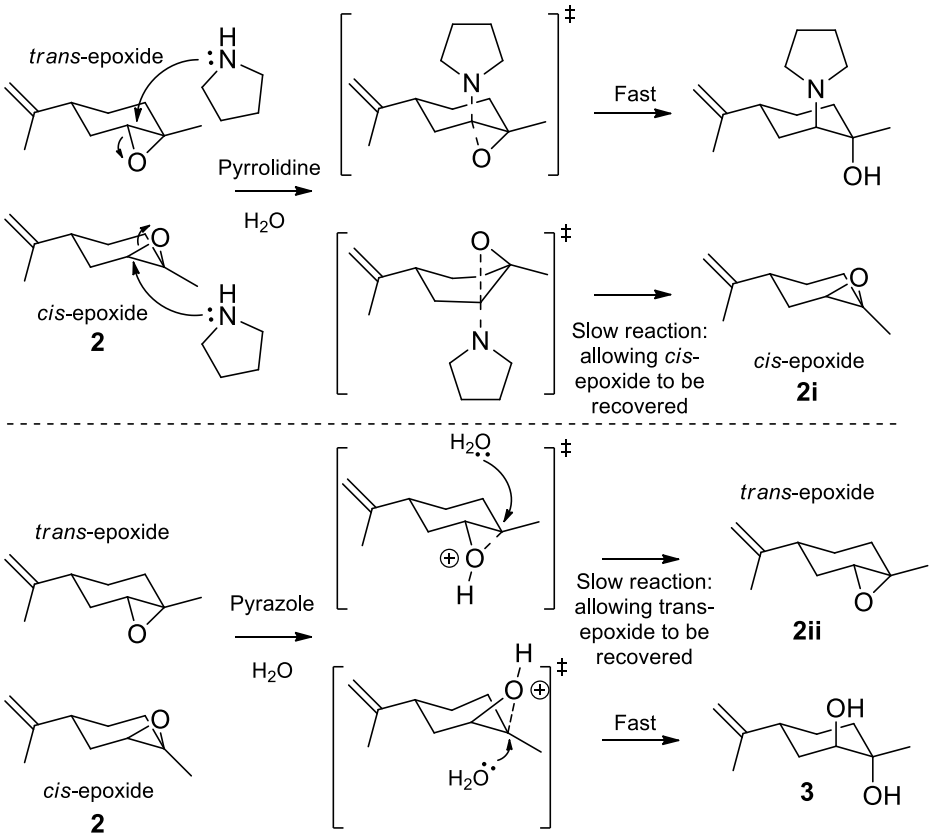

Scheme 210. Ring opening reactions used for isolation of each isomer of 1,2-limonene oxide

Each of the 1,2-limonene epoxide diastereoisomers were then reacted with one equivalent of AIP under solvent free conditions, with the *cis*-epoxide (2i) being ring-opened non-selectively to afford a 54:46 mixture of PAA (56) and carveol (58), whilst the *trans*-epoxide (2ii) gave a highly selective 98:2 mixture of PAA (56) and carveol (58), respectively (Scheme 211).

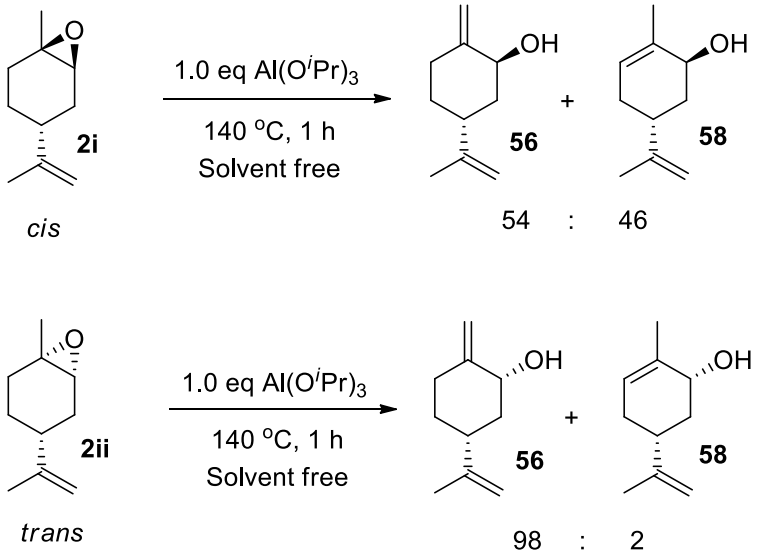

Scheme 211. Lewis acid mediated epoxide ring opening of pure 1,2-limonene epoxide diastereomers

These results confirmed that the conformation of the six-membered ring played an important role in determining which proton of each epoxide diastereomer eliminates to afford either PAA or carveol. The mechanism of the epoxide ring-opening mechanism is thought to involve coordination of the epoxide lone-pair to the aluminium Lewis acid to afford an -ate complex, with one of its isopropoxide ligands then acting as a base to deprotonate at its β-position to trigger epoxide ring-opening. Coordination of AIP to the *trans*-epoxide results in selective deprotonation at the methyl position to afford PAA because the isopropoxide ligand is unable to bridge to deprotonate the protons of the C_6 methylene group to afford carveol. Conversely, coordination of AIP to the *cis*-epoxide results in an -ate complex whose isopropoxide ligand can deprotonate both the methyl group and the methylene groups to afford a mixture of PAA and carveol (Scheme 212).[261]

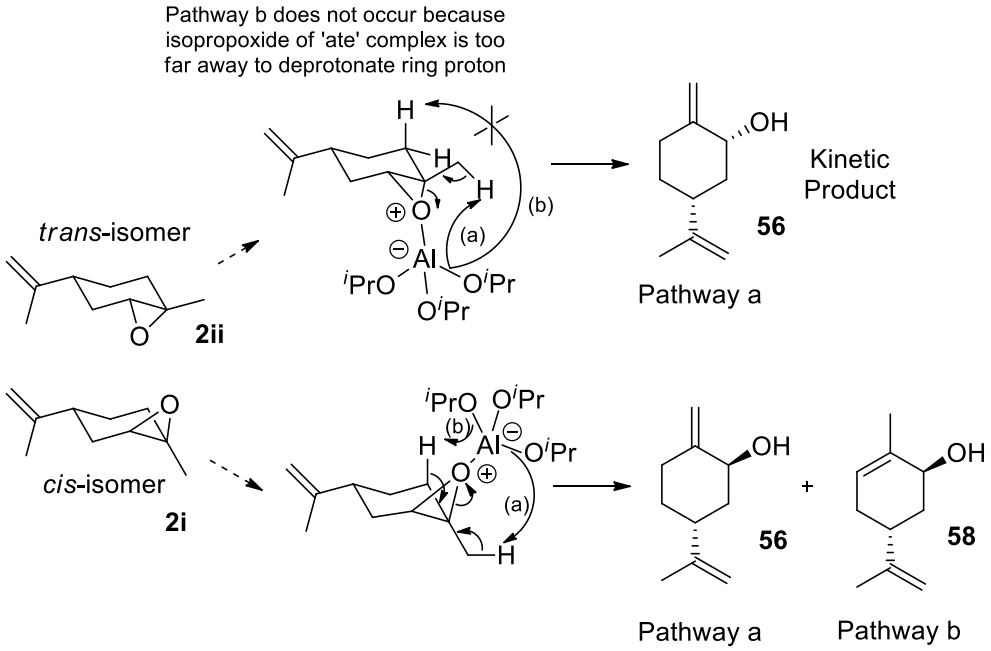

Scheme 212. Mechanistic explanation to explain the difference in ring-opening selectivity of *trans*- and *cis* 1,2-limonene epoxides

These results suggested that selective access to the *trans* epoxide would afford a high yielding route to the pseudo-limonene allylic alcohol (56) using AIP as a cheap Lewis acid in this ring-opening mediated ring opening methodology. A high yielding and selective synthesis of *trans*-1,2-limonene epoxide was previously reported by Greiner et al,[209] involving treatment of limonene with *N*-bromosuccinimide in acetone/water to give a bromohydrin (59) that was then cyclised to its epoxide *via* treatment with base (Scheme 213). The Greiner synthesis of *trans*-1,2-limonene epoxide (2ii) was repeated on a 10 g scale to give pure *trans*-1,2-limonene epoxide with no loss of selectivity. Workup of the first bromohydrin step involved salting with solid NaCl (to separate the acetone and water) followed by an acid wash to remove succinimide. The crude bromohydrin was then treated with aqueous 6M NaOH, resulting in ring-closure to afford *trans*-1,2-limonene epoxide in 72% yield over the two steps. Although, NBS is required in stoichiometric amounts in this protocol, the succinimide by-product may potentially be recycled to afford NBS, *via* treatment with bromine and base (Scheme 213).

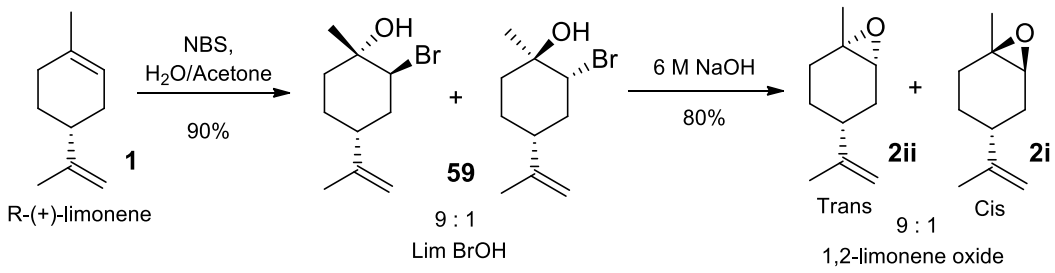

Scheme 213. Selective synthesis of *trans*-1,2-limonene epoxide (2ii)

Attempts to employ catalytic loadings of AIP to ring open *trans*-1,2-limonene epoxide under solvent free conditions were unsuccessful, with the reaction time taking 6h to reach 95% conversion, which afforded a complex reaction product containing multiple products that contained approximately 30% of the desired PAA product (Scheme 214).

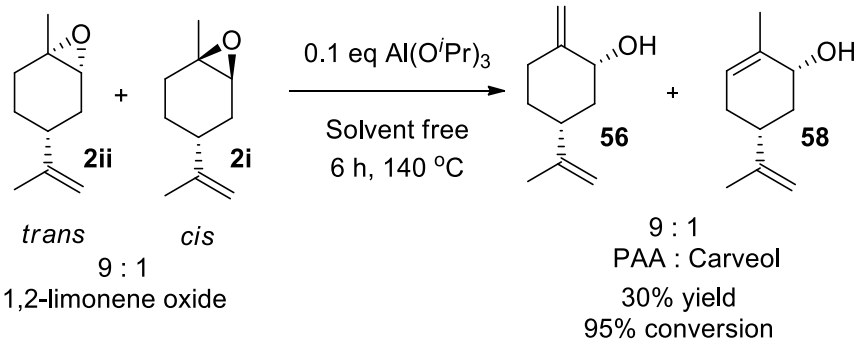

Scheme 214. Catalytic ring opening of *trans*-1,2-limonene epoxide with AIP

However, use of 1.0 eq of AIP resulted in full conversion of *cis*-1,2-limonene epoxide after 1.5 h to afford a good 70% yield of PAA after 1.5 h in the presence of 10% carveol and 5% of other uncharacterised minor products (Scheme 215). Using a stoichiometric loading of AIP is not ideal but is acceptable from an economic perspective due to the low cost of AIP ($3 per kg [Alibaba.com]). From a catalyst recycling perspective, magnetic nanoparticle supported AIP has previously been used by Jones et al,[262] for the catalytic ring opening of caprolactone, which enables easy recovery of the catalyst through application of a magnetic field.

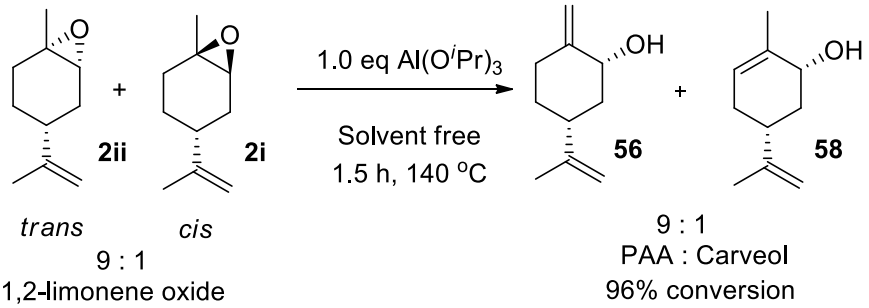

Scheme 215. Ring opening of *trans*-1,2-limonene epoxide with AIP

5.2.2 Step 3. Ozonolysis of PAA and PAA acetate

Ozonolysis is a robust methodology for transforming alkenes into carbonyl species that is effective on both cyclic and acyclic alkenes, which makes use of cheap molecular oxygen based processes that are amenable to scale up in batch and flow. For example, Brenek et al[263] demonstrated that 17 kg of β-pinene could be ozonolysed to afford nopinone in 65% yield (Scheme 216), whilst the microreactor technology team at Lonza[162] carried out ozonolysis in a 450 L loop flow reactor to produce 500 kg of a cyclopropyl aldehyde on a daily basis (Scheme 216).

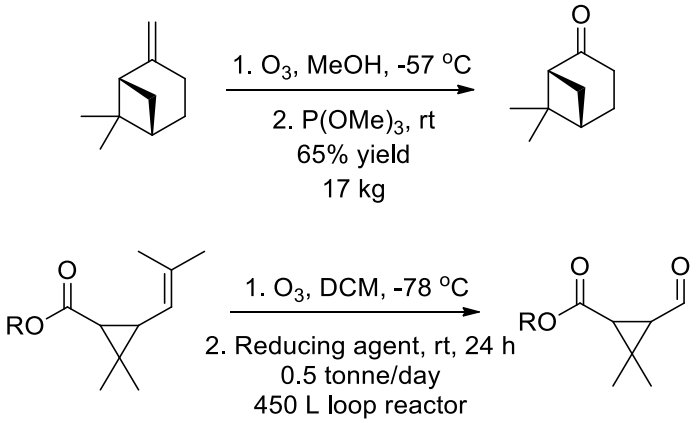

Scheme 216. Large scale batch and flow ozonolysis

PAA (56) was ozonolysed in CH_2Cl_2 at -78 °C under standard conditions (Scheme 217), with the ozone supply terminated once the solution had turned bright blue, which was taken as evidence that all the alkene bonds in the substrate had reacted to afford their respective ozonides (Scheme 217). The ozonolysis reaction was then worked up using a range of reducing agents (dimethyl sulfide, triphenylphosphine and triethylamine) which gave the desired diketone product (57) in a disappointing 32-38% yield (Scheme 217, Table 8). The 10% carveol by-product (58) was very difficult to separate from PAA by chromatography or distillation so we initially used this mixture in the ozonolysis experiments. Ozonolysis of carveol (58) produces a ring opened substrate as shown in Scheme 217 however this by-product was not isolated as the primary aim was the preparation of DKA.

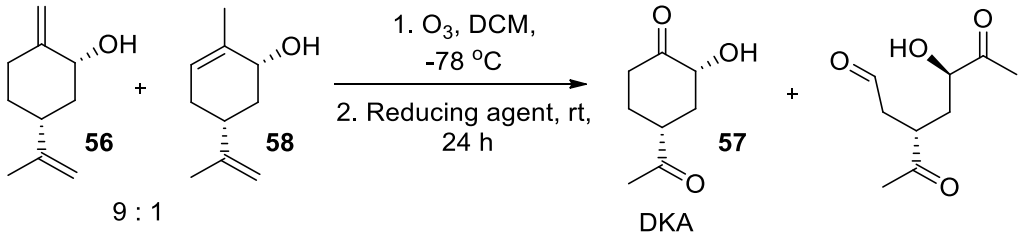

Scheme 217. Ozonolysis of PAA

Table 8. Conditions used for the reductive cleavage of ozonides

Ozonide degradation agent	Yield of DKA %[a]
DMS	38
PPh_3	32
NEt_3	37

[a]Isolated yields. Reactions run on 5 mmol scale using 5 eq of reducing agent.

The poor yield obtained for the double ozonolysis of PAA was initially puzzling; however a review of the literature revealed that the free hydroxyl group of allylic alcohols could participate in ozonolysis reactions. For example, Zvereva et al[264] have reported that ozonolysis of the alkene bond of an allylic alcohol group containing an exocyclic methylene group also gave poor yields of cyclohexanone products, due to competing formation of ring-opened carboxy-aldehyde products caused by its free alcohol group participating in the ozonolysis reaction (See Schemes 218 and 219 for details).

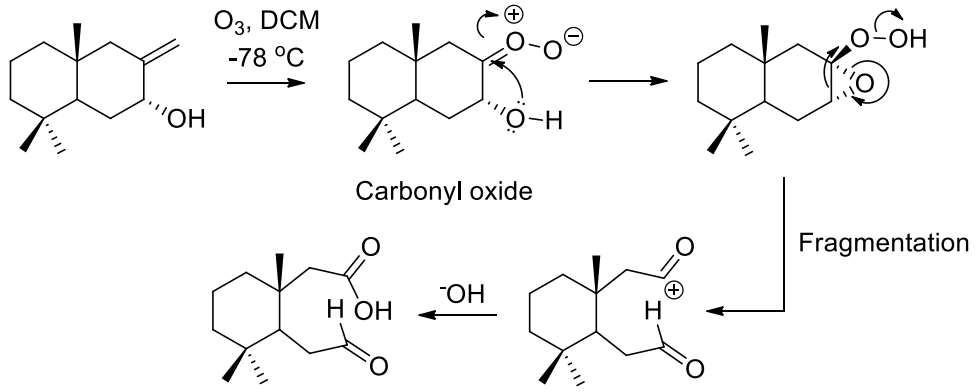

Scheme 218. Epoxide mechanism for competing formation of carboxy aldehyde

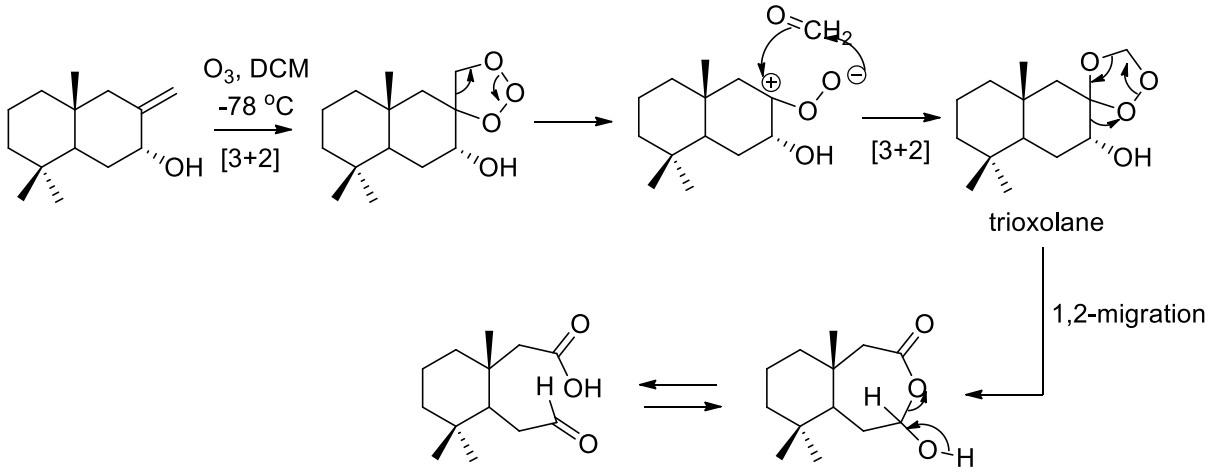

Scheme 219. Migration mechanism for competing formation of carboxy-aldehyde

Consequently, it was decided to repeat our ozonolysis reaction using methanol as a solvent, since it was reasoned that hydrogen bonding of methanol to the alcohol group might prevent it from participating in the ozonolysis reaction. Carrying out ozonolysis of PAA in methanol using zinc and acetic acid for reductive work-up[265] resulted in formation of the desired diketone

(DKA) in an improved 50% isolated yield after chromatography (Scheme 220), however, this yield was still too low for a synthesis of paracetamol to be economically feasible.

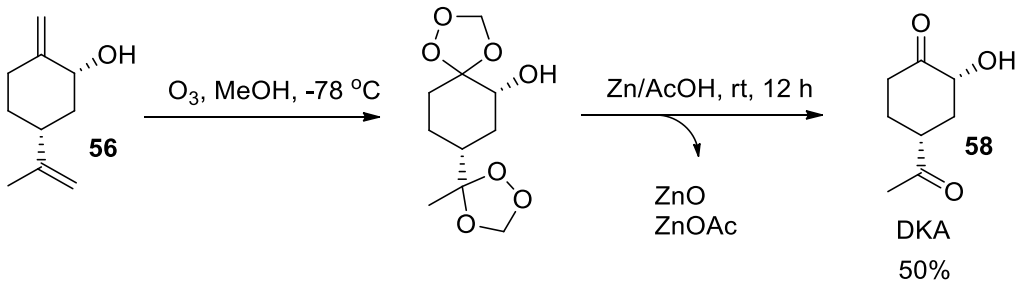

Scheme 220. Ozonolysis using a zinc/acetic acid workup

As only moderate yields had been observed for the ozonolysis of PAA (56) it was decided to protect its alcohol functionality as a simple acetate group to afford PAA-OAc (60), whose ozonolysis properties would then be investigated. This was achieved *via* treatment of PAA (56) with triethylamine and acetic anhydride in the presence of a catalytic amount of DMAP, which gave PAA-OAc (60) in an excellent 95% yield (Scheme 221).

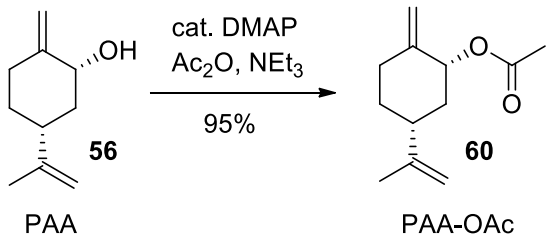

Scheme 221. Synthesis of PAA-OAc

The ozonolysis of PAA-OAc was then carried out in DCM at -78 °C using DMS as a quench to afford the desired diketone product (61) (DKA-OAc) in 85% isolated yield, providing further confirmation that the alcohol group of PAA was responsible for the low yields of its ozonolysis products. The DKA-OAc could then be hydrolysed under alkaline conditions *via* treatment with potassium methoxide in methanol, which gave DKA (57) in 80% yield (Scheme 222).

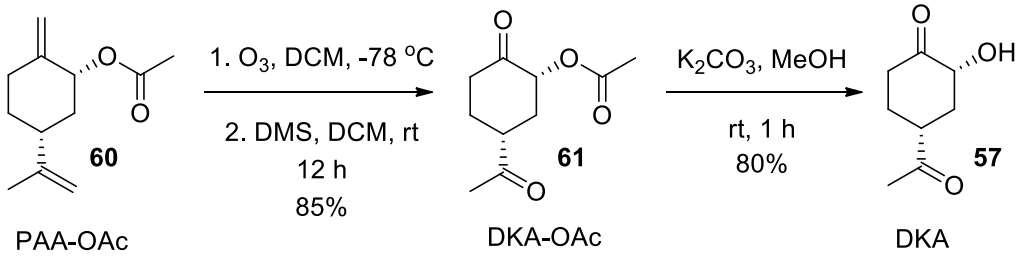

Scheme 222. Ozonolysis of PAA-OAc followed by acetate deprotection to afford DKA

5.2.3 Step 4. Unsuccessful dehydration reactions of DKA and DKA-OAc

The next step in the synthetic route to paracetamol involved dehydration of the α-alcohol group of the cyclic ketone to form an α,β-unsaturated ketone that would then be subsequently aromatised (*via* its enolic form) to afford 4-hydroxy-acetophenone (Scheme 223).

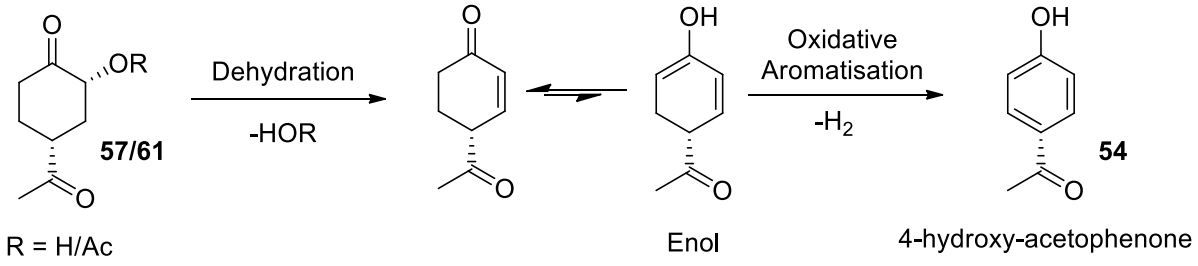

Scheme 223. Proposed elimination-aromatisation protocol

A review of the literature revealed a number of transformations where α-hydroxy groups of cyclohexyl ketones had been eliminated under acidic conditions to afford α,β-unsaturated ketones, albeit under relatively forcing thermal conditions (Scheme 224)[266- 58]. Therefore, it was hoped that carrying out this type of forcing dehydration reaction on PAA under an oxidative atmosphere might result in a one-pot dehydration-enolisation-aromatisation tandem reaction to directly afford *p*-hydroxy-acetophenone.

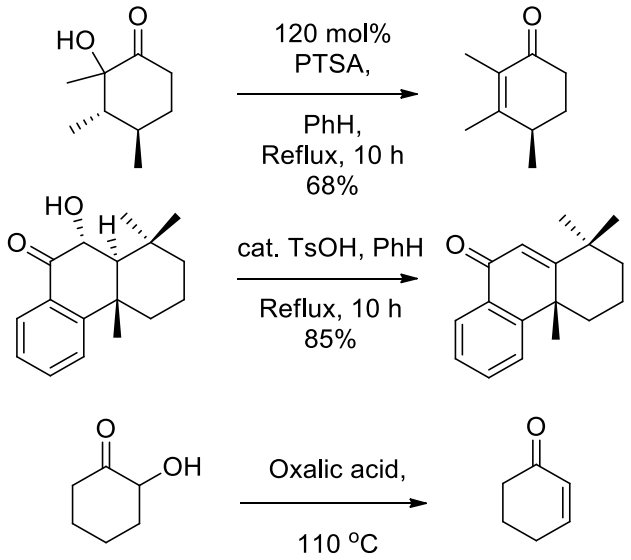

Scheme 224. Literature examples of acid catalysed alcohol elimination reactions to afford α-β-unsaturated cyclic ketone

Amberlyst-15 was initially chosen as chosen as a strong heterogeneous acid catalyst to trial the dehydration reaction of DKA, since this would facilitate easy recovery of the catalyst at the end of the reaction. As precedent, Frija et al[267] had previously used this acidic resin as a heterogeneous catalyst for the dehydration of a cyclohexyl tertiary alcohol to afford it's corresponding alkene (Scheme 225), so it was hoped that the secondary alcohol would also be amenable to elimination using this solid supported acid.

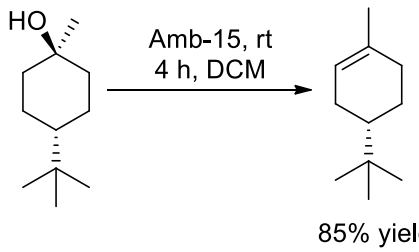

Scheme 225. Tertiary alcohol dehydration using Amberlyst-15

However, treatment of DKA with 10 mol% Amberlyst-15 in a range of solvents (acetone, EtOAc, MeOH, DCM, Et_2O) at reflux did not result in formation of the desired α,β-unsaturated ketone (or *p*-hydroxyacetophenone), affording either recovered DKA (Scheme 226) or a complex mixture of uncharacterisable products. Attempts to dehydrate DKA using 10 mol% homogeneous acid (phosphoric acid, oxalic acid, 10% H_2SO_4(aq), PTSA) in refluxing toluene were also unsuccessful affording complex mixture of products in each case.

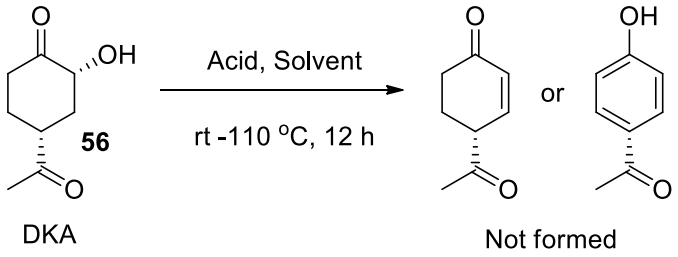

Scheme 226. Attempted acid mediated elimination of DKA

Since we had developed a viable route to DKA-OAc it was decided to determine whether we could develop acid catalysed conditions that would enable its acetate group (better leaving group) to be eliminated to afford the desired α,β-unsaturated ketone (Scheme 227).

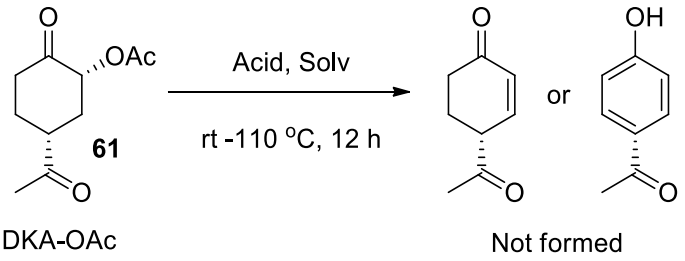

Scheme 227. Attempted acid mediated elimination of hydroxy-PAA

As precedent, Wysocki et al[268] had reported the acid catalysed deacetylation of an □-acetoxy-cyclohexyl ketone, albeit in a moderate 43% yield (Scheme 228). However, attempts to dehydrate DKA-OAc using 10 mol% homogeneous acid (phosphoric acid, oxalic acid, 10% H_2SO_4(aq), PTSA) in refluxing toluene were also unsuccessful affording complex mixtures of products in each case.

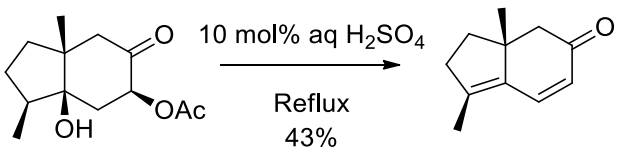

Scheme 228. Acid catalysed deacetylation of an α-acetoxy-cyclohexyl ketone

5.2.4 Step 4. Pseudo-limonene route to key diketone precursor

Since it was clear that an acid catalysed elimination strategy was not viable it was decided to explore an alternative Pd(0) catalysed elimination process for the reductive elimination of the acetate group of DKA-OAc. Tsuji et al[269] have developed a highly effective method for the hydrogenolysis of allylic compounds using palladium catalysis and ammonium formate as a hydride source, with excellent selectivity having been reported for the formation of less thermodynamically stable, terminal alkenes (Scheme 229). [270] In these reactions, a Pd(0) catalyst undergoes oxidative addition to the allylic acetate substrate to forms a π-allylic complex, with formate then attacking the palladium species to afford a formate complex that is then converted into a palladium-hydride *via* elimination of CO_2. Reductive elimination then occurs to regenerate the Pd(0) species, with hydride preferentially attacking the more substituted centre of the π-allyl complex to give the terminal alkene product (Scheme 230).[270]

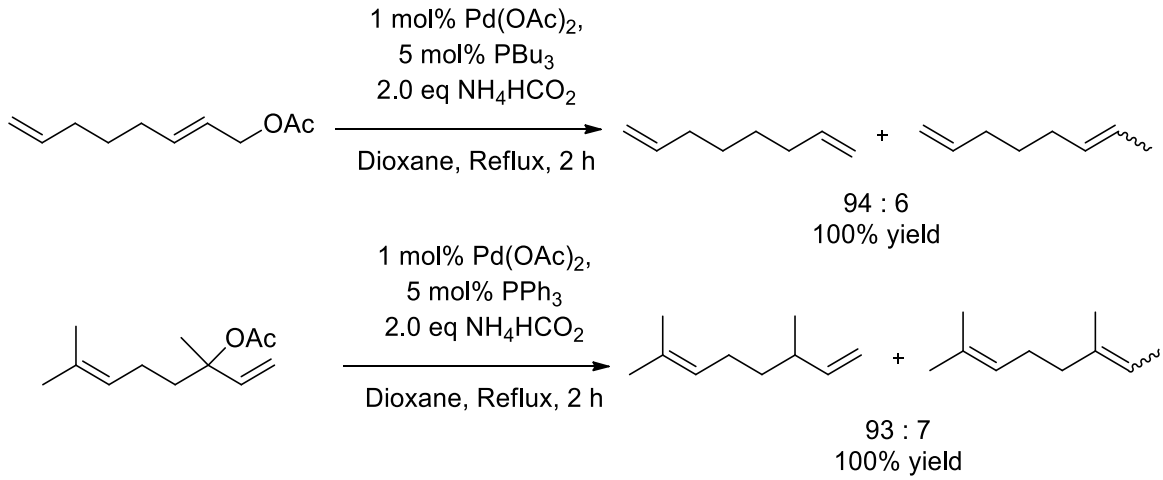

Scheme 229. Tsuji Pd(0) mediated reduction of allylic acetates.

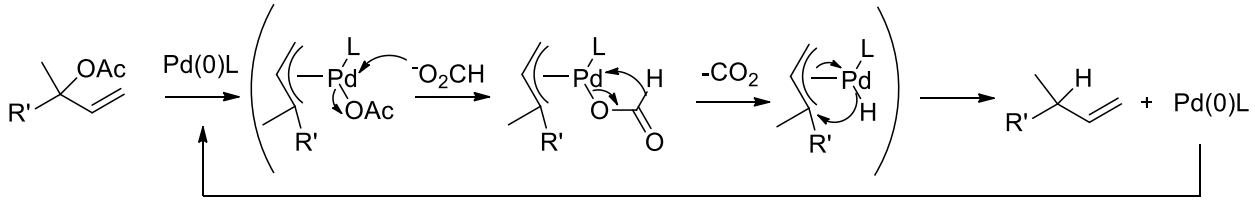

Scheme 230. Mechanism of Tsuji palladium catalysed reduction reaction[270]

To our delight, Tsuji's original conditions (dioxane as solvent) could be successfully applied to DKA-OAc (61) directly affording pseudo-limonene in a high 95% yield, with toluene then being used as a replacement solvent for dioxane (possible carcinogen/explosive hazard) to afford

pseudo-limonene (62) in an identical yield, with < 5% of 1,2-limonene (1) being present (Scheme 231).

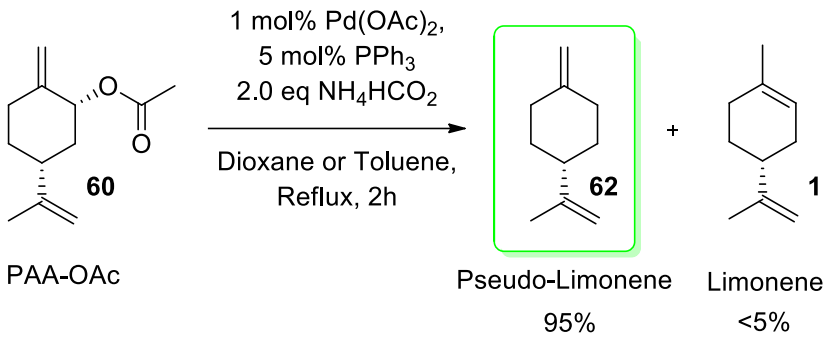

Scheme 231. Tsuji Pd(0) mediated reduction conditions applied to PAA-OAc

p-Mentha-1-(7)-8-diene (62) (pseudo-limonene) occurs widely in nature but is normally only present in very small amounts; however the essential oil obtained from Wormwood or *Artemisia absinthium* contains up to 9.0% pseudo-limonene[271]. Pseudo-limonene has a mild but distinctly different aroma compared to limonene that has potential use as a fragrance compound for perfumery applications.

Both alkene bonds of pseudo-limonene (62) were then doubly ozonolysed in DCM at -78 °C using dimethylsulfide for reductive cleavage of the ozonides to give the desired diketone product (63) in 88% yield on a multigram scale (Scheme 232).

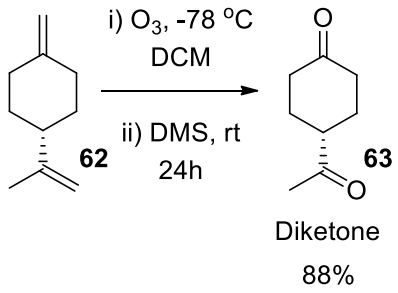

Scheme 232. Double ozonolysis reaction of pseudo-limonene

5.2.5 Step 5. Aromatisation Studies

The next step was to oxidatively aromatise the diketone (63) species into 4-hydroxyacetophenone (54), which would require conversion of the sp^3 centres of its cyclohexyl ring into the sp^2 atoms of the aromatic ring of 4-HAP (Scheme 233).

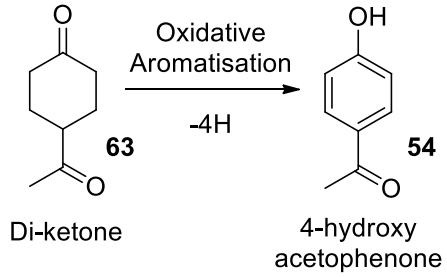

Scheme 233. Aromatisation of DK to 4-HAP

Work by Stahl et al[272] published in 2011 had demonstrated the use of palladium chemistry for the oxidative dehydrogenation of cyclohexanones to phenols. Their methodology was shown to work on a wide range of substrates (17 in total), with good functional groups tolerance, using a readily accessible palladium based catalyst and atmospheric pressure oxygen as a hydrogen acceptor (Scheme 234).

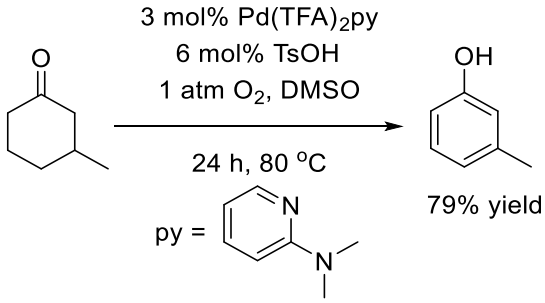

Scheme 234. Stahl et al optimised dehydrogenation/aromatisation conditions using a palladium catalyst and molecular oxygen

Stahl proposed an aromatisation mechanism (Scheme 235) involving formation of a palladium enolate, whose keto tautomer could undergo β-hydride elimination to produce an α-β-unsaturated cyclohexenone species. This species could then undergo two further rounds of Pd-enolate formation/β-hydride elimination to give the fully aromatised phenol species. High yields and selectivities were achieved in these aromatisation reactions, with use of oxygen ideal from a green perspective - however a relatively complex palladium ligand was required.

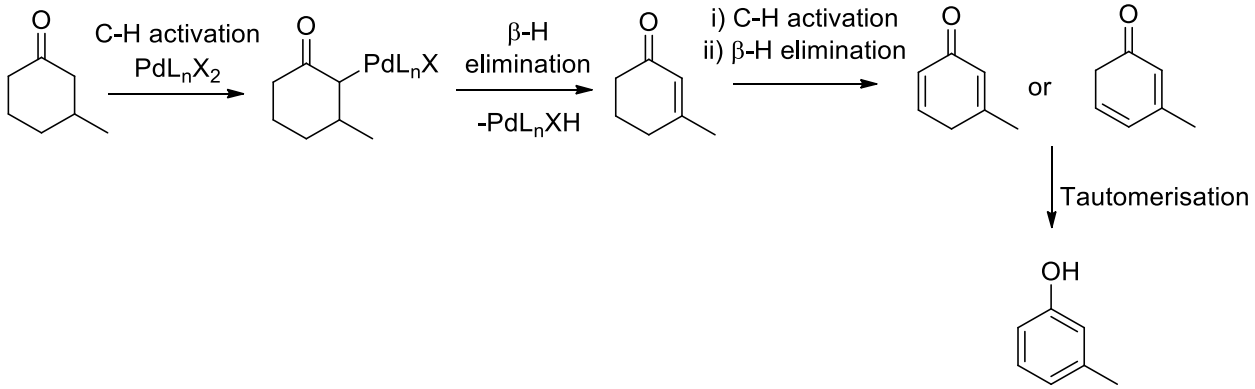

Scheme 235. Mechanism proposed by Stahl el al for palladium mediated dehydrogenation reactions of cyclohexanones

Liu et al.[273] expanded upon Stahl's methodology using palladium on carbon as a heterogeneous catalyst for the dehydrogenation/aromatisation of cyclohexanones, which had a number of benefits over Stahl's original dehydrogenative method (Scheme 236). Their catalytic system employed a simpler and cheaper heterogeneous catalyst; with no molecular oxygen required, producing good yields achieved for a range of 15 substrates containing a range of different substituents. The lack of dioxygen in this protocol is particularly useful because phenol products are susceptible to further oxidation, which can potentially give rise to by-products and lower yields.[273] Liu proposed an aromatisation mechanism whereby the hydrogen removed from the cyclohexanone substrate was used to reduce the palladium (0) species back into its active palladium (II) form (Scheme 237).

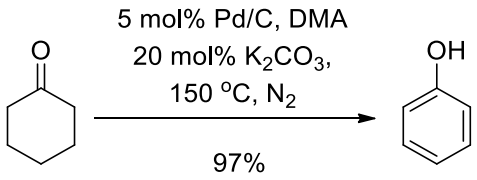

Scheme 236. Liu conditions applied to the aromatisation of cyclohexanone

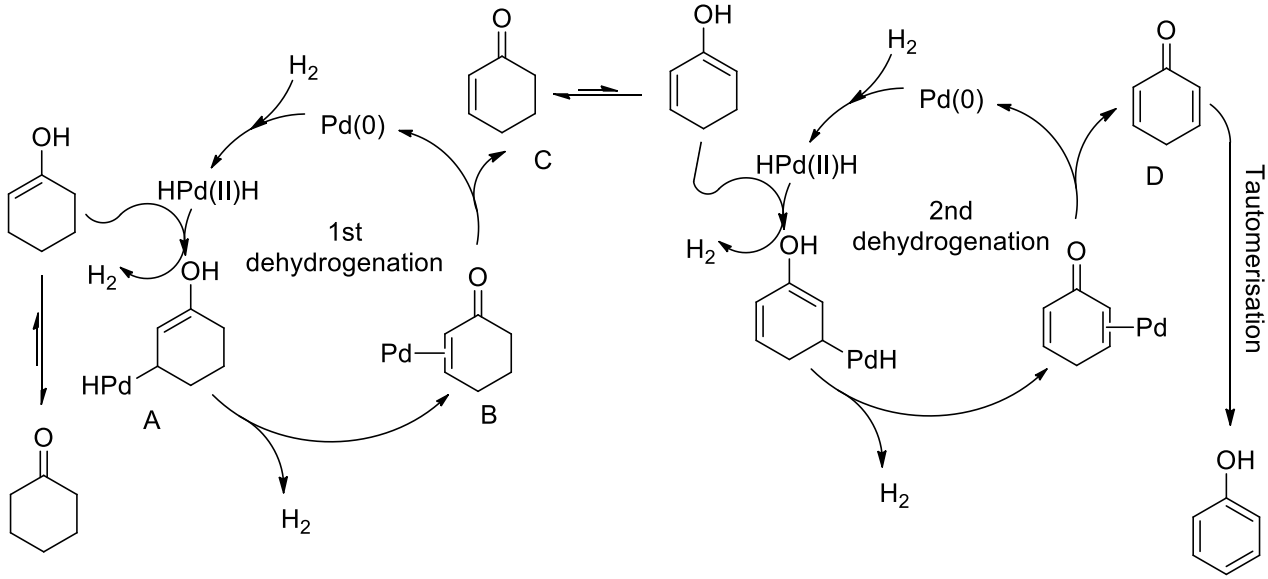

Scheme 237. Mechanism for Pd(0) mediated dehydrogenation reaction of cyclohexanones

Treatment of the diketone (63) with 5 mol% Pd/C, 20 mol% K_2CO_3 in refluxing dimethylacetamide at 150 ^oC under N_2 for 24 h resulted in clean conversion to give 4-hydroxyacetophenone (54) in 92% yield, with the Pd/C catalyst being easily recovered at the end of the reaction by filtration. This result contrasted with the result obtained using Stahl's homogeneous catalytic system (3 mol% $Pd(TFA)_2py$, 6 mol% TsOH, 1 atm O_2, DMSO, 100 ^oC, 24 h) which stalled at 60% conversion (Scheme 238).

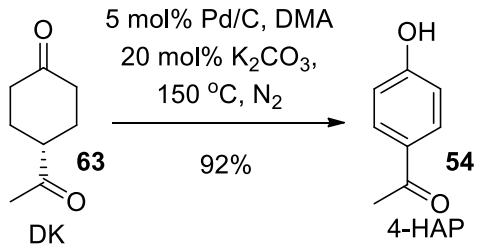

Scheme 238. Liu conditions applied to the aromatisation of DK to afford *p*-hydroxy-acetophenone

Due to the toxicity and hazards associated with using DMA as a solvent, an alternative solvent free system using Pd/C was investigated based upon the work by Frost et al[274] from 2014. They reported that 4-methyl-3-cyclohexenecarboxylic acid was aromatised to *p*-toluic acid using catalytic silica-Pd/C dispersed within glass wool that performed like a catalyst supported "packed bed" reactor. The substrate is heated at 250 ^oC under reduced pressure, resulting in vaporisation of the gaseous substrate through the glass wool supported Pd/C-Si mixture to perform the dehydrogenation process using a kugelrohr set-up. This reaction setup gave a 77% yield of *p*-toluic acid that was condensed directly into a collecting glass bulb (Scheme 239).

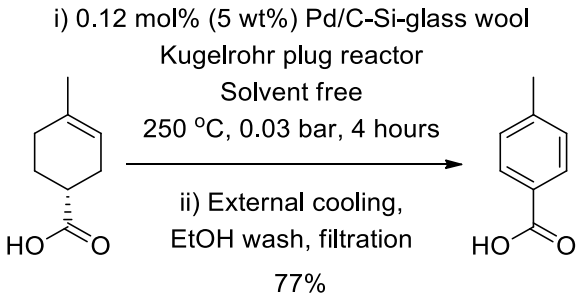

Scheme 239. Frost et al conditions applied for the aromatisation of 4-methyl-3-cyclohexenecarboxylic acid to afford *p*-toluic acid

We successfully applied the same approach to our DK substrate (63) which pleasingly gave 4-hydroxyacetophenone (54) as a white solid in a 79% yield over a period of 4 hours (Scheme 240). Importantly, a single batch of Pd/C-Si mixture could be successfully recycled to carry out 3 x 100 mmol aromatisation reactions, with no reduction in yield observed over successive 4 hour reaction times.

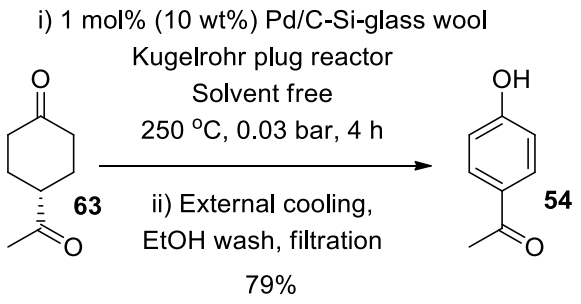

Scheme 240. Frost et al conditions applied for the aromatisation of diketone to afford *p*-hydroxy-acetophenone

5.2.6 Step 6. Synthesis of Paracetamol

One of the industrial syntheses of paracetamol involves using 4-hydroxyacetophenone (54) as a substrate for a Beckmann rearrangement, involving treatment of its ketone group with NH_2OH to give an oxime, followed by acid catalysed rearrangement to afford paracetamol (55) (Scheme 241). The most commonly used industrial acid is sulphuric acid, as the resultant bisulfate-amide salt can be neutralized by addition of ammonia to generate ammonium sulphate as a fertiliser by-product.[275]

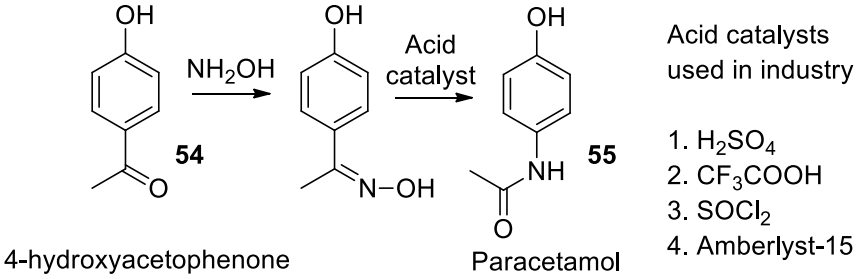

Scheme 241. Typical methods used to carry out the Beckmann rearrangement of 4-HAP

We employed two different literature methods to convert 4-hydroxy-acetophenone into paracetamol. The first approach involved heating 4-HAP with solid zinc oxide at 140 °C for 1 h under solvent free conditions, with the crude melt extracted with EtOAc to give paracetamol in 74% isolated yield (Scheme 242).[276] However reaction work-up was challenging when this reaction was scaled up, because the zinc melt solidified on cooling, making extraction of the paracetamol product inefficient.

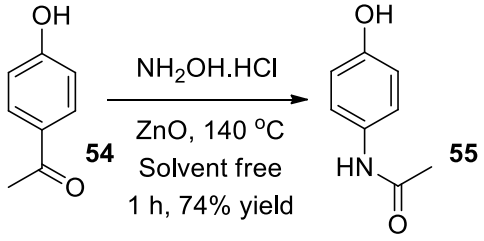

Scheme 242. Solvent free Beckmann rearrangement of 4-HAP

Consequently, we employed the protocol described by Vavasori et al[277] who described Beckmann rearrangement of 4-hydroxyacetophenone into paracetamol using hydroxyalamine hydrochloride at higher temperatures, without the need for any Lewis acid additives. Their one-pot synthesis (generating HCl *in-situ*) was performed in acetonitrile (1 eq, $NH_2OH.HCl$, 3 h, 70 ^oC) or under solvent-free conditions (3 eq, $NH_2OH.HCl$, 3 h, 110 ^oC) to afford paracetamol in 81% and 79% respectively (Scheme 243). The crude reaction mixture was cooled and washed with ice cold water and then recrystallized from hot water to yield paracetamol as a white solid.

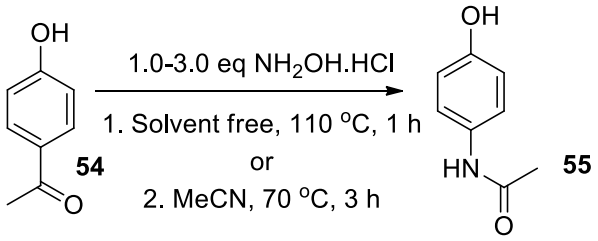

Scheme 243. Vavasori's one-pot Beckmann rearrangement of *para*-hydroxyacetophenone into Paracetamol

5.2.7 Summary of trans-limonene epoxide route to paracetamol

The seven step process that was developed for the conversion of limonene (1) into 4-HAP (54) is shown in Scheme 244. Firstly, *trans*-limonene epoxide (2ii) is selectively produced *via* base catalysed cyclisation of a bromohydrin intermediate (59), followed by regioselective Lewis acid catalysed ring opening to afford the less thermodynamically stable pseudo-limonene allylic alcohol (56). The allylic alcohol functionality of pseudo-limonene allylic alcohol is then protected as its acetate group, with the resultant allylic acetate (60) then undergoing a palladium mediated reduction reaction to afford pseudo-limonene (62). Pseudo-limonene is then subjected to a double ozonolysis reaction to afford a diketone (63) that undergoes a palladium catalysed dehydrogenation aromatisation to produce 4-HAP. 4-HAP could then be easily converted into paracetamol (55) *via* an established Beckmann rearrangement protocol.

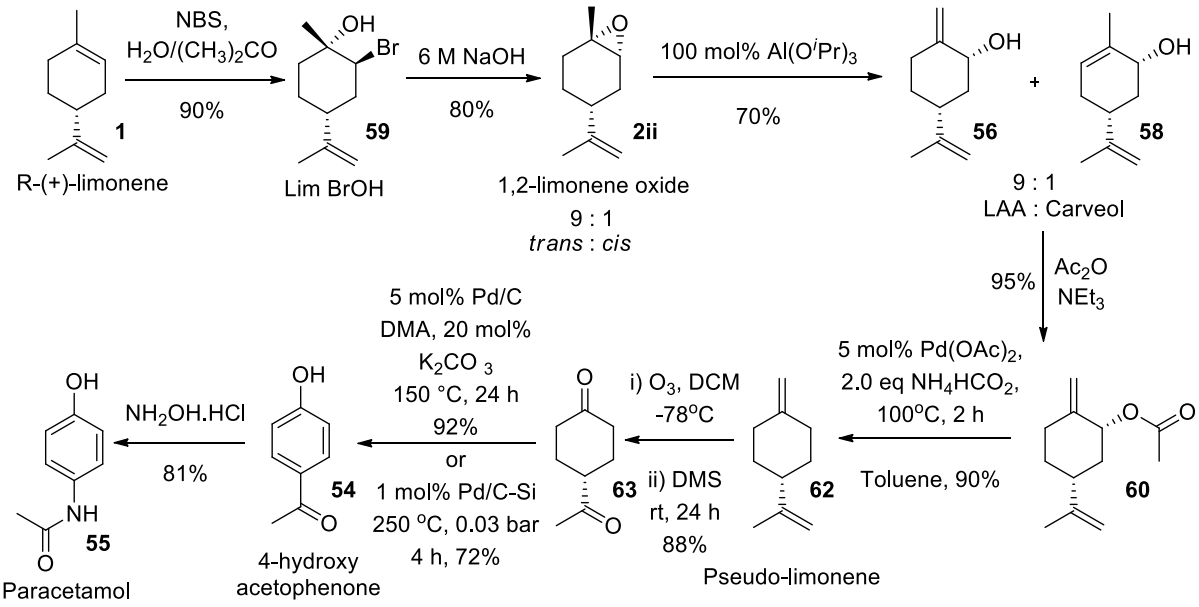

Scheme 244. Summary of *trans*-1,2-limonene epoxide route to paracetamol

This synthesis had successfully converted biorenewable limonene into the bulk commonly pharmaceutical paracetamol using scalable chemistry in an overall 29% yield with an overall atom economy of 8%. Unfortunately, 8 steps were required for its synthesis, which is 3 more than the 5 steps currently used to transform oil derived benzene into paracetamol. Consequently, it was decided to target a more efficient route to pseudo-limonene from a cheaper biorenewable terpene feedstock, with the ultimate aim of reducing the number of steps and cost required to reach our paracetamol target.

5.3 Target 2: Pseudo-limonene – 2nd Generation synthesis of Paracetamol

5.3.1 Syntheses using palladium catalysis, dehalogenation and dehydration methodologies

The first generation route to 4-HAP (54), shown in Scheme 245, proceeds through pseudo-limonene (62) and so it was decided to attempt to devise a more efficient synthesis of this key intermediate from a cheaper bulk monoterpene feedstock.

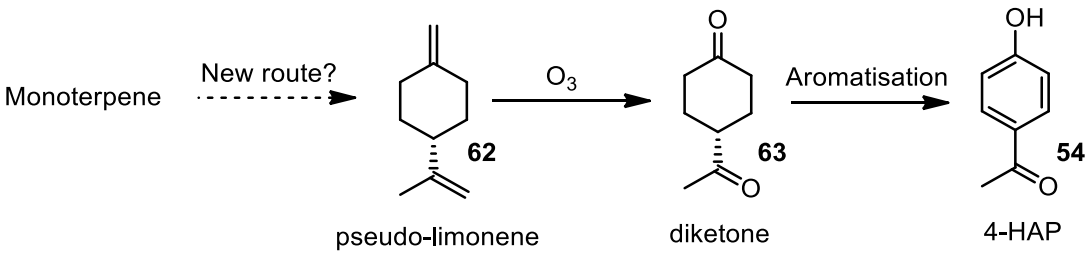

Scheme 245. Synthesis of 4-HAP from PL

5.3.1.1 Known literature synthetic routes to pseudo-limonene

The literature contained a few protocols for the synthesis of PL, however most of them had disadvantages that made them unsuitable for scale-up for the synthesis of paracetamol. Most of the literature methods for the synthesis of pseudo-limonene use perillyl alcohol as a starting material, which is only available in small amounts from plant species such as caraway, lavender, cranberries, cherries, sage, mint and lilac oil.[145] A number of routes have been developed that employ limonene as a precursor for the synthesis of perillyl alcohol, however multiple steps using stoichiometric reagents meant that these alternative routes could not be used as cheap and scalable routes to perillyl alcohol.[72] Similarly, other direct routes to pseudo-limonene from other monoterpene feed stocks were clearly not commercially viable, due to the cost and lack of availability of the raw starting materials[278], the number of steps required, or the fact that mixtures of pseudo-limonene and limonene were produced.[279,280,281]

5.3.2 Unsuccessful routes to pseudo-limonene using Dehydration methodologies

Bull et al[282] have previously developed a synthesis of δ-terpineol using β-pinene as a starting material which contained the same type of exocyclic methylene alkene present in pseudo-limonene. Therefore, it was proposed that selective dehydration of δ-terpineol would result in access to pseudo-limonene in 3 steps from cheap and abundant β-pinene (Scheme 246). Therefore, the synthesis of δ-terpineol was repeated involving treatment of β-pinene with NBS/H_2O to afford an allylic bromide (64) (70% yield) that was then treated with Zn/acetic acid to give δ-terpineol (65) in 80% yield.

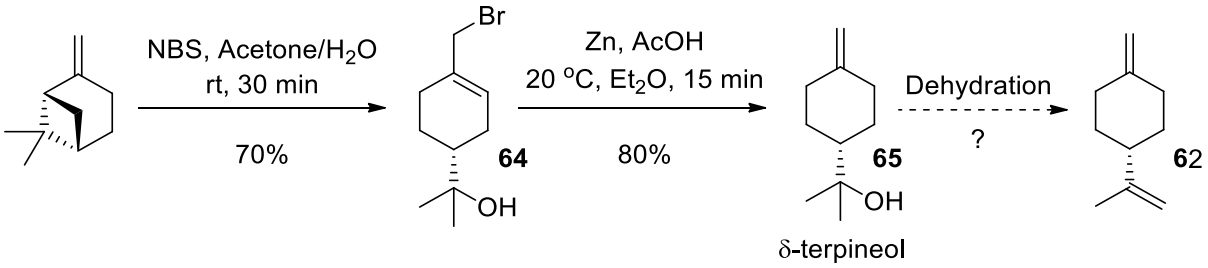

Scheme 246. Dehydration of δ-terpineol to afford pseudo-limonene

Rudloff et al.[283] had previously developed a dehydration method to convert α-terpineol into limonene *via* its treatment with neutral Al_2O_3 and pyridine at 220 °C, without any terpinolene having been formed (Scheme 247).

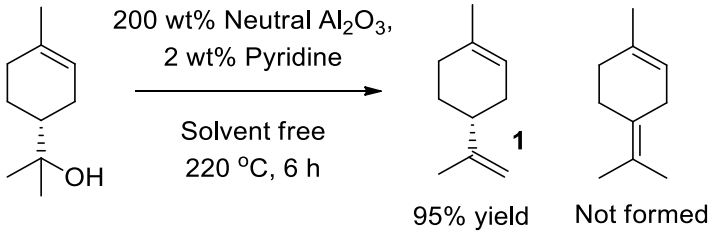

Scheme 247. Tertiary alcohol dehydration using alumina

However, attempts to selectively dehydrate δ-terpineol (65) to selectively afford the exocyclic methylene bond of pseudo-limonene (62) proved unsuccessful, affording mixtures of regioisomeric monoterpene isomers. These regioisomers were formed from competing isomerisation of the exocyclic double bond into its thermodynamically more stable endocyclic position to afford an inseparable 45:55 mixture of pseudo-limonene (62) and limonene (1) isomers (Scheme 248).

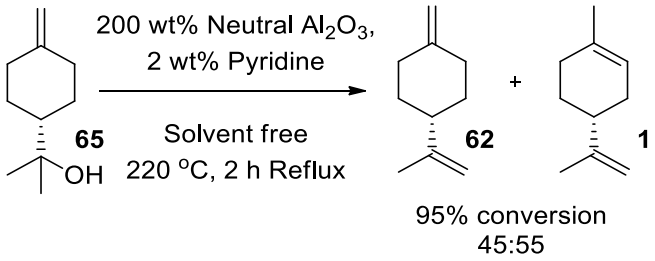

Scheme 248. Dehydration of δ-terpineol using alumina

5.3.3 Synthesis of pseudo-limonene *via* dehalogenation of perillyl chloride

Ceschi et al[284] had previously developed bi-phasic methodology for ring opening β-pinene using $InCl_3$ as a Lewis acid in DCM using aqueous NaOCl as an electrophilic source of chlorine, which resulted in facile ring opening of its bicyclic skeleton to afford the *p*-menthane skeleton of perillyl chloride (66). Therefore, this reaction was repeated to obtain perillyl chloride in 67% yield (Scheme 249). This indium mediated rearrangement was selective for the desired regioisomer of perillyl chloride, however, it required the use of stoichiometric amounts of expensive $InCl_3$ (£94 per 10 g, Sigma-Aldrich). Attempts to carry out this procedure using 0.5 equivalents of $InCl_3$ gave perillyl chloride in a much reduced 25% yield, therefore an alternative ring-opening protocol was pursued.

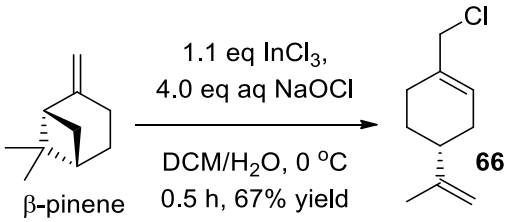

Scheme 249. Indium mediated ring opening of β-pinene

Liu et al[285] had reported previously that treatment of β-pinene with DMSO and phosphorus oxychloride (or phenyl dichlorophosphate) resulted in ring opening to afford quantitative yields of perillyl chloride (66) (Scheme 250). Attempts to repeat this literature procedure resulted in much lower yields than reported in this paper, with the original report providing no information on the order of reagent addition, length of reaction time or workup procedure. After carrying out extensive optimisation studies, it was found that dropwise addition of 1.0 equivalent of $POCl_3$ (£3.30 per 50 g, Sigma-Aldrich) to a mixture of 1.0 equivalent of β-pinene, 2.0 equivalents of DMSO and 2 equivalents of DCM at -15 °C resulted in formation of perillyl chloride in 70% yield (Scheme 251).

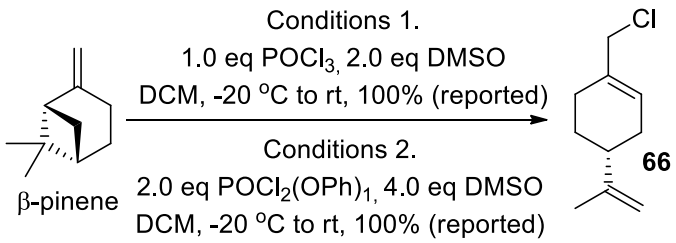

Scheme 250. Liu method for $POCl_3$ mediated rearrangement of β-pinene

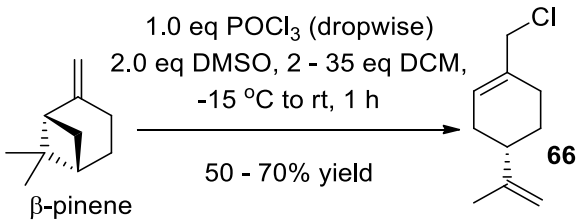

Scheme 251. Optimal $POCl_3$ mediated β-pinene ring opening conditions

Patil et al[286] have reported that phosphorus oxychloride and dimethylsulfoxide react together to form a highly reactive chloro-sulfoxonium intermediate which then acts as a highly electrophilic chlorine source that acts as a highly reactive chlorinating agent to initiate ring fragmentation of the β-pinene skeleton to afford perillyl chloride (Scheme 252).

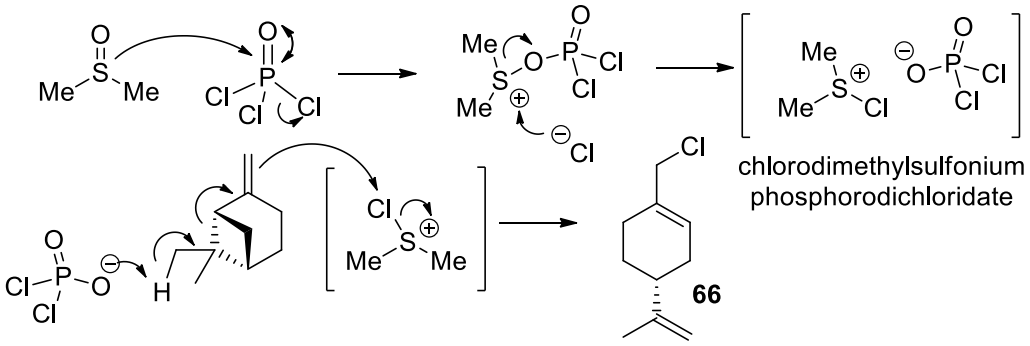

Scheme 252. Proposed mechanism for $POCl_3$ mediated β-pinene rearrangement

Treatment of perillyl chloride (66) with 5.0 eq of zinc and 10.0 eq of acetic acid in Et_2O at 20 °C for 12 h then afforded pseudo-limonene (62) in 80% isolated yield (56% yield over 2 steps from β-pinene, Scheme 253), that could then be converted into 4-HAP using the ozonolysis/aromatisation methodology discussed in the previous section.

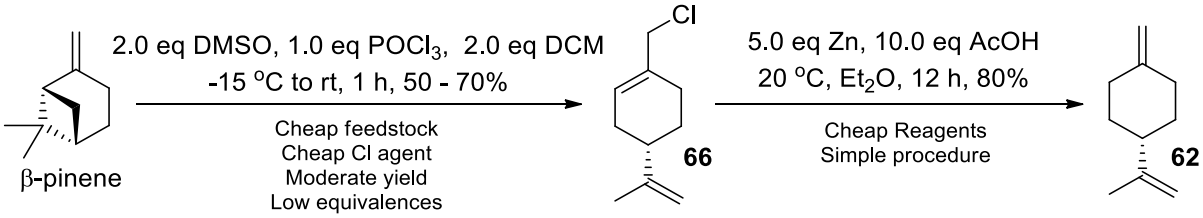

Scheme 253. 2 step synthesis of pseudo-limonene from β-pinene

Therefore, to summarise, Scheme 254 shows the final 2nd generation route from β-pinene to paracetamol (55) (*via* perillyl chloride (66)) that proceeds in 5 steps and 37% yield, using cheap reagents and conditions that are amenable to scale-up.

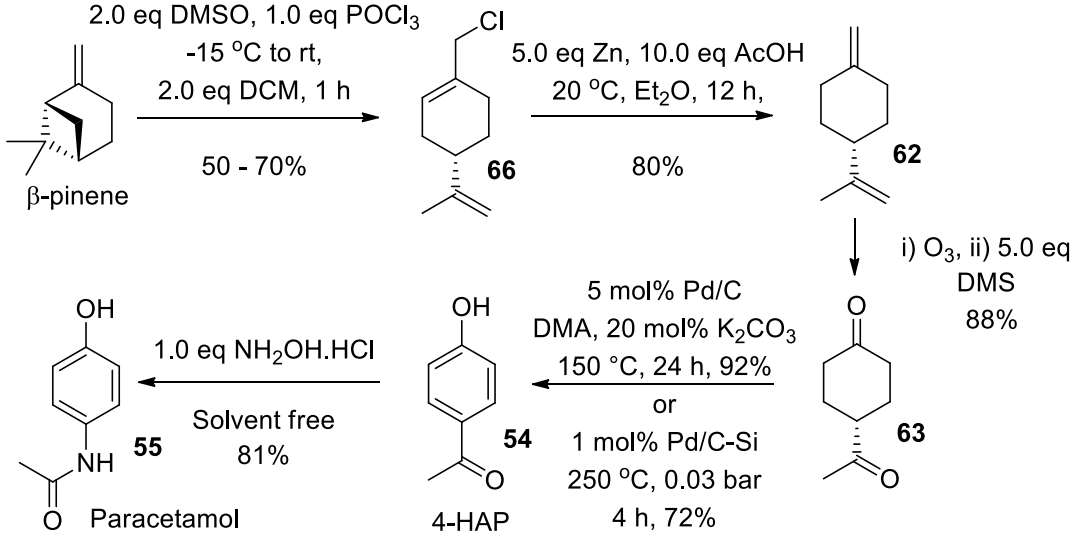

Scheme 254. 2nd generation Paracetamol route summary

5.4 Economics of 2nd generation paracetamol synthesis

The yield, atom economy and number of synthetic steps for each of the industrial routes and our two terpene derived routes for the synthesis paracetamol are summarised in Table 9. The lower 29% yield of our 1st generation route is primarily due to the overall length of the synthetic route (8 steps) with an atom economy of 8%, whilst this route also starts with limonene which is a more expensive terpene feedstock. The overall yield from β-pinene to paracetamol using the improved 2nd generation terpene route employing 5 steps is 37%, with an overall atom economy of 9%. Compared to the present industrial routes to Paracetamol the yield of our 2nd generation route is comparable, however its overall atom economy is lower. The first β-pinene ring opening step requires the introduction of a chlorine atom that is then eliminated from the molecule; however this step is necessary to mediate isomerisation of the alkene bond into an exocyclic position and so cannot be avoided. The zinc mediated dehalogenation step requires five equivalents of zinc and acetic acid which generates significant waste, whilst the ozonolysis step also generates atom waste due to the use of Me_2S as excess quenching agent. Nevertheless, we believe that our 2nd generation biorenewable route is competitive to current industrial routes to paracetamol from oil based feedstocks that use routes that generate large amounts of waste by-products.

Table 9. Comparison of paracetamol routes from non-renewable and biorenewable feedstocks

Route	Overall Yield	Atom Economy[b]	Number of Synthetic Steps
1. PNCB route	35% (75% from PNCB)[a]	38%	5
2. Phenol route	47% (52% from phenol)[a]	54%	5
3. Nitrobenzene route	52% [a]	52%	3
4. Hoeschst-Celenese	46% [a]	49%	4
5. 1st Generation from Limonene	29%	8%	8
6. 2nd Generation from β-pinene	37%	9% (20%)[c]	5

[a]Yields calculated using data reported in the literature relating to industrial processes. Values quoted may vary depending upon efficiencies of individual plant design and conditions used. Yields calculated by Eynde 2016[255] were determined using laboratory scale processes. [b]Atom economies calculated with routes using Ac_2O as the final acetylation step to paracetamol.[249] [c]Maximum possible atom economy if reaction condition equivalences were optimised further.

The 1st generation route from limonene is not likely to be a commercially viable synthetic route to paracetamol (*via* 4-HAP) due to the greater number of synthetic steps (8 steps), the use of expensive stoichiometric reagents such as NBS and the use of expensive and homogeneous palladium acetate that would be difficult to recover and reuse effectively.

However, the second-generation route to 4-HAP from β-pinene has much more potential as a commercially viable route with rough cost estimations are shown in Table 10. The cheap biorenewable feedstock β-pinene is used as a cheap starting material which can be purchased on industrial scale at a cost of $ 2 per 1 kg (all costings quoted as average prices from Alibaba.com) compared to $ 5 per 1 kg of limonene. The first ring-opening step ($POCl_3$, DMSO and CH_2Cl_2) and the second isomerisation step (Zn, AcOH, Et_2O) both employ cheap reagents, whilst variants of the ozonolysis process (O_3, Me_2S, CH_2Cl_2) have been widely used in industrial processes. The palladium catalysed isoaromatisation process uses a low loading of Pd/C as a cheap palladium catalyst, that we have shown can be recycled, whist the Beckmann reaction using NH_2OH that is already used in industry to convert 4-HAP into paracetamol.

The existing petrochemical-based industrial route to paracetamol is economically very efficient with each step employing low costing materials that enable paracetamol to be sold commercially in the cost range of $ 0.27 - $ 2.00 per packet of (16 x 500mg) tablets. Therefore, the current industrial price for paracetamol works out at around $ 0.03 - $ 0.25 per 1 g of paracetamol. However, from a sustainable perspective the commercial synthetic routes in current usage are far from ideal, with large amounts of waste generated by all current processes (e.g. 35,000 litres of aqueous waste per 1000 kg of paracetamol).[245]

An economic analysis of the viability of our new route to paracetamol is presented in Table 10, which uses industrial costings for reagents and solvents sourced from the Alibaba web-site to produce 50 g of paracetamol in an overall 37% yield from β-pinene (136g of β-pinene starting material). These costings reveal that our new 5-step biorenewable route could

potentially be used to prepare paracetamol at a cost of around $ 0.19 per gramme, which is less than the cost currently charged for premium-brand paracetamol ($ 0.20-0.25) on the open market. The major cost in this process is the price of the Pd/C catalyst used in the isoaromatisation reaction in step 4, however it should be noted that the costings in Table XX are based on its 'one-off' usage, with its proven recycling likely to reduce the costs of producing 'green' paracetamol further. Clearly, these costings, do not include costs associated with infrastructure, labour, transport, packaging and marketing, however, they clearly show that our synthetic route to biorenewable paracetamol could be produced at a competitive price. Although it is likely that our 'green' paracetamol would need to be sold at premium prices, we believe that highlighting the biorenewable origin of our 'green' paracetamol would result in customers being willing to pay higher prices, in the same way that 'green' cosmetics are currently marketed.

Table 10. Estimated cost using 136 g (1 mol) of β-pinene to produce 50 g of paracetamol using our 2nd generation route assuming an overall a 37% yield for the 5 steps.

Reaction Step	Reagent	Equiv	Moles / mol	Mw	Mass / g	Mass / kg	Average price quoted from Alibaba.com / $ per 1 kg	Estimated cost / $
1	β-pinene	1	1	136	136	0.136	2	0.27
1	DMSO	2	2	78	156	0.156	1	0.16
1	$POCl_3$	1	1	153	153	0.153	1.4	0.21
1	DCM	2	2	85	170	0.17	0.5	0.09
2	Zn	5	5	65	325	0.325	1	0.33
2	AcOH	10	10	60	600	0.6	0.05	0.03
2	Et_2O	20	20	74	1480	1.48	0.5	0.74
3	DMS	5	5	62	310	0.31	0.1	0.03
3	DCM	20	20	85	1700	1.7	0.5	0.85
4	Pd/C	5 mol% (of 10 wt% = 50g per 1 mol of substrate)	0.05	106	53	0.053	100 (variable 5-30wt% Pd content)	5.30[a]
4	DMA	20	20	87	1740	1.74	1	1.74
4	K_2CO_3	20 mol%	0.2	138	27.6	0.0276	0.12	0.003
5	$NH_2OH.HCl$	1	1	53	53	0.053	0.02	0.001
							$ per 50g of paracetamol[b]	9.75
							$ per 1g of paracetamol[b]	0.19

[a]Heterogeneous Pd/C used in step 4 has been recovered and recycled for the synthesis of subsequent batches of paracetamol production, thus lowering the cost of subsequent batches. [b]Hydrogen and oxygen gas costs omitted due to difficulty in estimation of exact volumes required.

Alternatively, this new route to 4-HAP (54) could potentially be used to provide a biorenewable feedstock for the synthesis of higher value, large volume bulk pharmaceuticals such as salbutamol. For example racemic salbutamol (in its hemisulfate form) is sold at a higher value of ca. $ 0.50 per 1 g (average price quoted on Alibaba.com) which as a consequence is an

even more economically feasible pharmaceutical target for using biorenewable 4-HAP as a substrate. A potential industrial route from biorenewable 4-HAP to green rac-Salbutamol, using known literature methodologies, is shown in Scheme 255.[242,287,240,288]

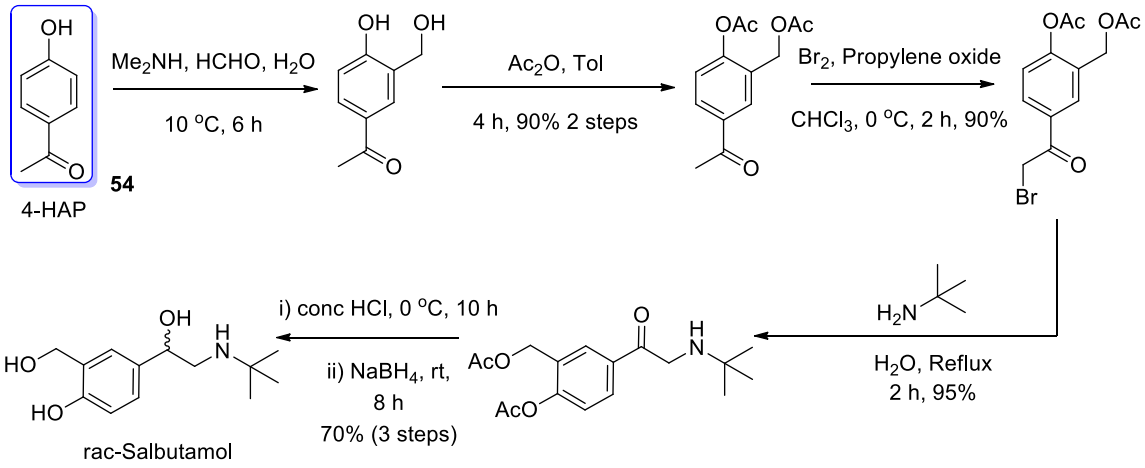

Scheme 255. Route to (*rac*)-salbutamol from 4-hydroxyacetophenone using known synthetic methodologies

5.5 Conclusions

In summary, two novel routes to paracetamol *via* the key pharmaceutical intermediate 4-HAP have been developed using sustainable reagents and catalytic methodologies. Unfortunately, the cost of the 1st generation route from limonene relies on two palladium catalysed steps (heterogeneous and homogeneous) making this approach potentially uneconomical. In comparison our 2nd generation route (Scheme 256) started from a cheaper renewable feedstock, β-pinene, required fewer steps (5 *vs* 8) and only required one step involving palladium catalysis (heterogeneous) making this 2nd generation route economically comparable to current petrochemically derived paracetamol synthetic routes.

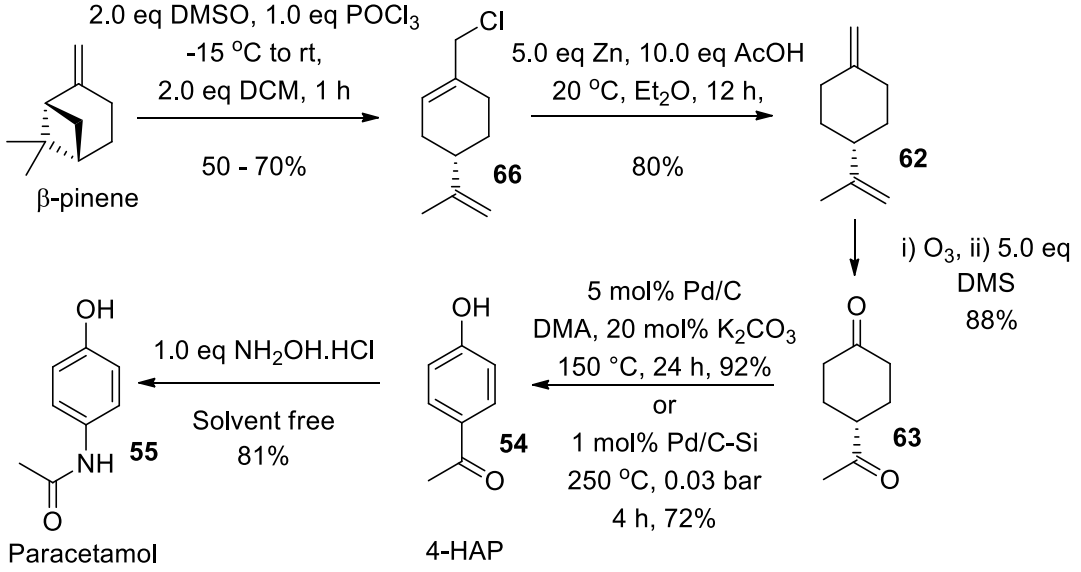

Scheme 256. 2nd generation synthesis of paracetamol.

This synthesis embraces the principle of employing a biorefinery approach for the conversion of readily available biorenewable substrates into multiple commercially valuable products, that provides sufficient flexibility that could cover the economic costs of investing in a new chemical process. Therefore, this new scalable synthetic route to paracetamol (55) also provides access to perillyl chloride (66), pseudo-limonene (62) and 4-hydroxy-acetophenone (54), all of which have significant commercial value as synthetic intermediates, fragrances or other pharmaceutical products. Access to 4-HAP is particularly noteworthy as this phenol is a key chemical intermediate in many chemical processes that is often used for the synthesis of drug-like molecules, with >6900 reports the SciFinder database, with >1750 patents describing its use for the synthesis of drugs, polymers and materials.

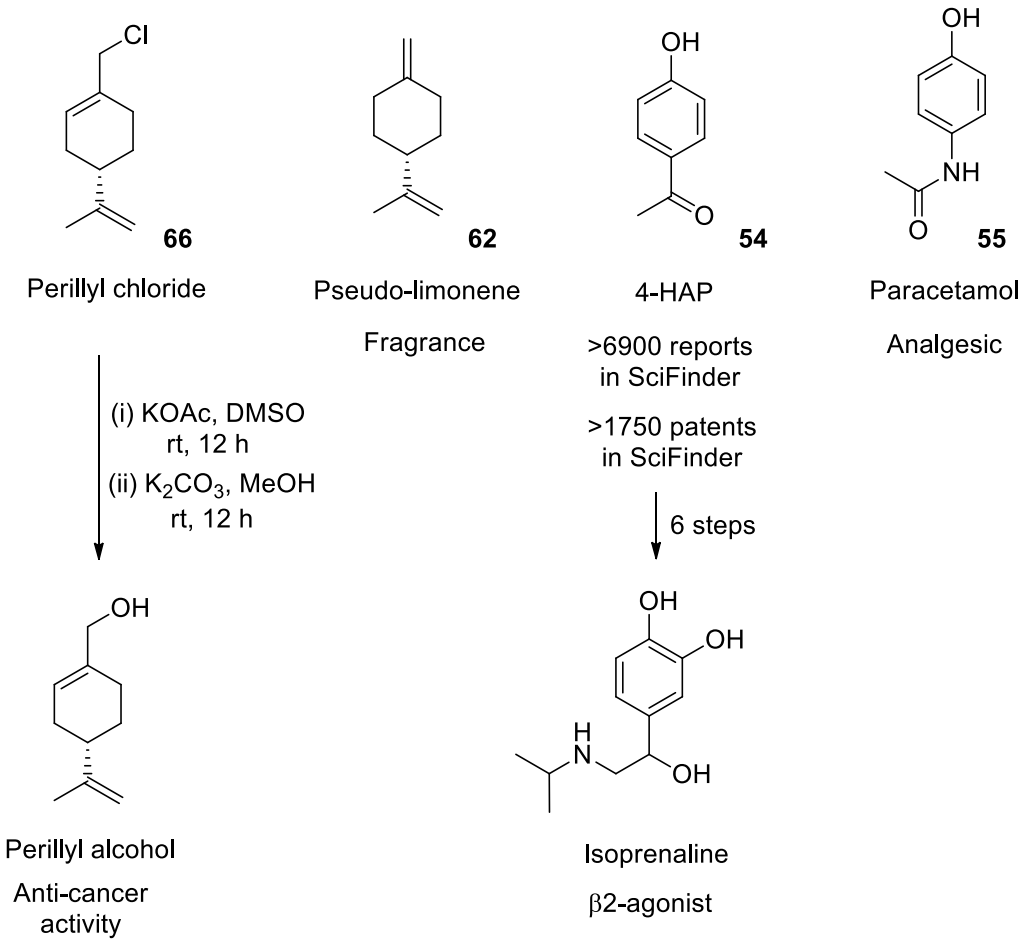

Scheme 257. Biorefinery approach to the synthesis of multiple products from a biorenewable feedstock.

6 Chapter 6: Stereoselective Synthesis of PMD diastereomers

6.1 Introduction – Insect repellents for the prevention of mosquito borne diseases

Approximately 700,000 people die each year worldwide due to effects caused by the effects of mosquito transmitted diseases, such as malaria, dengue fever and yellow fever.[289] The Zika virus has recently emerged as a major public health concern throughout South America, with increasing concerns that global warming will result in its spread into the southern parts of the United States and Mediterranean countries.

The Zika virus is part of the *Flaviviridae* family which was first identified in 1947[290] in the Zika Forest, Uganda,[291] which is spread by *Aedes* mosquitoes which that are present within a thin equatorial belt across the African and Asian continents. However, from 2007-2016 this virus spread to the Americas continent causing the 2015/2016 Zika virus epidemic in Brazil and other countries in South America. The Zika virus causes a range of symptoms ranging from minor effects (including fever and rash in adult patients), through to more damaging effects including Guillain–Barré syndrome which is a neurological illness that occurs in infected adults. More critically, infection of pregnant women with the Zika virus can result in fetal microcephaly resulting in severe brain malformations and birth defects in unborn children. 1.5 million people were infected between October 2015 and January 2016, with >3500 cases of infant microcephaly reported during this period.[292] WHO estimate that 4 million people in the Americas and 80-117 million worldwide were infected by the Zika virus by th end of 2017, including 1.5 million pregnant women.[292] Significant economic costs[293] are associated with Guillain–Barré syndrome and microcephaly, including costs from detecting and treating these diseases, lost productivity due to missed employment and lost income from tourism revenue. Short term estimates of the economic burden caused by this disease range from $7-18 billion,[294] depending upon the rate of virus transmission. Overall the lifetime costs of microcephaly and Guillain–Barré syndrome are predicted to range from $3-29 billion and $242 million to $10 billion,[294] respectively. Therefore, identifying efficient strategies to reduce the rate of transmission of the Zika virus is critical from both public health and economic perspectives. One of the most effective preventative measures to lower the rate of viral transmission that has been recommended by the Centre for Disease Control and Transmission in the USA is the frequent use of mosquito repellents.[295] Two of the most effective repellent agents are synthetic DEET and Citronella oil/ Lemon Eucalyptus oil that contains the active natural product ingredient *p*-menthane-3,8-diol (PMD), respectively (Figure 57).[296]

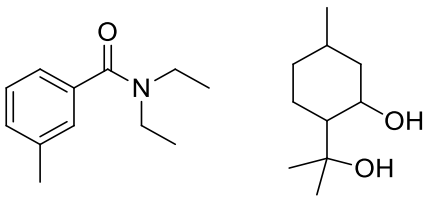

Figure 57. Structures of *N*,*N*-diethyl-*m*-toluamide (DEET) and *p*-menthane-3,8-diol (PMD).

PMD, is a naturally occurring monoterpene diol found in essential oils of the “lemon scented gum” tree or *Eucalyptus citriodora* that is found natively in Australia.[297] PMD was originally identified in China during the 1960s as an insect repellent after screening the extracts of the leaves of the lemon scented gum tree. It is currently prepared synthetically using a number of methodologies based on cyclisation of the acyclic monoterpene citronellal.[297] *Eucalyptus citriodora* leaves contain essential oil composed mainly of 70% citronellal, with PMD being present in low levels of just 0.7% (0.5%(+)-form, 0.2%(-)-form). Interestingly a 2016 study by Vaknin et al,[298] showed that *Eucalyptus citriodora* plants grown under shade had elevated levels of natural PMD in the essential oil from their leaves, which contained levels of up to 5% PMD (4%(+)-form, 1%(-)-form). It was found that the citronellal present in these leaves was gradually converted into the *cis*- and *trans*- isomers of *p*-menthane-3,8-diol (PMD) as the eucalyptus leaves aged over time.

PMD is a highly sought after monoterpene because of its excellent mosquito repellent properties[299] that are comparable to the petrochemically derived *N*,*N*-diethyl-*m*-toluamide (DEET).[300] DEET has been proposed to interfere with insect antenna receptors to prevent them from detecting carbon dioxide and lactic acid that stops them from being able to track down their host.[301] The exact mode of action of PMD is unknown, but it’s insecticidal activity has been proposed to be related to its ability to mask the insect attractant signals that humans emit, such as lactic acid, carbon dioxide, phenols, heat or humidity.[302] Further investigations into the mode of action of PMD would be useful for gaining a better understanding of each isomer’s individual efficacies and/or differences in performance, that would enable optimisation of PMD compositions to maximise their anti-mosquito repellency. However, PMD occurs naturally as a mixture of *cis*- and *trans*- isomers, with current synthetic routes resulting in a mixture of PMD stereoisomers that are difficult to separate, which makes assessment of the biological activity of individual PMD isomers impossible.

DEET is neurotoxic and has an unpleasant odour which means that it is unsuitable for long term use as an insect repellent in women and children.[300] PMD is an effective mosquito repellent which has no adverse side-effects, which is also known to repel other disease vectors such as fleas and ticks. PMD’s high insect repellent properties have resulted in the FDA approving PMD containing products for sale in the USA. PMD is currently sold as a mixture of isomers under the trade names Citriodiol®, Incognito™, Anti-mosquito and “Oil of lemon eucalyptus” variants contained in brands such as Trek Natural Repellent, Mosi-Guard Natural Insect Repellent and REPEL™. Citriodiol® is a high content PMD oil (containing a 64% mixture of *cis*- and *trans*- PMD) that is produced through steam distillation of leaves from *Eucalyptus citriodora* trees which affords an extract that is currently under review as an insect repellent with a range of regulatory agencies.[303] Other applications of PMD have also been investigated, with a patent published in 2005 describing PMD’s potent anti-viral properties against a variety of viral strains, such as Influenza, SARs and Herpes.[304]

PMD contains three chiral centres, which means that it has 8 different possible stereoisomers, all of which can potentially exhibit different insect repellent activity (Figure 58), with the biological activity of a number of the ‘non-natural’ stereoisomers currently unknown.

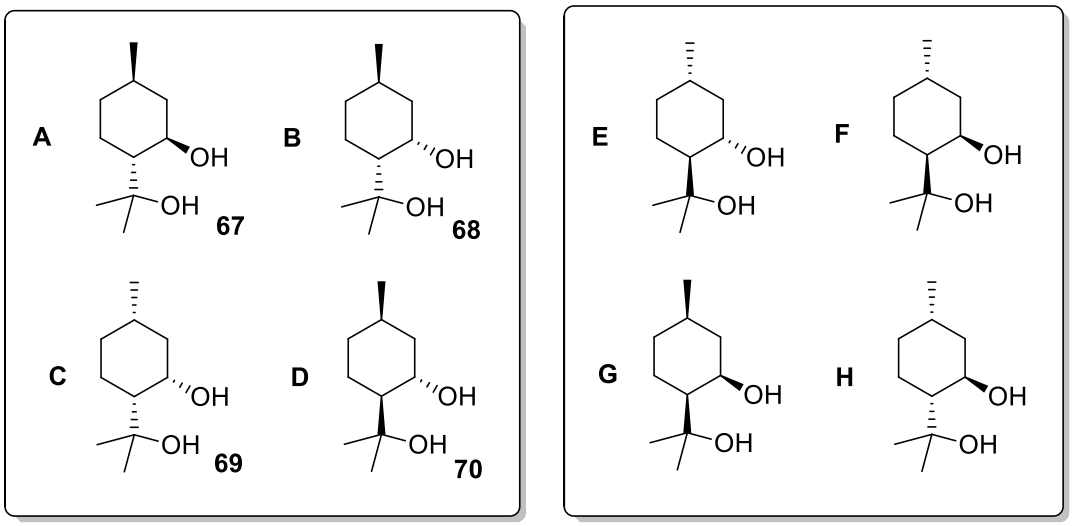

Figure 58. The eight possible diastereomers of PMD

Extraction of natural plant leaves generally produces very low quantities of PMD and restricts its usage to areas close to where the plants are grown, which has resulted in a a variety of synthetic methods having been developed for its synthesis. The earliest reported synthesis of PMD was by Barbier et al in 1896 who produced a mixture of PMD and isopulegol from the cyclisation of citronellal in aqueous dilute sulphuric acid.[299] Zimmerman et al[305] published the same route in 1953 involving mixing d-citronellal with 5% sulphuric acid for 27 hours to give a mixture of *cis* (68) and *trans* (67) PMD isomers, whose diastereomeric ratio was not disclosed (Scheme 2578.[305]

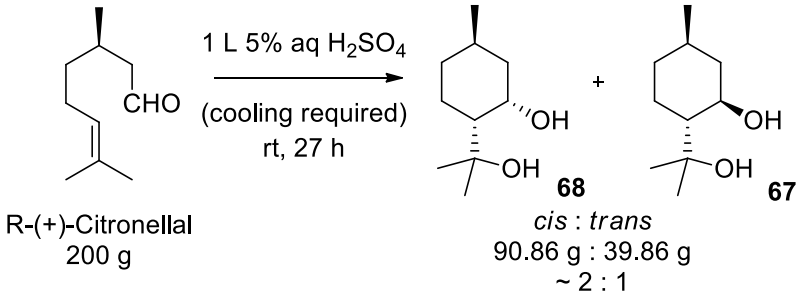

Scheme 258. Acid catalysed cyclisation of (*R*)-citronellal to afford *cis*- and *trans*- PMD

In 2000, Yuasa et al[297] working for Takasago Corporation developed an optimised, scalable route to PMD *via* acid catalysed cyclisation of citronellal that produced PMD as a mixture of four stereoisomers (Scheme 259). This acid catalysed route was used to prepare 500g of PMD (Scheme 259), however naturally occurring (*R*)-citronellal is expensive (£100 per gram), so a biorenewable route to PMD using a cheaper starting material would be highly desirable. Enantiopure citronellal itself is currently prepared from myrcene *via* the three step Takasago process as a precursor for the industrial synthesis of Menthol on a vast scale, or produced synthetically from petrochemical building block chemicals using the BASF process.[306]

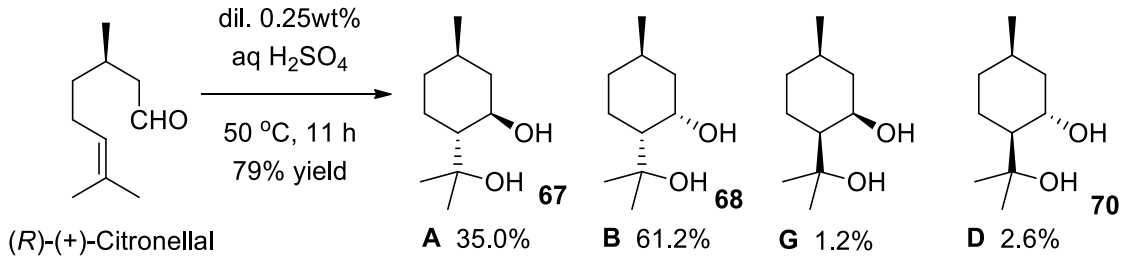

Scheme 259. Industrial cyclisation of (*R*)-citronellal to afford a mixture of 4 PMD diastereoisomers

Zhao et al[307] published the cyclisation of (*rac*)-citronellal in a mixed solvent of water and carbon dioxide, without the need for any other additives, reporting a six fold increase in reaction rate due to CO_2 dissolving in the water to form carbonic acid. The conversion rate achieved was lower than for sulphuric acid, however higher reaction temperatures enabledmoderate conversions to be achieved after 2 hours - compared to 11 hours using sulphuric acid (Scheme 260).

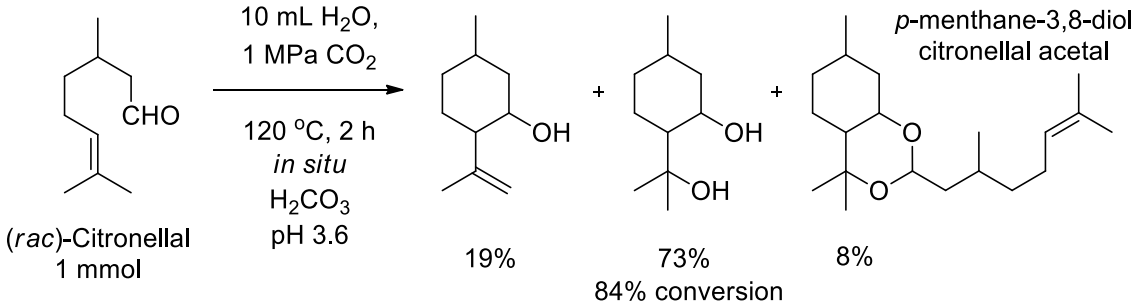

Scheme 260. “Green” cyclisation of citronellal to afford PMD using a CO_2/H_2O solvent.

In 2011 Kunz et al[308] developed a direct route to PMD from crude *Eucalyptus citriodora* oil using a similar acid catalysed approach, employing 7% aqueous citric acid to mediate cyclisation of an essential oil containing 74% (+)-citronellal in a biphasic aqueous system. The mixture was heated at 50 °C for 15 hours, with 82% conversion of citronellal being achieved with 80% selectivity for PMD. The exact ratio of each diastereomer of PMD was not identified, however the *cis* (68) to *trans* (67) ratio was reported to be 65:35 (Scheme 261).[308]

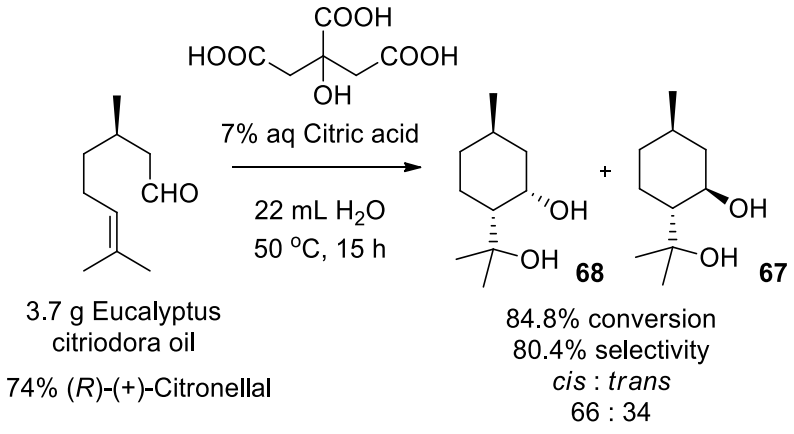

Scheme 261. Synthesis of PMD *via* acid catalysed cyclisation of *Eucalyptus citriodora* oil

All of these cyclisation reactions resulted in competing formation of a low percentage of PMD citronellal acetals produced (ranging from 2-10%) that are produced as a side product from reaction of PMD with citronellal. Each of these synthetic routes lack diasterocontrol with regards to control of their *cis* and *trans* selectivities, with the *cis* isomer generally favoured over its *trans* isomer by a ratio of 2:1.

Studies have shown that different PMD diastereomers have different repellent activities against mosquitoes, with Clarke et al reporting[309] that the *trans*-diol PMD isomer exhibited better repellent activity against mosquitos. However, its activity was shorter lived than its corresponding *cis*-diol isomer which had slightly less potency, but which exhibited greater activity over longer periods of time, with double the repellent effect being present after four hours[309]. Yuasa's synthesis of PMD currently produces a mixture of four of the possible eight diastereomers (**A**-**D**) from (*R*)-citronellal, with two isomers (**C** and **D**) only being produced in very small amounts. Therefore, there is currently a need to develop selective syntheses for each of these four PMD diastereomers (**A-D**), that could then be adapted for the synthesis of their antipodes (**E**-**H**) - the insect repellent activity of which have not yet been determined.

6.2 Selective synthesis of "trans-diol" PMD isomer A

We had previously epoxidised the 8,9-alkene bond of isopulegol using our optimised Venturello-Ishii epoxidation protocol which gave a 63% yield of diasteromeric epoxides (29) in a 60:40 ratio. This mixture of epoxides was then reduced using lithium aluminium hydride in Et_2O at rt for 12 h to afford the desired *trans*-p-menthane-3,8-diol **A** in 95% yield. The benefit of this approach is that reduction of both epoxide diastereomers results in removal of the chirality at their 8-positions, which results in formation of the same PMD diastereomer **A** (67) (Scheme 262).

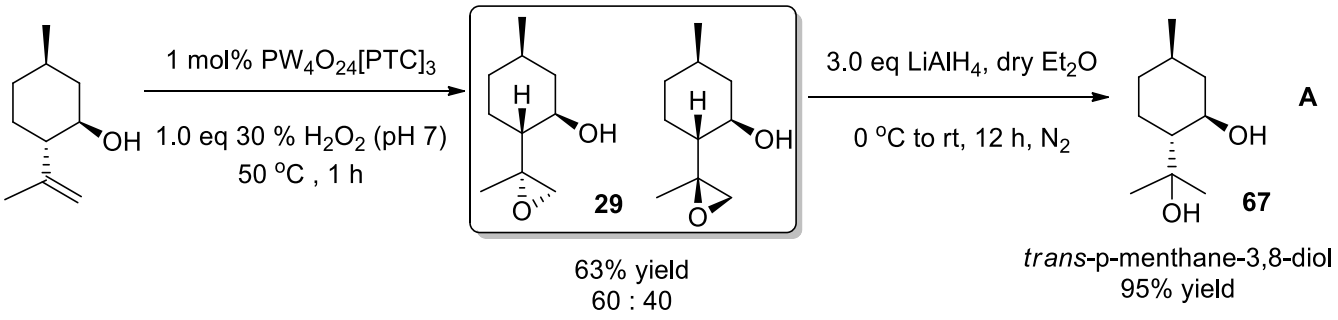

Scheme 262. Conversion of isopulegol epoxide diastereomers into *trans*-PMD isomer **A**

6.3 Selective synthesis of "cis-diol" PMD isomer B

With *trans*-PMD isomer **A** in hand, we next investigated whether we could employ an alcohol inversion strategy to prepare *cis*-p-menthane-3,8-diol **B** (68). Zhao et al[133] have previously reported the synthesis of (*Z*)-8-hydroxycitronellol from (+)-isopulegol (*ent*-isopulegol), involving epoxidation of its 8,9 alkene position, Mitsunobu inversion of its secondary alcohol group, followed by ring opening using a stoichiometric amount of aluminium isoproxide (Scheme 263).

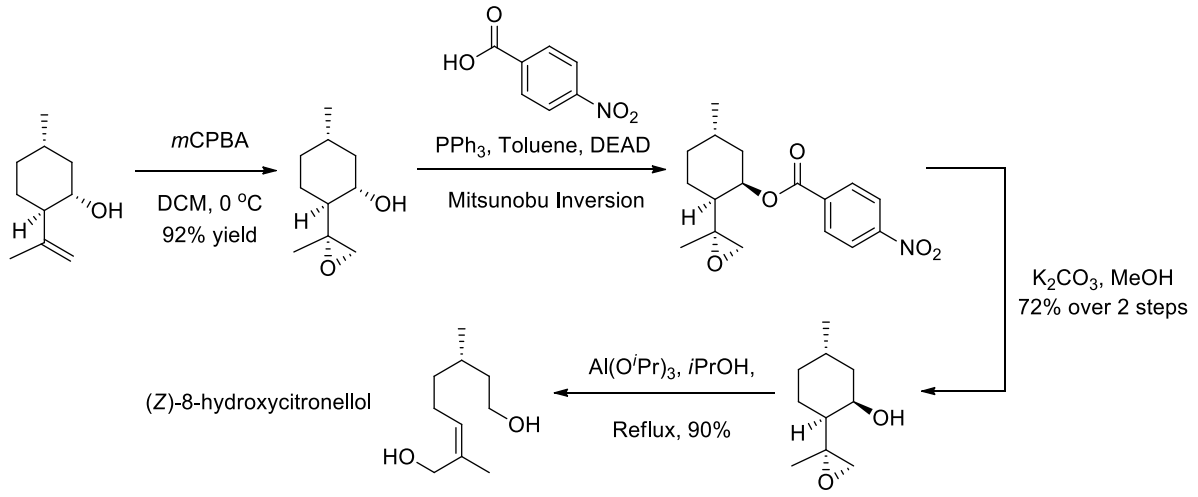

Scheme 263. Synthesis of (*Z*)-8-hydroxycitronellol from isopulegol

These Mitsunobu conditions were then applied to our 60:40 mixture of diastereomeric isopulegol epoxides (29), involving their reaction with *p*-nitrobenzoic acid, PPh_3 and DEAD to give a 60:40 mixture of diastereomeric esters (71) in 75% yield, indicating that clean inversion of their alcohol stereocentres had occurred. Treatment of this crude reaction mixture of diastereomeric benzoate esters with potassium methoxide in methanol resulted in transesterification of both diastereomers to give their corresponding alcohols (72), however one of these diastereomeric alcohols proved to be unstable under these conditions, decomposing to afford more polar products. This enabled a single diasteromeric epoxide alcohol (configuration not assigned) to be obtained in 50% yield, whose epoxide ring was then reduced with $LiAlH_4$ to afford the desired second *cis*-*p*-menthane-3,8-diol **B** (68) in 95% isolated yield (Scheme 264).

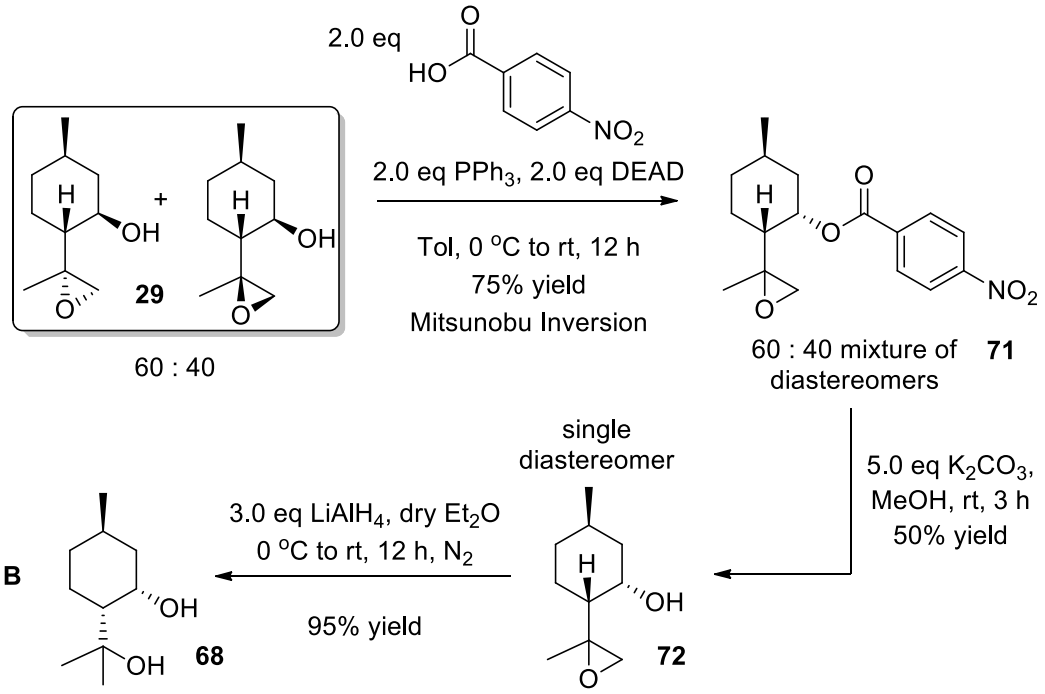

Scheme 264. Mitsunobu inversion strategy for the conversion of isopulegol epoxides into *cis*-PMD isomer **B**

6.4 Selective synthesis of “all cis” PMD isomer C

Our attention then turned to the synthesis of “all *cis*” PMD isomer **C** (*ent*-G) which contains a 1,4 *cis*-relationship across its cyclohexyl ring system using (*S*)-α-pinene as a cheap terpene substrate (Scheme 265). We anticipated that the key reaction in this six step synthesis would be step 3 which required selective fragmentation of the pinane skeleton to afford a *p*-menthane-3,8-diol acetonide (75). This would afford a bicyclic acetonide ring system that would enable diastereoselective hydrogenation of the alkene bond in Step 5 to occur from its least hindered concave face to introduce the 1,4-*cis* configuration of the *p*-menthane ring (76).

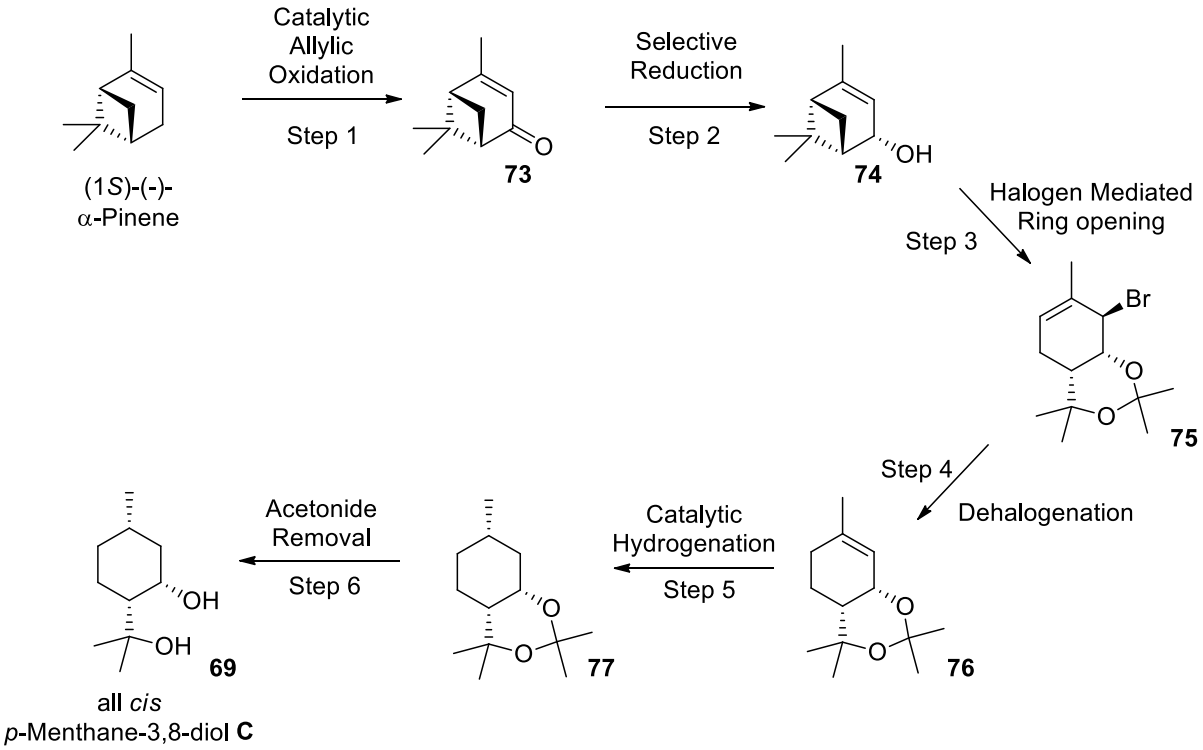

Scheme 265. Stereoselective synthesis of all-*cis*-PMD **C**

6.4.1 Step 1. Catalytic oxidation of α-Pinene

The first transformation targeted was the allylic oxidation of α-pinene to produce verbenone (73), which was carried out using the cheap cobalt catalyst [Co(pyr)$_2$Br$_2$] (Scheme 266) and molecular oxygen, employing a method first developed by Koskinen el al.[310] This methodology was reported to work at low catalyst loadings (0.13 mol%) on a 100 g scale using oxygen as an inexpensive oxidant under solvent free conditions.[310] This allylic oxidation reaction was repeated on a 10 g scale to afford an acceptable 50% yield of verbenone, with this reaction thought to proceed *via* a variation of the radical mechanism shown in Scheme 267.[26,28]

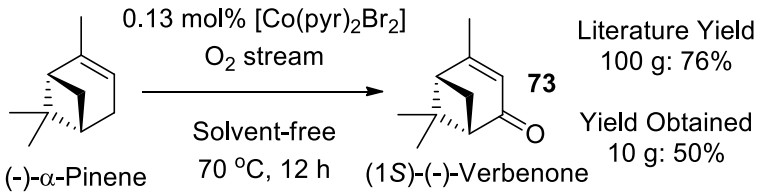

Scheme 266. Koskinen's allylic oxidation reaction of α-pinene

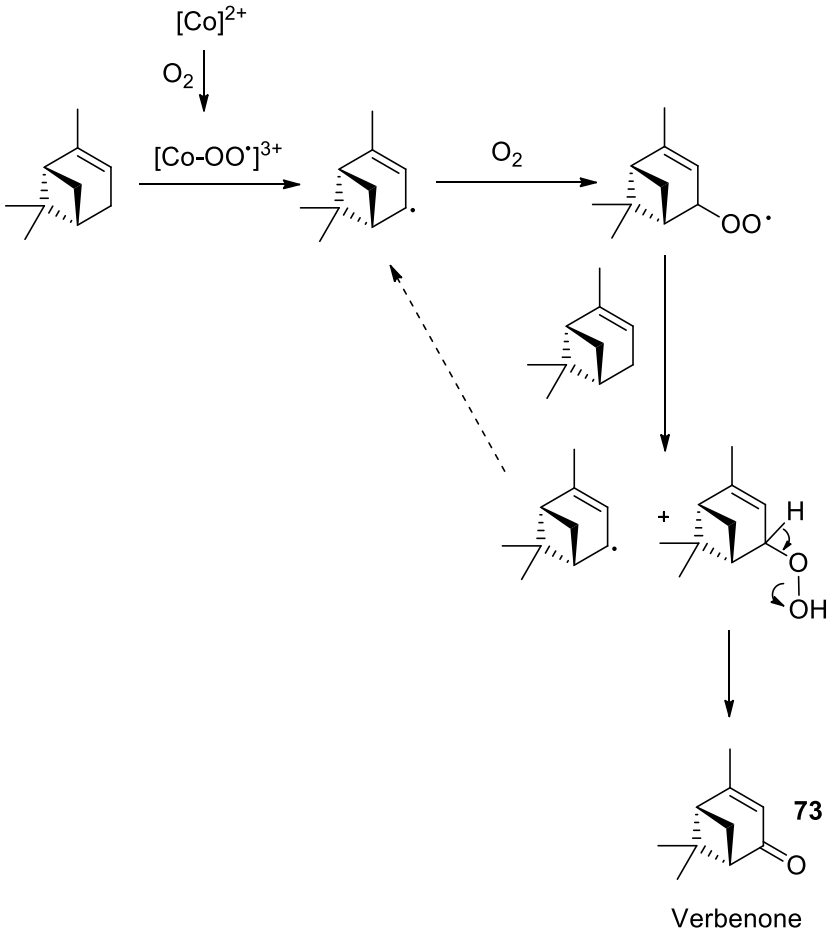

Scheme 267. Allylic radical mechanism for the oxidation of α-pinene into verbenone

6.4.2 Step 2. Reduction of Verbenone

The second step of our synthesis involved a standard stereoselective reduction of (1*S*)-verbenone (73) with diisobutylaluminium hydride at -70 °C in DCM for 2 h using methodology previously developed by Talipov et al,[311] which we repeated to afford *cis*-verbenol (74) as a single diastereomer in 62% yield (Scheme 268).

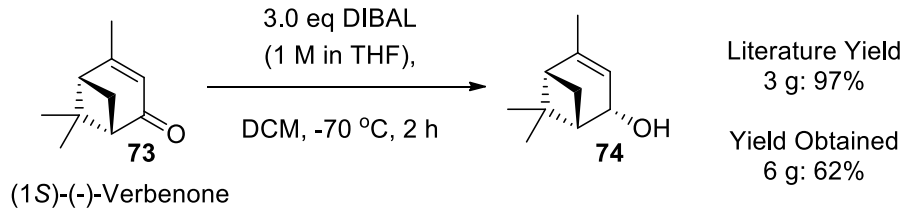

Scheme 268. Stereoselective reduction of verbenone to *cis*-verbenol

6.4.3 Step 3. Bromonium-mediated ring opening of Verbenol

Bulliard et al[312] had previously reported an *N*-bromosuccinimide mediated ring opening reaction of *cis*-verbenol (74) to give *trans*-BrAc (75) as a major product. This procedure was successfully repeated on a 3 g scale affording BrAc which resulted in formation of a mixture of diastereomeric *p*-menthane acetonides (*trans*-BrAc and *cis*-BrAc) in a 9 : 1 ratio in 68% yield (Scheme 269). The major *trans*-bromo-*cis*-acetonide BrAc was easily separated from its minor *cis*-bromo-*cis*-acetonide by chromatography, affording gram quantities that was then used as starting material in the subsequent debromination reaction.

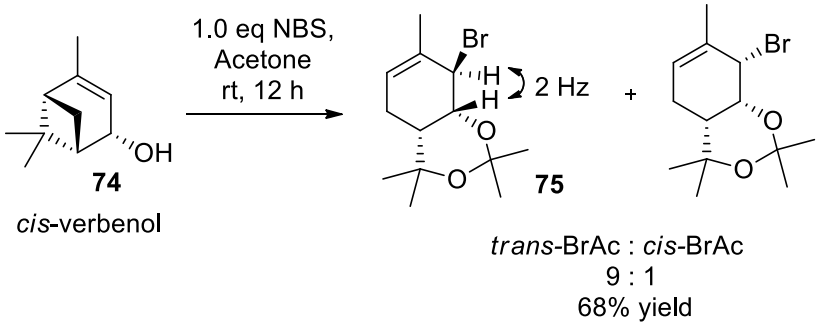

Scheme 269. NBS mediated ring opening of *cis*-verbenol

The major *trans*-BrAc diasteromer in this ring fragmentation reaction is formed *via* the mechanism shown in Scheme 270, with reaction of the alkene bond of *cis*-verbenol with NBS preferentially resulting in a bromonium ion being formed on its least hindered face. This bromonium species triggers fragmentation of the pinane skeleton to afford a *p*-menthane skeleton containing an isopropyl cation fragment that is rapidly intercepted by the alcohol group of a hemiacetal intermediate formed from reaction of the alcohol group of *cis*-verbenol with acetone to afford the observed bicyclic acetonide (*trans*-BrAc).

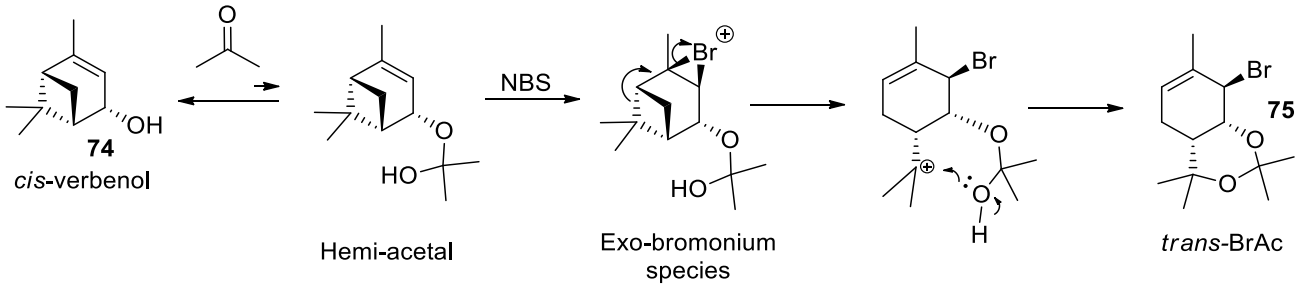

Scheme 270. Proposed mechanism for the NBS mediated ring opening reaction of *cis*-verbenol

6.4.4 Step 4. Dehalogenation of *trans*-BrAc intermediate

The next dehalogenation step was carried out using Brouchard's dehalogenation protocol for *trans*-BrAc (75) who had previously reported that its treatment with $LiAlH_4$ in Et_2O occurred *via* an S_N2 reaction to give homoallylic-Ace (76) in 65% yield.

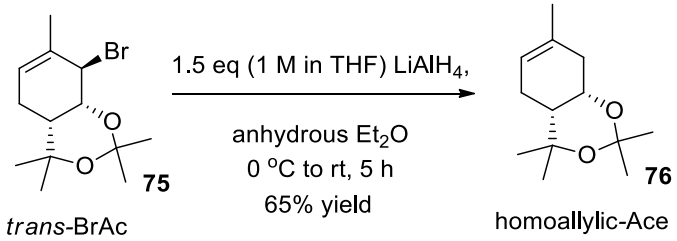

Scheme 271. Brouchard's conditions for the reduction of *trans*-BrAc to afford homoallylic-Ace

We repeated the reduction of the allylic bromide functionality of *trans*-BrAc according to this literature precedent (Scheme 271), involving dropwise addition of a solution of lithium aluminium hydride (1M in THF) to *trans*-BrAc in Et_2O at 0 °C, which we found gave the desired isomeric allylic-Ace in 64% yield (Scheme 272). This reductive debromination reaction can potentially react *via* an S_N2' reaction to afford our allylic Ace isomer (Scheme 273a), or *via* a direct S_N2 reaction to afford Brouchard's isomeric homoallylic Ace isomer (Scheme 273b). Consequently, 2D ^1H-^1H correlation COSY NMR spectroscopic analysis was carried out on our dehalogenated product, which showed a strong correlation peak between H_A and H_B that was consistent with formation of allylic-Ace (Figure 59). These interactions would not be expected for the alternative homallylic-Ace structure proposed by Brouchard, with no significant correlation peaks between H_A and H_C being obserbed that would have been expected if homoallylic Ace had been formed.[312] Therefore, we propose that an exclusive S_N2' mechanism occurs in this debromination reaction because the cyclic acetonide hinders direct backside S_N2 attack of the hydride at the σ*-orbital of the bromide, which results in hydride being preferentially directed to the alkene π*-orbital (Scheme 273).

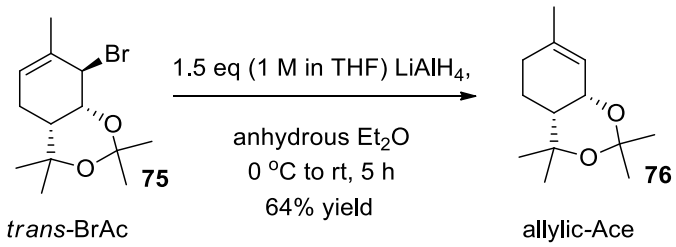

Scheme 272. Reductive debromination of *trans*-BrAc using $LiAlH_4$ to afford allylic-Ace

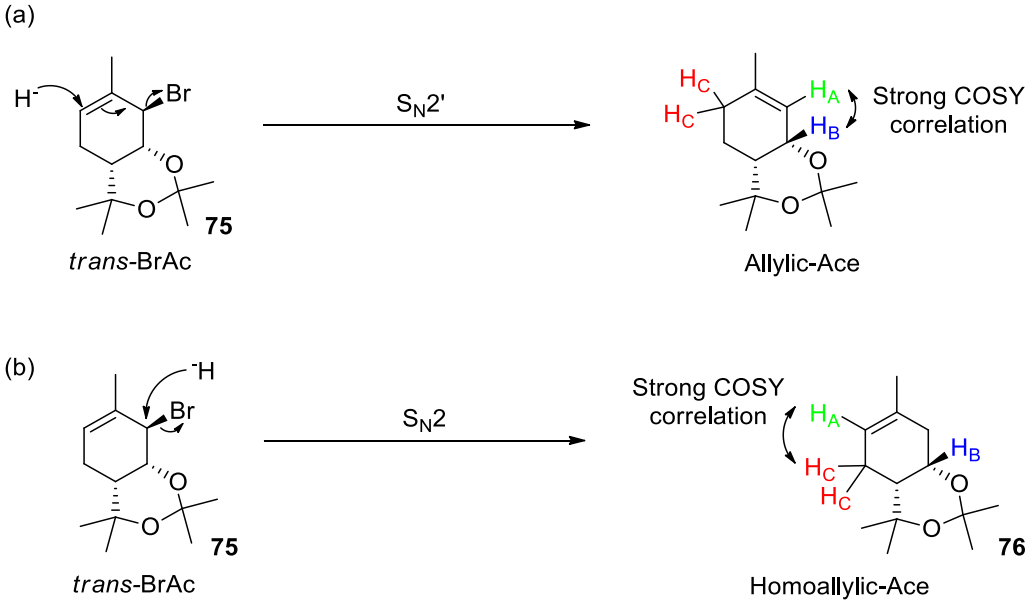

Scheme 273. Potential competing mechanisms for reductive dehalogenation of *trans*-BrAc. (a) S_N2' reduction affords an allylic Ace product that would give a strong COSY correlation between H_A and H_B. (b) S_N2 reduction affords a homoallylic Ace product that would give a strong COSY correlation between H_A and H_C.

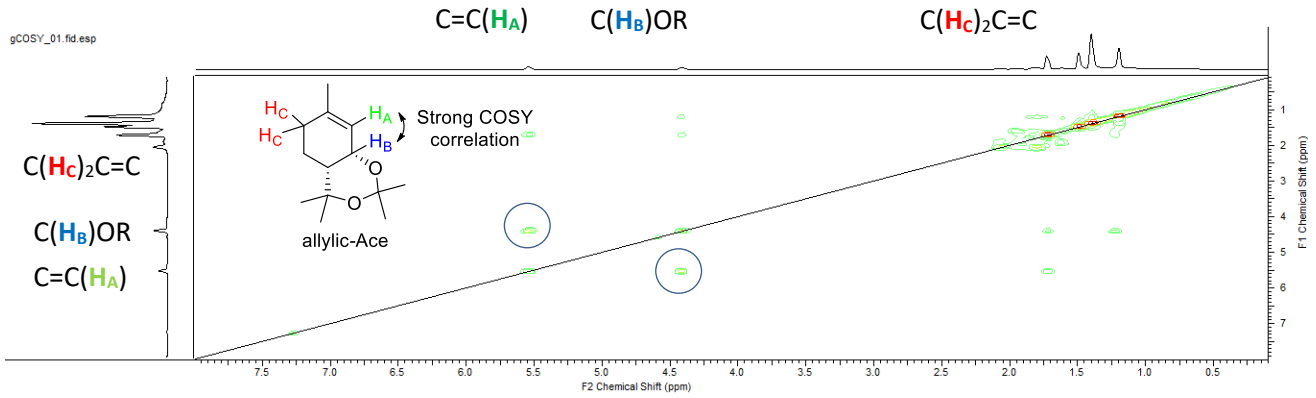

Figure 59. 2D COSY NMR of allylic Ace product showing a strong interaction between H_A and H_B

These results are consistent with related results reported by Borschberg et al,[313] who described that reduction of a related *trans*-BrAc derivative derived from *trans*-verbenol using $LiAlH_4$ gave a 2:1 mixture of allylic Ace (S_N2') and homoallylic Ace isomers (S_N2), respectively, and not the exclusive formation of homoallylic Ace isomer that was originally reported by Brouchard (Scheme 274).

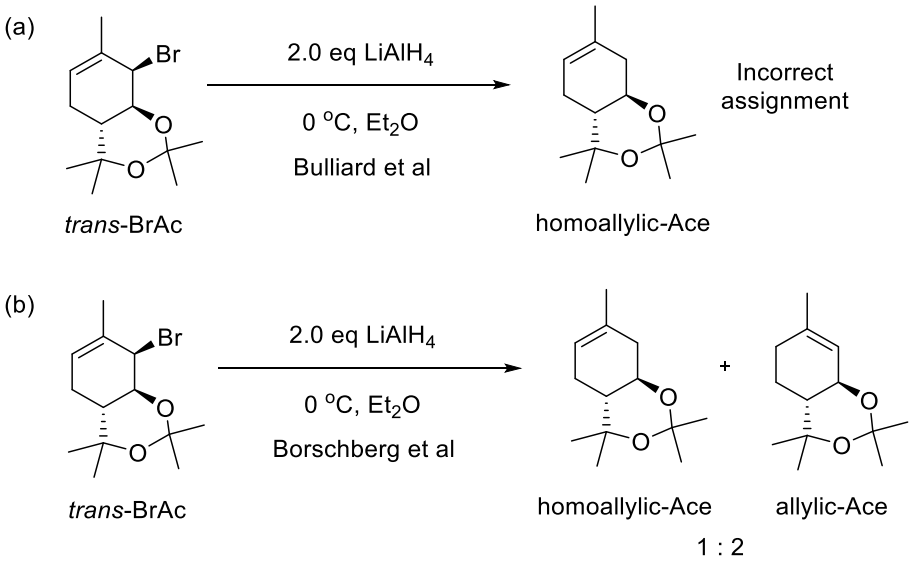

Scheme 274. Previous reports of $LiAlH_4$ mediated dehalogenation of *trans*-BrAc. (a) Bulliard et al[31] incorrectly reported that reduction of *trans*-BrAc with $LiAlH_4$ results in formation of homallylic-Ace (misassigned). (b) Borschberg et al. report that reduction of *trans*-BrAc affords a 1:2 mixture of homoallylic-Ace and allylic-Ace, whose ^1H NMR spectra were assigned using long range ^1H-^{13}C-HETCOR experiments.[313]

It is anticipated that access to allylic-Ace potentially provides an opportunity to prepare dehydro forms of PMD whose unsaturated ring systems are likely to adopt different conformations that may confer them with better insect repellent properties. Access to allylic-Ace also presents an opportunity for easily preparing triol derivatives of PMD that are likely to afford less volatile insect repellents that should retain repellent activity over longer periods of time (Scheme 275).

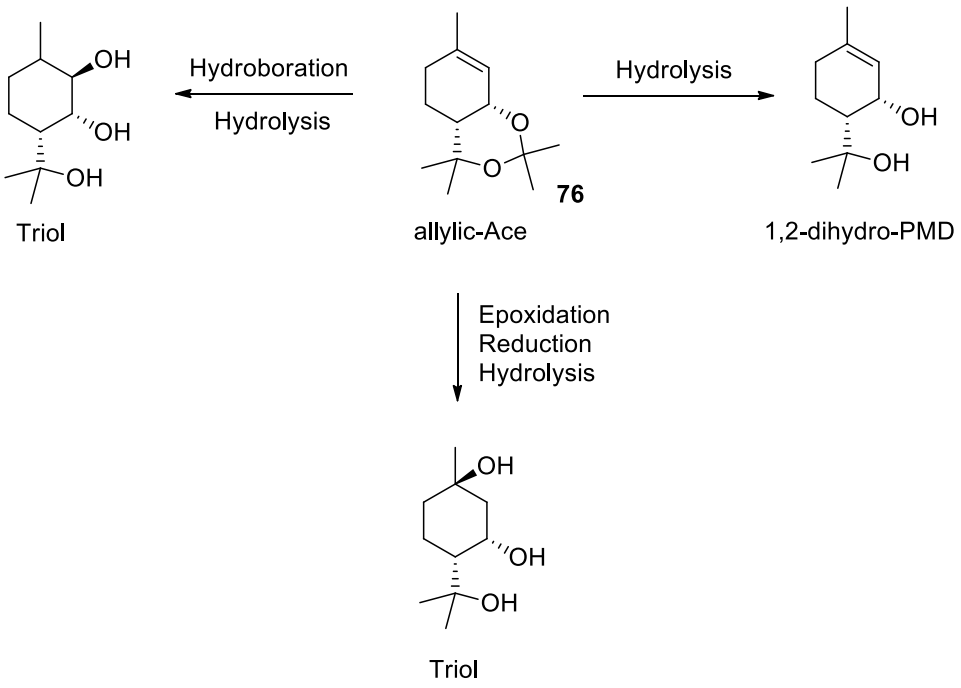

Scheme 275. Preparation of PMD analogues as potential insect repellents

6.4.5 Step 5. Catalytic hydrogenation of the alkene bond of allylic-Ace

The next step involved carrying out a diastereoselective hydrogenation reaction on the alkene bond of allylic-Ace (76) to give the all-*cis* stereochemistry of PMD-Ace (77). This was achieved *via* hydrogenation of allylic-Ace using 5 mol% of platinum oxide as catalyst in methanol under 1 atmosphere of hydrogen for 12 h at rt which gave PMD-Ace in 80% yield (Scheme 276). Hydrogenation of this alkene bond occurs exclusively from its convex face to afford the all *cis*-stereochemistry for the cyclohexyl substituents of PMD-Ace (Scheme 277).

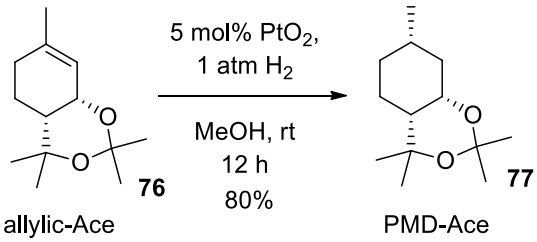

Scheme 276. Platinum oxide mediated hydrogenation of allylic-Ace using platinum oxide

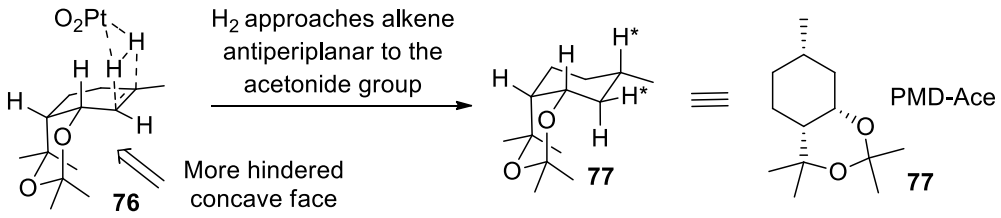

Scheme 277. Transition state model to explain the stereoselectivity of the allylic-Ace hydrogenation reaction

6.4.6 Step 6. Acid catalysed hydrolysis of the acetonide fragment of PMD-Ace

The final step of the synthesis involved acid catalysed deprotection of the acetonide group of PMD-Ace (77) to afford its unmasked diol functionality, which involved treatment with 10 mol% pyridinium tosylate at rt for 6 h which gave the all *cis*-PMD isomer **C** (69) (*ent*-**G**) in 70% yield (Scheme 278). Crystallisation of PMD **C** afforded a crystalline sample that was suitable for X-Ray crystallographic analysis which gave a structure that confirmed its all-*cis* stereochemistry, Figure 60. The cyclohexane ring adopts a chair conformation with its isopropyl substituent occupying an equatorial position that is stabilised by intramolecular hydrogen bonding between its two alcohol substituents.

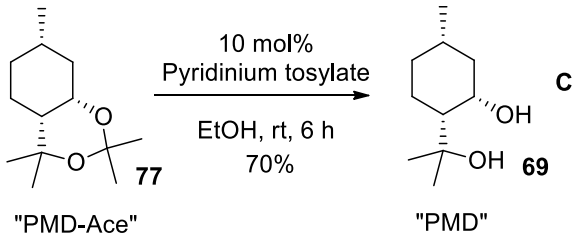

Scheme 278. Acid catalysed acetonide deprotection

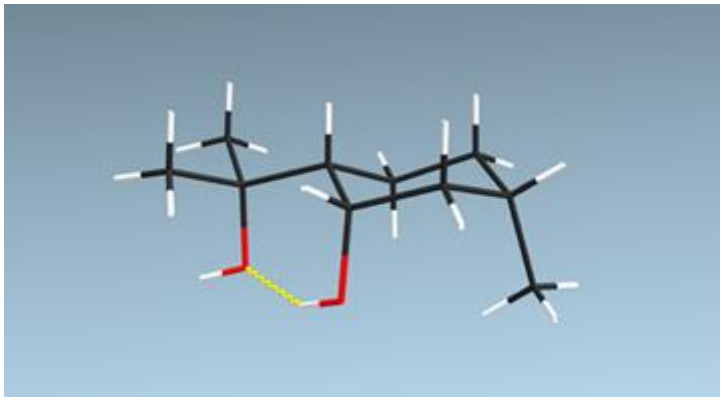

Figure 60. Crystal structure obtained of PMD **C**

Scheme 279 shows a summary of the six step route from α-pinene to the novel PMD diastereomer which can be used for the synthesis of gram quantities of unnatural all-*cis*-PMD C. This synthesis has been repeated using (*R*)-verbenol as a starting material to prepare the corresponding natural PMD antipode **C** in enantiopure form as an individual stereoisomer for screening as an insect repellent.

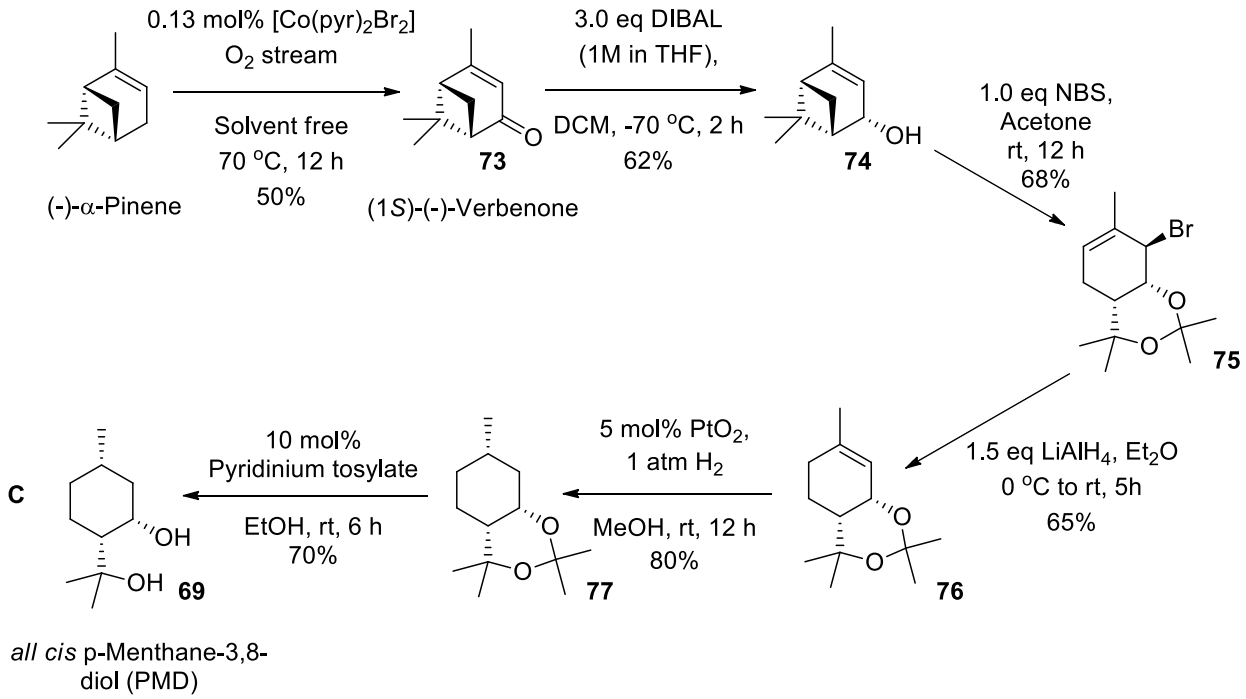

Scheme 279. Synthesis of all-*cis*-PMD diastereomer

6.5 Attempted syntheses of the remaining PMD isomer D

The all-*cis* PMD isomer **G** was then subjected to our previously established Mitsunobu inversion conditions, with the expectation that its secondary alcohol centre would be cleanly inverted to afford PMD isomer **D**. However, treatment of PMD isomer **C** with *p*-nitro-benzoic acid, PPh_3, DEAD in toluene did not afford any of the desired PMD nitrobenzoate ester, with all the starting material being consumed to produce a number of unidentified by-products (Scheme 280). It is proposed that the free tertiary alcohol group of **G** is probably responsible for the failure of this reaction, possibly *via* intramolecular displacement of the benzoate ester to afford cyclic ether bonds (diagnostic C-O resonances observed at δ 61.92 ppm and δ 62.06 ppm in the ^{13}C NMR spectrum of the crude reaction product).

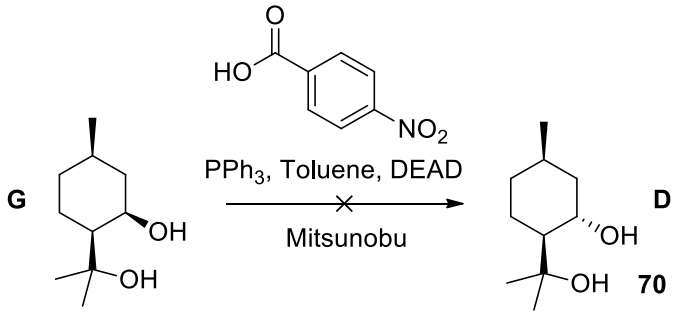

Scheme 280. Failed Mitsunobu reaction

Consequently, an alternative approach for the synthesis of PMD isomer **D** was attempted based on a report by Barrero et al[314] in 2010 for the synthesis of β-elemene analogues. The final step in one of their analogue syntheses involved a double dissolving metal reduction of an epoxy-ketone using lithium in ammonia/EtOH at low temperatures, which gave a *p*-menthane skeleton with a 1,4-*trans*- orientation between its secondary alcohol and isopropyloxy groups (Scheme 281).

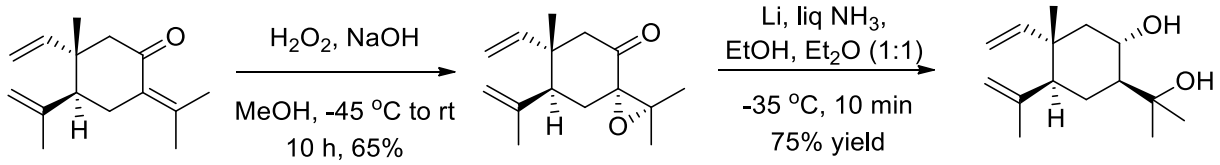

Scheme 281. Dissolving metal reduction of epoxide and ketone to *trans*-diol

It was proposed that this epoxidation/dissolving metal reduction approach could potentially be applied to commercially available pulegone to afford the desired *trans*-diol PMD isomer **D** (70) (Scheme 282). It was hoped that the 1,4-*cis*-stereochemistry of the PMD isomer would be fixed in the dissolving metal reduction step *via* kinetic protonation of an enolate intermediate occurring *anti* to its methyl substituent. The resultant ketone group would then be reduced to afford a thermodynamically more stable equatorial secondary alcohol group with a *trans*-orientation to its C_4 isopropyloxy group.

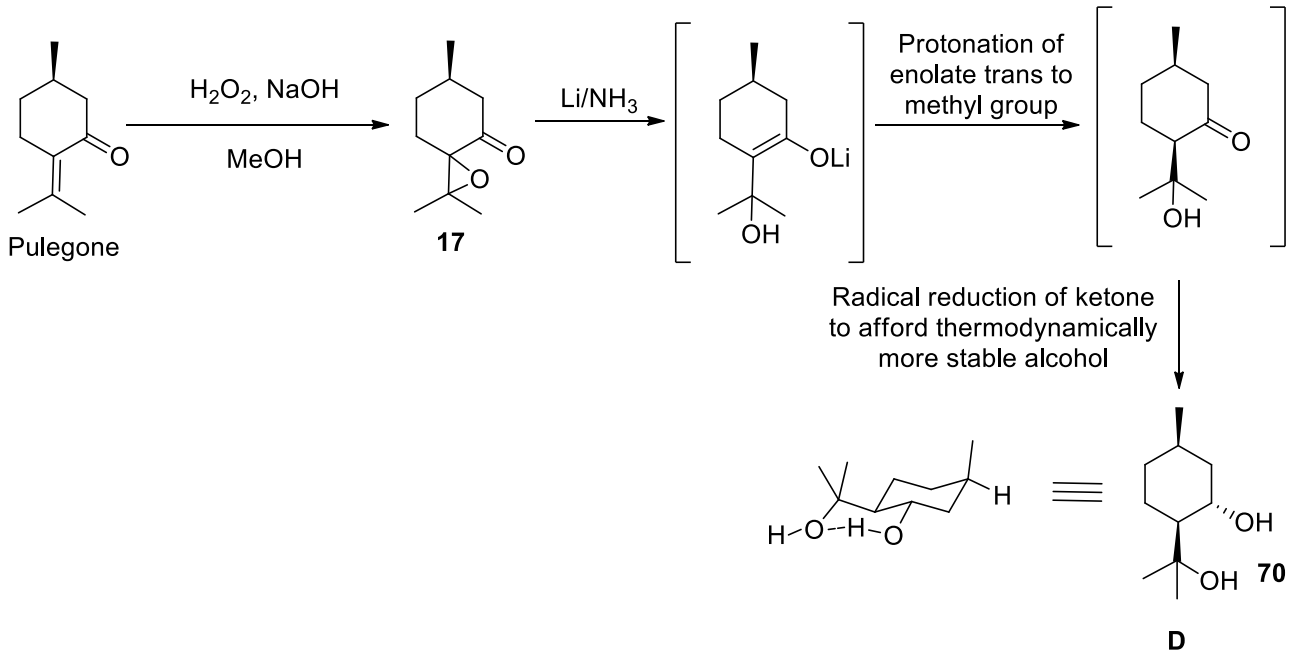

Scheme 282. Proposed synthesis of PMD isomer **D** *via* dissolving metal reduction of pulegone epoxide

Epoxidation of pulegone using H_2O_2/NaOH in MeOH resulted in a non-selective epoxidation reaction to afford a 3:2 mixture of diastereomeric epoxides (17) in 80% yield, that were not separated, because their C_4-stereocentres would be removed in the following dissolving metal reduction step. Unfortunately, although clean and high-yielding, treatment of this mixture of diastereomeric epoxides with Li in ammonia in EtOH/Et_2O at -35 °C resulted in formation of an inseparable 82:18 mixture of PMD **A** (67) and **D** (70) diastereomers in 70% yield. The

presence of the major diasteromer **A** was confirmed by comparison of the ^{1}H and ^{13}C NMR spectra of the crude reaction reduction product with the spectra of pure PMD **A** (67) prepared earlier using our pulegone epoxide/reduction method (see Scheme 283). The *trans*-3,4 stereochemistry of the minor PMD stereoisomer **D** formed in this reaction was evident from the bandwidth of its C*H*(OH) proton which indicated that it was comprised of two large vicinal *J* coupling constants, which also had a similar chemical shift and bandwidth to the C*H*(OH) proton of PMD **A**.

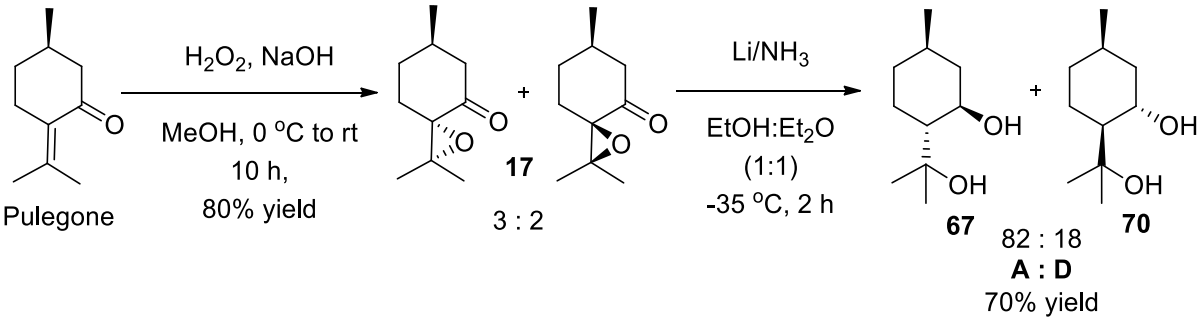

Scheme 283. Dissolving metal reduction of pulegone epoxides for the formation of 1,4-*trans*-PMD **A** and 1,4-*cis*-PMD **D**.

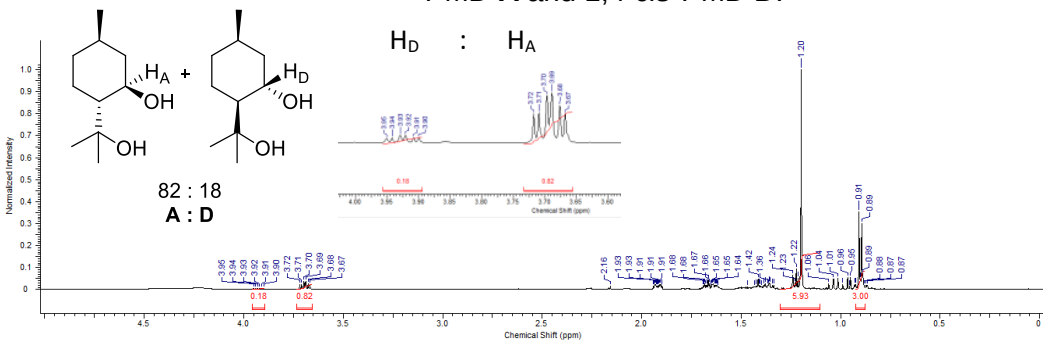

Figure 61. ^{1}H NMR spectra of crude reaction product obtained from dissolving metal reduction of pulegone epoxides that affords a 82:18 mixture of PMD **A** and PMD **D** diastereomers.

The mechanism (Scheme 284) of this dissolving metal reduction involves initial ring opening of the epoxide bonds of both pulegone epoxides to afford the same □-radical that combines with another electron to afford an enolate that is then protonated to afford a mixture of diasteroisomeric ketones. This enolate protonation step is ultimately responsible for fixing the C_4 stereocentre of the PMD product, which can potentially be formed under kinetic control (initial enolate protonation), or thermodynamic control (reversible sodium ethoxide mediated enolization). These 1,4-*trans* and 1,4-*cis* ketones are formed in a 82 : 18 ratio (Figure 61), with their ketone groups then reduced under thermodynamic control to afford anion radical intermediates that are protonated *anti* to their isopropyloxy groups to afford the respective *trans*-3,4-alcohol groups of PMD isomers **A** (82%) and **D** (18%).

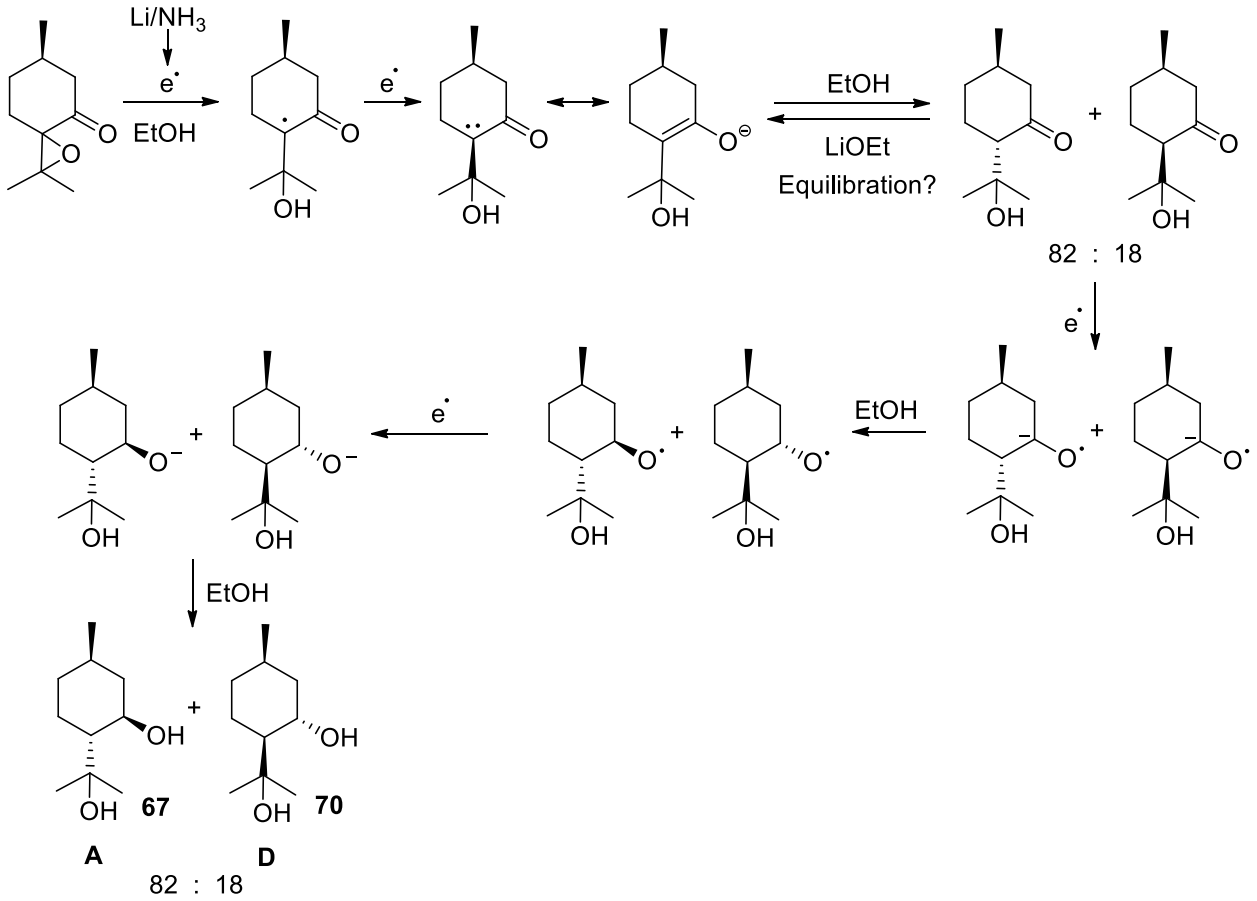

Scheme 284. Mechanism of the dissolving metal reduction reaction of pulegone epoxides.

6.6 Conclusion

In conclusion, we have successfully developed methodology that employs isopulegol and *α*-pinene as biorenewable starting materials for the stereoselective synthesis of three out of the four possible stereoisomers of PMD in enantiopure form (Figure 62). The all-*cis* PMD isomer **C** has been isolated and characterised for the first time, with each of the three routes being applicable to enantiomeric starting materials to enabling their corresponding PMD enantiomers (**E**-**G**) to be prepared. However, attempts to prepare the final PMD isomer **D** were only partially successful, with dissolving metal reduction of pulegone epoxide resulting in an inseparable mixture of PMD isomers **A** and **D**, with PMD isomer **D** being present as the minor component. ^{1}H and ^{13}C NMR spectra of the isolated pure PMD isomers **A**, **B** and **C** (and the 82 : 18 mixture of PMD isomers **A** and **D**) that have been prepared using the synthetic routes described in this chapter are shown on the following page for comparative purposes (Figure 63 and 64).

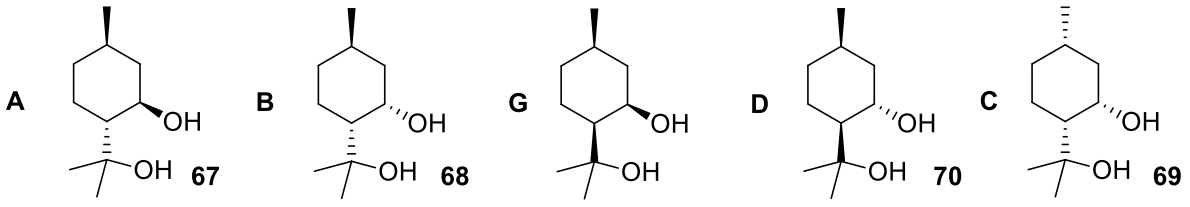

Figure 62: Naturally occurring isomers of PMD **A**,**B**,**G**,**D** and non-natural PMD **C**

Future work to develop a stereoselective synthesis of PMD-isomer **D** will concentrate on exploring two different routes, based on adaptation of the dissolving metal strategy already investigated, or through use of a directed reduction approach. In the first approach we will oxidise all-*cis*-PMD to its afford its corresponding ketone that will then be reduced selectively to afford PMD isomer **D** using dissolving metal reduction conditions (Scheme 285, Route A). An alternative approach using a reducing agent that can coordinate to the β-hydroxy group of the tertiary alcohol of this ketone will also be investigated, which should result in directed reduction of the ketone group from the same face to afford the equatorial alcohol of PMD isomer **D** (Scheme 285, Route B).

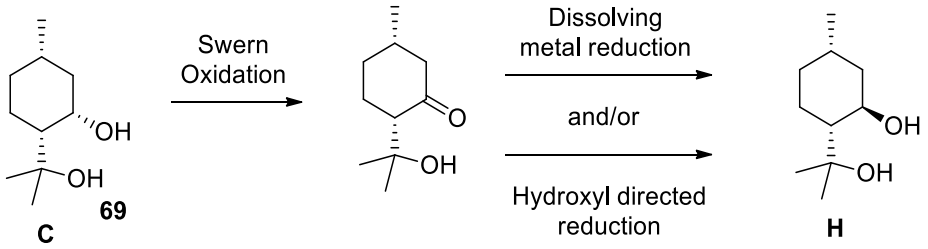

Scheme 285: Future work for the stereoselective synthesis of PMD isomer **D**

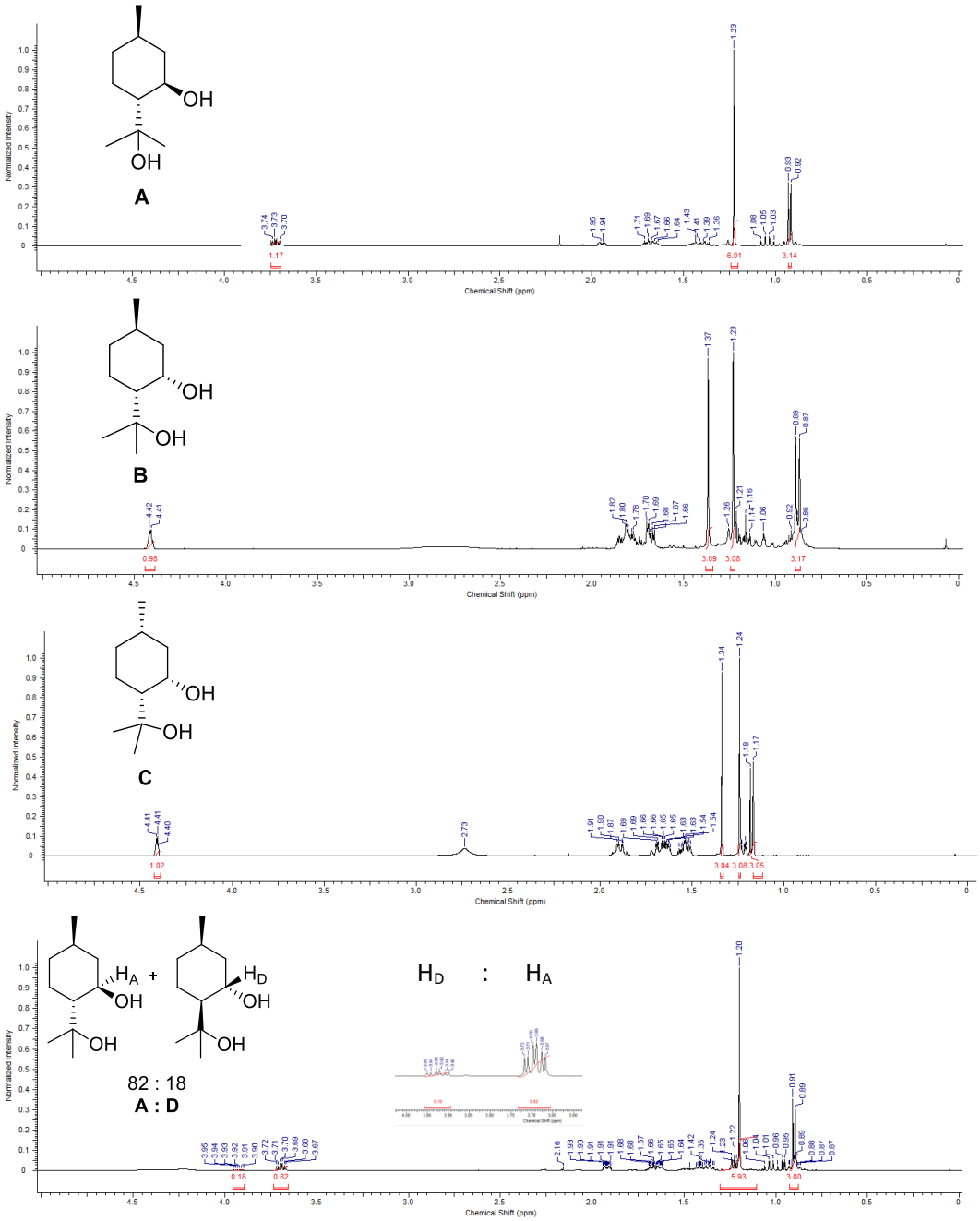

Figure 63. ^{1}H NMR spectra of PMD-isomers **A**-**D**

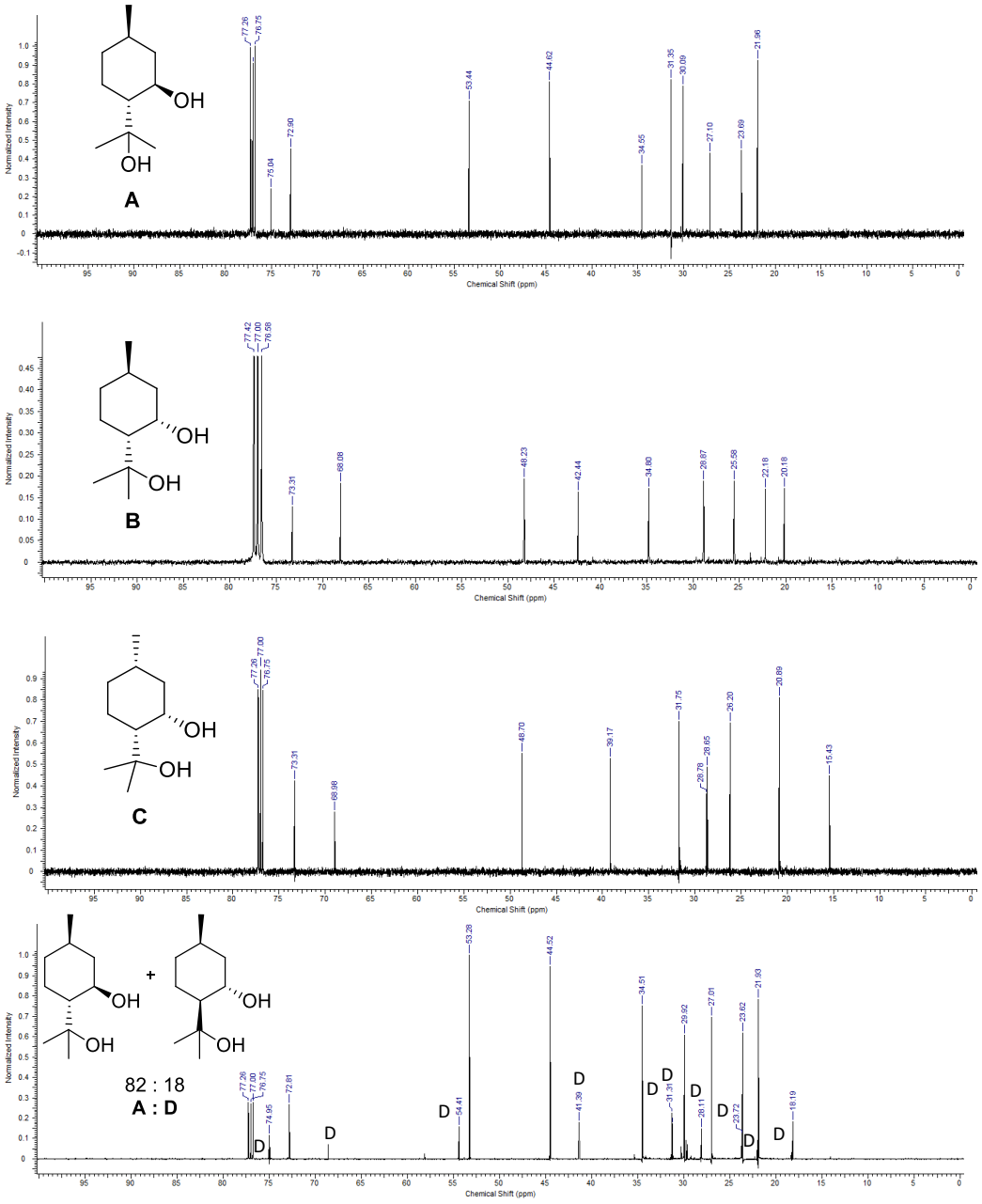

Figure 64. ^{13}C NMR spectra of PMD-isomers **A**-**D**

7 Experimental

7.1.1 Experimental Techniques

Reagents and solvents were sourced from commercial suppliers such as Acros Organics, Fluorochem, Fisher Scientific, Fluka Chemie, Lancaster, Sigma Aldrich and TCI. The chemicals received were used as received. When required inert conditions were achieved using dry solvents and nitrogen atmosphere.

Pre-coated aluminium backed commercial standard silica plates were used to carry out tlc analysis of compounds. Visualisation was carried out using 254 nm UV light and staining was performed using potassium permanganate and phosphomolybdic acid in ethanol solutions followed by gentle heating. 60 micron silica purchased from Sigma Aldrich was utilised during column chromatography of the compounds.

^{1}H and ^{13}C NMR spectra were recorded in $CDCl_3$, DMSO and D_2O at ambient temperature. Bruker Avance 250 (250 MHz) and Bruker 300 (300 MHz) or an Agilent Technologies 500 (500 MHz) NMR spectrometer instruments were used to perform the analysis and the ^{13}C NMR spectra were proton decoupled. The following abbreviations were used: s, d, t, q, quin, sext, m, and br to denote singlet, doublet, triplet, quartet, quintet, sextet, multiplet and broad respectively. Coupling constants were reported where known.

Mass spectrometry analysis was performed using a microTOF electrospray time-of-flight (ESI-TOF) mass spectrometer (Bruker Dlatonik GmbH, Bremen, Germany) and gas chromatography mass spectroscopy was performed using Agilent Technologies 7890B GC system. Infrared spectroscopy was performed using a PerkinElmer Spectrum 100 FT-IR Spectrometer.

A Radleys 12 Carosel and 20 mL Radleys carosel tubes and reduced volume 15 mL Radleys carosel tubes were used. Radleys tubes were also used as reaction vessels without loading within the carosel unit, for example when submerged within a water cooling bath and stirred using standard laboratory magnetic stirrer plates.

Flow equipment used was sourced from LTF gmbh (www.ltf-gmbh.com) and Kinesis. 2 x glass LTF microreactors (model number: XXL-ST-04) were used. 2 x Harvard apparatus PhD 2000 syringe pumps and 2 x 30 mL Luer lock tip style glass syringes were attached to the reactors using 1/16” PTFE tubing *via* Kinesis o-ring sealed 2- or 3- way PTFE adaptor twist valves.

7.2 Procedure for Catalytic Solvent-free Epoxidation of Terpene Substrates

7.2.1 Ishii-Venturello Catalyst preparation

The Venturello-A336 catalyst complex was prepared as follows. Tungstic acid, H_2WO_4 (15 g, 60 mmol) (£2.5 per 10 g (Fisher Scientific), was added to 30 wt% aqueous H_2O_2 (30 mL) diluted with distilled H_2O (12 mL). The solid acid fully dissolved and the bright yellow mixture was stirred for 1.5 h at 60°C until becoming a cloudy pale yellow-white coloured solution. The filtrate was allowed to cool to room temperature and 85% orthophosphoric acid, H_3PO_4 (1.86 mL) dissolved in distilled water (1.86 mL), was added alongside 180 mL distilled H_2O. After stirring for 30 min at room temperature a solution of Aliquat 336 (13.7 mL g, £0.80 per 10 mL (Fisher Scientific)) in CH_2Cl_2 (240 mL) was added slowly over 15 min. The resulting mixture was stirred vigorously for 1 h at room temperature after which the organic phase was separated, washed once with distilled H_2O then dried with $MgSO_4$ and concentrated under vacuum to give the Venturello-A336 catalyst complex as a viscous, transparent yellow syrup in a yield of 60% (16.5 g).

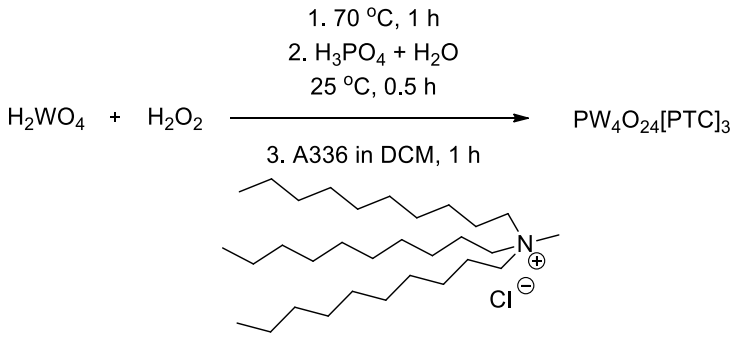

7.2.2 General Procedure for the organic solvent free Ishii-Venturello epoxidation

The following general epoxidation procedure is used for epoxidising the terpene substrates featured in the following sections:

Substrate X (5 mmol, 1.0 eq), $PW_4O_{24}[PTC]_3$ (0.11 g, 2259 $gmol^{-1}$, 0.05 mmol, 1 mol%) were added to a 20 ml glass Radleys carousel tube with a stirrer bar. The catalyst and substrate were stirred for 10 minutes to fully dissolve the catalyst and then stirring was lowered to a minimal amount whilst 30% aqueous hydrogen peroxide solution (0.5 mL, 5 mmol, 1.0 eq (per alkene motif desired to be epoxidised) (buffered to pH 7 with 0.5 M NaOH) was added slowly forming a biphasic mixture. To prevent exothermic runaway the tube was cooled with a water bath and slowly stirred. The reaction was stirred at room temperature for specified reaction times as described within each substrates respective scheme. The reaction was judged to be complete by tlc. The solution was left to settle with no stirring allowing the biphasic system to separate out into its two layers. The top organic layer was then pipetted or decanted off and purified *via* column chromatography (or fractional distillation under reduced pressure) to produce the desired epoxide as clear oils.

Description of modifications to general epoxidation protocol:

- Incorporation of this salt additive into our preformed Venturello catalyst protocol was achieved by dissolving 0.3 equivalents of Na_2SO_4 in the buffered hydrogen peroxide solution prior to its addition to the organic phase for bicyclic monoterpene substrates: α-Pinene, β-Pinene and Myrtenol respectively.
- Higher catalyst loadings were applied to certain substrates as described in the reaction schemes and the appropriate mass was dissolved in the organic substrate as with 1 mol%.
- Elevated temperature in the range of 35-50 ^oC were applied to enable epoxidation of lower activity alkenes as described in the reaction schemes.
- For substrates containing more than one alkene motif that is intended to be epoxidised an extra equivalence of H_2O_2 was added for example Squalene contains six tri-substituted alkene bonds desired to be epoxidised therefore six equivalents of H_2O_2 were added.

NOTE: Where possible ^1H and ^{13}C NMR data was compared to literature reported values which have been fully characterised previously. It is also important to note that cyclic terpene substrates have complex proton peak regions from 0 to 2 ppm within the ^1H NMR spectra. This has been recognised within previously reported literature with ring proton peaks possessing complex multiplet splitting patterns.

7.2.3 Procedure for the Epoxidation of a range of non-oxygenated cyclic terpenes

(R)-(+)-1,2-limonene oxide- (2)

1-methyl-4-(prop-1-en-2-yl)-7-oxabicyclo[4.1.0]heptane

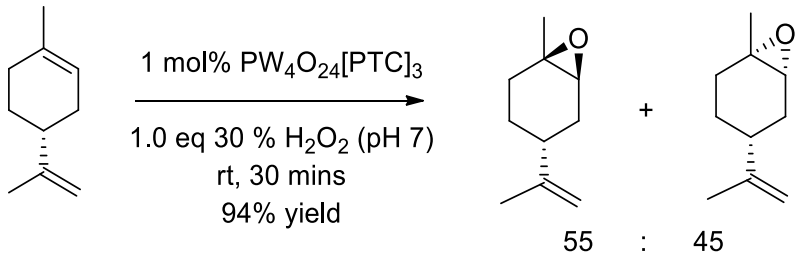

94%; 55:45; ^1H NMR (500 MHz, CHLOROFORM-d) δ (ppm) 1.13–2.13 (m, 7H, ring C**H**), 1.25 (s, 3H, CC**H**$_3$), 1.76 (m, 3H, CC**H**$_3$), 2.97 (t, J = 5.0 Hz, 1H, C(O)C**H**CH_2), 4.65 (s, 2H, CC**H**$_2$).

^{13}C NMR (500 MHz, CHLOROFORM-d) δ (ppm) 19.9 (CH_3), 20.9 (CH_3) , 25.7 (CH_2), 28.4 (CH_2), 30.1 (CH_2), 40.4 (CH), 57.0 (CH), 59.7 (C), 108.9 (CH_2), 148.8 (C). ^1H and ^{13}C NMR data matches that reported in the literature.[315]

α-Pinene epoxide- (5)

(1R,2R,4S,6R)-2,7,7-trimethyl-3-oxatricyclo[4.1.1.02,4]octane

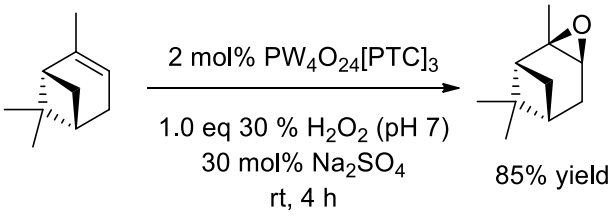

85%; 1:0; ^{1}H NMR (500 MHz, CHLOROFORM-d) δ (ppm) 0.92 (s, 3H, C**H**$_3$), 1.27 (s, 3H, C**H**$_3$), 1.34 (s, 3H, C**H**$_3$), 1.61 (d, J = 9.4 Hz, 1H, C**H**), 1.71–1.76 (br m, 1H, C**H**), 1.86–2.05 (m, 4H, ring C**H**), 3.06 (dd, J = 4.1, 1.5 Hz, 1H, C(O)C**H**).

^{13}C NMR (500 MHz, CHLOROFORM-d) δ (ppm) 20.1 (CH_3), 22.5 (CH_3), 25.8 (CH_3), 26.7 (CH_2), 27.6 (CH_2), 39.7 (CH), 40.5 (CH), 45.2 (C), 56.9 (CH), 60.4 (C). ^{1}H and ^{13}C NMR data matches that reported in the literature.

<u>3-Carene epoxide- (6)</u>

(1S,3S,5R,7R)-3,8,8-trimethyl-4-oxatricyclo[5.1.0.03,5]octane

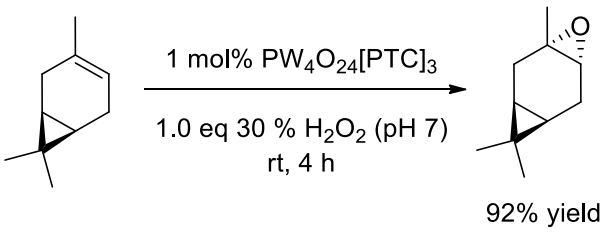

92%; 1:0; ^{1}H NMR (300 MHz, CHLOROFORM-d) δ (ppm) 0.44 (m, 1H, C**H**$_2$), 0.52 (m, 1H, C**H**$_2$), 0.72 (s, 3H. C**H**$_3$), 1.00 (s, 3H, C**H**$_3$), 1.25 (s, 3H, C**H**$_3$), 1.50 (dd, J = 16.5, 2.2 Hz, 1H, C**H**$_2$), 1.64 (dt, J = 16.5, 2.2 Hz, 1H, C**H**$_2$), 2.12 (m, 1H, C**H**), 2.26 (m, 1H, C**H**), 2.82 (s, 1H, C(O)C**H**).

^{13}C NMR (300 MHz, CHLOROFORM-d) δ (ppm) 13.8 (CH_3), 14.6 (CH_3), 16.0 (CH_3), 19.2 (CH_2), 19.1 (CH_2), 23.1 (CH), 23.3 (CH), 27.7 (C), 55.8 (C), 58.2 (CH). ^{1}H and ^{13}C NMR data matches that reported in the literature.[315]

<u>γ-Terpinene bis-epoxide- (7)</u>

(1S,3S,5R,7S)-1-isopropyl-5-methyl-4,8-dioxatricyclo[5.1.0.03,5]octane

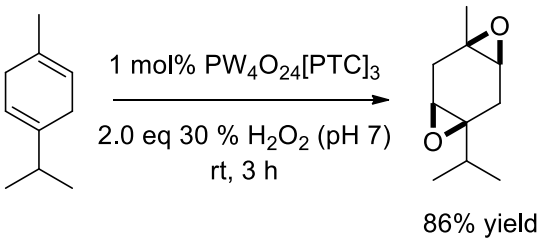

^{1}H NMR (500 MHz, CHLOROFORM-d) δ (ppm) 0.96 (s, 6H, C**H**$_3$), 1.32 (s, 3H, C**H**$_3$), 1.48 (m, 1H, C**H**), 2.20 (m, 4H, ring C**H**), 2.90 (s, 2H, C(O)**H**).

^{13}C NMR (500 MHz, CHLOROFORM-d) δ (ppm) 17.2 (CH_3), 18.17 (CH_3), 23.4 (CH_3), 24.8 (CH_3), 30.1 (Ar), 34.9 (Ar), 55.2 (C(O)H), 56.1 (C(O)H), 57.3 (C(O)H), 61.1 (C(O)H). I.R (thin film) $_{v}$max (cm^{-1}): C-O (1260), C-H (2962). HRMS (ESI): m/z calculated. $C_{10}H_{16}O_2$: requires 169.122855 for $[M+H]^+$; found: 169.1233; requires 191.104799 for $[M+Na]^{+;}$; found 191.1042.

<u>Valencene epoxide- (8)</u>

4,4a-dimethyl-6-(prop-1-en-2-yl)octahydro-1aH-naphtho[1,8a-b]oxirene

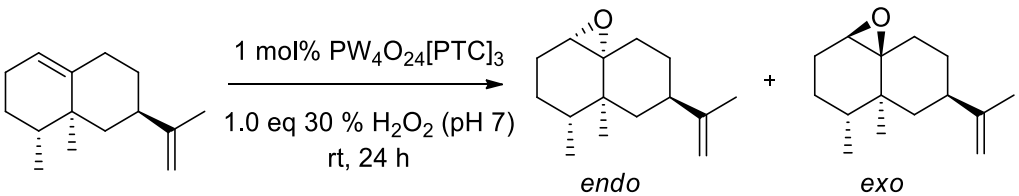

endo epoxy H = 3.0 ppm

exo epoxy H = 2.9 ppm

62% yield

72 : 28[a]

^{1}H NMR (300 MHz, CHLOROFORM-d) δ (ppm) 0.71 (d, *J* = 6.85 Hz, 1 H, ring C**H**), 0.85 (d, *J* = 6.85 Hz, 2 H, ring C**H**$_2$), 0.91 (d, *J* = 5.38 Hz, 1 H, ring C**H**), 0.98 - 1.02 (m, 3 H, CHC**H**$_3$), 1.14 - 1.32 (m, 5 H ring C**H**$_2$/ C**H**$_3$), 1.42 (d, *J* = 2.93 Hz, 1 H, ring C**H**), 1.74 - 1.76 (s, 3 H, C**H**$_3$), 1.87 (d, *J* = 13.21 Hz, 2 H, ring C**H**$_2$), 1.98 - 2.18 (m, 3 H, ring C**H**$_2$), 2.92 - 3.04 (m, 1 H, CH_2C**H**(O)C), 4.72 (s, 2 H, C=C**H**$_2$).

^{13}C NMR (300 MHz, CHLOROFORM-d) δ (ppm) 15.1, 16.0, 16.8, 21.0, 24.5, 24.5, 25.7, 30.7, 33.1, 33.4, 35.9, 39.9, 40.2, 40.5, 41.5, 45.8, 63.6, 64.1, 108.5, 150.0. Data consistent with previous literature[90]

β-Elemene bis-epoxide- (9)

(2R,2'S)-2,2'-((1R,3R,4S)-4-methyl-4-vinylcyclohexane-1,3-diyl)bis(2-methyloxirane)

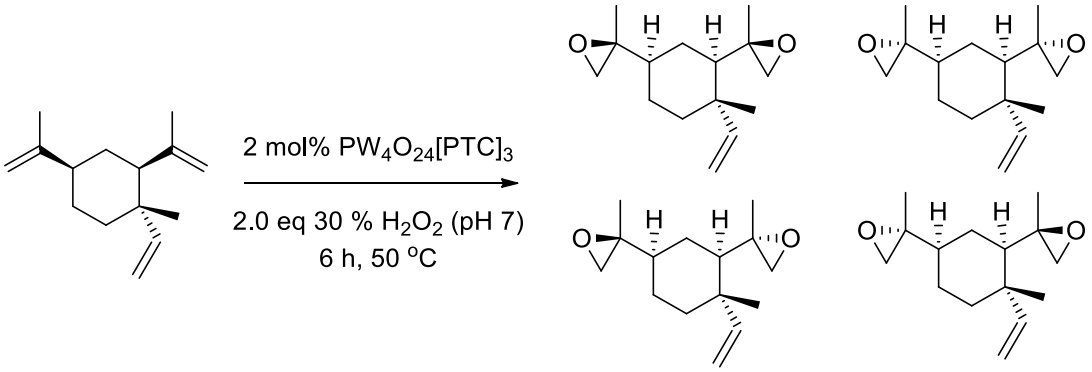

60% yield
40:40:10:10

^{1}H NMR (300 MHz, CHLOROFORM-d) δ (ppm) 1.04 – 1.08 (m, 1 H, ring C**H**), 1.12 (s, 3 H, C**H**$_3$), 1.21 (s, 3 H, C**H**$_3$), 1.23 - 1.29 (m, 3 H, ring C**H**$_2$), 1.31 (m, 3 H, C**H**$_3$), 1.32 – 1.41 (m, 3 H, ring C**H**$_2$), 1.57 – 1.64 (m, 1 H, ring C**H**), 2.54 - 2.63 (m, 2 H, C(O)C**H**$_2$), 2.67 (s, 2 H, C(O)C**H**$_2$), 4.97 (s, 2 H, C**H**$_2$=CH), 5.78 (d, *J* = 17.52 Hz, 1 H, CH$_2$=C**H**).

^{13}C NMR (300 MHz, CHLOROFORM-d) δ (ppm) 14.0, 18.2, 23.3, 25.9, 31.6, 39.8, 41.0, 44.0, 50.6, 57.9, 58.4, 58.6, 59.3, 110.7, 161.4. ^{1}H and ^{13}C NMR data matches that reported by PDRA M.Hutchby using stoichiometric *m*CPBA. I.R (thin film) $_v$max (cm^{-1}): C-H (2975), C=C (1665), C-O (1180).

7.2.4 Procedure for the Epoxidation of cyclic terpenes containing alcohol functionality

2,3-epoxyperillyl alcohol- (10)

(4-(prop-1-en-2-yl)-7-oxabicyclo[4.1.0]heptan-1-yl)methanol

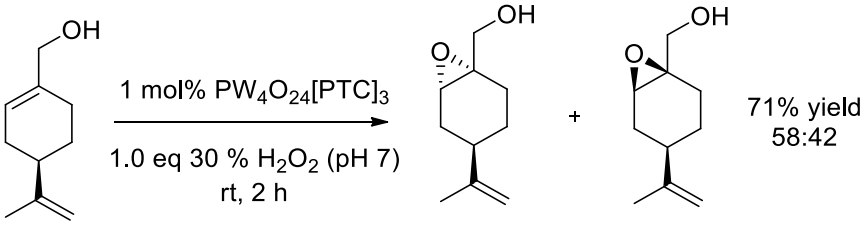

71% yield
58:42

^{1}H NMR (500 MHz, CHLOROFORM-d) δ (ppm) 1.21-1.45 (m, 2H, Ar), 1.61 (s, 2H, Ar), 1.73-1.90 (m, 2H, Ar), 2.05 (m, 1H, C**H**), 2.1-2.2 (m, 3H, C**H**$_3$), 3.29 (s, 1H, C(O)C**H**), 3.60 (m, 1H, CC**H**$_2$OH), 3.68 (m, 1H, CC**H**$_2$OH), 4.67-4.74 (m, 2H, CC**H**$_2$).

^{13}C NMR (500 MHz, CHLOROFORM-d) δ (ppm) 20.2 (CH$_2$), 20.9 (CH$_2$), 24.7 (CH$_2$), 25.9 (CH$_3$), 55.7 (CH), 56.7(C(O)H), 59.9(C), 64.2 (CH$_2$OH), 109.2 (CH$_2$), 148.7 (CCH$_2$) ^{1}H and ^{13}C NMR data matches that reported in the literature.[316]

Carveol 1,2 epoxide- (11)

1-methyl-4-(prop-1-en-2-yl)-7-oxabicyclo[4.1.0]heptan-2-ol

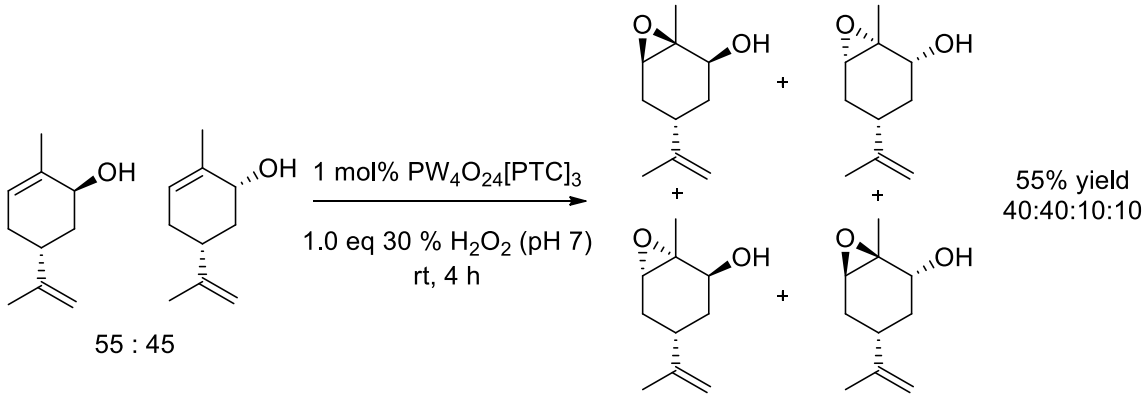

^{1}H NMR (500 MHz, CHLOROFORM-d) δ (ppm) 1.35-1.43 (m, 4H, C**H**$_2$), 1.65-1.69 (m, 3H, C**H**$_3$), 1.70 (m, 1H, C**H**), 2.16 (m, 3H, C**H**$_3$), 3.29 (s, 1H, C(O)C**H**), 3.97 (s, 1H, C(**H**)OH), 4.74 (m, 2H, CC**H**$_2$).

^{13}C NMR (500 MHz, CHLOROFORM-d) δ (ppm) 21.3 (CH_3), 30.1 (CH_3), 35.8 (CH_2), 40.3 (CH_2) 60.5 (C), 61.8 (C(O)H), 62.1 (C), 69.1 (CHOH), 109.6 (CH_2), 147.5 (C). I.R (thin film) $_{v}$max (cm^{-1}): O-H (b, 3407), C-H (2971), C=C (1645), C-O (1292). HRMS (ESI): m/z calculated. $C_{10}H_{16}O_2$: requires 167.1072 for $[M+H]^+$; found: 167.1079.

Myrtenol epoxide- (12)

(7,7-dimethyl-3-oxatricyclo[4.1.1.02,4]octan-2-yl)methanol

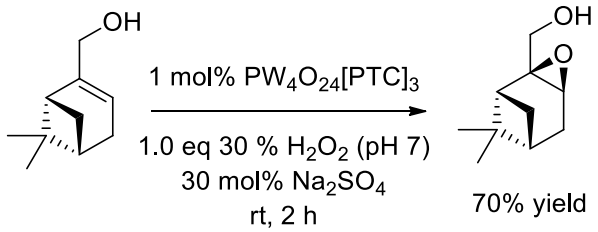

^{1}H NMR (300 MHz, CHLOROFORM-d) δ (ppm) 0.89 (s, 3 H, C**H**$_3$), 1.27 (s, 3 H, C**H**$_3$), 1.63 (d, *J* = 9.42 Hz, 1 H, ring C**H**), 1.71 - 1.79 (m, 1 H, ring C**H**), 1.84 - 2.09 (m, 4 H, ring C**H**$_2$), 2.37 (dd, *J* = 8.48, 4.33 Hz, 1 H, O**H**), 3.37 (dd, *J* = 4.14, 1.32 Hz, 1 H, C(O)C**H**), 3.57 (dd, *J* = 12.81, 8.48 Hz, 1 H, C**H**$_2$OH), 3.75 (dd, *J* = 12.72, 3.86 Hz, 1 H, C**H**$_2$OH).

^{13}C NMR (300 MHz, CHLOROFORM-d) δ (ppm) 20.0, 25.5, 26.4, 27.1, 40.1, 40.5, 40.5, 53.2, 62.9, 63.9. ^{1}H and ^{13}C NMR data matches that reported in the literature.[103]

4-carvomenthenol epoxide- (13)

3-isopropyl-6-methyl-7-oxabicyclo[4.1.0]heptan-3-ol

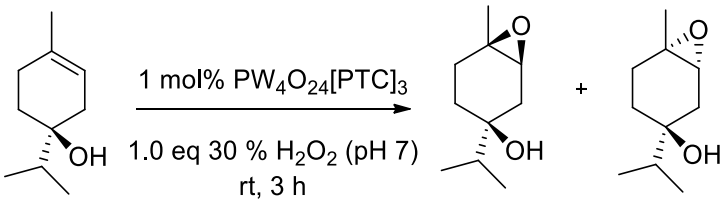

77% yield
90:10

^{1}H NMR (300 MHz, CHLOROFORM-d) δ (ppm) 0.90 (t, *J* = 6.69 Hz, 6 H, CHC**H**$_3$), 1.36 (s, 3 H, CC**H**$_3$), 1.56 (td, *J* = 13.89, 6.88 Hz, 2 H, ring C**H**$_2$), 1.76 - 1.95 (m, 2 H, ring C**H**$_2$), 1.99 - 2.09 (m, 1 H, C**H**), 3.21 (s, 1 H, C(O)C**H**), 3.54 (s, 1 H, O**H**).

^{13}C NMR (300 MHz, CHLOROFORM-d) δ (ppm) 16.6, 16.9, 24.0, 25.8, 29.4, 31.9, 37.1, 58.8, 62.3, 72.0. ^{1}H and ^{13}C NMR data matches that reported in the iterature.[317]

α-Terpineol epoxide- (14)

2-(6-methyl-7-oxabicyclo[4.1.0]heptan-3-yl)propan-2-ol -

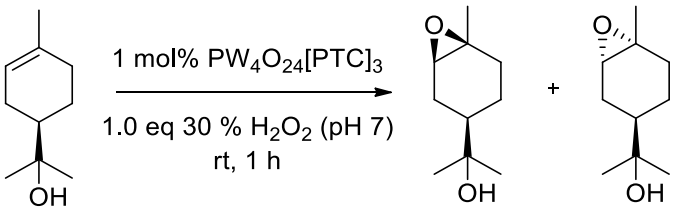

66% yield
56:44

^{1}H NMR (500 MHz, CHLOROFORM-d) δ (ppm) 1.13 (s, 3H, C**H**$_3$), 1.14 (s, 3H, C**H**$_3$), 1.32 (s, 3H, C**H**$_3$), 1.43– 1.50 (m, 2H, ring C**H**), 1.58–1.65 (m, 2H, ring C**H**), 2.00–2.08 (m, 2H, ring C**H**), 2.19–2.24 (m, 1H, C**H**), 3.00 (d, J = 5.4 Hz, 1H, C(O)**H**), 3.07 (br s, 1H, O**H**).

^{13}C NMR (500 MHz, CHLOROFORM-d) δ (ppm) 20.1, 22.8, 22.8, 24.4, 25.9, 26.3, 26.6, 27.18, 27.3, 27.4, 29.5, 30.8, 40.2, 44.1, 57.5, 57.5, 594, 61.2, 72.3, 72.4. Data is consistent with previously reported epoxides.[318]

7.2.5 Procedure for the Epoxidation of terpenes containing α-β-unsaturated functionality

α-ionone epoxide- (15)

4-(2,3-epoxy-2,6,6-trimethylcyclohexyl)-3-buten-2-one

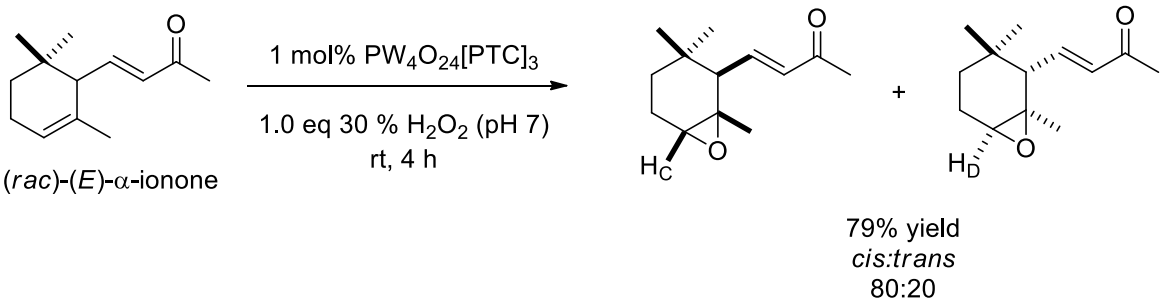

^{1}H NMR (500 MHz, CHLOROFORM-d) δ (ppm) 0.73 (s, 3H, C**H**$_3$), 0.91 (s, 3H, C**H**$_3$), 1.02 (m, 1H, C**H**), 1.23 (s, 3H, C**H**$_3$), 1.38 (m, 1H, C**H**$_2$), 1.85 (m, 1H, C**H**$_2$), 2.05 (m, 1H, C**H**$_1$), 2.09 (m, 1H, CH$_1$), 2.27 (s, 3H, C**H**$_3$), 3.05 (m, 1H, C(O)C**H**), 6.10 (m, 1H, CHC**H**CH), 6.69 (m, 1H, CHC**H**C(O)).

^{13}C NMR (500 MHz, CHLOROFORM-d) δ (ppm) 21.4 (CH$_3$), 21.6 (CH$_3$), 23.9 (CH$_3$), 27.5 (Ar), 27.7 (Ar), 28.3 (Ar), 31.1 (CH$_3$), 32.40 (CH), 52.3 (CH), 59.4 (C), 133.9 (CH), 145.9 (CH) ,198.5 (C(O)). ^{1}H and ^{13}C NMR data matches that reported in the literature.[318]

β-ionone epoxide- (16)

4-(1,2-epoxy-2,6,6-trimethylcyclohexyl)-3-buten-2-one

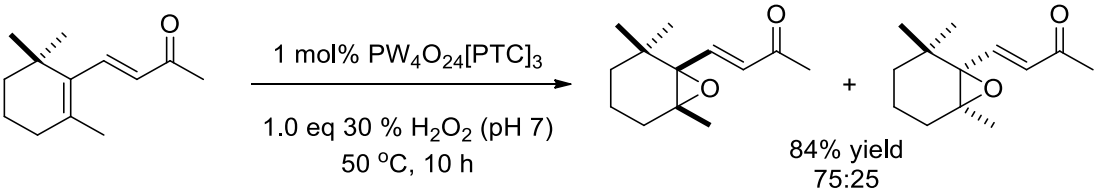

^{1}H NMR (500 MHz, CHLOROFORM-d) δ (ppm) 0.89 (s, 3H,C**H**$_3$), 1.10-1.30 (m, 6H, C**H**$_3$), 1.40 (m, 2H, ring C**H**), 1.75 (m, 4H, ring C**H**), 2.24 (s, 3H, C**H**$_3$), 6.25 (s, 1H, CC**H**CH), 6.98 (s, 1 H, CHC**H**C(O)).

^{13}C NMR (500 MHz, CHLOROFORM-d) δ (ppm) 16.7 (CH$_3$), 20.6 (CH$_3$), 25.7 (CH$_2$), 27.3 (CH$_2$), 29.6 (CH$_2$), 33.4 (CH$_3$), 33.5 (CH$_3$), 35.3 (CH$_3$), 65.7 (C(O)), 70.4 (C(O)), 132.37 (CH), 142.5 (CH), 197.4 (C(O)). ^{1}H and ^{13}C NMR data matches that reported in the literature.[319]

Pulegone epoxide- (17)

(3S,6R)-2,2,6-trimethyl-1-oxaspiro[2.5]octan-4-one

(3R,6R)-2,2,6-trimethyl-1-oxaspiro[2.5]octan-4-one

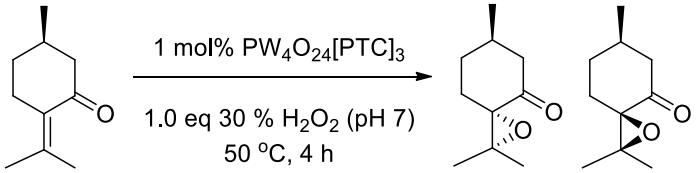

40% yield
55:45

^{1}H NMR (300 MHz, CHLOROFORM-d) δ (ppm) 1.03 - 1.09 (m, 3 H, C**H**$_3$), 1.20 (d, *J* = 3.39 Hz, 3 H, CHC**H**$_3$), 1.42 (s, 3 H, C**H**$_3$), 1.77 - 2.03 (m, 4 H, ring C**H**$_2$), 2.11 - 2.25 (m, 1 H, ring C**H**), 2.35 - 2.47 (m, 1 H, C**H**$_2$C(O)), 2.53 - 2.65 (m, 1 H, C**H**$_2$C(O)).

^{13}C NMR (300 MHz, CHLOROFORM-d) δ (ppm) 18.8, 19.7, 22.0, 29.9, 30.6, 33.9, 51.3, 63.2, 70.2, 207.6. ^{1}H and ^{13}C NMR data matches that reported in the literature.[320]

7.2.6 Procedure for the Epoxidation of acyclic terpenes

6,7-Myrcene epoxide- (18)

(R)-2,2-dimethyl-3-(3-methylenepent-4-en-1-yl)oxirane

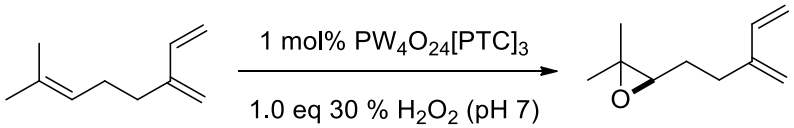

82% yield

^{1}H NMR (500 MHz, CHLOROFORM-d) δ (ppm) 1.25 (s, 3H, C**H**$_3$), 1.30 (s, 3H, C**H**$_3$), 1.65 - 1.79 (m, 2H, C**H**$_2$), 2.32 (d, 1H, C**H**), 2.42 (d, 1H, C**H**), 2.76 (t, J = 6.3 Hz, 1H, C(O)**H**), 5.01 - 5.11 (m, 3H, C**H**$_2$), 5.24 (d, J = 17.7 Hz, 1H, C**H**), 6.38 (m, 1H, C**H**).

^{13}C NMR (500 MHz, CHLOROFORM-d) δ (ppm) 18.3 (CH_3), 24.4 (CH_3), 27.1 (CH_2), 27.6 (CH_2), 58.0 (CH), 63.6 (C), 113.0 (CH_2), 115.7 (CH_2), 138.1 (CH), 144.9 (C); ^{1}H and ^{13}C NMR data matches that reported in the literature.[315]

Citronellal epoxide- (19)

5-((R)-3,3-dimethyloxiran-2-yl)-3-methylpentanal

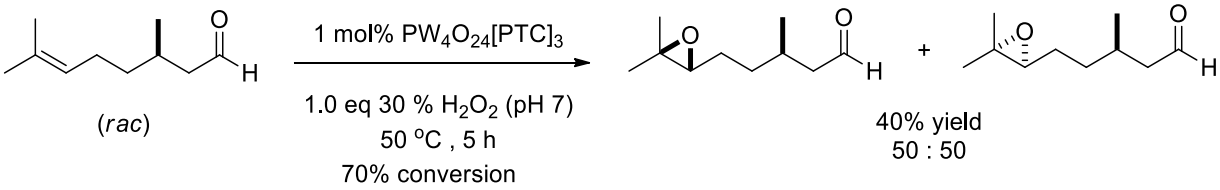

^{1}H NMR (500 MHz, CHLOROFORM-d) δ (ppm) 0.94 (d, J = 7 Hz, 3H, C**H**$_3$), 1.22 (s, 3H, C**H**$_3$), 1.27 (s, 3H, C**H**$_3$), 1.51 (m, 4H, C**H**$_2$), 2.36 (m, 1H, CH_2C**H**CH_3), 2.67 (m, 1H, C(O)C**H**), 9.72 (s, 1H, C**H**O) .

^{13}C NMR (500 MHz, CHLOROFORM-d) δ (ppm) 18.5 (CH_3), 19.6 (CH_3), 24.7 (CH_2), 27.8 (CH_2), 33.4 (CH_3), 50.7 (CH), 58.2 (CH(O)), 64.1 (C(O)), 202.4 (COH) ^{1}H and ^{13}C NMR data matches that reported in the literature.[318]

Citronellal diol- (20)

6,7-dihydroxy-3,7-dimethyloctanal / 6,7-Hydroxycitronellal

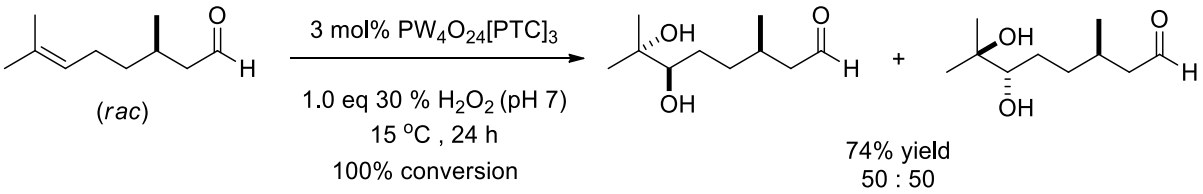

^{1}H NMR (500 MHz, CHLOROFORM-d) δ (ppm) 0.98 - 1.04 (m, 6 H, C**H**$_3$), 1.14 - 1.25 (m, 3H, C**H**$_3$), 1.27 - 1.35 (m, 4 H, C**H**$_2$), 1.42 - 1.60 (m, 2H, C**H**$_2$), 2.20 (s, 1H, C**H**$_2$), 2.35 (m, 1H, C**H**$_2$), 2.44 (m, 1H, C**H**$_2$), 3.32 - 3.43 (m, 1H, C**H**(OH)), 9.80 (t, J = 2.05 Hz, 1H, C**H**O).

^{13}C NMR (500 MHz, CHLOROFORM-d) δ (ppm) 19.6 (CH_3), 23.18 (CH_3), 26.4 (CH_3), 28.20 (CH_2), 29.74 (CH), 34.10 (CH_2), 39.56 (CH_2), 73.02 (C), 78.60 (CH), 202.84 (CH). ^{1}H and ^{13}C NMR data matches that reported in the literature.[321]

Farnesene bis-epoxide- (21)

2-(2-(3,3-dimethyloxiran-2-yl)ethyl)-2-methyl-3-(3-methylenepent-4-en-1-yl)oxirane -

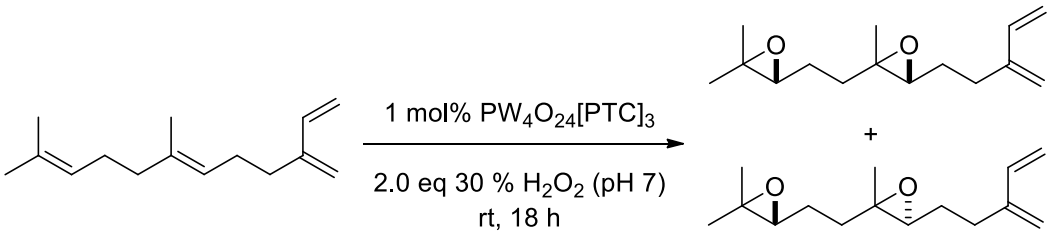

86% yield
50:50

^{1}H NMR (500 MHz, CHLOROFORM-d) δ (ppm) 1.23-1.28 (m, 9H, C**H**$_3$), 1.51-1.73 (m, 6H, C**H**$_2$), 2.65 (m, 2H, C**H**$_2$), 2.73 (m, 2H, C**H**$_2$), 5.02 (m, 3H, C**H**$_2$), 5.20 (m, 1H, C**H**$_2$), 6.33 (m, 1H, CC**H**CH$_2$).

^{13}C NMR (500 MHz, CHLOROFORM-d) δ (ppm) 16.2 (CH_3), 18.3 (CH_3), 24.2 (CH_3), 24.4 (CH_2), 26.95 (CH_2), 27.8 (CH_2), 35.3 (CH_2), 57.9 (CH), 60.2 (CH), 63.0 (C), 63.6 (C), 113.1 (CH_2), 115.8 (CH_2), 138.2 (CH), 145.0 (C); I.R (thin film) $_v$max (cm^{-1}): C-H (2962), C=C (1595), C-O (1249). HRMS (ESI): m/z calculated. $C_{15}H_{24}O_2$: requires 259.167400 for $[M+Na]^+$; found: 259.1692;

Squalene epoxide- (22)

Hexaepoxysqualene

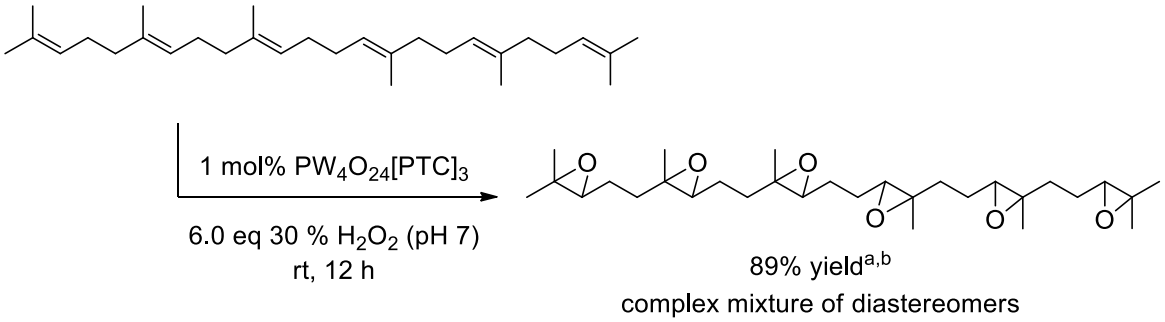

89% yield[a,b]
complex mixture of diastereomers

^{1}H NMR (500 MHz, CHLOROFORM-d) δ (ppm) 1.22-1.26 (m, 24H, C**H**$_3$), 1.34-1.68 (m, 20H, C**H**$_2$), 2.65-2.76 (m, 6H, C**H**(O)).

^{13}C NMR (500 MHz, CHLOROFORM-d) δ (ppm) 16.3 (CH_3), 16.3 (CH_3), 16.3 (CH_3), 16.5 (CH_3), 18.5 (CH_3), 18.6 (CH_3), 24.2 (CH_3), 24.4 (CH_3), 24.5 (CH_2), 24.6 (CH_2), 24.7 (CH_2), 25.6 (CH_2), 25.8 (CH_2), 25.9 (CH_2), 35.1 (CH_2), 35.4 (CH_2), 35.4 (CH_2), 35.5 (CH_2), 58.3 (CH), 58.3 (CH), 60.2 (CH), 60.3 (CH), 60.4 (CH), 60.4 (CH), 62.5 (C), 62.7 (C), 63.0 (C), 63.2 (C), 63.7 (C), 63.9 (C). I.R (thin film) $_v$max (cm^{-1}): C-H (2963), C-O (1249). HRMS (ESI): m/z calculated. $C_{30}H_{50}O_6$: requires 507.3686 for $[M+H]^+$; found: 507.3696;

7.2.7 Procedure for the Epoxidation of acyclic terpenes containing alcohol groups

Linalool 2,3 oxide- (23)

5-(3,3-dimethyloxiran-2-yl)-3-methylpent-1-en-3-ol

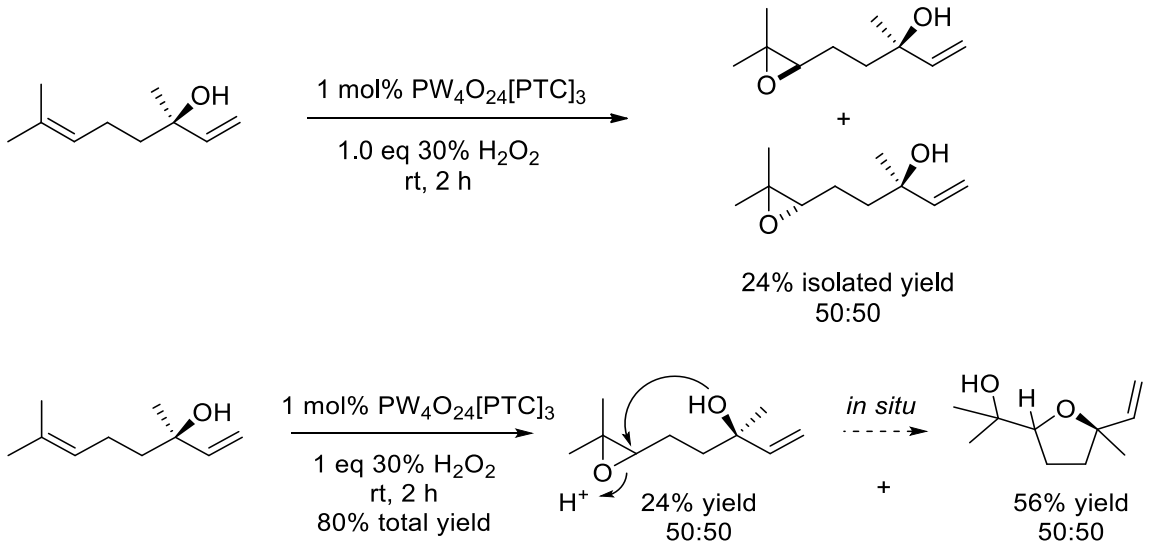

^{1}H NMR (500 MHz, CHLOROFORM-d) δ (ppm) 1.14 (s, 6H, C**H**$_3$), 1.22 (s, 3H, C**H**$_3$), 1.67-1.76 (m, 4H, C**H**$_2$), 2.11 (m, 1H, C(O)**H**), 3.40 (br s, 1H, O**H**), 4.97 (m, 2H, C**H**$_2$CH), 5.95 (m, 1H, CH$_2$C**H**).

^{13}C NMR (500 MHz, CHLOROFORM-d) δ (ppm) 20.7 (CH$_3$), 25.5 (CH$_3$), 25.6 (CH$_3$), 29.5 (CH$_2$), 32.4 (CH$_2$), 59.2 (C), 73.4 (CH), 74.7 (C), 110.6 (CH$_2$), 146.2 (CH). ^{1}H and ^{13}C NMR data matches that reported in the literature.[322,323]

2-(5-methyl-5-vinyltetrahydrofuran-2-yl)propan-2-ol- (24)

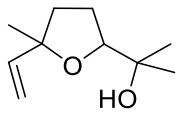

^{1}H NMR (500 MHz, CHLOROFORM-d) δ (ppm) 1.13 (s, 3H, C**H**$_3$), 1.23 (s, 3H, C**H**$_3$), 1.32 (s, 3H, C**H**$_3$), 1.83-1.89 (m, 4H, C**H**$_2$), 2.07 (br s, 1H, O**H**), 3.85 (m, 1H, C(O)**H**), 5.02 (m, 1H, CHC**H**$_2$), 5.21 (m, 1H, CHC**H**$_2$), 5.98 (m, 1H, CH$_2$C**H**C).

^{13}C NMR (500 MHz, CHLOROFORM-d) δ (ppm) 25.9 (CH$_3$), 26.5 (CH$_3$), 26.8 (CH$_3$), 37.4 (CH$_2$), 37.7 (CH$_2$), 71.1 (C) , 83.0 (CH), 85.5 (C(OH)), 111.3 (CH$_2$), 143.9 (CH); ^{1}H and ^{13}C NMR data matches that reported in the literature.[322]

(*rac*)-β-Citronellol epoxide- (25)

(*rac*)-6,7-Epoxy-3,7-dimethyloctanol

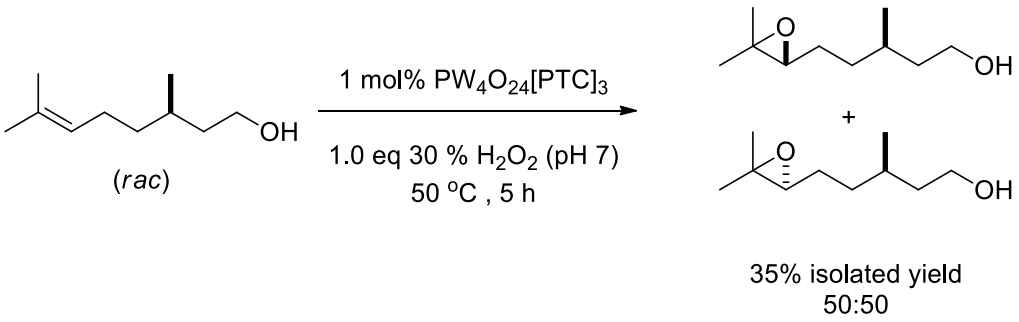

^{1}H NMR (500 MHz, CHLOROFORM-d) δ (ppm) 0.87 (s, 3H, C**H**$_3$), 1.22 (s, 3H, C**H**$_3$), 1.26 (s, 3H, C**H**$_3$), 1.35-158 (m, 6H, C**H**$_2$), 2.28 (s, 1H, C**H**), 2.66 (s, 1H, C(O)**H**), 3.63 (m, 2H, C**H**$_2$OH).

^{13}C NMR (500 MHz, CHLOROFORM-d) δ (ppm) 18.6 (CH_3), 19.3 (CH_3), 19.5 (CH_3), 24.8 (CH_2), 29.3 (CH_2), 33.5 (CH_2), 39.4 (CH), 39.7 (CH), 60.6 (C), 64.6 (CH_2OH). ^{1}H and ^{13}C NMR data matches that reported in the literature.[324]

7.2.7.1 Epoxidation of protected β-Citronellol

Protected β-citronellol epoxidation using Venturello catalyst –

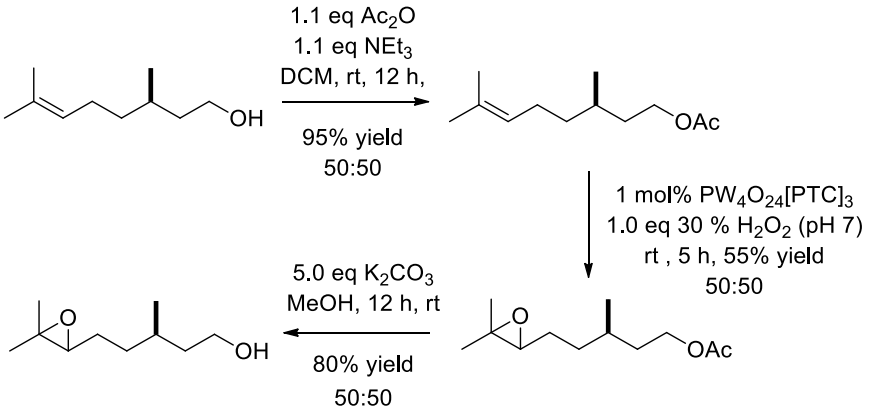

Acetylation of β-citronellol:

(*rac*)-3,7-dimethyloct-6-en-1-yl acetate- (26)

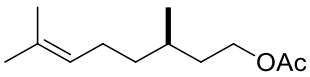

Acetylation of β-citronellol (1.1 g, 7 mmol) was carried out using Ac_2O (790 mg, 7.7 mmol) in triethylamine (710 mg, 8.9 mmol) at rt. After 12 hr, the reaction mixture was poured into MeOH 10 mL to degrade the excess Ac_2O into its methyl esters for removal *in vacuo*. After extraction with Et_2O (4 x 30 mL), the organic extracts were combined, washed with H_2O 30 mL, 10% HCl, saturated NaCl, dried with $MgSO_4$ and evaporated to give a colourless oil followed by column purification to give *O*-acetyl- β-citronellol in a 95% yield (1.3 g).

^{1}H NMR (300 MHz, CHLOROFORM-d) δ (ppm) 0.91 (d, *J* = 6.59 Hz, 3 H, C**H**$_3$), 1.11 - 1.25 (m, 1 H, C**H**), 1.30 - 1.58 (m, 4 H, C**H**$_2$), 1.59 - 1.64 (s, 3 H, C**H**$_3$), 1.64 - 1.69 (s, 3 H, C**H**$_3$), 1.92 - 2.03 (m, 2 H, C**H**$_2$), 2.03 - 2.06 (s, 3 H, C**H**$_3$), 3.99 - 4.15 (m, 2 H, C**H**$_2$OAc), 5.08 (tt, *J* = 7.09, 1.39 Hz, 1 H, C=C**H**).

^{13}C NMR (500 MHz, CHLOROFORM-d) δ (ppm) 17.6, 19.4, 21.0, 25.3, 25.7, 29.4, 35.3, 36.9, 63.0, 124.5, 131.3, 171.2. ^{1}H and ^{13}C NMR data matches that reported in the literature.[324]

Epoxidation method:

(*rac*)-β-Citronellol acetate epoxide- (27)

6,7-Epoxy-3,7-dimethyloctylacetate

O-acetyl- β-citronellol (495 mg, 2.5 mmol), $PW_4O_{24}[PTC]_3$ (51 mg, 2259 gmol^{-1}, 0.025 mmol, 1 mol%) and 30% aqueous hydrogen peroxide solution (0.25 mL, 2.5 mmol) were added to a radleys tube forming a biphasic mixture. The reaction was stirred at room temperature for 5 h. The reaction was judged to be complete by tlc. The solution was left to settle with no stirring allowing the biphasic system to separate out into its two layers. The top yellow organic layer was separated and purified *via* column chromatography to produce a clear oil 55% yield (294 mg).

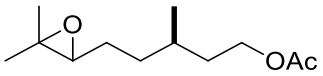

^{1}H NMR (500 MHz, CHLOROFORM-d) δ (ppm) 0.90 - 0.96 (m, 3 H, CC**H**$_3$), 1.25 - 1.32 (m, 6 H, CHC**H**$_3$), 1.39 - 1.62 (m, 5 H, C**H**/C**H**$_2$), 1.68 (dd, *J* = 13.21, 5.87 Hz, 1 H), 1.97 - 2.08 (m, 3 H, CC**H**$_3$), 2.65 - 2.74 (m, 1 H, C**H**(O)C), 4.02 - 4.17 (m, 2 H, C**H**$_2$OAc).

^{13}C NMR (500 MHz, CHLOROFORM-d) δ (ppm) 19.2 (CH_3), 19.3 (CH_3), 21.0 (CH_3), 24.9 (CH_2), 26.3 (CH_2), 29.7 (CH_2), 29.7 (CH_3), 35.4 (CH), 62.9 (CH(O)), 64.4 (C(O)), 64.5 (CH_2O), 171.4 (C(O)); ^{1}H and ^{13}C NMR data matches that reported in the literature.[324]

Deprotection method:

(*rac*)-5-(3,3-dimethyloxiran-2-yl)-3-methylpentan-1-ol- (25)

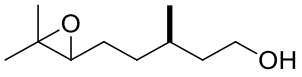

O-acetyl-β-citronellol epoxide (1 mmol, 214 mg) was dissolved in MeOH (5 mL) in a flask. The reaction mixture was stirred at room temperature and K_2CO_3 (360 mg, 5 mmol) was added and stirred for 12 hours at room temperature. The crude reaction mixture was filtered and evaporated to remove the MeOH and then diluted with DCM and washed with saturated NaCl. 3 x DCM washes were performed and the combined organic layers dried with magnesium sulfate and filtered. The residue obtained upon concentration *in vacuo* was purified by column chromatography to isolate a (*rac*)-β-Citronellol epoxide in 80% yield (137 mg). ^{1}H and ^{13}C NMR data matches that reported previously.

7.2.8 Procedure for the Epoxidation of terpenes containing disubstituted alkenes

Dihydrocarvone epoxide- (28)

2-methyl-5-(2-methyloxiran-2-yl)cyclohexanone

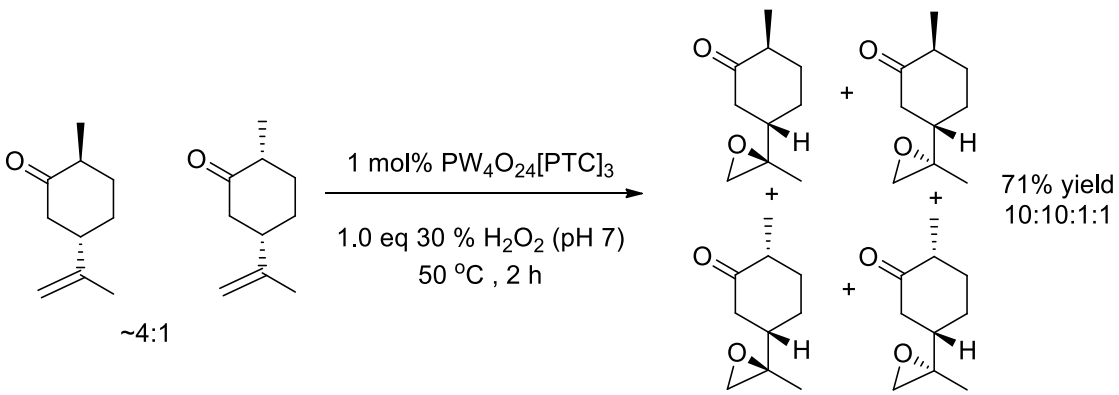

^{1}H NMR (500 MHz, CHLOROFORM-d) δ (ppm) 1.02 (dd, *J* = 6.85 Hz, 3 H, CHC**H**$_3$), 1.30 (d, *J* = 5.38 Hz, 3 H, CC**H**$_3$), 1.33 - 1.83 (m, 3 H, ring C**H**$_2$), 1.94 (dt, *J* = 12.47, 2.81 Hz, 1 H, ring C**H**), 2.08 - 2.23 (m, 2 H, ring C**H**$_2$), 2.34 (dd, *J* = 12.23, 6.36 Hz, 1 H, C**H**$_2$C(O)), 2.41 - 2.48 (m, 1 H, C**H**$_2$C(O)), 2.57 (dd, *J* = 10.27, 4.40 Hz, 1 H, C**H**$_2$C(O)), 2.66 (d, *J* = 4.89 Hz, 1 H, CC**H**$_2$).

^{13}C NMR (500 MHz, CHLOROFORM-d) δ (ppm) 14.2, 18.6, 27.2, 27.5, 30.8, 34.4, 45.2, 52.6, 53.3, 211.7. ^{1}H and ^{13}C NMR data matches that reported in the literature.[325]

(-)-Isopulegol epoxide- (29)

(1R,2R,5R)-5-methyl-2-((R)-2-methyloxiran-2-yl)cyclohexanol

(1R,2R,5R)-5-methyl-2-((S)-2-methyloxiran-2-yl)cyclohexanol

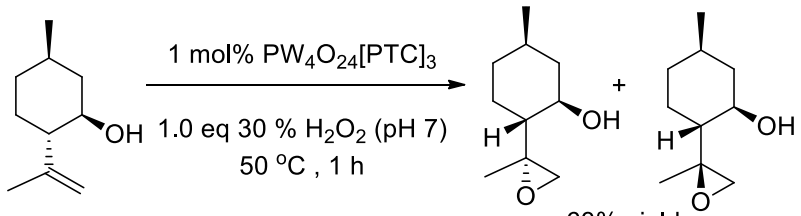

^{1}H NMR (500 MHz, CHLOROFORM-d) δ (ppm) 0.81 - 0.89 (m, 1 H), 0.90 - 0.92 (d, *J* =3.2 Hz, 3 H, CHC**H**$_3$), 0.93 - 1.08 (m, 2 H, ring C**H**$_2$), 1.21 (dd, *J* = 12.72, 3.42 Hz, 1 H, ring C**H**), 1.30 (s, 3 H, CC**H**$_3$), 1.38 - 1.49 (m, 1 H, ring C**H**), 1.62 - 1.73 (m, 2 H, ring C**H**$_2$), 1.96 - 2.05 (m, 1 H, ring C**H**), 2.52 (d, *J* = 4.89 Hz, 1 H, C(O)C**H**$_2$), 2.57 (d, *J* = 4.40 Hz, 1 H, C(O)C**H**$_2$), 3.69 (td, *J* = 10.52, 4.40 Hz, 1 H, C**H**(OH)).

^{13}C NMR (500 MHz, CHLOROFORM-d) δ (ppm) 16.9, 22.0, 27.6, 30.9, 33.9, 43.5, 51.1, 52.7, 59.1, 71.2^{1}H and ^{13}C NMR data matches that reported in the literature.[134]

Dihydromyrcenol epoxide- (30)

2-methyl-6-(oxiran-2-yl)heptan-2-ol

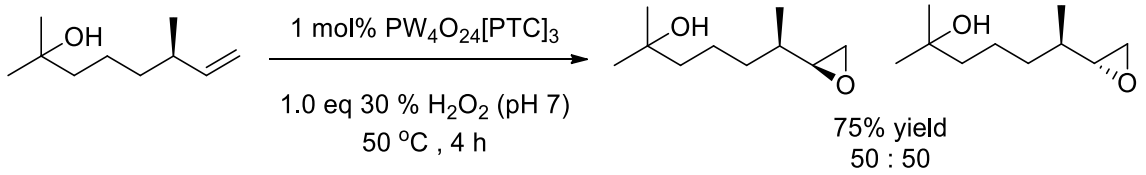

^{1}H NMR (300 MHz, CHLOROFORM-d) δ (ppm) 0.89 - 1.04 (m, 3 H, CHC**H**$_3$), 1.19 (s, 6 H, CC**H**$_3$), 1.23 - 1.61 (m, 8 H, alkyl C**H**$_2$), 2.42 - 2.56 (m, 1 H, CH$_2$(O)C**H**), 2.64 - 2.77 (m, 2 H, C**H**$_2$(O)CH).

^{13}C NMR (300 MHz, CHLOROFORM-d) δ (ppm) 15.7, 21.7, 29.0, 29.2, 35.0, 44.0, 46.9, 57.0, 57.0, 70.8. ^{1}H and ^{13}C NMR data matches that reported in the literature.[326]

7.2.9 Preparation of Mizuno catalyst

The Mizuno catalyst was prepared as shown in Figure 65.[141] A number of steps were required and was lengthier compared to the preparation of the Venturello catalyst however no anhydrous conditions, inert atmosphere or Schlenk techniques were necessary.

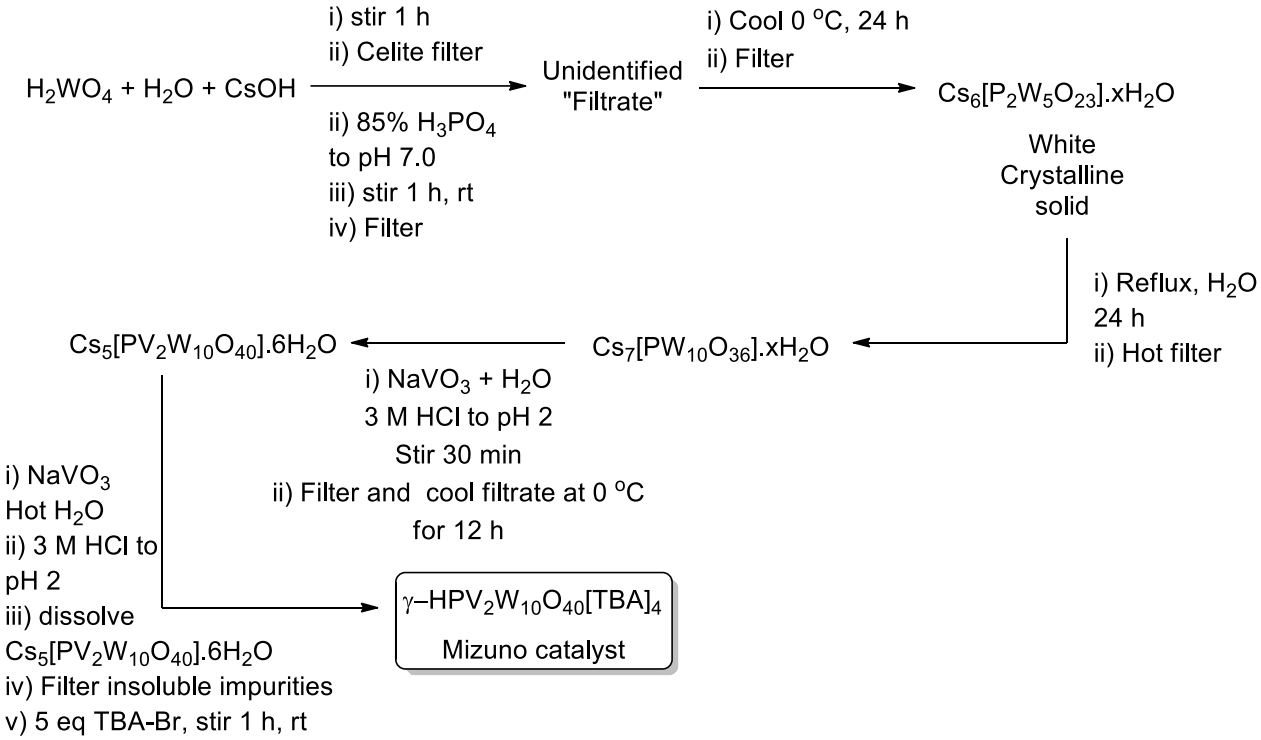

Figure 65. Preparation of Mizuno catalyst

11 mL of fresh (degrades easily) 50% aqueous cesium hydroxide solution was added to 6 g of tungstic acid in 40 mL of water until pH 13 is reached. This solution is stirred for 1 h at room temperature followed by filtration through celite to remove any remaining solid precipitate to give a clear colourless solution. 85% phosphoric acid is then added until the pH is lowered to pH 7, ca. 2.1 mL. The solution is stirred at room temperature for 1 h followed by gravity filtration to remove unwanted precipitates. The filtrate is then chilled at 0 °C for 24 hours within a refrigerator to give 9 g of white crystalline solid, $Cs_6[P_2W_5O_{23}].xH_2O$. This solid is filtered off and redissolved in 100 mL of water and refluxed for 24 h. The solution is filtered hot to give 1.8 g of insoluble solid precipitate, $Cs_7[PW_{10}O_{36}].xH_2O$.

0.1 g (0.82 mmol) of sodium metavanadate is dissolved in 4 ml of water and heated to 70 °C. The solution is cooled to 25 °C and 3 M HCl is added dropwise with vigorous stirring to reduce the pH to 2 followed by addition of 1.25 g of $Cs_7[PW_{10}O_{36}].xH_2O$ portionwise followed by stirring for 30 minutes. The solution is then filtered and the filtrate cooled at 0 °C for 12 hours. The precipitate is filtered to give 1 g of pale yellow $Cs_5[PV_2W_{10}O_{40}].6H_2O$ solid.

(0.015 g, 0.12 mmol) of sodium metavanadate is dissolved in 12ml of hot water (50-60 °C). Upon cooling, the pH of the solution was adjusted to 2.0 with 3 M HCl. Into the solution, $Cs_5[g\text{-}PV_2W_{10}O_{40}]\cdot 6H_2O$ (0.38 g, 0.11 mmol) was dissolved and the insoluble materials were

removed by filtration. Tetra-*n*-butylammonium bromide (0.18 g, 0.56 mmol) was added with vigorous stirring. The precipitate was collected by filtration, washed with water (40 mL), and dried *in vacuo*. The crude $[TBA]_4[g\text{-}HPV_2W_{10}O_{40}]$ (0.1 g) was dissolved in CH_3CN (10 mL) and the insoluble materials were removed by filtration. CH_3CN was removed by evaporation followed by addition of acetone (1 mL). The resulting yellow precipitate was collected by filtration to give $[TBA]_4[g\text{-}HPV_2W_{10}O_{40}]$ in a 70% yield (385 mg).[141]

7.2.10 Procedure for the 2-step, catalytic synthesis of limonene bis-epoxide

8,9-Limonene oxide- (31)

(R)-2-methyl-2-((R)-4-methylcyclohex-3-en-1-yl)oxirane

$[TBA]_4[g\text{-}HPV_2W_{10}O_{40}]$ (1 mol%, 70 mg), 70% $HClO_4$ (ca. 1 mol%, 1 drop), limonene (272 mg, 2 mmol) or carveol (304 mg, 2 mmol), and acetonitrile : ^{t}BuOH (3 mL : 3 mL) were successively placed into a round bottom flask. The reaction mixture was stirred at 25 ^{o}C, and 30% aqueous H_2O_2 (0.2 mL, 2 mmol) was added portionwise every 10 min over 50 minutes. After the addition was completed, the mixture was stirred at 25 ^{o}C for additional 20 min (total reaction time was 70 min). The product was purified by column chromatography giving a yield of 73% (221 mg).

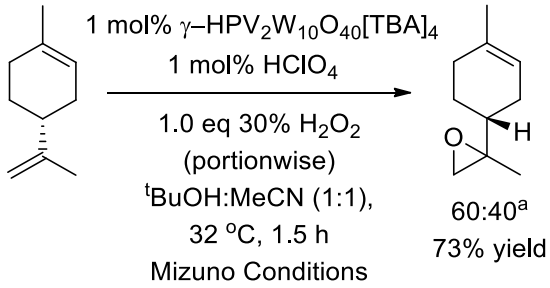

^{1}H NMR (300 MHz, CHLOROFORM-d) δ (ppm) 1.21 - 1.25 (m, 3H, C**H**$_3$), 1.34 - 1.41 (m, 2H, C**H**$_2$), 1.61 (s, 3H, C**H**$_3$), 1.70 - 2.03 (m, 5H, C**H**$_2$/C**H**), 2.48 - 2.55 (m, 1H, C(O)C**H**$_2$), 2.58 - 2.64 (m, 1H, C(O)C**H**$_2$), 5.33 (br. s., 1H, CC**H**); and

^{13}C NMR (300 MHz, CHLOROFORM-d) δ (ppm) 18.6 (CH_3), 23.3 (CH_3), 24.7 (CH_2), 27.3 (CH_2), 30.2 (CH_2), 40.1 (C), 53.3 (CH), 59.1 (C), 119.9 (CH), 134.0 (C); ^{1}H and ^{13}C NMR data matches that reported in the literature.[141]

8,9-Carveol epoxide- (32)

(5S)-2-methyl-5-((R)-2-methyloxiran-2-yl)cyclohex-2-enol

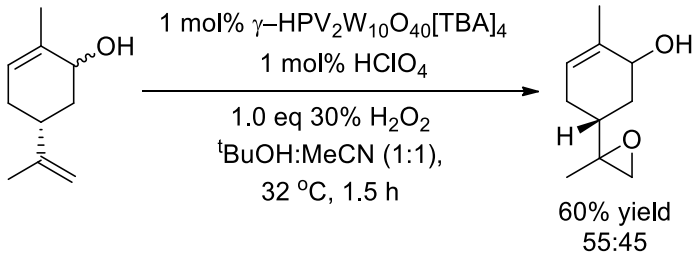

^{1}H NMR (300 MHz, CHLOROFORM-d) δ (ppm) 1.24 (s, 3H, C**H**$_3$), 1.71 (s, 3H, C**H**$_3$), 1.87 (m, 1H, C**H**), 2.19-2.27 (m, 4H, ring C**H**), 3.55-3.74 (m, 2H, C(O)C**H**$_2$), 4.05 (m, 1H, C(OH)**H**), 5.24 (s, 1H, CC**H**); and

^{13}C NMR (300 MHz, CHLOROFORM-d) δ (ppm) 21.4 (CH_3), 25.1 (CH_3), 29.4 (CH_2), 34.5 (CH_2), 40.5 (CH), 67.5 (CH), 67.6 (C), 84.7 (CH), 121.0 (CH), 139.6 (C). I.R (thin film) $_{v}$max (cm^{-1}): O-H (3407), C-H (2939), C=C (1667), C-O (1297). HRMS (ESI): m/z calculated. $C_{10}H_{16}O_2$: requires 169.122855 for $[M+H]^+$; found: 169.1233; requires 191.104799 for $[M+Na]^{+\cdot}$; found 191.1065.

<u>Limonene bis-epoxide- (4)</u>

(4R)-1-methyl-4-(2-methyloxiran-2-yl)-7-oxabicyclo[4.1.0]heptane

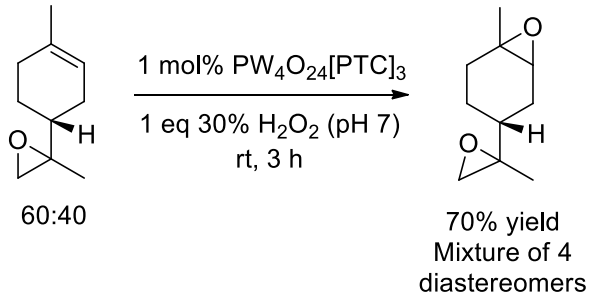

Yield = 70%; Mixture of four diastereomers – overlapping peaks.

^{1}H NMR (300 MHz, CHLOROFORM-d) δ (ppm) 1.22 (d, *J* = 3.39 Hz, 3 H, C**H**$_3$), 1.31 (s, 3 H, C**H**$_3$), 1.56 - 1.68 (m, 3 H, ring C**H**$_2$), 1.71 - 1.79 (m, 1 H, ring C**H**), 1.95 - 2.12 (m, 2 H, ring C**H**$_2$), 2.50 - 2.63 (m, 2 H, C**H**$_2$(O)C), 3.00 (t, *J* = 5.93 Hz, 1 H, C(O)C**H**).

^{13}C NMR (300 MHz, CHLOROFORM-d) δ (ppm) 17.5, 18.1, 21.3, 21.4, 23.0, 26.5, 26.6, 30.1, 30.2, 39.3, 40.0, 52.9, 53.4, 57.7, 57.8, 58.6, 58.7, 58.8. ^{1}H and ^{13}C NMR data matches that reported in the literature.[327]

7.2.11 Procedure for the 2-step synthesis of carvone bis-epoxide

1,2-Carvone epoxide- (35)

(1R,4R,6R)-1-methyl-4-(prop-1-en-2-yl)-7-oxabicyclo[4.1.0]heptan-2-one

Carvone (0.72 g, 4.8 mmol) was dissolved in 8 mL of methanol. The mixture was cooled to 0°C and 1.5 mL of 35% H_2O_2 was added. 1 mL of 6 M aq. NaOH solution was added over a period of 1-2 minutes. The mixture was stirred at 0 °C for 15 minutes and then at room temperature for 20 minutes. The mixture was dissolved in 10 mL of CH_2Cl_2 and washed twice with water (10 mL x 2) and saturated NaCl solution and then dried with $MgSO_4$. The mixture was dried, concentrated and purified using column chromotography.[36]

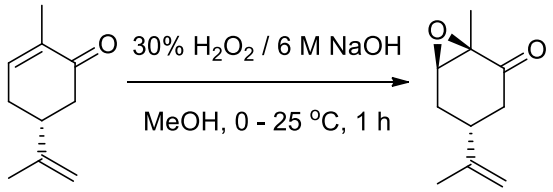

85% yield

^{1}H NMR (500 MHz, CHLOROFORM-d) δ (ppm) 1.38 (s, 3H, C**H**$_3$), 1.68 (s, 3H, C**H**$_3$), 1.88 (m, 1H, C**H**$_2$), 1.99 (m, 1H, C**H**$_2$), 2.33 (m, 1H, C**H**$_2$), 2.53 (m, 1H, C**H**$_2$), 2.56 (m, 1H, C**H**$_2$), 3.42 (s, 1H, C(O)**H**), 4.69 (s, 1H, CC**H**$_2$), 4.76 (s, 1H, CC**H**$_2$); and

^{13}C NMR (500 MHz, CHLOROFORM-d) δ (ppm) 15.2 (CH_3), 20.5 (CH_3), 28.6 (CH_2), 34.9 (CH_2), 41.7 (CH), 58.7 (CH), 61.2 (C), 110.4 (CH_2), 146.2 (C), 205.3 (C); ^{1}H and ^{13}C NMR data matches that reported in the literature.[328]

Carvone bis-epoxide- (34)

1-methyl-4-((S)-2-methyloxiran-2-yl)-7-oxabicyclo[4.1.0]heptan-2-one

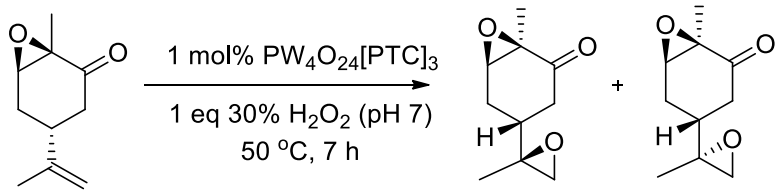

60% yield
55:45

^{1}H NMR (500 MHz, CHLOROFORM-d) δ (ppm) 1.28 (d, *J* = 12.72 Hz, 3 H, C**H**$_3$), 1.41 (s, 3 H, C(=O)CC**H**$_3$), 1.81 (dd, *J* = 14.43, 11.49 Hz, 1 H, ring C**H**), 1.91 - 2.00 (m, 1 H, ring C**H**), 2.13 - 2.20 (m, 1 H, ring C**H**), 2.31 - 2.42 (m, 1 H, C**H**$_2$(C=O), 2.50 - 2.60 (m, 2 H, C**H**$_2$(O)C/C**H**$_2$(C=O)), 2.66 (dd, *J* = 12.96, 4.65 Hz, 1 H, C**H**$_2$(O)C), 3.39 - 3.47 (m, 1 H, C**H**(O)C).

^{13}C NMR (500 MHz, CHLOROFORM-d) δ (ppm) 15.2, 19.0, 25.4, 33.6, 38.3, 52.2, 57.6, 59.0, 61.0, 204.7. ^{1}H and ^{13}C NMR data matches that reported in the literature.[329]

7.2.12 Procedure for the Large Scale Batch Solvent Free Epoxidation using modified Ishii-Venturello tungsten catalyst

Terpene substrate X (360 mmol), $PW_4O_{24}[PTC]_3$ (7.92 g, 2259 $gmol^{-1}$, 1 mol%) were added to a 1 L three necked round bottom flask with a stirrer bar. The catalyst and substrate were stirred for 10 minutes to fully dissolve the catalyst. A condenser was attached to the centre port, a thermometer was place in another to monitor the internal reaction temperature and a dropping funnel was attached to the third remaining port. The reaction vessel was cooled using a water bath and the temperature was never allowed to exceed 50 degrees Celcius. 30% aqueous hydrogen peroxide solution (37 mL, 360 mmol) (buffered to pH 7 with 0.5 M NaOH) was added dropwise in 5 mL portions forming a biphasic mixture. During hydrogen peroxide addition stirring was maintained at a slow rate and the temperature was continuously monitored. If the internal temperature exceeded 50 ^oC the dropwise addition was paused and restarted once the temperature had returned to 35 ^oC. The reaction was stirred at room temperature for 0.5 - 24 h. The reaction was judged to be complete following by tlc. The solution was left to settle with no stirring allowing the biphasic system to separate out into its two layers. The top yellow organic layer was separated and purified *via* distillation to produce a clear oil 86% yield (47 g). Epoxide products match previously discussed data.

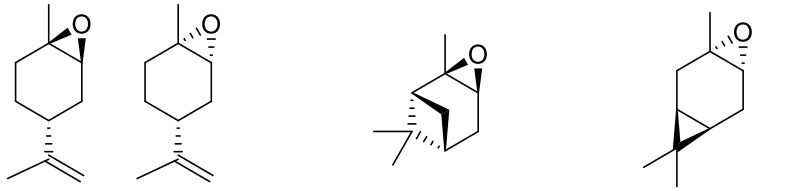

55 : 45

1 mol%, 2 h, rt

5 g: 90%, 15 g: 88%
50 g: 86%, 100 g: 85%

100 : 0

2 mol%, 5 h, rt
0.3 eq Na_2SO_4

15 g: 85%

100 : 0

1 mol%, 8 h, rt

15 g: 76%

7.2.13 Procedure for the Use of the Ishii-Venturello catalyst for epoxidation of β-pinene

β-pinene (0.68 g, 5 mmol, 1 eq), $PW_4O_{24}[PTC]_3$ (0.33 g, 2259 $gmol^{-1}$, 0.03 mmol, 3 mol%) were added to a 20 mL glass carousel tube with a stirrer bar submerged within a water bath. The catalyst and substrate were stirred for 10 minutes to fully dissolve the catalyst and then Na_2SO_4 (213 mg, 0.6 mmol) was dissolved in 30% aqueous hydrogen peroxide solution (0.5 mL, 5 mmol, 1 eq) and buffered to pH 7 with 0.5M NaOH. This aqueous solution was added dropwise over a 10 minute period forming a biphasic mixture accompanied by gentle stirring to prevent exothermic runaway. The reaction was stirred slowly at room temperature for 7 h. The reaction was judged to be complete following by tlc showing minimal starting material remaining alongside a moderate amount of polar by-products present lower on the tlc relative to the epoxide product spot. The solution was left to settle with no stirring allowing the biphasic system to separate out into its two layers. The top organic layer was then decanted off and purified *via* column chromatography to produce the desired β-pinene epoxide as a clear oil in 47% isolated yield.

β-pinene epoxide- (33)

2,10-epoxypinane

(1R,2S,5S)-6,6-dimethylspiro[bicyclo[3.1.1]heptane-2,2'-oxirane]

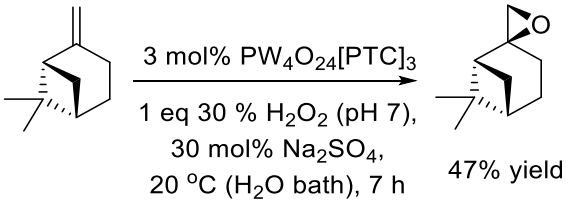

^{1}H NMR (300 MHz, CHLOROFORM-d) δ (ppm) 0.91 (s, 3 H, C**H**$_3$), 1.24 (s, 3 H, C**H**$_3$), 1.50 (t, *J* = 5.37 Hz, 1 H, ring C**H**), 1.65 (d, *J* = 10.17 Hz, 2 H, ring C**H**$_2$), 1.82 - 1.87 (m, 1 H, ring C**H**), 1.98 (d, *J* = 5.09 Hz, 1 H, ring C**H**), 2.25 (m, 3 H, ring C**H**$_2$), 2.61 (d, *J* = 4.71 Hz, 1 H, C**H**$_2$(O)C), 2.77 (d, *J* = 4.90 Hz, 1 H, C**H**$_2$(O)C).

^{13}C NMR (300 MHz, CHLOROFORM-d) δ (ppm) 21.1, 22.2, 23.5, 25.1, 26.0, 40.0, 40.7, 48.8, 56.5, 61.6. ^{1}H and ^{13}C NMR data matches that reported in the literature.[152]

7.2.14 Procedure for the Batch solvent free Ishii-Venturello epoxidation of Crude Sulphate Turpentine (CST)

CST (0.68 g, 5 mmol, 1 eq), $PW_4O_{24}[PTC]_3$ (0.11 g, 2259 gmol^{-1}, 0.05 mmol, 1 mol%) were added to a 20 mL glass carousel tube with a stirrer bar. The catalyst and substrate were stirred for 10 minutes to fully dissolve the catalyst and then 30% aqueous hydrogen peroxide solution (0.5 mL, 5 mmol, 1 eq) (buffered to pH 7 with 0.5 M NaOH) (inclusion of 0.3 eq Na_2SO_4 was varied and if included, was dissolved within the hydrogen peroxide before addition to the organic phase) was added slowly forming a biphasic mixture. During hydrogen peroxide addition if substrates were particularly exothermic the tube was cooled with a water bath and stirring was maintained at the lowest possible rpm. The reaction was stirred at room temperature for 0.5 - 24 h. The reaction was judged to be complete following by tlc. The solution was left to settle with no stirring allowing the biphasic system to separate out into its two layers. The top yellow organic layer was separated and purified *via* column chromatography to produce a clear oil (94% yield).

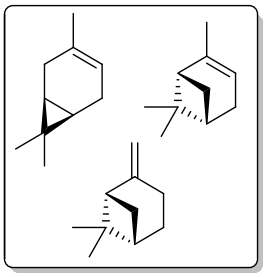

CST

2 mol% $PW_4O_{24}[PTC]_3$
2.0 eq 30 % H_2O_2 (pH 7)
Solvent free, rt, 2.5 h
No Na_2SO_4

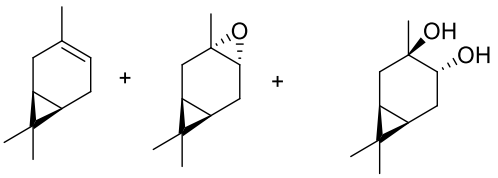

8 : 92 : 0
92% conversion

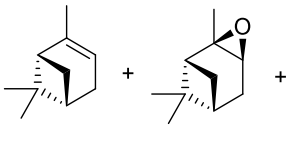

Pinane Diols + complex mixture of oxygenated terpenes

10 : 0 : 90
90% conversion

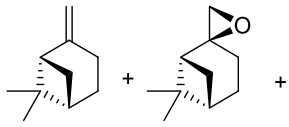

Pinane Diols + complex mixture of oxygenated terpenes

9 : 0 : 91
91% conversion

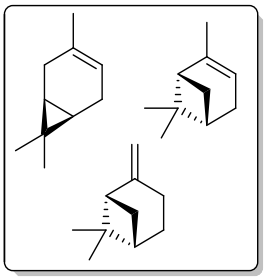

CST

2 mol% $PW_4O_{24}[PTC]_3$
2.0 eq 30 % H_2O_2 (pH 7)
Solvent free, rt, 4 h
0.3 eq Na_2SO_4

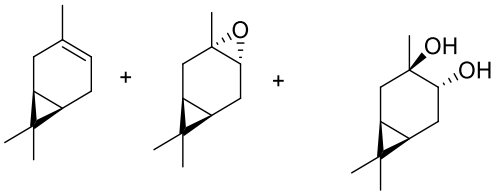

6 : 94 : 0
94% conversion

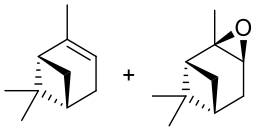

Pinane Diols + complex mixture of oxygenated terpenes

10 : 0 : 90
75% conversion

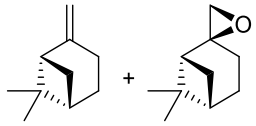

Pinane Diols + complex mixture of oxygenated terpenes

0 : 0 : 100
100% conversion

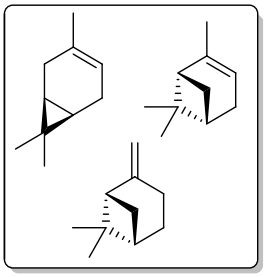

CST

1 mol% $PW_4O_{24}[PTC]_3$
1.0 eq 30 % H_2O_2 (pH 7)
Solvent free, rt, 7 h
0.3 eq Na_2SO_4

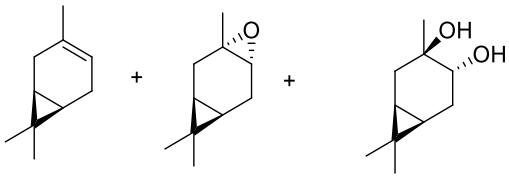

9 : 91 : 0
91% conversion

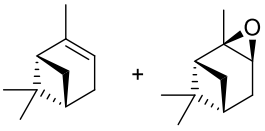

Pinane Diols + complex mixture of oxygenated terpenes

24 : 68 : 8
75% conversion

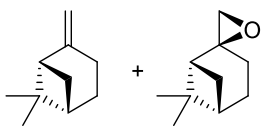

Pinane Diols + complex mixture of oxygenated terpenes

0 : 0 : 100
100% conversion

7.3 Procedure for Catalytic Solvent-free Flow Epoxidation Reactions of Terpene Substrates

Three initial flow epoxidation experiments were performed using limonene as a model terpene substrate to compare different flow reactor setups. The first setup involved using a coil of PTFE tubing (1/16" tube) and a Y-junction submerged in a heated water bath similar to the system used by Lapkin et al[172] to epoxidise cocoa butter in flow. The second setup involved a LTF glass millireactor with smooth channels; and the third setup was a LTF glass millireactor containing static mixer channels. A preformed catalyst loading of 2 mol% and a temperature of 50 ^{o}C was used in all reactor setups trialled. The first and second reactor designs gave 30% conversion to limonene epoxide after 5 minutes, however, the static mixer glass LTF millireactor gave significantly higher 65% conversion under these conditions, and so it was chosen for further flow epoxidation optimisation experiments.

1 mol% of preformed Ishii-Venturello catalyst was tested at a range of longer residence times in a static mixer glass LTF millireactor, using 1.6 equivalents of H_2O_2 at a constant temperature of 50 ^{o}C. Two glass milli-reactors fitted with static mixers with a volume of 4.5 mL were linked together to provide a combined reactor with a total reaction volume of 9 mL that enabled lower flow rates and longer residence times to be screened.

The Venturello catalyst (1.36 g, 1 mol%) was then dissolved in the limonene substrate (20 mL, 126 mmol) and the resultant solution loaded into a glass syringe. 30% hydrogen peroxide (11.7 mL) (buffered to pH 7.0 using 0.1M $NaOH_{(aq)}$) was then loaded into the second glass syringe. These syringes were then loaded onto their respective syringe pumps that could be programmed to pump solutions at different flow rates to achieve the desired reactor residence time and stoichiometries.

After flow reaction was commenced, the flow system was allowed to stabilise, before the composition of the flow solution was sampled at the outlet ports and immediately quenched by sampling the organic layer (and ending the reaction by preventing access to the aqueous hydrogen peroxide) and diluting with toluene or $CDCl_3$, followed by analysis using GCMS and NMR. The flow reactor setup that was employed in these flow reactions is shown below in Figure 66.

Sampling was performed by collecting reaction mixture from the appropriate exit port and stored in a vial, the organic layer settled within seconds and an aliquot transferred to a GCMS vial/NMR tube and quenched with the appropriate solvent, preventing further reaction of the organic substrate due to its lack of contact with the aqueous hydrogen peroxide oxidant. This simple two-feed flow set-up enabled flow rates and residency times to be adjusted to maximise conversion of limonene into its corresponding mixture of epoxides. The reaction product effluent was collected into a glass beaker, with its biphasic nature affording two layers - with the epoxide product present in the top organic layer. This enabled the limonene epoxide to be easily separated from the aqueous layer, without any solvent extraction procedures being required, with direct distillation *in vacuo* allowing for recovery of 'catalyst free' limonene epoxide in 70-75% isolated yield.

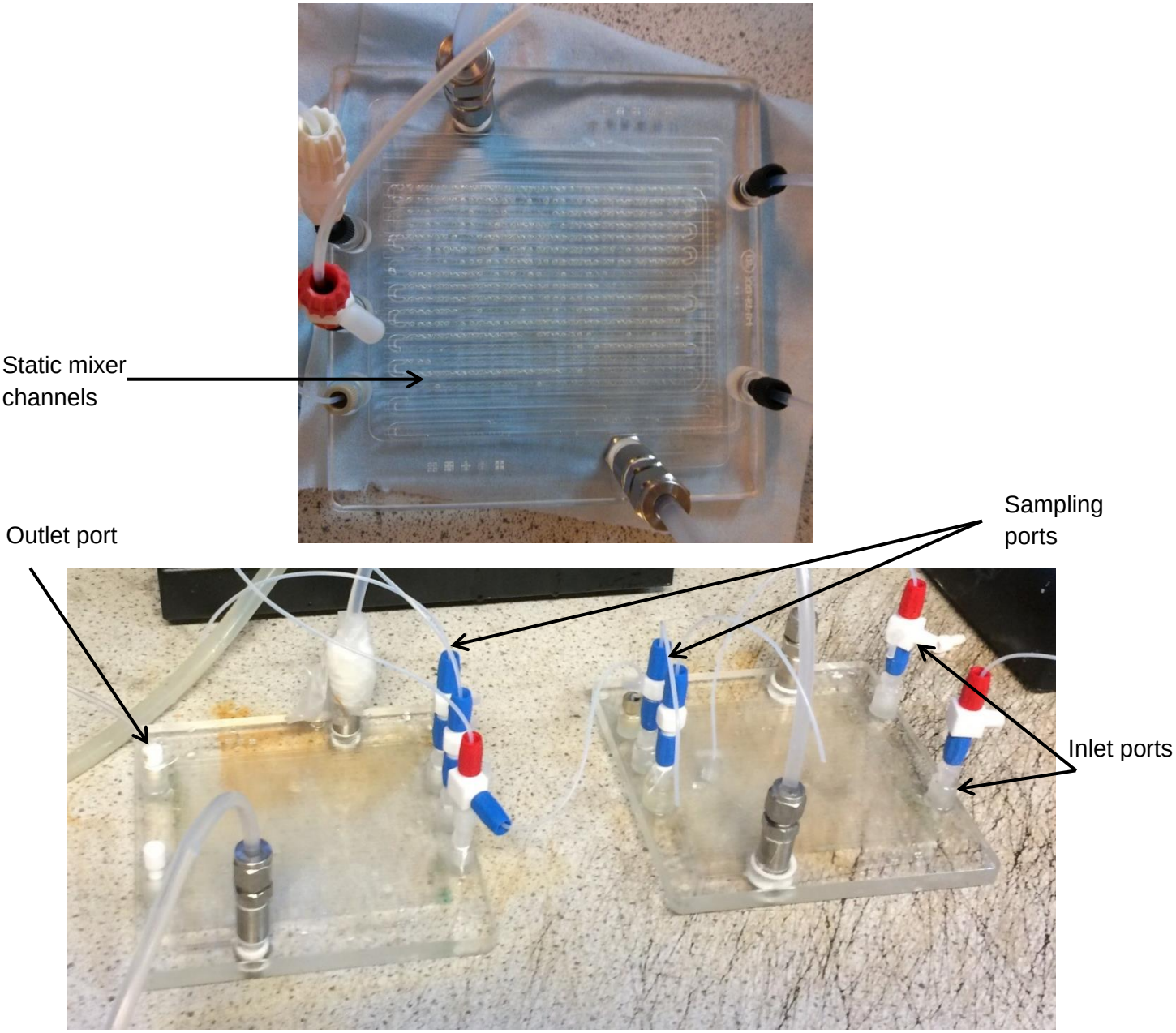

Figure 66. Photographs of flow reactor and LTF static mixer setup used for terpene epoxidation reactions

7.4 Procedure for *Anti*-dihydroxylation of Terpene Substrates

The appropriate terpene substrate (X g, 5 mmol, 1 eq), $PW_4O_{24}[PTC]_3$ (0.11 g, 2259 $gmol^{-1}$, 0.05 mmol, 1 mol%), unbuffered 30% aqueous H_2O_2 (0.51 mL, 5 mmol, 1 eq) and EtOAc (10 mmol, 1 mL) were added to a carousel tube forming a biphasic mixture. The reaction was stirred whilst heated for 1 h at 20 °C or 50 °C. The epoxidation reaction was judged to be complete by tlc after the appropriate number of hours shown within the corresponding schemes. Amberlyst-15 (0.13 mol%, 140 mg, 4.6 mmol/g) was then added and the reaction mixture was again stirred for 8-10 h at room temperature to ring open the epoxides to the anti-diol products, tlc was used to judge reaction progress. The solution was left to settle with no stirring allowing the biphasic system to separate out into two layers. 10 mL of EtOAc was added and the reaction mixture extracted with approximately 20 mL. The organic layer was dried with $MgSO_4$ and filtered to remove the Amberlyst-15 and drying agent. The solvent was then removed *in vacuo* to give the oil/solid diol products. The crude products were purified *via* column chromatography to produce a clean diols (XX% yield). The NMR spectra were compared with literature data where possible.

Limonene 1,2-*anti*- diol- (3)

(1S,2S,4R)-1-methyl-4-(prop-1-en-2-yl)cyclohexane-1,2-diol

(1R,2R,4R)-1-methyl-4-(prop-1-en-2-yl)cyclohexane-1,2-diol

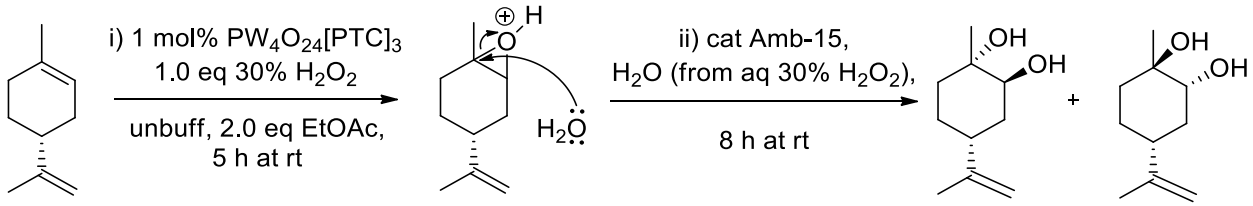

76% yield
55 : 45

^{1}H NMR (300 MHz, CHLOROFORM-d) δ (ppm) 1.26 (s, 3 H, CC**H**$_3$), 1.46 - 1.68 (m, 4 H,ring C**H**$_2$), 1.72 (s, 3 H, CC**H**$_3$), 1.92 (ddd, *J* = 13.94, 11.40, 2.92 Hz, 2 H, ring C**H**$_2$), 2.20 - 2.33 (m, 1 H, ring C**HC=**), 3.63 (t, *J* = 3.49 Hz, 1 H, C**H**OH), 4.64 - 4.77 (s, 2 H, C=C**H**$_2$).

^{13}C NMR (300 MHz, CHLOROFORM-d) δ (ppm) 21.1, 26.1, 26.5, 33.6, 33.9, 37.4, 71.4, 73.8, 109.0, 149.2. ^{1}H and ^{13}C NMR data matches that reported in the literature.[330]

Carene3,4--*anti*-diol- (36)

(1S,3R,4R,6R)-3,7,7-trimethylbicyclo[4.1.0]heptane-3,4-diol

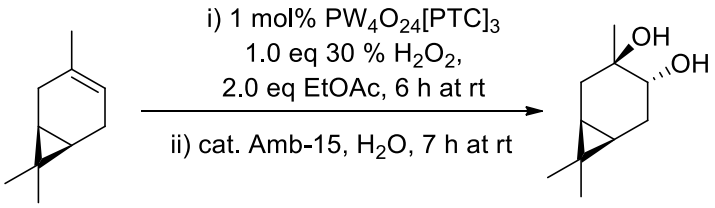

73% yield

^{1}H NMR (500 MHz, CHLOROFORM-d) δ (ppm) 0.61 - 0.75 (m, 2 H, ring C**H**$_2$), 0.95 (s, 3 H, CC**H**$_3$), 0.97 (s, 3 H, CC**H**$_3$), 1.18 (s, 3 H, C**H**$_3$C(OH)), 1.24 (m, 1 H, ring C**H**$_2$), 1.63 (m, 1 H, ring C**H**$_2$), 1.94 (m, 1 H, ring C**H**$_2$), 2.06 (dd, *J* = 14.51, 7.35 Hz, 1 H, ring C**H**$_2$), 2.72 – 3.14 (br s,. 2 H, O**H**), 3.32 (dd, *J* = 10.27, 7.44 Hz, 1 H, C**H**OH).

^{13}C NMR (500 MHz, CHLOROFORM-d) δ (ppm) 15.7, 17.6, 18.9, 19.9, 20.9, 27.8, 28.6, 33.6, 73.3, 74.3. ^{1}H and ^{13}C NMR data matches that reported in the literature.[331]

γ-terpinene-*anti*-tetrol – (37)

(1R,2S,4S,5S)-1-isopropyl-4-methylcyclohexane-1,2,4,5-tetraol

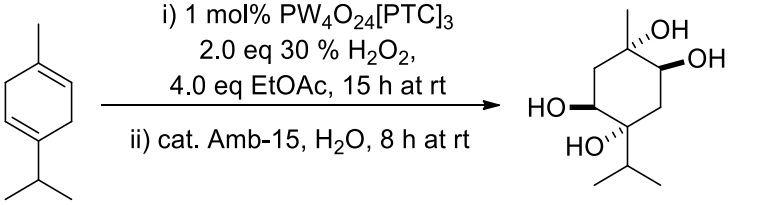

(rac)
mixture of diastereomers
62% yield

^{1}H NMR (500 MHz, DMSO-d$_6$) δ (ppm) 0.80 (d, *J* = 6.85 Hz, 3 H, C**H**$_3$CH), 0.85 (d, *J* = 6.85 Hz, 3 H, C**H**$_3$CH), 1.10 (s, 3 H, C**H**$_3$C(OH)), 1.42 - 1.50 (m, 1 H, ring C**H**), 1.67 (m, 1 H, ring C**H**$_2$), 1.79 - 1.88 (m, 2 H, ring C**H**$_2$), 2.00 (dd, *J* = 14.18, 2.93 Hz, 1 H, CH$_3$C**H**CH$_3$), 3.42 - 3.50 (m, 1 H, C**H**OH), 3.63 - 3.70 (m, 1 H, C**H**OH), 4.57 (s, 1 H, O**H**), 5.03 (d, *J* = 7.34 Hz, 1 H, O**H**), 5.12 (s, 1 H, O**H**), 5.38 (d, *J* = 6.36 Hz, 1 H, O**H**).

^{13}C NMR (500 MHz, DMSO-d$_6$) δ (ppm) 15.6, 16.2, 26.8, 31.1, 31.9, 34.2, 39.0, 39.2, 39.3, 39.6, 39.7, 39.8, 39.8, 39.9, 40.0, 70.4, 71.9, 73.7, 74.2. ^{1}H and ^{13}C NMR data matches that reported in the literature.[208]

Perillyl alcohol-1,2-*anti*-diol- (38)

(1R,2S,4R)-1-(hydroxymethyl)-4-(prop-1-en-2-yl)cyclohexane-1,2-diol

(1S,2R,4R)-1-(hydroxymethyl)-4-(prop-1-en-2-yl)cyclohexane-1,2-diol

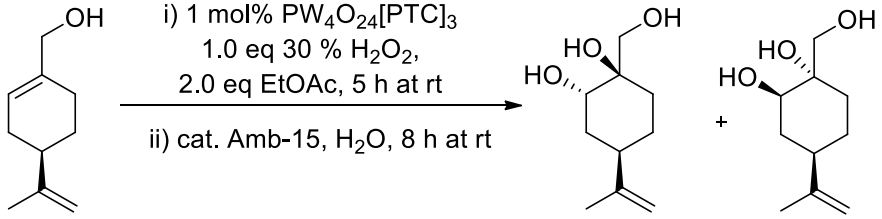

56% yield
58:42

^{1}H NMR (300 MHz, DMSO-d_6) δ (ppm) 1.09 - 1.39 (m, 2 H, ring C**H**$_2$), 1.39 - 1.54 (m, 3 H, ring C**H**$_2$), 1.64 (s, 3 H, CC**H**$_3$), 1.73 (m, 1 H, ring C**H**$_2$), 2.15 - 2.30 (m, 1 H, ring C**H**), 3.20 (d, *J* = 10.74 Hz, 1 H, C**H**$_2$OH), 3.38 (d, *J* = 10.74 Hz, 1 H, C**H**$_2$OH), 3.56 (br. s., 1 H, C**H**OH), 4.00 (br. s., 1 H, O**H**), 4.50 (br. s., 2 H, O**H**), 4.59 - 4.67 (s, 2 H, C=C**H**$_2$).

^{13}C NMR (300 MHz, DMSO-d_6) δ (ppm) 20.9, 25.5, 28.4, 33.8, 37.6 , 67.7, 68.8, 71.3, 108.3, 150.4. ^{1}H and ^{13}C NMR data matches that reported in the literature[332].

α-terpineol 1,2-*anti*-diol- (39)

(1R,2R,4R)-4-(2-hydroxypropan-2-yl)-1-methylcyclohexane-1,2-diol

(1S,2S,4R)-4-(2-hydroxypropan-2-yl)-1-methylcyclohexane-1,2-diol

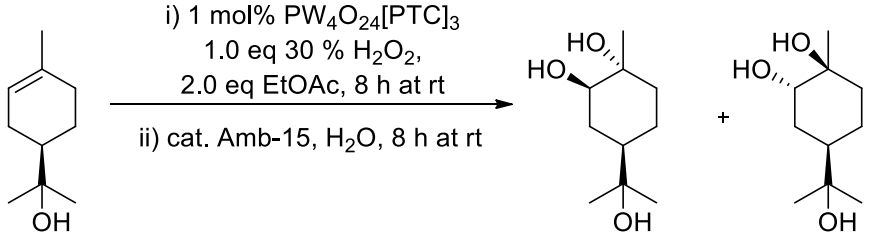

41% yield
56:44

^{1}H NMR (500 MHz, CHLOROFORM-d) δ (ppm) 1.20 (d, *J* = 9.29 Hz, 6 H, C(OH)C**H**$_3$), 1.28 (s, 3 H, C(OH)C**H**$_3$), 1.41 (br. s., 2 H, ring C**H**$_2$), 1.54 (m, 1 H, ring C**H**$_2$), 1.69 (m, 1 H, ring C**H**$_2$), 1.78 (m, 3 H, ring C**H**$_2$), 3.66 (s, 1 H, C(OH)**H**), 3.78 (br. s., 1 H, O**H**), 3.89 (br. s., 1 H, O**H**).

^{13}C NMR (500 MHz, CHLOROFORM-d) δ (ppm) 22.0, 26.8, 27.5, 27.5, 30.0, 33.5, 41.0, 70.8, 72.6, 74.0. ^{1}H and ^{13}C NMR data matches that reported in the literature.[213]

4-carvomenthenol-*anti*-diol- (40)

(1S,2S,4S)-4-isopropyl-1-methylcyclohexane-1,2,4-triol

(1R,2R,4S)-4-isopropyl-1-methylcyclohexane-1,2,4-triol

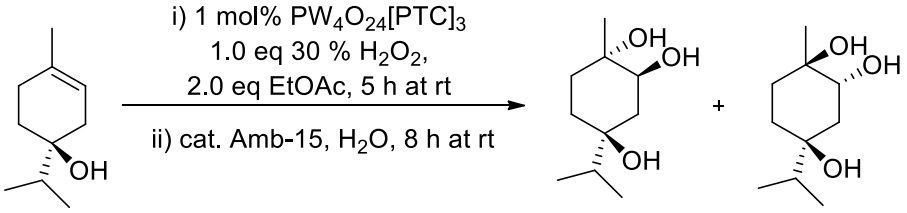

77% yield
90:10

^{1}H NMR (300 MHz, CHLOROFORM-d) δ (ppm) 0.94 (dd, *J* = 6.85, 0.98 Hz, 6 H, CHC**H**$_3$), 1.34 (s, 3 H, C(OH)C**H**$_3$), 1.39 - 1.53 (m, 2 H, ring C**H**$_2$), 1.58 - 1.62 (m, 1 H, CH_3(C**H**)CH_3), 1.79 - 1.83 (d, *J* = 3.91 Hz, 2 H, ring C**H**$_2$), 1.92 - 1.97 (m, 1 H, ring C**H**), 2.03 (s, 1 H, ring C**H**), 3.51 - 3.56 (m, 1 H, C**H**OH).

^{13}C NMR (300 MHz, CHLOROFORM-d) δ (ppm) 16.6, 16.7, 27.7, 29.2, 29.6, 33.8, 38.5, 71.6, 74.8, 75.3. ^{1}H and ^{13}C NMR data matches that reported in the literature.[317]

α-Ionone-*anti*-diol- (41)

(E)-4-((1R,2R,3R)-2,3-dihydroxy-2,6,6-trimethylcyclohexyl)but-3-en-2-one

(E)-4-((1S,2S,3S)-2,3-dihydroxy-2,6,6-trimethylcyclohexyl)but-3-en-2-one

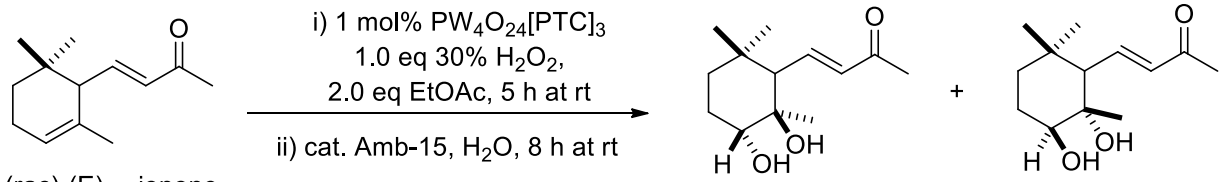

(rac)-(E)-α-ionone

70% yield[a]
cis:trans
80:20[b]

^{1}H NMR (500 MHz, CHLOROFORM-d) δ (ppm) 0.83 (s, 3 H, CC**H**$_3$), 1.06 (s, 3 H, CC**H**$_3$), 1.16 (s, 3 H, C(OH)C**H**$_3$), 1.25 (d, *J* = 15.65 Hz, 1 H, ring C**H**$_2$), 1.58 (s, 1 H, ring C**H**$_2$), 1.66 (m, 1 H, ring C**H**$_2$), 2.10 (s, 1 H, ring C**H**$_2$), 2.21 (s, 1 H, ring C**H**), 2.30 (s, 3 H, C(=O)C**H**$_3$), 3.58 (s, 1 H, C**H**OH), 6.09 (d, *J* = 16.14 Hz, 1 H, C=C**H**), 6.96 (d, *J* = 10.76 Hz, 1 H, C=C**H**).

^{13}C NMR (500 MHz, CHLOROFORM-d) δ (ppm) 22.2, 25.2, 27.0, 28.0, 32.2, 33.6, 33.9, 53.2, 73.4, 74.4, 134.8, 146.6, 198.6. ^{1}H and ^{13}C NMR data matches that reported in the literature.[139]

β-ionone-*anti*-diol- (42)

(E)-4-((1S,2R)-1,2-dihydroxy-2,6,6-trimethylcyclohexyl)but-3-en-2-one

(E)-4-((1R,2S)-1,2-dihydroxy-2,6,6-trimethylcyclohexyl)but-3-en-2-one

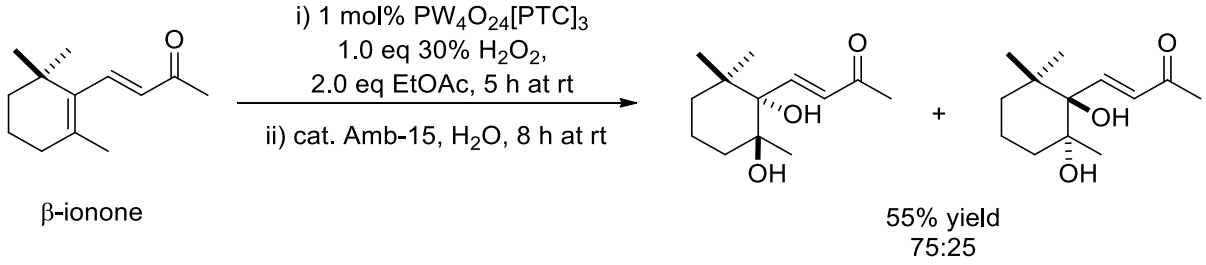

^{1}H NMR (500 MHz, CHLOROFORM-d) δ (ppm) 0.73 (s, 3 H, CC**H**$_3$), 1.03 (s, 3 H, CC**H**$_3$), 1.13 (s, 3 H, C**H**$_3$C(OH)), 1.40 (s, 3 H, ring C**H**$_2$), 1.49 (m, 3 H, ring CH$_2$), 1.73 (m, 2 H, ring C**H**$_2$), 2.21 (s, 3 H, C(=O)C**H**$_3$), 6.24 (d, *J* = 16.14 Hz, 1 H, C**H**=CH), 7.22 (d, *J* = 16.63 Hz, 1 H, CH=C**H**).

^{13}C NMR (500 MHz, CHLOROFORM-d) δ (ppm) 17.4, 24.7, 26.2, 27.1, 27.3, 36.0, 38.2, 53.2, 74.6, 79.2, 130.5, 149.0, 198.0. ^{1}H and ^{13}C NMR data matches that reported in the literature.[216]

(-)-Isopulegol-8,9-*anti*-diol- (43)

(S)-2-((1R,2R,4R)-2-hydroxy-4-methylcyclohexyl)propane-1,2-diol

(R)-2-((1R,2R,4R)-2-hydroxy-4-methylcyclohexyl)propane-1,2-diol

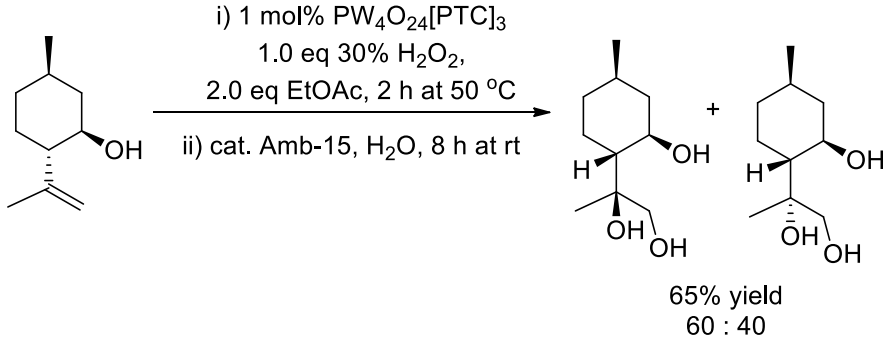

^{1}H NMR (500 MHz, CHLOROFORM-d) δ (ppm) 0.91 (m, 1 H, ring C**H**), 0.91 - 0.93 (m, 3 H, C(OH)C**H**$_3$), 0.95 - 1.03 (m, 1 H, ring C**H**), 1.03 - 1.12 (m, 1 H, ring C**H**), 1.15 (s, 3 H, C**H**$_3$), 1.40 - 1.48 (m, 1 H, ring C**H**), 1.57 - 1.81 (m, 3 H, ring C**H**$_2$), 1.92 - 2.00 (m, 1 H, C(OH)C**H**CH(OH)), 3.32 (br. s., 3 H, O**H**), 3.38 (s, 1 H, C**H**$_2$OH), 3.53 (d, *J* = 10.76 Hz, 1 H, C**H**$_2$OH), 3.79 (td, *J* = 10.52, 4.40 Hz, 1 H, C**H**OH).

^{13}C NMR (500 MHz, CHLOROFORM-d) δ (ppm) 19.6, 22.2, 26.5, 31.5, 34.4, 45.0, 48.0, 68.9, 72.5, 72.9. ^{1}H and ^{13}C NMR data matches that reported in the literature.[218]

Dihydrocarvone-8,9-*anti*-diol- (44)

5-(1,2-dihydroxypropan-2-yl)-2-methylcyclohexanone

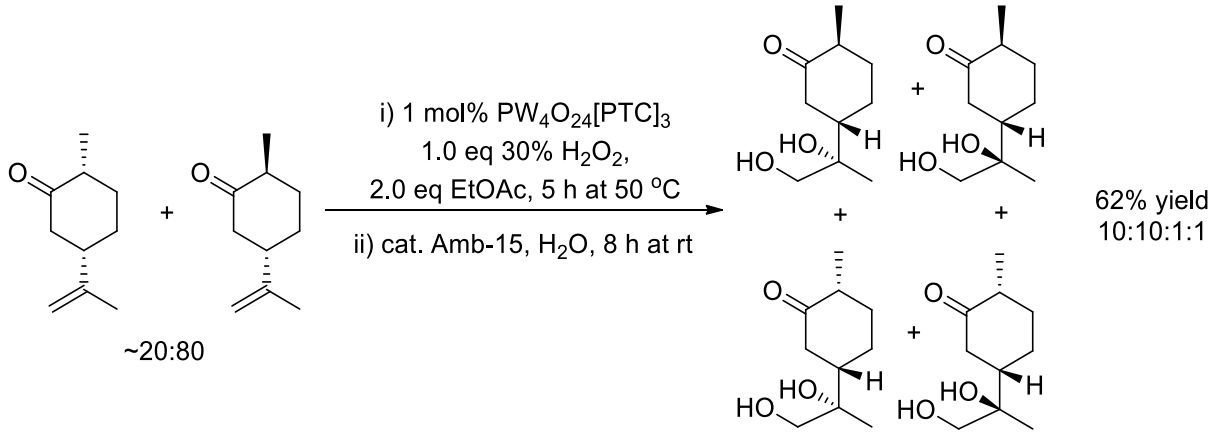

^{1}H NMR (300 MHz, CHLOROFORM-d) δ (ppm) 0.94 (dd, *J* = 6.40, 1.51 Hz, 3 H, CHC**H**$_3$), 1.01 - 1.09 (s, 3 H, C(OH)C**H**$_3$), 1.15 - 1.32 (m, 1 H, ring C**H**), 1.39 – 1.57 (m, 1 H, ring C**H**), 1.72 - 1.99 (m, 2 H, ring C**H**$_2$), 2.00 - 2.23 (m, 2 H, ring C**H**$_2$), 2.23 - 2.41 (m, 2 H, ring C**H**$_2$C=O), 3.34 (dd, *J* = 13.09, 11.21 Hz, 1 H, C(OH)C**H**$_2$OH), 3.43 - 3.53 (m, 1 H, C(OH)C**H**$_2$OH), 3.56 - 3.70 (br s., 2 H, O**H**).

^{13}C NMR (300 MHz, CHLOROFORM-d) δ (ppm) 14.1, 19.7, 25.5, 34.6, 43.3, 44.7, 46.2, 67.7, 73.8, 213.8. ^{1}H and ^{13}C NMR data matches that reported in the literature.[211]

<u>Myrcene-6,7-*anti*-diol- (45)</u>

(R)-2-methyl-6-methyleneoct-7-ene-2,3-diol

(S)-2-methyl-6-methyleneoct-7-ene-2,3-diol

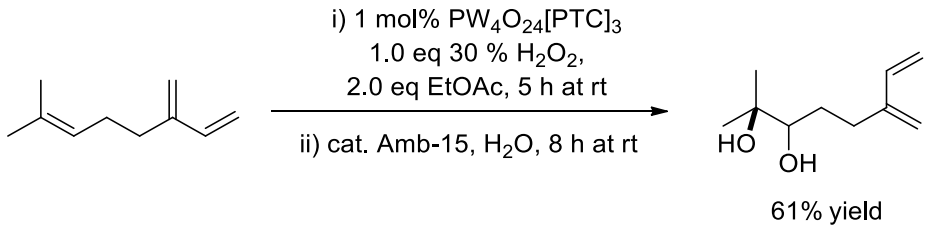

^{1}H NMR (500 MHz, CHLOROFORM-d) δ (ppm) 1.14 (s, 3 H, C**H**$_3$C(OH)), 1.18 (s, 3 H, C**H**$_3$C(OH)), 1.45 - 1.57 (m, 2 H, C**H**$_2$), 1.59 - 1.70 (m, 2 H, C**H**$_2$), 2.27 (d, *J* = 2.45 Hz, 1 H, C**H**$_2$CH(OH)), 2.53 (s, 1 H, C**H**$_2$CH(OH)), 3.38 (d, *J* = 11.74 Hz, 1 H, C**H**(OH)), 4.98 - 5.09 (m, 3 H, C**H**$_2$=C), 5.26 (d, *J* = 17.61 Hz, 1 H, C**H**$_2$=C), 6.32 - 6.40 (m, 1 H, CH$_2$=C**H**C).

^{13}C NMR (500 MHz, CHLOROFORM-d) δ (ppm) 23.1, 26.4, 28.4, 30.1, 73.7, 78.1, 113.5, 115.9, 138.6, 146.1. ^{1}H and ^{13}C NMR data matches that reported in the literature.[333]

7.4.1 Procedure for a*nti*-diol synthesis from non-renewable alkenes with Ishii-Venturello catalyst

The appropriate alkene substrate (X g, 5 mmol, 1 eq), $PW_4O_{24}[PTC]_3$ (0.11 g, 2259 $gmol^{-1}$, 0.05 mmol, 1 mol%) and unbuffered 30% aqueous H_2O_2 (0.51 mL, 5 mmol, 1 eq) were added to a carousel tube forming a biphasic mixture (organic solvent free). The reaction was stirred whilst heated for 1-3 h at 20 ^oC or 50 ^oC. The epoxidation-hydration reaction was judged to be complete by TLC. The solution was left to settle with no stirring allowing the biphasic system to separate out into its two layers. 20 mL of EtOAc was added and the reaction mixture extracted. The organic layer was dried with $MgSO_4$ and filtered to remove the drying agent. The solvent was then removed *in vacuo* to give the oil/solid diol products. The crude products were purified *via* column chromatography to produce a clean diols (XX% yield). The NMR spectra were compared with literature data where possible.

Phenylethane-1,2-*anti*-diol- (46)

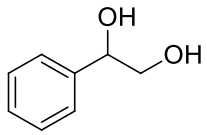

Yield = 82%; 50:50

^1H NMR (500 MHz, CHLOROFORM-d) δ (ppm) 3.68 - 3.81 (m, 2H, C**H**$_2$OH). 4.82 - 4.77 (m, 1H, C**H**OH), 7.27 - 7.35 (m, 5H, ring C**H**).

^{13}C NMR (500 MHz, CHLOROFORM-d) δ (ppm) 64.9, 68.1, 126.0, 127.0, 128.0, 128.6, 128.8, 140.5. ^1H and ^{13}C NMR data matches that reported in the literature.[334]

Phenylpropane-1,2-*anti*-diol- (47)

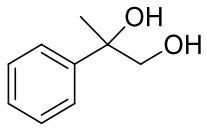

Yield = 84%; 50:50

^1H NMR (500 MHz, CHLOROFORM-d) δ (ppm) 1.54 (s, 3 H, C**H**$_3$OH), 3.65 (d, *J* = 11.25 Hz, 1 H, C**H**$_2$OH), 3.81 (d, *J* = 11.25 Hz, 1 H, C**H**$_2$OH), 7.33 - 7.48 (m, 5 H, ring C**H**).

^{13}C NMR (500 MHz, CHLOROFORM-d) δ (ppm) 26.6, 71.4, 74.3, 125.3, 125.9, 127.4, 128.7, 129.0, 145.2. ^1H and ^{13}C NMR data matches that reported in the literature.[334]

Cyclohexane-1,2-*anti*-diol- (48)

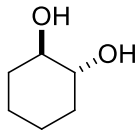

Yield = 72%; 50:50

^{1}H NMR (500 MHz, CHLOROFORM-d) δ (ppm) 1.25 - 1.28 (m, 4 H, C(OH)CH$_2$C**H**$_2$), 1.68 - 1.71 (m, 2 H, CH$_2$C**H**$_2$CH(OH)), 1.94 - 1.99 (m, 2 H, C**H**$_2$CHOH), 3.36 (td, *J* = 5.01, 2.20 Hz, 2 H, C**H**OH).

^{13}C NMR (500 MHz, CHLOROFORM-d) δ (ppm) 24.3, 32.8, 75.8. ^{1}H and ^{13}C NMR data matches that reported in the literature.[177]

1-methylcyclohexane-1,2-*anti*-diol- (50)

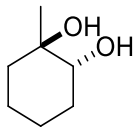

Yield = 73%; 50:50

^{1}H NMR (500 MHz, CHLOROFORM-d) δ (ppm) 1.20 (s, 3 H, CC**H**$_3$), 1.29 - 1.40 (m, 4 H, ring C**H**$_2$), 1.59 - 1.63 (m, 1 H, ring C**H**), 1.69 - 1.76 (m, 2 H, ring C**H**$_2$), 1.84 - 1.89 (m, 1 H, ring C**H**), 2.18 - 2.32 (m, 2 H, ring C**H**$_2$), 3.47 - 3.52 (m, 1 H, C**H**(OH)).

^{13}C NMR (500 MHz, CHLOROFORM-d) δ (ppm) 19.6, 23.2, 24.0, 31.0, 38.6, 74.0, 77.2. ^{1}H and ^{13}C NMR data matches that reported in the literature.[177]

4-methylcyclohexane-1,2-*anti*-diol- (49)

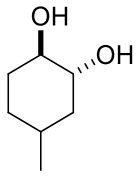

Yield = 75%; 50:50

^{1}H NMR (500 MHz, CHLOROFORM-d) δ (ppm) 0.99 (d, *J* = 7.34 Hz, 3 H, CHC**H**$_3$), 1.41 - 1.58 (m, 4 H, ring C**H**$_2$), 1.70 - 1.85 (m, 2 H, ring C**H**$_2$), 1.98 - 2.08 (m, 1 H, ring C**H**), 3.44 (br. s., 1 H, C**H**(OH)), 3.67 (br. s., 1 H, C**H**(OH)).

^{13}C NMR (500 MHz, CHLOROFORM-d) δ (ppm) 19.1, 27.5, 27.8, 29.4, 38.1, 71.4, 75.1. ^{1}H and ^{13}C NMR data matches that reported in the literature.[335]

7.4.1.1 Procedure for lower reactivity anti-diol synthesis from non-renewable alkenes with Ishii-Venturello catalyst

The appropriate alkene substrate (X g, 5 mmol, 1 eq), $PW_4O_{24}[PTC]_3$ (0.11 g, 2259 $gmol^{-1}$, 0.05 mmol, 1 mol%), unbuffered 30% aqueous H_2O_2 (0.51 mL, 5 mmol, 1 eq) and 1 mL EtOAc were added to a carousel tube forming a biphasic mixture. The reaction was stirred whilst heated for 1 h at 50 °C or 80 °C. The epoxidation reaction was judged to be complete by tlc. Amberlyst-15 (0.13 mol%, 140 mg, 4.6 mmol/g) was then added and the reaction mixture was again stirred for 5-6 h at the previous temperature to ring open the epoxides to the anti-diol products, tlc was used to judge reaction progress. The solution was left to settle with no stirring allowing the biphasic system to separate out into its two layers. 20 mL of EtOAc was added and the reaction mixture extracted. The organic layer was dried with $MgSO_4$ and filtered to remove the Amberlyst-15 and drying agent. The solvent was then removed *in vacuo* to give the oil/solid diol products. The crude products were purified *via* column chromatography to produce a clean diols (XX% yield). The NMR spectra were compared with literature data where possible.

Octane-1,2-*anti*-diol- (51)

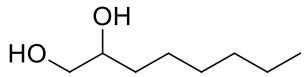

Yield = 75%, 50:50

^{1}H NMR (500 MHz, CHLOROFORM-d) δ (ppm) 0.80 - 0.96 (m, 3 H, CH_2CH_3), 1.28 - 1.38 (m, 6 H, CH_2CH_3), 1.44 (br. s., 2 H, CH_2CH_2), 2.15 – 2.48 (m, 2 H, CH_2CH_2), 3.39 - 3.47 (m, 1 H, CH_2CHOH), 3.65 (dt, *J* = 10.88, 2.63 Hz, 1 H, CH_2OH), 3.68 - 3.75 (m, 1 H, CH_2OH).

^{13}C NMR (500 MHz, CHLOROFORM-d) δ (ppm) 14.0, 22.6, 25.5, 29.3, 31.7, 33.2, 66.8, 72.4. ^{1}H and ^{13}C NMR data matches that reported in the literature.[334]

4-phenylbutane-1,2-*anti*-diol- (52)

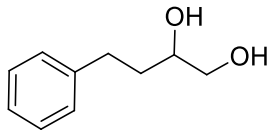

Yield = 75%, 50:50

^{1}H NMR (500 MHz, CHLOROFORM-d) δ (ppm) 1.72 - 1.80 (m, 2 H, CH_2Ar), 2.66 - 2.72 (m, 1 H, CH_2CHOH), 2.77 - 2.86 (m, 3 H, OH/CH_2CHOH), 3.46 (dd, *J* = 11.25, 7.83 Hz, 1 H, $CHOHCH_2OH$), 3.62 - 3.67 (m, 1 H, CH_2OH), 3.72 (tdd, *J* = 7.83, 4.89, 2.93 Hz, 1 H, CH_2OH), 7.14 - 7.24 (m, 3 H, ring CH), 7.24 - 7.34 (m, 2 H, ring CH).

^{13}C NMR (500 MHz, CHLOROFORM-d) δ (ppm) 31.8, 34.6, 66.7, 71.5, 125.9, 128.39, 128.44. ^{1}H and ^{13}C NMR data matches that reported in the literature.[336]

Cyclohexane-1,2,4,5-*anti*-tetrol- (53)

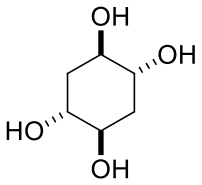

Yield = 70%, 50:50

^{1}H NMR (500 MHz, D_2O) δ (ppm) 1.81 - 1.89 (m, 4 H, C**H**$_2$), 3.78 (br. s., 4 H, C**H**OH).

^{13}C NMR (500 MHz, D_2O) δ (ppm) 33.7, 69.8. ^{1}H and ^{13}C NMR data matches that reported in the literature.[337]

7.5 Procedures for the 1st Generation route to paracetamol

7.5.1 Step 1. Procedure for the Ishii-Venturello catalysed epoxidation of limonene

(R)-(+)-1,2-limonene oxide- (2)

(4R)-1-methyl-4-(prop-1-en-2-yl)-7-oxabicyclo[4.1.0]heptane

(R)-(+)-limonene (0.68 g, 5 mmol, 1.0 eq), $PW_4O_{24}[MTCA]_3$ (0.11 g, 2259 $gmol^{-1}$, 0.05 mmol, 1 mol%) were added to a 20 mL glass carousel tube with a stirrer bar. The catalyst and substrate were stirred for 10 minutes to fully dissolve the catalyst and then 30% aqueous hydrogen peroxide solution (0.5 mL, 5 mmol, 1.0 eq) (buffered to pH 7 with 0.5 M NaOH) was added slowly forming a biphasic mixture. During hydrogen peroxide addition if substrates were particularly exothermic the tube was cooled with a water bath and stirring was maintained at a slow rate. The reaction was stirred at room temperature for 0.5 - 24 h. The reaction was judged to be complete following by tlc. The solution was left to settle with no stirring allowing the biphasic system to separate out into its two layers. The top yellow organic layer was separated and purified *via* column chromatography to produce a clear oil in a 94% yield (714 mg).

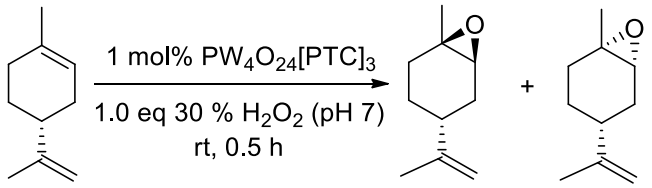

94% yield
55:45

^{1}H NMR (300 MHz, CHLOROFORM-d); δ ppm 1.13–2.13 (m, 7H, Ar**H**), 1.25 (s, 3H, CC**H**$_3$), 1.76 (m, 3H, CC**H**$_3$), 2.97 (t, J = 5.0 Hz, 1H, C(O)C**H**CH$_2$), 4.65 (s, 2H, CC**H**$_2$); and

^{13}C NMR (300 MHz, CHLOROFORM-d) δ ppm 19.9 (CH_3), 20.9 (CH_3) , 25.7 (CH_2), 28.4 (CH_2), 30.1 (CH_2), 40.4 (CH), 57.0 (CH), 59.7 (C), 108.9 (CH_2), 148.8 (C). ^{1}H and ^{13}C NMR data matches that reported in the literature.[315]

7.5.2 Step 2. Procedure for the ring opening of 1,2-limonene epoxide using organo-aluminium reagents

Pseudo-limonene allylic alcohol (PAA)- (56)

(5R)-2-methylene-5-(prop-1-en-2-yl)cyclohexanol

Tetramethylpiperidine (1.66 mL, 9.86 mmol) was diluted with benzene/solvent (15 mL), the resulting solution was cooled to 0 ^{o}C, *n*-butyllithium (4.27 mL, 9.86 mmol, 2.30 M solution in hexanes) was then added, and the colourless solution turned yellow. After 30 min of stirring, diethylaluminum chloride (11.3 mL, 11.29 mmol, 1.00 M solution in hexanes) was added, the yellow colour disappeared, and a cloudy opaque yellow solution formed. After a further 40 min of stirring at 0 ^{o}C, 1,2-limonene oxide (0.75 g, 4.92 mmol) was added as a solution in benzene/solvent (5 mL). The reaction mixture was stirred for 45 min at 0 ^{o}C and then for 2 h at rt. The reaction was quenched with the slow addition of saturated $NaHCO_3$ (20 mL) at 0 ^{o}C, the product was extracted with $CHCl_3$ (20 mL x 3), washed with brine (30 mL), dried using $MgSO_4$, filtered, and concentrated *in vacuo* to give the crude product. Purification by column chromatography (pentane/Et_2O; 4/1) gave the product, limonene allylic alcohol, as a mixture of diastereoisomers as a colourless oil in a 83% yield (623 mg).

^{1}H and ^{13}C NMR data matches that reported in the literature.[257]

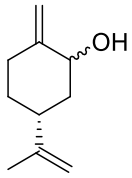

55:45

^{1}H NMR (300 MHz, CHLOROFORM-d) diastereomer mixture; δ ppm 1.11 - 1.36 (m, 2 H, ring C**H**$_2$), 1.38 - 1.61 (m, 1 H, ring C**H**), 1.69 (d, *J* = 0.95 Hz, 3 H, CC**H**$_3$), 1.75 - 1.88 (m, 1 H, ring C**H**), 1.91 - 2.04 (m, 1 H, ring C**H**), 2.04 - 2.24 (m, 2 H, ring C**H**$_2$), 2.34 - 2.57 (m, 2 H, ring C**H**$_2$), 4.32 (t, *J* = 3.16 Hz, 1 H, C(**H**)OH), 4.63 - 4.87 (m, 4 H, =C**H**$_2$)

^{13}C NMR (300 MHz, CHLOROFORM-d) diastereomer mixture; δ ppm 20.6, 20.8, 21.0, 29.8, 32.4, 32.5, 33.6, 34.6, 37.2, 37.9, 38.9, 41.8, 44.0, 65.3, 71.8, 72.0, 103.9, 108.7, 108.9, 109.0, 109.5, 148.4, 149.2, 149.7, 150.9. ^{1}H and ^{13}C NMR data matches that reported in the literature.[72]

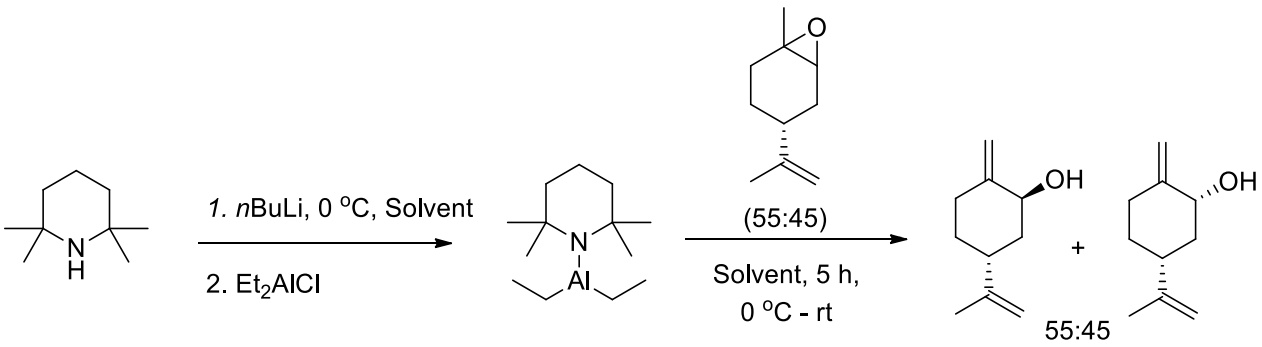

Table 13. Aluminium-TMP procedure solvent screen

Solvent	**Yield % of LPAA[a]**
Benzene	83
Toluene	86
Hexane	77
THF	83

[a]Isolated yields with 1:1 PAA diastereomer selectivity, reactions carried out in 15 mL solvent, 750 mg LO, 1.7 mL 2,2,6,6-tetramethylpiperidine, 4.3 mL 2.3 M *n*BuLi in hexanes, 11.3 mL diethyl aluminium chloride solution (1.0 M in hexanes), 0 °C to rt, 5 h.

7.5.2.1 Procedure for the ring opening of 1,2-limonene epoxide using lithium-amine reagents

Amine screen procedure for epoxide ring opening

Tetramethylpiperidine/Amine (1.66 mL, 9.86 mmol) was diluted with diethyl ether (15 mL), the resulting solution was cooled to -78°C, *n*-butyllithium (4.27 mL, 9.86 mmol, 2.30 M solution in hexanes) was then added, and the colourless solution turned yellow. After 30 min of stirring, the yellow colour disappeared, and a cloudy opaque yellow solution formed. After a further 40 min of stirring at 0 °C, 1,2-limonene oxide (0.75 g, 4.92 mmol) was added as a solution in diethyl ether (5 mL). The reaction mixture was stirred for 3 hours at 35°C. The reaction was quenched with the slow addition of saturated $NaHCO_3$ (20 mL) at 0 °C, the product was extracted with $CHCl_3$ (20 mL x 3), washed with brine (30 mL), dried using $MgSO_4$, filtered, and concentrated *in vacuo* to give the crude product. Purification by column chromatography (pentane/Et_2O; 4/1) gave the product, limonene allylic alcohol, as a mixture of diastereoisomers as a colourless oil in a 89% yield (668 mg).

^1H and ^{13}C NMR spectra consistent with previously reported PAA and carveol species also as reported in the literature[257]. GCMS analysis identified mixture containing mainly PAA with minor carveol components.

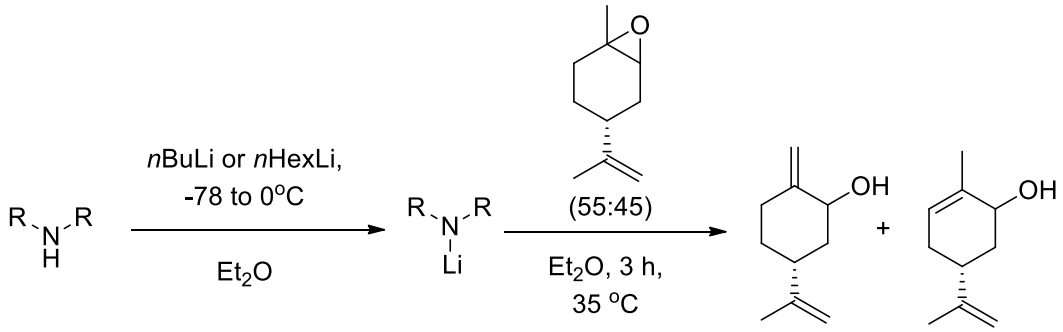

Table 14. Screen of lithium amides used as bases for ring opening of 1,2-limonene epoxide

Amine	**Yield**	**Selectivity to PAA**	**Selectivity to Carveol**
TMP	95	94	6
*i*Pr	90	90	10
Et	91	80	20

[a]Isolated yields; reactions carried out using 750 mg 1,2-limonene epoxide in 15 mL Et_2O

7.5.3 Step 2. Procedure for ring opening using Lewis acids

Lewis acid ring opening General Procedure

Solid lewis acids/Al(O^iPr)$_3$ (0.02-6.12 g, 0.1-3 mmol) was added to a stirred solution of (+)-1,2-limonene oxide (0.3 g, 1 mmol) dissolved in toluene (6.5 mL) and refluxed at 140 ^oC for 4 h. The solution was left to cool with no stirring. The contents of the flask were transferred to a separation funnel with toluene (20 mL). The organic solution was extracted with saturated $NaHCO_3$ (2 × 10 mL) and saturated brine (2 × 10 mL). The toluene layer was dried with anhydrous $MgSO_4$ and filtered into a 100 mL, round-bottom flask. The toluene was removed *in vacuo*. The crude limonene allylic alcohol mixture was then purified using column chromatography however PAA was inseparable from its regioisomer carveol.

^1H and ^{13}C NMR spectra, MS and IR data were consistent with the organoaluminium procedure product and literature data.[257]

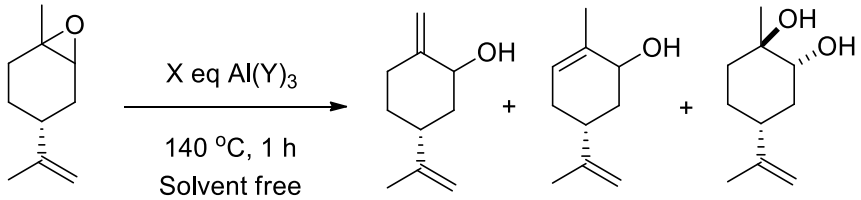

55:45

Table 15. Alternative Lewis acid screen at 140 ^oC

Lewis acid / Y	**Equivalence of Lewis acid / X**	**Yield % (both isomers)**[a]	**Selectivity to desired isomer**
Aluminium Isopropoxide	1	94	61
Aluminium Isopropoxide	0.1	86	60
Titanium Isopropoxide	1	-	-
Aluminium Ethoxide	1	-	-
Aluminium Ethoxide	3	-	-
Aluminium *tert* butoxide	1	83	59

[a]Isolated yields after following the reaction *via* tlc. Reactions carried out in 6.5 mL toluene, 304 mg 1,2-limonene oxide, specified eq of Lewis acid, 4 h, 140 ^oC.

7.5.3.1 Lewis acid ring opening procedure optimisation:

Solvent / Temperature screen and results with AIP – performed according to General Procedure

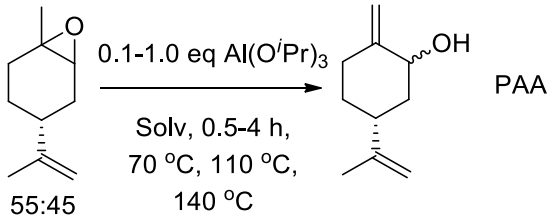

Table 16. Temperature screen using AIP

Solvent	**Temperature, °C**	**Equivalence of Al(O^{i}Pr)$_3$**	**Yield % (both isomers)**	**Selectivity to desired isomer PAA**
Xylene	140	0.1	50	55
Toluene	70	1.0	-	-
Toluene	110	0.1	61	66
Solvent free	140	0.1	86	60

[a]Isolated yields after following the reaction *via* tlc. Reactions carried out in 0.6 mL solvent, 204 mg 1,2-limonene epoxide, 0.5 – 4 h, temperature and Lewis acid equivalence as stated in table.

Solvent free temperature screen and results with AIP - performed according to General Procedure

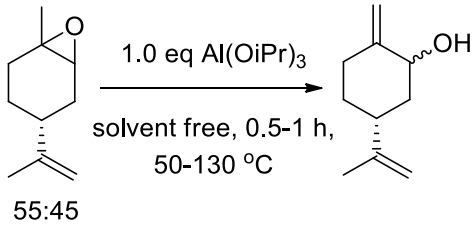

Table 17. Temperature screen of solvent free AIP system

Temperature/ °C	**Yield % of PAA[a]**
50	-
70	25
90	40
110	51
120	50
130	51

[a]Yields calculated by GCMS and ^{1}H NMR integration. tlc was used to monitor reaction progress, reactions carried out in solvent free conditions, 0.5 – 1.0 h, 1 eq of AIP (408 mg), 304 mg 1,2-limonene oxide and temperature was varied as stated in table.

7.5.3.2 Procedures for the kinetic resolution of 1,2-limonene epoxide isomers:

7.5.3.3 Procedure for cis-(+)-limonene epoxide

cis-(+)-limonene epoxide- (2i)

(1R,4R,6S)-1-methyl-4-(prop-1-en-2-yl)-7-oxabicyclo[4.1.0]heptane

Pyrrolidine (8.35 mL, 0.10 mol), (R)-(+)-limonene epoxide (16.4 mL, 0.10 mol), and deionized water (1.5 mL, 0.08 mol) were added to a 50 mL round-bottom flask equipped with a magnetic stir bar and a reflux condenser. The reaction mixture was heated to reflux and stirred under reflux for 24 h. The contents of the round-bottom were transferred to a separatory funnel with pentane (50 mL). The organic solution was extracted with deionized water (2 × 50 mL). The pentane layer was dried with anhydrous magnesium sulfate and gravity filtered into a 100 mL, round-bottom flask. The pentane was removed *in vacuo* and purified by column chromatography to yield 5.05 g of *cis*-(+)-limonene epoxide.

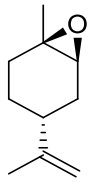

cis

^{1}H NMR (300 MHz, CHLOROFORM-d) δ ppm 1.26 (s, 3H, CC**H**$_3$), 1.49 (m, 2H, ring C**H**), 1.65 (s, 3H, CC**H**$_3$), 1.68 (m, 1H, ring C**H**), 1.80 (m, 2H, ring C**H**), 2.06 (m, 2H, ring C**H**), 3.01 (t, 1H, *J*= 2.4 Hz, C(O)C**H**CH$_2$), 4.65 (d, 2H, *J*=14.8 Hz ,CC**H**$_2$). NMR data consistent with literature.[260]

7.5.3.4 Procedure for trans-(+)-limonene epoxide

A 50 mL, round-bottom flask equipped with a magnetic stir bar and a reflux condenser had (R)-(+)-limonene epoxide (3.06 g, 0.02 mol), pyrazole (0.23 g, 0.003 mol), and deionized water (11 mL) added to it. The mixture was heated to 100 °C (reflux) and heated under reflux for 5 h. The reaction mixture was then placed in a water bath heated to approximately 80 °C. The mixture was then transferred to a separation funnel and extracted with warm (80 °C) deionized water (2 × 30 mL) to remove the diol. Excess pentane was then added to the separation funnel containing the organic layer and a slurry of white solid formed immediately. The mixture was vacuum filtered to remove the solid and further solid formed upon evaporative cooling from the vacuum. The mixture was filtered for a second time removing the remainder of 1,2-limonene diol. The pentane remained clear and was dried over anhydrous magnesium sulfate and gravity filtered into a 100 mL, round-bottom flask. The pentane was removed *in vacuo* leaving *trans*-R-(+)-limonene epoxide (1.15 g).

trans-(+)-limonene epoxide- (2ii)

(1S,4R,6R)-1-methyl-4-(prop-1-en-2-yl)-7-oxabicyclo[4.1.0]heptane

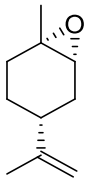

trans

^{1}H NMR (300 MHz, CHLOROFORM-d) δ (ppm) 1.06 - 1.35 (m, 1H, ring C**H**), 1.20 (s, 3H, CC**H**$_3$), 1.58 - 1.76 (m, 5H, ring C**H**/C**H**$_2$), 1.55 (s, 3H, C(OC)C**H**$_3$), 1.89 (s, 1H, ring C**H**), 2.87 (d, *J*=5.3 Hz, 1H, C(O)C**H**), 4.55 (s, 2H, C=C**H**$_2$). NMR data spectra consistent with literature.[260]

7.5.3.5 Limonene bromination/hydration to Limonene Bromohydrin

Limonene bromohydrin (LimBrOH)- (59)

(4R)-2-bromo-1-methyl-4-(prop-1-en-2-yl)cyclohexanol

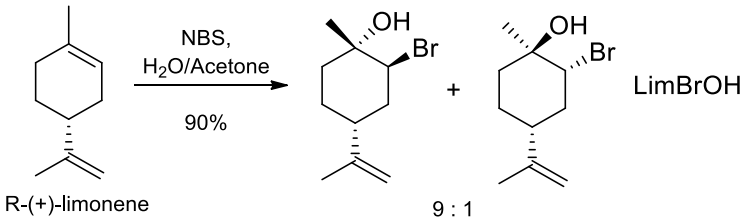

To synthesise *trans*-limonene oxide, a modified procedure from Greiner *et al.* was used [338]. A volume of 1.4 mL (8.8 mmol, 1.0 eq) limonene, 1 mL water and 4.5 mL acetone were added into a 25 mL round bottom flask. The mixture was cooled down to 0 °C and (1.6 g, 9.2 mmol, 1.05 eq) *N*-bromosuccinimide was added and stirred at rt for 2 hours when reaction progress was judged complete by tlc. Saturated NaCl was added to cause the aqueous and organic layers to separate and the aqueous layer was washed three times with 30 mL diethyl ether and dried with anhydrous magnesium sulphate followed by evaporation *in vacuo* to give a crude oil in a 90% yield (1.84 g).

^{1}H NMR (300 MHz, CHLOROFORM-d) δ (ppm), 1.23 (d, *J*=3.4 Hz, 1H, ring C**H**), 1.39 (s, 3H, CC**H**3), 1.50 - 1.67 (m, 1H, ring C**H**), 1.71 (s, 3H, C(OH)C**H**$_3$) 1.93 - 2.15 (m, 5H, ring C**H**/C**H**$_2$), 4.18 (br. s., 1H, CBr(**H**)), 4.73 (d, *J*=6.8 Hz, 2H, C=C**H**$_2$).

^{13}C NMR (300 MHz, CHLOROFORM-d) δ (ppm) 21.3, 26.0, 29.4, 33.1, 35.7, 38.3, 60.1, 71.7, 109.5, 148.4. ^{1}H NMR and ^{13}C NMR spectra consistent with previous NMR data and literature data.[209]

7.5.3.6 Limonene Bromohydrin elimination to trans-limonene epoxide

<u>*trans*-(+)-limonene epoxide- (2ii)</u>

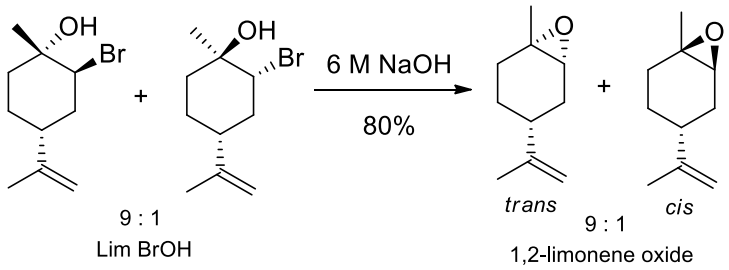

After removing the aqueous phase and acetone solvent, the crude bromohydrin oil was converted directly to the epoxide with 2 mL of a 6 M NaOH solution at 25 °C for 2h. The alkaline solution was removed, and the crude product was diluted with 10 mL diethyl ether before it was washed with 15 mL of a saturated sodium bicarbonate solution and, subsequently, 15 mL of water. After evaporating the solvent, 1.4 g of the crude product was obtained as a yellow viscous liquid. Gas chromatography analysis revealed a *trans*-limonene epoxide selectivity of 90%, with 10% *cis*-LO. The final product was purified using column chromatography giving an 80% yield (963 mg (72% yield over 2 steps)).

^{1}H NMR (300 MHz, CHLOROFORM-d) δ (ppm) 1.06 - 1.35 (m, 1H, ring C**H**), 1.20 (s, 3H, CC**H**$_3$), 1.58 - 1.76 (m, 5H, ring C**H**/C**H**$_2$), 1.55 (s, 3H, C(OC)C**H**$_3$), 1.89 (s, 1H, ring C**H**), 2.87 (d, *J*=5.3 Hz, 1H, C(O)C**H**), 4.55 (s, 2H, C=C**H**$_2$).

^{13}C NMR (300 MHz, CHLOROFORM-d) δ (ppm) 20.1, 23.0, 24.2, 29.8, 30.7, 40.6, 57.3, 59.0, 109.0, 148.9. ^{1}H NMR and ^{13}C NMR spectra consistent with previous NMR data and literature data.[209]

7.5.3.7 Step 2. Ring opening with AIP

<u>Pseudo-limonene allylic alcohol (PAA)- (56)</u>

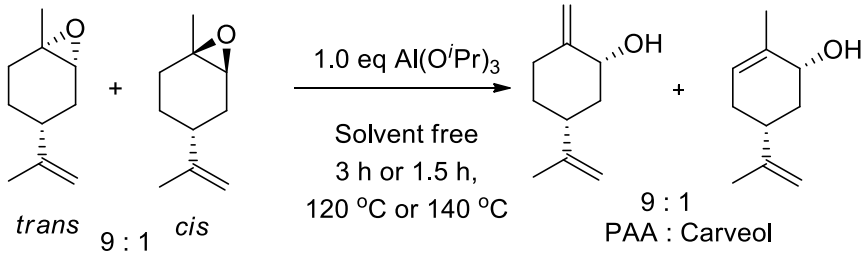

Al(O^{i}Pr)$_3$ (612 mg/61.2 mg, 3.0 mmol/0.3 mmol, 1.0/0.1 eq) was added to a stirred solution of *trans*-limonene oxide (456 mg, 3 mmol, 1.0 eq) and refluxed at 120 °C or 140 °C for 3 or 1.5 h in a reduced volume radleys glass carousel tube. The solution was left to cool with no stirring. The contents of the flask were transferred to a separation funnel with ethyl acetate (30 mL). The organic solution was washed with water and saturated ammonium chloride, approximately 20 mL. The ethyl acetate layer was dried with anhydrous $MgSO_4$ and filtered into a 100 mL,

round-bottom flask. The ethyl acetate was removed *in vacuo*. The crude limonene allylic alcohol mixture was then purified using column chromatography giving the desired PAA product in a 70% yield (320 mg). The regioisomer impurity carveol was inseparable from PAA by chromatography or distillation.

^{1}H NMR and ^{13}C NMR spectra consistent with previous NMR data and literature data.[257]

Note: Be sure to use fresh $Al(O^{i}Pr)_3$ as this can degrade to $Al(OH)_3$ over time producing lowered yields of PAA.

7.5.4 Step 3. Ozonolysis procedures

Diketone alcohol (DKA)- (57)

(2R,4R)-4-acetyl-2-hydroxycyclohexanone

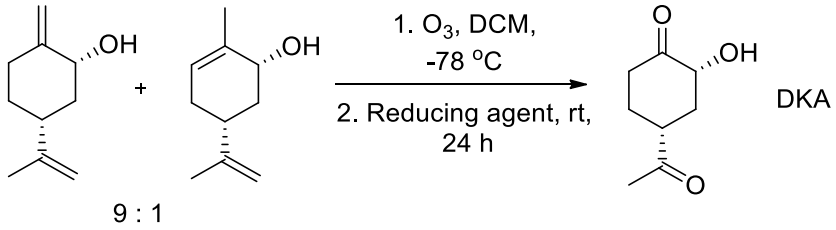

The alkene substrate, PAA (5 mmol, 760 mg) was dissolved in dry CH_2Cl_2 (10 mL) in a flask. The solution was cooled to -78 °C, and a stream of O_3/O_2 was introduced through a disposable glass pipet for a period until the solution turned pale blue in colour which varied with the amount of alkene. Once judged to be complete (tlc and pale blue colour), the reaction was sparged with N_2 for 2 mins. The reaction mixture was warmed to room temperature and the ozonide degradation agent (5 mmol) was added and stirred for 24 hours at rt. The crude reaction mixture was diluted with CH_2Cl_2 and saturated $NaHCO_3$. The separated aqueous layer was extracted with additional CH_2Cl_2. The combined organic layers were dried with magnesium sulfate and filtered. The residue obtained upon concentration *in vacuo* was purified *via* column chromatography with pentane/ethyl acetate to isolate the diketone alcohol diastereomer products.

^{1}H NMR (300 MHz, CHLOROFORM-d) δ (ppm) 1.53 - 1.67 (m, 1 H, ring C**H**), 1.71 - 1.82 (m, 1 H, ring C**H**), 2.19 - 2.25 (s, 3 H, CC**H**$_3$), 2.32 - 2.56 (m, 2 H, ring C**H**$_2$), 2.58 - 2.69 (m, 2 H, C**H**$_2$), 2.93 (tt, *J* = 12.48, 3.32 Hz, 1 H, C**H**), 3.65 (br. s., 1 H, O**H**), 4.22 (ddd, *J* = 12.32, 6.63, 1.26 Hz, 1 H, C**H**(OH)).

^{13}C NMR (300 MHz, CHLOROFORM-d) δ (ppm) 28.2, 28.7, 37.5, 37.7, 48.0, 73.8, 208.0, 209.7.

IR (thin film) v max (cm^{-1}): 3391 (O-H alcohol), 1702 (C=O ketone). HRMS (ESI): m/z calculated for $C_8H_{12}O_3$: requires 179.1798 for $[M+Na]^+$; found: 179.0135.

Table 18. Yields obtained with a variety of ozonide reducing agents

Ozonide reducing agent	Yield of DKA %[a]
DMS	38
PPh_3	32
NEt_3	37

[a]Isolated yields. Reactions run on 5 mmol scale using 5 eq of reducing agent.

7.5.4.1 Zinc and acetic acid ozonolysis procedure[265]

Diketone alcohol (DKA)- (57)

(2R,4R)-4-acetyl-2-hydroxycyclohexanone

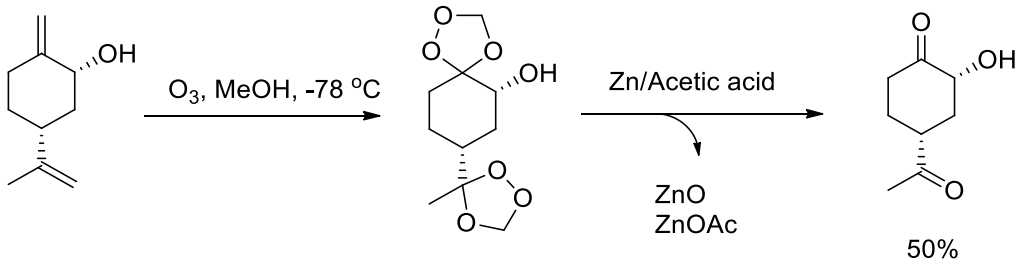

The alkene substrate, PAA (5 mmol, 760 mg) was dissolved in dry MeOH (10 mL) in a flask. The solution was cooled to -78 °C, and a stream of O_3/O_2 was introduced through a disposable glass pipet for a period until the solution turned pale blue in colour which varied with the amount of alkene. Once judged to be complete (tlc and pale blue colour), the reaction was sparged with N_2 for 2 mins. The reaction mixture was warmed to room temperature and the ozonide degradation agent zinc dust (5 eq, 5 mmol, 325 mg) with acetic acid (10 eq, 10 mmol, 0.57 mL) was added and stirred for 24 hours. The zinc acetate was filter and the MeOH solution collected and evaporated *in vacuo*. The crude product was diluted with ethyl acetate and washed with saturated $NaHCO_3$. The separated aqueous layer was extracted with additional ethyl acetate. The combined organic layers were dried with magnesium sulfate and filtered. The residue obtained upon concentration *in vacuo* was purified *via* column chromatography to isolate the diketone alcohol diastereomer products in a 50% yield (390 mg). ^1H and ^{13}C NMR spectra data consistent with previously reported data.

7.5.4.2 Acetylation of Pseudo-limonene Allylic Alcohol to Pseudo-Limonene Allylic Acetate

Pseudo-limonene allylic alcohol (PAA-OAc)- (60)

(1R,5R)-2-methylene-5-(prop-1-en-2-yl)cyclohexyl acetate

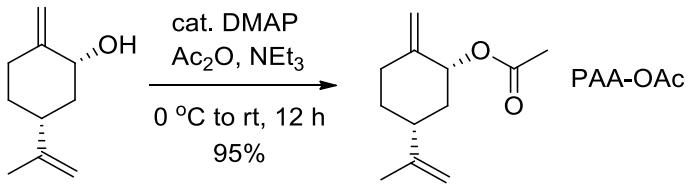

DMAP (55 mg, 0.45 mmol, 0.03 eq.) and NEt_3 (4.59 mL, 33 mmol, 2.2 eq) were added to a round bottom flask containing stirred solution of PAA (2.3 g, 15 mmol, 1.0 eq) and dry DCM (45 mL). The solution was cooled to 0 ºC in an ice bath. Then Ac_2O (3.37 g, 33 mmol, 2.2 eq) was then added drop wise for 5 min and was allowed to warm to rt and stirred overnight. Reaction was deemed to be complete by tlc. Methanol was added to crude reaction mixture and stirred for 2 h at rt, which reacts with any excess Ac_2O forming a methyl ester which is easily removed *in vacuo*. Diethyl ether was added to extract the product and then was washed with 1 M HCl to remove triethylamine. The product was concentrated *in vacuo* and then purified using column chromatography to give PAA-OAc in a 95% yield (2.76 g).

^{1}H NMR (300MHz, CHLOROFORM-d) δ (ppm) 1.16 - 1.31 (m, 3H, ring C**H**/C**H**$_2$), 1.65 (s, 3H, CC**H**$_3$), 1.64 – 1.93 (m, 1H, ring C**H**), 2.05 (s, 3H, C(=O)C**H**$_3$), 2.12 - 2.42 (m, 3H, ring C**H**/C**H**$_2$), 4.64 – 4.89 (m, 4H, C=C**H***2*), 5.15 - 5.35 (m, 1H, C(**H**)OAc),

^{13}C NMR (300 MHz, CHLOROFORM-d) δ 20.5, 20.8, 30.5 32.2, 38.7, 43.5, 73.2, 109.2, 112.2, 130.7, 147.8, 169.7. ^{1}H NMR and ^{13}C NMR spectra consistent with literature.[72]

7.5.4.3 Ozonolysis of limonene allylic acetate to Diketone acetate

Diketone acetate (DKA-OAc)- (61)

(1R,5R)-5-acetyl-2-oxocyclohexyl acetate

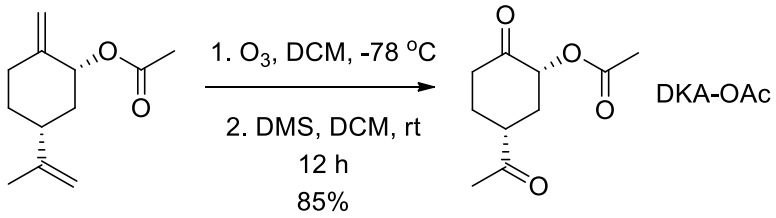

The alkene substrate, PAA-OAc (0.194 g, 1 mmol, 1.0 eq) was dissolved in dry DCM (5 mL) in a flask. The solution was cooled to -78 ºC, and a stream of O_3/O_2 was introduced through a disposable glass pipet for a period until the solution turned pale blue in colour which varied with the amount of alkene. Once judged to be complete (pale blue colour), the reaction was

sparged with N_2 for 2 mins. The reaction mixture was warmed to room temperature and the ozonide reducing agent, DMS (0.36 mL, 5 mmol, 5 eq) was added and stirred for 12 hours. The crude reaction mixture was diluted with DCM and saturated $NaHCO_3$.The separated aqueous layer was extracted with additional DCM. The combined organic layers were dried with magnesium sulfate and filtered. The residue obtained upon concentration *in vacuo* was purified *via* column chromatography with pet ether and ethyl acetate to isolate the diketone alcohol acetate (DKA-OAc) diastereomer products in 85% yield (168 mg).

^{1}H NMR (300 MHz, CHLOROFORM-d) δ (ppm) 1.75 - 2.02 (m, 4H, ring C**H**$_2$), 2.13 (s, 3H, C(=O)C**H**$_3$), 2.26 (s, 3H, C(=O)C**H**$_3$), 2.42 – 2.55 (m, 3H, ring C**H**/C**H**$_2$), 2.96 (m, 1H, C(**H**)), 5.25 (m, 1H, C(**H**)OAc).

^{13}C NMR (300 MHz, CHLOROFORM-d) δ (ppm) 20.5, 27.4, 28.5, 33.9, 38.7, 48.2, 74.7, 169.8, 202.7, 207.4. IR (thin film) v max (cm^{-1}): 1707.57 (C=O ketone), 1221.83 (C-O ether). HRMS (ESI): m/z calculated for $C_{10}H_{14}O_4$ requires 221.07898 for $[M+Na]^+$ found 221.0825.

7.5.4.4 Deprotection of diketone acetate

Diketone alcohol (DKA)- (57)

(2R,4R)-4-acetyl-2-hydroxycyclohexanone

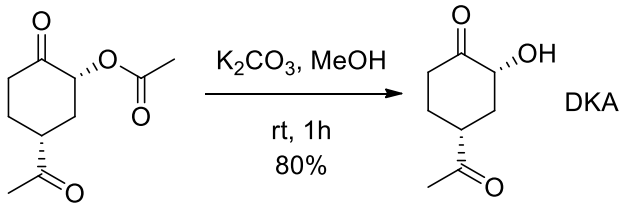

The acetate substrate, diketone acetate (198 mg, 1 mmol, 1.0 eq) was dissolved in MeOH (5 mL) in a flask. The reaction mixture was stirred at room temperature and the K_2CO_3 (690 mg, 5 mmol, 5 eq) was added and stirred for 1 hour. The crude reaction mixture was evaporated to remove the MeOH and then diluted with DCM, filtered and washed with saturated NaCl. Multiple DCM washes were performed and the combined organic layers dried with magnesium sulfate and filtered. The residue obtained upon concentration *in vacuo* was purified *via* column chromatography to isolate the diketone alcohol product in 80% yield (124 mg). ^{1}H NMR and ^{13}C NMR spectra consistent with previous DKA NMR data.

7.5.5 Step 4. Unsuccessful dehydration reactions of PAA and PAA-Ac

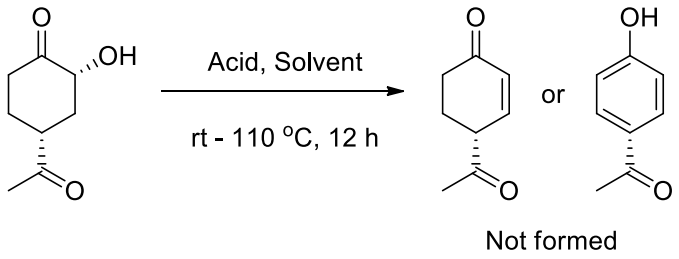

Table 19. Room temperature solvent screen with Amberlyst-15 system*

Solvent	**Yield of keto-enone %[a]**
Acetone	-
Ethyl acetate	-
Methanol	-
Dichloromethane	-
Diethyl ether	-

[a]Yields calculated by ^{1}H NMR integration, reactions carried out in 1 mL solvent, 10 mg Amberlyst-15 (4.6 mmol/g), 60mg (0.38 mmol) DKA, Reflux, 4 h.

Amberlyst-15 (10 mg) was added to a stirred solution of diketone alcohol (60 mg) dissolved in the appropriate solvent (1 mL) and reacted under reflux for 4 h. The contents of the flask was diluted with solvent (10 mL), filtered and transferred to a separation funnel and washed with saturated NaCl (2 × 10 mL). The organic solvent layer was dried with anhydrous magnesium sulfate and filtered into a 50 mL, round-bottom flask. The solvent was removed *in vacuo*. No desired product was obtained during this screen with only recovered PAA or a complex mixture of uncharacterisable products obtained.

Extended acid screen using toluene:

Table 20. Acid screen for dehydration/de-acetylation reactions

Acid	**Yield of keto-enone starting from DKA[b] %[a]**	**Yield of keto-enone starting from DKA-OAc[b] %[a]**
Amberlyst-15	-[b]	-[b]
Phosphoric acid	-[b]	-[b]
Oxalic acid	-[b]	-[b]
10% H_2SO_4 aq	-[b]	-[b]
PTSA	-[b]	-[b]

[a]Yields calculated by ^{1}H NMR integration, reactions carried out in 1 mL toluene solvent, 0.1 eq acid, 60 mg/75 mg (0.38 mmol) DKA/DKA-OAc, refluxed at 110 °C for 12 h.

The appropriate acid (10 mol%, 0.1 eq, 0.038 mmol) was added to a stirred solution of diketone alcohol / acetate (60 mg / 75 mg, 0.38 mmol) dissolved in the appropriate solvent (1 mL) and reacted under reflux for 12 h. The contents of the flask was diluted with solvent (10 mL), filtered

and transferred to a separation funnel and neutralised with saturated $NaHCO_3$ (3 × 10 mL). The organic solvent layer was dried with anhydrous magnesium sulfate and filtered into a 50 mL, round-bottom flask. The toluene was removed *in vacuo*. No desired product was obtained during these screens with only recovered PAA or a complex mixture of uncharacterisable products obtained.

7.5.6 Step 4. Procedure for palladium catalysed hydrogenolysis to diketone precursor *via* pseudo-limonene

Pseudo-limonene (PL)- (62)

1-methylene-4-(prop-1-en-2-yl)cyclohexane

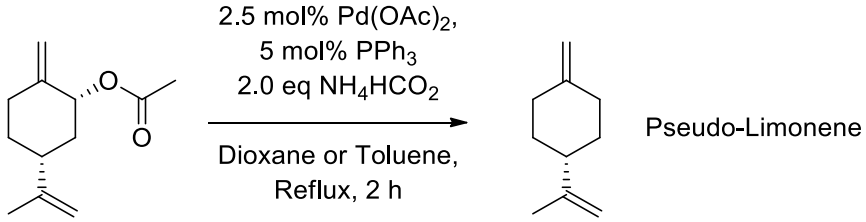

Palladium acetate (10 mg, 0.045 mmol, 2.5 mol%), ammonium formate (252 mg, 4 mmol) , PPh_3 (26 mg, 0.1 mmol, 5 mol%) were added to a 10 ml round bottomed flask containing a stirred solution of limonene allylic acetate (2 mmol, 388 mg) and the solvents (6 mL), dioxane or toluene. The solution refluxed for 20 min at 100 ^oC and then the resulting mixture was filtered through celite. To workup, a saturated solution of NaCl was added, extracted with diethyl ether, and filtered into a 10 mL, round-bottom flask. This was then dried with anhydrous $MgSO_4$, filtered, and concentrated *in vacuo* followed by purification by column chromatography giving pseudo-limonene in 95% yield (258 mg). Mixture analysis was carried out by GCMS and NMR showing 5% inseparable limonene.

^1H NMR (300 MHz, CHLOROFORM-d) δ (ppm) 1.30 (m, 2H, ring C**H**$_2$), 1.72 (s, 3H, CC**H**$_3$), 1.38 – 2.88 (m, 7H, ring C**H**$_2$/C*H*), 4.63 (s, 2H, C=C**H**$_2$), 4.69 (s, 2H, C=C**H**$_2$).

^{13}C NMR (300 MHz, CHLOROFORM-d) δ (ppm) 20.8, 20.9, 33.1, 34.8, 34.9, 45.1, 107.0, 108.5, 149.4, 150.2. ^1H and ^{13}C NMR data matches that reported in the literature reported by Shim et al.[339]

7.5.6.1 Procedure for the ozonolysis of pseudo-Limonene to Diketone

Diketone (DK)- (63)

4-acetylcyclohexanone

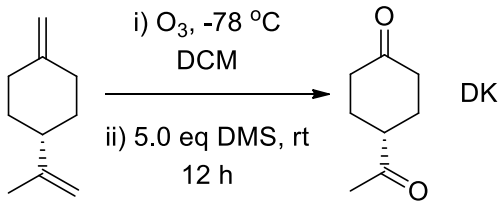

88%

Pseudo-limonene (1.36 g, 10 mmol) was dissolved in dry DCM (10 mL) in a flask. The solution was cooled to -78 °C, and a stream of O_3/O_2 was introduced through a disposable glass pipet for a period until the solution turned pale blue in colour which varied with the amount of alkene. Once judged to be complete (pale blue colour), the reaction was sparged with N_2 for 2 mins. The reaction mixture was warmed to room temperature and the ozonide quencher agent, DMS (3.7 mL, 50 mmol) was added dropwise and stirred for 12 hours. The crude reaction mixture was diluted with DCM and washed with water and saturated NaCl.The separated aqueous layer was extracted with additional DCM. The combined organic layers were dried with magnesium sulfate and filtered. The residue obtained upon concentration *in vacuo* was purified *via* column chromatography with pet ether and ethyl acetate to isolate the diketone product in 88% yield (1.23 g).

^{1}H NMR (300 MHz, CHLOROFORM-d) δ (ppm) 1.75 – 1.91 (m, 2H, ring C**H**$_2$), 2.19 (s, 3H, CC**H**$_3$), 2.25 – 2.44 (m, 6H, ring C**H**$_2$/C**H**), 2.75 (m, 1H, ring C**H**).

^{13}C NMR (300 MHz, CHLOROFORM-d) δ (ppm) 27.7, 28.1, 39.6, 48.3, 53.3, 53.4, 209.9, 210.4. ^{1}H and ^{13}C NMR data matches that reported in the literature reported by Trost et al.[340]

7.5.7 Step 5. Procedures for the oxidative aromatisation of DK to 4-HAP

7.5.7.1 Stahl et al conditions.[341]

4-hydroxyacetophenone (4-HAP)- (54)

1-(4-hydroxyphenyl)ethanone

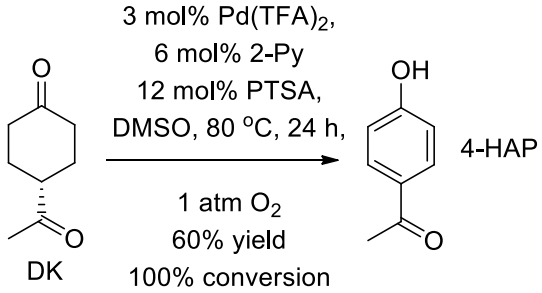

To a two-necks flask loaded with a stir bar was added the cyclic ketone (140 mg, 1 mmol), PTSA (20 mg, 0.12 mmol), 3 mol% $Pd(TFA)_2$ (0.03 mmol, 10 mg), 2-(Dimethylamino)pyridine (0.06 mmol, 8 mg) and DMSO (1 ml). The flask was first degassed and then sealed with O_2 gas balloon. The reaction was heated in an oil bath to 80 °C with vigorous stirring for 24 h. After the reaction was completed, Pd was filtrated through celite. Then 10 ml of water was added to the filtrate followed by extraction with EtOAc (10 ml × 3) and the combined organic layer was dried over anhydrous $MgSO_4$. The solvent was removed under reduced pressure. Purification by column chromatography gave 4-HAP in a yield of 60% (81 mg).

^{1}H NMR (300 MHz, DMSO-d_6) δ (ppm) 2.52 (s, 3 H, C**H**$_3$ 6.82 - 6.91 (m, *J* = 8.85 Hz, 2 H, Ar**H**), 7.80 - 7.91 (m, *J* = 8.85 Hz, 2 H, Ar**H**), 10.39 (s, 1 H, O**H**).

^{13}C NMR (300 MHz, DMSO-d_6) δ (ppm) 26.3, 115.2, 128.6, 130.8, 162.0, 196.1. ^{1}H and ^{13}C NMR data matches that reported in the literature data.[342]

7.5.7.2 Liu et al conditions.[273]

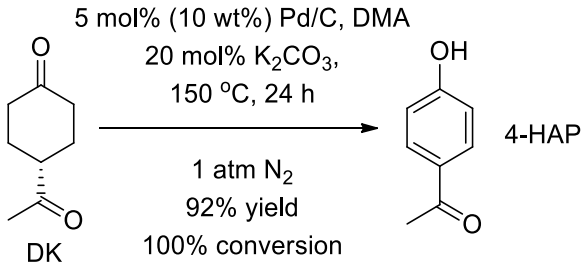

To a two-necks flask loaded with a stir bar was added the diketone (140 mg, 1 mmol), K_2CO_3 (28 mg, 0.2 mmol), 10 wt% Pd/C (52 mg, 0.052 mmol Pd) and DMA (1 ml). The flask was first degassed and then sealed with N_2 gas balloon. The reaction was heated in an oil bath to 150

°C with vigorous stirring for 24 h. After the reaction was completed, Pd/C was filtrated and 2 ml water was added to the filtrate and was washed with saturated $NaHCO_3$. The filtrate was extracted with EtOAc (6 ml ×3) and the combined organic layer was dried over anhydrous $MgSO_4$. The product was concentrated *in vacuo* and the crude residue purified by column chromatography to give 4-HAP in a 92% yield (126 mg).

7.5.7.3 Frost et al conditions.[274]

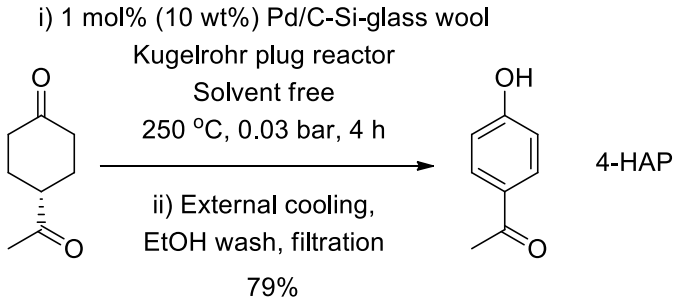

High purity grade silica gel (Sigma Aldrich), 60 Å pore size, 200-400 mesh particle size (8.5 g) was oven dried (150 °C) overnight before being cooled under an inert atmosphere and thoroughly mixed with (10 wt%) Pd/C (1 g, 1 mmol). This material was then packed into a small Kugelrohr bulb (20 mL capacity using glass wool to plug the bulb and immobilize the supported catalyst. The diketone (14 g, 100 mmol) was charged to a 50 mL Kugelrohr bulb attached prior to the catalyst containing bulb with a 25 mL receiver flask positioned after the catalyst bulb. The flasks containing the diketone and the catalyst were then inserted into the Kukelrohr oven and heated to 250 °C under a constant vacuum (0.03 bar) with slow rotation for 4 h. The receiver flask was continuously cooled and a white solid accumulated over a period of several hours which was recovered by washing with methanol. Evaporation *in vacuo* gave a 79% yield (10.7 g) of a white solid that can either be used directly in the subsequent step or purified *via* recrystallized from water.

7.5.8 Step 6. Procedures for the Beckmann rearrangement

7.5.8.1 Solvent free hydroxylamine hydrochloride Beckmann method – Vavasori method

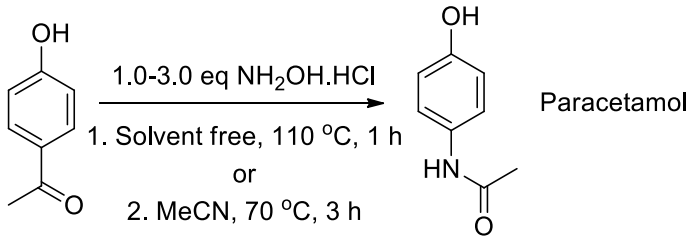

Paracetamol- (55)

N-(4-hydroxyphenyl)acetamide

4-hydroxyacetophenone (680 mg, 5 mmol), $NH_2OH.HCl$ (350 mg, 5 mmol) were mixed solvent free and upon heating turned into a melt mixture. The reaction flask was heated to 110 °C for 1 h and reaction progress monitored by tlc. Upon cooling, the mixture was washed with ice cold water and then recrystallized from hot water to give pure paracetamol as a white solid in 81% yield (611 mg).

^{1}H NMR (300 MHz, DMSO-d_6) δ ppm; 1.97 (s, 3H, C(O)C**H**$_3$), 6.66 (d, 1H, *J*= 8.7 Hz Ar**H**), 7.33 (d, 1H, *J*= 9.0 Hz, Ar**H**), 9.16 (s, 1H, CHC(O**H**)CH), 9.66 (s, 1H, C(N**H**)C(O)).

^{13}C NMR (300 MHz, DMSO-d_6) δ ppm; 23.79, 115.03, 120.82, 131.07, 153.15, 167.57. ^{1}H and ^{13}C NMR data matches that reported in the literature.[277]

7.5.8.2 Zinc oxide method

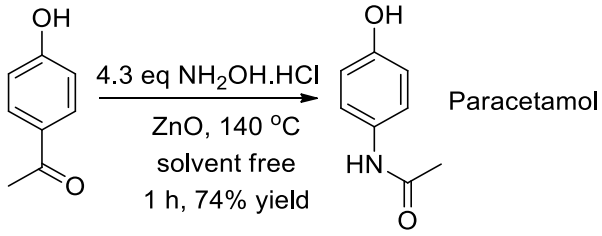

4-hydroxyacetophenone (1 mmol), $NH_2OH.HCl$ (0.3 g, 4.3 mmol) and ZnO (0.16 g, 2 mmol) were mixed sufficiently in a 10 mL round-bottomed flask equipped with a magnetic stirrer and heated in an oil bath at 140 °C for 2 h solvent free. Reaction progress was monitored by tlc and the resulting mixture was extracted with ethyl acetate (15 mL) and filtered to remove ZnO whilst still warm. The solvent was removed *in vacuo* to give the product which was purified by column chromatography (ethyl acetate-pet ether). Purification by column chromatography gave pure Paracetamol.

^{1}H and ^{13}C NMR data matches that reported in the literature data[277].

7.6 Procedures for the 2nd Generation synthesis of Paracetamol

7.6.1 Unsuccessful routes to pseudo-limonene using Dehydration methodologies

7.6.1.1 δ-terpineol synthesis

δ-terpineol- (65)

2-(4-methylenecyclohexyl)propan-2-ol

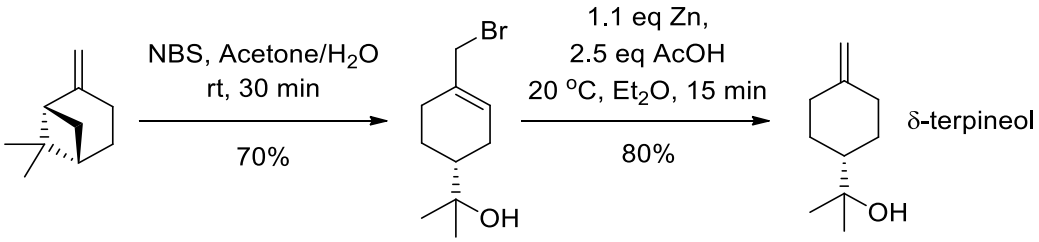

N-Bromosuccinimide (15.0 g, 85 mmol) was added in small portions to a rapidly stirred ice-cold solution of β-pinene (10 g, 75 mol) in acetone:water (4:1, 250 ml). After 30 min the mixture was poured onto water (250 ml), extracted into ether and dried ($MgSO_4$). Evaporation of the ether gave a pale yellow oil (16 g). This intermediate degraded with loss of bromine very quickly therefore used immediately to form delta terpineol. Zinc dust (5 g, 76 mmol) was added to a rapidly stirred ice-cold solution of this oil dissolved in diethyl ether (200 ml) and acetic acid (50 ml, 190 mmol). After 30 min the reaction mixture was extracted repeatedly with sodium bicarbonate solution (saturated aqueous), and then dried ($MgSO_4$), and the solvent was removed to afford a yellow oil (12 g). Purification by silica column chromatography in 1:4 EtOAc:Pet Ether afforded δ-terpineol 56% yield over 2 steps (6.4 g).

^{1}H NMR (300 MHz, CHLOROFORM-d) δ (ppm) 1.11 (dd, *J* = 12.43, 4.14 Hz, 2 H, ring **H**), 1.17 (s, 6 H, C**H**$_3$), 1.36 - 1.53 (m, 2 H, ring **H**), 1.89 - 1.93 (m, 1 H, C**H**), 1.96 (dd, *J* = 4.80, 1.98 Hz, 1 H, C**H**), 2.01 - 2.07 (m, 2 H, ring C**H**$_2$), 2.31 - 2.41 (m, 2 H, ring C**H**$_2$), 4.61 (t, *J* = 1.60 Hz, 2 H, =C**H**$_2$).

^{13}C NMR (300 MHz, CHLOROFORM-d) δ (ppm) 27.0, 28.8, 34.8, 48.8, 72.8, 106.8, 149.4. ^{1}H and ^{13}C NMR data matches that reported in the literature.[282]

7.6.1.2 Unsuccessful alumina mediated dehydration of δ-terpineol

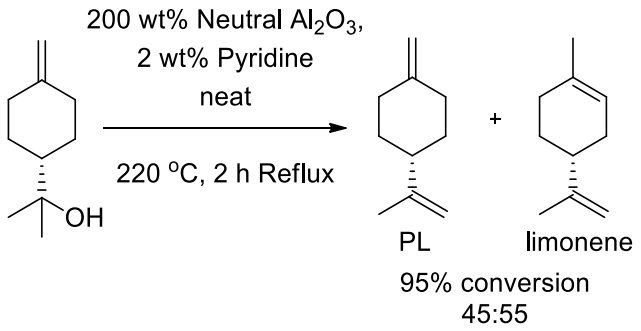

Neutral alumina (Woelm, activity grade) (2.0 g) was placed into a 25-ml flask. To this was added pyridine (0.02 to 0.04 g) and δ-terpineol (1.0 g) and the mixture was heated under reflux at 220 °C (oil bath) for 6 hours. The crude solid reaction mixture was then washed with EtOAc and filtered to remove the alumina. The product was concentrated *in vacuo* to give a crude oil that was analysed using ^{1}H NMR.

Pseudo-limonene and limonene ^{1}H and ^{13}C NMR data matches that reported previously and in the literature.[339]

7.6.2 Synthesis of pseudo-limonene *via* dehalogenation of perillyl chloride

7.6.2.1 $InCl_3$ mediated β-pinene fragmentation conditions

<u>Perillyl Chloride (PerCl)- (66)</u>

(R)-1-(chloromethyl)-4-(prop-1-en-2-yl)cyclohex-1-ene

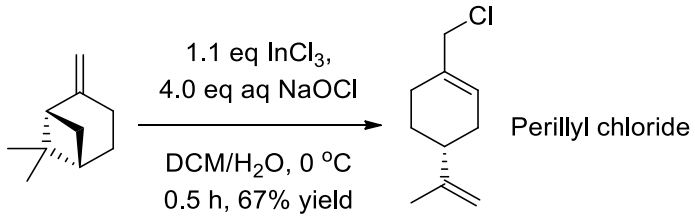

β-pinene (68 mg, 0.5 mmol) in 2.5 mL of DCM was added to a vigorously stirred solution of $InCl_3$ (121.7 mg, 0.55 mmol) in water, cooled externally with an ice bath. To the resulting mixture was added (2.5 mL, 2 mmol) of aqueous NaClO (10-13% m/v) and the reaction mixture was stirred at 0°C for 30 min. The reaction was quenched by the slow addition of saturated aqueous Na_2SO_3. The layers were separated and the aqueous layer was extracted with DCM (2 x 8 mL). The combined organic layers was dried over $MgSO_4$, and concentrated *in vacuo* and the chlorinated product was purified by column chromatography to give perillyl chloride as a pale yellow oil in a 67% yield (127 mg).

^{1}H NMR (300 MHz, CHLOROFORM-d) δ (ppm) 1.42 - 1.58 (m, 1 H, C**H**), 1.74 (s, 3 H, C**H**$_3$), 1.82 - 2.04 (m, 2 H, C**H**$_2$), 2.10 - 2.24 (m, 5 H, C**H**$_2$), 4.01 (s, 2 H, CC**H**$_2$Cl), 4.72 (dt, *J* = 6.36, 1.15 Hz, 2 H, CC**H**$_2$), 5.77 - 5.87 (m, 1 H, CC(**H**)CH$_2$).

^{13}C NMR (300 MHz, CHLOROFORM-d) δ (ppm) 20.6, 26.3, 27.2, 30.5, 40.5, 50.1, 108.8, 126.9, 134.0, 149.2. ^{1}H and ^{13}C NMR data matches that reported in the literature.[284]

7.6.3 Optimised $POCl_3$ mediated β-pinene fragmentation conditions

Perillyl Chloride (PerCl)

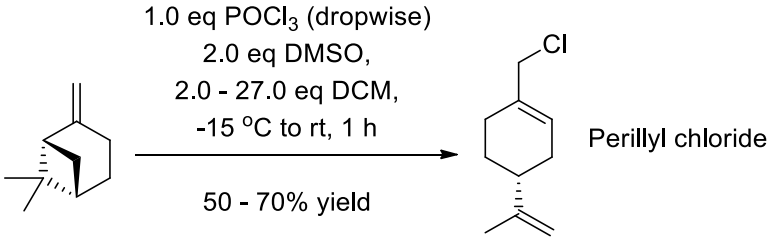

β-pinene (136 mg, 1.0 mmol) was added to a stirred solution of anhydrous dimethyl sulfoxide (0.14 mL, 2.0 mmol) in DCM (0.12 mL, 2.0 mmol) and cooled to -15 °C using an acetone bath and dry ice chips added individually. The temperature of the internal reaction mixture was monitored using a low temperature thermometer. Phosphorus oxychloride (0.093 mL, 1.0 mmol) was then added dropwise slowly over 5 minutes dropwise to the stirred solution that was then stirred for a further 1 h over an internal temperature range of -15 °C to +20 °C. 10.0 mL of EtOAc was added and the crude mixture followed by distilled water to remove DMSO. The aqueous layer was extracted three times with EtOAc and then the organic layers were then combined and dried with $MgSO_4$ followed by concentration *in vacuo* to give a pale yellow oil. This was dissolved immediately in approximately 20 mL pentane and flushed through a silica plug. A purple precipitate collects at the top of the silica plug column. The pure perillyl chloride is then concentrated once more i*n vacuo* to give perillyl chloride as a pale yellow oil in 70% yield (119 mg). ^{1}H and ^{13}C NMR data matches data previously discussed and that reported in the literature.[284]

Upon dropwise addition of $POCl_3$ an increase in temperature is observed even at low temperatures. Cooling below -20 °C halted reaction progress and led to build up of unreacted $POCl_3$ and DMSO that upon warming reacted very vigorously leading to low yields ~10-20%.

Large scale by using to the following protocol:

β-pinene (2.31 mL, 15 mmol) was added to a stirred solution of anhydrous dimethyl sulfoxide (2.13 mL, 30 mmol) in 20 mL DCM and cooled to -15 °C using an acetone bath and dry ice chips added individually. The temperature of the internal reaction mixture was monitored using a low temperature thermometer. Phosphorus oxychloride (1.4 mL, 15 mmol) was dissolved in 5 mL of DCM and then added dropwise at a rate of approximately 1 drop per second slowly over 25 minutes to the stirred solution. The internal temperature was maintained between -15

and -10 °C throughout the addition of $POCl_3$. Reaction progress was monitored by tlc. Upon complete addition of $POCl_3$ the reaction vessel was removed from the cooling bath and the internal temperature increased to rt. All starting material had reacted by tlc at which point 50 mL of DCM was added followed by 20 mL of distilled water was added slowly over 5 minutes. The reaction mixture was then transferred to a separation funnel and additional water was added to wash out the DMSO. The aqueous layer was extracted three times with DCM and the organic layers were then combined and dried with $MgSO_4$ that turned the cloudy white organic solution clear. Gravity filtration to remove the drying agent and concentration *in vacuo* gave a pale yellow oil. This was dissolved immediately in approximately 20 mL pentane and flushed through a silica plug that was further flushed with pentane. A purple precipitate collected at the top of the silica plug column. The semi-pure perillyl chloride was then concentrated once more i*n vacuo* and purified by column chromatography to give pure perillyl chloride as a pale yellow oil in 50% yield (1.24 g). ^{1}H and ^{13}C NMR data matched data previously discussed and that reported in the literature.[284]

7.6.4 Zinc/AcOH mediated dehalogenation of perillyl chloride to pseudo-limonene

Pseudo-limonene- (62)

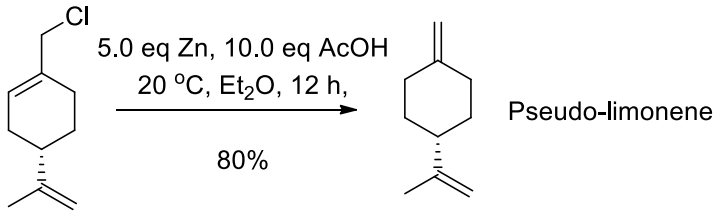

To a stirred solution of perillyl chloride (850 mg, 5 mmol) Zinc dust (1.65 g, 25 mmol) dissolved in Et_2O (10 ml) at 0 °C was added acetic acid (28 ml, 50 mmol) dropwise. The reaction mixture was warmed to room temperature and after 12 hours stirring at room temperature the reaction mixture was extracted repeatedly with sodium bicarbonate solution (saturated aqueous), and then dried $MgSO_4$, and the solvent was removed with *in vacuo* (no heating and light vacuum due to pseudo-limonene volatility) to afford a yellow oil that was purified by chromatography through a silica plug with a 100% petroleum ether flush to afford pseudo-limonene in a 80% yield (540 mg).

^{1}H NMR (500 MHz, CHLOROFORM-d) δ (ppm) 1.30 (m, 2H, C**H**$_2$), 1.72 (s, 3H, C**H**$_3$), 1.38 – 2.88 (m, 7H, C**H**$_2$/C**H**), 4.63 (s, 2H, C=C**H**$_2$), 4.69 (s, 2H, C=C**H**$_2$).

^{13}C NMR (500 MHz, CHLOROFORM-d) δ (ppm) 20.8, 20.9, 33.1, 34.8, 34.9, 45.1, 107.0, 108.5, 149.4, 150.2. ^{1}H and ^{13}C NMR data matches that discussed earlier and reported in the literature.[339]

7.7 Procedures for the Stereoselective Synthesis of PMD isomers

7.7.1 Procedure for the selective synthesis of "trans-diol" PMD isomer A

7.7.1.1 Epoxidation of (−)-Isopulegol

(-)-Isopulegol epoxide – (29)

5-methyl-2-((R)-2-methyloxiran-2-yl)cyclohexanol

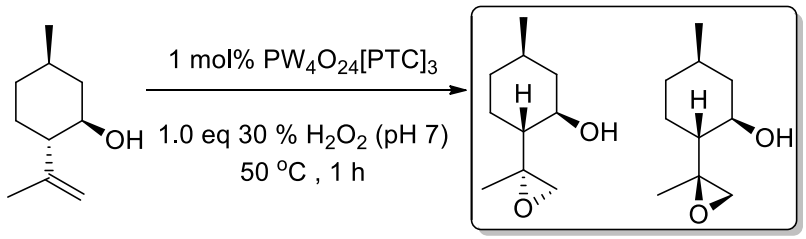

63% yield
60 : 40
(-)-Isopulegol epoxide

(−)-Isopulegol (0.77 g, 5 mmol), $PW_4O_{24}[PTC]_3$ (0.11 g, 2259 $gmol^{-1}$, 0.05 mmol, 1 mol%) were added to a 20 mL glass carousel tube with a stirrer bar. The catalyst and substrate were stirred for 10 minutes to fully dissolve the catalyst and then 30% aqueous hydrogen peroxide solution (0.5 mL, 5 mmol) (buffered to pH 7 with 0.5M NaOH) was added slowly forming a biphasic mixture. To prevent exothermic runaway the tube was cooled with a water bath and stirring was maintained at the lowest possible rpm. The reaction was stirred at room temperature for 1 h at 50°C. The reaction was judged to be complete following by tlc. The solution was left to settle with no stirring allowing the biphasic system to separate out into its two layers. The top organic layer was then decanted off and purified *via* column chromatography (or fractional distillation under reduced pressure) to produce the desired (−)-Isopulegol epoxide as a clear oil in 63% yield (0.53 g).

^{1}H NMR (500 MHz, CHLOROFORM-d); δ (ppm) 0.81 - 0.89 (m, 1 H), 0.90 - 0.92 (d, *J* =3.2 Hz, 3 H, CHC**H**$_3$), 0.93 - 1.08 (m, 2 H, ring C**H**$_2$), 1.21 (dd, *J* = 12.72, 3.42 Hz, 1 H, ring C**H**), 1.30 (s, 3 H, CC**H**$_3$), 1.38 - 1.49 (m, 1 H, ring C**H**), 1.62 - 1.73 (m, 2 H, ring C**H**$_2$), 1.96 - 2.05 (m, 1 H, ring C**H**), 2.52 (d, *J* = 4.89 Hz, 1 H, C(O)C**H**$_2$), 2.57 (d, *J* = 4.40 Hz, 1 H, C(O)C**H**$_2$), 3.69 (td, *J* = 10.52, 4.40 Hz, 1 H, C**H**(OH)).

^{13}C NMR (500 MHz, CHLOROFORM-d); δ (ppm) 16.9, 22.0, 27.6, 30.9, 33.9, 43.5, 51.1, 52.7, 59.1, 71.2. ^{1}H and ^{13}C NMR data matches that reported in the literature.[134]

7.7.1.2 Procedure for the reduction of (−)-Isopulegol epoxide diastereomer mixture

<u>*trans*-p-menthane-3,8-diol A (PMD-A)- (67)</u>

(1R,2R,5R)-2-(2-hydroxypropan-2-yl)-5-methylcyclohexanol

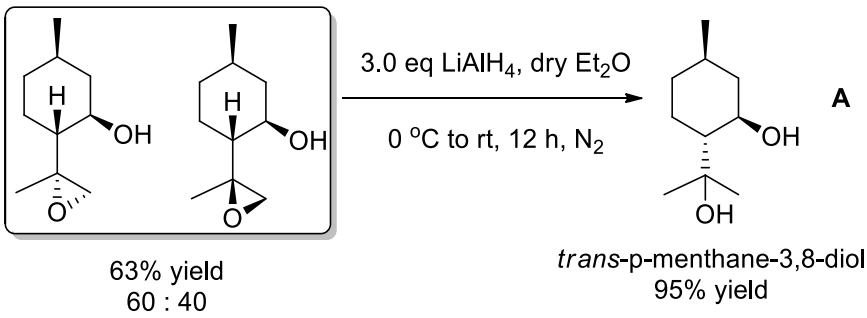

(−)-Isopulegol epoxide (85 mg, 0.5 mmol) was added to a solution of 3 ml of anhydrous Et_2O and the flask purged with N_2 gas. The mixture was cooled to 0°C and 1 M $LiAlH_4$ in THF (1.5 ml, 1.5 mmol) was added dropwise over 5 minutes the stirred epoxide solution. The reaction mixture was stirred for 12 hours and allowed to warm slowly to room temperature. The reaction was judged complete by tlc and distilled water was added dropwise over 20 minutes to quench the excess $LiAlH_4$. The crude mixture was then transferred to a separation funnel and extracted with excess Et_2O and the combined organic layers washed with saturated ammonium chloride and dried using $MgSO_4$ and concentrated *in vacuo* and purified by column chromatography to give a white crystalline solid PMD diastereomer A in a 78% yield (67 mg).

^{1}H NMR (500 MHz, CHLOROFORM-d) δ (ppm) 0.87 - 0.92 (m, 1 H, ring C**H**), 0.92 (d, *J* = 6.85 Hz, 3 H, CHC**H**$_3$), 0.97 (m, 1 H, ring C**H**), 0.99 - 1.10 (m, 1 H, ring C**H**), 1.19 - 1.29 (m, 6 H, CC**H**$_3$), 1.34 - 1.47 (m, 2 H, ring C**H**$_2$), 1.62 - 1.73 (m, 2 H, ring C**H**$_2$), 1.92 - 1.98 (m, 1 H, ring C**H**), 3.73 (dt, *J* = 10.27, 5.14 Hz, 1 H, C**H**(OH)).

^{13}C NMR (500 MHz, CHLOROFORM-d) δ (ppm) 22.0, 23.7, 27.1, 30.1, 31.4, 34.5, 44.6, 53.4, 72.9, 75.0. ^{1}H and ^{13}C NMR data matches that reported in the literature.[297]

7.7.2 Procedures for the selective synthesis of "cis-diol" PMD isomer B

7.7.2.1 Preparation of isopulegol benzoate ester

(-)-Isopulegol benzoate ester- (71)

(1S,2R,5R)-5-methyl-2-((S)-2-methyloxiran-2-yl)cyclohexyl 4-nitrobenzoate

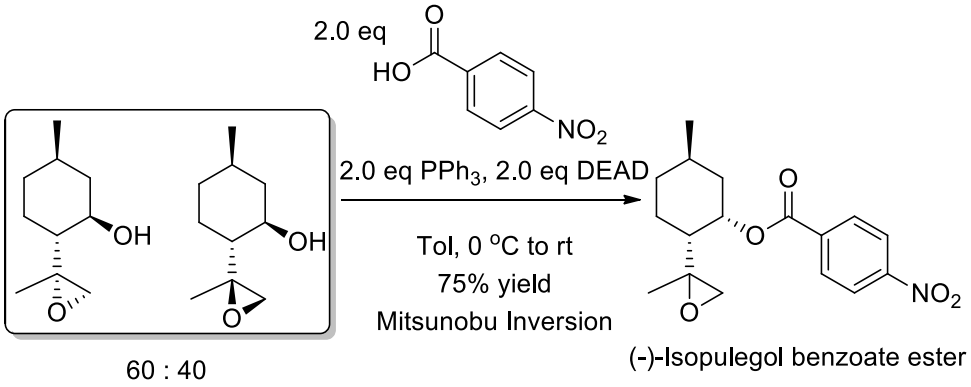

To a stirred solution of (-)-isopulegol epoxide (340 mg, 2 mmol), 4-nitrobenzoic acid (668 mg, 4 mmol), and PPh_3 (1.05 g, 4 mmol) in toluene (10 mL) was added DEAD (696 mg, 0.62 ml, 4 mmol) at 0 °C. The reaction mixture was allowed to warm to rt and stirred at that temperature for 2 h before it was diluted with diethyl ether (20 mL) and filtered. The filter cake was washed with diethyl ether (30 mL). The filtrate was concentrated under vacuum, and the residue was purified by silica column chromatography to give a crystalline white product in a 75% yield (0.48 g).

^{1}H NMR (500 MHz, CHLOROFORM-d) diastereomer mixture; δ (ppm) 0.91 (dd, *J* = 6.36, 5.38 Hz, 3 H, CHC**H**$_3$), 0.98 - 1.13 (m, 1 H, ring C**H**), 1.24 - 1.32 (m, 3 H, CC**H**$_3$), 1.35 (s, 1 H, ring C**H**), 1.49 - 1.60 (m, 1 H, ring C**H**), 1.71 - 1.93 (m, 3 H, ring C**H**/**H**$_2$), 2.10 (dd, *J* = 14.18, 3.42 Hz, 1 H, ring C**H**), 2.43 (d, *J* = 4.40 Hz, 1 H, ring C**H**), 2.50 (d, *J* = 4.89 Hz, 1 H, C(O)C**H**$_2$), 2.64 - 2.75 (m, 1 H, C(O)C**H**$_2$), 5.57 (br. s., 1 H, C**H**(OH)), 8.13 - 8.34 (m, 4 H, Ar**H**).

^{13}C NMR (500 MHz, CHLOROFORM-d) diastereomer mixture; δ (ppm) 20.0, 20.8, 22.0, 22.0, 26.7, 27.0, 34.0, 39.1, 45.5, 45.9, 51.9, 52.0, 72.4, 72.7, 123.7, 123.7, 130.5, 130.7.

7.7.2.2 Nitrobenzoate ester cleavage to isopulegol epoxide

(+)-Isopulegol epoxide- (72)

(1S,2R,5R)-5-methyl-2-((S)-2-methyloxiran-2-yl)cyclohexanol

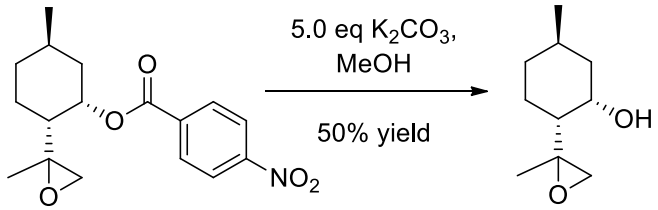

Isopulegol nitrobenzoate (1 mmol, 319 mg) was dissolved in MeOH (5 mL) in a flask. The reaction mixture was stirred at room temperature and K_2CO_3 (360 mg, 5 mmol) was added and stirred for 1 hour at room temperature. The crude reaction mixture was filtered and evaporated to remove the MeOH and then diluted with DCM and washed with 2 M NaOH followed by saturated NaCl (upon which one epoxide diastereomer proved unstable and degraded to a more polar species. Three DCM washes were performed and the combined organic layers dried with magnesium sulfate and filtered. The residue obtained upon concentration *in vacuo* was purified by column chromatography to isolate a single stable inverted isopulegol epoxide diastereomer product in 50% yield (85 mg).

^{1}H NMR (500 MHz, CHLOROFORM-d) δ (ppm) 0.85 - 0.89 (m, 3 H, CHC**H**$_3$), 0.89 - 0.95 (m, 1 H), 1.01 - 1.09 (m, 1 H), 1.12 - 1.19 (m, 1 H), 1.21 (s, 1 H), 1.39 - 1.41 (s, 3 H, CC**H**$_3$), 1.46 - 1.55 (m, 2 H), 1.73 (dt, *J* = 13.08, 2.75 Hz, 1 H), 1.81 (d, *J* = 6.36 Hz, 1 H), 2.49 (d, *J* = 4.40 Hz, 1 H, C(O)C**H**$_2$), 2.62 (br. s., 1 H, O**H**), 2.81 (d, *J* = 4.40 Hz, 1 H, C(O)C**H**$_2$), 4.32 (br. s., 1 H, C**H**(OH)).

^{13}C NMR (500 MHz, CHLOROFORM-d) δ (ppm) 21.8, 22.1, 22.2, 25.5, 34.5, 41.9, 44.2, 51.3, 60.2, 67.8. ^{1}H and ^{13}C NMR data matches that reported in the literature.[343]

7.7.2.3 Reduction of Isopulegol epoxide diastereomer to PMD isomer B

<u>*cis*-p-menthane-3,8-diol B (PMD-B)- (68)</u>

(1S,2R,5R)-2-(2-hydroxypropan-2-yl)-5-methylcyclohexanol -

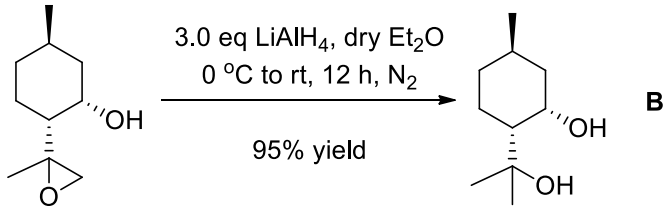

(+)-Isopulegol epoxide (85 mg, 0.5 mmol) was added to a solution of 3 ml of anhydrous Et_2O and the flask purged with N_2 gas. The mixture was cooled to 0 °C and 1 M $LiAlH_4$ in THF (1.5 ml, 1.5 mmol) was added dropwise over 5 minutes the stirred epoxide solution. The reaction mixture was stirred for 12 hours and allowed to warm slowly to room temperature. The reaction was judged complete by tlc and distilled water was added dropwise over 20 minutes to quench the excess $LiAlH_4$. The crude mixture was then transferred to a separation funnel and extracted with excess Et_2O and saturated ammonium chloride. The combined organic layers were then washed with brine and dried using $MgSO_4$ and concentrated *in vacuo* to give a white crystalline solid PMD diastereomer B in a 95% yield (82 mg).

^{1}H NMR (300 MHz, CHLOROFORM-d) δ (ppm) 0.87 - 0.89 (m, 3 H, CHC**H**$_3$), 1.06 (s, 1 H, ring C**H**), 1.10 - 1.21 (m, 2 H, ring C**H**$_2$), 1.23 (s, 3 H, CC**H**$_3$), 1.37 (s, 3 H, CC**H**$_3$), 1.63 - 1.74 (m, 2 H, ring C**H**$_2$), 1.74 - 1.89 (m, 3 H, ring C**H**/**H**$_2$), 4.41 (d, *J* = 2.64 Hz, 1 H, C**H**(OH)).

^{13}C NMR (300 MHz, CHLOROFORM-d) δ (ppm) 20.2, 22.2, 25.6, 28.9, 28.9, 34.8, 42.4, 48.2, 68.1, 73.3. ^{1}H and ^{13}C NMR data matches that reported in the literature.[343]

7.7.3 Procedures for the selective synthesis of "all cis" PMD isomer C

7.7.3.1 Step 1.Allylic oxidation of (-)-α-Pinene

7.7.3.1.1 $[Co(pyr)_2Br_2]$ Catalyst Preparation:
A hot ethanolic solution of hydrated cobalt bromide (1.0 mol) was mixed with a hot ethanolic solution of 4-methylpyridine (2.5 mol.). On cooling, blue crystals separated. The Product was recrystallised from ethanol, washed with cold DCM, and dried in air to give pure, blue solid $[Co(pyr)_2Br_2]$.[344]

7.7.3.1.2 Allylic oxidation using molecular oxygen method:[345]

<u>(1S)-(-)-Verbenone- (73)</u>

(1S,5S)-4,6,6-trimethylbicyclo[3.1.1]hept-3-en-2-one

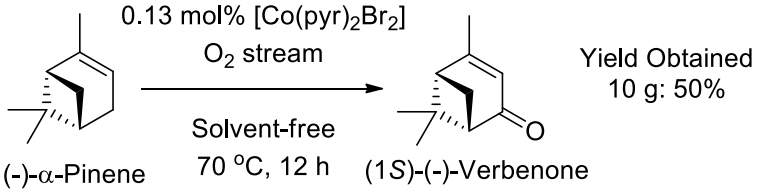

(-)-α-Pinene (5.0 g, 0.037 mol) air oxidation was performed in a glass rbf with a condenser attached and a needle delivering oxygen directly into the pinene organic layer. An oil bath heated to 70 °C heated the organic/catalyst solution. Co(II) catalyst (0.15 mol%) was added to the neat pinene and molecular oxygen was passed through the solution to achieve vigorous bubbling under atmospheric pressure. Heating and oxygen bubbling was continued for 12 hours at 70 °C. The crude verbenone was then diluted with diethylether and filtered through celite to remove the catalyst. The solvent was removed *in vacuo* and purified by column chromatography to give (S)-(-)-Verbenone in a 50% yield[345].

^{1}H NMR (300 MHz, CHLOROFORM-d) δ (ppm) 1.00 (s, 3 H, CC**H**$_3$), 1.48 (s, 3 H, CC**H**$_3$), 1.96 - 2.02 (m, 3 H, =CC**H**$_3$), 2.07 (d, *J* = 9.04 Hz, 1 H, CH_2C**H**), 2.41 (t, *J* = 5.84 Hz, 1 H, CH_2C**H**), 2.63 (t, *J* = 5.84 Hz, 1 H, CHC**H$_2$**), 2.79 (dt, *J* = 9.23, 5.46 Hz, 1 H, CHC**H$_2$**), 5.71 (s, 1 H, =C**H**).

^{13}C NMR (300 MHz, CHLOROFORM-d) δ (ppm) 22.0, 23.5, 26.5, 40.8, 49.6, 54.0, 57.5, 121.1, 170.2, 204.0. ^{1}H and ^{13}C NMR data matches that reported in the literature.[346]

$[\alpha]^{20}_D$: -185° (MeOH)

7.7.3.2 Step 2. Procedure for the reduction of verbenone

<u>*cis*-(S)-verbenol- (74)</u>

(1S,2S,5S)-4,6,6-trimethylbicyclo[3.1.1]hept-3-en-2-ol

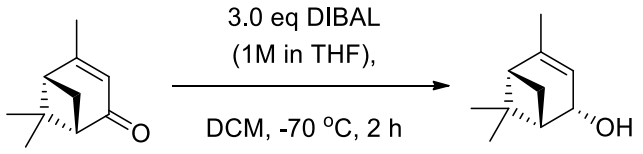

(1S)-(-)-Verbenone *cis*-(S)-verbenol

To a solution of verbenone (0.50 g, 3.3 mmol) in 50 mL of anhydrous DCM was added dropwise at -70 °C in an nitrogen atmosphere 4 mL of 1 M $(i\text{-}Bu)_2AlH$ solution in hexane, the mixture was stirred for 2 h at the same temperature. 10 mL of H_2O was added and the stirring was continued for 0.5 h. The separated precipitate was washed with EtOAc and saturated ammonium chloride. The solid precipitate was filtered and re-washed with excess EtOAc three times. The organic layers were combined and washed with brine and then were dried with $MgSO_4$ and evaporated. The crude mixture was purified by column chromatography to give pure verbenol in a yield of 62% (0.31 g).

Note the verbenol Rf value is very similar to the starting material, mini NMR the reaction mixture to check fully reacted.

^{1}H NMR (300 MHz, CHLOROFORM-d) δ (ppm) 1.09 (s, 3 H, CC**H**$_3$), 1.30 (s, 1 H, C**H**), 1.36 (s, 3 H, CC**H**$_3$), 1.61 (s, 1 H, C**H**), 1.74 (t, *J* = 1.70 Hz, 3 H, =CC**H**$_3$), 1.93 - 2.02 (m, 1 H, =CC**H**), 2.30 (dd, *J* = 3.39, 2.07 Hz, 1 H, CC**H**$_2$), 2.45 (ddd, *J* = 9.04, 6.22, 5.27 Hz, 1 H, (OH)CC**H**), 4.47 (br. s., 1 H, O**H**), 5.37 (td, *J* = 3.01, 1.51 Hz, 1 H, =C**H**).

^{13}C NMR (300 MHz, CHLOROFORM-d) δ (ppm) 22.3, 22.4, 26.6, 35.3, 38.7, 47.5, 48.0, 73.3, 119.1, 147.2. ^{1}H and ^{13}C NMR data matches that reported in the literature.[311]

$[\alpha]^{20}_D$: +12° (MeOH)

7.7.3.3 Step 3. Procedure for bromine mediated ring opening

<u>*Trans*-Bromoacetonide (*trans*-BrAc)- (75)</u>

(4aR,8R,8aR)-8-bromo-2,2,4,4,7-pentamethyl-4a,5,8,8a-tetrahydro-4H-benzo[d][1,3]dioxine

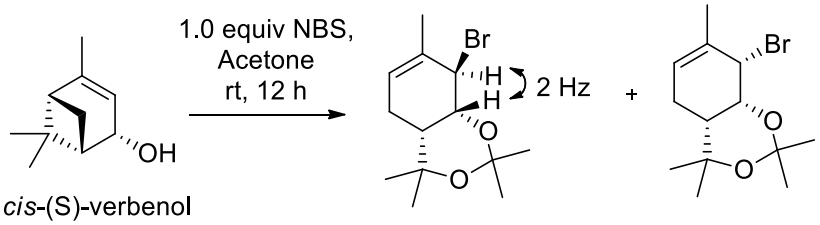

cis-(S)-verbenol

trans-BrAc : *cis*-BrAc
9 : 1
68% yield

To a solution of NBS (3.6 g, 20 mmol) in acetone (40 mL) is added a solution of verbenol (3.0 g, 20 mmol) in acetone (40 mL) dropwise over 15 minutes. The mixture is stirred at room temperature for 24 h, acetone is then evaporated and the residual crude paste is dissolved in pentane (40 mL). The succinimide is filtered off and the solvent evaporated. The BrAce can degrade over time so is stored within the freezer and may be columned quickly to purify. The BrAce diastereomers can be separated on the column, they appear as two spots near each other on the tlc plate. Care must be taken when performing and working up this reaction to prevent any acid coming in contact with the BrAce as this leads to rapid deprotection of the acetonide. Buchi and glassware should be rinsed with sat $NaHCO_3$ before use. The crude mixture was purified by column chromatography to give pure bromo-acetonide in a yield of 68% (4.1 g).[312]

^{1}H NMR (300 MHz, CHLOROFORM-d) δ (ppm) 1.17 (s, 3 H, OCC**H**$_3$), 1.36 (s, 3 H, OCC**H**$_3$), 1.46 (s, 3 H, OCC**H**$_3$), 1.50 (s, 3 H, OCC**H**$_3$), 1.83 - 1.90 (m, 4 H, CH/=CC**H**$_3$), 2.01 - 2.15 (m, 1 H, C**H**), 2.31 - 2.47 (m, 1 H, (O)CHC**H**), 4.40 (s, 1 H, C**H**O(C)), 4.59 (t, *J* = 1.88 Hz, 1 H, C**H**Br), 5.66 (dd, *J* = 2.92, 1.41 Hz, 1 H, C=**H**C).

^{13}C NMR (300 MHz, CHLOROFORM-d) δ (ppm) 21.6, 22.7, 24.7, 27.4, 28.5, 31.6, 32.6, 53.2, 68.8, 73.8, 99.5, 126.9, 130.3. ^{1}H and ^{13}C NMR data matches that reported in the literature.[312]

$[\alpha]^{20}_D$: -209° ($CHCl_3$)

7.7.3.4 *Step 4. Procedure for dehalogenation using $LiAlH_4$*

Allylic-Ace- (76)

(4aR,8aS)-2,2,4,4,7-pentamethyl-4a,5,6,8a-tetrahydro-4H-benzo[d][1,3]dioxine

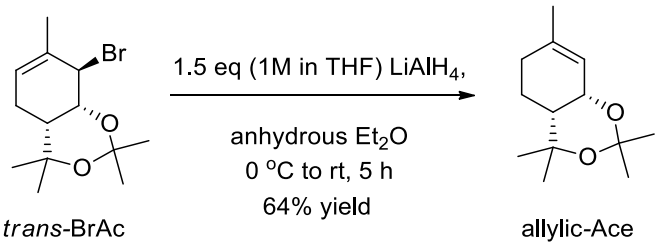

A solution of crude BrAce (1.44 g, 5 mmol) in dry Et_2O (10 mL) is added dropwise to a stirred solution of 1M $LiAlH_4$ in THF (7.5 ml, 7.5 mmol) in dry Et_2O (10 mL) at 0 °C. Stirring is continued at room temperature for 5 h, water is then carefully added to hydrolyse the hydride and the mixture is extracted with Et_2O, washed with saturated ammonium chloride and dried with $MgSO_4$. The solvent is evaporated to give crude AlkAce which was purified by column chromatography to give pure AlkAce in a 64% yield (0.74 g).

^{1}H NMR (300 MHz, CHLOROFORM-d) δ (ppm) 1.17 (s, 3 H, OCC**H**$_3$), 1.21 (t, *J* = 3.30 Hz, 1 H, ring C**H**$_2$), 1.37 (d, *J* = 2.64 Hz, 6 H, OCC**H**$_3$), 1.46 (s, 3 H, OCC**H**$_3$), 1.55 - 1.65 (m, 1 H, ring C**H**$_2$), 1.69 (s, 3 H, =CC**H**$_3$), 1.72 - 1.83 (m, 1 H, OCC**H**), 2.02 (d, *J* = 5.27 Hz, 2 H, ring C**H**$_2$), 4.34 - 4.43 (m, 1 H, OC**H**), 5.47 - 5.56 (m, 1 H, =C**H**).

^{13}C NMR (300 MHz, CHLOROFORM-d) δ (ppm) 18.4, 23.4, 24.7, 29.0, 29.6, 30.8, 31.8, 40.3, 61.6, 72.9, 98.2, 120.6, 141.3. ^{1}H and ^{13}C NMR data matches that reported in the literature.[312]

$[\alpha]^{20}_D$: +48° ($CHCl_3$)

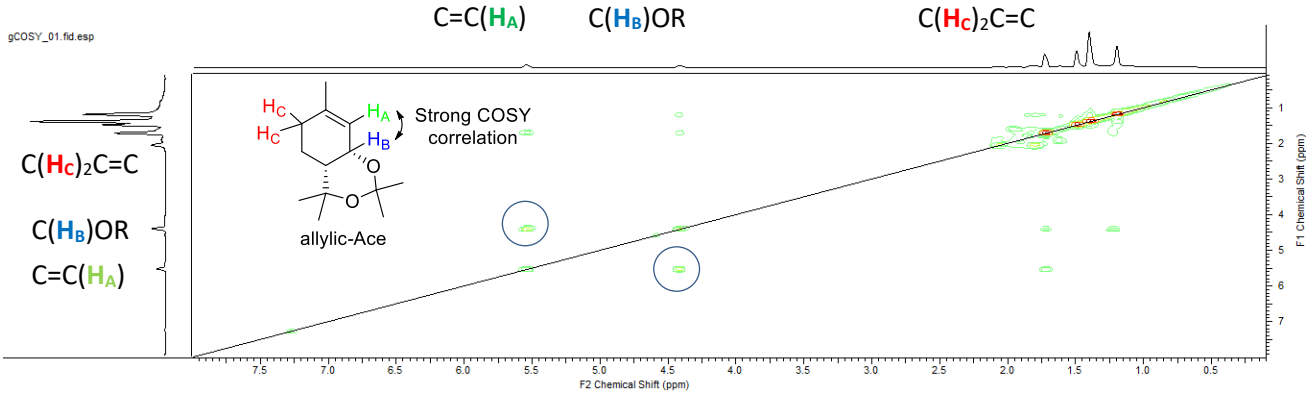

Figure 67. 2D COSY NMR of allylic Ace product showing a strong interaction between H_A and H_B

7.7.3.5 Step 5. Procedure for the catalytic hydrogenation of the alkene bond of allylic-Ace

PMD-Ace- (77)

(4aR,7S,8aS)-2,2,4,4,7-pentamethylhexahydro-4H-benzo[d][1,3]dioxine

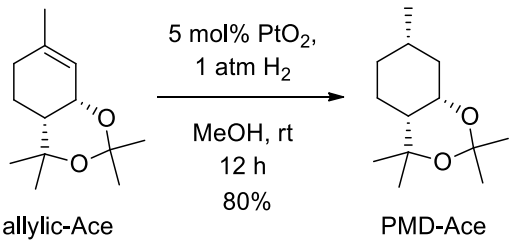

A solution of crude AlkAce (210 mg, 1 mmol) in MeOH (2 mL) is added to a stirred suspension of PtO_2 (5 mol%, 15 mg, 0.05 mmol) in MeOH (3 mL) at room temperature. A balloon of hydrogen bubbling into the reaction solution is then added and the solution flushed with hydrogen for 5 minutes. The balloon needle is left within the reaction solution throughout the duration of the reaction. Stirring is continued at room temperature for 12 h overnight. The crude reaction mixture is filtered through celite and the solvent evaporated to give pure hydrogenated product in a 80% yield (169 mg).

^{1}H NMR (300 MHz, CHLOROFORM-d) δ (ppm) 1.12 - 1.16 (m, 6 H, CHC**H**$_3$/ring C**H**$_2$), 1.35 (s, 3 H, OCC**H**$_3$), 1.39 (s, 3 H, OCC**H**$_3$), 1.43 (s, 3 H, OCC**H**$_3$), 1.45 (s, 3 H, OCC**H**$_3$), 1.46 - 1.60 (m, 2 H, ring C**H**/C**H**$_2$), 1.60 - 1.73 (m, 2 H, ring C**H**$_2$), 1.85 (s, 2 H, ring C**H**$_2$), 4.28 (d, *J* = 3.39 Hz, 1 H, OC**H**).

^{13}C NMR (300 MHz, CHLOROFORM-d) δ (ppm) 16.7, 16.8, 20.4, 24.6, 28.6, 28.9, 31.3, 32.0, 41.9, 42.0, 64.5, 73.5, 98.1. ^{1}H and ^{13}C NMR data matches that reported in the literature.[312]

$[\alpha]^{20}_{D}$: -6º ($CHCl_3$)

7.7.3.6 Step 6. Procedure for PMD-acetonide deprotection

All-*cis*-PMD (PMD-C)- (69)

(1S,2R,5S)-2-(2-hydroxypropan-2-yl)-5-methylcyclohexanol

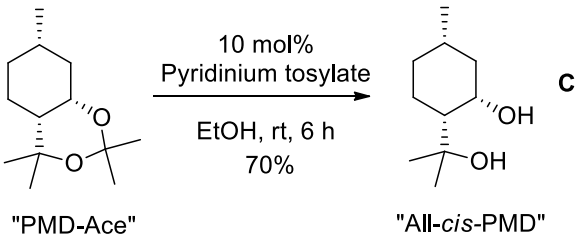

A solution of crude PMD-Ace (212 mg, 1 mmol) in EtOH (5 mL) is added to a stirred suspension of pyridinium tosylate (10 mol%, 0.1 mmol, 30 mg) in EtOH (5 mL) at room temperature and the solution is stirred for 6 h. The reaction mixture is evaporated, re-dissolved in Et_2O / DCM (3:1) and flushed through a silica plug and evaporated to give pure PMD in 70% yield (120 mg), a white crystalline solid once cooled to room temperature.

(1S,2R,5S)-2-(2-hydroxypropan-2-yl)-5-methylcyclohexanol

^{1}H NMR (500 MHz, CHLOROFORM-d) δ (ppm) 1.18 (d, *J* = 7.34 Hz, 3 H, CHC**H**$_3$), 1.22 (d, *J* = 9.29 Hz, 1 H, ring C**H**), 1.24 (s, 3 H, (OH)CC**H**$_3$), 1.34 (s, 3 H, (OH)CC**H**$_3$), 1.49 - 1.60 (m, 2 H, ring C**H**$_2$), 1.61 - 1.74 (m, 3 H, ring C**H**/C**H**$_2$), 1.89 (dd, *J* = 12.72, 3.42 Hz, 2 H, ring C**H**$_2$), 4.41 (d, *J* = 3.42 Hz, 1 H, C**H**OH)

^{13}C NMR (500 MHz, CHLOROFORM-d) δ (ppm) 15.4, 20.9, 26.2, 28.7, 28.8, 31.8, 39.2, 48.7, 69.0, 73.3.

I.R (thin film) $_{\nu}$max (cm^{-1}): O-H (3275) br, C-H (2911), C-O (1243). HRMS (ESI): m/z calculated. $C_{10}H_{20}O_2$: requires 195.1356 for $[M+Na]^+$; found: 195.1339;

$[\alpha]^{20}_D$: +17º ($CHCl_3$)

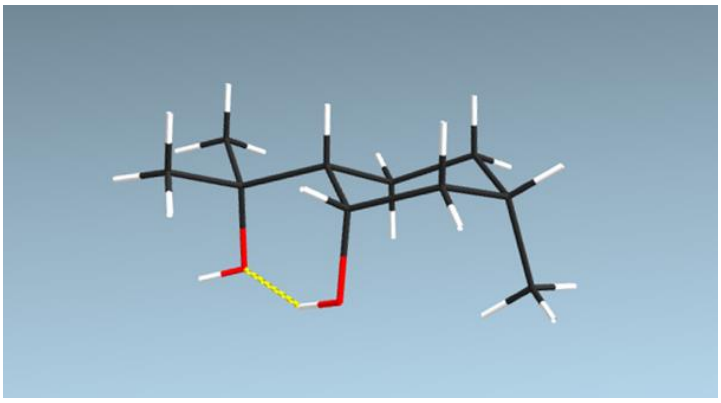

Figure 68. Crystal structure obtained of PMD isomer C

7.7.4 Procedures for the attempts towards a selective synthesis of “trans-diol” PMD isomer D

7.7.4.1 Epoxidation of pulegone

Pulegone epoxide- (17)

2,2,6-trimethyl-1-oxaspiro[2.5]octan-4-one

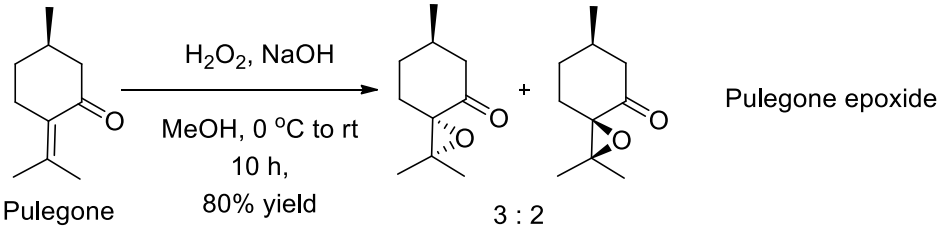

Pulegone (304 mg, 2 mmol) was dissolved in 8 ml of methanol. The mixture was cooled to 0 °C and 1.5 mL of 35% H_2O_2 was added. 1 mL of 6M aq. NaOH solution was added over a period of 1-2 minutes. The mixture was stirred at 0 °C for 15 minutes and then at room temperature for 20 minutes. The mixture was dissolved in 10 mL of CH_2Cl_2 and washed twice with water (10 mL x 2) and saturated NaCl solution and then dried with $MgSO_4$. The mixture was dried, concentrated and purified using column chromatography to give pure pulegone epoxide in a 80% yield (268 mg).[36]

^{1}H NMR (300 MHz, CHLOROFORM-d) δ (ppm) 1.03 - 1.09 (m, 3 H, C**H**$_3$), 1.20 (d, *J* = 3.39 Hz, 3 H, CHC**H**$_3$), 1.42 (s, 3 H, C**H**$_3$), 1.77 - 2.03 (m, 4 H, ring C**H**$_2$), 2.11 - 2.25 (m, 1 H, ring C**H**), 2.35 - 2.47 (m, 1 H, C**H**$_2$C(O)), 2.53 - 2.65 (m, 1 H, C**H**$_2$C(O)).

^{13}C NMR (300 MHz, CHLOROFORM-d) δ (ppm) 18.8, 19.7, 22.0, 29.9, 30.6, 33.9, 51.3, 63.2, 70.2, 207.6. ^{1}H and ^{13}C NMR data matches that reported in the literature.[320]

7.7.4.2 Unsuccessful Birch reduction of pulegone epoxide to PMD isomer mixture- (67) / (70)

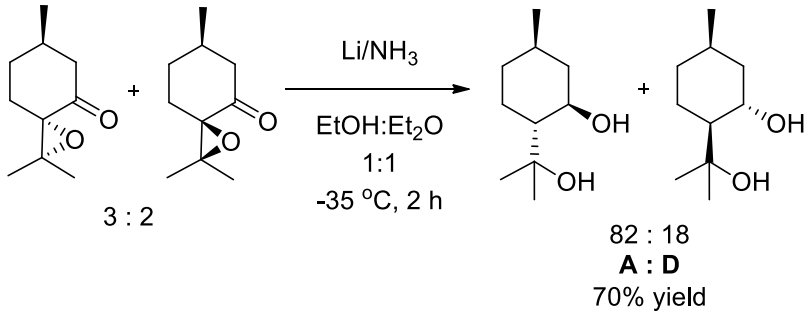

A solution of pulegone epoxide (336 mg, 2 mmol) in a (1:1) mixture of diethyl ether:absolute ethanol (40 ml) and lithium (170 mg, 24 mmol) were successively added to a cold (-35 °C) stirred liquid ammonia (120 ml) under nitrogen over 40 minutes with each addition turning the stirred solution deep blue, that dissipated after thorough mixing, returning to its clear state. The mixture was warmed to room temperature and the excess of ammonia evaporated. The residue obtained was extracted with diethyl ether, washed with brine and concentrated *in vacuo* to give the crude product that was then purified by column chromatography to obtain pure inseparable diastereomer mixture of PMD isomers A and D in a 71% yield (315 mg).

^{1}H NMR (500 MHz, CHLOROFORM-d) diastereomer mixture; δ (ppm) 0.88 - 0.92 (m, 3 H, C**H**$_3$), 0.92 - 1.08 (m, 2 H, ring C**H**$_2$), 1.10 - 1.31 (m, 6 H, C**H**$_3$), 1.31 - 1.54 (m, 2 H, ring C**H**$_2$), 1.56 - 1.73 (m, 2 H, ring C**H**$_2$), 1.86 - 1.97 (m, 2 H, ring C**H**$_2$), 3.69 (td, *J* = 10.27, 4.40 Hz, 0.82 H, C**H**OH), 3.94 (m, 0.18H, C**H**OH).

^{13}C NMR (500 MHz, CHLOROFORM-d) diastereomer mixture; δ (ppm) 18.2, 21.9, 22.0, 23.6, 23.7, 27.0, 28.1, 29.6, 29.8, 29.9, 30.3, 31.2, 31.3, 34.5, 41.4, 44.5, 53.3, 54.4, 68.6, 72.8, 75.0, 75.0. ^{1}H and ^{13}C NMR data for isomer A[297] and D[347] consistent with previous literature.

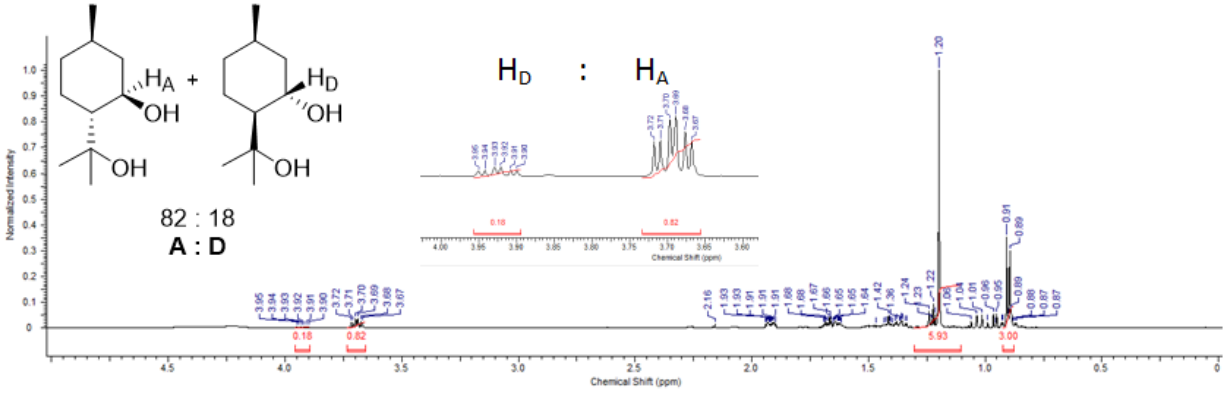

Figure 69. ^{1}H NMR of PMD isomer mixture

8 Appendix

Table. Optimisation of Venturello conditions for monoterpene epoxidations in flow

Experiment	Catalyst loading / %	Equiv H_2O_2	H_2O_2 / %	pH	Equiv Na_2SO_4	Temp / °C	Reactor Volume / mL	Residence time / min	Flow rate Organic / mL/hr	Flow rate H_2O_2 / mL/hr	Conv / %	Epoxide Yield / %
1. Limonene	1	1.6	30	7	-	50	9.0	30	11.6	6.4	77	71
2. Limonene	3	1.6	30	7	-	50	4.5	15	11.6	6.4	100	85
3. 3-carene	1	1.6	30	7	-	50	9.0	30	11.6	6.4	75	73
4. 3-carene	3	1.6	30	7	-	50	9.0	30	11.6	6.4	100	97
5. α-pinene	1	1.6	30	7	0.3	50	9.0	40	8.7	4.8	36	36
6. α-pinene	3	1.6	30	7	0.3	60	9.0	30	11.6	6.4	70	70
7. α-pinene	6	1.6	30	7	0.3	60	6.0	20	11.6	6.4	88	81
8. β-pinene	5	2.6	50	7	0.3	75	1.5	1.65	34.6	19.4	55	55
9. β-pinene	5	2.6	50	7	0.3	75	1.5	0.83	69.2	38.8	41	41
10. β-pinene	5	2.6	50	7	0.3	75	3.0	1.65	69.2	38.8	49	5
11. CST	5	1.6	30	7	0.3	60	4.5	15	11.6	6.4		α-p: 60% 3-car : 98%
12. CST	5	1.6	30	7	0.3	60	7.5	25	11.6	6.4		3-car : 90%

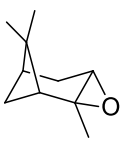

α-Pinene epoxide

81% yield
20 minutes

β-Pinene epoxide

55% yield
1.65 minutes

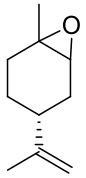

1,2 limonene epoxide

85% yield
15 minutes

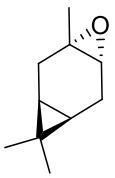

3-Carene epoxide

97% yield
30 minutes

Table 12. Optimisation of Venturello conditions for β-pinene epoxidation in flow

Entry	Venturello Cat Loading (mol%) X	H_2O_2 eq Y	H_2O_2 Strength (%)	Res Time (min)	Temp (°C) Z	Reactor Volume (mL)	Sm Remaining (%)	Complex by-product mixture 3.5-4.0 ppm	Yield of β-Pinene Epoxide (%)[a]
1 964	1	2.6	50	30	50	9	93	-	6[a]
2 964	1	2.6	50	40	50	9	+90[b]	Present	0[c]
3 965	1	2.6	50	30	25	9	97	-	3[a]
4 965	1	2.6	50	30	35	9	+90[b]	Present	0[c]
5 965	1	2.6	50	40	35	9	+90[b]	Present	0[c]
6 966	1	2.6	50	5	50	4.5	93	-	7[a]
7 966c	1	2.6	50	5	65	4.5	82	-	18[a]
8 967c	1	2.6	50	5	75	4.5	78	-	22[a]
9 967c'	1	2.6	50	3.3	75	3.0	82	-	18[a]
10 967e	1	2.6	50	6.6	75	6.0	76	-	24[a]
11 967g	1	2.6	50	10	75	9	+70[b]	Present	>16[b]
12 974a	2	2.6	50	1.25	70	4.5	76	-	24[a]
13 974a''	2	2.6	50	1.95	70	7	+70[b]	Present	>9[b]
14 983a	5	2.6	50	1.67	75	1.5	45	-	55[a]
15 983b	5	2.6	50	3.3	75	3.0	+40[b]	Present, Sig[n]	>50[b]
16	5	2.6	50	6.6	75	6.0	+30[b]	Present, Sig[n]	0[c]
17	10	2.6	50	1.67	75	1.5	+40[b]	Present	>52[b]

[a]Yields were determined by monitoring substrate consumption *via* ^{1}H NMR and calculated using starting material 4.63 ppm ^{1}H alkene peak : product 2.79 ppm ^{1}H epoxy peak ratios, x%

conversion x 100% selectivity = yield. [b]Approximated starting material/epoxide % amounts determined by ^{1}H NMR integrations. Presence of unknown by-product complex mixture prevented exact starting material/epoxide % amount calculations. [c]Absolute yields of epoxide determined by absence of epoxy H at 2.79ppm *via* ^{1}H NMR.

8.1 X-ray Crystallography data for PMD isomer C

Table 1. Crystal data and structure refinement for s17sdb1.

Identification code	s17sdb1	
Empirical formula	C10 H20 O2	
Formula weight	172.26	
Temperature	150.00(10) K	
Wavelength	1.54184 Å	
Crystal system	Orthorhombic	
Space group	$P2_12_12_1$	
Unit cell dimensions	a = 10.9450(7) Å	□= 90°.
	b = 10.3459(7) Å	□= 90°.
	c = 9.1458(5) Å	□ = 90°.
Volume	1035.63(11) Å^3	
Z	4	
Density (calculated)	1.105 Mg/m^3	
Absorption coefficient	0.587 mm^{-1}	
F(000)	384	
Crystal size	0.300 x 0.150 x 0.050 mm^3	
Theta range for data collection	5.885 to 72.987°.	
Index ranges	-12<=h<=13, -12<=k<=12, -8<=l<=11	
Reflections collected	7018	
Independent reflections	2042 [R(int) = 0.0420]	
Completeness to theta = 67.684°	99.9 %	
Absorption correction	Semi-empirical from equivalents	
Max. and min. transmission	1.00000 and 0.57769	
Refinement method	Full-matrix least-squares on F^2	
Data / restraints / parameters	2042 / 0 / 120	
Goodness-of-fit on F^2	1.070	
Final R indices [I>2sigma(I)]	R1 = 0.0400, wR2 = 0.0929	
R indices (all data)	R1 = 0.0497, wR2 = 0.0957	
Absolute structure parameter	-0.02(15)	
Extinction coefficient	n/a	
Largest diff. peak and hole	0.146 and -0.163 e.Å^{-3}	

9 References

1. G. H. Brundtland, *Report of the World Commission on Environment and Development : Our Common Future*, 1987.

2. U. of York, *The Chemicals Industry, CIECPromotingScience.com, Date Accessed 30.8.15*, 2013.

3. P. T. Anastas and J. C. Warner, *Green Chemistry: Theory and Practice*, Oxford University Press, 1998.

4. A. J. D. Silvestre and A. Gandini, *Terpenes : Major Sources , Properties and Applications*, 2008.

5. M. A. Takita, I. J. Berger, A. C. Basílio-palmieri, K. M. Borges, J. M. De Souza, and M. L. N. P. Targon, *Genet. Mol. Biol.*, 2007, **30**, 841–847.

6. A. Behr and L. Johnen, *ChemSusChem*, 2009, **2**, 1072–95.

7. L. Caputi and E. Aprea, *Recent Patents Food, Nutr. Agric.*, 2011, **3**, 9–16.

8. C. S. Sell, *A Fragrant Introduction to Terpenoid Chemistry*, .

9. S. Tippmann, Y. Chen, V. Siewers, and J. Nielsen, *Biotechnol. J.*, 2013, **8**, 1435–44.

10. W. Schwab, C. Fuchs, and F.-C. Huang, *Eur. J. Lipid Sci. Technol.*, 2013, **115**, 3–8.

11. A. Karl and A. Swift, *Top. Catal.*, 2004, **27**, 143 –155.

12. K. Ukkonen, *Pine Chemicals- Global view Pine Chemicals- Global View - Nopek Oy*, 2016.

13. J. Zhou, G. Du, and J. Chen, *Curr. Opin. Biotechnol.*, 2014, **25**, 17–23.

14. G. Grigoropoulou and J. H. Clark, *Tetrahedron Lett.*, 2006, **47**, 4461–4463.

15. G. Sienel, R. Rieth, and K. Rowbottom, *Ullmann's Encyclopedia of Industrial Chemistry - Epoxides*, 2012.

16. R. E. Parker and N. S. Isaacs, *Chem. Rev.*, 1959, **59**, 737–799.

17. S. A. Hauser, M. Cokoja, and F. E. Ku, *Catal. Sci. Technol.*, 2013, **3**, 552–561.

18. G. D. Yadav and A. A. Pujari, *Org. Process Res. Dev.*, 2000, **4**, 88–93.

19. K. Kamata, K. Sugahara, R. Ishimoto, S. Nojima, M. Okazaki, T. Matsumoto, and N. Mizuno, *ChemCatChem*, 2014, **6**, 2327–2332.

20. A. Padwa and S. S. Murphree, *Arkivoc*, 2006, **3**, 6–33.

21. E. Griffith, Z. Su, S. Niwayama, C. Ramsay, Y.-H. Chang, and J. o Liu, *Proc. Natl. Acad. Sci. USA*, 1998, **95**, 15183–15188.

22. E. Kraka and D. Cremer, *Chem. Phys. Lett.*, 2002, **361**, 129–135.

23. R. K. Pandey, R. K. Upadhyay, and P. Kumar, *Arkovic*, 2006, **xiv**, 10–14.

24. E. J. Corey and M. Chaykovsky, *J. Am. Chem. Soc.*, 1965, **87**, 1353–1364.

25. J. Clayden, N. Greeves, and S. Warren, *Organic Chemisty, p503-520*, Oxford University Press, 2012.

26. A. Igor, G. Kerry, and P. Paul, *Wiley Interdiscip. Rev. Comput. Mol. Sci.*, 2011, **1**, 109–141.

27. J. Clayden, N. Greeves, and S. Warren, *Organic Chemistry, p431-433*, Oxford University Press, 2012.

28. J. Clayden, N. Greeves, and S. Warren, *Organic Chemistry, p430*, Oxford University Press, 2012.

29. V. G. Dryuk, *Tetrahedron*, 1976, **32**, 2855–2866.

30. A. Azman, B. Borstnik, and B. Plesnicar, *J. Org. Chem.*, 1969, **34**, 971–972.

31. H. B. Henbest and R. A. L. Wilson, *J. Chem. Soc.*, 1957, 1958–1965.

32. K. Herbert, G. P. H., S. Rainer, and M. Wilfried, *Ullmann's Encycl. Ind. Chem.*, 2000.

33. J. Davarpanah and A. R. Kiasat, *Catal. Commun.*, 2014, **46**, 75–80.

34. S. Sakaguchi, Y. Nishiyama, and Y. Ishii, *J. Org. Chem*, 1996, **61**, 5307–5311.

35. F. Fringuelli, R. Germani, F. Pizzo, and G. Savelli, *Tetrahedron Lett.*, 1989, **30**, 1427–1428.

36. K. K. W. Mak, Y. M. Lai, and Y. Siu, *J. Chem. Educ.*, 2006, **83**, 1058–1061.

37. T. Geller, A. Gerlach, and M. Kr, *Tetrahedron Lett.*, 2004, **45**, 5065–5067.

38. A. Waldemar, S.-M. C. R., and Z. Cong-Gui, *Org. React.*, 2004.

39. Y. Shi, *Acc. Chem. Res.*, 2004, **37**, 488–496.

40. G. Bellucci, C. Chiappe, G. Lo Moro, and G. Ingrosso, *J. Org. Chem.*, 1995, **60**, 6214–6217.

41. T. Itoh, K. Jitsukawa, K. Kaneda, and S. Teranishi, *J. Am. Chem. Soc.*, 1979, **101**, 159–169.

42. T. Katsuki and K. B. Sharpless, *J. Am. Chem. Soc.*, 1980, **102**, 5974–5976.

43. E. Jacobsen, P. Reider, C. Senanayake, K. Ryan, T. Verhoeven, E. Roberts, and J. Larrow, *Org. Synth.*, 2004, **76**, 46.

44. W. Zhang, J. L. Loebach, and S. R. Wilson, *J. Am. Chem. Soc*, 1990, **112**, 2801–2803.

45. E. N. Jacobsen, W. Zhang, A. R. Muci, J. R. Ecker, and L. Deng, *J. Am. Chem. Soc.*, 1991, **113**, 7063–7064.

46. T. Linker, *Angew. Chemie Int. Ed. English*, 1997, **36**, 2060–2062.

47. Y. Xu, N. R. B. J. Khaw, and Z. Li, *Green Chem.*, 2009, **11**, 2047.

48. B. S. Lane and K. Burgess, *Chem. Rev.*, 2003, **103**, 2457–2471.

49. A. Mouret, L. Leclercq, A. Muhlbauer, and V. Nardello-Rataj, *Green Chem.*, 2014, **16**, 269–278.

50. N. Mizuno and K. Yamaguchi, *Chem. Rec.*, 2006, **6**, 12–22.

51. W. R. Sanderson, *Pure Appl. Chem.*, 2000, **72**, 1289–1304.

52. K. Kamata, T. Hirano, S. Kuzuya, and N. Mizuno, *J. Am. Chem. Soc*, 2009, **131**, 6997–7004.

53. D. Limnios and C. G. Kokotos, *J. Org. Chem*, 2014, **79**, 4270–4276.

54. J. W. Kück, M. R. Anneser, B. Hofmann, A. Pçthig, M. Cokoja, and F. E. Kühn, *ChemSusChem*, 2015, **8**, 4056–4063.

55. R. A. Moretti, J. Du Bois, and T. D. P. Stack, *Org. Lett.*, 2016, **18**, 2528–2531.

56. B. S. Lane and K. Burgess, *J. Am. Chem. Soc*, 2001, **123**, 2933–2934.

57. J. A. Hyatt, G. S. Kottas, and J. Effler, *Org. Process Res. Dev.*, 2002, **6**, 782–787.

58. A. Gerlach and T. Geller, *Adv. Synth. Catal.*, 2004, **346**, 1247–1249.

59. G. R. Ebrahimian, X. Mollat, and P. L. Fuchs, *Org. Biomol. Chem.*, 2012, **14**, 2630–2633.

60. R. M. Hindupur, H. N. Pati, A. M. Thompson, D. Launay, and D. Martin, *Org. Process Res. Dev.*, 2017, **21**, 52–59.

61. Y. Wang, K. Kamata, R. Ishimoto, Y. Ogasawara, K. Suzuki, K. Yamaguchi, and N. Mizuno, *Catal. Sci. Technol.*, 2015, **5**, 2602–2611.

62. J. A. Cox and P. J. Kulesza, in *Catalytic Surfaces for Electroanalysis*, 2009.

63. G. Lewandowski and E. Milchert, *Ind. Eng. Chem. Res.*, 2011, **50**, 7101–7108.

64. C. Venturello, J. A. N. C. J. Bart, and M. Ricci, *J. Mol. Catal.*, 1985, **32**, 107–110.

65. C. Venturello, E. Alneri, and M. Ricci, *J. Org. Chem*, 1983, **48**, 3831–3833.

66. C. Venturello and R. D'Aloisio, *J. Org. Chem.*, 1988, **53**, 1553–1557.

67. K. Sato, M. Aoki, and M. Ogawa, *J. Org. Chem*, 1996, **61**, 8310–8311.

68. B. F. Sels, D. E. De Vos, A. V. de P, and P. A. Jacobs, *J. Org. Chem*, 1999, **64**, 7267–7270.

69. Y. Kon, H. Hachiya, Y. Ono, T. Matsumoto, and K. Sato, *Synthesis (Stuttg).*, 2011, 1092–1098.

70. H. Hachiya, Y. Kon, Y. Ono, K. Takumi, N. Sasagawa, Y. Ezaki, and K. Sato, *Synthesis (Stuttg).*, 2012, **44**, 1672–1678.

71. Y. Kon, Y. Ono, T. Matsumoto, and K. Sato, *Synlett*, 2009, **7**, 1095–1098.

72. K. Geoghegan and P. Evans, *Tetrahedron Lett.*, 2014, **55**, 1431–1433.

73. P. Yang, M. Yao, J. Li, Y. Li, and A. Li, *Angew. Chem., Int. Ed.*, 2016, **55**, 6964–6968.

74. J. White, J. Ruppert, M. Avery, S. Torii, and J. Nokami, *J. Am. Chem. Soc*, 1981, **103**, 1813–1821.

75. C. M. Byrne, S. D. Allen, E. B. Lobkovsky, and G. W. Coates, *J. Am. Chem. Soc.*, 2004, **126**, 11404–11405.

76. O. Hauenstein, S. Agarwal, and A. Greiner, *Nat. Commun.*, 2016, **7**, 1–7.

77. P. Levecque, D. W. Gammon, H. H. Kinfe, P. Jacobs, D. De Vos, and B. Sels, *Adv. Synth. Catal.*, 2008, **350**, 1557–1568.

78. Y. Kon, H. Hachiya, Y. Ono, T. Matsumoto, and K. Sato, *Synthesis (Stuttg).*, 2011, 1092–1098.

79. H. Hachiya, Y. Kon, Y. Ono, K. Takumi, N. Sasagawa, Y. Ezaki, and K. Sato, *Synlett*, 2011, 2819–2822.

80. Z. Xu and J. Qu, *Chem. Eur. J.*, 2013, **19**, 314–323.

81. M. Uroos, P. Pitt, L. M. Harwood, W. Lewis, A. J. Blake, and C. J. Hayes, *Org. Biomol. Chem.*, 2017, **15**, 8523–8528.

82. G. J. McGarvey, in *Encyclopedia of Reagents for Organic Synthesis*, John Wiley & Sons, Ltd, 2001.

83. H. Pamingle and K. Schulte-Elte, *Helv. Chim. Acta*, 1989, **72**, 1158–1163.

84. A. Srikrishna and G. Neetu, *Tetrahedron: Asymmetry*, 2010, **21**.

85. A. N. A. Kumar, G. Joshi, and H. Y. M. Ram, *Curr. Sci.*, 2012, **103**.

86. I. S. C. King, Cardiff University Thesis, On the Synthesis of Furan-Containing Fragrance Compounds, p12, 2011.

87. V. Srirajan, B. M. Bhawal, and A. R. A. . Deshmukh, *Tetrahedron*, 1996, **52**, 5585–5590.

88. F. Z. Macaev and A. V. Malkov, *ChemInform*, 2006, **37**, 9–29.

89. M. H. Shastri, D. G. Patil, and V. D. Patil, *Tetrahedron*, 1985, **41**, 3083–3090.

90. G. Shaffer, E. Eschinasi, K. Purzycki, and A. Doerr, *J. Org. Chem*, 1975, **40**, 2181–2185.

91. R. J. Sowden, S. Yasmin, N. H. Rees, S. G. Bell, and L. Wong, *Org. Biomol. Chem.*, 2005, **3**, 57–64.

92. M. Youssef, A. Itto, M. A. Ali, A. Karim, and J. Daran, *Tetrahedron Lett.*, 2002, **43**, 8769–8771.

93. A. Shamsizadeh, A. Roohbakhsh, F. Ayoob, and A. Moghaddamahmadi, in *Chapter 25 – The Role of Natural Products in the Prevention and Treatment of Multiple Sclerosis*, Academic Press, 2017, pp. 249–260.

94. D. Prat, B. Delpech, and R. Lett, *Tetrahedron Lett.*, 1986, **27**, 711–714.

95. J. A. Marshall and E. A. Van Devender, *J. Org. Chem*, 2001, **66**, 8037–8041.

96. J. A. Marshall, G. S. Bartley, and E. M. Wallace, *J. Org. Chem*, 1996, **61**, 5729–5735.

97. D. Tanner, P. Andersson, L. Tedenborg, and P. Somfai, *Tetrahedron*, 1994, **50**, 9135–9144.

98. J. Becker, K. Bergander, R. Fröhlich, and D. Hoppe, *Angew. Chem., Int. Ed.*, 2008, **47**, 1654–1657.

99. K. Mori, *Tetrahedron: Asymmetry*, 2006, **17**, 2133–2142.

100. Q. Wang, Q. Huang, B. Chen, J. Lu, H. Wang, and X. She, *Angew. Chem., Int. Ed.*, 2006, **45**, 3651–3653.

101. C. Still, S. Murata, G. Revial, and K. Yoshihara, *J. Am. Chem. Soc*, 1983, **105**, 625–627.

102. J. Loureiro, M. A. Maestro, A. Mouriño, and R. Sigüeiro, *J. Steroid Biochem. Mol. Biol.*, 2016, **164**, 56–58.

103. V. Il, K. P. Volcho, D. V Korchagina, V. A. Barkhash, and F. Nariman, *Helv. Chim. Acta*, 2007, **90**, 353–368.

104. W. Liu and J. P. N. Rosazza, *Synth. Commun.*, 2006, 2731–2735.

105. S. Tighe, Y.-Y. Gao, and S. C. G. Tseng, *Transl. Vis. Sci. Technol.*, 2013, **2**, 2.

106. R. M. Carman and M. T. Fletcher, *Aust. J. Chem*, 1984, 1117–1122.

107. C. Villa, B. Trucchi, R. Gambaro, and S. Baldassari, *Int. J. Cosmet. Sci.*, 2008, **30**, 139–144.

108. M. E. Amato, F. P. Ballistreri, A. Pappalardo, G. A. Tomaselli, R. M. Toscano, G. T. Sfrazzetto, S. Chimiche, U. Catania, and V. A. Doria, *Molecules*, 2013, **18**, 13754–13768.

109. G. P. More and S. V Bhat, *Tetrahedron Lett.*, 2013, **54**, 4148–4149.

110. H. Ye, G. Deng, J. Liu, and F. G. Qiu, *Org. Lett.*, 2009, **11**, 5442–5444.

111. S. Serra and V. Lissoni, *Eur. J. Org. Chem.*, 2015, 2226–2234.

112. C. Herna, A. Rosales, I. Rodrı, and M. Mun, *Tetrahedron*, 2009, **65**, 9542–9549.

113. L. Yu, Z. Bai, X. Zhang, X. Zhang, Y. Ding, and Q. Xu, *Catal. Sci. Technol.*, 2016, **6**, 1804–1809.

114. I. F. and Fragrances, *Discov. tomorrow's ingredients today*, 2018, 1.

115. A. Bosser, E. Paplorey, J. Belin, L. Recherche-développement, and M. A. Industries, *Bioteechnol. Prog.*, 1995, **11**, 689–692.

116. A. Srikrishna, G. Satyanarayana, and K. R. Prasad, *Synth. Commun.*, 2007, **37**, 1511–1516.

117. A. Srikrishna, L. Shaktikumar, and G. Satyanarayana, *Arkivoc*, 2003, 69–74.

118. M. Ansari and S. Emami, *Eur. J. Med. Chem.*, 2016, **123**, 141–154.

119. K. Yamaguchi, K. Mori, T. Mizugaki, K. Ebitani, and K. Kaneda, *J. Org. Chem*, 2000, **65**, 6897–6903.

120. L. Majidi and M. El Idrissi, *Phys. Chem. News*, 2003, **9**, 122–124.

121. K. Ngo, K. Cheung, and G. D. Brown, *J. Chem. Res.*, 1998, 80–81.

122. H. Ishida, S. Kimura, N. Kogure, M. Kitajima, and H. Takayama, *Org. Biomol. Chem.*, 2015, **13**, 7762–7771.

123. B. Riss, M. Garreau, P. Fricero, P. Podsiadly, N. Berton, and S. Buchter, *Tetrahedron*, 2017, **73**, 3202–3212.

124. D. Batzel and F. Woolard, 2012, PCT Int. Appl. (2012), WO 2012158250 A1 20121122.

125. S. Caillol, G. David, B. Boutevin, J. Pascault, and U. De Lyon, *Chem. Rev.*, 2014, **114**, 1082–1115.

126. G. Fiorani, M. Stuck, C. Martín, M. Belmonte, E. Martin, E. C. Escudero-adµn, and A. W. Kleij, *ChemSusChem*, 2016, **9**, 1304–1311.

127. J. E. Starrett, S. Weinreb, and M. Y. Kim, *J. Org. Chem.*, 1981, **46**, 5383–5389.

128. L. Thijs, E. Stokkingreef, J. Lemmens, and B. Zwanenburg, *Tetrahedron*, 1985, **41**, 2949–2956.

129. J. Xin, M. Li, R. Li, M. P. Wolcott, and J. Zhang, *ACS Sustain. Chem. Eng.*, 2016, **4**, 2754–2761.

130. A. Murphy, A. Pace, T. D. P. Stack, and S. U. V, 2004, 1–4.

131. J. R. Lowe, W. B. Tolman, and M. A. Hillmyer, *Biomacromolecules*, 2009, **10**, 2003–2008.

132. T.-L. Ho and Z. U. Din, *Synth. Commun.*, 2006, **19**, 813–816.

133. X. Z. Zhao, Y. Q. Tu, L. Peng, X. Q. Li, and Y. X. Jia, *Tetrahedron Lett.*, 2004, **45**, 3713–3716.

134. J. H. Kim, H. J. Lim, and S. H. Cheon, *Tetrahedron*, 2003, **59**, 7501–7507.

135. S. Gill, P. Kocienski, A. Kohler, A. Pontirolia, and L. Qunb, *Chem. Commun.*, 1996, 1743–1744.

136. L. Pen, C. Mart, and A. W. Kleij, *Macromolecules*, 2017, **50**, 5337–5345.

137. V. Schimpf, B. S. Ritter, P. Weis, and K. Parison, *Macromolecules*, 2017, **50**, 944–955.

138. A. L. V. De P, D. E. De Vos, C. M. De C, and P. A. Jacobs, *Tetrahedron Lett.*, 1998, **39**, 8521–8524.

139. F. A. Bermejo, D. Clemente-tejeda, and L. Alejandro, *Tetrahedron*, 2013, **69**, 2977–2986.

140. V. V Fomenko, O. V Bakhvalov, V. F. Kollegov, and N. F. Salakhutdinov, 2017, EP 2324690, p1–3.

141. K. Kamata, K. Sugahara, K. Yonehara, R. Ishimoto, and N. Mizuno, *Chemistry*, 2011, **17**, 7549–59.

142. Y. Nakagawa, K. Kamata, M. Kotani, K. Yamaguchi, and N. Mizuno, *Angew. Chem., Int. Ed.*, 2005, **44**, 5136–5141.

143. O. Smitt and H. Ho, *Tetrahedron*, 2002, **58**, 7691–7700.

144. A. Murphy, G. Dubois, T. D. P. Stack, and S. U. V, *J. Am. Chem. Soc*, 2003, **125**, 5250–5251.

145. T. C. Chen, C. O. Da Fonseca, and A. H. Schönthal, *Am J Cancer Res*, 2015, **5**, 1580–1593.

146. D. Gamba, C. Liberato, S. Pisoni, D. Amorim, M. Antonio, P. Lunardi, C. Alberto, and S. Gonçalves, *Eur. J. Med. Chem.*, 2010, **45**, 526–535.

147. T. C. Chen, N. Chan, S. Labib, J. Yu, H. Cho, F. M. Hofman, and A. H. Schönthal, *Int. J. Mol. Sci*, 2018, **19**, 1–18.

148. K. Geoghegan and P. Evans, *J. Org. Chem*, 2013, **78**, 3410–3415.

149. B. N. Bluthe, J. Ecoto, M. Fetizon, S. Lazare, and E. Polytechnique, *J.C.S Perkin I*, 1980, **2**, 1747–1751.

150. P. Taylor, R. Pellegata, P. Ventura, M. Villa, G. Palmisano, and G. Lesma, *Synth. Commun.*, 2006, **15**, 165–170.

151. M. Stekrova, I. Paterova-Dudkova, E. Vyskocilova-Leitmannova, and L. Cerveny, *Res. Chem. Intermed.*, 2012, **38**, 2075–2084.

152. L. E. Nikitina, S. A. Dieva, V. V Plemenkov, O. A. Lodochnikova, A. T. Gubaidullin, O. N. Kataeva, and I. A. Litvinov, *Russ. J. Gen. Chem.*, 2001, **71**, 1233–1237.

153. V. V Fomenko, O. V Bakhvalov, V. F. Kollegov, and N. F. Salakhutdinov, *Russ. J. Gen. Chem.*, 2017, **87**, 1675–1679.

154. N. D. Sathikge, *CSIR Biosci. Confid.*, 2008, **1**, 1–44.

155. C. S. Sell, *Kirk-Othmer Encyclopedia of Chemical Technology - Terpenoids*, John Wiley & Sons, Inc., 2006.

156. N. Anderson, *Org. Process Res. Dev.*, 2001, **5**, 613–621.

157. T. Illg, P. Löb, and V. Hessel, *Bioorg. Med. Chem.*, 2010, **18**, 3707–19.

158. S. G. Newman and K. F. Jensen, *Green Chem.*, 2013, **15**, 1456–1472.

159. M. Colombo and I. Peretto, *Drug Discov. Today*, 2008, **13**, 677–84.

160. N. G. Anderson, *Org. Process Res. Dev.*, 2012, **16**, 852–869.

161. S. B. Broek, J. R. Leliveld, R. Becker, M. E. Delville, P. J. Nieuwland, K. Koch, and F. P. J. T. Rutjes, *Org. Process Res. Dev.*, 2012, **16**, 934–938.

162. M. Nobis, D. R. Roberge, M. Nobis, and D. M. Roberge, *Chim. Oggi / Chem. Today*, 2011, **29**, 56–58.

163. X. Zhang, S. Stefanick, and F. J. Villani, *Org. Process Res. Dev.*, 2004, **8**, 455–460.

164. B. P. Mason, K. E. Price, J. L. Steinbacher, A. R. Bogdan, and D. T. Mcquade, *Chem. Rev.*, 2007, **107**, 2300–2318.

165. M. Struempel, B. Ondruschka, R. Daute, and A. Stark, *Green Chem.*, 2008, **10**, 41.

166. A. Harsanyi, A. Conte, L. Pichon, A. Rabion, S. Grenier, and G. Sandford, *Org. Process Res. Dev.*, 2017, **21**, 273–276.

167. P. B. Cranwell, M. O'Brien, D. L. Browne, P. Koos, A. Polyzos, M. Pena-Lopez, and S. V Ley, *Org. Biomol. Chem.*, 2012, **10**, 5774–5779.

168. B. A. M. W. Van Den Broek, R. Becker, F. Kçssl, M. E. Delville, P. J. Nieuwland, K. Koch, and F. P. J. T. Rutjes, *ChemSusChem*, 2012, **5**, 289–292.

169. W. He, Z. Fang, Q. Tian, W. Shen, and K. Guo, *Ind. Eng. Chem. Res.*, 2016, **55**, 1373–1379.

170. S.-P. Kee and A. Gavriilidis, *Org. Process Res. Dev.*, 2009, **13**, 941–951.

171. P. Fernandez-rodriguez, J. Haber, F. Kleinbeck, S. Kamptmann, F. Susanne, P. Hoehn, M. Lanz, L. Pellegatti, F. Venturoni, J. Robertson, and C. Willis, *Green Chem.*, 2017, **19**, 1439–1448.

172. D. Plaza, V. Strobel, P. K. Heer, A. Sellars, S. Hoong, J. Clark, and A. A. Lapkin, *J. Chem. Technol. Biotechnol.*, 2017, **92**, 2254–2266.

173. G. Mouzin, H. Cousse, and J. M. Autin, *Synth. Commun.*, 1980, 54–55.

174. W. F. Richter, B. R. Whitby, and R. C. Chou, *Xenobiotica*, 1996, **26**, 243–254.

175. M. Kawamura, A. Talero, J. Santiago, E. Garambel-Vilca, I. Rosset, and A. Burtoloso, *J. Org. Chem.*, 2016, **81**, 10569–10575.

176. Z. Li and R. Tong, *J. Org. Chem.*, 2017, **82**, 1127–1135.

177. A. Rosatella and C. Afonso, *Adv. Bio. Res*, 2011, **353**, 2920 – 2926.

178. C. J. R. Bataille and T. J. Donohoe, *Chem. Soc. Rev.*, 2011, **40**, 114–128.

179. H. C. Kolb, M. S. VanNieuwenhze, and K. B. Sharpless, *Chem. Rev.*, 1994, **94**, 2483–2547.

180. B. Plietker and M. Niggemann, *Org. Lett.*, 2003, **5**, 3353–3356.

181. L. Emmanuvel, T. Mahammad, A. Shaikh, and A. Sudalai, *Org. Lett.*, 2005, **7**, 5071 – 5074.

182. C. Alamillo-ferrer, S. C. Davidson, M. J. Rawling, N. H. Theodoulou, M. Campbell, P. G. Humphreys, A. R. Kennedy, and N. C. O. Tomkinson, *Org. Lett.*, 2015, **17**, 5132–5135.

183. S. I. Okovityi, R. G. Gaponova, Y. A. Seredyuk, and L. I. Kas, *Russ. J. Org. Chem.*, 2002, **38**, 160–164.

184. A. Gangjee, Y. Zhao, S. Raghavan, C. C. Rohena, S. L. Mooberry, and E. Hamel, *J. Med. Chem*, 2013, **56**, 6829–6844.

185. F. Fringuelli, R. Germani, F. Pizzo, and G. Savelli, *Synth. Commun.*, 1989, **19**, 1939 – 1943.

186. W. Zhu and W. T. Ford, *J. Org. Chem.*, 1991, **56**, 7022–7026.

187. P. Gogoi, S. Das Sharma, and D. Konwar, *Lett. Org. Chem.*, 2007, **4**, 249–252.

188. S. Wu, A. Li, Y. S. Chin, and Z. Li, *ACS Catal*, 2013, **3**, 752–759.

189. Q. Neng, J. Zhang, T. Hua, and X. Ping, *Catal. Commun.*, 2009, **10**, 1279–1283.

190. Y. Usui, K. Sato, and M. Tanaka, *Angew. Chem., Int. Ed.*, 2003, **42**, 5623–5625.

191. A. Theodorou, L. Triandafillidi, and C. Kokotos, *Eur. J. Org. Chem.*, 2017, 1502–1509.

192. R. Saladino, A. Andreoni, and C. Crestini, *Tetrahedron*, 2005, **61**, 1069–1075.

193. V. Singh and P. T. Deota, *Synth. Commun.*, 1988, 617–624.

194. C. Venturello and M. Gambaro, *Synth. Commun.*, 1989, 295–297.

195. Beat Ernst and C. Leumann, *Modern synthetic methods, p202*, 1995.

196. S.-H. Wei and S.-T. Liu, *Catal Lett*, 2009, **127**, 143–147.

197. S. S. Balula, I. C. M. S. Santos, L. Cunha-silva, A. P. Carvalho, J. Pires, C. Freire, J. A. S. Cavaleiro, B. De Castro, and A. M. V Cavaleiro, *Catal. Today*, 2013, **203**, 95–102.

198. C. M. Plummer, P. Kraft, J. Froese, O. A. H. Jones, and H. M. Hügel, *Asian J. Org. Chem*, 2015, **6**, 1075–1084.

199. X. Feng, A. J. East, W. B. Hammond, Y. Zhang, and M. Jaffe, *Polym. Adv. Technol*, 2011, **22**, 139–150.

200. F. Kido, M. Kato, and T. Abiko, *J. Chem. Soc., Perkin Trans. 1*, 1995, **1**, 2989–2994.

201. Y. Shono, K. Watanabe, and H. Sekihachi, 1998, EP 0 476 885 B1, p1–29.

202. V. V. Costa, K. a. da Silva Rocha, I. V. Kozhevnikov, E. F. Kozhevnikova, and E. V. Gusevskaya, *Catal. Sci. Technol.*, 2013, **3**, 244.

203. Y. Takeuchi, H. Fujisawa, and R. Noyori, *Org. Lett.*, 2004, **6**, 6318–6320.

204. M. Mitsuyasu and M. Tadakatsu, 2000, JP2000072644 (A), p1–3.

205. K. Piatkowski, S. Lochynski, Szalkowska-Pagowska, and A. Hieronima; Siemieniuk, 1995, Method of manufacturing novel (–)–cis–3–hydroxy–tr.

206. A. Hendrich and K. Piatkowski, 1987.

207. Z. Muljiani, A. Deshmukh, and S. Gadre, *Synth. Commun.*, 2014, **17**, 25–32.

208. Y. Hikino, *Yakugaku Zasshi*, 1965, **85**, 477–480.

209. O. Hauenstein, M. Reiter, S. Agarwal, B. Rieger, and A. Greiner, *Green Chem.*, 2015, **18**, 760–770.

210. I. Kiran, *Nat. Prod. Commun.*, 2011, **6**, 1805–1806.

211. T. Ishikawa, M. Kudo, and J. Kitajima, *Chem. Pharm. Bull.*, 2002, **50**, 501–507.

212. T. Four, R. M. Carman, and M. T. Fletcher, *Aust. J. Chem*, 1984, **37**, 2129–1236.

213. W. Abraham, B. Stumpf, and K. Kieslich, *Appl Microbiol Biotechnol*, 1986, **24**, 24–30.

214. A. Srivastava and T. Shivanandappa, *Nutr. Neurosci.*, 2014, **17**, 164–174.

215. D. Clemente-tejeda and F. A. Bermejo, *Tetrahedron*, 2014, **70**, 9381–9386.

216. W. Eschenrnoser, P. Uehelhart, and U. Zurich, *Helv. Chim. Acta*, 1981, **64**, 2681–2690.

217. Y. Liu, G. Shi, X. Wang, C. Zhang, Y. Wang, R. Chen, and D. Yu, *J. Asian Nat. Prod. Res.*, 2016, **6020**, 1–11.

218. Y. Yuasa and Y. Yuasa, *Helv. Chim. Acta*, 2004, **87**, 2602–2607.

219. F. M. Nunes, F. Gabriel, N. N. Saraiva, M. A. Trapp, M. C. De Mattos, M. Conceic, F. Oliveira, and E. Rodrigues-filho, *Appl. Catal. A Gen.*, 2013, **468**, 88–94.

220. Y. Hirai, M. Ikeda, T. Murayama, and T. Ohata, *Biosci. Biotechnol. Biochem*, 1998, **62**, 1364–1368.

221. H. Hioki, H. Ooi, M. Hamano, Y. Mimura, and S. Yoshio, *Tetrahedron*, 2001, **57**, 1235–1246.

222. E. Steinreiber, S. F. Mayer, and K. Faber, *Synthesis (Stuttg).*, 2001, 2035–2039.

223. D. C. Braddock, A. X. Gao, A. J. P. White, and M. Whyte, *Chem. Commun.*, 2014, **50**, 13725–13728.

224. G. Wang, W. Tang, and R. R. Bidigare, *Terpenoids As Therapeutic Drugs and Pharmaceutical Agents*, 2005.

225. V. J. J. Martin, D. J. Pitera, S. T. Withers, J. D. Newman, and J. D. Keasling, *Nat. Biotechnol.*, 2003, **21**, 796–802.

226. J. Bohlmann and C. I. Keeling, *Plant J.*, 2008, **54**, 656–69.

227. S. Malik, R. M. Cusidó, M. H. Mirjalili, E. Moyano, J. Palazón, and M. Bonfill, *Process Biochem.*, 2011, **46**, 23–34.

228. J. Turconi, R. Guevel, G. Oddon, R. Villa, A. Geatti, M. Hvala, K. Rossen, R. Go, and A. Burgard, *Org. Process Res. Dev.*, 2014, **18**, 417–422.

229. A. Ghosh and K. Xi, *J. Org. Chem.*, 2009, **74**, 1–19.

230. J. G. Hubert, D. P. Furkert, and M. A. Brimble, *J. Org. Chem.*, 2015, **80**, 2231–2239.

231. E. Elamparuthi, C. Fellay, M. Neuburger, and K. Gademann, *Angew. Chem., Int. Ed.*, 2012, **51**, 4071–4073.

232. R. S. Kumaran and G. Mehta, *Tetrahedron*, 2015, **71**, 1718–1731.

233. N. A. Meanwell, in *A Synopsis of the Properties and Applications of Heteroaromatic Rings in Medicinal Chemistry*, eds. E. F. V Scriven and C. A. B. T.-A. in H. C. Ramsden, Academic Press, 2017, vol. 123, pp. 245–361.

234. B. Schaefer, *Natural Products in the Chemical Industry*, 2014.

235. A. H. Payne and D. B. Hales, *Endocr. Rev.*, 2004, **25**, 947–970.

236. J. Lange and S. G. Solutions, *Biofuels, Bioprod. Bioref.*, 2007, **1**, 39–48.

237. R. Ciriminna, M. Lomeli-Rodriguez, P. Demma Carà, J. a. Lopez-Sanchez, and M. Pagliaro, *Chem. Commun.*, 2014, **50**, 15288–15296.

238. F. Beran, P. Rahfeld, K. Luck, R. Nagel, H. Vogel, N. Wielsch, S. Irmisch, S. Ramasamy, J. Gershenzon, D. G. Heckel, and T. G. Köllner, *Proc. Natl. Acad. Sci.* , 2016, **113** , 2922–2927.

239. M. Q. Styles, E. A. Nesbitt, S. Marr, M. Hutchby, and D. J. Leak, *FEBS J.*, 2017, **284**, 1700–1711.

240. M. Muthukrishnan, D. R. Garud, R. R. Joshi, and R. A. Joshi, *Tetrahedron*, 2007, **63**, 1872–1876.

241. E. Palmer - Top 20 Generic molecules worldwide, *FiercePharma.com*, 2011, 1.

242. Y. Lu, X. Xu, X. Zhang, Y. Lu, X. Xu, and X. Zhang, *Org. Prep. Proced. Int.*, 2015, **47**, 168–172.

243. C. Mattia and F. Coluzzi, *Minerva Anestesiol.*, 2009, **75**, 644.

244. L. S. Bertolini A., Ferrari A., Ottani A., Guerzoni S., Tacchi R., *CNS Drug Rev.*, 2006, **12**, 250–275.

245. N. P. C. Company, *DRUGS & PHARMACEUTICAL TECHNOLOGY HANDBOOK - Paracetamol An analysis of technologies for cleaner production*, Asia Pacific Business Press Inc., 2004.

246. N. Fleming - Does paracetamol do you more harm than good? The Guardian, 2015.

247. B. Latli, Ã. M. Hrapchak, H. Switek, D. M. Retz, D. Krishnamurthy, and C. H. Senanayake, *J. Label. Compd. Radiopharm.*, 2010, **53**, 15–23.

248. J. M. Fortunak and C. King - Green chemistry synthesis of the malerial drug Amodiaquine and the analogs thereof PCT/US2013/030005, 2013, 1–37.

249. R. Joncour, N. Duguet, M. Lemaire, E. Metay, and A. Ferreira, *Green Chem.*, 2014, **16**, 2997–3002.

250. E. Friderichs, T. Christoph, and H. Buschmann, in *Ullmann's Encyclopedia of Industrial Chemistry*, Wiley-VCH Verlag GmbH & Co. KGaA, 2000.

251. *Paracetamol Production in India - Government of Andhra Pradesh*, 2002.

252. DSIR, *Technology in Indian Paracetamol Industry p1-20*, 2000.

253. S. Basu, M. S. Kumar, G. Amitava, and D. S. G, 2013, **2**, 20–25.

254. Z. Research, *Acetaminophen (Paracetamol) Market for Pharmaceuticals, Dye Industry and Chemical Industry - Global Industry Perspective, Comprehensive Analysis, Size, Share, Growth, Segment, Trends and Forecast, 2014 – 2020*, 2016.

255. J. Jacques and V. Eynde, *Pharmaceuticals*, 2016, **9**, 1–16.

256. BASF Preparation of O-Acylphenols C07C 45/46, 1985.

257. M. Uroos, W. Lewis, A. J. Blake, and C. J. Hayes, *J. Org. Chem.*, 2010, **75**, 8465–70.

258. A. Yasuda, H. Yamamoto, and H. Nozaki, *Bull. Chem. Soc. Jpn.*, 1979, **52**, 1705.

259. P. Basabe, a. Blanco, O. Bodero, M. Martín, I. S. Marcos, D. Díez, F. Mollinedo, and J. G. Urones, *Tetrahedron*, 2010, **66**, 2422–2426.

260. D. Steiner, L. Ivison, C. T. Goralski, R. B. Appell, and R. Gojkovic, 2002, **13**, 2359–2363.

261. C. Raptis, H. Garcia, and M. Stratakis, *Angew. Chem. Int. Ed. Engl.*, 2009, **48**, 3133–6.

262. W. Long, C. S. Gill, and C. W. Jones, *Dalt. trans.*, 2010, **39**, 1470–1472.

263. T. Fisher and P. H. Dussault, *Tetrahedron*, 2017, **73**, 4233–4258.

264. T. I. Zvereva, V. G. Kasradze, O. B. Kazakova, and O. S. Kukovinets, *Russ. J. Org. Chem.*, 2010, **46**, 1431–1451.

265. L. Chen and D. F. Wiemer, *J. Org. Chem*, 2002, **67**, 7561–7564.

266. C. Sha, H. Liao, and P. Cheng, *J. Org. Chem*, 2003, **68**, 8704–8707.

267. L. M. T. Frija and C. a. M. Afonso, *Tetrahedron*, 2012, **68**, 7414–7421.

268. R. Bonikowski, J. Kula, A. Bujacz, A. Wajs-bonikowska, and M. Zakłos-szyda, 2012, **23**, 1038–1045.

269. J. Tsuji, *Pure Appl. Chem.*, 1986, **58**, 869–878.

270. J. Tsuji and T. Yamakawa, *Tetrahedron Lett.*, 1979, 613–616.

271. M. D. Berechet, M. D. Stelescu, E. Manaila, and G. Craciun, *Rev. Chim.*, 2015, **66**, 1814–1818.

272. Y. Izawa, D. Pun, and S. S. Stahl, *Science*, 2011, **333**, 209–214.

273. J. Zhang, Q. Jiang, D. Yang, X. Zhao, Y. Dong, and R. Liu, *Chem. Sci.*, 2015, **6**, 4674–4680.

274. K. K. Miller, P. Zhang, Y. Nishizawa-brennen, and J. W. Frost, *ACS Sustain. Chem. Eng.*, 2014, **2**, 2053–2056.

275. M. A. E. Ggersdorfer and B. Aktiengesellschaft, *Ullmann's Encyclopedia of Industrial Chemistry - Terpenes*, 2012.

276. M. H. H. Sharghi, *Synthesis (Stuttg).*, 2002, **8**, 1057–1059.

277. E. Rancan, F. Aricò, G. Quartarone, L. Ronchin, P. Tundo, and A. Vavasori, *Catal. Commun.*, 2014, **54**, 11–16.

278. T. Mandai, T. Matsumoto, and J. Tsuji, *Synlett*, 1993, **2**, 113–114.

279. K. Shibuya and M. Shiratsuchi, *Synth. Commun.*, 1995, **25**, 431–449.

280. A. Noujima, T. Mitsudome, T. Mizugaki, K. Jitsukawa, and K. Kaneda, *Chem. Commun.*, 2012, **48**, 6723–6725.

281. A. Srlkrlshna, R. Viswajanani, J. A. Sattigeri, and C. V. Yelamaggad, *Tetrahedron Lett.*, 1995, **36**, 2347–2350.

282. S. Bull and R. M. Carman, *Aust. J. Chem*, 1992, **45**, 2077–2081.

283. E. von Rudloff, *Can. J. Chem*, 1961, **30**, 1860–1864.

284. D. S. Pisoni, D. Gamba, C. V Fonseca, J. S. Costa, C. L. Petzhold, E. R. De Oliveira, and M. A. Ceschi, *J. Braz. Chem. Soc*, 2006, **17**, 321–327.

285. H.-J. Liu and J. M. Nyangulu, *Tetrahedron Lett.*, 1989, **30**, 5097–5098.

286. S. M. Patil, S. Kulkarni, M. Mascarenhas, R. Sharma, S. M. Roopan, and A. Roychowdhury, *Tetrahedron*, 2013, **69**, 8255–8262.

287. B. Schaefer, *Natural Products in the Chemical Industry*, Springer Berlin Heidelberg, Berlin, Heidelberg, 2014.

288. G. Shang, D. Liu, S. E. Allen, Q. Yang, and X. Zhang, *Chem. Eur. J.*, 2007, **13**, 7780–7784.

289. E. J. Norris and J. R. Coats, *Int. J. Environ. Res. Public Heal.*, 2017, **14**, 1–15.

290. V. Sikka, V. Chattu, R. Popli, S. Galwankar, D. Kelkar, S. Sawicki, S. Stawicki, and T. Papadimos, *J. Glob. Infect. Dis.*, 2016, **8**, 3–15.

291. R. W. Malone, J. Homan, M. V Callahan, J. Glasspool-Malone, L. Damodaran, A. D. B. Schneider, R. Zimler, J. Talton, R. R. Cobb, I. Ruzic, J. Smith-Gagen, D. Janies, J. Wilson, and Z. R. W. Group, *PLoS Negl. Trop. Dis.*, 2016, **10**, e0004530.

292. WHO, *Zika virus microcephaly and Guillain-Barre syndrome Situation Report April 2016*, 2016.

293. M. Z. Mehrjardi, *Virol. Res. Treat.*, 2017, **8**, 1178122X17708993.

294. A. Bruno, *A SOCIO-ECONOMIC IMPACT ASSESSMENT OF THE ZIKA VIRUS IN LATIN AMERICA AND THE CARIBBEAN : with a focus on Brazil , Colombia and Suriname*, 2017.

295. CDC, *Zika Virus*, 2018, 1 – Prevention and Transmission.

296. S. D. Rodriguez, H.-N. Chung, K. K. Gonzales, J. Vulcan, Y. Li, J. A. Ahumada, H. M. Romero, M. De La Torre, F. Shu, and I. A. Hansen, *J. Insect Sci.*, 2017, **17**, 24.

297. Y. Yuasa, H. Tsuruta, and Y. Yuasa, *Org. Process Res. Dev.*, 2000, **4**, 1999–2001.

298. A. V Degani, N. Dudai, A. Bechar, and Y. Vaknin, 2018, **5026**.

299. I. T. Dell - Composition containing p-menthane-3, 8 diol and its use as insect repellent PCT/GB2008/003113, 2009, 1–23.

300. S. P. Carroll and J. Loye, *J. Am. Mosq. Control Assoc.*, 2006, **22**, 507–514.

301. S. B McIver, *A Model for the Mechanism of Action of the Repellent Deet on Aedes Aegypti (Diptera: Culicidae)*, 1981, vol. 18.

302. B. P. Factsheet, *Beyond Pestic.*, 2010, **30**, 1–23.

303. Citrefine, *www.citrefine.com*, 2018, 1.

304. P. D. Clarke - Antiviral composition comprising p-menthane-3, 8-diol WO 2005/087209 A1, 2005, 1–37.

305. H. Zimmerman and J. English, *J. Am. Chem. Soc*, 1953, **1308**, 2367–2370.

306. K. Tani, T. Yamagata, S. Akutagawa, and H. Kumobayashi, *J. Am. Chem. Soc*, 1984, **106**, 5208–5217.

307. H. Cheng, X. Meng, R. Liu, Y. Hao, and Y. Yu, *Green Chem.*, 2009, **11**, 1227–1231.

308. J. Drapeau, M. Rossano, D. Touraud, U. Obermayr, M. Geier, A. Rose, and W. Kunz, *Comptes Rendus Chim.*, 2011, **14**, 629–635.

309. P. D. Clarke - Insect Repellent Compositions GB 2282534, 1995, 1–11.

310. M. Lajunen and A. M. P. Koskinen, *Tetrahedron Lett.*, 1994, **35**, 4461–4464.

311. G. Y. Ishmuratov, V. S. Tukhvatshin, M. P. Yakovleva, and R. F. Talipov, *Russ. J. Gen. Chem.*, 2016, **52**, 755–756.

312. M. Bulliard, G. Balme, and J. Gore, *Synth. Commun.*, 1988, **12**, 972–975.

313. R. Galli, M. Dobler, R. Stahl, R. Guller, and H.-J. Borschberg, *Helv. Chim. Acta*, 2002, **85**, 3400–3413.

314. A. F. Barrero, M. M. Herrador, P. Arteaga, N. Meine, M. P. Carmen, and J. V Catal, *Org. Biomol. Chem.*, 2011, **9**, 1118–1125.

315. Y. Kon, Y. Ono, T. Matsumoto, and K. Sato, *Synlett*, 2009, **7**, 1095–1098.

316. J. M. Schomaker, V. R. Pulgam, and B. Borhan, *J. Am. Chem. Soc.*, 2004, **126**, 13600–13601.

317. S. Yamazaki, *J. Org. Chem.*, 2012, **77**, 9884–9888.

318. G. Majetich, J. Shimkus, and Y. Li, *Tetrahedron Lett.*, 2010, **51**, 6830–6834.

319. E. Negishi and F. Luo, *J. Org. Chem.*, 1983, **97**, 1562–1564.

320. B. Benjilali, D. Buisson, and R. Azerad, *Tetrahedron Lett.*, 1992, **33**, 2349–2352.

321. B. Suess, W. Meyerhof, and T. Hofmann, *J. Agric. Food Chem.*, 2016.

322. S. Yamazaki, *Org. Biomol. Chem.*, 2010, **8**, 2377–2385.

323. H. Rudler, *J. Mol. Catal. A Chem.*, 1998, **133**, 255–265.

324. C. E. Davis, J. L. Bailey, J. W. Lockner, and R. M. Coates, *J. Org. Chem.*, 2003, **68**, 75–82.

325. A. Murphy, A. Pace, and T. D. P. Stack, *Org. Lett.*, 2004, **6**, 3119–3122.

326. M. Mityazawa and T. Murata, *J. Oleo. Sci*, 2001, **50**, 921–925.

327. R. M. Carman and K. D. Klika, *Aust. J. Chem*, 1991, **44**, 1803–1808.

328. K. R. Muralidharan, A. R. De Lera, S. D. Isaeff, A. W. Norman, and W. H. O. Jb, *J. Org. Chem*, 1993, **58**, 1895–1899.

329. S. Rozen and M. Kol, *J. Org. Chem*, 1990, **55**, 5155–5159.

330. P. C. Andrews, B. H. Fraser, C. M. Forsyth, P. C. Junk, M. Massi, and K. L. Tuck, *Synthesis (Stuttg).*, 2007, 1523–1527.

331. Y. Takeuchi, H. Fujisawa, and R. Noyori, *Org. Lett.*, 2004, **6**, 4607–4610.

332. M. N. Gould, P. Crowell, and Z. Ren, *Biochem. Pharmacol.*, 1994, **47**, 1405–1415.

333. C. Gally, B. M. Nestl, and B. Hauer, *Angew. Chemie Int. Ed.*, 2015, **54**, 12952–12956.

334. A. Farre, K. Soares, R. A. Briggs, A. Balanta, and D. M. Benoit, *Chem. Eur. J.*, 2016, **22**, 17552–17556.

335. L. Habala, C. Dworak, A. A. Nazarov, C. G. Hartinger, S. A. Abramkin, V. B. Arion, W. Lindner, M. Galanski, and B. K. Keppler, *Tetrahedron*, 2008, **64**, 137–146.

336. Y. Monguchi*, F. Wakayama, H. Takada, Y. Sawama, and H. Sajiki, *Synlett*, 2015, **26**, 700–704.

337. L. M. Geary, T. Chen, T. P. Montgomery, and M. J. Krische, *J. Am. Chem. Soc*, 2014, **136**, 5920–5922.

338. O. Hauenstein, M. Reiter, S. Agarwal, B. Rieger, and A. Greiner, *Green Chem.*, 2016, **18**, 760–770.

339. S. C. Shim, D. S. Kim, D. J. Yoo, T. Wada, and Y. Inoue, *J. Org. Chem*, 2002, **67**, 5718–5726.

340. B. Trost, W. Vladuchick, and A. Bridges, *J. Am. Chem. Soc.*, 1980, **102**, 3554–3572.

341. D. Pun, T. Diao, and S. S. Stahl, *J. Am. Chem. Soc*, 2013, **135**, 8213–8221.

342. E. J. Rayment, N. Summerhill, and E. A. Anderson, *J. Org. Chem.*, 2012, **77**, 7052–7060.

343. E. Nazimova, A. Pavlova, O. Mikhalchenko, I. Il, D. Korchagina, T. Tolstikova, K. Volcho, and N. Salakhutdinov, *Med. Chem. Res.*, 2016, **25**, 1369–1383.

344. H. King, E. Koros, and S. Nelson, *J. Chem. Soc. A Inorganic, Phys. Theor.*, 1963, 5449–5459.

345. M. K. Lajunen, T. Maunula, and A. M. P. Koskinen, *Tetrahedron*, 2000, **56**, 8167–8171.

346. E. J. Horn, B. R. Rosen, Y. Chen, J. Tang, K. Chen, M. D. Eastgate, and P. S. Baran, *Nature*, 2016, **533**, 77–81.

347. Y. Asakawa, R. Matsuda, M. Tori, and T. Hashimoto, *Phytochemistry*, 1988, **27**, 3861–3869.